Microbiology Monographs

Series Editor: Alexander Steinbüchel

Michael Hippler *Editor*

Chlamydomonas: Molecular Genetics and Physiology

Springer

Microbiology Monographs

Volume 30

Series editor
Alexander Steinbüchel
Münster, Germany

More information about this series at http://www.springer.com/series/7171

Michael Hippler
Editor

Chlamydomonas: Molecular Genetics and Physiology

Springer

Editor
Michael Hippler
Institute of Plant Biology and Biotechnology
Universität Münster
Münster, Germany

ISSN 1862-5576 ISSN 1862-5584 (electronic)
Microbiology Monographs
ISBN 978-3-319-66363-0 ISBN 978-3-319-66365-4 (eBook)
DOI 10.1007/978-3-319-66365-4

Library of Congress Control Number: 2017958132

Printed on acid-free paper

This Springer imprint is published by Springer Nature
The registered company is Springer International Publishing AG
The registered company address is: Gewerbestrasse 11, 6330 Cham, Switzerland

Contents

Genomics and Functional Genomics in *Chlamydomonas reinhardtii*

Ian K. Blaby and Crysten E. Blaby-Haas

Abstract The availability of the *Chlamydomonas reinhardtii* nuclear genome sequence continues to enable researchers to address biological questions relevant to algae, land plants, and animals in unprecedented ways. As we continue to characterize and understand biological processes in *C. reinhardtii* and translate that knowledge to other systems, we are faced with the realization that many genes encode proteins without a defined function. The field of functional genomics aims to close this gap between genome sequence and protein function. Transcriptomes, proteomes, and phenomes can each provide layers of gene-specific functional data while supplying a global snapshot of cellular behavior under different conditions. Herein we present a brief history of functional genomics, the present status of the *C. reinhardtii* genome, how genome-wide experiments can aid in supplying protein function inferences, and provide an outlook for functional genomics in *C. reinhardtii*.

1 Introduction

The first bacterial genome sequence, completed in the mid-1990s (Fleischmann et al. 1995), was rapidly followed by a succession of milestone accomplishments [e.g., the first eukaryote in 1996 (Goffeau et al. 1996), the first plant genome in 2000 (Kaul et al. 2000), and the first mammalian genome in 2002 (Waterston et al. 2002)]. These achievements marked the beginning of a new era in biological sciences. The resulting post-genomic age has equipped researchers with the genetic blueprints for thousands of organisms. Unfortunately, however, it is not immediately clear how these blueprints translate into complex, thriving, and adaptable organisms. Indeed, a key observation made with early genome sequences, and subsequently echoed with each new genome, is that we have complete functional understanding for a small percentage of the encoded proteins [although this perhaps came as little surprise (Bork et al. 1992a, b)]. Increases in the speed of sequence acquisition, accuracy (due in large part to increased depth, or coverage, of

I.K. Blaby (✉) • C.E. Blaby-Haas
Biology Department, Brookhaven National Laboratory, 50 Bell Avenue, Building 463, Upton, NY 11973, USA
e-mail: iblaby@bnl.gov

M. Hippler (ed.), *Chlamydomonas: Molecular Genetics and Physiology*,
Microbiology Monographs 30, DOI 10.1007/978-3-319-66365-4_1

sequence), reductions in cost per genome, and the required sample size have resulted in the pace of genome sequencing far outstripping experimental validation of gene function. Consequently, biologists are presently working with a growing parts list without the knowledge as to what the pieces do, how they interact and how this results in a functioning cell.

1.1 What Is Functional Genomics?

Fortunately, a key development that came with the first genome sequences was the birth of functional genomics (Hieter and Boguski 1997). Functional genomics lies at the interface of two revelations: first, each genome encodes a plethora of proteins with unknown or poorly defined function; second, each genome provides a list of those proteins enabling the scale-up of experiments to simultaneously inform on the function of as many of them as possible (Fig. 1). Determining protein function plays a large part in modern biology generally, but what distinguishes functional genomics from other fields is that protein function is informed by genome-wide studies, such as transcriptomics and proteomics, and high-throughput screening including protein-protein interactions, global protein localization efforts, and mutant library phenotyping (phenomics) (Fig. 1).

As of yet, no single functional genomics approach has come close to deciphering the function of every protein in a given genome. Instead each experiment provides a single, global (but condition-specific) snapshot. The field therefore also encompasses computational analyses that endeavor to establish bridges between the mountains of high-throughout (HTP) genome-wide experimental data and protein function. Integration of functional genomics experiments and other genome-based analyses such as comparative genomics can generate functional inferences. Functional genomics can overlap significantly with systems biology, since both fields employ global approaches to experimentation. Accordingly, systems-wide studies can be highly informative to

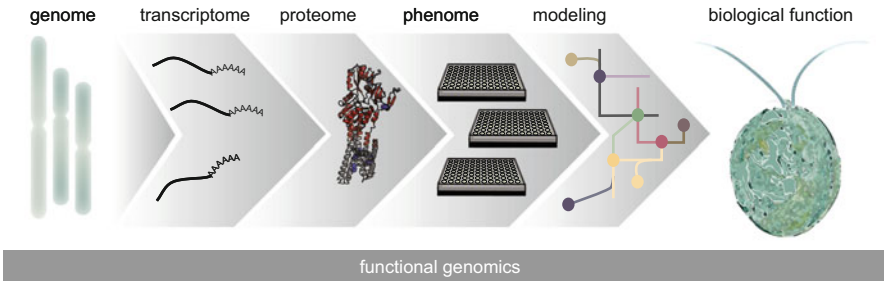

Fig. 1 The genome provides the raw sequence to which genes can be mapped. The function of proteins encoded by those genes can be informed through functional genomics experiments that relate biological information such as changes in transcript or protein abundance and phenotypes to each locus. In order to maximize the value of genome-wide studies, computational analyses and modeling are needed to gain a systems-level understanding of biological function from these experimental pieces

protein function where data is accumulated and interpreted from a holistic perspective. Thereupon, functional genomics and systems biology can form the basis of, and inform the design of, metabolic engineering and synthetic biology approaches.

1.2 What Is Protein Function?

Function is a multifaceted description of a protein's role in the cell. This description has both biochemical and biological elements. For an enzyme, the function would require understanding the reaction(s) catalyzed, the pathway or process the protein participates in, the location of the protein within the cell, how the gene and encoded protein are regulated, and what cofactors are required for activity. As experimental evidence for each of these attributes is provided, the annotation approaches a "gold-standard" level. By virtue of the detailed level of genetic/biochemical characterization to achieve this status, these experiments tend to be performed in laboratories with expertise in the process or pathway under examination, adding an additional level of robustness to the resulting functional annotations.

1.3 The Functional Annotation Problem

Traditionally, functional characterization of proteins has largely been performed one protein at a time. As the number of uncharacterized proteins (individual proteins and protein families) increases with each new genome sequence, the detailed but time-consuming characterization of one protein at a time is an impracticable approach to understanding the function of every protein in every organism. A compromise has been to transfer, or propagate, experimentally determined functions (called functional annotations) to non-experimentally characterized proteins employing sequence similarity. In an age where protein sequences are at our fingertips and bioinformatics play an increasingly large part in biological research, automated functional annotations abound in online databases. It is often difficult to know where annotations originated (i.e., by whom and in which organism the experimental validation was performed) and how reliable they are.

The logic of most automated protein functional annotation is based on the evolutionary concepts of orthology and ancestral relationships; a function may be shared among members of a protein family. Such methods are routinely implemented using BLAST (Altschul et al. 1990, 1997). While some estimates for reliability of similarity-based approaches have been determined (Tian and Skolnick 2003), this mechanism of annotation is generally confounded by the fact that function may not be conserved between even highly similar sequences. Conversely, proteins with dissimilar sequences may have the same function (for example, due to convergent evolution). Furthermore, as a consequence of runaway annotation propagation from genome to genome, 60% of database-deposited functional annotations are estimated to be incorrect for some protein families (Schnoes et al. 2009).

At some point, the genome being automatically annotated is so phylogenetically distant from the organism in which the original function-determining experiment was actually performed that the annotation becomes less relevant and ultimately invalid. This problem is particularly acute for organisms that are evolutionarily distant from very well experimentally characterized model organisms. Automated, structured classifications comprising strictly controlled vocabularies, such as those provided by the gene ontology (GO), and plant-specific tools such as MapMan (Thimm et al. 2004) and Mercator (Lohse et al. 2014) mitigate this annotation error to some extent but generally fail to link an annotation to a specific piece of evidence (Rhee et al. 2008).

1.4 Why Use Functional Genomics?

Each type of functional genomics experiment provides a snapshot of some functional data for many, if not all, genes in an organism at relatively little expense (in terms of time and finance). Although highly detailed protein characterization necessitates expert experimental validation, functional genomics can quickly provide testable hypotheses that drastically reduce the time at the bench it takes for detailed characterization of protein function.

2 *Chlamydomonas reinhardtii* Genomics

2.1 The Status of Protein Function Annotation in Chlamydomonas

A wide range of biological phenomena is studied in *C. reinhardtii* (herein Chlamydomonas), resulting in a wealth of information about Chlamydomonas and by extension plants and animals (Harris 2001, 2009; Goodenough 2015). The Chlamydomonas nuclear genome encodes roughly 19,500 proteins (17,741 loci with 19,526 putative transcripts in JGI 5.5/Phytozome 10 gene model version). The sequence of each protein is predicted from a gene model, which is derived from a combination of prediction tools and sequenced transcript data (such as expressed sequence tags (ESTs), full-length cDNAs, and RNA-Seq reads). Some of these genes are possibly pseudogenes, but it is expected that the number of non-expressed genes is less than 2500 (Zones et al. 2015). All other genes perform some role ensuring that each Chlamydomonas cell survives to the next generation.

Yet, despite intensive study for more than half a century, the role of many genes in Chlamydomonas is unknown (Table 1). This situation is not uncommon. The first eukaryotic genome sequenced, belonging to *Saccharomyces cerevisiae* (Goffeau et al. 1996) and by far the most characterized eukaryotic genome to date, contains 30% of genes that are not associated with a biological process and 40% that are not associated

Table 1 Gene annotation status in Chlamydomonas

Annotation type[a]	Number of genes	Fraction (of primary transcripts[b]) (%)
Primary gene symbol[c]	1815	10.2
Defline and/or description[c]	7834	44.2
PFAM domain[c]	9242	52.1
GO ontology[c]	6636	37.4
MapMan ontology[d]	5685	32.0
Loci that have none of the above	5699	32.1

[a]Determined using v5.5 models, data collected March 2016
[b]Since alternate transcripts (i.e., splice variants) are almost entirely predicted, only primary transcripts are analyzed here
[c]Data sourced from Phytozome (Goodstein et al. 2012)
[d]Thimm et al. (2004)

with a molecular function even though nearly 80% of genes are linked with some form of experimental evidence (as of 24 March 2016; http://www.yeastgenome.org/genomesnapshot). One can imagine that the state of gene function knowledge in more complex eukaryotes such as plants, which have many more genes, is by comparison limited (Chlamydomonas has nearly 10,000 more genes than *S. cerevisiae*, although there is likely some functional redundancy due to gene duplications).

To a certain extent experimental characterization in other organisms can provide some functional information. For instance, about 10,000 Chlamydomonas proteins have at least one PFAM domain (Table 1; however, some of these domains are not associated with a known function). A combination of sequence similarity, more stringent bioinformatics analyses, and experimental evidence has led to annotation of approximately 10% of predicted Chlamydomonas transcripts (Table 1). Making inroads into deciphering complete function of the remaining 90% of genes and placing these genes in a biological context requires functional genomics approaches.

2.2 *The Chlamydomonas Nuclear Genome and Gene Models*

Since many techniques in functional genomics rely on accurate gene models and protein sequences, we start our discussion of functional genomics in Chlamydomonas with a prelude on structural genomics. Raw genome sequence indicates little of biological function. A critical step prior to assigning and defining functional annotations, which describe the role of an encoded protein, is to physically annotate a genome (otherwise known as structural genomics). Physical annotations define the structural attributes of the genome, such as the number and size of chromosomes/scaffolds, positions (i.e., coordinates) of genes on chromosomes, intron/exon junctions, transcription start/stop sites, and translation start/stop sites. Since the accuracy of the predicted protein sequence is dependent upon the quality of the raw genome sequence and accuracy of the gene models, it is crucial for the physical annotations to be of a very high standard before functional annotations can be reliably applied. Fortunately, as a result of numerous efforts integrating

new computational algorithms and the incorporation of experimental datasets, the quality of the Chlamydomonas genome and its gene models are of a high level, as described herein.

After initiation of the Chlamydomonas genome project in the early 2000s and subsequent to two early releases, the draft Chlamydomonas genome (v3) was published in 2007 (Merchant et al. 2007), achieving an averaged 13x coverage by Sanger-based sequencing of 2.1 million reads (Table 2). The draft genome assembly was annotated with the aid of de novo gene prediction tools. This suite of tools comprised statistical models, which computationally scanned the genome for occurrences of putative open reading frames (as determined by translational start and stop sites) and possible intron/exon splice junctions. These models incorporated homology data of translated sequence to known proteins/conserved domains and were supported in conjunction with ~0.25 million ESTs (Haas et al. 2003, 2008; Holt and Yandell 2011). These methods resulted in the JGI v3 generation of gene models, released in 2005 (Table 2). The collection consisted of 15,143 predicted transcripts, of which 82 had manually annotated alternate splice forms, and was deposited in NCBI databases under accession number ABCN01000000 (Merchant et al. 2007). For nomenclature purposes each transcript was assigned a unique six-digit ID. Concurrently with the JGI-led effort, an independent investigation was performed in which a collection of >2000 cDNAs was used as a training set for ab initio gene identification. This study resulted in the GreenGenie2 catalog of gene models (Kwan et al. 2009). As an indication of robustness of these two gene model collections, most (78%) putative transcripts overlapped between the two collections, although many were unique to either the GreenGenie2 (23%) or JGI v3 (22%) collections, suggesting additional work was necessary to capture the complete coding sequence.

A series of successive generations incorporating new methods, data, and algorithms have built upon these early releases resulting in improvements to both the genome assembly and the gene models (Blaby et al. 2014). These post-publication updates started with targeted Sanger-based sequencing of regions with low quality in combination with manual attempts at gap closing. The new sequence attained from these approaches was assisted by a genetic map (Rymarquis et al. 2005), aiding the positioning of scaffolds onto chromosomes. These approaches enabled

Table 2 History of Chlamydomonas genome assemblies and generations of gene models

Genome assemble (release date)	Number of scaffolds (of which chromosomes)	Total sequence Mb (% gaps)	Gene model version (release date)	Number of transcripts (alternate transcripts)
3 (2006)	1557 (na)	120.2 (12.5%)	JGI v3	15,143 (82)
4 (2008)	88 (17)	112.3 (7.5)	JGI v4	16,709 (0)
			Aug u5	15,818 (1070)
			Aug u9	15,935 (0)
			JGI v4.3	17,114 (0)
5 (2012)	54 (17)	111.1 (3.6%)	JGI v5.3.1	17,737 (1789)
			JGI v5.5	17,741 (1785)

significant forward strides to be made; the total number of scaffolds reduced from 1557 in v3 to 88 in the v4 assembly, providing the basis for several rounds of gene model improvements. The first generation of gene models made available for assembly v4, known as JGI v4, constituted 16,709 transcripts. Although this collection of models did not officially support alternate transcripts, analysis by Labadorf et al. inferred 611 alternative splice variants (Labadorf et al. 2010). Subsequent updates were made possible by incremental improvements in the Augustus algorithm, which supported inclusion of EST data (Stanke et al. 2008), and proteomic data (Specht et al. 2011). Consequently, these model collections, released between 2008 and 2012, saw the predicted transcript number increase from 15,818 with the Aug5 release to 17,114 with the Aug10.2 release (Table 1). This latter release, known as JGI v4.3, benefited significantly from the advent of second-generation sequencing technologies, and the inclusion of >6 million ESTs sequenced on the 454 platform, as well as homology to the then-recently sequenced *Volvox carteri* genome (Prochnik et al. 2010). The adoption of Augustus for gene model identification also marked the transition to the now-standardized (and permanent) system for Chlamydomonas loci ID, written in the format Cre*X*.g*Y*. In similar fashion to Arabidopsis loci identifiers (written as AT*X*G*Y*), Cre indicates the organism (*Chlamydomonas reinhardtii*), *X* denotes the chromosome/scaffold, and *Y* is a unique six-digit identifier, which proceeds in numerical order from the "beginning" of chromosome 1 to the "end" of the final scaffold. Initially this identifier increased in increments of 50, thus allowing for the incorporation of new genes without the need for all subsequent loci ID to be reshuffled. JGI v4.3 represented the final gene model version to be based upon the v4 genome.

Work on the next (and, presently, the most up-to-date) revisions to both the nuclear genome sequence and gene models, v5 and v5.5, respectively, took full advantage of advances in second-generation sequencing technologies and was released in mid-2012. Efforts were made to close remaining gaps in the genome sequence by construction of new genomic fragment libraries of differing insert sizes [as a means of compromising between achieving some sequence (with small inserts) and sequencing across repetitive sequence (with long inserts)] with a combination of Sanger and 454-based technologies. These endeavors resulted in reducing the total number of scaffolds from 88 in v4 to 54 in v5 (Table 2). In its present state (v5), the genome totals 111.1 Mbp, averages 65% GC, and comprises 17 chromosomes plus additional 37 repeat-rich non-anchored scaffolds. These chromosomes and scaffolds range ~1–10 Mbp and 0.1–0.8 Mbp, respectively. Common metrics used to describe the quality of a draft genome are the N50 and L50 statistics. N50 describes the smallest number of sequenced fragments required to make 50% of the complete assembly, and L50 is the size of the smallest fragment within the fragments comprising N50. Thus, a more complete genome will have a higher N50 and a lower L50 than a less complete genome of the same size. As work on the Chlamydomonas genome has progressed, the N50 has reduced from 24 to 7, and the L50 has increased from 1.7 to 8 Mb between v3 and v5.

Building upon the JGI v4 gene model inventory, extensive revisions, incorporating more than a billion reads from 59 independent RNA-Seq experiments, including paired reads and stranded libraries (enabling direction and strand of the model to be

determined), were incorporated into an updated Augustus algorithm (Aug11.6) and resulted in the v5.3.1 gene model catalog. During this transition, many complex revisions to gene models were made, such as splitting a single-gene model into multiple models and fusing several models into one (causing additional complications if a named gene is split; in such cases, the name migrated with the conserved domain). Consequently, 28% of loci could not be easily mapped forward and were provisioned with a temporary loci ID in the format g.*X*, where *X* provided a unique placeholder ID. Another, relatively minor, update released in 2014 (v5.5) amended these temporary loci by employing a more robust technique to map ~74% of loci from v4.3 resulting in gene models v5.5. Approximately 15% of gene models were given a new locus as a result of movement between chromosomes/scaffolds. The remaining ~12% could not easily be mapped from the v4 assembly to v5 and were also provided with a new locus. Minor changes were also made to a handful of gene models, with four loci each splitting into two in going from v5.3.1 to v5.5.

As it currently stands in this most recent iteration, the Chlamydomonas reference genome encodes 17,741 transcripts plus 1785 alternate transcripts resulting from splice variants. The coding sequence has an average GC skew of 68% although there is significant deviation between genes. More than 10% (2388) of predicted transcripts have a GC content of $\geq$75%; astonishingly, a handful (66) contain $\geq$80% GC. At the other end of the scale, 138 contain $\leq$55%. These outliers may represent recent acquisitions by horizontal gene transfer and have potentially not yet ameliorated to the average GC content. On the whole, it appears that genes containing a slight skew toward high GC content are more highly expressed, at least at the level of mRNA. By ranking genes by mRNA abundance (i.e., reads per kb per million bases; RPKM) and identifying the top 200 transcripts conserved in five RNA-Seq experiments (Castruita et al. 2011; Boyle et al. 2012; Urzica et al. 2012; Malasarn et al. 2013; Wakao et al. 2014), the codon usage of genes highly expressed in diverse conditions was determined (Table 3). The average GC content in these genes was 64%, with 88% GC at the third base. This codon usage data may aid in efforts for high expression of genes in metabolic engineering.

2.3 *Present and Future Directions for the Chlamydomonas Nuclear Genome*

As with all draft genomes, work continues on both the assembly (continued gap closing) and gene models. Chlamydomonas loci IDs are now static (or will deviate only marginally to allow for transfer of loci as required for future updates). However, the complicated history and the number of studies conducted using earlier generations of gene models necessitate the need to translate between versions. Correspondence tables are available to download for this purpose (http://phytozome.jgi.doe.gov/pz/portal.html). Several studies have highlighted potential directions for future exploration, including a recent genomic analysis suggesting that a fraction of gene models could be extended at the N-terminus (Cross 2015). Although the analysis is entirely of an informatic nature, the implications this may have on

Table 3 Codon usage of highly expressed genes in Chlamydomonas

	Codon	aa	%	Codon	aa	%	Codon	aa	%	Codon	aa	%	
U	UUU	F	0.33	UCU	S	0.46	UAU	Y	0.20	UGU	C	0.06	**U**
	UUC	F	3.18	UCC	S	1.80	UAC	Y	2.51	UGC	C	1.50	**C**
	UUA	L	0.05	UCA	S	0.11	UAA	STOP	0.31	UGA	STOP	0.45	**A**
	UUG	L	0.14	UCG	S	1.83	UAG	STOP	0.33	UGG	W	1.08	**G**
C	CUU	L	0.30	CCU	P	0.60	CAU	H	0.14	CGU	R	0.69	**U**
	CUC	L	1.01	CCC	P	3.34	CAC	H	1.70	CGC	R	4.75	**C**
	CUA	L	0.10	CCA	P	0.16	CAA	Q	0.16	CGA	R	0.05	**A**
	CUG	L	6.25	CCG	P	1.00	CAG	Q	3.31	CGG	R	0.59	**G**
A	AUU	I	1.15	ACU	T	0.64	AAU	N	0.13	AGU	S	0.13	**U**
	AUC	I	3.05	ACC	T	3.50	AAC	N	3.30	AGC	S	1.75	**C**
	AUA	I	0.04	ACA	T	0.14	AAA	K	0.08	AGA	R	0.03	**A**
	AUG	M	2.79	ACG	T	0.78	AAG	K	7.37	AGG	R	0.19	**G**
G	GUU	V	0.68	GCU	A	2.13	GAU	D	0.69	GGU	G	1.43	**U**
	GUC	V	2.32	GCC	A	6.12	GAC	D	4.21	GGC	G	6.29	**C**
	GUA	V	0.06	GCA	A	0.33	GAA	E	0.09	GGA	G	0.17	**A**
	GUG	V	4.61	GCG	A	2.10	GAG	E	5.68	GGG	G	0.28	**G**
	U			**C**			**A**			**G**			

predicted protein sequence warrant further attention. Another study suggests exonic regions are not included in the present reference assembly genome, potentially indicating that the complete coding sequence (and consequently protein sequences) is not represented (Tulin and Cross 2015). A further issue requiring attention is the omission of a number of gene models, possibly numbering on the order of a few hundred, that were represented in v4.3 but are not present in v5.5 (Blaby, unpublished). It is presently unknown as to why these models were not picked up by the Augustus 11.6 algorithm as many are highly supported by ESTs/RNA-Seq datasets and include, for example, *PSBW*, encoding the W protein of photosystem II.

3 Functional Genomics in Chlamydomonas

Here, we define a functional genomics dataset as the cumulative results of a genome-wide experiment. Specifically, the data has to be linked directly to precise gene loci or proteins. Needless to say, a functional genomics experiment attempts to inform on every gene, transcript or protein in the cell. However, the extent to which a global investigation is truly genome-wide is dependent on the technique used. In this section, we discuss the three predominant types of functional genomics studies in Chlamydomonas: mRNA quantification (transcriptomics), protein detection and quantification (proteomics), and mutant phenotype screening (phenomics). Transcriptomic methods (mainly microarray and RNA-Seq) enable high-throughput examination of gene expression, identifying genes whose mRNA abundance alters significantly between experimental conditions (environment) or strains (wild-type/mutant comparisons). In Chlamydomonas, RNA-Seq, a deep-sequencing technology, comes the closest to providing quantitative data on every gene on the genome (theoretically informing on every gene model, assuming sequencing depth is sufficient). Proteomic methods can provide information on where proteins are in the cell, an indication of where they perform their function, and can provide information of the differential abundance of proteins between conditions or strains. Proteomic approaches have been able to inform on the presence of 3500 Chlamydomonas proteins in a single study and differential abundance demonstrated for approaching 1000 proteins (Park et al. 2015). Phenomic methods traditionally rely on availability of a library of single-gene deletions or disruptions. The library is screened for mutant phenotypes that deviate from the parent strain used to construct the library (growth defect, colony morphology, chlorophyll content, etc.) when grown under precise conditions (such as high light, low nutrient availability, etc.). Efforts are being made to provide a sequenced insertional library (Li et al. 2016), which may enable functional genomics studies of mutant phenotypes. In the meantime, phenomic studies in Chlamydomonas are limited to forward genetic screens of un-sequenced libraries, isolation of mutants with desired phenotypes, and the subsequent identification of the site of mutation.

3.1 Transcriptomics

Transcriptomes offer a valuable tool in the functional genomics arsenal by providing a snapshot of transcript abundance under well-defined conditions for a large number of transcripts. Transcript abundance changes can be used in several ways to infer function. Higher mRNA abundance in one growth condition (e.g., low-sulfur medium) compared to a second growth condition (such as sulfur-replete medium) can give an indication as to when the gene product is needed (growth during sulfur starvation). There are however several assumptions being made in this simplistic type of function deduction. It can be difficult to know if the observed transcript changes are due to the experimental variable (presence/absence of sulfur) or an indirect consequence of the variable (perhaps redox stress), leading to the question "is the corresponding protein involved in sulfur metabolism or a downstream process?" Also, in some cases, transcript abundance may be linked to a feedback response involving activity of the encoded protein during the experimental condition. For instance, under iron starvation, the abundances of transcripts encoding several iron-dependent proteins increase, while the protein's abundance decreases; it appears that the increase in transcript abundance is responding to the reduced activity of these iron-dependent proteins during iron deprivation rather than a role for these proteins in acclimating to poor iron nutrition (Urzica et al. 2012). The identification of co-expressed genes can also inform function using the "guilt-by-association" principle (Niehrs and Pollet 1999), whereby the function of a gene is inferred by its co-expression with another gene of known function.

Transcriptomics in Chlamydomonas can be traced back to the first DNA microarrays containing probes to detect the differential abundance of ~3000 assembled ESTs (Fig. 2) (Im et al. 2003). These early transcriptomes provided data on the influence of several environmental conditions on transcript abundance, including light and CO_2 (Im et al. 2003), sulfur nutrition (Zhang et al. 2004), and photooxidative stress (Ledford et al. 2004). As the EST library grew (Asamizu et al. 2004), DNA microarrays grew to measure over 10,000 ESTs. After the release of the draft Chlamydomonas nuclear genome in the early 2000s, genomic information in addition to ESTs was used in the design of microarrays (Eberhard et al. 2006). The first "whole genome" microarray was published in 2005 and based on gene models associated with draft v2 of the nuclear genome (Stolc et al. 2005). Subsequent microarrays have been designed and employed as more accurate genome sequence drafts and accompanying gene models were released, but in large part, microarray technology has been supplanted by quantitative cDNA sequencing (i.e., RNA-Seq).

Reductions in cost and sample size, fast turnaround, and streamlined bioinformatic applications (reviewed in Van Verk et al. 2013) have resulted in a swelling stream of Chlamydomonas RNA-Seq datasets. Furthermore, RNA-Seq datasets adapt to changes in gene models, since the raw sequenced reads can be realigned should updates occur subsequent to the experiment being performed. The types of experiments published over the past 5 years reflect the status of Chlamydomonas as a popular microbial experimental system for studying photosynthesis, nutrition, cilia, and abiotic stresses.

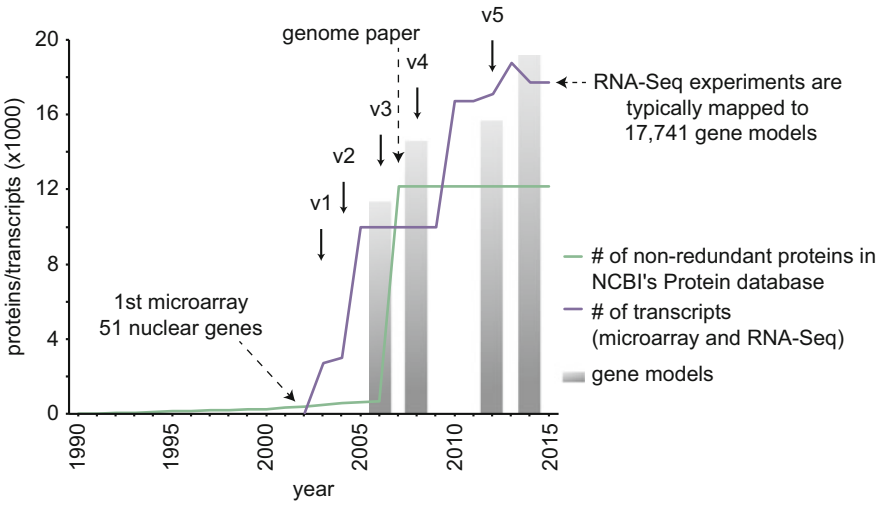

Fig. 2 Progress of genomics and transcriptomics in Chlamydomonas. The *green line* represents number of nuclear-encoded protein sequences in GenBank starting at 1990. Because of the redundancy caused by duplicated entries, protein entries from each year were mapped to JGI 5.5. If the sequence could not be mapped forward, it was not included in the graph. The number of entries in GenBank significantly increased with deposition of predicted proteins associated with the genome publication (Merchant et al. 2007), with only a handful of new sequences deposited subsequently. Presently, about 70% of Chlamydomonas proteins in the Phytozome 11 database are represented in GenBank, and the gene models associated with many of those deposited in 2007 have changed as a result of more accurate genome assemblies and gene model prediction algorithms. *Gray bars* indicate the number of gene models released to the public in the indicated years that map onto the v5.5 gene models. The *purple line* represents the progress of transcriptomics in Chlamydomonas; the number of "gene-specific" probes reported for each microarray is given, but it should be noted that there are potential redundancies and artifacts due to the limited availability of accurate gene models when many of these microarrays were designed. Starting in 2002 (Lilly et al. 2002) with a microarray that included probes for 51 nuclear genes, transcriptomics of the nuclear genome progressively increased in scope over the next decade. As EST libraries were made public followed by the first drafts of the nuclear genome, the size of microarrays continued to increase, while the publication of Chlamydomonas RNA-Seq experiments began in 2010. Although the present release of JGI gene models includes alternative transcripts, most RNA-Seq analyses only include mapping to the primary transcripts

3.2 Proteomics

One must remember that transcriptome data only gives an indication of transcriptional and post-transcriptional regulation of mRNA abundance. Many proteins in the cell, however, are regulated at the posttranslational level either through post-translational modifications or degradation. The detection and quantification of these condition-specific changes require analysis of proteins. The history of proteomics in Chlamydomonas is similar to that of transcriptomics: the number of proteins identified and quantified in a typical experiment has increased with time largely due to availability of the genome sequence (for identification of peptides/proteins) and technological advancements (Rolland et al. 2009).

To gain a functional genomics insight, differential abundance measurements from a quantitative proteomics study utilize the same logic as a transcriptomics study. The assumption is that proteins that are more abundant in a test condition verses standard growth conditions are involved in acclimating to that test condition thus inferring a functional role. Several studies have been performed in Chlamydomonas where researchers quantify changes in the transcriptome and proteome. In general, RNA-Seq and microarrays are able to quantify transcripts from an order of magnitude more genes than proteins using shotgun proteomics (Hsieh et al. 2013; Mettler et al. 2014; Schmollinger et al. 2014).

Unlike transcriptomics, proteomics can inform function by cataloging the location of proteins within the cell. In this case, proteins are identified after purification of the target compartment or structure. MS-based identification has been performed on proteins present in (and from a functional genomics perspective assumed to carry out a biological role in) the chloroplast (Allmer et al. 2006; Terashima et al. 2010, 2011; Bienvenut et al. 2011), the eyespot (Schmidt et al. 2006; Wagner et al. 2008; Eitzinger et al. 2015), flagella (Keller et al. 2005; Pazour et al. 2005; Diener et al. 2015), mitochondria (Atteia et al. 2009), nucleus (Winck et al. 2012), and lipid bodies (Moellering and Benning 2010; Nguyen et al. 2011).

3.3 Phenomics

For geneticists, a condition-specific phenotype resulting from the disruption of a single gene represents the Holy Grail in understanding the function of that disrupted gene. Given this, it comes as little surprise that for many organisms, the creation of an indexed, genome-wide mutant library [typically defined as containing independent disruptions in 85% of predicted genes (Carpenter and Sabatini 2004)] follows shortly after attainment of the genome sequence (Winzeler et al. 1999; Alonso et al. 2003; Baba et al. 2006). With such a library in hand, researchers begin screening the library under various growth conditions and cataloging the measured phenotypes associated with each disrupted locus. HTP phenotypic profiling enables systematic genotype-to-phenotype relations to be generated. This approach differs from the classical forward genetic screen, where researchers are seeking the genetic basis for a particular phenotype. With reverse genetics, researchers are seeking phenotypes associated with each genotype.

Typically, a large number of parameters are collected, either sequentially or simultaneously, to generate comprehensive datasets for each mutant strain's phenome. Similar logic as with gene co-expression can be applied: if two strains deleted for different genes display similar phenotypes under the same conditions, there may be a functional linkage. This field is presently in its infancy in Chlamydomonas, although it is primed to come online in the near future as the known site-of-insertion mutant libraries become available (Li et al. 2016).

Table 4 Summary of data repositories and online tools enabling genomics and functional genomics in Chlamydomonas

			Purpose for using			
Tool/database	Location	Chlamydomonas genome assembly/ gene model generation[a]	Genomic/functional genomics data repository	Functional genomics analysis abilities	Comparative genomics abilities[b]	Tools for validating functional analysis
Phytozome (Goodstein et al. 2012)	http://www.phytozome.net	v5/v5.5	Primary repository of Chlamydomonas genome/gene models. Can bulk download data as well as obtain correspondence tables to translate gene model IDs	Contains user-validated annotations, and PFAM, Panther and GO predicted annotations. Gene co-expression tool utilizing some transcriptomes	Genomic data for >40 plants/photosynthetic organisms	
UCLA algal genomics portal	http://genomes.mcdb.ucla.edu/	v3–v5/ (transcriptomes presently available mapped to v4/v4.3)	Chlamydomonas genome browser, based on the UCSC browser (Kent et al. 2002). Can bulk download some genomic data	Multiple transcriptomes available to view in genome browser	Can compare relative mRNA abundances of genes in different conditions	
Algal Annotation Tool (Lopez et al. 2011)	http://pathways.mcdb.ucla.edu/algal/index.html	v3–v5	Batch conversion of gene identifiers	Bulk annotation prediction via Kegg, MapMan, GO, Panther, Metacyc. Gene co-expression tool utilizing some transcriptomes		

NCBI	http://blast.ncbi.nlm.nih.gov/Blast.cgi?PAGE=Proteins	v3/JGIv3	Presently the only online resource to query Chlamydomonas using PsiBlast[c] (Altschul et al. 1997)			
Predalgo (Tardif et al. 2012)	https://giavap-genomes.ibpc.fr/cgi-bin/predalgodb.perl?page=main	N/A (dependent upon user-provided sequence)		Green algal-specific protein localization predictions		
Plant Transcription factor database (Pérez-Rodríguez et al. 2010)	http://plntfdb.bio.uni-potsdam.de/v3.0/index.php?sp_id=CRE4	v4/v4.3		Prediction of all genome-encoded transcription factors	Database covers 20 photosynthetic organisms	
PLANTTFDB (Jin et al. 2014)	http://planttfdb.cbi.pku.edu.cn/	v4/v4.3		Predicted genome-encoded transcription factors	Database covers 83 photosynthetic species	
cis-regulatory site prediction tool (Ding et al. 2012)	http://hulab.ucf.edu/research/projects/Microalgae/sdcre/motifcomb.html	v4/JGIv4.3		Gene regulatory element prediction		
AlgaePath (Zheng et al. 2014)	http://algaepath.itps.ncku.edu.tw/algae_path/home.html	v5/v5.3.1		Maps mRNA abundance from a number of transcriptomes to KEGG pathway maps	Analysis can also be performed on *Neodesmus* sp. UTEX 2219–4	

(continued)

Table 4 (continued)

			Purpose for using			
Tool/database	Location	Chlamydomonas genome assembly/ gene model generation[a]	Genomic/functional genomics data repository	Functional genomics analysis abilities	Comparative genomics abilities[b]	Tools for validating functional analysis
ALCOdb (Aoki et al. 2016)	http://alcodb.jp/	v5/v5.5		Microalgal gene co-expression networks	Identifies orthologs in *Cyanidioschyzon merolae*, for which (microarray-based) co-expression networks are also present	
ChlamyChem (Alfred et al. 2012)	http://chlamychem.utoronto.ca/ChlamyChem/download.php			Phenotypic and chemical screen resource		
ChlamyCyc5 (May et al. 2009)	http://pmn.plantcyc.org/organism-summary?object=CHLAMY	v3/JGIv3				
PlantSEED (Seaver et al. 2014)	http://bioseed.mcs.anl.gov/~seaver/FIG/seedviewer.cgi?page=PlantSEED	v3/JGIv3			Comparative platform embodying the "subsystem" approach for genome annotation (Overbeek et al. 2005)	
pico-PLAZA (Vandepoele et al. 2013)	http://bioplaza/plaza/versions/pico-plaza/	v4/JGI4.3			Comparative platform for genomics analysis of Chlamydomonas	

PlantGDB (Duvick et al. 2008)	http://www.plantgdb.org/	v4/JGIv4.3	Genome repository and browser		Comparative genomics platform for >100 plants, genome browser for 14 species	
ChlamyNET (Romero-Campero et al. 2016)	http://viridiplantae.ibvf.csic.es/ChlamyNet/	v5/v5.5		Chlamydomonas gene co-expression networks, putative transcription factor binding site predictions		
Chlamydomonas Resource Center	http://chlamycollection.org/					Distributes >5000 cataloged Chlamydomonas strains, in addition to phenotyped and sequenced mutant collections (Dent et al. 2015; Li et al. 2016). Also stocks, plasmids, cDNA libraries, kits, etc.
ChlamyStation	http://chlamystation.free.fr/					Paris (IBPC) Collection of photosynthesis mutants

[a]As of March 2016
[b]Defined here as a tool that can directly comparatively analyze data between (1) organisms or (2) conditions within an organism
[c]Later versions of the genome/gene models can be queried by running PsiBLAST on a local terminal; source code is available at https://blast.ncbi.nlm.nih.gov/Blast.cgi?PAGE_TYPE=BlastDocs&DOC_TYPE=Download

3.4 Other "Omics" Experimental Types

Other global studies, such as metabolomes and lipidomes, have been conducted in Chlamydomonas. These investigations can illuminate changes within the cell on the systems level. From a functional genomics perspective of linking function to specific proteins, the data generated from these types of experiments can be useful when viewed in the context of other datasets (such as those described in this section) that can ascribe each observation to a specific loci. Several studies in Chlamydomonas have taken this multi-"omic" approach to understanding how Chlamydomonas acclimates to different growth conditions, such as rapamycin treatment (Kleessen et al. 2015), nutrient deprivation (Schmollinger et al. 2014; Park et al. 2015), oxygen status (Subramanian et al. 2014), temperature (Légeret et al. 2016), and light (Mettler et al. 2014).

3.5 Databases and Resources for Chlamydomonas Genomics and Functional Genomics

A growing number of online resources are available to curate, disseminate, and interpret Chlamydomonas genomics datasets, as well as catalogs for resource distribution (such as strains and vectors). These tools range from data repositories to sophisticated platforms enabling integrative analysis of different data types, including comparative analyses with other organisms. We have summarized a number of the available tools, their uses, and the genome assembly/gene model version they presently employ (Table 4). Ideally, the most recent gene models should be used since these represent the most accurate predicted protein sequences. However, many tools offering unique modes of analysis utilize legacy gene model versions, and model generation conversion is necessary.

4 Outlook and Future Directions

4.1 Integrative Approaches to Analysis

Since it is unlikely that a single genome-wide technique will definitively enable function to be assigned to proteins, a key concept of functional genomics is the need to assimilate and exploit each piece of evidence relating to any given gene to generate function inferences. As more compatible inferences are made, confidence is gained and function predictions can be made. These predictions can be experimentally tested by applying appropriate targeted genetic and/or biochemical analysis to generate "gold-standard" annotations. As new global datasets are generated and newer technologies (for instance, Chip-Seq or ribosome profiling) are applied,

the integration of data becomes increasingly powerful, as the likelihood of any given gene displaying differential behavior relative to background increases. In any case, analysis of datasets in isolation may result in incorrect conclusions due to potential false positives and negatives. Consequently an integrative approach to analysis is important (Vidal 2001; Ge et al. 2003; Joyce and Palsson 2006) although the inherent difficulties in integrating datasets have also been highlighted (Palsson and Zengler 2010). Specifically, although large-scale repositories exist for specific data types [such as SRA and GEO (Edgar et al. 2002; Leinonen et al. 2011)], no system is in place for depositing all datasets. Furthermore experimental variables, such as precise genotypes, lighting conditions, media recipes, and temperature, are likely to vary to a greater or lesser extent between studies even when performed within the same laboratory. Stringent record keeping and documentation of experimental conditions are therefore critical but can be overlooked.

Several online tools catering to Chlamydomonas do present multiple data types (Table 4), in particular, expression and co-expression data coupled with genomics. Additional integration of datasets, including proteomes, phenotype, and other genome-wide studies, will aid these analyses. More recently, big-data approaches are being considered to deploy machine learning techniques to gain maximal knowledge from datasets (Ma et al. 2014).

4.2 Comparative Algal Genomics

Recently, two *C. reinhardtii* genome comparison studies have offered an appreciation for genome diversity of both commonly used laboratory strains and natural variation in wild isolates (Flowers et al. 2015; Gallaher et al. 2015). Both investigations compared their re-sequenced genomes to the published reference genome of strain CC-503 and identified significant genotypic diversity between strains. Although the relatively small number of strains analyzed in these two investigations prevented GWAS-style linkage of genotype to phenotype, a combination of sequencing more genomes, for example, of field isolates, and phenomics approaches of all sequenced strains may help to elucidate these relations. As more Chlamydomonas genomes become available, the quality of their assembly and critically gene model accuracy improve, and -omic methods are applied to them, the ability to confidently apply the principles outlined herein becomes more powerful.

Algae comprise a large, diverse group of organisms. Although Chlamydomonas remains by far the most studied and the most "genomically advanced," a growing number of algal genomes are now available enabling genomes to be interpreted comparatively. Logically, where clear orthologs exist between organisms, indicating vertical evolutionary descent, functional inferences and annotations can be legitimately transferred with higher confidence than simple similarity-based methods. Furthermore, this data transfer can be contextualized by the lifestyle,

growth requirements, and habitat of the respective organisms as well as by experimentally gathered data.

It is important to note that application of the approaches discussed here only provides functional inferences and that experimental validation is crucial to be certain of such inferences and should be considered a requisite before very high confidence (i.e., gold-standard) annotations can be applied. Experimental procedures available in the Chlamydomonas molecular toolbox for performing this next step have been reviewed recently (Jinkerson and Jonikas 2015; Mussgnug 2015).

Acknowledgments IKB and CEB-H are supported by the Office of Biological and Environmental Research of the Department Of Energy.

References

Alfred SE, Surendra A, Le C, Lin K, Mok A, Wallace IM, Proctor M, Urbanus ML, Giaever G, Nislow C (2012) A phenotypic screening platform to identify small molecule modulators of *Chlamydomonas reinhardtii* growth, motility and photosynthesis. Genome Biol 13:R105

Allmer J, Naumann B, Markert C, Zhang M, Hippler M (2006) Mass spectrometric genomic data mining: novel insights into bioenergetic pathways in *Chlamydomonas reinhardtii*. Proteomics 6:6207–6220

Alonso JM, Stepanova AN, Leisse TJ, Kim CJ, Chen H, Shinn P, Stevenson DK, Zimmerman J, Barajas P, Cheuk R, Gadrinab C, Heller C, Jeske A, Koesema E, Meyers CC, Parker H, Prednis L, Ansari Y, Choy N, Deen H, Geralt M, Hazari N, Hom E, Karnes M, Mulholland C, Ndubaku R, Schmidt I, Guzman P, Aguilar-Henonin L, Schmid M, Weigel D, Carter DE, Marchand T, Risseeuw E, Brogden D, Zeko A, Crosby WL, Berry CC, Ecker JR (2003) Genome-wide insertional mutagenesis of *Arabidopsis thaliana*. Science 301:653–657

Altschul SF, Gish W, Miller W, Myers EW, Lipman DJ (1990) Basic local alignment search tool. J Mol Biol 215:403–410

Altschul SF, Madden TL, Schäffer AA, Zhang J, Zhang Z, Miller W, Lipman DJ (1997) Gapped BLAST and PSI-BLAST: a new generation of protein database search programs. Nucleic Acids Res 25:3389–3402

Aoki Y, Okamura Y, Ohta H, Kinoshita K, Obayashi T (2016) ALCOdb: gene coexpression database for microalgae. Plant Cell Physiol 57:e3

Asamizu E, Nakamura Y, Miura K, Fukuzawa H, Fujiwara S, Hirono M, Iwamoto K, Matsuda Y, Minagawa J, Shimogawara K, Takahashi Y, Tabata S (2004) Establishment of publicly available cDNA material and information resource of *Chlamydomonas reinhardtii* (Chlorophyta) to facilitate gene function analysis. Phycologia 43:722–726

Atteia A, Adrait A, Brugière S, Tardif M, van Lis R, Deusch O, Dagan T, Kuhn L, Gontero B, Martin W, Garin J, Joyard J, Rolland N (2009) A proteomic survey of *Chlamydomonas reinhardtii* mitochondria sheds new light on the metabolic plasticity of the organelle and on the nature of the alpha-proteobacterial mitochondrial ancestor. Mol Biol Evol 26:1533–1548

Baba T, Ara T, Hasegawa M, Takai Y, Okumura Y, Baba M, Datsenko KA, Tomita M, Wanner BL, Mori H (2006) Construction of *Escherichia coli* K-12 in-frame, single-gene knockout mutants: the Keio collection. Mol Syst Biol 2:2006.0008

Bienvenut WV, Espagne C, Martinez A, Majeran W, Valot B, Zivy M, Vallon O, Adam Z, Meinnel T, Giglione C (2011) Dynamics of post-translational modifications and protein stability in the stroma of *Chlamydomonas reinhardtii* chloroplasts. Proteomics 11:1734–1750

Blaby IK, Blaby-Haas CE, Tourasse N, Hom EF, Lopez D, Aksoy M, Grossman A, Umen J, Dutcher S, Porter M, King S, Witman GB, Stanke M, Harris EH, Goodstein D, Grimwood J,

Schmutz J, Vallon O, Merchant SS, Prochnik S (2014) The Chlamydomonas genome project: a decade on. Trends Plant Sci 19:672–680

Bork P, Ouzounis C, Sander C, Scharf M, Schneider R, Sonnhammer E (1992a) What's in a genome? Nature 358:287

Bork P, Ouzounis C, Sander C, Scharf M, Schneider R, Sonnhammer E (1992b) Comprehensive sequence analysis of the 182 predicted open reading frames of yeast chromosome III. Protein Sci 1:1677–1690

Boyle NR, Page MD, Liu B, Blaby IK, Casero D, Kropat J, Cokus S, Hong-Hermesdorf A, Shaw J, Karpowicz SJ, Gallaher S, Johnson S, Benning C, Pellegrini M, Grossman A, Merchant SS (2012) Three acyltransferases and a nitrogen responsive regulator are implicated in nitrogen starvation-induced triacylglycerol accumulation in Chlamydomonas. J Biol Chem 287:15811–15825

Carpenter AE, Sabatini DM (2004) Systematic genome-wide screens of gene function. Nat Rev Genet 5:11–22

Castruita M, Casero D, Karpowicz SJ, Kropat J, Vieler A, Hsieh SI, Yan W, Cokus S, Loo JA, Benning C, Pellegrini M, Merchant SS (2011) Systems biology approach in Chlamydomonas reveals connections between copper nutrition and multiple metabolic steps. Plant Cell 23(4): 1273–1292

Cross FR (2015) Tying down loose ends in the chlamydomonas genome: functional significance of abundant upstream open reading frames. G3 (Bethesda) 6(2):435–446

Dent RM, Sharifi MN, Malnoë A, Haglund C, Calderon RH, Wakao S, Niyogi KK (2015) Large-scale insertional mutagenesis of Chlamydomonas supports phylogenomic functional prediction of photosynthetic genes and analysis of classical acetate-requiring mutants. Plant J 82:337–351

Diener DR, Lupetti P, Rosenbaum JL (2015) Proteomic analysis of isolated ciliary transition zones reveals the presence of ESCRT proteins. Curr Biol 25:379–384

Ding J, Li X, Hu H (2012) Systematic prediction of cis-regulatory elements in the *Chlamydomonas reinhardtii* genome using comparative genomics. Plant Physiol 160:613–623

Duvick J, Fu A, Muppirala U, Sabharwal M, Wilkerson MD, Lawrence CJ, Lushbough C, Brendel V (2008) PlantGDB: a resource for comparative plant genomics. Nucleic Acids Res 36:D959–D965

Eberhard S, Jain M, Im CS, Pollock S, Shrager J, Lin Y, Peek AS, Grossman AR (2006) Generation of an oligonucleotide array for analysis of gene expression in *Chlamydomonas reinhardtii*. Curr Genet 49:106–124

Edgar R, Domrachev M, Lash AE (2002) Gene expression omnibus: NCBI gene expression and hybridization array data repository. Nucleic Acids Res 30:207–210

Eitzinger N, Wagner V, Weisheit W, Geimer S, Boness D, Kreimer G, Mittag M (2015) Proteomic analysis of a fraction with intact eyespots of *Chlamydomonas reinhardtii* and assignment of protein methylation. Front Plant Sci 6:1085

Fleischmann RD, Adams MD, White O, Clayton RA, Kirkness EF, Kerlavage AR, Bult CJ, Tomb JF, Dougherty BA, Merrick JM (1995) Whole-genome random sequencing and assembly of *Haemophilus influenzae* Rd. Science 269:496–512

Flowers JM, Hazzouri KM, Pham GM, Rosas U, Bahmani T, Khraiwesh B, Nelson DR, Jijakli K, Abdrabu R, Harris EH, Lefebvre PA, Hom EF, Salehi-Ashtiani K, Purugganan MD (2015) Whole-genome resequencing reveals extensive natural variation in the model green alga *Chlamydomonas reinhardtii*. Plant Cell 27:2353–2369

Gallaher SD, Fitz-Gibbon ST, Glaesener AG, Pellegrini M, Merchant SS (2015) Chlamydomonas genome resource for laboratory strains reveals a mosaic of sequence variation, identifies true strain histories, and enables strain-specific studies. Plant Cell 27:2335–2352

Ge H, Walhout AJ, Vidal M (2003) Integrating 'omic' information: a bridge between genomics and systems biology. Trends Genet 19:551–560

Goffeau A, Barrell BG, Bussey H, Davis RW, Dujon B, Feldmann H, Galibert F, Hoheisel JD, Jacq C, Johnston M, Louis EJ, Mewes HW, Murakami Y, Philippsen P, Tettelin H, Oliver SG (1996) Life with 6000 genes. Science 274(546):563–547

Goodenough U (2015) Historical perspective on Chlamydomonas as a model for basic research: 1950–1970. Plant J 82:365–369

Goodstein DM, Shu S, Howson R, Neupane R, Hayes RD, Fazo J, Mitros T, Dirks W, Hellsten U, Putnam N, Rokhsar DS (2012) Phytozome: a comparative platform for green plant genomics. Nucleic Acids Res 40:D1178–D1186

Haas BJ, Delcher AL, Mount SM, Wortman JR, Smith RK, Hannick LI, Maiti R, Ronning CM, Rusch DB, Town CD, Salzberg SL, White O (2003) Improving the Arabidopsis genome annotation using maximal transcript alignment assemblies. Nucleic Acids Res 31:5654–5666

Haas BJ, Salzberg SL, Zhu W, Pertea M, Allen JE, Orvis J, White O, Buell CR, Wortman JR (2008) Automated eukaryotic gene structure annotation using EVidenceModeler and the Program to Assemble Spliced Alignments. Genome Biol 9:R7

Harris EH (2001) Chlamydomonas as a model organism. Annu Rev Plant Physiol Plant Mol Biol 52:363–406

Harris E (2009) The Chlamydomonas sourcebook, 2nd edn. Academic Press, San Diego, CA

Hieter P, Boguski M (1997) Functional genomics: it's all how you read it. Science 278:601–602

Holt C, Yandell M (2011) MAKER2: an annotation pipeline and genome-database management tool for second-generation genome projects. BMC Bioinf 12:491

Hsieh SI, Castruita M, Malasarn D, Urzica E, Erde J, Page MD, Yamasaki H, Casero D, Pellegrini M, Merchant SS, Loo JA (2013) The proteome of copper, iron, zinc, and manganese micronutrient deficiency in *Chlamydomonas reinhardtii*. Mol Cell Proteomics 12:65–86

Im CS, Zhang Z, Shrager J, Chang CW, Grossman AR (2003) Analysis of light and CO(2) regulation in *Chlamydomonas reinhardtii* using genome-wide approaches. Photosynth Res 75: 111–125

Jin J, Zhang H, Kong L, Gao G, Luo J (2014) PlantTFDB 3.0: a portal for the functional and evolutionary study of plant transcription factors. Nucleic Acids Res 42:D1182–D1187

Jinkerson RE, Jonikas MC (2015) Molecular techniques to interrogate and edit the Chlamydomonas nuclear genome. Plant J 82:393–412

Joyce AR, Palsson B (2006) The model organism as a system: integrating 'omics' data sets. Nat Rev Mol Cell Biol 7:198–210

Kaul S, Koo HL, Jenkins J, Rizzo M, Rooney T, Tallon LJ, Feldblyum T, Nierman W, Benito MI, Lin X, Town CD (2000) Analysis of the genome sequence of the flowering plant *Arabidopsis thaliana*. Nature 408:796–815

Keller LC, Romijn EP, Zamora I, Yates JR, Marshall WF (2005) Proteomic analysis of isolated chlamydomonas centrioles reveals orthologs of ciliary-disease genes. Curr Biol 15:1090–1098

Kent WJ, Sugnet CW, Furey TS, Roskin KM, Pringle TH, Zahler AM, Haussler D (2002) The human genome browser at UCSC. Genome Res 12:996–1006

Kleessen S, Irgang S, Klie S, Giavalisco P, Nikoloski Z (2015) Integration of transcriptomics and metabolomics data specifies the metabolic response of Chlamydomonas to rapamycin treatment. Plant J 81:822–835

Kwan AL, Li L, Kulp DC, Dutcher SK, Stormo GD (2009) Improving gene-finding in *Chlamydomonas reinhardtii*: GreenGenie2. BMC Genomics 10:210

Labadorf A, Link A, Rogers MF, Thomas J, Reddy AS, Ben-Hur A (2010) Genome-wide analysis of alternative splicing in *Chlamydomonas reinhardtii*. BMC Genomics 11:114

Ledford HK, Baroli I, Shin JW, Fischer BB, Eggen RI, Niyogi KK (2004) Comparative profiling of lipid-soluble antioxidants and transcripts reveals two phases of photo-oxidative stress in a xanthophyll-deficient mutant of *Chlamydomonas reinhardtii*. Mol Gen Genomics 272: 470–479

Légeret B, Schulz-Raffelt M, Nguyen HM, Auroy P, Beisson F, Peltier G, Blanc G, Li-Beisson Y (2016) Lipidomic and transcriptomic analyses of *Chlamydomonas reinhardtii* under heat stress

unveil a direct route for the conversion of membrane lipids into storage lipids. Plant Cell Environ 39:834–847

Leinonen R, Sugawara H, Shumway M, Collaboration, I.N.S.D. (2011) The sequence read archive. Nucleic Acids Res 39:D19–D21

Li X, Zhang R, Patena W, Gang SS, Blum SR, Ivanova N, Yue R, Robertson JM, Lefebvre P, Fitz-Gibbon ST, Grossman AR, Jonikas MC (2016) An indexed, mapped mutant library enables reverse genetics studies of biological processes in *Chlamydomonas reinhardtii*. Plant Cell 28(2):367–387

Lilly JW, Maul JE, Stern DB (2002) The *Chlamydomonas reinhardtii* organellar genomes respond transcriptionally and post-transcriptionally to abiotic stimuli. Plant Cell 14:2681–2706

Lohse M, Nagel A, Herter T, May P, Schroda M, Zrenner R, Tohge T, Fernie AR, Stitt M, Usadel B (2014) Mercator: a fast and simple web server for genome scale functional annotation of plant sequence data. Plant Cell Environ 37:1250–1258

Lopez D, Casero D, Cokus SJ, Merchant SS, Pellegrini M (2011) Algal functional annotation tool: a web-based analysis suite to functionally interpret large gene lists using integrated annotation and expression data. BMC Bioinf 12:282

Ma C, Zhang HH, Wang X (2014) Machine learning for big data analytics in plants. Trends Plant Sci 19:798–808

Malasarn D, Kropat J, Hsieh SI, Finazzi G, Casero D, Loo Ja, Pellegrini M, Wollman F-A, Merchant SS (2013) Zinc deficiency impacts CO2 assimilation and disrupts copper homeostasis in *Chlamydomonas reinhardtii*. J Biol Chem 288:10672–10683

May P, Christian JO, Kempa S, Walther D (2009) ChlamyCyc: an integrative systems biology database and web-portal for *Chlamydomonas reinhardtii*. BMC Genomics 10:209

Merchant SS, Prochnik SE, Vallon O, Harris EH, Karpowicz SJ, Witman GB, Terry A, Salamov A, Fritz-Laylin LK, Maréchal-Drouard L, Marshall WF, Qu L-H, Nelson DR, Sanderfoot AA, Spalding MH, Kapitonov VV, Ren Q, Ferris P, Lindquist E, Shapiro H, Lucas SM, Grimwood J, Schmutz J, Cardol P, Cerutti H, Chanfreau G, Chen C-L, Cognat V, Croft MT, Dent R, Dutcher S, Fernández E, Fukuzawa H, González-Ballester D, González-Halphen D, Hallmann A, Hanikenne M, Hippler M, Inwood W, Jabbari K, Kalanon M, Kuras R, Lefebvre Pa, Lemaire SD, Lobanov AV, Lohr M, Manuell A, Meier I, Mets L, Mittag M, Mittelmeier T, Moroney JV, Moseley J, Napoli C, Nedelcu AM, Niyogi K, Novoselov SV, Paulsen IT, Pazour G, Purton S, Ral J-P, Riaño-Pachón DM, Riekhof W, Rymarquis L, Schroda M, Stern D, Umen J, Willows R, Wilson N, Zimmer SL, Allmer J, Balk J, Bisova K, Chen C-J, Elias M, Gendler K, Hauser C, Lamb MR, Ledford H, Long JC, Minagawa J, Page MD, Pan J, Pootakham W, Roje S, Rose A, Stahlberg E, Terauchi AM, Yang P, Ball S, Bowler C, Dieckmann CL, Gladyshev VN, Green P, Jorgensen R, Mayfield S, Mueller-Roeber B, Rajamani S, Sayre RT, Brokstein P, Dubchak I, Goodstein D, Hornick L, Huang YW, Jhaveri J, Luo Y, Martínez D, Ngau WCA, Otillar B, Poliakov A, Porter A, Szajkowski L, Werner G, Zhou K, Grigoriev IV, Rokhsar DS, Grossman AR (2007) The Chlamydomonas genome reveals the evolution of key animal and plant functions. Science (New York, NY) 318:245–250

Mettler T, Mühlhaus T, Hemme D, Schöttler MA, Rupprecht J, Idoine A, Veyel D, Pal SK, Yaneva-Roder L, Winck FV, Sommer F, Vosloh D, Seiwert B, Erban A, Burgos A, Arvidsson S, Schönfelder S, Arnold A, Günther M, Krause U, Lohse M, Kopka J, Nikoloski Z, Mueller-Roeber B, Willmitzer L, Bock R, Schroda M, Stitt M (2014) Systems analysis of the response of photosynthesis, metabolism, and growth to an increase in irradiance in the photosynthetic model organism Chlamydomonas reinhardtii. Plant Cell 26:2310–2350

Moellering ER, Benning C (2010) RNA interference silencing of a major lipid droplet protein affects lipid droplet size in Chlamydomonas reinhardtii. Eukaryot Cell 9:97–106

Mussgnug JH (2015) Genetic tools and techniques for Chlamydomonas reinhardtii. Appl Microbiol Biotechnol 99:5407–5418

Nguyen HM, Baudet M, Cuiné S, Adriano JM, Barthe D, Billon E, Bruley C, Beisson F, Peltier G, Ferro M, Li-Beisson Y (2011) Proteomic profiling of oil bodies isolated from the unicellular

green microalga Chlamydomonas reinhardtii: with focus on proteins involved in lipid metabolism. Proteomics 11:4266–4273

Niehrs C, Pollet N (1999) Synexpression groups in eukaryotes. Nature 402:483–487

Overbeek R, Begley T, Butler RM, Choudhuri JV, Chuang HY, Cohoon M, de Crécy-Lagard V, Diaz N, Disz T, Edwards R, Fonstein M, Frank ED, Gerdes S, Glass EM, Goesmann A, Hanson A, Iwata-Reuyl D, Jensen R, Jamshidi N, Krause L, Kubal M, Larsen N, Linke B, McHardy AC, Meyer F, Neuweger H, Olsen G, Olson R, Osterman A, Portnoy V, Pusch GD, Rodionov DA, Rückert C, Steiner J, Stevens R, Thiele I, Vassieva O, Ye Y, Zagnitko O, Vonstein V (2005) The subsystems approach to genome annotation and its use in the project to annotate 1000 genomes. Nucleic Acids Res 33:5691–5702

Palsson B, Zengler K (2010) The challenges of integrating multi-omic data sets. Nat Chem Biol 6: 787–789

Park JJ, Wang H, Gargouri M, Deshpande RR, Skepper JN, Holguin FO, Juergens MT, Shachar-Hill Y, Hicks LM, Gang DR (2015) The response of *Chlamydomonas reinhardtii* to nitrogen deprivation: a systems biology analysis. Plant J 81:611–624

Pazour GJ, Agrin N, Leszyk J, Witman GB (2005) Proteomic analysis of a eukaryotic cilium. J Cell Biol 170:103–113

Pérez-Rodríguez P, Riaño-Pachón DM, Corrêa LG, Rensing SA, Kersten B, Mueller-Roeber B (2010) PlnTFDB: updated content and new features of the plant transcription factor database. Nucleic Acids Res 38:D822–D827

Prochnik SE, Umen J, Nedelcu AM, Hallmann A, Miller SM, Nishii I, Ferris P, Kuo A, Mitros T, Fritz-Laylin LK, Hellsten U, Chapman J, Simakov O, Rensing SA, Terry A, Pangilinan J, Kapitonov V, Jurka J, Salamov A, Shapiro H, Schmutz J, Grimwood J, Lindquist E, Lucas S, Grigoriev IV, Schmitt R, Kirk D, Rokhsar DS (2010) Genomic analysis of organismal complexity in the multicellular green alga *Volvox carteri*. Science 329:223–226

Rhee SY, Wood V, Dolinski K, Draghici S (2008) Use and misuse of the gene ontology annotations. Nat Rev Genet 9:509–515

Rolland N, Atteia A, Decottignies P, Garin J, Hippler M, Kreimer G, Lemaire SD, Mittag M, Wagner V (2009) Chlamydomonas proteomics. Curr Opin Microbiol 12:285–291

Romero-Campero FJ, Perez-Hurtado I, Lucas-Reina E, Romero JM, Valverde F (2016) ChlamyNET: a Chlamydomonas gene co-expression network reveals global properties of the transcriptome and the early setup of key co-expression patterns in the green lineage. BMC Genomics 17:227

Rymarquis LA, Handley JM, Thomas M, Stern DB (2005) Beyond complementation. Map-based cloning in *Chlamydomonas reinhardtii*. Plant Physiol 137:557–566

Schmidt M, Gessner G, Luff M, Heiland I, Wagner V, Kaminski M, Geimer S, Eitzinger N, Reissenweber T, Voytsekh O, Fiedler M, Mittag M, Kreimer G (2006) Proteomic analysis of the eyespot of *Chlamydomonas reinhardtii* provides novel insights into its components and tactic movements. Plant Cell 18:1908–1930

Schmollinger S, Mühlhaus T, Boyle NR, Blaby IK, Casero D, Mettler T, Moseley JL, Kropat J, Sommer F, Strenkert D, Hemme D, Pellegrini M, Grossman AR, Stitt M, Schroda M, Merchant SS (2014) Nitrogen-sparing mechanisms in Chlamydomonas affect the transcriptome, the proteome, and photosynthetic metabolism. Plant Cell 26(4):1410–1435

Schnoes AM, Brown SD, Dodevski I, Babbitt PC (2009) Annotation error in public databases: misannotation of molecular function in enzyme superfamilies. PLoS Comput Biol 5:e1000605

Seaver SM, Gerdes S, Frelin O, Lerma-Ortiz C, Bradbury LM, Zallot R, Hasnain G, Niehaus TD, El Yacoubi B, Pasternak S, Olson R, Pusch G, Overbeek R, Stevens R, de Crécy-Lagard V, Ware D, Hanson AD, Henry CS (2014) High-throughput comparison, functional annotation, and metabolic modeling of plant genomes using the PlantSEED resource. Proc Natl Acad Sci U S A 111:9645–9650

Specht M, Stanke M, Terashima M, Naumann-Busch B, Janssen I, Höhner R, Hom EF, Liang C, Hippler M (2011) Concerted action of the new Genomic Peptide Finder and AUGUSTUS

allows for automated proteogenomic annotation of the *Chlamydomonas reinhardtii* genome. Proteomics 11:1814–1823

Stanke M, Diekhans M, Baertsch R, Haussler D (2008) Using native and syntenically mapped cDNA alignments to improve de novo gene finding. Bioinformatics 24:637–644

Stolc V, Samanta MP, Tongprasit W, Marshall WF (2005) Genome-wide transcriptional analysis of flagellar regeneration in *Chlamydomonas reinhardtii* identifies orthologs of ciliary disease genes. Proc Natl Acad Sci U S A 102:3703–3707

Subramanian V, Dubini A, Astling DP, Laurens LM, Old WM, Grossman AR, Posewitz MC, Seibert M (2014) Profiling Chlamydomonas metabolism under dark, anoxic H2-producing conditions using a combined proteomic, transcriptomic, and metabolomic approach. J Proteome Res 13:5431–5451

Tardif M, Atteia A, Specht M, Cogne G, Rolland N, Brugière S, Hippler M, Ferro M, Bruley C, Peltier G, Vallon O, Cournac L (2012) PredAlgo: a new subcellular localization prediction tool dedicated to green algae. Mol Biol Evol 29:3625–3639

Terashima M, Specht M, Naumann B, Hippler M (2010) Characterizing the anaerobic response of *Chlamydomonas reinhardtii* by quantitative proteomics. Mol Cell Proteomics 9:1514–1532

Terashima M, Specht M, Hippler M (2011) The chloroplast proteome: a survey from the *Chlamydomonas reinhardtii* perspective with a focus on distinctive features. Curr Genet 57: 151–168

Thimm O, Bläsing O, Gibon Y, Nagel A, Meyer S, Krüger P, Selbig J, Müller La, Rhee SY, Stitt M (2004) Mapman: a user-driven tool to display genomics data sets onto diagrams of metabolic pathways and other biological processes. Plant J 37:914–939

Tian W, Skolnick J (2003) How well is enzyme function conserved as a function of pairwise sequence identity? J Mol Biol 333:863–882

Tulin F, Cross F (2015) Patching holes in the Chlamydomonas genome (bioRxiv)

Urzica EI, Casero D, Yamasaki H, Hsieh SI, Adler LN, Karpowicz SJ, Blaby-Haas CE, Clarke SG, Loo JA, Pellegrini M, Merchant SS (2012) Systems and trans-system level analysis identifies conserved iron deficiency responses in the plant lineage. Plant Cell 24(10):3921–3948

Van Verk MC, Hickman R, Pieterse CM, Van Wees SC (2013) RNA-Seq: revelation of the messengers. Trends Plant Sci 18:175–179

Vandepoele K, Van Bel M, Richard G, Van Landeghem S, Verhelst B, Moreau H, Van de Peer Y, Grimsley N, Piganeau G (2013) Pico-PLAZA, a genome database of microbial photosynthetic eukaryotes. Environ Microbiol 15:2147–2153

Vidal M (2001) A biological atlas of functional maps. Cell 104:333–339

Wagner V, Ullmann K, Mollwo A, Kaminski M, Mittag M, Kreimer G (2008) The phosphoproteome of a *Chlamydomonas reinhardtii* eyespot fraction includes key proteins of the light signaling pathway. Plant Physiol 146:772–788

Wakao S, Chin BL, Ledford HK, Dent RM, Casero D, Pellegrini M, Merchant SS, Niyogi KK (2014) Phosphoprotein SAK1 is a regulator of acclimation to singlet oxygen in *Chlamydomonas reinhardtii*. elife 3:e02286

Waterston RH, Lindblad-Toh K, Birney E, Rogers J, Abril JF, Agarwal P, Agarwala R, Ainscough R, Alexandersson M, An P, Antonarakis SE, Attwood J, Baertsch R, Bailey J, Barlow K, Beck S, Berry E, Birren B, Bloom T, Bork P, Botcherby M, Bray N, Brent MR, Brown DG, Brown SD, Bult C, Burton J, Butler J, Campbell RD, Carninci P, Cawley S, Chiaromonte F, Chinwalla AT, Church DM, Clamp M, Clee C, Collins FS, Cook LL, Copley RR, Coulson A, Couronne O, Cuff J, Curwen V, Cutts T, Daly M, David R, Davies J, Delehaunty KD, Deri J, Dermitzakis ET, Dewey C, Dickens NJ, Diekhans M, Dodge S, Dubchak I, Dunn DM, Eddy SR, Elnitski L, Emes RD, Eswara P, Eyras E, Felsenfeld A, Fewell GA, Flicek P, Foley K, Frankel WN, Fulton LA, Fulton RS, Furey TS, Gage D, Gibbs RA, Glusman G, Gnerre S, Goldman N, Goodstadt L, Grafham D, Graves TA, Green ED, Gregory S, Guigó R, Guyer M, Hardison RC, Haussler D, Hayashizaki Y, Hillier LW, Hinrichs A, Hlavina W, Holzer T, Hsu F, Hua A, Hubbard T, Hunt A, Jackson I, Jaffe DB, Johnson LS, Jones M, Jones TA, Joy A, Kamal M, Karlsson EK, Karolchik D, Kasprzyk A,

Kawai J, Keibler E, Kells C, Kent WJ, Kirby A, Kolbe DL, Korf I, Kucherlapati RS, Kulbokas EJ, Kulp D, Landers T, Leger JP, Leonard S, Letunic I, Levine R, Li J, Li M, Lloyd C, Lucas S, Ma B, Maglott DR, Mardis ER, Matthews L, Mauceli E, Mayer JH, McCarthy M, McCombie WR, McLaren S, McLay K, McPherson JD, Meldrim J, Meredith B, Mesirov JP, Miller W, Miner TL, Mongin E, Montgomery KT, Morgan M, Mott R, Mullikin JC, Muzny DM, Nash WE, Nelson JO, Nhan MN, Nicol R, Ning Z, Nusbaum C, O'Connor MJ, Okazaki Y, Oliver K, Overton-Larty E, Pachter L, Parra G, Pepin KH, Peterson J, Pevzner P, Plumb R, Pohl CS, Poliakov A, Ponce TC, Ponting CP, Potter S, Quail M, Reymond A, Roe BA, Roskin KM, Rubin EM, Rust AG, Santos R, Sapojnikov V, Schultz B, Schultz J, Schwartz MS, Schwartz S, Scott C, Seaman S, Searle S, Sharpe T, Sheridan A, Shownkeen R, Sims S, Singer JB, Slater G, Smit A, Smith DR, Spencer B, Stabenau A, Stange-Thomann N, Sugnet C, Suyama M, Tesler G, Thompson J, Torrents D, Trevaskis E, Tromp J, Ucla C, Ureta-Vidal A, Vinson JP, Von Niederhausern AC, Wade CM, Wall M, Weber RJ, Weiss RB, Wendl MC, West AP, Wetterstrand K, Wheeler R, Whelan S, Wierzbowski J, Willey D, Williams S, Wilson RK, Winter E, Worley KC, Wyman D, Yang S, Yang SP, Zdobnov EM, Zody MC, Lander ES, Consortium MGS (2002) Initial sequencing and comparative analysis of the mouse genome. Nature 420:520–562

Winck FV, Riaño-Pachón DM, Sommer F, Rupprecht J, Mueller-Roeber B (2012) The nuclear proteome of the green alga *Chlamydomonas reinhardtii*. Proteomics 12:95–100

Winzeler EA, Shoemaker DD, Astromoff A, Liang H, Anderson K, Andre B, Bangham R, Benito R, Boeke JD, Bussey H, Chu AM, Connelly C, Davis K, Dietrich F, Dow SW, El Bakkoury M, Foury F, Friend SH, Gentalen E, Giaever G, Hegemann JH, Jones T, Laub M, Liao H, Liebundguth N, Lockhart DJ, Lucau-Danila A, Lussier M, M'Rabet N, Menard P, Mittmann M, Pai C, Rebischung C, Revuelta JL, Riles L, Roberts CJ, Ross-MacDonald P, Scherens B, Snyder M, Sookhai-Mahadeo S, Storms RK, Véronneau S, Voet M, Volckaert G, Ward TR, Wysocki R, Yen GS, Yu K, Zimmermann K, Philippsen P, Johnston M, Davis RW (1999) Functional characterization of the S. cerevisiae genome by gene deletion and parallel analysis. Science 285:901–906

Zhang Z, Shrager J, Jain M, Chang CW, Vallon O, Grossman AR (2004) Insights into the survival of *Chlamydomonas reinhardtii* during sulfur starvation based on microarray analysis of gene expression. Eukaryot Cell 3:1331–1348

Zheng HQ, Chiang-Hsieh YF, Chien CH, Hsu BK, Liu TL, Chen CN, Chang WC (2014) AlgaePath: comprehensive analysis of metabolic pathways using transcript abundance data from next-generation sequencing in green algae. BMC Genomics 15:196

Zones JM, Blaby IK, Merchant SS, Umen JG (2015) High-resolution profiling of a synchronized diurnal transcriptome from *Chlamydomonas reinhardtii* reveals continuous cell and metabolic differentiation. Plant Cell 27:2743–2769

Nuclear Transformation and Toolbox Development

Jan H. Mussgnug

Abstract More than 99% of all genes of *C. reinhardtii* are encoded in the nuclear DNA. Over the past decades, classical genetic techniques and molecular biological strategies have been established that allow manipulation of the nuclear DNA for fundamental research and applied tasks. The nuclear genome is haploid during the vegetative stage of the green microalga's life cycle, a feature promoting the elucidation of specific genotype–phenotype interrelations in genetic studies. Supported by the general progress of molecular technologies, the toolbox for *C. reinhardtii* nuclear genome transformation and engineering has been greatly expanded, and, today, a substantial arsenal of tools and techniques is available which can be utilized to approach individual molecular research tasks.

Several important aspects of nuclear genetic engineering with *C. reinhardtii* will be addressed in this chapter. Since in many cases, the prerequisite for genetic engineering is the transformation of DNA, strategies for nuclear DNA delivery will be introduced within the historical context. Furthermore, established DNA elements, transformation selection markers, strategies to achieve modulation of gene expression, and examples of versatile vectors will be summarized. Finally, cell line-specific considerations will be addressed before future perspectives are presented.

1 Introduction

Eukaryotic *C. reinhardtii* microalgae store DNA, the basic chemical compound comprising the cells' genetic information, in three types of organelles: nuclei, chloroplasts, and mitochondria. Efficient techniques for stable DNA transformation have been established for all three genomes some 25 years ago; therefore, all three compartments are easily accessible for genetic engineering today.

By far most of the approximately 19,500 predicted protein-coding transcripts (including splice variants) originate from the cell nucleus (Joint Genome Institute

J.H. Mussgnug (✉)
Faculty of Biology, Center for Biotechnology (CeBiTec), Bielefeld University, Universitätsstrasse 27, 33615 Bielefeld, Germany
e-mail: jan.mussgnug@uni-bielefeld.de

M. Hippler (ed.), *Chlamydomonas: Molecular Genetics and Physiology*, Microbiology Monographs 30, DOI 10.1007/978-3-319-66365-4_2

2015). Here, the genetic information is stored as DNA, eventually transcribed into RNA and, in the case of protein-coding genes, decoded in the cytosol to guide formation of protein macromolecules. These functional units are then individually distributed to the compartments of the microalgal cell and participate in regulating life functions.

The very first successful DNA transformation of *C. reinhardtii* was published in the year 1982 (Rochaix and van Dillewijn 1982), and since then, the development and utilization of a versatile toolbox for genetic engineering has been a major focus of molecular biologists working with this model organism. Genetic engineering strategies have greatly been aided by the fast technical progress related to DNA sequencing, DNA synthesis, bioinformatics, and chemical component analysis over the last decades. Many regulatory genetic elements promoting stable transgene (TG) expression are known today, and, furthermore, regulatory sequences have been identified that allow modulated TG expression for more complex gene expression trials.

Several positive and negative transformation markers allow fast and easy selection of successfully transformed algal cells. Depending on the individual TG and the host cell line, however, nuclear gene expression can still be challenging, and the efficiency has to be evaluated on a case-by-case basis.

2 Methods for Nuclear DNA Transformation

Stable integration of recombinant DNA into the nuclear genome is well established, and three methods are commonly used to achieve DNA transfer: biolistic particle bombardment, vortexing in the presence of small particles, and electroporation. The choice of the preferred method mainly depends on the parental cell line characteristics, especially on the presence or absence of an outer cell wall, and potential constraints with respect to the available laboratory equipment. In addition to the three main methods, T-DNA transformation mediated by *Agrobacterium tumefaciens* was described to be possible as well (Kumar et al. 2004) but does not seem to be commonly applied. Micro- and nanoinjection (Nichols and Rikmenspoel 1978; Hennig et al. 2015) could also be feasible methods but apparently have not yet been applied for stable transfer of nucleic acid into *C. reinhardtii* cells. Since it has been shown that the efficiency of DNA transformation was increased when vector sequences were omitted from nuclear transformation setups (Meslet-Cladiere and Vallon 2011), it is reasonable to recommend avoiding unnecessary DNA regions from transformation experiments.

2.1 Biolistic Transformation

Biolistic particle bombardment of plant cells was first demonstrated by Klein et al. (1987), who used a particle gun to deliver tungsten particles previously coated with nucleic acids (DNA or RNA) into onion (*Allium cepa*) cell tissue (Klein et al. 1987). In the following year, this technique was successfully applied to achieve the first stable and efficient DNA transformation of *C. reinhardtii* cells. Since codon optimized and reliable dominant selectable markers promoting antibiotic resistance were not yet established, most initial trials relied on transformation of photosynthetic or auxotrophic Chlamydomonas mutants with the respective endogenous genes to restore photosynthetic competence or nutrient prototrophy, respectively. Boynton et al. (1988) were the first to succeed with this strategy by restoring an *atpB*-deficient chloroplast mutant (Boynton et al. 1988), a method later also applied to introduce embedded foreign genes (Blowers et al. 1989).

Shortly thereafter, several examples of successful biolistic transformation of the nuclear genome followed. For nuclear transformants selection, Debuchy et al. (1989) used the argininosuccinate lyase gene (ARG7), whereas Kindle et al. (1989) chose the nitrate reductase gene (NIT1) to restore the corresponding nuclear mutant cell lines (Debuchy et al. 1989; Kindle et al. 1989). In a related work, it was shown that DNA co-transformation into the nuclear genome was also possible with this method (Day et al. 1990). The presence of a wild-type (wt) cell wall does not prevent biolistic DNA transformation, and nonhomologous insertion of the transformed DNA at apparently random loci is far more common than integration by homologous recombination. An early work estimated a ratio of 24:1 (random vs. homologous events) (Sodeinde and Kindle 1993), but more recent work indicates an even higher ratio in favor of random integration (Zorin et al. 2005).

2.2 Agitation of Cells in the Presence of DNA and Microparticles

A disadvantage of the biolistic method is that sample preparation is quite time-consuming, and comparably sophisticated technical equipment is necessary. Karen L. Kindle therefore adopted an alternative method, which had been established for yeast before, with great success to generate nuclear transformants cheaply and efficiently (Kindle 1990). This method, often referred to as "glass bead transformation," relies on agitation of *C. reinhardtii* cells in the presence of DNA and small (diameter of ca. 0.5 mm) glass beads. Polyethylene glycol (PEG) can be added to increase the transformation efficiency, and as an alternative to glass beads, silicon carbide whiskers have also been used (Dunahay 1993). The hydroxyproline-rich outer wt cell wall inhibits DNA uptake, so it has to be removed via autolysin treatment before agitation, or, alternatively, a cell wall-deficient cell line can be used. Despite this constraint, this method is well suited for many research

applications, and because of its simplicity, it furthermore represents an ideal choice for teaching environments, e.g., school or university courses.

The overwhelming majority of transformation events occur at random locations, and a ratio of 1000:1 (nonhomologous vs. homologous events) (Sodeinde and Kindle 1993) or even less (Gumpel et al. 1994; Nelson and Lefebvre 1995) has been estimated. Zorin et al. (2005) demonstrated that nonhomologous DNA integration events were more than 100-fold reduced when single-stranded, instead of double-stranded, DNA was used, therefore dramatically decreasing the ratio of nonhomologous vs. homologous events (Zorin et al. 2005). Although the method was further improved by the authors (Zorin et al. 2009), it still did not gain traction, most likely due to the accompanying technical difficulties.

2.3 Electroporation

The application of electric impulses for reversible membrane breakdown and stable DNA transformation was first demonstrated by Neumann and colleagues in 1982, who successfully used this technique to transfer a herpes simplex thymidine kinase gene into LTK^- mouse cells (Neumann et al. 1982). Most likely, the main reason behind the increased membrane permeability after electric field application is that aqueous pores are formed, which allow transmembrane molecule transport otherwise prevented by an intact lipid bilayer (Yarmush et al. 2014).

An advantage of the electroporation method is that it is fast and can be achieved with rather inexpensive equipment. It therefore has been used to transform many pro- and eukaryotic species, including Chlamydomonas cell lines, both with and without an outer cell wall (Brown et al. 1991; Shimogawara et al. 1998). Recently published, large-scale analyses of nuclear insertions sites after electroporation of cell wall-deficient *C. reinhardtii* strain CC-4533 (CMJ030) revealed that DNA insertion occurs at apparently random loci. Furthermore, sequence evidence suggests that endonucleolytic events can occur during mutagenesis and lead to DNA rearrangements before integration, resulting in misleading flanking sequence identifications in subsequent insertion site analyses (Zhang et al. 2014; Li et al. 2016). A notable feature of the electroporation method is that it can also be applied to introduce exogenous proteins into *C. reinhardtii* (Hayashi et al. 2001).

3 Recombinant DNA Expression

Plasmids are most commonly used as vectors for Chlamydomonas nuclear transformation, and some selected examples are presented in a later section of this chapter. Transformation plasmids usually consist of a cloning vector backbone and one or more TG inserts. A typical insert comprises promoter/5′UTR, coding region, and 3′UTR sequences and can contain one or more introns. The regulatory

5′ and 3′ sequences are often derived from endogenous or foreign genes with high natural expression levels, including several inducible genes (see Sect. 3.2). If the TG confers a selectable phenotype, positive transformant identification is straightforward. In case the TG does not confer a selectable phenotype, it can be co-transformed on a second plasmid, be cloned into the selectable vector plasmid as a separate expression cassette, or it can be fused with a reporter protein. In addition, viral 2A peptides were recently successfully employed to express multicistronic transgenes. Importantly, these 2A peptides allow direct coupling of a gene of interest to a selection marker. By applying this strategy, Rasala et al. (2012) demonstrated that coupling of xylanase1 with the FMDV 2A peptide resulted in a ~100-fold increase of enzyme activity, compared to the unlinked control (Rasala et al. 2012). Many combinations of promoter DNA regions, selection markers, introns, and 3′UTR regions have been generated, and an updated overview of successfully used vector elements is presented in the following sections.

3.1 Promoter Elements

Gene expression is dependent on DNA elements which promote binding of the transcription factors necessary to control initiation of RNA polymerase activity. Several promoter elements like TATA boxes, initiator (Inr), B recognition (BRE), and downstream promoter elements (DPE) have been identified in plants (Porto et al. 2014); however, flexibility of location and sequence variability can make motif assignment difficult. A genome-wide computational study was performed by Ding et al. (2012) to identify potential cis-regulatory elements within the nuclear genome of *C. reinhardtii*. In this work, a novel algorithm called MERCED ("modeling evolution rate across species for cis-regulatory element discovery") was applied, predicting a total of 66,530 cis-regulatory elements, corresponding to 317 element motifs (Ding et al. 2012).

Most of the DNA regions used to drive heterologous nuclear gene expression in Chlamydomonas originate from only very few hosts. An extended list of promoters is presented in Table 1.

3.2 Modulation of Recombinant DNA Expression

Depending on the goal, modulated or constitutive recombinant gene expression can be aimed for, and several regulatory elements have been characterized which can direct gene expression rates.

Table 1 List of promoters used for recombinant DNA expression in *C. reinhardtii* from nuclear genomes

Name	Organism, annotation	References
ARG7	*C. reinhardtii*, argininosuccinate lyase	Specht et al. (2014)
ATX1	*C. reinhardtii*, copper chaperone *antioxidant*	Fei and Deng (2007)
ß2TUB	*C. reinhardtii*, β2-tubulin	Brunke et al. (1984)
C3	*C. reinhardtii*, C3	Voytsekh et al. (2008)
CAH1	*C. reinhardtii*, carbonic anhydrase	Kucho et al. (1999), Ferrante et al. (2011)
CaMV 35S	*Cauliflower mosaic virus*, 35S	Kumar et al. (2004), Guilley et al. (1982), Ruecker et al. (2008)
CHOP2	*C. reinhardtii*, channelopsin-2	Fuhrmann et al. (2004)
CPX1	*C. reinhardtii*, coproporphyrinogen oxidase	Quinn et al. (2003)
CYC6	*C. reinhardtii*, cytochrome c_6	Quinn et al. (2003), Ferrante et al. (2011)
FDX5	*C. reinhardtii*, ferredoxin	Lambertz et al. (2010)
FEA1 (H43)	*C. reinhardtii*, FEA1 (H43)	Baba et al. (2011), Fei et al. (2009)
FOX1	*C. reinhardtii*, multi-copper oxidase	Deng et al. (2014)
FTR1	*C. reinhardtii*, iron transporter	Fei et al. (2010)
GPXH (GPX5)	*C. reinhardtii*, glutathione peroxidase	Leisinger et al. (2001)
HSP70A	*C. reinhardtii*, heat shock factor 1	Schroda et al. (2000)
HSP70A/ RBCS2	*C. reinhardtii*, hybrid promoter HSP70A/RBCS2	Schroda et al. (2000), Strenkert et al. (2013), Lodha et al. (2008)
HSP70A/ RBCS3	*Volvox carteri*, hybrid promoter HSP70A/RBCS3	Hallmann and Wodniok (2006)
HYDA1	*C. reinhardtii*, [FeFe]-hydrogenase isoform1	Pape et al. (2012)
LHCBM6	*C. reinhardtii*, LHCBM6 (CABII-1, LHCB1)	Blankenship and Kindle (1992), Hahn and Kück (1999)
LHCBM9	*C. reinhardtii*, LHCBM9	Grewe et al. (2014), Sawyer et al. (2015)
LIP	*Dunaliella tertiolecta*, light-inducible protein	Park et al. (2013)
METE	*C. reinhardtii*, B_{12}-independent methionine synthase	Helliwell et al. (2014), Croft et al. (2005)
NAB1	*C. reinhardtii*, nucleic acid-binding protein 1	Berger et al. (2014), Mussgnug et al. (2005)
NIT1	*C. reinhardtii*, nitrate reductase	Ohresser et al. (1997)
nos	*Agrobacterium tumefaciens*, nopaline synthase	Diaz-Santos et al. (2013), Hall et al. (1993)
PSAD	*C. reinhardtii*, photosystem I subunit	Fischer and Rochaix (2001)
RBCS2	*C. reinhardtii*, RUBISCO small subunit	Goldschmidt-Clermont and Rahire (1986), Kozminski et al. (1993)

(continued)

Table 1 (continued)

Name	Organism, annotation	References
RBCS2	*Dunaliella tertiolecta*, RUBISCO small subunit	Walker et al. (2005)
saps	Synthetic algal promoters	Scranton et al. (2016)
SQD2	*C. reinhardtii*, sulphoquinovosyltransferase	Iwai et al. (2014)
SV 40	*Simian virus 40*, early promoter	Hasnain et al. (1985), Ladygin and Butanaev (2002)

Alternative names are indicated in brackets. Table modified from (Mussgnug 2015)

3.2.1 High-Level Transgene Expression

Arguably the most prominent option for high TG expression in Chlamydomonas currently is the HSP70A/RBCS2 hybrid promoter. This promoter fusion element was introduced by Schroda et al. (2000), since the HSP70A element was observed to activate TG-driving promoters located further downstream (Schroda et al. 2000). Detailed investigations showed that this activating effect is mediated by distinct cis-regulatory elements within the promoter (TATA-box and heat shock elements), indicating that associated chromatin structure modulations are responsible for the observed stimulating effects (Lodha et al. 2008; Strenkert et al. 2013). The *C. reinhardtii* ARG7 promoter is another example promoting comparatively high TG expression capacity, and it was recently demonstrated that the respective 1425 promoter/5′UTR region promotes similar TG expression efficiency as the chimeric HSP70A/RBCS2 promoter (Specht et al. 2014). Further potentially highly efficient promoter regions, e.g., derived from the ubiquitin regulatory protein (UBIRP), were identified in a promoter trapping approach (Vila et al. 2012). Since these novel promoters have not yet been systematically characterized, it is reasonable to suggest that additional improvements, e.g., addition of enhancing cis-regulatory elements, will result in establishment of further improved TG expression vectors. In this context, Scranton et al. (2016) very recently identified specific cis-motifs present within native *C. reinhardtii* promoters of genes with high expression levels via the POWRS software (Davis et al. 2012). This information was used to generate a set of novel synthetic algal promoters (saps), and 7 of the 25 investigated saps were described to promote higher average and maximum reporter gene expression than the HSP70A/RBCS2 hybrid promoter (Scranton et al. 2016).

3.2.2 Inducible Transgene Expression

For certain target proteins, constitutive high-level expression might not be desirable, e.g., in case dose-dependent phenotypes are investigated or if cytotoxic side effects of the product cannot be excluded. Analyses of individual genes and full transcriptomes have led to the identification of a great number of transcriptionally regulated *C. reinhardtii* genes. Despite this fact, not many tightly controlled

inducible promoters have been studied thoroughly for versatile recombinant DNA expression. Three of the prominent examples will briefly be depicted in the following paragraphs; however, it should be noted that novel, effective "on/off" promoters are still in demand.

One of the best characterized inducible genes of Chlamydomonas is cytochrome c_6, for which studies on transcriptional regulation were performed already 25 years ago (Merchant et al. 1991). Since then, it was demonstrated that the respective promoter is silenced if copper is present, but transcription is strongly induced if copper is completely absent or upon nickel addition (Quinn et al. 2003). A 428 bp promoter sequence was subsequently used to build a versatile system for inducible control of chloroplast genes (Surzycki et al. 2007), mediated by the factor NAC2 (Nickelsen et al. 1994).

The nitrate reductase NIT1 represents another strongly inducible *C. reinhardtii* gene, and the promoter region has been studied in recombinant setups for many years (Zhang and Lefebvre 1997). Here, transcription is repressed in the presence of ammonium and induced when ammonium is replaced by nitrate. The NIT1 promoter was used for inducible transcript silencing via RNAi (Koblenz and Lechtreck 2005), and a 791 bp 5′ sequence was subsequently used to create a versatile inducible microRNA expression system (Schmollinger et al. 2010). Interestingly, the NIT1 promoter was also tested in the work of Surzycki et al. but was found not to be effective in their setup (Surzycki et al. 2007).

The methionine synthase gene METE was shown to be repressed in the presence of vitamin B_{12} (Croft et al. 2005), and Ramundo et al. used a 1213 bp region upstream of this gene as an inducible promoter for a vitamin-controlled expression/repression system for chloroplast genes (Ramundo et al. 2013). They found, however, that complete silencing of gene expression could not be achieved via vitamin B_{12} addition alone but was only possible via the additional activity of the thiamine pyrophosphate-responsive riboswitch THI4 (Ramundo et al. 2013). This riboswitch was originally identified by Croft and colleagues in the 5′UTR of the THI4 gene and shown to regulate thiamine biosynthesis in vivo (Croft et al. 2007). Since effective, inducible riboswitches can evidently be found in the *C. reinhardtii* genome, it is possible that the discovery of additional riboswitches will lead to the development of further, independent options to modulate recombinant TG expression in the future.

3.3 Introns

In addition to the aforementioned cis-regulatory promoter elements located upstream of the TG coding region, enhancing elements present within endogenous introns have also been identified. The general relevance of introns is reflected by the fact that 92% of the *C. reinhardtii* genes contain at least one intron (Merchant et al. 2007). The introns of the highly expressed RBCS2 gene were analyzed in detail. Lumbreras and colleagues demonstrated that the RBCS2 intron 1 enhances TG

expression and that this effect is not dependent on the orientation or localization relative to the promoter of the TG (Lumbreras et al. 1998). Kovar and colleagues observed that adequate expression of an engineered ALS protein was dependent on the presence of the respective set of introns (Kovar et al. 2002). Eichler-Stahlberg et al. performed a luciferase-based reporter study on the relevance of the individual RBCS2 introns and demonstrated that highest levels of reporter activity were obtained when introns 1, 2, and 3 were inserted in the correct order (Eichler-Stahlberg et al. 2009). Furthermore, preliminary data from a systematic study in our lab showed that the gene expression can significantly be enhanced by strategical distribution of multiple RBCS2 introns into a target transgene-coding sequence. Interestingly, an enhancing effect was not detected for all introns tested, indicating the presence of specific enhancer elements. These examples clearly show that intron characteristics of a given target transgene is a factor that should be taken into account for nuclear gene expression approaches.

3.4 3′UTRs

Shen and colleagues performed a large-scale computational study and showed that the average length of *C. reinhardtii* 3′UTRs is 595 nucleotides (with several extending 1450 nucleotides), which is roughly twice as long as the average 3′UTRs of *Arabidopsis thaliana* (Shen et al. 2008). Polyadenylation of the 3′ends of nuclear pre-mRNAs is a crucial step for functional gene expression, and cis-elements guiding this process can regularly be detected within the 3′UTRs. Recent bioinformatic (Zhao et al. 2014) and experimental (Bell et al. 2016) investigations clearly confirmed the earlier notion that (UGUAA) is the dominant polyadenylation signal for *C. reinhardtii* nuclear genes. Interestingly, the sequence data indicated that alternative polyadenylation of nuclear mRNAs can occur (Zhao et al. 2014), although extend and relevance for functional gene expression are still under debate (Bell et al. 2016).

With regard to recombinant gene expression approaches, the 3′UTR derived from the RBCS2 gene was applied most often (Lumbreras et al. 1998; Cerutti et al. 1997); however, many more were successfully used, including the 3′UTRs from PSAD (Fischer and Rochaix 2001), COP (Sizova et al. 2001), ARS (Davies et al. 1992), and ALS (Kovar et al. 2002). Furthermore, TG expression was demonstrated to be possible even without inclusion of a defined 3′UTR (Meslet-Cladiere and Vallon 2011). Enhancement of TG expression via optimization of the respective 3′UTR could be a feasible strategy, but this was not yet investigated systematically.

3.5 G+C Content

In contrast to the mitochondrial (~45% G+C) and chloroplast (~35% G+C) genomes, the nuclear genome of *C. reinhardtii* is biased toward high-G+C content (overall ~64%, coding sequence ~68% G+C content) (Merchant et al. 2007). Since it was observed that foreign gene expression was poor in many early trials, it was suggested that important factors for efficient heterologous nuclear gene expression in *C. reinhardtii* are G+C content and codon composition of the respective TGs. Fuhrmann et al. (1999) tested this hypothesis with an *Aequorea victoria* gene encoding a GFP protein. An adapted version of the gene was synthesized, which was composed entirely of codons that are present in naturally well-expressed Chlamydomonas genes, concomitantly raising the G+C content from 39.5% to 61.6% and thus more closely resembling the average nuclear G+C content. In contrast to the original gene, the synthetic GFP could be expressed efficiently as part of fusion proteins, suggesting a positive effect of the codon adjustment (Fuhrmann et al. 1999). In a similar approach, Heitzer et al. (2007) compared the expression of AT-rich and GC-rich GFP variants, fused in frame with the BLE protein marker. As a result, the number of positive transformants and the transformants' individual resistances toward the selection reagent zeocin was significantly higher for the codon optimized variants, indicating more pronounced gene-silencing effects in case of the not-adapted TG version. In this study, however, it was not possible to correlate these effects with elevated cellular recombinant protein levels (Heitzer et al. 2007).

Very recently, a systematic study was published that further verified the value of codon adjustment for efficient TG expression in *C. reinhardtii*. This study was set up to unravel the individual contributions of codon composition and G+C content to recombinant DNA expression (Barahimipour et al. 2015). Four gene variants of the YFP reporter protein were synthesized, each varying in relative codon adaptation and/or the G+C content, cloned into a PSAD expression cassette (Fischer and Rochaix 2001) and separately transformed into two Chlamydomonas strains, the expression strain UVM11 and its progenitor, Elow47 (Neupert et al. 2009). Ten clones, each containing the respective complete expression cassette, were then randomly selected, and the relative YFP expression levels determined via RNA gel blot analysis, in-gel protein fluorescence imaging, and confocal laser-scanning microscopy. The results demonstrated that even with equal G+C content and varying numbers of vector integration events, a clear correlation of TG expression and relative codon usage could be observed. The authors concluded that not the G+C content per se but that optimum codon usage seems to be a key factor for efficient nuclear TG expression (Barahimipour et al. 2015, 2016).

Gene design for expression studies is common practice today and companies like *Thermo Fisher Scientific Inc.* or *GenScript USA Inc.* offer bioinformatic tools that generate gene variants optimized for several expression hosts. Since costs for gene syntheses have continuously been declining over the last decades, rational gene sequence design and codon adaptation will certainly lead to a rapid increase of the

number of foreign proteins efficiently expressed from the nuclear genome of *C. reinhardtii*.

3.6 Selectable Markers and Reporters

A very important aspect for genetic engineering is the development of suitable transformation markers and reporter genes, and continuing progress has been made since the first transformation trials were performed. Today, at least 23 nuclear transformation selection markers (Table 2) and 12 reporters based on color or light-emission (Table 3) are established for *C. reinhardtii*.

Since it is possible to generate numerous combinations of the established genetic elements, increasingly complex projects can be realized, further confirming the status of *C. reinhardtii* as a prime candidate for recombinant TG expression in microalgae.

3.7 Recombinant Protein Production and Targeting

As mentioned above, proteins can be produced from nuclear, chloroplast, and mitochondrial genomes, and a growing number of recombinant proteins with potential as high-value products are successfully expressed from the nuclear or chloroplast genomes [recently reviewed by Rasala and Mayfield (2015)]. In general, higher levels of total soluble target protein accumulation can be reached from chloroplast expression systems, with a typical range of between 1 and 10% of the total protein. Nuclear-encoded target proteins typically accumulate to lower levels of below 0.25% of the total protein (Rasala and Mayfield 2015); however, in contrast to the chloroplast expression systems, options are available to target the proteins to specific subcellular compartments or for secretion.

Targeting in general is dependent on the presence of specific signals, and software tools like TargetP (Emanuelsson et al. 2000) and PredAlgo, a software more suited for green algae (Tardif et al. 2012), have been developed for computer-based prediction of the subcellular localization of specific proteins in chloroplasts, mitochondria, or the secretory pathway.

Successful efforts to generate versatile vectors for recombinant protein targeting from the cytosol to variable subcellular destinations were described in two recent articles (Rasala et al. 2014; Lauersen et al. 2015) (see Table 4).

Nuclear localization could be reached by C-terminal addition of one copy or a tandem repeat of the seven amino acid (AA) SV40 large T-antigen nuclear localization signal. Targeting to chloroplast, mitochondria, or endoplasmic reticulum (ER) was achieved via addition of various N-terminal peptide sequences. Addition of the 37 N-terminal AA of the PSAD protein or the 45 AA of the RBCS1 protein led to import into the chloroplast, whereas addition of a 47 AA peptide derived from the ATPA gene resulted in targeting to the mitochondrial network (Lauersen et al. 2015;

Table 2 List of positive transformation markers applied for *C. reinhardtii* nuclear transformation experiments

Name	Organism, annotation	Activity	References
aadA	*Escherichia coli*, *pR538–1*, aminoglycoside adenyltransferase	Resistance to spectinomycin and streptomycin	Cerutti et al. (1997), Meslet-Cladiere and Vallon (2011)
AC29 (ALB3.1)	*C. reinhardtii*, ALBINO3.1	Complementation of yellow, acetate-requiring phenotype	Ferris (1995), Bellafiore et al. (2002)
ALS	*C. reinhardtii*, acetolactate synthase	Resistance to sulfometuron methyl and related sulfonylurea herbicides	Kovar et al. (2002)
aph 7″	*Streptomyces hygroscopicus*, aminoglycoside phosphotransferase	Resistance to hygromycin B	Berthold et al. (2002)
aphVIII	*Streptomyces rimosus*, aminoglycoside phosphotransferase	Resistance to paromomycin	Sizova et al. (1996, 2001)
ARG7	*C. reinhardtii*, argininosuccinate lyase	Complementation of arginine auxotrophy	Debuchy et al. (1989)
ARG9	*Arabidopsis thaliana*/*C. reinhardtii*, N-acetyl ornithine aminotransferase	Complementation of arginine auxotrophy	Remacle et al. (2009)
ATPC	*C. reinhardtii*, ATP synthase subunit	Restoration of photosynthetic competence	Smart and Selman (1993)
ble	*Streptoalloteichus hindustanus*, BLE (BRP) protein	Resistance to bleomycin, phleomycin and zeo(my)cin	Stevens et al. (1996), Lumbreras et al. (1998)
cat	Transposon *Tn9*, chloramphenicol acetyltransferase	Resistance to chloramphenicol	Tang et al. (1995)
CRY1	*C. reinhardtii*, ribosomal protein S14	Resistance to emetine and cryptopleurine	Nelson et al. (1994)
gat	Synthetic glyphosate acetyltransferase	Resistance to glyphosate	Bruggeman et al. (2014), Castle et al. (2004)
hpt	*E. coli*, hygromycin phosphotransferase	Resistance to hygromycin B	Butanaev (1994), Kumar et al. (2004)
NIC7	*C. reinhardtii*, quinolinate synthetase A	Complementation of nicotinamide auxotrophy	Ferris (1995), Ferris et al. (2002)
NIT1 (NIA1)	*C. reinhardtii*, nitrate reductase	Restoration of growth on nitrate	Fernandez et al. (1989), Kindle et al. (1989)
NIT2	*C. reinhardtii*, nitrogen metabolism transcription factor	Restoration of growth on nitrate	Schnell and Lefebvre (1993), Camargo et al. (2007)

(continued)

Table 2 (continued)

Name	Organism, annotation	Activity	References
nptII	Transposon *Tn5*, neomycin phosphotransferase	Resistance to kanamycin, G418, and paromomycin	Hall et al. (1993), An et al. (1985), Barahimipour et al. (2016)
OEE1	*C. reinhardtii*, oxygen-evolving enhancer protein 1	Restoration of photosynthetic competence	Mayfield and Kindle (1990)
PDS	*C. reinhardtii*, phytoene desaturase	Resistance to norflurazon	Bruggeman et al. (2014)
PPX (PPO)	*C. reinhardtii*, protoporphyrinogen oxidase	Resistance to oxyfluorfen	Bruggeman et al. (2014), Randolph-Anderson et al. (1998)
PSY	*C. reinhardtii*, phytoene synthase	Restoration of carotenoid-less phenotype	McCarthy et al. (2004)
TETX	*Enterobacteriaceae bacterium SL1*, tetracycline resistance protein	Resistance to tetracycline	Garcia-Echauri and Cardineau (2015)
THI10	*C. reinhardtii*, hydroxyethylthiazole kinase	Complementation of thiamine auxotrophy	Ferris (1995), Ferris et al. (2002)

Alternative names are indicated in brackets. Table modified from (Mussgnug 2015)

Table 3 List of reporters used for color or light-emission detection in *C. reinhardtii* nuclear transformation experiments

Name	Organism, annotation	Activity	References
ARS2	*C. reinhardtii*, arylsulfatase	Color reaction with, e.g., X-Sulf	Davies et al. (1992), de Hostos et al. (1989), Specht et al. (2014)
xyn1	*Trichoderma reesei*, xylanase 1	Fluorescence from, e.g., DiFMUX$_2$ substrate	Rasala et al. (2012)
BFP, CFP, GFP, OPF, RFP, YFP	*Entacmaea quadricolor (blue)*, *Aequorea victoria (cyan*, *green*, *yellow)*, *Discosoma sp. (orange, red)* fluorescent proteins	Blue, cyan, green, orange, red, or yellow fluorescence	Fuhrmann et al. (1999), Franklin et al. (2002), Rasala et al. (2013), Neupert et al. (2009), Lauersen et al. (2015)
GLUC RLUC LUCCP LUXCT	*Gaussia princeps*, luciferase *Renilla reniformis*, luciferase *Photinus pyralis*, luciferase *Vibrio harveyi*, luciferase	Chemiluminescence	Fuhrmann et al. (2004), Shao and Bock (2008), Ruecker et al. (2008), Minko et al. (1999), Matsuo et al. (2006), May field and Schultz (2004)

DiFMUX$_2$: 6,8-difluoro-4-methylumbelliferyl beta-D-xylobioside; X: 5-Bromo-4-chloro-3-indolyl. Table modified from (Mussgnug 2015)

Table 4 Options for subcellular targeting of recombinant protein as described by Rasala et al. 2014 (1) and Lauersen et al. 2015 (2)

Subcellular target location	Signal peptide origin	Signal peptide sequence	Signal peptide orientation	References
Nucleus	SV40 large T-antigen	*PKKKRKV*	C-terminal	1, 2
Chloroplast	PSAD	*MAVMMRTQAPAATRASSRVAVAARPAARRAVVVRAEA*	N-terminal	1, 2
Chloroplast	RBCS1	*MAAVIAKSSVSAAVARPARSSVRPMAALKPAVKAAPVAAPAQANQ*	N-terminal	2
Mitochondria	ATPA	*MRSQALSLARAGLLQLSSQTGASLEGGFALSKRAEQALIRASRAFAS*	N-terminal	1, 2
ER-secretion	ARS1	*MHARKMGALAVLAVACLAAVASVAHAADTK*	N-terminal	1
ER-secretion	BIP1	*MAQWKAAVLLLALACASYGFGVWAEEEKLGTVIG*	N-terminal	1
ER-secretion	CAH1	*MARTGALLLVALALAGCAQAC*	N-terminal	2
ER retention		*HDEL*	C-terminal	1
Peroxisomal microbodies	PTS1 (*Cucurbita sp.*)	*IHHPRELSRL*	C-terminal	2
Peroxisomal microbodies	PTS1 (*C. reinhardtii*)	*HIVTKTPSRM*	C-terminal	2
Peroxisomal microbodies	PTS1-like peptide	*SWRRSLI*	C-terminal	2

ER endoplasmic reticulum

Rasala et al. 2014). ER targeting was observed with three signal peptides, derived from the arylsulfatase ARS1 (30 AA), the BIP1 chaperon protein (34 AA), or the *C. reinhardtii* carbonic anhydrase CAH1 (21 AA), respectively. C-terminal addition of an ER retention signal (*HDEL*) was demonstrated to prevent secretion and retain the recombinant protein in the ER.

Five of the six enzymes associated with the glyoxylate cycle were recently shown to reside in peroxisomal microbodies (Lauersen et al. 2016), one of which being the malate synthase PTS1. C-terminal addition of the respective 10 AA signal peptides derived from the pumpkin or Chlamydomonas malate synthase, as well as a 7 AA PTS1-like peptide, resulted in successful targeting into these microstructures (Table 4).

It should be noted that the establishment of expression vectors facilitating controlled subcellular protein targeting is an important step in terms of nuclear tool development, because this will allow implementation of increasingly complex metabolic pathway engineering projects in *C. reinhardtii*.

4 Gene Expression Inhibition

The generation of mutants deficient in specific nuclear gene expression has been invaluable to study gene functions. In principle, random or targeted mutagenesis strategies can be applied, and variable mutagens and vector tools have been established for this purpose.

4.1 Random Mutation Strategies

Mutagenesis of the nuclear genome of *C. reinhardtii* can be induced via application of ionizing radiation, mutagenic chemicals, or by DNA insertion. Irrespective of the mutagen, the nuclear genome modifications occur at apparently random loci, however, notable mutagen-dependent characteristics of the resulting cell lines should be taken into account.

4.1.1 Mutagenesis Via Radiation or Chemicals

Treatment of Chlamydomonas with X-rays or UV irradiation dates back to the 1950s (Ebersold 1956; Nybom 1953), and the mutagenic effect is based on physically induced DNA damage, e.g., DNA breakage or lesions resulting from the formation of pyrimidine dimers. Incomplete repair of the DNA damage can then result in the appearance of aberrant, heritable mutant phenotypes.

Many chemicals have the potential to react with DNA and induce mutagenesis, and prominent agents applied for *C. reinhardtii* include methylnitronitrosoguanidine

(MNNG), methyl methanesulfonate (MMS), and ethylmethanesulfonate (EMS) (Harris 2009). These substances induce mutagenesis by DNA alkylation [here: addition of methyl or ethyl groups (Rhaese and Boetker 1973)], resulting in the occurrence of mismatched base pairs and potentially other forms of DNA damage.

Although the underlying mechanism that cause the DNA modifications differ, the resulting cell lines after physical or chemical mutagenesis show several common characteristics. A notable feature of mutagenesis by radiation or chemicals is that the resulting strains are not considered to be genetically modified organisms (GMO). This is important because strict regulations apply for GMOs in many countries, making outdoor or commercial applications difficult and cost-intensive. In addition, in contrast to insertional mutagenesis, both mutagenic strategies commonly result in locally confined DNA alterations and therefore can create gain-of-function or loss-of-function gene mutations (Dent et al. 2001). Other mutual features are that the individual DNA mutation event *per se* does not allow positive selection and that the subsequent determination of the mutation event number and the respective affected DNA region, if desired, pose substantial difficulties. Although several methods like, e.g., classical genetic mapping, *TILLING* [targeting induced local lesions in genomes (McCallum et al. 2000)], or even full-genome sequencing can be applied for this purpose, the implementation is technically challenging and labor-intensive (Dutcher et al. 2012; Schierenbeck et al. 2015; Harris 2009).

4.1.2 Insertional Mutagenesis

As mentioned in Sect. 2, foreign DNA molecules integrate at apparently random nuclear loci, irrespective of the method applied for DNA transformation. Insertional mutagenesis offers notable advantages compared to mutagenesis by chemicals or irradiation. Most importantly, identification of the nuclear insertion sites is rather easy because knowledge of the introduced DNA sequence allows application of several PCR-based methods aiming for amplification of the flanking nuclear region (Galvan et al. 2007; Strauss et al. 2001; Zhang et al. 2014), therefore facilitating functional genomic approaches (Dent et al. 2005, 2015; Li et al. 2016).

The insertion events are of rather uncontrolled nature, as vividly evidenced by the fact that large nuclear deletions in the range of 50 kb can occur, fragments of the transgene construct can be lost or rearranged during the procedure, and multiple plasmid insertions are observed on a regular basis (Harris 2009; Gumpel and Purton 1994). Recent high-throughput genotyping studies showed that uncontrolled DNA digestion and ligation events can take place, which are probably caused by enzymes from lysed cells (Zhang et al. 2014; Li et al. 2016). Although it is quite easy to determine the number of plasmid DNA insertions via DNA gel blot analyses after transformation, confirmation of cosegregation of marker and phenotype by crossing experiments is an important step for functional genomics approaches. Dent et al. (2005) isolated random plasmid insertion mutants with photosynthesis-related phenotypes after biolistic particle bombardment and sequenced the flanking DNA

Table 5 Notable features of nuclear random mutation strategies

Mutagenesis via irradiation or chemicals	Mutagenesis via DNA insertion
Considered non-GMO	Considered GMO
Can be applied to create loss-of-function and gain-of-function mutations	Not well suited to create gain-of-function mutations
Mutation event does not *per se* create a positive selection marker	Usage of appropriate markers allows direct selection for positive transformants
Determination of the number of mutation events can be difficult	Determination of the number of DNA insertions is comparably easy, but untagged mutants regularly occur
Localization of the altered DNA region responsible for a mutant phenotype is difficult	Identification of the nuclear regions flanking the DNA insertion site is comparably easy

regions via TAIL-PCR. Sequence data could be determined for 50 mutants; however, backcrossing of 17 of these mutants revealed that only ~50% showed molecular marker and phenotype cosegregation (Dent et al. 2005), thus demonstrating that half of the cell lines represented untagged mutants. A related but larger-scale study was published recently. Here, glass bead transformation was performed to generate a collection of ~49,000 mutants. After prescreening for photosynthesis-related phenotypes, 459 flanking DNA sequences derived from 439 mutants could be isolated. Interestingly, cosegregation of 17 out of 20 mutants was reported in this study, corresponding to 85% (Dent et al. 2015).

It is not possible to draw a general conclusion regarding a typical ratio of cosegregation at this point, because the overall number of cell lines analyzed still is comparably low, and it is very likely that the ratio can depend on several experimental parameters. The fact, however, that untagged mutants are found quite often is a clear indication that an unknown number of background mutation events can take place during DNA insertional mutagenesis, potentially triggered by the transformation procedure or by spontaneous events. Since the overall mutation event number can therefore apparently be significantly higher than the number of DNA plasmid insertions determined by concomitant DNA gel blot analyses, assignment of specific gene functions will generally require further experiments, e.g., functional complementation.

Since small or large deletions often occur at the insertion site (Dent et al. 2015), insertional mutagenesis is not well suited to generate gain-of-function mutants, and the presence of foreign DNA classifies the mutants as GMO.

Some key considerations discussed in this paragraph are summarized in Table 5.

4.2 Targeted Mutation Strategies

Two general options are currently available if reduction of the expression of a specific nuclear Chlamydomonas gene is desired: (a) RNA-dependent gene silencing or (b) direct gene disruption via DNA insertion, homologous recombination, or

directed endonuclease activity. Since two recently published review articles describe this topic in greater detail (Jinkerson and Jonikas 2015; Mussgnug 2015), a compact summary will be provided here.

4.2.1 RNA-Dependent Gene Silencing

Gene-silencing strategies based on expression of antisense RNA (Schroda et al. 1999), inverted repeats (Fuhrmann et al. 2001), and micro-RNAs (miRNAs) (Hu et al. 2014; Molnar et al. 2009; Zhao et al. 2009) have all been successfully applied in *C. reinhardtii*, and even a few customizable vectors for this purpose were developed (see Sect. 5 for two examples). Furthermore, conditional gene silencing has been achieved by incorporation of inducible silencing construct (Schmollinger et al. 2010; Koblenz and Lechtreck 2005). This can be advantageous compared to knockout strategies, because the silencing effect can be temporarily induced, and the subsequent alleviation of gene repression can prevent long-term cellular adaptation reactions. A notable characteristic of gene-silencing strategies is that the silencing is often incomplete (Schroda 2006). This might in some cases be an advantage, e.g., in case essential genes are investigated; however, residual gene expression can substantially complicate unambiguous phenotype assignments. The stability of gene silencing can also be an issue, and loss of the silencing phenotype has often been observed (Schroda 2006). Therefore, for several research tasks, generation of stable knockout cell lines by direct gene disruption is a desired alternative.

4.2.2 Direct Gene Disruption

Homologous recombination is a principle option to delete specific genes, and Zorin et al. (2005) applied a method based on the use of single-stranded DNA to the nuclear genome of *C. reinhardtii*. The authors succeeded in increasing the ratio of site-specific vs. random integration events and successfully isolated two mutants of the PHOT gene. Identification of specific deletion mutants with this method, however, appears to be quite challenging since only very few successful examples were reported since then (Zorin et al. 2005, 2009).

Site-specific endonucleases have been used to create mutants of many pro- and eukaryotes, and the three main strategies have been approached for Chlamydomonas: zinc-finger nucleases (ZFNs), transcription activator-like effector nucleases (TALENs), and clustered regularly interspaced short palindromic repeats (CRISPR)/CRISPR-associated (Cas) system. A ZFN approach was successfully performed by Sizova et al. (2013), who used this method to knockout the COP3 gene (Sizova et al. 2013). TALE proteins were applied successfully to activate endogenous gene expression (Gao et al. 2014, 2015); however, FokI nuclease domain coupling for targeted gene knockout was not yet demonstrated.

The first trials to introduce the CRISPR/Cas9 system for *C. reinhardtii* were published by Jiang et al. (2014), and it was shown that the system is functional, but lack of surviving transformants indicated possible toxicity issues (Jiang et al. 2014). Work of Greiner (Humboldt University Berlin), however, provided evidence that expression of a Cas9-YFP fusion protein in *C. reinhardtii* was possible, and specific Cas9 nuclease activity was detectable (Greiner 2014). Very recently, Shin et al. (2016) demonstrated the successful generation of knockout and knock-in mutants via direct intracellular delivery of commercially manufactured, specific sgRNA/Cas9 ribonucleoproteins (RNPs) by electroporation (Shin et al. 2016). As a proof of concept, the authors independently targeted the loci of MAA7, CpSRP43, and ChlM, with the idea that knockout of these targets would lead to easily detectable phenotypes. Indeed, mutants of all three target loci could be isolated; however, currently unknown events led to curious in-frame indel patterns, or when co-transformation was performed to enhance RNP delivery, unexpected DNA vector insertions at the Cas9 cut sites (Shin et al. 2016). In a similar approach, Baek and colleagues used CRISPR-Cas ribonucleoproteins to generate a two-gene knockout cell line that constitutively produced the pigment zeaxanthin (Baek et al. 2016). Despite this proof of principle, a versatile CRISPR-Cas-based DNA tool is not yet available for Chlamydomonas. The range of microalgal species accessible via CRISPR-Cas-based methods, however, is rapidly expanding and already includes the oleaginous species *Nannochloropsis oceanica* (Wang et al. 2016) and the marine diatom *Phaeodactylum tricornutum* (Nymark et al. 2016).

An alternative strategy to obtain knockout cell lines for a specific gene is the generation of large-scale random DNA insertion mutant collections and subsequent identification of the cell line affected in expression of the gene of interest. This strategy has been applied with notable success. Gonzales-Ballester and colleagues (2011) created two large-scale mutant collections with a total of ~122,000 cell lines by insertional mutagenesis of the AphVIII marker gene, conferring resistance to the antibiotic paromomycin. Systematic DNA superpools from these mutants were generated, which allowed subsequent PCR-based screenings and identification of individual cell lines with specifically affected target regions (Gonzalez-Ballester et al. 2011).

Zhang et al. (2014) introduced a promising new method designated *ChlaMmeSeq* (*Chlamydomonas MmeI-based insertion site sequencing*) and showed that this method can be applied to simultaneously map thousands of insertion sites in pooled mutant cell lines. The technique is based on the extraordinary characteristics of the *Mme*I restriction enzyme, which can be exploited for the high-throughput identification of 20–21 bp flanking genomic DNA sequence tags (Zhang et al. 2014). The procedure recently was applied as part of an advanced mapping approach in a CC-4533 cell line background. Despite notable difficulties based on cassette truncations and interfering DNA rearrangements resulting in no or misleading flanking site identifications, an initial indexed library of 1935 mutants (representing 1562 genes) could successfully be established (Li et al. 2016). Since then, the total number of mutants of this library has been increased to ~37,000

(as of April 2016), and access is possible via the website https://www.chlamylibrary.org/.

It should be noted that generation and maintenance of large-scale Chlamydomonas mutant collections is still very labor-intensive, and in case the generation of a knockout cell line within a specific cellular background is aimed for, de novo setup of such a strategy is not a practical option for many laboratories.

As a conclusion, a major current limitation of Chlamydomonas genetic engineering remains the absence of an efficient and easily adaptable tool to generate a specific nuclear knockout mutation in a distinct Chlamydomonas cell line.

5 Customizable Vectors and Expression Strain

5.1 Selected Vectors for Diverse Practical Applications

The construction or modification of DNA plasmid vectors is a routine procedure in genetic engineering projects. The number of vectors comprising one or more of the elements listed in Tables 1, 2, and 3 has been growing very fast, and it is beyond the scope of this article to present a comprehensive overview of these plasmids. It should be noted that most of the vectors were applied for a specific purpose within a research project, and only a limited number has been designed for versatile, customizable applications. The following selected examples, all being available at the *Chlamydomonas Resource Center*, represent versatile vectors that are applicable for diverse nuclear genetic engineering tasks, ranging from tagged recombinant protein expression to inducible gene silencing.

5.1.1 pGenD

The *pGenD* vector was introduced by Fischer and Rochaix (2001) as a versatile nuclear gene expression vector. The expression cassette is based on the intron-free *PsaD* gene and comprises 822 bp of the *PsaD* 5′ upstream region, 591 bp coding region, and 624 bp of the 3′ downstream region (Fischer and Rochaix 2001). Versatility of the vector was reached by introducing the unique *Nde*I and *Eco*RI restriction sites into the expression cassette, allowing fast and easy replacement of the coding sequence. The same regulatory elements were used for the derived pJR38/39 expression vectors (Neupert et al. 2009).

5.1.2 Maa7/X IR (NE-537)

This construct was created by Rohr et al. (2004) and can be used for target gene silencing via RNA interference (RNAi). The expression cassette is controlled by the

RBCS2 promoter and the 35S terminator and comprises an inverted repeat derived from the endogenous MAA7 3′UTR. The inverted repeat region is separated by a DNA spacer which can easily be replaced by a target sequence via DNA restriction (*Eco*RI) and insert ligation. The target insert must comprise an inverted repeat sequence derived from the target gene and should be separated by a DNA spacer. The final silencing cassette therefore is constructed to allow the formation of a double-stranded RNA hairpin-loop structure that triggers co-silencing of the endogenous MAA7 and the specific target gene. MAA7 encodes the Chlamydomonas tryptophan synthase ß subunit, and silencing of this gene confers resistance to 5-fluoroindole, since the enzymatic conversion into the toxic 5-fluorotryptophan is prevented (Rohr et al. 2004). This allows direct selection for cell lines which show efficiently co-silenced marker and target genes, even facilitating the identification of cell lines with efficiently silenced gene families (Mussgnug et al. 2007).

5.1.3 pProm-Chlamy (pHsp70A/RbcS2-Chlamy)

Although it is possible to introduce a nonselectable gene present on one vector by co-transformation with a selectable marker present on a second vector, efficiency strongly increases if both cassettes are present on the same plasmid. Heitzer and Zschoernig (2007) introduced a strategy for construction of Chlamydomonas tandem expression vectors utilizing in vitro plasmid fusion via *Cre*/*loxP* recombination. The *pProm-Chlamy* vectors furthermore were designed to contain unique restriction sites to allow modular replacement of promoter, coding region, and 3′UTR (Heitzer and Zschoernig 2007).

5.1.4 pChlamiRNA1–3

Molnar et al. (2009) developed a versatile plasmid vector system for miRNA-mediated gene silencing. The *pChlamiRNA* vectors are based expression of the miRNA *cre-MIR1157*, and the most versatile versions allow easy targeting of specific genes of interest. The authors provide detailed instructions for vector customization as supporting information, including target site identification (Ossowski et al. 2008), amiRNA design and respective DNA oligonucleotide preparation, and vector assembly (Molnar et al. 2009). This tool was further modified by Schmollinger et al. (2010) to include the inducible NIT1 promoter, thus allowing conditional amiRNA expression, a strategy successfully applied before for an inverted repeat RNAi gene-silencing construct (Schmollinger et al. 2010; Koblenz and Lechtreck 2005).

5.1.5 pOptimized (pOpt)

The *pOpt* plasmid toolkit for recombinant protein synthesis was designed *in silico* and constructed in a strictly modular fashion (Lauersen et al. 2015). The vector system is based on two tandem expression cassettes, one destined for the selection marker and the other for the recombinant protein, which can furthermore be customized by tagging and modified for subcellular targeting. The inclusion of unique restriction sites for each of the modules prior to de novo DNA synthesis of the vector and the exchangeable elements allows highly flexible and simple adaptation of both expression cassettes. The initial version of the *pOpt* toolkit comprised two selectable transformation markers, five reporter tagging, and six subcellular localization options. Because of the modular design, it can easily be expanded by additional modules.

5.2 Cell Lines Promoting Nuclear Transgene Expression

Recombinant TG expression from the nuclear *C. reinhardtii* genome has proven to be difficult in many cases. One approach to overcome this problem is the development of cell lines with improved expression characteristics, and Neupert et al. (2009) successfully devised a sophisticated genetic screen for this purpose. Briefly, co-transformation of an arginine auxotroph cell line (cw15-302) was performed with two plasmids, one restoring arginine prototrophy and the other conferring resistance to the antibiotic emetine. A cell line was then selected which could tolerate low emetine concentrations (5–25 μg ml^{-1}) but died when exposed to elevated antibiotic levels. This cell line, designated Elow47, was then exposed to UV radiation and the resulting mutants screened on high emetine concentrations (60 μg ml^{-1}), with the idea to select cell lines where initial transcriptional repression was alleviated. Indeed, two cell lines, designated UVM4 and UVM11, could be isolated that efficiently expressed foreign transgenes (Neupert et al. 2009; Barahimipour et al. 2015, 2016; Lauersen et al. 2013). In addition to the UVM strains, improved TG expression was recently also shown for an insertional mutant of the putative maintenance-type DNA cytosine methyltransferase MET1 (Kong et al. 2015), which therefore represents an interesting alternative.

6 Concluding Remarks and Future Perspectives

As outlined in this article, nuclear mutagenesis of *C. reinhardtii* is a routine procedure today, and screening of mutant collections comprising many thousands of cell lines has been successfully performed (Terashima et al. 2015; Gonzalez-Ballester et al. 2011; Zhang et al. 2014; Dent et al. 2015; Li et al. 2016). It can be expected that ongoing and future large-scale approaches will lead to the isolation of further defined mutants invaluable for the elucidation of currently unknown cellular processes and regulatory

networks. Conservation of such large cell line collections, however, is still technically challenging, despite recent progress in developing high-throughput procedures for cell line propagation and cryopreservation (Li et al. 2016). Furthermore, as long as a knockout mutant is not available for a desired cell line, the lack of an efficient tool applicable for generation of targeted nuclear knockout strains or site-specific genome editing still represents a major drawback.

The utilization of the bacterial CRISPR/Cas system has been a major technological breakthrough in the field of genetic engineering for many pro- and eukaryotes. Unfortunately, adaptation of the original method comprising the Cas9 enzyme from *Streptococcus pyogenes* (SpCas9) (Jinek et al. 2012) to Chlamydomonas seems to be rather difficult. Due to the impressively fast progress in this research field, including the generation of rationally engineered SpCas9 variants (Slaymaker et al. 2016; Kleinstiver et al. 2016) and identification of alternative nucleases like the Cas9 homologue from *Staphylococcus aureus* (SaCas9) (Ran et al. 2015) or the programmable Cpf1 endonucleases from *Acidaminococcus sp. BV3L6* and *Lachnospiraceae bacterium ND2006* (Zetsche et al. 2015), it seems likely that establishment of such a versatile editing tool for Chlamydomonas—a major goal for decades—will eventually be achieved in the near future.

Metabolic pathway engineering of *C. reinhardtii*, especially when several engineering steps or multiple cellular compartments are involved, is still very much in its infancy. The emerging efforts to create modular and more versatile genetic tools, combined with novel options for TG expression modification, e.g., via riboswitches, enhancer elements, or 2A peptide sequences, have opened the doors to tackle increasingly sophisticated engineering tasks. In this context, the further development and community-wide implementation of standardized procedures, from cell cultivation to cloning methods like, e.g., *Golden Gate* assembly (Engler et al. 2008, 2014), would be advisable.

Given that *C. reinhardtii* combines several features common to plants, bacteria, and yeast, the establishment of *C. reinhardtii* as an industrial biotechnology platform by implementing synthetic biology and modular DNA device strategies (Scaife et al. 2015) represents a logical next step to advance fundamental and applied microalgal research.

Acknowledgments I thank Dr. Lutz Wobbe for critical comments on the manuscript and the German state North Rhine-Westphalia for funding.

Conflict of Interest I declare no conflict of interest.

References

An G, Watson BD, Stachel S, Gordon MP, Nester EW (1985) New cloning vehicles for transformation of higher plants. EMBO J 4(2):277–284

Baba M, Hanawa Y, Suzuki I, Shiraiwa Y (2011) Regulation of the expression of H43/Fea1 by multi-signals. Photosynth Res 109(1–3):169–177

Baek K, Kim DH, Jeong J, Sim SJ, Melis A, Kim JS, Jin E, Bae S (2016) DNA-free two-gene knockout in Chlamydomonas reinhardtii via CRISPR-Cas9 ribonucleoproteins. Sci Rep 6:30620

Barahimipour R, Strenkert D, Neupert J, Schroda M, Merchant SS, Bock R (2015) Dissecting the contributions of GC content and codon usage to gene expression in the model alga Chlamydomonas reinhardtii. Plant J. doi:10.1111/tpj.13033

Barahimipour R, Neupert J, Bock R (2016) Efficient expression of nuclear transgenes in the green alga Chlamydomonas: synthesis of an HIV antigen and development of a new selectable marker. Plant Mol Biol. doi:10.1007/s11103-015-0425-8

Bell SA, Shen C, Brown A, Hunt AG (2016) Experimental genome-wide determination of RNA polyadenylation in Chlamydomonas reinhardtii. PLoS One 11(1):e0146107. doi:10.1371/journal.pone.0146107

Bellafiore S, Ferris P, Naver H, Gohre V, Rochiax JD (2002) Loss of Albino3 leads to the specific depletion of the light-harvesting system. Plant Cell 14(9):2303–2314

Berger H, Blifernez-Klassen O, Ballottari M, Bassi R, Wobbe L, Kruse O (2014) Integration of carbon assimilation modes with photosynthetic light capture in the green alga Chlamydomonas reinhardtii. Mol Plant 7(10):1545–1559

Berthold P, Schmitt R, Mages W (2002) An engineered Streptomyces hygroscopicus aph 7″ gene mediates dominant resistance against hygromycin B in Chlamydomonas reinhardtii. Protist 153(4):401–412

Blankenship JE, Kindle KL (1992) Expression of chimeric genes by the light-regulated cabII-1 promoter in Chlamydomonas reinhardtii: a cabII-1/nit1 gene functions as a dominant selectable marker in a nit1- nit2-strain. Mol Cell Biol 12(11):5268–5279

Blowers AD, Bogorad L, Shark KB, Sanford JC (1989) Studies on Chlamydomonas chloroplast transformation: foreign DNA can be stably maintained in the chromosome. Plant Cell 1 (1):123–132

Boynton JE, Gillham NW, Harris EH, Hosler JP, Johnson AM, Jones AR, Randolph-Anderson BL, Robertson D, Klein TM, Shark KB, Sanford JC (1988) Chloroplast transformation in Chlamydomonas with high velocity microprojectiles. Science 240(4858):1534–1538

Brown LE, Sprecher SL, Keller LR (1991) Introduction of exogenous DNA into Chlamydomonas reinhardtii by electroporation. Mol Cell Biol 11(4):2328–2332

Bruggeman AJ, Kuehler D, Weeks DP (2014) Evaluation of three herbicide resistance genes for use in genetic transformations and for potential crop protection in algae production. Plant Biotechnol J 12(7):894–902

Brunke KJ, Anthony JG, Sternberg EJ, Weeks DP (1984) Repeated consensus sequence and pseudopromoters in the four coordinately regulated tubulin genes of Chlamydomonas reinhardi. Mol Cell Biol 4(6):1115–1124

Butanaev AM (1994) Use of the hygromycin phosphotransferase gene as the dominant selective marker for Chlamydomonas reinhardtii transformation. Mol Biol 28(5):1061–1068

Camargo A, Llamas A, Schnell RA, Higuera JJ, Gonzalez-Ballester D, Lefebvre PA, Fernandez E, Galvan A (2007) Nitrate signaling by the regulatory gene NIT2 in Chlamydomonas. Plant Cell 19(11):3491–3503

Castle LA, Siehl DL, Gorton R, Patten PA, Chen YH, Bertain S, Cho HJ, Duck N, Wong J, Liu DL, Lassner MW (2004) Discovery and directed evolution of a glyphosate tolerance gene. Science 304(5674):1151–1154

Cerutti H, Johnson AM, Gillham NW, Boynton JE (1997) A eubacterial gene conferring spectinomycin resistance on Chlamydomonas reinhardtii: integration into the nuclear genome and gene expression. Genetics 145(1):97–110

Croft MT, Lawrence AD, Raux-Deery E, Warren MJ, Smith AG (2005) Algae acquire vitamin B12 through a symbiotic relationship with bacteria. Nature 438(7064):90–93

Croft MT, Moulin M, Webb ME, Smith AG (2007) Thiamine biosynthesis in algae is regulated by riboswitches. Proc Natl Acad Sci USA 104(52):20770–20775

Davies JP, Weeks DP, Grossman AR (1992) Expression of the arylsulfatase gene from the beta-2-tubulin promoter in Chlamydomonas reinhardtii. Nucleic Acids Res 20(12):2959–2965
Davis IW, Benninger C, Benfey PN, Elich T (2012) POWRS: position-sensitive motif discovery. PLoS One 7(7):e40373
Day A, Debuchy R, Vandillewijn J, Purton S, Rochaix JD (1990) Studies on the maintenance and expression of cloned DNA fragments in the nuclear genome of the green alga Chlamydomonas reinhardtii. Physiol Plant 78(2):254–260
de Hostos EL, Schilling J, Grossman AR (1989) Structure and expression of the gene encoding the periplasmic arylsulfatase of Chlamydomonas reinhardtii. Mol Gen Genet 218(2):229–239
Debuchy R, Purton S, Rochaix JD (1989) The argininosuccinate lyase gene of Chlamydomonas reinhardtii: an important tool for nuclear transformation and for correlating the genetic and molecular maps of the ARG7 locus. EMBO J 8(10):2803–2809
Deng XD, Yang JH, Wu XX, Li YJ, Fei XW (2014) A C2H2 zinc finger protein FEMU2 is required for fox1 expression in Chlamydomonas reinhardtii. PLoS One 9(12). doi:10.1371/journal.pone.0112977
Dent RM, Han M, Niyogi KK (2001) Functional genomics of plant photosynthesis in the fast lane using Chlamydomonas reinhardtii. Trends Plant Sci 6(8):364–371
Dent RM, Haglund CM, Chin BL, Kobayashi MC, Niyogi KK (2005) Functional genomics of eukaryotic photosynthesis using insertional mutagenesis of Chlamydomonas reinhardtii. Plant Physiol 137(2):545–556
Dent RM, Sharifi MN, Malnoe A, Haglund C, Calderon RH, Wakao S, Niyogi KK (2015) Large-scale insertional mutagenesis of Chlamydomonas supports phylogenomic functional prediction of photosynthetic genes and analysis of classical acetate-requiring mutants. Plant J. doi:10.1111/tpj.12806
Diaz-Santos E, de la Vega M, Vila M, Vigara J, Leon R (2013) Efficiency of different heterologous promoters in the unicellular microalga Chlamydomonas reinhardtii. Biotechnol Prog 29 (2):319–328
Ding J, Li XM, Hu HY (2012) Systematic prediction of cis-regulatory elements in the Chlamydomonas reinhardtii genome using comparative genomics. Plant Physiol 160(2):613–623
Dunahay TG (1993) Transformation of Chlamydomonas reinhardtii with silicon-carbide whiskers. BioTechniques 15(3):452–460
Dutcher SK, Li L, Lin H, Meyer L, Giddings TH Jr, Kwan AL, Lewis BL (2012) Whole-genome sequencing to identify mutants and polymorphisms in Chlamydomonas reinhardtii. G3 Genes Genomes Genetics 2(1):15–22
Ebersold WT (1956) Crossing over in Chlamydomonas reinhardi. Am J Bot 43(6):408–410
Eichler-Stahlberg A, Weisheit W, Ruecker O, Heitzer M (2009) Strategies to facilitate transgene expression in Chlamydomonas reinhardtii. Planta 229(4):873–883
Emanuelsson O, Nielsen H, Brunak S, von Heijne G (2000) Predicting subcellular localization of proteins based on their N-terminal amino acid sequence. J Mol Biol 300(4):1005–1016
Engler C, Kandzia R, Marillonnet S (2008) A one pot, one step, precision cloning method with high throughput capability. PLoS One 3(11):e3647
Engler C, Youles M, Gruetzner R, Ehnert TM, Werner S, Jones JD, Patron NJ, Marillonnet S (2014) A golden gate modular cloning toolbox for plants. ACS Synth Biol 3(11):839–843
Fei XW, Deng XD (2007) A novel Fe deficiency-responsive element (FeRE) regulates the expression of atx1 in Chlamydomonas reinhardtii. Plant Cell Physiol 48(10):1496–1503
Fei XW, Eriksson M, Yang JH, Deng XD (2009) An Fe deficiency responsive element with a core sequence of TGGCA regulates the expression of FEA1 in Chlamydomonas reinhardtii. J Biochem 146(2):157–166
Fei XW, Eriksson M, Li YJ, Deng XD (2010) A novel negative Fe-deficiency-responsive element and a TGGCA-type-like FeRE control the expression of FTR1 in Chlamydomonas reinhardtii. J Biomed Biotechnol. doi:10.1155/2010/790247
Fernandez E, Schnell R, Ranum LPW, Hussey SC, Silflow CD, Lefebvre PA (1989) Isolation and characterization of the nitrate reductase structural gene of Chlamydomonas reinhardtii. Proc Natl Acad Sci USA 86(17):6449–6453

Ferrante P, Diener DR, Rosenbaum JL, Giuliano G (2011) Nickel and low CO_2-controlled motility in Chlamydomonas through complementation of a paralyzed flagella mutant with chemically regulated promoters. BMC Plant Biol 11. doi:10.1186/1471-2229-11-22

Ferris PJ (1995) Localization of the nic-7, ac-29 and thi-10 genes within the mating-type locus of Chlamydomonas reinhardtii. Genetics 141(2):543–549

Ferris PJ, Armbrust EV, Goodenough UW (2002) Genetic structure of the mating-type locus of Chlamydomonas reinhardtii. Genetics 160(1):181–200

Fischer N, Rochaix JD (2001) The flanking regions of PsaD drive efficient gene expression in the nucleus of the green alga Chlamydomonas reinhardtii. Mol Gen Genomics 265(5):888–894

Franklin S, Ngo B, Efuet E, Mayfield SP (2002) Development of a GFP reporter gene for Chlamydomonas reinhardtii chloroplast. Plant J 30(6):733–744

Fuhrmann M, Oertel W, Hegemann P (1999) A synthetic gene coding for the green fluorescent protein (GFP) is a versatile reporter in Chlamydomonas reinhardtii. Plant J 19(3):353–361

Fuhrmann M, Stahlberg A, Govorunova E, Rank S, Hegemann P (2001) The abundant retinal protein of the Chlamydomonas eye is not the photoreceptor for phototaxis and photophobic responses. J Cell Sci 114(21):3857–3863

Fuhrmann M, Hausherr A, Ferbitz L, Schodl T, Heitzer M, Hegemann P (2004) Monitoring dynamic expression of nuclear genes in Chlamydomonas reinhardtii by using a synthetic luciferase reporter gene. Plant Mol Biol 55(6):869–881

Galvan A, Gonzalez-Ballester D, Fernandez E (2007) Insertional mutagenesis as a tool to study genes/functions in Chlamydomonas. In: Leon R, Galvan A, Fernandez E (eds) Transgenic microalgae as green cell factories, vol 616. Landes Bioscience, pp 77–89

Gao H, Wright DA, Li T, Wang YJ, Horken K, Weeks DP, Yang B, Spalding MH (2014) TALE activation of endogenous genes in Chlamydomonas reinhardtii. Algal Res 5:52–60

Gao H, Wang Y, Fei X, Wright DA, Spalding MH (2015) Expression activation and functional analysis of HLA3, a putative inorganic carbon transporter in Chlamydomonas reinhardtii. Plant J. doi:10.1111/tpj.12788

Garcia-Echauri SA, Cardineau GA (2015) TETX: a novel nuclear selection marker for Chlamydomonas reinhardtii transformation. Plant Methods 11:27

Goldschmidt-Clermont M, Rahire M (1986) Sequence, evolution and differential expression of the two genes encoding variant small subunits of ribulose bisphosphate carboxylase/oxygenase in Chlamydomonas reinhardtii. J Mol Biol 191(3):421–432

Gonzalez-Ballester D, Pootakham W, Mus F, Yang W, Catalanotti C, Magneschi L, de Montaigu A, Higuera JJ, Prior M, Galvan A, Fernandez E, Grossman AR (2011) Reverse genetics in Chlamydomonas: a platform for isolating insertional mutants. Plant Methods 7:24

Greiner A (2014) CRISPR/Cas9 und Zinkfinger-Nukleasen für die gezielte Genstilllegung in Chlamydomonas reinhardtii. Dissertation, Humboldt University Berlin, Berlin

Grewe S, Ballottari M, Alcocer M, D'Andrea C, Blifernez-Klassen O, Hankamer B, Mussgnug JH, Bassi R, Kruse O (2014) Light-harvesting complex protein LHCBM9 is critical for photosystem II activity and hydrogen production in Chlamydomonas reinhardtii. Plant Cell 26(4):1598–1611

Guilley H, Dudley RK, Jonard G, Balazs E, Richards KE (1982) Transcription of Cauliflower mosaic virus DNA: detection of promoter sequences, and characterization of transcripts. Cell 30(3):763–773

Gumpel NJ, Purton S (1994) Playing tag with Chlamydomonas. Trends Cell Biol 4(8):299–301

Gumpel NJ, Rochaix JD, Purton S (1994) Studies on homologous recombination in the green alga Chlamydomonas reinhardtii. Curr Genet 26(5–6):438–442

Hahn D, Kück U (1999) Identification of DNA sequences controlling light- and chloroplast-dependent expression of the lhcb1 gene from Chlamydomonas reinhardtii. Curr Genet 34(6):459–466

Hall LM, Taylor KB, Jones DD (1993) Expression of a foreign gene in Chlamydomonas reinhardtii. Gene 124(1):75–81

Hallmann A, Wodniok S (2006) Swapped green algal promoters: aphVIII-based gene constructs with Chlamydomonas flanking sequences work as dominant selectable markers in Volvox and vice versa. Plant Cell Rep 25(6):582–591

Harris EH (2009) The Chlamydomonas sourcebook: introduction to Chlamydomonas and its laboratory use, 2nd edn. Academic Press, Oxford

Hasnain SE, Manavathu EK, Leung WC (1985) DNA-mediated transformation of Chlamydomonas reinhardtii cells: use of aminoglycoside 3′-phosphotransferase as a selectable marker. Mol Cell Biol 5(12):3647–3650

Hayashi M, Hirono M, Kamiya R (2001) Recovery of flagellar dynein function in a Chlamydomonas actin/dynein-deficient mutant upon introduction of muscle actin by electroporation. Cell Motil Cytoskeleton 49(3):146–153

Heitzer M, Zschoernig B (2007) Construction of modular tandem expression vectors for the green alga Chlamydomonas reinhardtii using the Cre/lox-system. BioTechniques 43(3):324–332

Heitzer M, Eckert A, Fuhrmann M, Griesbeck C (2007) Influence of codon bias on the expression of foreign genes in microalgae. In: Leon R, Galvan A, Fernandez E (eds) Transgenic microalgae as green cell factories, vol 616. Landes Bioscience, pp 46–53

Helliwell KE, Scaife MA, Sasso S, Araujo AP, Purton S, Smith AG (2014) Unraveling vitamin B12-responsive gene regulation in algae. Plant Physiol 165(1):388–397

Hennig S, van de Linde S, Lummer M, Simonis M, Huser T, Sauer M (2015) Instant live-cell super-resolution imaging of cellular structures by nanoinjection of fluorescent probes. Nano Lett 15(2):1374–1381

Hu JL, Deng X, Shao N, Wang GH, Huang KY (2014) Rapid construction and screening of artificial microRNA systems in Chlamydomonas reinhardtii. Plant J 79(6):1052–1064

Iwai M, Ikeda K, Shimojima M, Ohta H (2014) Enhancement of extraplastidic oil synthesis in Chlamydomonas reinhardtii using a type-2 diacylglycerol acyltransferase with a phosphorus starvation-inducible promoter. Plant Biotechnol J 12(6):808–819

Jiang WZ, Brueggeman AJ, Horken KM, Plucinak TM, Weeks DP (2014) Successful transient expression of Cas9 and single guide RNA genes in Chlamydomonas reinhardtii. Eukaryot Cell 13(11):1465–1469

Jinek M, Chylinski K, Fonfara I, Hauer M, Doudna JA, Charpentier E (2012) A programmable dual-RNA-guided DNA endonuclease in adaptive bacterial immunity. Science 337(6096):816–821

Jinkerson RE, Jonikas MC (2015) Molecular techniques to interrogate and edit the Chlamydomonas nuclear genome. Plant J. doi:10.1111/tpj.12801

Joint Genome Institute (2015) Phytozome v10.1, Chlamydomonas reinhardtii v5.5, US Department of Energy. http://phytozome.jgi.doe.gov.

Kindle KL (1990) High-frequency nuclear transformation of Chlamydomonas reinhardtii. Proc Natl Acad Sci USA 87(3):1228–1232

Kindle KL, Schnell RA, Fernandez E, Lefebvre PA (1989) Stable nuclear transformation of Chlamydomonas using the Chlamydomonas gene for nitrate reductase. J Cell Biol 109 (6):2589–2601

Klein TM, Wolf ED, Wu R, Sanford JC (1987) High-velocity microprojectiles for delivering nucleic-acids into living cells. Nature 327(6117):70–73

Kleinstiver BP, Pattanayak V, Prew MS, Tsai SQ, Nguyen NT, Zheng Z, Joung JK (2016) High-fidelity CRISPR-Cas9 nucleases with no detectable genome-wide off-target effects. Nature

Koblenz B, Lechtreck KF (2005) The NIT1 promoter allows inducible and reversible silencing of centrin in Chlamydomonas reinhardtii. Eukaryot Cell 4(11):1959–1962

Kong F, Yamasaki T, Kurniasih SD, Hou L, Li X, Ivanova N, Okada S, Ohama T (2015) Robust expression of heterologous genes by selection marker fusion system in improved Chlamydomonas strains. J Biosci Bioeng. doi:10.1016/j.jbiosc.2015.01.005

Kovar JL, Zhang J, Funke RP, Weeks DP (2002) Molecular analysis of the acetolactate synthase gene of Chlamydomonas reinhardtii and development of a genetically engineered gene as a dominant selectable marker for genetic transformation. Plant J 29(1):109–117

Kozminski KG, Diener DR, Rosenbaum JL (1993) High level expression of nonacetylatable alpha-tubulin in Chlamydomonas reinhardtii. Cell Motil Cytoskeleton 25(2):158–170

Kucho K, Ohyama K, Fukuzawa H (1999) CO_2-responsive transcriptional regulation of CAH1 encoding carbonic anhydrase is mediated by enhancer and silencer regions in Chlamydomonas reinhardtii. Plant Physiol 121(4):1329–1337

Kumar SV, Misquitta RW, Reddy VS, Rao BJ, Rajam MV (2004) Genetic transformation of the green alga Chlamydomonas reinhardtii by Agrobacterium tumefaciens. Plant Sci 166 (3):731–738

Ladygin VG, Butanaev AM (2002) Transformation of Chlamydomonas reinhardtii CW-15 with the hygromycin phosphotransferase gene as a selective marker. Genetika 38(9):1196–1202

Lambertz C, Hemschemeier A, Happe T (2010) Anaerobic expression of the ferredoxin-encoding FDX5 gene of Chlamydomonas reinhardtii is regulated by the Crr1 transcription factor. Eukaryot Cell 9(11):1747–1754

Lauersen KJ, Berger H, Mussgnug JH, Kruse O (2013) Efficient recombinant protein production and secretion from nuclear transgenes in Chlamydomonas reinhardtii. J Biotechnol 167 (2):101–110

Lauersen KJ, Kruse O, Mussgnug JH (2015) Targeted expression of nuclear transgenes in Chlamydomonas reinhardtii with a versatile, modular vector toolkit. Appl Microbiol Biotechnol 99:3491–3503

Lauersen KJ, Willamme R, Coosemans N, Joris M, Kruse O, Remacle C (2016) Peroxisomal microbodies are at the crossroads of acetate assimilation in the green microalga Chlamydomonas reinhardtii. Algal Res 16:266–274

Leisinger U, Rufenacht K, Fischer B, Pesaro M, Spengler A, Zehnder AJB, Eggen RIL (2001) The glutathione peroxidase homologous gene from Chlamydomonas reinhardtii is transcriptionally up-regulated by singlet oxygen. Plant Mol Biol 46(4):395–408

Li XB, Zhang R, Patena W, Gang SS, Blum SR, Ivanova N, Yue R, Robertson JM, Lefebvre PA, Fitz-Gibbon ST, Grossman AR, Jonikas MC (2016) An indexed, mapped mutant library enables reverse genetics studies of biological processes in Chlamydomonas reinhardtii. Plant Cell 28(2):367–387

Lodha M, Schulz-Raffelt M, Schroda M (2008) A new assay for promoter analysis in Chlamydomonas reveals roles for heat shock elements and the TATA box in HSP70A promoter-mediated activation of transgene expression. Eukaryot Cell 7(1):172–176

Lumbreras V, Stevens DR, Purton S (1998) Efficient foreign gene expression in Chlamydomonas reinhardtii mediated by an endogenous intron. Plant J 14(4):441–447

Matsuo T, Onai K, Okamoto K, Minagawa J, Ishiura M (2006) Real-time monitoring of chloroplast gene expression by a luciferase reporter: evidence for nuclear regulation of chloroplast circadian period. Mol Cell Biol 26(3):863–870

Mayfield SP, Kindle KL (1990) Stable nuclear transformation of Chlamydomonas reinhardtii by using a C. reinhardtii gene as the selectable marker. Proc Natl Acad Sci USA 87(6):2087–2091

Mayfield SP, Schultz J (2004) Development of a luciferase reporter gene, luxCt, for Chlamydomonas reinhardtii chloroplast. Plant J 37(3):449–458

McCallum CM, Comai L, Greene EA, Henikoff S (2000) Targeted screening for induced mutations. Nat Biotechnol 18(4):455–457

McCarthy SS, Kobayashi MC, Niyogi KK (2004) White mutants of Chlamydomonas reinhardtii are defective in phytoene synthase. Genetics 168(3):1249–1257

Merchant S, Hill K, Howe G (1991) Dynamic interplay between two copper-titrating components in the transcriptional regulation of cyt c6. EMBO J 10(6):1383–1389

Merchant SS, Prochnik SE, Vallon O, Harris EH, Karpowicz SJ, Witman GB, Terry A, Salamov A, Fritz-Laylin LK, Marechal-Drouard L, Marshall WF, Qu LH, Nelson DR, Sanderfoot AA, Spalding MH, Kapitonov VV, Ren QH, Ferris P, Lindquist E, Shapiro H, Lucas SM, Grimwood J, Schmutz J, Cardol P, Cerutti H, Chanfreau G, Chen CL, Cognat V, Croft MT, Dent R, Dutcher S, Fernandez E, Fukuzawa H, Gonzalez-Ballester D, Gonzalez-Halphen D, Hallmann A, Hanikenne M, Hippler M, Inwood W, Jabbari K, Kalanon M, Kuras R, Lefebvre PA, Lemaire SD, Lobanov AV, Lohr M, Manuell A, Meir I, Mets L, Mittag M, Mittelmeier T, Moroney JV, Moseley J, Napoli C, Nedelcu AM, Niyogi K, Novoselov SV, Paulsen IT, Pazour G,

Purton S, Ral JP, Riano-Pachon DM, Riekhof W, Rymarquis L, Schroda M, Stern D, Umen J, Willows R, Wilson N, Zimmer SL, Allmer J, Balk J, Bisova K, Chen CJ, Elias M, Gendler K, Hauser C, Lamb MR, Ledford H, Long JC, Minagawa J, Page MD, Pan JM, Pootakham W, Roje S, Rose A, Stahlberg E, Terauchi AM, Yang PF, Ball S, Bowler C, Dieckmann CL, Gladyshev VN, Green P, Jorgensen R, Mayfield S, Mueller-Roeber B, Rajamani S, Sayre RT, Brokstein P, Dubchak I, Goodstein D, Hornick L, Huang YW, Jhaveri J, Luo YG, Martinez D, Ngau WCA, Otillar B, Poliakov A, Porter A, Szajkowski L, Werner G, Zhou KM, Grigoriev IV, Rokhsar DS, Grossman AR, Annotation C, Team JA (2007) The Chlamydomonas genome reveals the evolution of key animal and plant functions. Science 318(5848):245–251

Meslet-Cladiere L, Vallon O (2011) Novel shuttle markers for nuclear transformation of the green alga Chlamydomonas reinhardtii. Eukaryot Cell 10(12):1670–1678

Minko I, Holloway SP, Nikaido S, Carter M, Odom OW, Johnson CH, Herrin DL (1999) Renilla luciferase as a vital reporter for chloroplast gene expression in Chlamydomonas. Mol Gen Genet 262(3):421–425

Molnar A, Bassett A, Thuenemann E, Schwach F, Karkare S, Ossowski S, Weigel D, Baulcombe D (2009) Highly specific gene silencing by artificial microRNAs in the unicellular alga Chlamydomonas reinhardtii. Plant J 58(1):165–174

Mussgnug JH (2015) Genetic tools and techniques for Chlamydomonas reinhardtii. Appl Microbiol Biotechnol 99(13):5407–5418

Mussgnug JH, Wobbe L, Elles I, Claus C, Hamilton M, Fink A, Kahmann U, Kapazoglou A, Mullineaux CW, Hippler M, Nickelsen J, Nixon PJ, Kruse O (2005) NAB1 is an RNA binding protein involved in the light-regulated differential expression of the light-harvesting antenna of Chlamydomonas reinhardtii. Plant Cell 17(12):3409–3421

Mussgnug JH, Thomas-Hall S, Rupprecht J, Foo A, Klassen V, McDowall A, Schenk PM, Kruse O, Hankamer B (2007) Engineering photosynthetic light capture: impacts on improved solar energy to biomass conversion. Plant Biotechnol J 5(6):802–814

Nelson JAE, Lefebvre PA (1995) Targeted disruption of the NIT8 gene in Chlamydomonas reinhardtii. Mol Cell Biol 15(10):5762–5769

Nelson JAE, Savereide PB, Lefebvre PA (1994) The Cry1 gene in Chlamydomonas reinhardtii: structure and use as a dominant selectable marker for nuclear transformation. Mol Cell Biol 14 (6):4011–4019

Neumann E, Schaefer-Ridder M, Wang Y, Hofschneider PH (1982) Gene transfer into mouse lyoma cells by electroporation in high electric fields. EMBO J 1(7):841–845

Neupert J, Karcher D, Bock R (2009) Generation of Chlamydomonas strains that efficiently express nuclear transgenes. Plant J 57(6):1140–1150

Nichols KM, Rikmenspoel R (1978) Control of flagellar motion in Chlamydomonas and Euglena by mechanical microinjection of Mg2+ and Ca2+ and by electric current injection. J Cell Sci 29:233–247

Nickelsen J, van Dillewijn J, Rahire M, Rochaix JD (1994) Determinants for stability of the chloroplast psbD RNA are located within its short leader region in Chlamydomonas reinhardtii. EMBO J 13(13):3182–3191

Nybom N (1953) Some experiences from mutation experiments in Chlamydomonas. Hereditas 39 (1–2):317–324

Nymark M, Sharma AK, Sparstad T, Bones AM, Winge P (2016) A CRISPR/Cas9 system adapted for gene editing in marine algae. Sci Rep 6:24951

Ohresser M, Matagne RF, Loppes R (1997) Expression of the arylsulphatase reporter gene under the control of the nit1 promoter in Chlamydomonas reinhardtii. Curr Genet 31(3):264–271

Ossowski S, Schwab R, Weigel D (2008) Gene silencing in plants using artificial microRNAs and other small RNAs. Plant J 53(4):674–690

Pape M, Lambertz C, Happe T, Hemschemeier A (2012) Differential expression of the Chlamydomonas [FeFe]-hydrogenase-encoding HYDA1 gene is regulated by the COPPER RESPONSE REGULATOR1. Plant Physiol 159(4):1700–1712

Park S, Lee Y, Lee JH, Jin E (2013) Expression of the high light-inducible Dunaliella LIP promoter in Chlamydomonas reinhardtii. Planta 238(6):1147–1156

Porto MS, Pinheiro MPN, Batista VGL, dos Santos RC, Melo PD, de Lima LM (2014) Plant promoters: an approach of structure and function. Mol Biotechnol 56(1):38–49

Quinn JM, Kropat J, Merchant S (2003) Copper response element and Crr1-dependent Ni2+-responsive promoter for induced, reversible gene expression in Chlamydomonas reinhardtii. Eukaryot Cell 2(5):995–1002

Ramundo S, Rahire M, Schaad O, Rochaix JD (2013) Repression of essential chloroplast genes reveals new signaling pathways and regulatory feedback loops in Chlamydomonas. Plant Cell 25(1):167–186

Ran FA, Cong L, Yan WX, Scott DA, Gootenberg JS, Kriz AJ, Zetsche B, Shalem O, Wu XB, Makarova KS, Koonin EV, Sharp PA, Zhang F (2015) In vivo genome editing using Staphylococcus aureus Cas9. Nature 520(7546):186–191

Randolph-Anderson BL, Sato R, Johnson AM, Harris EH, Hauser CR, Oeda K, Ishige F, Nishio S, Gillham NW, Boynton JE (1998) Isolation and characterization of a mutant protoporphyrinogen oxidase gene from Chlamydomonas reinhardtii conferring resistance to porphyric herbicides. Plant Mol Biol 38(5):839–859

Rasala BA, Mayfield SP (2015) Photosynthetic biomanufacturing in green algae; production of recombinant proteins for industrial, nutritional, and medical uses. Photosynth Res 123 (3):227–239

Rasala BA, Lee PA, Shen ZX, Briggs SP, Mendez M, Mayfield SP (2012) Robust expression and secretion of Xylanase1 in Chlamydomonas reinhardtii by fusion to a selection gene and processing with the FMDV 2A peptide. PLoS One 7(8). doi:10.1371/journal.pone.0043349

Rasala BA, Barrera DJ, Ng J, Plucinak TM, Rosenberg JN, Weeks DP, Oyler GA, Peterson TC, Haerizadeh F, Mayfield SP (2013) Expanding the spectral palette of fluorescent proteins for the green microalga Chlamydomonas reinhardtii. Plant J 74(4):545–556

Rasala BA, Chao SS, Pier M, Barrera DJ, Mayfield SP (2014) Enhanced genetic tools for engineering multigene traits into green algae. PLoS One 9(4). doi:10.1371/journal.pone.0094028

Remacle C, Cline S, Boutaffala L, Gabilly S, Larosa V, Barbieri MR, Coosemans N, Hamel PP (2009) The ARG9 gene encodes the plastid-resident N-acetyl ornithine aminotransferase in the green alga Chlamydomonas reinhardtii. Eukaryot Cell 8(9):1460–1463

Rhaese HJ, Boetker NK (1973) The molecular basis of mutagenesis by methyl and ethyl methanesulfonates. Eur J Biochem 32(1):166–172

Rochaix JD, van Dillewijn J (1982) Transformation of the green alga Chlamydomonas reinhardtii with yeast DNA. Nature 296(5852):70–72

Rohr J, Sarkar N, Balenger S, Jeong BR, Cerutti H (2004) Tandem inverted repeat system for selection of effective transgenic RNAi strains in Chlamydomonas. Plant J 40(4):611–621

Ruecker O, Zillner K, Groebner-Ferreira R, Heitzer M (2008) Gaussia-luciferase as a sensitive reporter gene for monitoring promoter activity in the nucleus of the green alga Chlamydomonas reinhardtii. Mol Gen Genomics 280(2):153–162

Sawyer AL, Hankamer BD, Ross IL (2015) Sulphur responsiveness of the Chlamydomonas reinhardtii LHCBM9 promoter. Planta. doi:10.1007/s00425-015-2249-9

Scaife MA, Nguyen GT, Rico J, Lambert D, Helliwell KE, Smith AG (2015) Establishing Chlamydomonas reinhardtii as an industrial biotechnology host. Plant J. doi:10.1111/tpj.12781

Schierenbeck L, Ries D, Rogge K, Grewe S, Weisshaar B, Kruse O (2015) Fast forward genetics to identify mutations causing a high light tolerant phenotype in Chlamydomonas reinhardtii by whole-genome-sequencing. BMC Genomics 16(1):57

Schmollinger S, Strenkert D, Schroda M (2010) An inducible artificial microRNA system for Chlamydomonas reinhardtii confirms a key role for heat shock factor 1 in regulating thermotolerance. Curr Genet 56(4):383–389

Schnell RA, Lefebvre PA (1993) Isolation of the Chlamydomonas regulatory gene NIT2 by transposon tagging. Genetics 134(3):737–747

Schroda M (2006) RNA silencing in Chlamydomonas: mechanisms and tools. Curr Genet 49 (2):69–84

Schroda M, Vallon O, Wollman FA, Beck CF (1999) A chloroplast-targeted heat shock protein 70 (HSP70) contributes to the photoprotection and repair of photosystem II during and after photoinhibition. Plant Cell 11(6):1165–1178

Schroda M, Blocker D, Beck CF (2000) The HSP70A promoter as a tool for the improved expression of transgenes in Chlamydomonas. Plant J 21(2):121–131

Scranton MA, Ostrand JT, Georgianna DR, Lofgren SM, Li D, Ellis RC, Carruthers DN, Dräger A, Masica DL, Mayfield SP (2016) Synthetic promoters capable of driving robust nuclear gene expression in the green alga Chlamydomonas reinhardtii. Algal Res 15:135–142

Shao N, Bock R (2008) A codon-optimized luciferase from Gaussia princeps facilitates the in vivo monitoring of gene expression in the model alga Chlamydomonas reinhardtii. Curr Genet 53 (6):381–388

Shen YJ, Liu YS, Liu L, Liang C, Li QSQ (2008) Unique features of nuclear mRNA Poly (A) signals and alternative polyadenylation in Chlamydomonas reinhardtii. Genetics 179 (1):167–176

Shimogawara K, Fujiwara S, Grossman A, Usuda H (1998) High-efficiency transformation of Chlamydomonas reinhardtii by electroporation. Genetics 148(4):1821–1828

Shin SE, Lim JM, Koh HG, Kim EK, Kang NK, Jeon S, Kwon S, Shin WS, Lee B, Hwangbo K, Kim J, Ye SH, Yun JY, Seo H, Oh HM, Kim KJ, Kim JS, Jeong WJ, Chang YK, Jeong BR (2016) CRISPR/Cas9-induced knockout and knock-in mutations in Chlamydomonas reinhardtii. Sci Rep 6:27810

Sizova IA, Lapina TV, Frolova ON, Alexandrova NN, Akopiants KE, Danilenko VN (1996) Stable nuclear transformation of Chlamydomonas reinhardtii with a Streptomyces rimosus gene as the selective marker. Gene 181(1–2):13–18

Sizova I, Fuhrmann M, Hegemann P (2001) A Streptomyces rimosus aphVIII gene coding for a new type phosphotransferase provides stable antibiotic resistance to Chlamydomonas reinhardtii. Gene 277(1–2):221–229

Sizova I, Greiner A, Awasthi M, Kateriya S, Hegemann P (2013) Nuclear gene targeting in Chlamydomonas using engineered zinc-finger nucleases. Plant J 73(5):873–882

Slaymaker IM, Gao L, Zetsche B, Scott DA, Yan WX, Zhang F (2016) Rationally engineered Cas9 nucleases with improved specificity. Science 351(6268):84–88

Smart EJ, Selman BR (1993) Complementation of a Chlamydomonas reinhardtii mutant defective in the nuclear gene encoding the chloroplast coupling factor 1 (CF1) gamma-subunit (atpC). J Bioenerg Biomembr 25(3):275–284

Sodeinde OA, Kindle KL (1993) Homologous recombination in the nuclear genome of Chlamydomonas reinhardtii. Proc Natl Acad Sci USA 90(19):9199–9203

Specht EA, Nour-Eldin HH, Hoang KT, Mayfield SP (2014) An improved ARS2-derived nuclear reporter enhances the efficiency and ease of genetic engineering in Chlamydomonas. Biotechnol J 10(3):473–479

Stevens DR, Rochaix JD, Purton S (1996) The bacterial phleomycin resistance gene ble as a dominant selectable marker in Chlamydomonas. Mol Gen Genet 251(1):23–30

Strauss C, Mussgnug JH, Kruse O (2001) Ligation-mediated suppression-PCR as a powerful tool to analyse nuclear gene sequences in the green alga Chlamydomonas reinhardtii. Photosynth Res 70(3):311–320

Strenkert D, Schmollinger S, Schroda M (2013) Heat shock factor 1 counteracts epigenetic silencing of nuclear transgenes in Chlamydomonas reinhardtii. Nucleic Acids Res 41(10):5273–5289

Surzycki R, Cournac L, Peltier G, Rochaix JD (2007) Potential for hydrogen production with inducible chloroplast gene expression in Chlamydomonas. Proc Natl Acad Sci USA 104(44):17548–17553

Tang DKH, Qiao SY, Wu M (1995) Insertion mutagenesis of Chlamydomonas reinhardtii by electroporation and heterologous DNA. Biochem Mol Biol Int 36(5):1025–1035

Tardif M, Atteia A, Specht M, Cogne G, Rolland N, Brugiere S, Hippler M, Ferro M, Bruley C, Peltier G, Vallon O, Cournac L (2012) PredAlgo: a new subcellular localization prediction tool dedicated to green algae. Mol Biol Evol 29(12):3625–3639

Terashima M, Freeman ES, Jinkerson RE, Jonikas MC (2015) A fluorescence-activated cell sorting-based strategy for rapid isolation of high-lipid Chlamydomonas mutants. Plant J 81(1):147–159

Vila M, Diaz-Santos E, de la Vega M, Rodriguez H, Vargas A, Leon R (2012) Promoter trapping in microalgae using the antibiotic paromomycin as selective agent. Mar Drugs 10(12):2749–2765

Voytsekh O, Seitz SB, Iliev D, Mittag M (2008) Both subunits of the circadian RNA-binding protein CHLAMY1 can integrate temperature information. Plant Physiol 147(4):2179–2193

Walker TL, Becker DK, Collet C (2005) Characterisation of the Dunaliella tertiolecta RbcS genes and their promoter activity in Chlamydomonas reinhardtii. Plant Cell Rep 23(10–11):727–735

Wang Q, Lu Y, Xin Y, Wei L, Huang S, Xu J (2016) Genome editing of model oleaginous microalgae Nannochloropsis spp. by CRISPR/Cas9. Plant J. doi:10.1111/tpj.13307

Yarmush ML, Golberg A, Sersa G, Kotnik T, Miklavcic D (2014) Electroporation-based technologies for medicine: principles, applications, and challenges. Annu Rev Biomed Eng 16:295–320

Zetsche B, Gootenberg JS, Abudayyeh OO, Slaymaker IM, Makarova KS, Essletzbichler P, Volz SE, Joung J, van der Oost J, Regev A, Koonin EV, Zhang F (2015) Cpf1 Is a single RNA-guided endonuclease of a class 2 CRISPR-Cas system. Cell 163(3):759–771

Zhang D, Lefebvre PA (1997) FAR1, a negative regulatory locus required for the repression of the nitrate reductase gene in Chlamydomonas reinhardtii. Genetics 146(1):121–133

Zhang R, Patena W, Armbruster U, Gang SS, Blum SR, Jonikas MC (2014) High-throughput genotyping of green algal mutants reveals random distribution of mutagenic insertion sites and endonucleolytic cleavage of transforming DNA. Plant Cell 26(4):1398–1409

Zhao T, Wang W, Bai X, Qi YJ (2009) Gene silencing by artificial microRNAs in Chlamydomonas. Plant J 58(1):157–164

Zhao ZX, Wu XH, Kumar PKR, Dong M, Ji GL, Li QSQ, Liang C (2014) Bioinformatics analysis of alternative polyadenylation in green alga Chlamydomonas reinhardtii using transcriptome sequences from three different sequencing platforms. G3 Genes Genomes Genetics 4(5):871–883

Zorin B, Hegemann P, Sizova I (2005) Nuclear-gene targeting by using single-stranded DNA avoids illegitimate DNA integration in Chlamydomonas reinhardtii. Eukaryot Cell 4(7):1264–1272

Zorin B, Lu YH, Sizova I, Hegemann P (2009) Nuclear gene targeting in Chlamydomonas as exemplified by disruption of the PHOT gene. Gene 432(1–2):91–96

Mitochondrial Bioenergetics Pathways in Chlamydomonas

Simon Massoz, Pierre Cardol, Diego González-Halphen, and Claire Remacle

Abstract Mitochondrion is the site where the Krebs cycle and *ox*idative *phos*phorylation (OXPHOS) take place. After a brief overview of Krebs cycle and acetate metabolism in Chlamydomonas, this chapter focuses on OXPHOS components. OXPHOS is composed of five major multiprotein complexes: NADH:ubiquinone oxidoreductase (complex I), succinate dehydrogenase (complex II), ubiquinone: cytochrome *c* oxidoreductase (complex III), cytochrome *c* oxidase (complex IV), and ATP synthase. Three complexes (complexes I, III, and IV) pump protons from the matrix to the *i*nter*m*embrane *s*pace (IMS) and build a gradient which is used by ATP synthase to produce ATP. In Chlamydomonas and other eukaryotes, proteins forming these complexes have a dual genetic origin. A few proteins, mostly hydrophobic polypeptides, are mitochondrion-encoded, while the vast majority are nucleus-encoded and imported from the cytoplasm. Here we will review our current knowledge about these complexes.

List of Abbreviations

acetyl CoA	Acetyl coenzyme A
ADP	Adenosine diphosphate
ATP	Adenosine triphosphate
BNC	Binuclear center
FAD	Flavin adenine dinucleotide
Fe-S	Iron-sulfur
FMN	Flavin mononucleotide
IMS	Intermembrane space
NAD+	Nicotinamide adenine dinucleotide

S. Massoz • P. Cardol • C. Remacle (✉)
Liège University, Genetics and Physiology of Microalgae, Chemin de la Vallée 4, 4000 Liège 1, Belgium
e-mail: c.remacle@ulg.ac.be

D. González-Halphen
Universidad Nacional Autónoma de México, Instituto de Fisiología Celular, México DF, Mexico

M. Hippler (ed.), *Chlamydomonas: Molecular Genetics and Physiology*,
Microbiology Monographs 30, DOI 10.1007/978-3-319-66365-4_3

NADH	Reduced form of nicotinamide adenine dinucleotide
NADP+	Nicotinamide adenine dinucleotide phosphate
NADPH	Reduced form of nicotinamide adenine dinucleotide phosphate
OXPHOS	Oxidative phosphorylation
Q	Ubiquinone
QH_2	Ubiquinol
Pi	Inorganic phosphate
PLS	Proton-loading site
ROS	Reactive oxygen species

1 Krebs Cycle and Acetate Metabolism

The mitochondrion houses the Krebs cycle in the matrix and OXPHOS in the inner mitochondrial membrane (Fig. 1). Pyruvate, the end product of glycolysis, is imported inside the mitochondria by crossing both the outer and the inner mitochondrial membrane. Similar to most ions and metabolites, pyruvate is hypothesized to cross the outer membrane through the *v*oltage-*d*ependent *a*nion *c*hannel (VDAC) based on the fact that humans deficient of VDAC1 show impaired pyruvate oxidation and ATP production (McCommis and Finck 2015). In Chlamydomonas, two VDAC proteins have been identified in the genome, ASC1 and ASC2, sharing 64% of sequence identity to each other (Salinas, unpublished). In contrast, specific pyruvate carriers for the inner mitochondrial membrane have been identified in yeast, Drosophila, and humans (Bricker et al. 2012). Accordingly, two genes described as encoding mitochondrial pyruvate carriers are present in version 5.5 of the Chlamydomonas genome (https://phytozome.jgi.doe.gov): Cre02.g113100.t1.1 and Cre10.g433400.t1.1. Once pyruvate enters the matrix, it is converted into acetyl CoA by the mitochondrial *p*yruvate *deh*ydrogenase complex (PDH, composed of three subunits encoded by *PDC1*, *PDC2*, and *PDH1* genes; Fig. 1). Acetyl CoA then enters the Krebs cycle, consisting of eight mitochondrial enzymes, whose presence has been confirmed in the mitochondria by proteomic analysis (Atteia et al. 2009). The following genes encode the components of Chlamydomonas Krebs cycle (Atteia et al. 2009): (1) *Fum*arase (FUM, Fig. 1) is encoded by *FUM1*; (2) *m*alate *deh*ydrogenase (MDH, Fig. 1) is represented by two isoforms encoded by the *MDH3* and *MDH4* genes; (3) *ci*trate *s*ynthase (CIS, Fig. 1) is represented by one isoform encoded by *CIS1*; (4) aconitase (ACH, Fig. 1) is represented by the lone isoform encoded by *ACH1*; (5) *is*ocitrate *deh*ydrogenase (IDH, Fig. 1) is represented by three isoforms, two are NAD-dependent and encoded by *IDH1* and *IDH2*, while one isoform encoded by *IDH3* is NADP-dependent; (6) the 2-*ox*o*g*lutarate *deh*ydrogenase complex (OGDH, Fig. 1) is composed of three subunits, encoded by *OGD1*, *OGD2*, and *OGD3*; (7) *s*uccinyl-*C*oA *s*ynthase (SCS, Fig. 1) is composed of two subunits encoded by *SCLA1* and *SCLB1* genes; (8) *s*uccinate *deh*ydrogenase (complex II/SDH, Fig. 1) will be described in the OXPHOS section.

Exchange of metabolites between cellular compartments involves different transporters (Fig. 1). Thirteen genes corresponding to *mit*ochondrial substrate

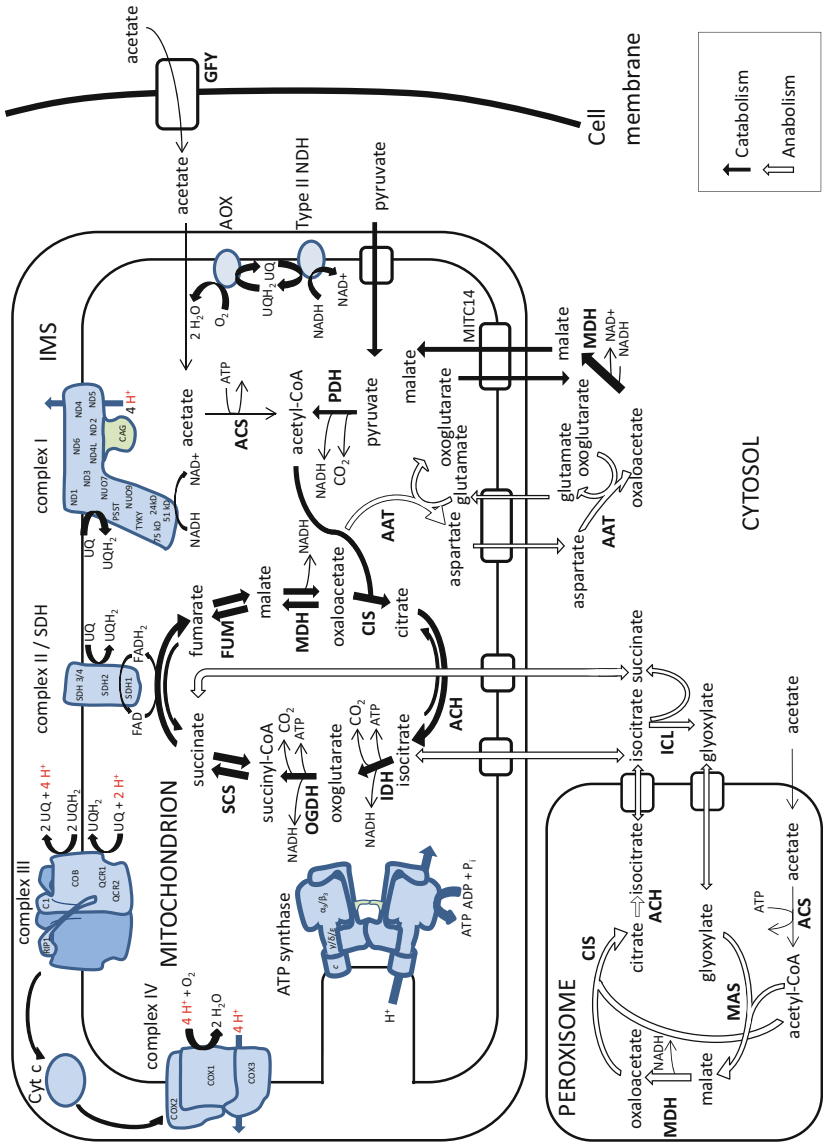

Fig. 1 General scheme of mitochondrial carbon metabolism in *C. reinhardtii*. OXPHOS: only bacterial core subunits and Chlamydomonas-specific modules (*green*) are represented. Only H^+ involved in ΔpH (*red*) are depicted in complexes I, III, and IV. *AAT* aspartate aminotransferase, *ACH* aconitase, *ACS* acetyl CoA synthase, *CIS* citrate synthase, *FUM* fumarase, *GFY* putative acetate transporters, *ICL* isocitrate lyase, *IDH* isocitrate dehydrogenase, *MAS* malate synthase, *MDH* malate dehydrogenase, *MITC14* oxoglutarate/malate carrier, *OGDH* 2-oxoglutarate dehydrogenase, *PDH* pyruvate dehydrogenase complex, *SCS* succinyl coenzyme A synthetase

*c*arrier proteins (MITC) are identified in the Phytozome 5.5 version of Chlamydomonas nuclear genome. In particular, MITC10, 11, and 14 have been found by proteomics analysis of mitochondria (Atteia et al. 2009). *MITC14* codes for a putative 2-oxoglutarate/malate carrier.

One particularity of Chlamydomonas is its ability to sustain heterotrophic growth (growth in the dark) through acetate assimilation. Five putative acetate transporters belonging to the *G*RP1/*F*UN34/*Y*aa family (GFY, Fig. 1) have been recently identified in Chlamydomonas (Goodenough et al. 2014) based on homology to fungal acetate permease A. These proteins bear six transmembrane segments, suggesting membrane localization. Once inside the cell, acetate is metabolized into acetyl CoA by acetyl CoA synthase. Three isoforms of *a*cetyl *C*oA *s*ynthase are present: ACS1 is cytosolic (Lauersen et al. 2016), ACS2 is chloroplastic (Terashima et al. 2010), while ACS3 would be colocalized in mitochondria (Atteia et al. 2009) and peroxisomes (Lauersen et al. 2016) (Fig. 1). Acetyl CoA can be used in the glyoxylate cycle to fuel gluconeogenesis and other anabolic pathways or in the Krebs cycle to produce NADH for the respiratory chain and ATP production, both processes being necessary for effective growth in the dark (Salinas et al. 2014; Plancke et al. 2014). Indeed, respiratory-deficient mutants and the recently characterized mutant deficient of isocitrate lyase (*icl1*), one of the two specific enzymes of the glyoxylate cycle (Fig. 1), are unable to grow under heterotrophic conditions. The localization of the enzymes of the glyoxylate cycle has been recently elucidated (Lauersen et al. 2016). Five of the six enzymes associated with the glyoxylate cycle are located within peroxisomal microbodies: one of the isoforms of malate dehydrogenase (MDH1), citrate synthase (CIS2), and acetyl CoA synthase (ACS3) and the lone form of *ma*late *s*ynthase (MAS1) and of aconitase (ACH1), which defines for the first time a central role of peroxisomal microbodies in acetate assimilation. Only the single form of *isoc*itrate *l*yase (ICL1) was found in the cytosol, which implies shuttling of metabolites such as isocitrate, succinate, and glyoxylate between peroxisomal microbodies, cytosol, and mitochondria (Fig. 1). Pore-like membrane structures and specific transporters would permit these exchanges, but the molecular identity of such channel proteins remains undetermined (Kunze and Hartig 2013).

2 OXPHOS

2.1 Complex I

Complex I (EC 1.6.5.3), the first complex of OXPHOS, catalyzes the reaction

$$[\mathrm{NADH} + \mathrm{H}^+] + \mathrm{Q} + 4\ \mathrm{H}^+_{\mathrm{matrix}} \Rightarrow \mathrm{NAD}^+ + \mathrm{QH}_2 + 4\ \mathrm{H}^+_{\mathrm{IMS}} (\mathrm{Q} = \text{ubiquinone})$$

In all organisms investigated so far, complex I is an L-shaped multiprotein complex (Vinothkumar et al. 2014) with a molecular mass of ~1 MDa and

45 subunits (in humans), out of which 41 are conserved among eukaryotes (Cardol 2011). Fourteen of these subunits represent the core of the complex as they form the structure of the most simplistic bacterial complex I (type I NDH) (Efremov et al. 2010; Berrisford et al. 2016) and are conserved in all eukaryotic complex I. Among these 14 core subunits, the mitochondrially encoded subunits ND1, ND2, ND4, ND5, ND6, ND3 (NUO3), and ND4L (NUO11) form the membrane arm of the complex. The nucleus-encoded 75 kDa (NUOS1), 51 kDa (NUO6), 24 kDa (NUO5), 49 kDa (NUO7), 30 kDa (NUO9), TYKY (NUO8), and PSST (NUO10) subunits form the matrix part of the complex (bovine and Chlamydomonas nomenclature). In addition to these core subunits, around 30 supernumerary subunits are present in the eukaryotic complex I. Though their role remains unclear, these subunits are thought to stabilize and protect complex I (Hirst et al. 2003).

In complex I, electrons are channeled from NADH to a ubiquinone molecule through a flavin mononucleotide (FMN) and seven iron-sulfur (Fe-S) clusters named N3, N1b, N4, N5, N6a, N6b, and N2. An eighth Fe-S cluster is located near the FMN, named N1a, and thought to serve as an electron store meant to avoid an excessive reactive oxygen species (ROS) production (Zickermann et al. 2015). These Fe-S clusters are mostly reduced under physiological conditions (Kotlyar et al. 1990). The FMN with a midpoint redox potential at pH 7 of ~ −340 mV serves as the first electron acceptor from NADH; the N3, N1b, N4, N5, N6a, and N6b are equipotential at ∼−250 mV and serve as a path for electron transport (Ohnishi 1998; Brandt 2011). The high-potential N2 cluster (−120 mV) serves as final electron acceptor and catalyzes electron transfer to the ubiquinone molecule.

The prokaryotic core complex I is divided into modules based on function and position within the complex (Fig. 2). The N module, located at the most distal part of the matrix arm, is related to NAD+-reducing hydrogenases (Friedrich and Weiss 1997). It is responsible for NADH oxidation and is composed of the 75 kDa, 51 kDa, and 24 kDa subunits. The 51 kDa subunit bears the FMN and the N1b Fe-S cluster. The 24 kDa bears the N1a Fe-S cluster. The large 75 kDa bears the N3, N4, and N5 Fe-S clusters.

The Q module, or quinone reduction module, is composed of the 49 kDa, 30 kDa, TYKY, and PSST subunits. This module allows electron transfer to the ubiquinone through the N6a and N6b Fe-S clusters located on the TYKY subunit and through N2 reaction center cluster. The 49 kDa, TYKY, and PSST subunits are thought to be derived from a Ni-Fe-type hydrogenase (Friedrich and Weiss 1997; Vignais and Billoud 2007) where the proximal Fe-S cluster from the Ni-Fe reaction center became the current N2 cluster (Kerscher et al. 2001). It is interesting to note that the N2 cluster, long thought to be harbored by the 49 kDa and PSST subunits, has been shown to be only linked to the PSST subunit (Sazanov and Hinchliffe 2006) with the 49 kDa subunit being at the interface of this cluster. Despite the fact that the 49 kDa and 30 kDa proteins are the only core subunits of the matrix arm that do not provide ligands for cofactors, Chlamydomonas cells inactivated for their expression fail to assemble whole complex I as also observed in all species (*Neurospora* and *E. coli*) investigated so far (Schulte and Weiss 1995; Duarte et al. 1998; Massoz et al. 2014).

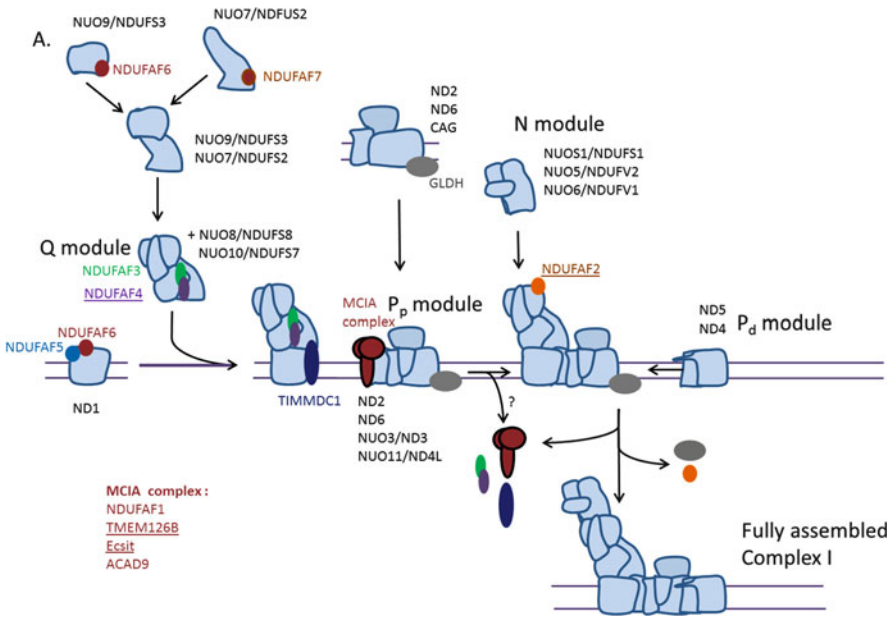

Fig. 2 Hypothetical assembly model for complex I in Chlamydomonas. Nomenclature for Chlamydomonas/humans is used for core subunits, and human nomenclature is used for assembly factors. One name indicated means similar nomenclature. The plant-specific assembly factor (GLDH) is also shown. Underlined assembly factors have been identified in humans, but no homologs have been found in *C. reinhardtii*

The P module, often divided into the proximal (P_p) and distal region (P_d), is composed of the remaining membrane subunits. The ND1, ND2, ND3, ND4L, and ND6 subunits compose the P_p module (Fig. 1). The P_d module is composed of the ND4 and ND5 subunits. ND2, ND4, and ND5 are homologous to the *E. coli* cation/H^+ antiporter MrpA/MrpD (Mathiesen and Hägerhäll 2002). These three subunits are responsible for three out of four proton-pumping sites in complex I. The fourth site is thought to be a channel located in the small ND subunits (ND3, ND4L, and ND6) with maybe part of the ND1 subunit (Zickermann et al. 2015; Berrisford et al. 2016).

The current proton-pumping mechanism model for complex I is supported by crystal structures in the bacterium *Thermus thermophilus* [reviewed in Sazanov (2015)], the fungus *Yarrowia lipolytica* (Zickermann et al. 2015), and mammals (Vinothkumar et al. 2014). The proton-pumping channels through the membrane domain are distant from the redox-active groups mediating electron transfer through the hydrophilic domain (Efremov and Sazanov 2011). As a consequence, the proton-coupled electron transfer in complex I is expected to differ mechanistically from that in other respiratory complexes. The current model for proton pumping is based on a two-stage stabilization-change mechanism. This model proposes that the stabilization of a negatively charged ubiquinone drives a conformational change causing energy transmission to the membrane arm and resulting in proton pumping (Brandt

2011). This model combines computational simulations with biochemical experiments based on bacterial complex I (Sharma et al. 2015; Hummer and Wikström 2016). The bacterial complex I structure revealed an unusual ubiquinone-binding cavity (Baradaran et al. 2013). The reduction of bound ubiquinone would create a significant charge imbalance in the catalytic cavity. The charge imbalance would be transmitted to the antiporter-like subunits by long-range conformational transmission. The antiporter-like subunits define a central flexible axis containing charged and polar residues which extend from the ubiquinone-binding site at the junction between the two main domains to the tip of the hydrophobic arm and thus represent a hydrophilic central axis along the hydrophobic domain by which these concerted conformational changes are transmitted. This would lead to changes in exposure to solvent and in the pKa of key residues in the antiporter subunits, allowing proton translocation (Berrisford et al. 2016; Hummer and Wikström 2016). Displaced ubiquinone would then be protonated. Once protonated, the charge imbalanced would be compensated, and the newly formed ubiquinol would exit the cavity.

Complex I is the biggest complex of OXPHOS, with a large number of proteins encoded in both the mitochondrial and the nuclear genomes. The assembly of complex I is expected to involve of lot of chaperones and is not yet fully understood. Because most data on complex I assembly were obtained in mammals, assembly description will here be explained based on knowledge gained in humans. Thus, human nomenclature will be used for the assembly description. As many other OXPHOS complexes, complex I seems to be orderly assembled into subcomplexes before these subcomplexes are assembled together to form the holoenzyme (Fig. 2). The process starts with the assembly of the Q module containing NDUFS2, NDUFS3, NDUFS8, and NDUFS7. This requires the intervention of at least four factors named NDUFAF7, NDUFAF3, NDUFAF4, and NDUFAF6. NDUFAF7 is a methyltransferase which methylates NDUFS2 (Rhein et al. 2013). NDUFAF6 has been shown to stabilize NDUFS3 and ND1. NDUFAF3 and NDUFAF4 are interdependent factors that recruit the subunits of the Q module to assemble them with the ND1 membrane subunit (Saada et al. 2009), ND1 being itself stabilized by the NDUFAF5/NDUFAF6 assembly factors. The Q module + ND1 represent an early 400 kDa subcomplex. The second subcomplex (460 kDa) is composed of the small ND subunits (ND3, ND4L, and ND6) and ND2 and assembles independently from the 400 kDa. The four assembly factors NDUFAF1, ACAD9, TMEM126B, and ECSIT (also called MCIA complex) are known to allow the assembly of this 460 kDa subcomplex [reviewed in Sánchez-Caballero et al. (2016)]. The two subcomplexes merge together with the help of TIMMDC1 (Guarani et al. 2014) into a 650 kDa subcomplex. Following these events, the assembled P_d module merges with the rest of the subunits into a 830 kDa subcomplex stabilized by the Foxred1 assembly factor. The assembled N module also proceeds to merge with the now complete complex I with the help of the NDUFAF2 assembly factors (not present in *C. reinhardtii*), though the role of the NDUFAF2 in N module assembly has been contested in recent years (Kmita et al. 2015) where it was speculated to potentially maintain the Q module into a proper conformation until later stage of assembly. The completion of the assembly triggers the release of all remaining

assembly factors. Recombinant assembly factor Ind1 from humans (huInd1) (also called NUBPL, Table 1) expressed in *E. coli* has been shown to bind Fe-S clusters in vitro, and depletion of huInd1 was shown to be responsible for decreased complex I assembly (Sheftel et al. 2009). These results point toward a role of huInd1 in Fe-S cluster insertions. The *a*poptosis-*i*nducing *f*actor (AIF) also plays a role in complex I assembly since cells depleted for this factor display decreased complex I activity (Mimaki et al. 2012), though the exact role of this assembly factor remains unknown.

Whether plant complex I assembly follows the same pathway as in humans or not is difficult to say. On the one hand, on the 14 assembly factors described in humans, 11 have putative homologs in Arabidopsis (Table 1), suggesting that similar patterns of assembly could be found. On the other hand, as plant complex I contains an additional gamma carbonic anhydrase module attached to the Pp module (Sunderhaus et al. 2006; Klodmann et al. 2010; Fromm et al. 2016), this suggests that the assembly should follow a different assembly pattern than that found in humans at least for the attachment of these subunits to complex I. Indeed, the carbonic anhydrase subunits of the module seem to be crucial for the beginning of assembly of complex I in *A. thaliana* (Fromm et al. 2016). At that stage, our knowledge is extremely limited since only two assembly factors have been demonstrated to participate in complex I assembly in plants: IND1 (homolog of huInd1) and L-*g*alactono-1,4-*l*actone *de**h*ydrogenase (GLDH). The role of IND1 in complex I assembly of *A. thaliana* is more complex than in humans as the factor has been suggested to participate to both complex I assembly and mitochondrial translation (Wydro et al. 2013). GLDH catalyzing the last step of ascorbate biosynthesis is found in 400–850 kDa subcomplexes in *A. thaliana* and has been shown to be necessary for the assembly of the membrane arm of the complex (Schimmeyer et al. 2016). GLDH thus represents the first plant-specific assembly factor since GLDH is not conserved in humans (Schimmeyer et al. 2016).

In *C. reinhardtii*, gamma carbonic anhydrase subunits are found by proteomic analysis of complex I (Cardol et al. 2004). These subunits should also form a domain like in Arabidopsis, as a gamma carbonic domain similar to that of Arabidopsis has been found in *Polytomella* (Sunderhaus et al. 2006), a very close relative of Chlamydomonas. This suggests that insertion of these subunits in the complex should follow similar pattern to that proposed in plants. Ten out of the fourteen assembly factors found in humans have putative homologs (Table 1), and the plant-specific factor (GLDH) has also a homolog in *C. reinhardtii* (Table 1), but no functional analysis has never been undertaken on these putative factors. Nevertheless, subcomplexes observed in mutants obtained in the core subunits allow us to suggest a pattern for complex I assembly. Indeed, in *nd5* or *nd4* mutants and in a mutant affected in the nucleus-encoded NUOB10 subunit (PDSW), a 700 kDa subcomplex assembles and contains all modules except the P_d module, as proteomic analysis suggested (Cardol et al. 2002, 2008; Barbieri et al. 2011). A 200 kDa soluble subcomplex, bearing NADH dehydrogenase activity, is observed in wild-type, *nd4* and *nd5* mutants and is the only module detected in *nd1*, *nd6*, *nd3*, and *nd4L* mutants (Cardol et al. 2002, 2006). It has been shown to contain at least the NUOS1 (75 kDa) subunit (N module) and the NUO7 (ND7) subunit (Q module) (Cardol et al. 2002)

Table 1 Gene name of subunits and assembly factors of the mitochondrial OXPHOS chain

Homo sapiens	*Saccharomyces cerevisiae*	*Arabidopsis thaliana*	*Chlamydomonas reinhardtii*	Reference
Complex I				
Core subunits				
NDUFS7	nuo19.3 [j]	PSST	*NUO10* (PSST)	a,f
NDUFS8	nuo21.3c [j]	TYKY	*NUO8* (TYKY)	a,f
NDUFV2	nuo24 [j]	24 kDa	*NUO5* (24 kDa)	a,f
NDUFS1	nuo78 [j]	75 kDa	*NUOS1* (75 kDa)	a,f
NDUFV1	Nuo51 [j]	51 kDa	*NUO6* (51 kDa)	a,f
NDUFS2	nuo49 [j]	Nad7	*NUO7* (ND7)	a,f
NDUFS3	nuo30.4 [j]	Nad9	*NUO9* (ND9)	a,f
ND1	ndh-1 [j]	Nad1	*nd1*	a,f
ND2	ndh-2 [j]	Nad2	*nd2*	a,f
ND3	ndh-3 [j]	Nad3	*NUO3* (ND3)	a,f
ND4	ndh-4 [j]	Nad4	*nd4*	a,f
ND4L	Mt-nd4l [j]	Nad4L	*NUO11* (ND4L)	a,f
ND5	ndh-5 [j]	Nad5	*nd5*	a,f
ND6	ndh-6 [j]	Nad6	*nd6*	a,f
Supernumerary subunits				
NDUFA1	nuo9.8 [j]	MWFE	*NUOA1*	a,f
NDUFA2	nuo10.5 [j]	B8	*NUOB8*	a,f
NDUFB3	nuo10.6 [j]	B12	*NUOB12*	a,f
NDUFA5	nuo29.9 [j]	B13	*NUOB13*	a,f
NDUFS6	nuo18.4 [j]	13 kDa	*NUOS6*	a,f
NDUFA6	nuo14.8 [j]	B14	*NUOB14*	a,f
NDUFA11	nuo21.3b [j]	B14.7	*TIM17*	a,f
NDUFB11	nuo11.7 [j]	NDU12	*NUO17*	a,f
NDUFS5	nuo11.5 [j]	15 kDa	*NUOS5*	a,f
NDUFB4	nuo6.6 [j]	NDU8	*NUOB4*	a,f
NDUFA12	nuo13.4 [j]	DAP13 / B17.2	*NUO13*	a,f
NDUFA13	nuo14 [j]	B16.6	*NUOB16*	a,f
NDUFB7	NCU11348 [j]	B18	*NUOB18*	a,f
NDUFS4	nuo21 [j]	18 kDa	*NUOS4*	a,f
NDUFA8	nuo20.8 [j]	PGIV	*NUOA8*	a,f
NDUFB9	NCU11258 [j]	B22	*NUOB22*	a,f
NDUFB10	Nuo12.3 [j]	PDSW	*NUOB10*	a,f
NDUFA9	Nuo40 [j]	39 kDa	*NUOA9*	a,f
NDUFB8	Nuo20.1 [j]	ASHI	*TEF29*	a,f
NDUFB2	NCU01436 [j]	AGGG	_	a,f
NDUFB1	Nuo20.9 [j]	20.9 kDa	*NUO21*	a,f
NDUFC2	Nuo10.4 [j]	NDU9	*NUOP1*	a,f
NDUFC1	NCU08300 [j]	NDU10	Cre17.g725400	a,f

(continued)

Table 1 (continued)

Homo sapiens	*Saccharomyces cerevisiae*	*Arabidopsis thaliana*	*Chlamydomonas reinhardtii*	Reference
NDUFA3	nuo9.5 [j]	B9	Cre12.g537050	a,f
NDUFAB1	SDAP [j]	_	*ACP1*	a,f
NDUFA7	NCU08930 [j]	B14.5a	Cre12.g484700	a,f
NDUFA4	NCU02016 [j]	At3g29970	_	a,f
NDUFB5	nuo17.8 [j]	SGDH	_	a,f
NDUFA10		ATDNK	*DNK1*	a,f
_	_	CA1	*CAG1*,*CAG2*, *CAG3*	a,f
_	_	CA2		
_	_	CA3		
_	_	CAL1		
_	_	CAL2		
_	_	P1	_	a,f
_	_	P2	_	a,f
_	_	_	*NUOP4*	a,f
_	_	_	*NUOP5*	a,f
_	_	At3g07480	*NUOP3*	a,f
Candidate plant-specific subunits			_	
_	_	At1g68680	_	a,f
_	_	P3	_	a,f
_	_	TIM23–2	TIM23	a,f
_	_	At2g28430	_	a,f
_	_	DUF543	_	a,f
Assembly factors				
NDUFAF1	CIA30 [j]	At1g17350	*NUOAF1*	a,f
_	CIA84 [j]	_	_	a
NUBPL	IND1 [k]	IND1	*MNP1*	a,f
Foxred1	_	At2g24580	Cre16.g671450	a,f
NDUFAF2	NCU00278 [j]	At4g26965	_	a,f
NDUFAF3	_	At3g60150	Cre12.g496800	a,f
NDUFAF4	_	_	_	f
NDUFAF5	_	At1g22800	Cre13.g584750	f
NDUFAF6	NCU09517 [j]	At1g62730	Cre03.g194300	f
NDUFAF7	_	At3g28700	Cre02.g096400	f
TIMMDC1	_	At1g20350	Cre10.g452650	f
TMEM126B	_	_	_	f
Ecsit	_	_	_	f
_	_	GLDH	GLDH	f,g
ACAD9	NCU06543 [j]	IVD	Cre06.g296400	f
AIF	_	MDAR4	*MDAR1*	f

(continued)

Table 1 (continued)

Homo sapiens	*Saccharomyces cerevisiae*	*Arabidopsis thaliana*	*Chlamydomonas reinhardtii*	Reference
Complex II				
SDHA	SDH1	SDH1–1, SDH1–2	*SDH1*	a
SDHB	SDH2	SDH2–1, SDH2–2	*SDH2*	a
SDHC	SDH3	SDH3–1	*SDH3*	a
SDHD	SDH4	SDH4	*SDH4*	a
_	_	SDH5	_	a
_	_	SDH6	_	a
Assembly factors				
SDHAF1	SDH6	At2g39725	*LYR1*	a,b
SDHAF2	SDH5	SDHAF2	Cre12.g550750	a,b
SDHAF3	SDH7	_	_	b
SDHAF4	SDH8	_	_	b
_	FLX1	_	Cre04.g217913	a
_	TCM62	_	_	a
Complex III				
UQCRC1	COR1	COR1	*QCR1*	a
UQCRC2	QCR2	At3g16480, At1g51980	*MPPA2*	a
_	_	_	*MPPA1*	a
MT-CYB	COB	AtMg00220	*cob*	a
CYC1	CYT1	At3g27240, At5g40810	*CYC1*	a
UQCRCFS1	ISP	At5g13440, At5g13430	*RIP1*	a
UQCRQ	QCR7	At4g32470, At5g25450	*QCR7*	a
UQCRB	QCR8	At3g10860, At5g05370	*QCR8*	a
UQCRH	QCR6	At2g01090, At1g15120	*QCR6*	a
UQCR10	QCR9	At3g52730	*QCR9*	a
UQCR10	QCR10	At2g40765	*QCR10*	a
UQCRFS1	_	_	_	a
Assembly factors				
BCS1	BCS1	At5g17760	*BCS1*	a
ABC1	COQ8	At4g01660	*COQ8*	a
_	BCA1	_	_	a
UQCC1	CBP3	At5g51220	Cre01.g052050	a
UQCC3	CBP4	_	_	a,d
UQCC2	CBP6	_	_	a,c
TTC19	_	_	_	a
_	CYC2	_	_	a

(continued)

Table 1 (continued)

Homo sapiens	*Saccharomyces cerevisiae*	*Arabidopsis thaliana*	*Chlamydomonas reinhardtii*	Reference
LYRM7	MZM1	_	Cre07.g332150	a
Cytochrome c				
CYC	CYC1	At1g22840, At4g10040	*CYC*	a
Assembly factors				
System III	System III	System I	System III	a
CCHL	CYT2	_	*HCS1*	a
_	CYC2	_		a
_	CYC3	_	*HCS2*	a
_	_	_	*HCS3*	a
_	_	AtMg00830	_	a
_	_	AtMg00900	_	a
_	_	AtMg00960	_	a
_	_	AtMg00110	_	a
_	_	AtMg00180	_	a
_	_	At1g15220, At3g51790	_	a
Complex IV				
MT-CO1	COX1	COX1	cox1	a
MT-CO2	COX2	COX2	*COX2a*	a
_	_	_	*COX2b*	a
MT-CO3	COX3	COX3	*COX3*	a
COX5b	COX4	_	*COX4/5b*	a
COX4I-1	COX5a	_	_	a
COX4I-2	COX5b	COX5B-1, COX5B-2	_	a
_	_	At3g62400, At2g47380, COX5C	*COX5C*	a
COX5a	COX6	_	_	a
COX7a	COX7	_	_	a
COX7c	COX8	_	_	a
COX6c	COX9	_	_	a
COXVIIb	_	_	_	a
COX8	_	_	_	a
COX6b	COX12	COX6B-1, COX6B-3	*COX12*	a
COX6a	COX13	COX6A	*COX13*	a
_	_	_	*COX90*	a
Assembly factors				
Membrane insertion and processing of complex IV subunits				
OXA1L	OXA1	OXA1	*OXA1*	a
COX20	COX20	_	_	a

(continued)

Table 1 (continued)

Homo sapiens	*Saccharomyces cerevisiae*	*Arabidopsis thaliana*	*Chlamydomonas reinhardtii*	Reference
COX18	COX18	_	*COX18*	a
_	MSS2	_	_	a
_	MSS51	_	_	a
_	PNT1	_	_	a
_	IMP1	_	*IMP1*	a
IMMP2L	IMP2	At3g08980	*IMP2*	a
_	SOM1	_	_	a
Copper metabolism and insertion into complex IV				a
COX17	COX17	COX17–2	*COX17*	a
SCO1, SCO2	SCO1, SCO2	HCC1, HCC2	*SCO1*	a
COX11	COX11	COX11	*COX11*	a
COX19	COX19	COX19–1	*COX19*	a
COX23	COX23	At1g02160	*COX23*	a
PET191	PET191	At1g10865	*PET191*	a
CMC1/CMC2	CMC1/CMC2	At2g07681, ccmC	_	a
Heme A biosynthesis				a
COX10	COX10	COX10	*COX10*	a
COX15	COX15	COX15	*COX15*	a
FDX2	YAH1	MFDX1, MFDX2	*MFDX*	a
ADR	ARH1	_	*ARH1*	a
Assembly				a
_	PET100	At4g14615, At1g52821	_	a
SURF1	SHY1	SURF1	*SUR1*	a
_	COX14	_	_	a
_	COA1/2/3	_	_	a
_	COX25	_	_	a
_	CMC3	_	_	a
_	COA4	_	_	a
CCDC90A	FMP32	_	_	e
Unknown function				a
COX16	COX16	At4g14145	*COX16*	a
CSRP2BP	PET117	_	_	a
ATP synthase				
Fo subcomplex				
ATP6	ATPA	ATP-1	*ATP6*	a
_	_	ATP6–2	_	a
ATP5F1	ATPB	AtMg00640	_	a
ATP5G3	ATPC	AtMg01080, At2g07671	*ATP9A*	a

(continued)

Table 1 (continued)

Homo sapiens	*Saccharomyces cerevisiae*	*Arabidopsis thaliana*	*Chlamydomonas reinhardtii*	Reference
_	_	_	*ATP9B*	a
ATP5H	ATPD	At3g52300	_	a
ATP5I	ATPE	At5g15320	_	a
ATP5J2	ATPF	At4g30010	_	a
ATP5L	ATPG	At2g19680	_	a
ATP5J	ATPH	_	_	a
ATP8	ATP8	AtMg00480		a
ATP5O	ATP5	At5g13450	*ATP5*	a
ATPI	INH1, STF1	At5g04750	_	a
_	STF2	_	_	a
_	ATPJ/I	_	_	a
F1 subcomplex				
ATP5A1	α	AtMg01190, At2g07698	*ATP1(α)*	a
ATP5B	β	At5g08670, At5g08680	*ATP2 (β)*	a
		At5g08690		a
ATP5C1	γ	At2g33040	*ATP3 (γ)*	a
ATP5D	δ	At5g47030	*ATP16 (δ)*	a
ATP5E	ε	At1g51650	*ATP15 (ε)*	a
_	ATPK	_	_	a
_	_	At2g21870	_	a
_	_	_	*ASA1*	a
_	_	_	*ASA2*	a
_	_	_	*ASA3*	a
_	_	_	*ASA4*	a
_	_	_	*ASA5*	a
_	_	_	*ASA6*	a
_	_	_	*ASA7*	a
_	_	_	*ASA8*	a
_	_	_	*ASA9*	a
Assembly factors				
Fo subcomplex				
_	ATP10	AAF18252	_	a
ATP23	ATP23	_	_	a
_	ATP25	At3g03420.1	Cre17.g697934	a
OXA1L	OXA1	OXA1	*OXA1*	a
_	ATP22	_	_	i
F1 subcomplex				
ATPAF1	ATP11	At2g34050	*ATP11*	a
ATPAF2	ATP12	At5g40660	*ATP12*	a
_	FMC1	_	*FMC1*	a

(continued)

Table 1 (continued)

Homo sapiens	*Saccharomyces cerevisiae*	*Arabidopsis thaliana*	*Chlamydomonas reinhardtii*	Reference
_	HSP90	_	*HSP90*	h
Alternative oxidase				
_	AOX-AAC37481 [j]	AOX1a,AOX1b, AOX1c,AOX1d,	*AOX1*	a
_		AOX2	*AOX2*	
Type-II NAD(P)H dehydrogenase family				
_	NDAe1, NDAe2, NDAi1	NDA1, NDA2	*NDA1*, *NDA5*	a
		NDB, NDB2	*NDA6*, *NDA7*	
		NDB3, NDB4		
		NDC		

Adapted from (a) Salinas et al. (2014), (b) Van Vranken et al. (2015), (c) Tucker et al. (2013), (d) Brand et al. (2014), (e) Paupe et al. (2015), (f) Subrahmanian et al. (2016), (g) Klodmann and Braun (2011), (h) Francis and Thorsness (2011), (i) Helfenbein et al. (2003)

[j]Data retrieved from *N. crassa*

[k]Data retrieved from *Y. lipolytica*

Gene names of complex I subunits of *A. thaliana* follow bovine nomenclature for the core and supernumerary subunits. P1, P2, At3g07480 and gamma carbonic anhydrase (CA1, CA2, CA3, CAL1, CAL2) do not have bovine counterparts but are not plant-specific either

and was postulated to be an early assembly intermediate (Subrahmanian et al. 2016). Interestingly, recent studies showed that a *NUO7*-RNAi cell line still possesses the 200 kDa module (Massoz et al. 2014) despite the strong downregulation of the *NUO7* transcript and the absence of a whole complex I. In addition, the NUOS1 subunit (75 kDa subunit) was detected in the *NUO7*-RNAi cell line by immunoblotting on membrane extracts, while the NUO8 (TYKY) and NUO10 (PSST) subunits of the Q module were absent (Massoz et al. 2014). Thus, the question of the nature of the 200 kDa module arises. Considering that both the N module and an early Q module would have similar size (Fig. 2), they would co-migrate in BN-PAGE. We thus propose that the subunit identification made in 2002 when we isolated the subcomplex at 200 kDa was performed on both modules, which explains the presence of NUO7 (Q module) and NUOS1 (75 kDa subunit) (N module) in this previous analysis. This co-migration also explains that the *NUO7*-RNAi cell line would still present the 200 kDa module (N module) while the Q module would be absent. Together these results suggest that the Q and N module assembles independently.

In conclusion, we suggest, three subcomplexes could be detected in Chlamydomonas complex I mutants isolated so far: (1) a 700 kDa subcomplex still possessing NADH dehydrogenase activity and barely attached to the membrane. A subcomplex similar to the 700 kDa subcomplex has been identified in maize deficient of ND4 (Karpova and Newton 1999), while in human cell lines, ND4-deficient cell lines do not assemble the membrane components of complex I (Hofhaus and Attardi 1993). (2) A 200 kDa module maintaining a NADH

dehydrogenase activity would correspond to the N module alone; such module containing NDUFS1, NDUFV2, and NDUFV1 was reported to accumulate in TIMMDC1-deficient knockdown cell lines in humans (Guarani et al. 2014); and (3) a putative ±200 kDa early intermediate corresponding to the Q module and containing at least NUO7/NUO8/NUO9/NUO10. It could be similar to the "subcomplex 3" observed in various organisms including humans during complex I assembly (Vogel et al. 2007; Guarani et al. 2014). These elements are summarized in Fig. 2.

In Chlamydomonas, complex I is a 950 kDa complex composed of up to 47 subunits (Subrahmanian et al. 2016). All core subunits are conserved, but the NUO3 (ND3) and NUO11 (ND4L) subunits are nucleus-encoded, as opposed to their mammalian counterparts (Cardol et al. 2006). In addition to the 14 core subunits, *C. reinhardtii* complex I is also composed of up to 33 supernumerary subunits (see Table 1). Two subunits, NUOP4 and NUOP5, are specific to *C. reinhardtii* and *Volvox* sp. (see https://phytozome.jgi.doe.gov/). The CAG1, CAG2, and CAG3 subunits are homologous to the gamma carbonic anhydrase (CA) subunits of *A. thaliana* where two additional subunits (CAL1, CAL2) are also present (see above).

C. reinhardtii is attractive for studying complex I because algae deficient of that complex survive due to the support of alternative NADH dehydrogenases (Lecler et al. 2012) and photosynthesis. Many mutants have been identified, mostly impaired in core mitochondrion- or nucleus-encoded subunits, and some of them in supernumerary ones [reviewed in Salinas et al. (2014), Subrahmanian et al. (2016)] including the NUOP4 subunit specific to *C. reinhardtii* (Massoz et al. 2015). Complex I mutants are generally screened based on their slow growth in the dark phenotype. Indeed, their growth is significantly slower than wild type in these conditions because they only retain two of the three phosphorylation sites that are operational when electron transfer proceeds through the whole respiratory chain. In contrast complex III and complex IV mutants do not grow in the dark (see further) because they lack the cytochrome pathway and thus only retain one of the proton-pumping enzymes of the respiratory chain. The less affected phenotype of complex I mutants compared to complex III and complex IV mutants is also observed in the light under mixotrophic conditions (light + acetate) for the same reason (Remacle et al. 2001; Cardol et al. 2002; Massoz et al. 2014). As a consequence, very little changes of their proteome are observed while a decreased ROS production of about 30% is found (Massoz et al. 2014). Overall, this phenotype is much less severe than that observed in vascular plants like maize, tobacco, and *Arabidopsis thaliana*, which are male sterile and/or display abnormal leaf development [reviewed in Subrahmanian et al. (2016)].

2.2 Complex II

Complex II (1.3.5.1) catalyzes the reversible conversion of succinate into fumarate and as such is also part of the Krebs cycle (Fig. 1):

$$\text{succinate} + Q \Leftrightarrow \text{fumarate} + QH_2$$

It is a small multiprotein complex of about 110 kDa composed of four subunits in most eukaryotes, including Chlamydomonas. The two matrix subunits, Sdh1 and Sdh2, are anchored to the membrane by the Sdh3 and Sdh4 membrane subunits. The Sdh1 subunit contains a flavin adenine dinucleotide (FAD) cofactor. The Sdh2 subunit is an iron-sulfur-containing protein bearing three Fe-S centers (2Fe-2S, 4Fe-4S, and 3Fe-4S). Sdh3 and Sdh4 harbor two ubiquinone reduction sites and a *b*-type heme at the interface of both subunits. Only the high-affinity ubiquinone reduction site (Q_p) is used during electron transport, and the crystal structure of complex II has shown that the Q_p is formed by Sdh3 and Sdh4 but also part of the Sdh2 domain (Sun et al. 2005). The role of both the *b*-type heme and low-affinity ubiquinone reduction (Q_d) sites remains unclear. Yeasts deprived of their *b*-type heme are still able to assemble a functional complex II (Oyedotun et al. 2007).

Unlike complexes I, III, or IV, complex II does not contribute to the formation of the proton gradient. The succinate oxidation into fumarate has been described to function as a two-state "free-occupied mechanism" (Cheng et al. 2015) where the reaction would go as follows: Binding of succinate to complex II induces conformational changes of the enzyme from free to occupied. During occupied conformation, the FAD cofactor is reduced. The occupied conformation becomes unstable once the FAD is reduced into $FADH^-$, and the conformational equilibrium is shifted toward free again, where fumarate binding is unfavorable and thus released. The electron can then be transferred to the nearest Fe-S cluster (2Fe-2S) and then to the 4Fe-4S and 3Fe-4S centers, and the cycle is repeated.

In OXPHOS complexes, the most hydrophobic subunits are encoded in the mitochondrial genome, while most hydrophilic subunits are encoded in the nuclear genome. In contrast, all four subunits, including the membrane-anchored Sdh3 and Sdh4, are usually encoded in the nuclear genome except in primitive mitochondrial genomes such as the one of *Reclinomonas americana* where Sdh3 is found (Lang et al. 1997). The exact mechanism for the assembly of complex II has yet to be fully comprehended, but clues have been given by studies on yeast. We currently know six assembly factors involved in complex II biogenesis [reviewed in Rutter et al. (2010), and Van Vranken et al. (2015)]. It is accepted that Sdh1 and Sdh2 matrix proteins dimerize prior to the assembly with Sdh4 and Sdh3 membrane proteins. The first step of the assembly process is the maturation of the Sdh1 and Sdh2 subunits. The insertion of the FAD cofactor to Sdh1 requires Flx1, a protein involved in maintaining the mitochondrial matrix balance in flavin nucleotide (Tzagoloff et al. 1996). The flavinylation of FAD requires Sdh5, a mitochondrial assembly factor (Hao et al. 2009), which is only found associated with Sdh1, when the latter is not dimerized with Sdh2. Sdh5 is likely to interact with Sdh1 but not directly with the FAD group. Interestingly, loss of Sdh5 does not lead to complete impairment of complex II (Van Vranken et al. 2015; Eletsky et al. 2012). During this stage, the Sdh8 assembly factor has been shown to be associated with Sdh1

until dimerization occurs. Its role has been speculated to protect FAD and to maintain Sdh1 in an assembly-competent state (Van Vranken et al. 2015).

Regarding Sdh2 maturation, incorporation of the Fe-S clusters is needed prior to dimerization. This step involves at least two assembly factors named Sdh6 and Sdh7. Despite the fact that both proteins possess a LYR motif, recently identified as interacting with Fe-S centers in mammals (Rouault 2015), no direct evidence currently points at those proteins as actually playing a role in Fe-S cluster transfer into the Sdh2 subunits. These two assembly factors are thought to protect the Sdh2 subunits and the Sdh1/Sdh2 dimers before assembly with Sdh3 and Sdh4 (Un et al. 2014). Little is known about the Sdh3 and Sdh4 subunits assembly process, beside the fact that Sdh1 and Sdh2 seem to be needed for Sdh3 and Sdh4 to assemble. At last, a protein named Tcm62 has been shown to play a role in complex II assembly. A mutant isolated in yeast was shown to be depleted in complex II activity (Dibrov et al. 1999). The exact role of Tcm62 is still under discussion, but it has been suggested to support protein folding, most likely primarily Sdh2 (Rutter et al. 2010; Dibrov et al. 1999).

In *C. reinhardtii* three out of these six assembly factors have been predicted based on genome analysis (Table 1), but little is known about eventual similarities or differences in the assembly steps. To our knowledge, no complex II mutants have been characterized so far, but a mutant potentially affected of Sdh3 has been identified in the indexed mutant library recently produced (Li et al. 2016). It is interesting to note that even though *C. reinhardtii* is part of the green lineage, its complex II doesn't share the complexity of complex II in land plants which is composed of eight subunits (Salinas et al. 2014).

2.3 Complex III

Complex III (EC 1.10.2.2), the third complex of the OXPHOS chain and the second proton-pumping complex, catalyzes the following reaction:

$$2QH_2 + 2\,\text{ferricytochrome}\ c + 2H^+{}_{\text{Matrix}} \Rightarrow QH_2 + 2\,\text{ferrocytochrome}\ c + 4H^+{}_{\text{IMS}}$$

It functions as a multiprotein homodimeric structure of approximately 490 kDa, each monomer containing ten to eleven subunits in yeast and mammals. Among these, the three core subunits are homologs to the three subunits of prokaryotic complex III (Trumpower 1990b): *cyto*chrome *b* (COB), *cy*tochrome c_1 (CYC1), and Rieske *i*ron-*s*ulfur *p*rotein (ISP), while eight subunits are supernumerary subunits. Cytochrome *b* contains the ubiquinone oxidation site (Q_o) and ubiquinone reduction site (Q_i) separated by two *b*-type hemes. One heme (b_L) is close to the Q_o site and has a low redox potential, and the other heme (b_H) has a high potential heme (Wenz et al. 2009). The Rieske protein contains a 2Fe-2S center allowing transfer from cytochrome *b* to cytochrome c_1. Cytochrome c_1 contains a *c*-type heme.

Complex III participates to proton gradient formation through the Q cycle (Trumpower 1990a). In short, upon oxidation of ubiquinol at the Q_o site (on the IMS side), two protons are released into the IMS while two electrons are transferred through complex III. The first electron will be transferred successively to iron-sulfur Rieske protein, to cytochrome c_1, and then to soluble cytochrome c. The second electron will be transferred on the b_L heme and then on the b_H heme. This electron will then reduce a ubiquinone into a semiquinone at the Q_i site on the matrix side. The newly oxidized ubiquinone will then leave the Q_o site, and the cycle is repeated when a second ubiquinol enters and gets oxidized, leading to a second electron being transferred to cytochrome c and the semiquinone to be fully reduced into ubiquinol on the Q_i site by the second electron. In terms of protons, the result of this four-electron transfer is four protons being ejected into the IMS and two protons from the matrix being used to reduce a ubiquinone on the Q_i site. The key to the Q cycle is the correct routing of both electrons to either the Rieske protein or the b_L heme. The flexibility of the Rieske protein and its dual conformation in oxidizing and reducing competent positions (Zhang et al. 1998) seem to be one of the main elements for the Q cycle. Recently, the so-called surface-affinity-modulated ISP-ED (extrinsic domain of iron-sulfur protein) motion switch hypothesis (Xia et al. 2013) proposes that the binding of a ubiquinol into the Qo site will trigger conformational changes, maybe due to the widening of Qo to accept the substrate. This would transmit a signal to an alpha-helix around Qo to switch into "on" position, increasing the affinity of the Rieske protein for cytochrome b. This will lock the Rieske protein in a position where it can receive an electron from cytochrome b but cannot give it to cytochrome c_1, now too far away. The Rieske protein is locked in docking position with cytochrome b until ubiquinone has been released. This will force the second electron to go through b_L. Once both electrons are transferred and the ubiquinone released, the Rieske protein is freed from its interactions with cytochrome b, allowing it to move to a closer position to cytochrome c_1 and transfer its electron. It has been proposed that the reduction events in both Rieske and b_L happen simultaneously (Zhu et al. 2007).

In complex III, only the COB subunit is synthesized inside the mitochondrion: all other proteins are imported from the cytosol. Currently, our knowledge about complex III assembly is scarce. Indeed, only a limited number of assembly factors have been described from the investigation in yeast. Accordingly, the yeast nomenclature will be used for the following description.

COB is known to be the first protein in the assembly process. Cpb6 and Cpb3 assembly factors are known to be part of the COB assembly process. These proteins have been proposed to interact early in the assembly process directly with the ribosome and to be needed for efficient translation (Gruschke et al. 2011); these two assembly factors are also important for complex III maturation since they are found on early subcomplex intermediates (Gruschke et al. 2012). The Cpb4p assembly factor has also been shown to be part of an early COB subcomplex, though it does not interact with the Cpb3 and Cbp6 assembly factors (Brand et al. 2014). During this first stage of assembly, Qcr7 and Qcr8 supernumerary subunits are added to the newly synthetized COB subunit. Qcr7 and Qcr8 seem important for the progress of

assembly, since the deletion of the corresponding genes prevent further subcomplexes to be produced (Zara et al. 2007). The next step is the assembly of the core protein 1 (encoded by COR1) and core protein 2 (encoded by QCR2) subunits and cytochrome c_1. There is currently no data on how these subunits are assembled, but because their absence prevents the assembly of later subcomplexes, they might be incorporated simultaneously (Zara et al. 2007). It has also been shown that these subunits are able to interact together and form small complexes if the initial COB subcomplex is not present. The incorporation of core proteins 1 and 2 triggers the release of the Cpb4 assembly factor (Gruschke et al. 2012). This stage of assembly is referred to as the late core assembly stage. In addition to the core proteins 1 and 2 and cytochrome c_1 subunits, this intermediary subcomplex also contains the Qcr6 and Qcr9 supernumerary subunits and an additional assembly factor called Bcs1. Bcs1 is an AAA ATPase needed for the latter insertion of ISP (Rieske) protein (Conte et al. 2015). The Bca1 assembly factor has also been shown to play a role in the formation of the late core assembly stage though its exact role is still unknown (Mathieu et al. 2011). At this stage, complex III has been shown to already be in its dimeric conformation (Conte et al. 2015). The last stage of assembly consists in the addition of the ISP (Rieske) protein and the Qcr10 subunits and requires the Bcs1p and Mmz1p assembly factors. Qcr9, along with Mzm1, has been shown to be able to interact specifically with ISP in yeast and in strains where early assembly intermediates are stalled (Phillips et al. 1993; Smith et al. 2012). The Mzm1p possesses a LYR motif that might interact with the Fe-S center of ISP (Smith et al. 2012). The Coq8 protein has been predicted to be a chaperone for complex III (Brasseur et al. 1997) and was also linked to coenzyme Q synthesis pathways (Do et al. 2001). Its role in complex III assembly has thus been proposed to be related to quinone availability. Though only known to be present in metazoans, TTC19, an inner membrane protein possessing a tetratricopeptide motif, has been shown to be involved in complex III assembly (Ghezzi et al. 2011), possibly as a chaperone. In *C. reinhardtii*, only four assembly factors have been identified so far in the genomic sequence (Table 1).

Cytochromes *c* are redox-active proteins containing a *c*-type heme covalently bound by two cysteine residues. In mitochondria, cytochromes *c* are represented by cytochrome c_1 in complex III and soluble cytochrome *c*. Various assembly mechanisms have been identified and described for cytochromes *c* (Mavridou et al. 2013; Allen et al. 2008). In mitochondria, system III is used to import and mature cytochrome *c*, while cytochrome *c1* is imported differently through the TIM/TOM machineries (Mavridou et al. 2013). System III requires the intervention of a unique enzyme for the cytochrome *c* maturation, the cytochrome *c* heme lyase, or the cytochrome *c1* heme lyase. In yeast, Cyt2 has been shown to be a cytochrome c_1 heme lyase (Zollner et al. 1992), and Cyc3 have been shown to be a cytochrome *c* heme lyase (Dumont et al. 1987), though the latter was shown to also be active on cytochrome c_1 (Bernard et al. 2003). In *C. reinhardtii*, cytochrome *c* and cytochrome c_1 lyases are also present (Bernard et al. 2003). Humans only possess one gene with both functions (Prakash et al. 2002). In yeast, Cyc2 is also involved in cytochrome c/c_1 maturation. Cyc2 was proposed to regulate Cyc3 activity and

participate in heme attachment. It seems to be essential when Cyt2 is inactive (Bernard et al. 2003; Smith et al. 2012). No Cyc2 homolog was found in *C. reinhardtii* (Salinas et al. 2014).

Complex III in *C. reinhardtii* probably possesses eleven subunits (Table 1). Among them, ten are conserved between *C. reinhardtii*, humans, and *A. thaliana*, MPPA1 being the only protein specific to *C. reinhardtii*. Core protein 1 and core protein 2 from higher plants possess a proteolytic activity (mitochondrial processing peptidase or MPP) that cleaves the transit peptide of preproteins when they are imported into mitochondria (Glaser and Dessi 1999). In Chlamydomonas, QCR1 (homolog of core 1 protein) exhibits consensus sequences typical of β-MPP protein, while MPPA2 (homolog of core 2 protein) does not share consensus sequences for α-MPP activity (van Lis et al. 2003). Nevertheless, a third component, with the characteristics of an MPP α-subunit (MPPA1), is also encoded in Chlamydomonas (Cardol et al. 2009a). The question of the in vivo mitochondrial processing activity of complex III in *C. reinhardtii* remains thus open.

In *C. reinhardtii*, only *cob* mutants have ever been produced (listed in Salinas et al. 2014), resulting in a lack of complex III activity and assembly due to the central position of cytochrome *b* subunit. Chlamydomonas complex III mutants lack the whole cytochrome pathway of respiration due to the colinearity of both complexes III and IV. The resulting lack of ATP caused by the loss of the two proton-pumping enzymes leads to the inability of such mutants to grow under heterotrophic condition (acetate + dark) (Salinas et al. 2014). This inability to grow in the dark is the main screening method currently used to obtain complex III mutants. Mutants can also be identified using a TTC (triphenyltetrazolium chloride) reducing test (Dorthu et al. 1992). In *C. reinhardtii*, complex III deficiencies have been shown to be impactful enough to disturb photosynthesis (Cardol et al. 2003). When coupled with a *stt7* mutation, leading to the lack of flexibility in energy redistribution between photosystems, complex III mutants display a drop in photosynthetic efficiency when measured both in the dark and the light. This phenotype allows easy identification of complex III mutants using fluorescence measurements (Cardol et al. 2009b; Massoz et al. 2015).

2.4 Complex IV

Complex IV (1.9.3.1) is the last proton-pumping complex of the OXPHOS chain with a size of approximately 200 kDa. It catalyzes the reaction:

$$4 \text{ ferrocytochrome } c + O_2 + 8H^+_{\text{matrix}} \rightarrow 4 \text{ ferricytochrome } c + 2H_2O + 4H^+_{\text{IMS}}$$

The Cox1, Cox2, and Cox3 subunits are the core subunits of complex IV. The Cox1 subunit bears heme *a*, heme a_3, and the Cu_B center. The Cox2 subunit carries the Cu_A center, while the Cox3 subunit does not bear any prosthetic groups. In most organisms, Cox1, Cox2, and Cox3 are encoded in the mitochondrial genome as they

are membrane-embedded subunits. In addition, around seven to eleven supernumerary subunits have been identified in mammals, yeasts, or plants [reviewed in Salinas et al. (2014)].

In complex IV, four electrons are transported onto molecular oxygen to produce two water molecules, while four protons are transferred into the IMS. Two proton-transfer channels have been identified in the Cox1 protein. They are called D and K channels, based on the presence of conserved Asp (D) and Lys (K) residues at the beginning of each channel, respectively. The D channel is filled with a series of ordered water molecules forming a proton-conductive pathway and helping to reach a conserved Glu residue at its end. Electrons are transferred from soluble cytochrome *c* through Cu_A and heme *a* toward the binuclear center (Cu_B and heme a_3; BNC). The proton-transfer mechanisms contain several steps involving the BNC and are reviewed in Kaila et al. (2010). In short, the ligation of the molecular oxygen to the BNC leads to a split of the molecule. Following that event, four cycles of one-electron reduction step occur, accompanied by the pumping of two protons each time: one into the proton-loading site (PLS) and one into the BNC for chemistry. Though the four cycles have identical chemical balance, they all possess different kinetics. The proton pumped into the PLS is transferred into the IMS by a still unknown mechanism. It has been shown that the K channel only participates in one (maybe two) proton transfer(s) (Wikström et al. 2000; Svensson-Ek et al. 2002). Notably, during the reductive phase when the heme a_3 might be already bound to a water molecule, (the) proton(s) would be pumped through the K channel which is the closest to the Cu_B center. This would lead the D channel to effectively pump the four protons leading to the PLS and at least two of the protons leading to the BNC. From this perspective, one can ask how protons from the same channel can be routed toward PLS or BNC. Water wire pathways would form leading preferentially toward one site or another (Wikström et al. 2000). This water gate phenomenon has been shown to be dependent on the redox state of the two hemes of the enzyme and helps redirect proton toward the right site. The Cox3 subunit is a major subunit of complex III, but it does not carry any redox component. It has been shown that a mutant in COIII (Cox3 homolog) of *Paracoccus denitrificans* might assemble a COI and COII (Cox1 and Cox2 homolog) subcomplex, though not properly functional (Haltia et al. 1989). Studies showed that Cox3 was important for maintaining the correct function of the D channel (Hosler 2004). The Cox3 area surrounding the conserved Asp in the D channel has been proposed to raise the proton affinity for this conserved amino acid to trap protons. In addition, COXIII has been shown to stabilize a hydrocarbon chain in close proximity to the water chain inside the D channel, potentially helping them to maintain a correct arrangement inside the channel. COXIII also plays a key role in maintaining the exit proton pathway.

Complex IV biogenesis is by far the most understood assembly process among OXPHOS complexes in yeast with more than 30 assembly factors identified so far, with various functions from RNA stabilization to heme maturation. Unfortunately, most of these identified proteins have no equivalents in Chlamydomonas (Table 1). It is accepted that the three Cox subunits assemble and mature independently of each

other before being assembled together. This process is reviewed in Soto et al. (2012). The Cox1 subunit is the first to be inserted in the membrane, a process which requires at least the conserved Oxa1 protein. Cox2 is then inserted and processed in the membrane, thanks to at least Oxa1 in addition to the Cox20 and Cox18 assembly factors. The two proteins will then be attached to each other. The Cox3 subunit will then be assembled and attached to the Cox1 and Cox2 subcomplex. Unlike the Cox assembly process, the heme insertion and maturation assembly seem much more conserved between yeast and Chlamydomonas. The current knowledge is reviewed in Barrientos et al. (2009) and Soto et al. (2012). The copper cofactor maturation pathway involved the Cox17, Cox19, and Cox23 assembly factors; these three soluble proteins possess copper-binding motifs and are thought to be part of a copper distribution pathway. The Cox17 assembly factor would also transfer copper to Sco1 and Cox11, two membrane chaperones proposed to facilitate copper insertion into the Cox1 and Cox2 subunits. *Cox17* mutants have been produced in Chlamydomonas (Remacle et al. 2010). In *cox17* mutants, total amount of complex IV was found unchanged, but complex IV activity was decreased, an observation that was explained by a diminished copper availability. Inside complex IV, hemes *a* are present. These hemes are derived from heme *b* transformed into heme *O* and then finally into heme *a*. The conversion from heme *b* to heme *O* is processed by at least Cox10, while the conversion from heme *O* to heme *a* is processed through two discrete monooxygenase steps. The first step is catalyzed by at least Cox15, Mfdx (Yah1 in yeast) (Barros et al. 2001), and Arh1 (Soto et al. 2012). No enzyme has been yet identified as candidate for the subsequent oxidation step (Soto et al. 2012). Interestingly, a *C. reinhardtii* mutant (called w17) was recently identified in a hydroxylase/monooxygenase with a partial dark growth defect phenotype (Massoz et al. 2015). It was later shown that this mutant possessed a 30% reduced complex IV activity (Massoz, unpublished data), though a clear relationship between the depleted gene and the actual phenotype remains to be demonstrated.

In *C. reinhardtii*, ten subunits have been confirmed to compose complex IV, and eight potential subunits homologous to those found in other eukaryotes were found in the genome (Cardol et al. 2005; van Lis et al. 2003) including the subunit COX90 specific to Chlamydomonas (Lown et al. 2001). COX2 and COX3 are encoded in the nucleus in *C. reinhardtii* (Perez-Martinez et al. 2001, 2002). In addition, the *COX2* gene is split into *COX2a* and *COX2b* genes, a characteristic shared by all chlorophycean algae (Rodriguez-Salinas et al. 2012). Both *COX3* and *COX2a*/*b* have gained attributes from nuclear genomes, proper codon usage and introns, and an overall decreased hydrophobicity in the corresponding gene products compared to their mitochondria-encoded counterparts (Perez-Martinez et al. 2001).

Complex IV nuclear mutant (*cox3* mutant) or mitochondrial mutant (*cox1* mutant) in *C. reinhardtii* shows no complex IV activity or assembly altogether (Colin et al. 1995; Remacle et al. 2010) and, like complex III mutants, lack the whole cytochrome pathway of respiration.

2.5 ATP Synthase

Mitochondrial F_1Fo-ATP synthase (EC 3.6.1.3) has a pivotal role in OXPHOS by catalyzing the reaction ADP + Pi + $n{H^+}_{IMS}$ <=> ATP + $n{H^+}_{Matrix}$. The complex is present in the inner mitochondrial membrane and forms oligomers that are believed to determine the morphology of the yeast mitochondrial cristae (Paumard et al. 2002). Although exhibiting some differences, the well-characterized yeast and the beef heart enzymes share a similar subunit composition. The enzyme works as a molecular motor (Oster and Wang 2003) with a central rotary axis [formed by subunits γ/δ/ε/*c*-ring] and several fixed elements that include the catalytic core (subunits α_3/β_3), a peripheral stalk (OSCP/*b*/*d*/F6), a dimerization module (A6L/*e*/*f*/*g*), and other fixed elements (subunit *a*) (Arselin et al. 2004; Walker and Dickson 2006). Proton passage through both subunit *a* and the *c*-ring induces the rotation of the γ/δ/ε central stalk (Wächter et al. 2011). The rotation of subunit γ impels the three catalytic β-subunits to form ATP from ADP + Pi (Yasuda et al. 1998). The peripheral stalk impedes rotation of the α_3/β_3 moiety while counteracting the torque generated by the rotation of the γ-subunit (Dickson et al. 2006). Regulatory polypeptides, such as the inhibitory protein IF_1, prevent the enzyme from hydrolyzing ATP (Gledhill and Walker 2005).

The mitochondrial ATP synthase of chlorophycean algae has diverged substantially from the yeast and bovine enzymes and exhibits salient differences in terms of subunit composition and structural features. For example, both the *C. reinhardtii* β- and α-subunits exhibit atypical sequence extensions of 70 residues in the C-terminus and of 18 residues in the N-terminus, respectively (Franzén and Falk 1992; Nurani and Franzén 1996). Much has been learned on the structure and function of the mitochondrial ATP synthase from algae by studying the enzyme from *Polytomella* sp., a colorless, close relative of Chlamydomonas that lacks chloroplasts and a cell wall (Figueroa-Martinez et al. 2015). Lauryl maltoside-solubilized mitochondrial F_1Fo-ATP synthases of *C. reinhardtii* and *Polytomella* sp. migrate in blue-native electrophoresis as a 1600 kDa dimer (van Lis et al. 2003; Villavicencio-Queijeiro et al. 2009). When the *C. reinhardtii* genome became known (Merchant et al. 2007), the components of the enzyme whose N-terminal sequences had been previously obtained by Edman degradation (Funes et al. 2002) were identified. Thus, the enzyme was found to be constituted by the classical subunits α, β, γ, δ, *a* (ATP6), *c* (ATP9), and OSCP, while no homologs of the ε, *b*, *d*, *e*, *f*, *g*, IF_1, A6L, and F6 subunits could be found encoded in the algal genome. In addition, the enzyme contained polypeptides with no known counterparts in the databases, and these were named Asa1 to Asa9, for "ATP synthase associated components" (Fig. 3). The polypeptide composition of the mitochondrial ATP synthase of *Polytomella* sp. was found to be similar to the one of *C. reinhardtii* enzyme (Vazquez-Acevedo et al. 2006; van Lis et al. 2007). Although the biochemical characterization of the mitochondrial ATP synthase has been carried out mainly with *C. reinhardtii* and *Polytomella* sp., genes encoding homologs of Asa subunits are found in other chlorophycean algae including members of the genera Chlamydomonas,

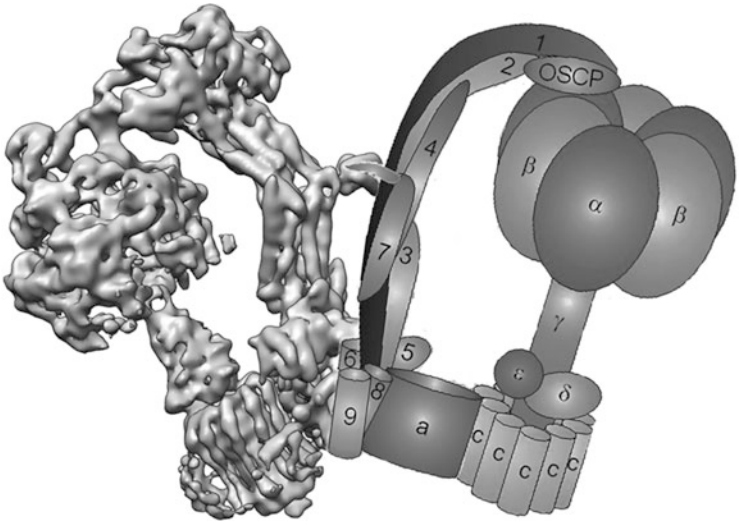

Fig. 3 Subunit composition and localization of Chlamydomonas mitochondrial ATP synthase

Chloroccocum, *Dunaliella*, *Polytomella*, *Scenedesmus*, and *Volvox* (Lapaille et al. 2010; Colina-Tenorio et al. 2015). The idea that these unique proteins could be the main constituents of the peripheral stalk of the complex and the elements responsible of the enzyme's dimeric nature was formulated (Lapaille et al. 2010; Colina-Tenorio et al. 2015). All the subunits that form the mitochondrial ATP synthase of chlorophycean algae seem to be nucleus-encoded; to date, no genes encoding a subunit of the enzyme has been identified in the corresponding algal mitochondrial genomes (Vahrenholz et al. 1993; Smith and Lee 2009; Smith et al. 2010; Hamaji et al. 2013), not even the three mitochondrial genes frequently present in mtDNA: *atp6*, *atp8*, and *atp9*.

The isolated mitochondrial ATPases from the green alga *C. reinhardtii* exhibited a specific activity of 2.9 U/mg with only 40% sensitivity to oligomycin (Nurani and Franzén 1996), an antibiotic that usually fully inhibits the enzyme. The *Polytomella* sp. enzyme showed a very low ATPase activity that markedly increased up to 3.8 U/mg when nonionic detergents are present in the activity assay. The hydrolytic activity is sensitive to the classical inhibitors oligomycin and DCCD (Villavicencio-Queijeiro et al. 2015), although oligomycin seems to bind loosely. Indeed, while oligomycin readily inhibits algal growth, respiration, and ATP levels in several classes of chlorophytes, chlorophycean algae seem not to be affected (Lapaille et al. 2010).

Neighboring interactions of Asa subunits in the ATP synthase of *Polytomella* sp. have been studied by silencing the expression of Asa subunits, generating subcomplexes by partial dissociation of complex V, reconstituting subcomplexes using recombinant subunits in vitro, cross-linking the purified enzyme, and modeling the complex by EM image reconstruction. Knockdown experiments using RNA

interference abolished expression of the Asa7 subunit in *C. reinhardtii*. Although neither growth nor OXPHOS of the alga was affected, the intact enzyme could not be isolated, since it dissociated upon lauryl maltoside solubilization (Lapaille et al. 2010). Therefore, Asa7 was proposed to play a pivotal role in maintaining the stability of the peripheral stalk. Asa1 is thought to be the main support of the peripheral stalk, playing a structural role analogous to subunit *b* in orthodox enzymes (Colina-Tenorio et al. 2015), probably making a bridge between the OSCP subunit and other polypeptides that may be embedded in or closer to the membrane (Asa3, Asa5, Asa8, *a* and c_{10}-ring). Subunits Asa2, Asa4, and Asa7 interact to form an Asa2/Asa4/Asa7 subcomplex that establishes contacts with Asa1 and with OSCP (Miranda-Astudillo et al. 2014); thus, the peripheral stalk seems to be formed by the intertwining of several polypeptides, including Asa1, Asa2, Asa4, and Asa7. In contrast, the smaller subunits Asa6, Asa8, and Asa9 are predicted to have transmembrane stretches and to form the dimerization domain of the algal mitochondrial ATP synthase. An updated model for the topological disposition of the 17 polypeptides that constitute the algal enzyme has been proposed recently (Vázquez-Acevedo et al. 2016) and is shown in Fig. 3.

The dimeric algal ATP synthase has been observed in several electron microscopy studies including 3D tomography (Dudkina et al. 2005, 2010; Cano-Estrada et al. 2010). The ATP synthase oligomers seem to make helical arrangements along the cristae membranes, confirming the role of complex V in determining the shape of the inner mitochondrial membrane (Dudkina et al. 2006). An electron cryomicroscopy map of the *Polytomella* sp. dimeric ATP synthase at 6.2 Å resolution (Allegretti et al. 2015) has revealed some finer architectural details (Fig. 3). A salient feature is that the peripheral stalks are very robust and constituted by alpha-helices that seem to form coil-coiled structures that contact the F_1 sector more than once. The overall dimeric structure is further reinforced by protein-protein contacts that unite the two peripheral stalks in their middle region. Subunit *a* was found to contain four alpha-helices that are embedded in the bilayer almost horizontally, partially surrounding the *c*-ring. A high-resolution structure of the algal mitochondrial ATP synthase is still needed in order to learn about the detailed topology of all its components.

Although some studies have addressed the biogenesis of the CF_1-CFo chloroplast ATP synthase of Chlamydomonas (Drapier et al. 2007), almost nothing is known about the assembly of its mitochondrial counterpart. Nevertheless, the mitochondrial enzyme is expected to follow the almost universal three-module process that has been described for the F_1Fo-ATPases of bacteria, chloroplasts, and mitochondria (Rühle and Leister 2015). The biogenesis of the mitochondrial system has been studied in depth in yeast, where complex V assembles in distinct independent modules (Rak et al. 2011): (1) the soluble F_1 module comprising subunits $\alpha_3/\beta_3/\gamma/\delta/\varepsilon$, (2) the c_{10}-ring of the Fo sector, and (3) a stator module comprising subunits *a*/*b*/*d*/*h*/8. In consecutive steps, the F_1 module associates to the membrane-bound c_{10}-ring forming a $\alpha_3/\beta_3/\gamma/\delta/\varepsilon/c_{10}$ subcomplex and subsequently to subunit *a* of the stator module, giving rise to a $\alpha_3/\beta_3/\gamma/\delta/\varepsilon/c_{10}$/*a*/*b*/*d*/*h*/8 subcomplex. The possibility of futile proton efflux in early stages of the assembly of such a complex enzyme driven by the chemiosmotic potential is avoided by the late addition of the c_{10}-ring to the proton-translocating subunit *a*. The whole complex is

then completely stabilized by the further incorporation of the membrane-bound subunit *f* and of the OSCP subunit, the latter one binding to the peripheral stalk and to the α_3/β_3 catalytic core, therefore fixing together all the stator components of the ATP synthase. Dimerization of the enzyme must occur upon the incorporation of the membrane-bound subunits *e* and *g*. One can only speculate that the *C. reinhardtii* complex V will follow a similar biogenesis pathway with a three-module assembly process; nevertheless, it is clear that it will exhibit some distinct features, since the highly robust peripheral arm and the dimerization sector must be assembled through sequential incorporation of all the atypical Asa subunits found only in chlorophycean algae.

The complex assembly of the mitochondrial F_1Fo-ATP synthase is assisted at all stages by several chaperones and assembly factors. The biogenesis of the soluble F_1 module (subunits $\alpha_3/\beta_3/\gamma/\delta/\varepsilon$) is facilitated by the matrix-localized chaperones Fmc1p, Hsp90, Atp11p, and Atp12p (Lefebvre-Legendre et al. 2001; Wang et al. 2001; Francis and Thorsness 2011). Homologs of all these four proteins are present in *C. reinhardtii* (see Table 1). In addition, other players in the formation of the Fo sector have also been identified in the green alga: Atp25 that participates in the expression and oligomerization of subunit *c* (Zeng et al. 2008) and Oxa1 that plays a role in the association of the *c*-ring with subunit *a* (Jia et al. 2007). In contrast, other assembly factors previously characterized in the yeast system including Atp22 (that promotes synthesis of subunit *a*), Atp23 (that is involved in the maturation of subunit *a*), and Atp10 (that promotes the association of subunit *a* with subunit 8) seem not to be present in the green alga.

3 Alternative Pathways

In addition to the four main complexes, alternative type-II NAD(P)H dehydrogenases can transfer electrons from NADH to ubiquinone and alternative oxidase (AOX) from ubiquinone to molecular oxygen (Fig. 1). These alternative enzymes do not participate in the formation of a proton gradient. Mitochondrial type-II NAD(P)H dehydrogenases located on the surface of the mitochondrial inner membrane face either the intermembrane space or the matrix. They are monomeric enzymes of 40–60 kDa contrary to the multimeric type-I NADH dehydrogenases (complex I) and usually contain one non-covalently bound FAD as prosthetic group (Møller et al. 1993). Alternative oxidases are homodimeric, and the monomeric unit has a size of about 40 kDa. They contain a covalently bound diiron center that catalyzes the four-electron reduction of dioxygen to water by ubiquinol (Siedow et al. 1995; Shiba et al. 2013). The presence of these two types of enzymes allows for better survival of *C. reinhardtii* mutants affected in complex I, III, or IV and partly explains why isolating mutants deficient of OXPHOS complexes in *C. reinhardtii* is possible.

In *C. reinhardtii*, alternative oxidase is encoded by two genes: *AOX1* and *AOX2* (Dinant et al. 2001), with *AOX1* being the most abundant transcript. Multiple roles are assigned to alternative oxidase. First it serves as security valve preventing

over-reduction of the ubiquinone pool and thus acting as against ROS accumulation (Milani et al. 2001) and allowing a better functioning for complex III, since ubiquinone is required in the Q cycle. Second, the AOX pathway, serving as a modular exit point for electrons, would allow a more constant reoxidation of NADH, which is used as electron acceptor upstream of the OXPHOS. Such functions are reflected in Chlamydomonas AOX-RNAi cell lines (Mathy et al. 2010), where ROS production is increased up to fivefold and the ROS scavenging enzymes are overexpressed. The mutant cell lines also exhibit heavy metabolic changes (Mathy et al. 2010) with an overall decrease in the catabolic pathways such as glycolysis, Krebs cycle, and glyoxylate cycle and a shift toward anabolic pathways. These metabolic changes lead to increased cell size and biomass without any impact on growth rate. In complex III mutants or WT strain exposed to H_2O_2, *AOX1* transcripts exhibit increased expression (Dinant et al. 2001) correlated to an increased amount of proteins (Molen et al. 2006).

AOX has also been shown to be induced in Chlamydomonas by a variety of stresses including cold, ROS exposure, change in the source of nitrogen source (Molen et al. 2006), or heat (Zalutskaya et al. 2015). All these external conditions are likely to activate several specific transcription factors, since a reporter gene built with a 1073 bp fragment of the *AOX1* promoter would not respond to all stresses (Molen et al. 2006). Posttranscriptional regulations are also involved since the complex III inhibitor antimycin A leads to an increase at the transcript level but not at the protein level (Molen et al. 2006).

Alternative NADH dehydrogenase transfers electrons from NADH to the ubiquinone pool. Among the six type-II NADH dehydrogenases identified in Chlamydomonas (Cardol et al. 2005), the 53 kDa NDA1 has been shown to be localized at the inner side of the mitochondrial membrane (Lecler et al. 2012) (Fig. 1), while NDA2 and NDA3 were found to be located in the chloroplast (Jans et al. 2008; Terashima et al. 2010). The loss of NDA1 was correlated to a slight decrease of NADH dehydrogenase activity, but no impact on heterotrophic growth was observed. However, when coupled to a complex I mutation, severe respiratory and growth defects could be observed, underlining the importance of the enzyme in NADH oxidation in the absence of complex I (Lecler et al. 2012).

Acknowledgments Simon Massoz is a recipient of PhD FRIA fellowship (Fond pour la formation à la Recherche dans l'Industrie et dans l'Agriculture). Pierre Cardol is a research associate from F.R.S.-FNRS (Fond de la Recherche Scientifique). Technical support from Q.B.P. Miriam Vázquez-Acevedo and financial support from grants 245486 from CONACyT-F.R.S.-FNRS (Mexico-Belgium) and from grants 239219 (CONACyT, Mexico), IN203311-3 (DGAPA-UNAM, Mexico) and MIS F.4520, FRFC 2.4597, CDR J.0032 and CDR J.0265.17 (Belgian F.R.S.-FNRS) are also gratefully acknowledged.

References

Allegretti M, Klusch N, Mills DJ et al (2015) Horizontal membrane-intrinsic α-helices in the stator a-subunit of an F-type ATP synthase. Nature 521:237–240. doi:10.1038/nature14185

Allen JWA, Jackson AP, Rigden DJ et al (2008) Order within a mosaic distribution of mitochondrial c-type cytochrome biogenesis systems? FEBS J 275:2385–2402. doi:10.1111/j.1742-4658.2008.06380.x

Arselin G, Vaillier J, Salin B et al (2004) The modulation in subunits e and g amounts of yeast ATP synthase modifies mitochondrial cristae morphology. J Biol Chem 279:40392–40399. doi:10.1074/jbc.M404316200

Atteia A, Adrait A, Brugire S et al (2009) A proteomic survey of Chlamydomonas reinhardtii mitochondria sheds new light on the metabolic plasticity of the organelle and on the nature of the α-proteobacterial mitochondrial ancestor. Mol Biol Evol 26:1533–1548. doi:10.1093/molbev/msp068

Baradaran R, Berrisford JM, Minhas GS, Sazanov LA (2013) Crystal structure of the entire respiratory complex I. Nature 494:443–448. doi:10.1038/nature11871

Barbieri MR, Larosa V, Nouet C, Subrahmanian N, Remacle C, Hamel PP (2011) A forward genetic screen identifies mutants deficient for mitochondrial complex I assembly in Chlamydomonas reinhardtii. Genetics 188:349–358. doi:10.1534/genetics

Barrientos A, Gouget K, Horn D et al (2009) Suppression mechanisms of COX assembly defects in yeast and human: Insights into the COX assembly process. Biochim Biophys Acta, Mol Cell Res 1793:97–107. doi:10.1016/j.bbamcr.2008.05.003

Barros MH, Carlson CG, Glerum DM, Tzagoloff A (2001) Involvement of mitochondrial ferredoxin and Cox15p in hydroxylation of heme O. FEBS Lett 492:133–138. doi:10.1016/S0014-5793(01)02249-9

Bernard DG, Gabilly ST, Dujardin G et al (2003) Overlapping specificities of the mitochondrial cytochrome c and c 1 heme lyases. J Biol Chem 278:49732–49742. doi:10.1074/jbc.M308881200

Berrisford JM, Baradaran R, Sazanov LA (2016) Structure of bacterial respiratory complex I. Biochim Biophys Acta Bioenergetics. doi:10.1016/j.bbabio.2016.01.012

Brandt U (2011) A two-state stabilization-change mechanism for proton-pumping complex i. Biochim Biophys Acta Bioenerg 1807:1364–1369. doi:10.1016/j.bbabio.2011.04.006

Brasseur G, Tron P, Dujardin G, Slonimski P (1997) The nuclear ABCl gene is essential for the correct conformation and functioning of the cytochrome bc, complex and the neighbouring complexes II and IV in the mitochondrial respiratory chain. Eur J Biochem 246:103–111

Bricker DK, Taylor EB, Schell JC et al (2012) A mitochondrial pyruvate carrier required for pyruvate uptake in yeast, Drosophila, and humans. Science 337:96–100. doi:10.1126/science.1218099

Cano-Estrada A, Vazquez-Acevedo M, Villavicencio-Queijeiro A et al (2010) Subunit-subunit interactions and overall topology of the dimeric mitochondrial ATP synthase of Polytomella sp. Biochim Biophys Acta Bioenerg 1797:1439–1448. doi:10.1016/j.bbabio.2010.02.024

Cardol P (2011) Mitochondrial NADH:Ubiquinone oxidoreductase (complex I) in eukaryotes: a highly conserved subunit composition highlighted by mining of protein databases. Biochim Biophys Acta Bioenerg 1807:1390–1397. doi:10.1016/j.bbabio.2011.06.015

Cardol P, Matagne RF, Remacle C (2002) Impact of mutations affecting ND mitochondria-encoded subunits on the activity and assembly of complex I in chlamydomonas. Implication for the structural organization of the enzyme. J Mol Biol 319:1211–1221. doi:10.1016/S0022-2836(02)00407-2

Cardol P, Gloire G, Havaux M et al (2003) Photosynthesis and state transitions in mitochondrial mutants of Chlamydomonas reinhardtii affected in respiration. Plant Physiol 133:2010–2020. doi:10.1104/pp.103.028076.transition

Cardol P, Vanrobaeys F, Devreese B et al (2004) Higher plant-like subunit composition of mitochondrial complex I from Chlamydomonas reinhardtii: 31 conserved components among eukaryotes. Biochim Biophys Acta Bioenerg 1658:212–224. doi:10.1016/j.bbabio.2004.06.001

Cardol P, González-Halphen D, Reyes-Prieto A et al (2005) The mitochondrial oxidative phosphorylation proteome of Chlamydomonas reinhardtii deduced from the Genome Sequencing Project. Plant Physiol 137:447–459. doi:10.1104/pp.104.054148

Cardol P, Lapaille M, Minet P et al (2006) ND3 and ND4L subunits of mitochondrial complex I, both nucleus encoded in Chlamydomonas reinhardtii, are required for activity and assembly of the enzyme. Eukaryot Cell 5:1460–1467. doi:10.1128/EC.00118-06

Cardol P, Boutaffala L, Memmi S et al (2008) In Chlamydomonas, the loss of ND5 subunit prevents the assembly of whole mitochondrial complex I and leads to the formation of a low abundant 700 kDa subcomplex. Biochim Biophys Acta Bioenerg 1777:388–396. doi:10.1016/j.bbabio.2008.01.001

Cardol P, Alric J, Girard-bascou J, Franck F et al (2009a) Impaired respiration discloses the physiological significance of state transitions in Chlamydomonas. Proc Natl Acad Sci USA 106:15979–15984

Cardol P, Figueroa F, Remacle C, et al (2009b). Oxidative phosphorylation: building blocks and related component. The *Chlamydomonas* sourcebook, 2nd edn, 2, pp 469–503

Cheng VWT, Piragasam RS, Rothery RA et al (2015) Redox state of flavin adenine dinucleotide drives substrate binding and product release in Escherichia coli succinate dehydrogenase. Biochemistry 54:1043–1052. doi:10.1021/bi501350j.Redox

Colin M, Dorthu MP, Duby F et al (1995) Mutations affecting the mitochondrial genes encoding the cytochrome oxidase subunit I and apocytochrome b of Chlamydomonas reinhardtii. Mol Gen Genet 249:179–184. doi:10.1007/bf00290364

Colina-Tenorio L, Miranda-Astudillo H, Cano-Estrada A et al (2015) Subunit Asa1 spans all the peripheral stalk of the mitochondrial ATP synthase of the chlorophycean alga polytomella sp. Biochim Biophys Acta Bioenerg 1857:359–369. doi:10.1016/j.bbabio.2015.11.012

Conte A, Papa B, Ferramosca A, Zara V (2015) The dimerization of the yeast cytochrome bc 1 complex is an early event and is independent of Rip1. Biochim Biophys Acta Mol Cell Res 1853:987–995. doi:10.1016/j.bbamcr.2015.02.006

Dibrov E, Fu S, Lemire BD (1999) The Saccharomyces cerevisiae TCM62 gene encodes a chaperone necessary for the assembly of the mitochondrial succinate dehydrogenase (complex II). J Biol Chem 273:32042–32048. doi:10.1074/jbc.273.48.32042

Dickson VK, Silvester JA, Fearnley IM et al (2006) On the structure of the stator of the mitochondrial ATP synthase. EMBO J 25:2911–2918. doi:10.1038/sj.emboj.7601177

Dinant M, Baurain D, Coosemans N et al (2001) Characterization of two genes encoding the mitochondrial alternative oxidase in Chlamydomonas reinhardtii. Curr Genet 39:101–108. doi:10.1007/s002940000183

Do TQ, Hsu AY, Jonassen T et al (2001) A defect in coenzyme Q biosynthesis is responsible for the respiratory deficiency in Saccharomyces cerevisiae abc1 mutants. J Biol Chem 276:18161–18168. doi:10.1074/jbc.M100952200

Dorthu MP, Remy S, Michel-Wolwertz MR et al (1992) Biochemical, genetic and molecular characterization of new respiratory-deficient mutants in Chlamydomonas reinhardtii. Plant Mol Biol 18:759–772

Drapier D, Rimbault B, Vallon O et al (2007) Intertwined translational regulations set uneven stoichiometry of chloroplast ATP synthase subunits. EMBO J 26:3581–3591. doi:10.1038/sj.emboj.7601802

Duarte M, Mota N, Pinto L, Videira A (1998) Inactivation of the gene coding for the 30.4-kDa subunit of respiratory chain NADH dehydrogenase: Is the enzyme essential for Neurospora? Mol Gen Genet 257:368–375. doi:10.1007/s004380050659

Dudkina NV, Heinemeyer J, Keegstra W et al (2005) Structure of dimeric ATP synthase from mitochondria: An angular association of monomers induces the strong curvature of the inner membrane. FEBS Lett 579:5769–5772. doi:10.1016/j.febslet.2005.09.065

Dudkina NV, Sunderhaus S, Braun HP, Boekema EJ (2006) Characterization of dimeric ATP synthase and cristae membrane ultrastructure from Saccharomyces and Polytomella mitochondria. FEBS Lett 580:3427–3432. doi:10.1016/j.febslet.2006.04.097

Dudkina NV, Oostergetel GT, Lewejohann D et al (2010) Row-like organization of ATP synthase in intact mitochondria determined by cryo-electron tomography. Biochim Biophys Acta Bioenerg 1797:272–277. doi:10.1016/j.bbabio.2009.11.004

Dumont ME, Ernst JF, Hampsey DM, Sherman F (1987) Identification and sequence of the gene encoding cytochrome c heme lyase in the yeast Saccharomyces cerevisiae. EMBO J 6:235–241

Efremov RG, Sazanov LA (2011) Structure of the membrane domain of respiratory complex I. Supplementary information. Nature 476:414–420. doi:10.1038/nature10330

Efremov RG, Baradaran R, Sazanov LA (2010) The architecture of respiratory complex I. Nature 465:441–445. doi:10.1038/nature09066

Eletsky A, Jeong M, Kim H et al (2012) Solution NMR structure of yeast succinate dehydrogenase flavinylation factor Sdh5 reveals a putative Sdh1 binding site. Biochemistry 51:8475–8477. doi:10.1038/nature13314.A

Figueroa-Martinez F, Nedelcu AM, Smith DR, Reyes-Prieto A (2015) When the lights go out: the evolutionary fate of free-living colorless green algae. New Phytol 206:972–982. doi:10.1111/nph.13279

Francis BR, Thorsness PE (2011) Hsp90 and mitochondrial proteases Yme1 and Yta10/12 participate in ATP synthase assembly in Saccharomyces cerevisiae. Mitochondrion 11:587–600. doi:10.1016/j.mito.2011.03.008

Franzén LG, Falk G (1992) Nucleotide sequence of cDNA clones encoding the β subunit of mitochondrial ATP synthase from the green alga Chlamydomonas reinhardtii: the precursor protein encoded by the cDNA contains both an N-terminal presequence and a C-terminal extension. Plant Mol Biol 19:771–780. doi:10.1007/BF00027073

Friedrich T, Weiss H (1997) Modular evolution of the respiratory NADH:ubiquinone oxidoreductase and the origin of its modules. J Theor Biol 187:529–540. doi:10.1006/jtbi.1996.0387

Fromm S, Braun H, Peterhansel C (2016) Mitochondrial gamma carbonic anhydrases are required for complex I assembly and plant reproductive development. New Phytol 211:194–207. doi:10.1111/nph.13886

Funes S, Davidson E, Gonzalo Claros M et al (2002) The typically mitochondrial DNA-encoded ATP6 subunit of the F1F0-ATPase is encoded by a nuclear gene in Chlamydomonas reinhardtii. J Biol Chem 277:6051–6058. doi:10.1074/jbc.M109993200

Ghezzi D, Arzuffi P, Zordan M et al (2011) Mutations in TTC19 cause mitochondrial complex III deficiency and neurological impairment in humans and flies. Nat Genet 43:259–263. doi:10.1038/ng.761

Glaser E, Dessi P (1999) Integration of the mitochondrial-processing peptidase into the cytochrome bc1 complex in plants. J Bioenerg Biomembr 31:259–274. doi:10.1023/A:1005475930477

Gledhill JR, Walker JE (2005) Inhibition sites in F1-ATPase from bovine heart mitochondria. Biochem J 386:591–598. doi:10.1042/BJ20041513

Goodenough U, Blaby I, Casero D et al (2014) The path to triacylglyceride obesity in the sta6 strain of Chlamydomonas reinhardtii. Eukaryot Cell 13:591–613. doi:10.1128/EC.00013-14

Gruschke S, Kehrein K, Römpler K et al (2011) Cbp3-Cbp6 interacts with the yeast mitochondrial ribosomal tunnel exit and promotes cytochrome b synthesis and assembly. J Cell Biol 193:1101–1114. doi:10.1083/jcb.201103132

Gruschke S, Römpler K, Hildenbeutel M et al (2012) The Cbp3–Cbp6 complex coordinates cytochrome. J Cell Biol 199:137–150. doi:10.1083/jcb.201206040

Guarani V, Paulo J, Zhai B et al (2014) TIMMDC1/C3orf1 functions as a membrane-embedded mitochondrial complex I assembly factor through association with the MCIA complex. Mol Cell Biol 34:847–861. doi:10.1128/MCB.01551-13

Haltia T, Finel M, Harms N et al (1989) Deletion of the gene for subunit III leads to defective assembly of bacterial cytochrome oxidase. EMBO J 8:594–596

Hamaji T, Smith DR, Noguchi H et al (2013) Mitochondrial and plastid genomes of the colonial green alga gonium pectorale give insights into the origins of organelle DNA architecture within the volvocales. PLoS One. doi:10.1371/journal.pone.0057177

Hao H, Khalimonchuk O, Schraders M et al (2009) SDH5, a gene required for flavination of succinate dehydrogenase is mutated in paraganglioma. Science 325:1139–1142

Helfenbein KG, Ellis TP, Dieckmann CL, Tzagoloff A (2003) ATP22, a nuclear gene required for expression of the F0 sector of mitochondrial ATPase in Saccharomyces cerevisiae. J Biol Chem 278:19751–19756. doi:10.1074/jbc.M301679200

Hirst J, Carroll J, Fearnley IM et al (2003) The nuclear encoded subunits of complex I from bovine heart mitochondria. Biochim Biophys Acta Bioenerg 1604:135–150. doi:10.1016/S0005-2728(03)00059-8

Hofhaus G, Attardi G (1993) Lack of assembly of mitochondrial DNA-encoded subunits of respiratory NADH dehydrogenase and loss of enzyme activity in a human cell mutant lacking the mitochondrial ND4 gene product. EMBO J 12:3043–3048

Hosler JP (2004) The influence of subunit III of cytochrome c oxidase on the D pathway, the proton exit pathway and mechanism-based inactivation in subunit I. Biochim Biophys Acta Bioenerg 1655:332–339. doi:10.1016/j.bbabio.2003.06.009

Hummer G, Wikström M (2016) Molecular simulation and modeling of complex I. Biochim Biophys Acta Bioenerg:1–7. doi:10.1016/j.bbabio.2016.01.005

Jans F, Mignolet E, Houyoux P-A et al (2008) A type II NAD(P)H dehydrogenase mediates light-independent plastoquinone reduction in the chloroplast of Chlamydomonas. Proc Natl Acad Sci USA 105:20546–20551. doi:10.1073/pnas.0806896105

Jia L, Dienhart MK, Stuart RA (2007) Oxa1 directly interacts with Atp9 and mediates its assembly into the mitochondrial F1Fo-ATP synthase complex. Mol Biol Cell 18:986–994. doi:10.1091/mbc.E06

Kaila VR, Verkhovsky MI, Wikström M (2010) Proton-coupled electron transfer in cytochrome oxidase. Chem Rev 110:7062–7081. doi:10.1021/cr1002003

Karpova OV, Newton KJ (1999) A partially assembled complex I in NAD4-deficient mitochondria of maize. Plant J 17:511–521. doi:10.1046/j.1365-313X.1999.00401.x

Kerscher S, Kashani-poor N, Zwicker K et al (2001) Exploring the catalytic core of complex I by Yarrowia lipolytica yeast genetics. J Bioenerg Biomembr 33(3):187–196

Klodmann J, Braun H-P (2011) Proteomic approach to characterize mitochondrial complex I from plants. Phytochemistry 72:1071–1080. doi:10.1016/j.phytochem.2010.11.012

Klodmann J, Sunderhaus S, Nimtz M et al (2010) Internal architecture of mitochondrial complex I from Arabidopsis thaliana. Plant Cell 22:797–810. doi:10.1105/tpc.109.073726

Kmita K, Wirth C, Warnau J et al (2015) Accessory NUMM (NDUFS6) subunit harbors a Zn-binding site and is essential for biogenesis of mitochondrial complex I. Proc Natl Acad Sci 112:201424353. doi:10.1073/pnas.1424353112

Kotlyar AB, Sled VD, Burbaev DS et al (1990) Coupling site I and the rotenone-sensitive ubisemiquinone in tightly coupled submitochondrial particles. FEBS Lett 264:17–20. doi:10.1016/0014-5793(90)80753-6

Kunze M, Hartig A (2013) Permeability of the peroxisomal membrane: lessons from the glyoxylate cycle. Front Physiol 4:1–12. doi:10.3389/fphys.2013.00204

Lang FB, Burger G, O'Kelly CJ, Cedergren R et al (1997) An ancestral mitochondrial genome resembling a eubacterial genome in miniature. Nature 387:493–497

Lapaille M, Escobar-Ramírez A, Degand H et al (2010) Atypical subunit composition of the chlorophycean mitochondrial F 1FO-ATP synthase and role of asa7 protein in stability and oligomycin resistance of the enzyme. Mol Biol Evol 27:1630–1644. doi:10.1093/molbev/msq049

Lauersen K, Willamme R, Coosemans N et al (2016) Peroxisomal microbodies are at the crossroads of acetate assimilation in the green microalga Chlamydomonas reinhardtii. Algal Res 16:266–274

Lecler R, Cardol P, Remacle C, Barbare E (2012) Characterization of an internal type-II NADH dehydrogenase from Chlamydomonas reinhardtii mitochondria. Curr Genet 58:205–216. doi:10.1007/s00294-012-0378-2

Lefebvre-Legendre L, Vaillier J, Benabdelhak H et al (2001) Identification of a nuclear gene (FMC1) required for the assembly/stability of yeast mitochondrial F(1)-ATPase in heat stress conditions. J Biol Chem 276:6789–6796. doi:10.1074/jbc.M009557200

Li X, Zhang R, Patena W et al (2016) An indexed, mapped mutant library enables reverse genetics studies of biological processes in Chlamydomonas reinhardtii. Plant Cell. doi:10.1105/tpc.16.00465

Lown FJ, Watson AT, Purton S (2001) Chlamydomonas nuclear mutants that fail to assemble respiratory or photosynthetic electron transfer complexes. Biochem Soc Trans 29:452–455. doi:10.1042/BST0290452

Massoz S, Larosa V, Plancke C et al (2014) Inactivation of genes coding for mitochondrial Nd7 and Nd9 complex I subunits in Chlamydomonas reinhardtii. Impact of complex I loss on respiration and energetic metabolism. Mitochondrion 19:365–374. doi:10.1016/j.mito.2013.11.004

Massoz S, Larosa V, Horrion B et al (2015) Isolation of Chlamydomonas reinhardtii mutants with altered mitochondrial respiration by chlorophyll fluorescence measurement. J Biotechnol 215:27–34. doi:10.1016/j.jbiotec.2015.05.009

Mathiesen C, Hägerhäll C (2002) Transmembrane topology of the NuoL, M and N subunits of NADH:quinone oxidoreductase and their homologues among membrane-bound hydrogenases and bona fide antiporters. Biochim Biophys Acta Bioenerg 1556:121–132. doi:10.1016/S0005-2728(02)00343-2

Mathieu L, Marsy S, Saint-Georges Y et al (2011) A transcriptome screen in yeast identifies a novel assembly factor for the mitochondrial complex III. Mitochondrion 11:391–396. doi:10.1016/j.mito.2010.12.002

Mathy G, Cardol P, Dinant M et al (2010) Proteomic and functional characterization of a Chlamydomonas reinhardtii mutant lacking the mitochondrial alternative oxidase. J Proteome Res 9:2825–2838. doi:10.1021/pr900866e

Mavridou DAI, Ferguson SJ, Stevens JM (2013) Cytochrome c assembly. IUBMB Life 65:209–216. doi:10.1002/iub.1123

McCommis KS, Finck BN (2015) Mitochondrial pyruvate transport: a historical perspective and future research directions. Biochem J 466:229–262. doi:10.1007/978-1-4614-5915-6

Merchant SS, Prochnik SE, Vallon O et al (2007) The Chlamydomonas genome reveals the evolution of key animal and plant functions. Science 318:245–252

Milani G, Jarmurszkiewicz W, Sluse-Goffart CM et al (2001) Respiratory chain network in mitochondria of Candida parapsilosis: ADP/O appraisal of the multiple electron pathways. FEBS Lett 508:231–235

Mimaki M, Wang X, McKenzie M et al (2012) Understanding mitochondrial complex I assembly in health and disease. Biochim Biophys Acta Bioenerg 1817:851–862. doi:10.1016/j.bbabio.2011.08.010

Miranda-Astudillo H, Cano-Estrada A, Vazquez-Acevedo M et al (2014) Interactions of subunits Asa2, Asa4 and Asa7 in the peripheral stalk of the mitochondrial ATP synthase of the chlorophycean alga Polytomella sp. Biochim Biophys Acta Bioenerg 1837:1–13. doi:10.1016/j.bbabio.2013.08.001

Molen TA, Rosso D, Piercy S, Maxwell DP (2006) Characterization of the alternative oxidase of Chlamydomonas reinhardtii in response to oxidative stress and a shift in nitrogen source. Physiol Plant 127:74–86. doi:10.1111/j.1399-3054.2006.00643.x

Møller IM, Rasmusson AG, Fredlund KM (1993) NAD(P)H-ubiquinone oxidoreductases in plant mitochondria. J Bioenerg Biomembr 25:377–384. doi:10.1007/BF00762463

Nurani G, Franzén LG (1996) Isolation and characterization of the mitochondrial ATP synthase from *Chlamydomonas reinhardtii*. cDNA sequence and deduced protein sequence of the alpha subunit. Plant Mol Biol 31:1105–1116

Ohnishi T (1998) Iron-sulfur clusters/semiquinones in complex I. Biochim Biophys Acta Bioenerg 1364:186–206. doi:10.1016/S0005-2728(98)00027-9

Oster G, Wang H (2003) Rotary protein motors. Trends Cell Biol 13:114–121. doi:10.1016/S0962-8924(03)00004-7

Oyedotun KS, Sit CS, Lemire BD (2007) The Saccharomyces cerevisiae succinate dehydrogenase does not require heme for ubiquinone reduction. Biochim Biophys Acta Bioenerg 1767:1436–1445. doi:10.1016/j.bbabio.2007.09.008

Paumard P, Vaillier J, Coulary B et al (2002) The ATP synthase is involved in generating mitochondrial cristae morphology. EMBO J 21:221–230. doi:10.1093/emboj/21.3.221

Paupe V, Prudent J, Dassa EP et al (2015) CCDC90A (MCUR1) is a cytochrome c oxidase assembly factor and not a regulator of the mitochondrial calcium uniporter. Cell Metab 21:109–116. doi:10.1016/j.cmet.2014.12.004

Perez-Martinez X, Antaramian A, Vazquez-Acevedo M et al (2001) Subunit II of cytochrome c oxidase in Chlamydomonas algae is a heterodimer encoded by two independent nuclear genes. J Biol Chem 276:11302–11309. doi:10.1074/jbc.M010244200

Perez-Martinez X, Funes S, Tolkunova E et al (2002) Structure of nuclear-localized cox3 genes in Chlamydomonas reinhardtii and in its colorless close relative Polytomella sp. Curr Genet 40:399–404. doi:10.1007/s00294-002-0270-6

Phillips JD, Graham LA, Trumpower BL (1993) Subunit 9 of the Saccharomyces cerevisiae cytochrome bc1 complex is required for insertion of EPR-detectable iron-sulfur cluster into the Rieske iron-sulfur protein. J Biol Chem 268:11727–11736

Plancke C, Vigeolas H, Höhner R et al (2014) Lack of isocitrate lyase in Chlamydomonas leads to changes in carbon metabolism and in the response to oxidative stress under mixotrophic growth. Plant J 77:404–417. doi:10.1111/tpj.12392

Prakash SK, Cormier TA, Mccall AE et al (2002) Loss of holocytochrome c-type synthetase causes the male lethality of X-linked dominant microphthalmia with linear skin defects (MLS) syndrome. Hum Mol Genet 11:3237–3248

Rak M, Gokova S, Tzagoloff A (2011) Modular assembly of yeast mitochondrial ATP synthase. EMBO J 30:920–930. doi:10.1038/emboj.2010.364

Remacle C, Baurain D, Cardol P, Matagne F (2001) Mutants of Chlamydomonas reinhardtii deficient in mitochondrial complex I: characterization of two mutations affecting the nd1 coding sequence. Genetics 158:1051–1060

Remacle C, Coosemans N, Jans F et al (2010) Knock-down of the COX3 and COX17 gene expression of cytochrome c oxidase in the unicellular green alga Chlamydomonas reinhardtii. Plant Mol Biol 74:223–233. doi:10.1007/s11103-010-9668-6

Rhein VF, Carroll J, Ding S et al (2013) NDUFAF7 methylates arginine 85 in the NDUFS2 subunit of human complex i. J Biol Chem 288:33016–33026. doi:10.1074/jbc.M113.518803

Rodriguez-Salinas E, Riveros-Rosas H, Li Z et al (2012) Lineage-specific fragmentation and nuclear relocation of the mitochondrial cox2 gene in chlorophycean green algae (Chlorophyta). Mol Phylogenet Evol 64:166–176. doi:10.1016/j.ympev.2012.03.014

Rouault TA (2015) Mammalian iron-sulphur proteins: novel insights into biogenesis and function. Nat Rev Mol Cell Biol 16:45–55. doi:10.1038/nrm3909

Rühle T, Leister D (2015) Assembly of F1F0-ATP synthases. Biochim Biophys Acta 1847:849–860. doi:10.1016/j.bbabio.2015.02.005

Rutter J, Winge DR, Schiffman JD (2010) Succinate dehydrogenase – assembly, regulation and role in human disease. Mitochondrion 10:393–401. doi:10.1016/j.mito.2010.03.001

Saada A, Vogel RO, Hoefs SJ et al (2009) Mutations in NDUFAF3 (C3ORF60), encoding an NDUFAF4 (C6ORF66)-interacting complex I assembly protein, cause fatal neonatal mitochondrial disease. Am J Hum Genet 84:718–727. doi:10.1016/j.ajhg.2009.04.020

Salinas T, Larosa V, Cardol P et al (2014) Biochimie respiratory-deficient mutants of the unicellular green alga Chlamydomonas: a review. Biochimie 100:207–218. doi:10.1016/j.biochi.2013.10.006

Sánchez-Caballero L, Guerrero-Castillo S, Nijtmans L (2016) Unraveling the complexity of mitochondrial complex I assembly; a dynamic process. Biochim Biophys Acta Bioenerg. doi:10.1016/j.bbabio.2016.03.031

Sazanov LA (2015) A giant molecular proton pump: structure and mechanism of respiratory complex I. Nat Rev Mol Cell Biol 16:375–388. doi:10.1038/nrm3997

Sazanov LA, Hinchliffe P (2006) Structure of the hydrophilic domain. Science 311:1430–1437
Schimmeyer J, Bock R, Meyer EH (2016) l-Galactono-1,4-lactone dehydrogenase is an assembly factor of the membrane arm of mitochondrial complex I in Arabidopsis. Plant Mol Biol 90:117–126. doi:10.1007/s11103-015-0400-4
Schulte U, Weiss H (1995) Generation and characterization of NADH: ubiquinone oxidoreductase mutants in Neurospora crassa. Methods Enzymol 260:3–13
Sharma V, Belevich G, Gamiz-Hernandez AP et al (2015) Redox-induced activation of the proton pump in the respiratory complex I. Proc Natl Acad Sci USA 112:11571–11576. doi:10.1073/pnas.1503761112
Sheftel AD, Stehling O, Pierik AJ et al (2009) Human ind1, an iron-sulfur cluster assembly factor for respiratory complex I. Mol Cell Biol 29:6059–6073. doi:10.1128/MCB.00817-09
Shiba T, Kido Y, Sakamoto K et al (2013) Structure of the trypanosome cyanide-insensitive alternative oxidase. Proc Natl Acad Sci USA 110:4580–4585. doi:10.1073/pnas.1218386110
Siedow JN, Umbach AL, Moore AL (1995) The active site of the cyanide-resistant oxidase from plant mitochondria contains a binuclear iron center. FEBS Lett 362:10–14. doi:10.1016/0014-5793(95)00196-G
Smith DR, Lee RW (2009) The mitochondrial and plastid genomes of Volvox carteri: bloated molecules rich in repetitive DNA. BMC Genomics 10:132. doi:10.1186/1471-2164-10-132
Smith DR, Hua J, Lee RW (2010) Evolution of linear mitochondrial DNA in three known lineages of Polytomella. Curr Genet 56:427–438. doi:10.1007/s00294-010-0311-5
Smith PM, Fox JL, Winge DR (2012) Biogenesis of the cytochrome bc 1 complex and role of assembly factors. Biochim Biophys Acta Bioenerg 1817:276–286. doi:10.1016/j.bbabio.2011.11.009
Soto IC, Fontanesi F, Liu J, Barrientos A (2012) Biogenesis and assembly of eukaryotic cytochrome c oxidase catalytic core. Biochim Biophys Acta Bioenerg 1817:883–897. doi:10.1016/j.bbabio.2011.09.005
Subrahmanian N, Remacle C, Hamel PP (2016) Plant mitochondrial complex I composition and assembly: a review. Biochim Biophys Acta Bioenerg. doi:10.1016/j.bbabio.2016.01.009
Sun F, Huo X, Zhai Y et al (2005) Crystal structure of mitochondrial respiratory membrane protein complex II. Cell 121:1043–1057. doi:10.1016/j.cell.2005.05.025
Sunderhaus S, Dudkina NV, Jansch L et al (2006) Carbonic anhydrase subunits form a matrix-exposed domain attached to the membrane arm of mitochondrial complex I in plants. J Biol Chem 281:6482–6488. doi:10.1074/jbc.M511542200
Svensson-Ek M, Abramson J, Larsson G et al (2002) The X-ray crystal structures of wild-type and EQ(I-286) mutant cytochrome c oxidases from Rhodobacter sphaeroides. J Mol Biol 321:329–339. doi:10.1016/S0022-2836(02)00619-8
Terashima M, Specht M, Naumann B, Hippler M (2010) Characterizing the anaerobic response of Chlamydomonas reinhardtii by quantitative proteomics. Mol Cell Proteomics 9:1514–1532. doi:10.1074/mcp.M900421-MCP200
Trumpower B (1990a) The protonmotive Q cycle. J Biol Chem 265:11409–11412. doi:10.3109/10409239409086800
Trumpower BL (1990b) Cytochrome bc1 complexes of microorganisms. Microbiol Rev 54:101–129
Tucker EJ, Wanschers BFJ, Szklarczyk R et al (2013) Mutations in the UQCC1-interacting protein, UQCC2, cause human complex III deficiency associated with perturbed cytochrome b protein expression. Genetics. doi:10.1371/journal.pgen.1004034
Tzagoloff A, Jang J, Glerum M, Wu M (1996) FLX1 codes for a carrier protein involved in maintaining a proper balance of flavin nucleotides in yeast mitochondria. J Biol Chem 271:7392–7397
Un N, Yu YD, Cox J et al (2014) The LYR factors SDHAF1 and SDHAF3 mediate maturation of the iron-sulfur subunit of succinate dehydrogenase. Cell Metab:253–266. doi:10.1021/jf104742n.Biological

Vahrenholz C, Riemen G, Pratje E et al (1993) Mitochondrial DNA of Chlamydomonas reinhardtii: the structure of the ends of the linear 15.8-kb genome suggests mechanisms for DNA replication. Curr Genet 24:241–247. doi:10.1007/BF00351798

Van Den Brand AM, Jonckheere A, Wanschers BFJ et al (2014) A mutation in the human CBP4 ortholog UQCC3 impairs complex III assembly, activity and cytochrome b stability. Hum Mol Genet 23:6356–6365. doi:10.1093/hmg/ddu357

van Lis R, Atteia A, Mendoza-hernández G, González-halphen D (2003) Identification of novel mitochondrial protein components of Chlamydomonas reinhardtii. A proteomic approach. Plant Physiol 132:318–330. doi:10.1104/pp.102.018325.proteins

van Lis R, Mendoza-Hernández G, Groth G, Atteia A (2007) New insights into the unique structure of the F0F1-ATP synthase from the chlamydomonas algae Polytomella sp. and Chlamydomonas reinhardtii. Plant Physiol 144:1190–1199. doi:10.1104/pp.106.094060

Van Vranken J, Na U, Winge DR, Rutter J (2015) Protein-mediated assembly of succinate dehydrogenase and its cofactors. Crit Rev Biochem Mol Biol 50:168–180. doi:10.1530/ERC-14-0411.Persistent

Vazquez-Acevedo M, Cardol P, Cano-Estrada A et al (2006) The mitochondrial ATP synthase of chlorophycean algae contains eight subunits of unknown origin involved in the formation of an atypical stator-stalk and in the dimerization of the complex. J Bioenerg Biomembr 38:271–282. doi:10.1007/s10863-006-9046-x

Vázquez-Acevedo M, Vega-deLuna F, Sánchez-Vásquez L et al (2016) Dissecting the peripheral stalk of the mitochondrial ATP synthase of chlorophycean algae. Biochim Biophys Acta Bioenerg. doi:10.1016/j.bbabio.2016.02.003

Vignais PM, Billoud B (2007) Occurrence, classification, and biological function of hydrogenases: an overview. Chem Rev 107:4206–4272

Villavicencio-Queijeiro A, Vázquez-Acevedo M, Cano-Estrada A, Zarco-Zavala M, Tuena de Gómez M, Mignaco JA, Freire MM, Scofano HM, Foguel D, Cardol P, Remacle C, González-Halphen D (2009) The fully-active and structurally-stable form of the mitochondrial ATP synthase of Polytomella sp. is dimeric. J Bioenerg Biomembr 41:1–13. doi:10.1007/s10863-009-9203-0

Villavicencio-Queijeiro A, Pardo JP, Gonzalez-Halphen D (2015) Kinetic and hysteretic behavior of ATP hydrolysis of the highly stable dimeric ATP synthase of Polytomella sp. Arch Biochem Biophys 575:30–37. doi:10.1016/j.abb.2015.03.018

Vinothkumar KR, Zhu J, Hirst J (2014) Architecture of mammalian respiratory complex I. Nature 515:80–84. doi:10.1038/nature13686.Architecture

Vogel RO, Dieteren CEJ, Van Den Heuvel LP et al (2007) Identification of mitochondrial complex I assembly intermediates by tracing tagged NDUFS3 demonstrates the entry point of mitochondrial subunits. J Biol Chem 282:7582–7590. doi:10.1074/jbc.M609410200

Wächter A, Bi Y, Dunn SD et al (2011) Two rotary motors in F-ATP synthase are elastically coupled by a flexible rotor and a stiff stator stalk. Proc Natl Acad Sci USA 108:3924–3929. doi:10.1073/pnas.1011581108

Walker JE, Dickson VK (2006) The peripheral stalk of the mitochondrial ATP synthase. Biochim Biophys Acta Bioenerg 1757:286–296. doi:10.1016/j.bbabio.2006.01.001

Wang ZG, White PS, Ackerman SH (2001) Atp11p and Atp12p are assembly factors for the F1-ATPase in human mitochondria. J Biol Chem 276:30773–30778. doi:10.1074/jbc.M104133200

Wenz T, Hielscher R, Hellwig P et al (2009) Role of phospholipids in respiratory cytochrome bc1 complex catalysis and supercomplex formation. Biochim Biophys Acta Bioenerg 1787:609–616. doi:10.1016/j.bbabio.2009.02.012

Wikström M, Jasaitis A, Backgren C et al (2000) The role of the D- and K-pathways of proton transfer in the function of the haem-copper oxidases. Biochim Biophys Acta Bioenerg 1459:514–520. doi:10.1016/S0005-2728(00)00191-2

Wydro MM, Sharma P, Foster JM et al (2013) The evolutionarily conserved iron-sulfur protein INDH is required for complex I assembly and mitochondrial translation in Arabidopsis. Plant Cell 25:4014–4027. doi:10.1105/tpc.113.117283

Xia D, Esser L, Tang WK et al (2013) Structural analysis of cytochrome bc1 complexes: Implications to the mechanism of function. Biochim Biophys Acta Bioenerg 1827:1278–1294. doi:10.1016/j.bbabio.2012.11.008

Yasuda R, Noji H, Kinosita K, Yoshida M (1998) F1-ATPase is a highly efficient molecular motor that rotates with discrete 120 degree steps. Cell 93:1117–1124. doi:10.1016/S0092-8674(00)81456-7

Zalutskaya Z, Lapina T, Ermilova E (2015) The Chlamydomonas reinhardtii alternative oxidase 1 is regulated by heat stress. Plant Physiol Biochem 97:229–234. doi:10.1016/j.plaphy.2015.10.014

Zara V, Conte L, Trumpower BL (2007) Identification and characterization of cytochrome bc1 subcomplexes in mitochondria from yeast with single and double deletions of genes encoding cytochrome bc1 subunits. FEBS J 274:4526–4539. doi:10.1111/j.1742-4658.2007.05982.x

Zeng X, Barros MH, Shulman T, Tzagoloff A (2008) ATP25, a new nuclear gene of Saccharomyces cerevisiae required for expression and assembly of the Atp9p subunit of mitochondrial ATPase. Mol Biol Cell 19:308–317. doi:10.1091/mbc.E07

Zhang Z, Huang L, Shulmeister VM et al (1998) Electron transfer by domain movement in cytochrome bc1. Nature 392:677–684. doi:10.1038/33612

Zhu J, Egawa T, Yeh S-R et al (2007) Simultaneous reduction of iron-sulfur protein and cytochrome b(L) during ubiquinol oxidation in cytochrome bc(1) complex. Proc Natl Acad Sci USA 104:4864–4869. doi:10.1073/pnas.0607812104

Zickermann V, Wirth C, Nasiri H, et al (2015) Mechanistic insight from the crystal structure of mitochondrial complex I. 5:4–10

Zollner A, Rödel G, Haid A (1992) Molecular cloning and characterization of the Saccharomyces cerevisiae CYT2 gene encoding cytochrome-c1-heme lyase. Eur J Biochem 207:1093–1100

Bioenergetic Pathways in the Chloroplast: Photosynthetic Electron Transfer

Philipp Gäbelein, Laura Mosebach, and Michael Hippler

Abstract In this review, we address bioenergetic pathways in the chloroplast of *Chlamydomonas reinhardtii*, with a focus on photosynthetic electron transfer. The conversion of solar energy into chemical energy by oxygenic photosynthesis, as performed by plants, green algae and cyanobacteria, supports the life on this planet. The production of oxygen (O_2) and the assimilation of carbon dioxide (CO_2) into organic matter determine, to a large extent, the composition of our atmosphere. Plant photosynthesis is conducted by a series of reactions that occur mainly in the chloroplast, resulting in light-dependent H_2O oxidation, $NADP^+$ reduction and ATP formation. NADPH and ATP, produced by linear electron flow (LEF), are required for carbon fixation via the Calvin-Benson-Bassham (CBB) cycle. Besides, photosynthetic electron transfer may operate in a cyclic electron flow (CEF) mode to satisfy the cellular ATP demand. Electrons derived from LEF may also be diverted to various other metabolic pathways, e.g. via ferredoxin (FDX). In addition, photosynthesis evolved to maximize its outcome while minimizing photooxidative stress. In this regard, mechanisms such as non-photochemical quenching (NPQ) and state transitions regulate energy influx at different light availabilities, which feedback to the proton-motive force (pmf) and the redox state of the plastoquinone/plastoquinol (PQ) pool, thereby also regulating LEF and CEF. To overcome possible limitations in electron transfer at the acceptor side of photosystem (PSI), alternative electron transfer pathways evolved, including flavodiiron proteins (FDPs), allowing safe utilization of O_2 as alternative electron acceptor, as well as the hydrogenase, which utilizes two electrons and two protons to produce H_2. Nevertheless, reactive oxygen species (ROS) may be formed, e.g. via the Mehler reaction at the acceptor side of PSI, which is why photosynthetic electrons are also utilized in detoxification mechanisms to prevent excessive damage. In conclusion, photosynthetic electron transfer is interwoven in a regulatory network that is aimed at adjusting ATP and NADPH production in a way that electron transfer is not harmful to the cell.

Authors Philipp Gäbelein and Laura Mosebach contributed equally to the work.

P. Gäbelein • L. Mosebach • M. Hippler (✉)
Institute of Plant Biology and Biotechnology, University of Münster, Schlossplatz 8, 48143 Münster, Germany
e-mail: mhippler@uni-muenster.de

M. Hippler (ed.), *Chlamydomonas: Molecular Genetics and Physiology*,
Microbiology Monographs 30, DOI 10.1007/978-3-319-66365-4_4

1 LEF Operation

The photosynthetic machinery, which resides in the thylakoid membrane of the chloroplast, comprises transmembrane protein complexes as the two photosystems (PS) II and I with their light-harvesting complexes (LHC) and the cytochrome b_6f complex (Cyt b_6f complex), together harbouring the essential components mediating light-induced charge separation and subsequent electron transfer along with proton translocation. The chloroplast CF_1-F_0-ATP-synthase (ATPase), another integral protein complex, transforms energy stored in the form of an electrochemical gradient into biologically useful free energy (Mitchell 1961). These major protein complexes are distributed across the thylakoid membrane in a heterogeneous way, with PSII and the Cyt b_6f being localized in the stacked domains, the Cyt b_6f and PSI coinciding at the intermediate areas and the Cyt b_6f, PSI and the ATPase residing in the unstacked regions. Still, thylakoid stacking is less pronounced in the *C. reinhardtii* chloroplast compared to vascular plants (see chapter "Thylakoid Ultrastructure: Visualizing the Photosynthetic Machinery"). Furthermore, the photosynthetic apparatus features peripheral protein complexes, such as the ferredoxin:$NADP^+$ oxidoreductase (FNR) and the mobile electron carriers plastoquinone/plastoquinol (PQ/PQH_2), plastocyanin (PC), cytochrome c_6 and ferredoxin (FDX), all being involved in photosynthetic electron transfer (Nelson and Ben-Shem 2004; Nelson and Yocum 2006).

1.1 PSII and PSI

Light energy absorbed by the photosynthetic pigments of LHC antenna proteins is transmitted to the reaction centre subunits of PSII and PSI via energy resonance transfer. *C. reinhardtii* features four major trimeric LHCII proteins (type I–IV, encoded by *LhcbM3*, *LhcbM4*, *LhcbM6*, *LhcbM8* and *LhcbM9*; *LhcbM5*; *LhcbM2* and *LhcbM7*; and *LhcbM1*, respectively) as well as two minor monomeric LHCII proteins (CP29 and CP26, encoded by *Lhcb4* and *Lhcb5*, respectively), contributing to the formation of PSII-LHCII supercomplexes with three LHCII trimers attached to both sides of the dimeric core ($C_2S_2M_2L_2$) (Tokutsu et al. 2012; Drop et al. 2014a). In contrast, nine LHCI proteins (encoded by *Lhca1–Lhca9*) constitute a double-layered, heterogeneous belt associated with one side of the monomeric PSI core (Drop et al. 2011). At the reaction centres, where the special chlorophyll *a* pairs P680 (PSII) and P700 (PSI) represent the primary electron donors, photochemical charge separation occurs: At P680, excited electrons are transferred towards a tightly bound PQ at the Q_A site via the primary electron acceptor pheophytine. From the loosely bound PQ at the Q_B site, electrons enter the PQ pool by successive PQ reduction during two photochemical cycles, involving the uptake of protons from the thylakoid stroma. The resulting electron gap at $P680^+$

provides a redox potential sufficient to oxidize H_2O, giving rise to O_2 evolution, which is accompanied by the release of protons to the thylakoid lumen. This process is mediated by a manganese cluster (Mn_4CaO_5) at the luminal side, serving as a charge accumulator passing through five intermediate states (S_0–S_4) and thereby connecting the four electron oxidation of two H_2O via tyrosine Y_Z of the D1 subunit with the one electron event at P680 (Vinyard et al. 2013). At PSI, light-induced excitation of P700 facilitates electron donation to one of two primary acceptors chlorophyll *a* A_0. Subsequently, electrons are transmitted towards the stromal side along two parallel branches via phylloquinone A_1, rejoining at the [4Fe-4S] clusters F_X, F_A and F_B, where the reduction of the [2Fe-2S] electron carrier FDX occurs. Completing the process of LEF, electrons are successively transferred within a ternary complex from FDX to $NADP^+$ via the FAD-containing enzyme FNR, consuming one proton per NADPH (Kurisu et al. 2001). The resulting reducing equivalents facilitate assimilatory pathways, in particular the Calvin-Benson-Bassham (CBB) cycle, which involves CO_2 fixation.

Electron transfer between FDX1 and PSI depends on protein-protein interactions between the subunits PsaC, PsaD and PsaE (Busch and Hippler 2011). $P700^+$ in turn is reduced via PC, a copper-containing electron carrier at the luminal side of the thylakoid membrane. For electron transfer between PC and PSI, a detailed protein-protein interaction model has been depicted by Sommer et al. (2004). Herein, efficient electron transfer between PC and PSI is dependent on hydrophobic as well as electrostatic interactions [see also Busch and Hippler (2011)]. Long range electrostatic attractions between basic patches of PsaF and acidic regions of PC (Nordling et al. 1991; Haehnel et al. 1994; Hippler et al. 1996, 1997, 1998) as well as hydrophobic contact between the electron transfer site of the donors and of PSI including PsaA-W651 and PsaB-W627 in *C. reinhardtii* (Haehnel et al. 1994; Sommer et al. 2002) are required for stable electron transfer complex formation and efficient electron transfer. Mutations of PsaB-Glu613 to Asn or PsaB-Asp612 and PsaB-Glu613 to His result in a clear acceleration of electron transfer rates and improved binding of PC to PSI in comparison to wild type (Sommer et al. 2002; Kuhlgert et al. 2012). Structural data clearly show that the negative charge provided by PsaB-Glu613 is exposed on the surface of PSI (Ben-Shem et al. 2003). Thus, it is possible that a change of Asp/Glu to Asn/His results in tighter binding of the donor to PSI, since this mutation decreases the electrostatic repulsion between the negatively charged donors and PSI, which in turn might result in slower unbinding of oxidized PC (Finazzi et al. 2005), leading to slower electron transfer between PSI and the Cyt b_6f complex.

1.2 Cyt b_6f Complex

Being functionally interposed between PSII and PSI in LEF, the homodimeric Cyt b_6f complex pursues the photosynthetic electron transport chain at the level of the PQ pool via successive PQH_2 oxidation at the Q_o site, involving the release of

protons into the thylakoid lumen. Subsequently, electrons follow two bifurcating routes: either they pass through the high potential chain starting from the [2Fe-2S] centre of the Rieske subunit via heme c at Cyt f to finally reduce PC or they return to the PQ pool joining a modified Q-cycle via the Cyt b_6 low potential chain from heme b_l over heme b_h to the Q_i site, where successive PQ reduction occurs, including the uptake of protons from the thylakoid stroma. In addition, a heme c_i on the stromal face near the Q_i site has been described, although its function is elusive so far (Kurisu et al. 2003; Stroebel et al. 2003; Baniulis et al. 2008).

1.3 Transmembrane Electrochemical Proton Gradient

Besides supplying NADPH for downstream metabolic reactions, LEF contributes to the generation of a transmembrane electrochemical proton gradient: Via H_2O splitting at PSII, four protons per two molecules H_2O are released into the lumen. At the level of the Cyt b_6f complex, Q-cycle operation facilitates proton translocation from the stromal to the luminal side of the thylakoid membrane with an efficiency of two protons per electron. NADPH production consumes one proton per molecule in the stroma. In the end, three protons are translocated across the thylakoid membrane per electron passing through the electron transport chain. The resulting proton-motive force (pmf) is utilized by the ATPase to produce ATP. Moreover, the electric component ($\Delta\Psi$) of the pmf impacts the ATPase activity, which is further regulated via thiol modulation by the chloroplast thioredoxin (TRX) system.

As the *C. reinhardtii* CF_0 subunit of the ATPase features a 13-fold rotational symmetry, the pmf promotes the synthesis of 1.38 ATP per NADPH (Meyer Zu Tittingdorf et al. 2004; Alric 2010). However, the CBB cycle demands a ratio of 3 ATP per 2 NADPH. This demand is further increased to 4 ATP per 2 NADPH, when the carbon-concentrating mechanism (CCM) is active under ambient CO_2 conditions in *C. reinhardtii* (Lucker and Kramer 2013). Diverse auxiliary electron flow pathways compensating for this ATP deficit will be discussed in the subsequent sections.

2 LEF Regulation

C. reinhardtii is exposed to fluctuating light intensities and varying nutrient availabilities, so that a fine-tuned regulation of light harvesting and subsequent electron transfer processes via feedback loops is essential to balance energy provision and energy consumption in a tightrope walk between optimally satisfying the demands of downstream metabolic reactions on the one hand and protecting the organism from photodamage on the other hand. Singlet-excited chlorophylls decay to the ground state via various potential routes: fluorescence emission, energy resonance

transfer at the antenna, photochemical quenching at the reaction centres, non-photochemical quenching (NPQ) and relaxation via the triplet-excited state promoting the formation of singlet oxygen ($^1O_2$) (Müller et al. 2001). NPQ of PSII chlorophyll fluorescence may be differentiated into three distinct components based on their relaxation kinetics (Baker 2008): (1) energy-dependent quenching (qE), i.e. thermal energy dissipation; (2) state transition-related quenching (qT), i.e. redistribution of incident excitation flux between the two photosystems; and (3) irreversible photoinhibition-associated quenching (qI).

2.1 State Transitions

In *C. reinhardtii*, state transitions and thermal energy dissipation play complementary roles: At low light intensities, balancing the relative absorption cross-sections of the photosystems is integral to sustain photosynthetic electron transfer. Furthermore, in *C. reinhardtii*, the initial part of glycolysis and the degradation of starch are localized in the chloroplast (Terashima et al. 2010, 2011; Johnson and Alric 2012), and the habitat of *C. reinhardtii* is prone to hypoxia or anoxia, resulting in amplified reduction of the PQ pool via light-independent reactions (Yang et al. 2015a). The redox state of the PQ pool, sensed at the Q_o site of the Cyt b_6f complex (Zito et al. 1999), controls the activity of the serine-threonine kinase Stt7 (Depège et al. 2003), which is presumably also regulated via a trans-thylakoid thiol-reducing pathway mediated by the chloroplast TRX system (Lemeille et al. 2009). Alternatively, reduction of Stt7 might occur via superoxide ($O_2^{\bullet -}$), known to be generated at the Cyt b_6f complex by PQH_2 oxidation (Singh et al. 2016). Stt7 reversibly phosphorylates LHCII proteins, ensuing the lateral migration of phosphorylated LHCIIs from PSII to PSI (Rochaix 2014; Goldschmidt-Clermont and Bassi 2015). This equilibrates the redox state of the PQ pool, alleviating the reduction pressure exerted by PSII and enhancing the oxidation pressure arising from PSI photochemistry (Delosme et al. 1996). Strictly speaking, the resulting chlorophyll fluorescence quenching at PSII is not of a non-photochemical nature in this case but rather occurs in a photochemical way at the reaction centre of PSI. This concept has been challenged by several recent studies (Iwai et al. 2010b; Nagy et al. 2014; Ünlü et al. 2014, 2015), which proposed phosphorylated LHCII antenna disconnected from PSII to form non-photochemically quenching aggregates. Yet, another current study (Nawrocki et al. 2016) substantiates the established concept and concludes, based on in vivo absorption spectroscopy in agreement with structural (Drop et al. 2014b) and biochemical data (Takahashi et al. 2014), that upon state transitions either two LHCII trimers and one monomeric antenna protein, or two type II LHC trimers, two CP29 and one CP26 associate with the PSI core. From a physiological point of view, state transition has been demonstrated to play a critical role in the acclimation to anoxic conditions or high-light stress (Cardol et al. 2009; Bergner et al. 2015).

2.2 qE-Dependent NPQ

In contrast to qT, the capacity to dissipate excitation energy as heat is not always present in *C. reinhardtii* [opposed to the situation in vascular plants, where qE-dependent NPQ is constitutive (Rochaix 2014; Wobbe et al. 2015)], but largely depends on the availability of LHCSR3 (Peers et al. 2009). LHCSR3 expression is induced in response to environmental conditions promoting photooxidative stress, i.e. high light, being sensed by a blue light photoreceptor (Petroutsos et al. 2016). In addition, LHCSR3 expression is induced in response to low CO_2 availability, requires functional photosynthetic electron transfer and is regulated via Ca^{2+} and the Ca^{2+} sensor CAS (Petroutsos et al. 2011; Maruyama et al. 2014; Wang et al. 2016). Binding of LHCSR3 to the PSII-LHCII supercomplex is facilitated by the PSII subunit R (PSBR) (Xue et al. 2014). The resulting PSII-LHCII-LHCSR3 supercomplex is proposed to exist in two distinct states: the light-harvesting state and the photoprotective state. A transition from the high fluorescent to the energy dissipative state is triggered by the protonation of LHCSR3 (Liguori et al. 2013; Tokutsu and Minagawa 2013; Ballottari et al. 2016). Until lately, it had been established that the luminal pH sensor PSII subunit S (PsbS), being essential for qE-dependent NPQ induction in land plants (Li et al. 2000, 2004; Fan et al. 2015), played no role in *C. reinhardtii*, as the *PsbS* gene product was not detected under a wide range of growth conditions (Bonente et al. 2008). Recent studies however revisited the biological function of PsbS in *C. reinhardtii*, reporting a rapid but transient accumulation of PsbS in response to high-light stress (Correa-Galvis et al. 2016; Tibiletti et al. 2016). Importantly, a knockdown of PsbS resulted in diminished NPQ capacity and LHCSR3 accumulation, implicating that LHCSR3-dependent NPQ in *C. reinhardtii* partially depends on the presence of PsbS (Correa-Galvis et al. 2016). Intriguingly, PsbS expression is induced in response to UV-B light via the photoreceptor UVR8 and acclimation to UV-B light primes *C. reinhardtii* for photoprotection during subsequent high-light stress (Allorent et al. 2016).

The induction of qE-dependent NPQ is tightly coupled to the osmotic component of the pmf (ΔpH) and hence creates a regulatory feedback loop between electron transfer and light harvesting: Once the excitation flux exceeds the capacity of downstream metabolic reactions, the arising acidification of the thylakoid lumen initiates a downregulation of PSII photochemistry, thereby alleviating the reducing pressure exerted on downstream components of the photosynthetic electron transport chain (Kramer et al. 2004a). State transitions and qE-dependent NPQ play complementary roles in the acclimation to high-light stress in *C. reinhardtii* (Allorent et al. 2013).

2.3 Photosynthetic Control

Furthermore, intensified acidification of the thylakoid lumen provokes the release of Ca^{2+} from the H_2O-splitting complex, thereby inactivating O_2 evolution (Hochmal et al. 2015). Besides regulating the activity of PSII, the ΔpH controls the rate-limiting step of LEF, i.e. the oxidation of PQH_2 at the Q_o site (Stiehl and Witt 1969; Finazzi and Rappaport 1998; Rott et al. 2011). Alternatively, it has been proposed that the activity of the Cyt b_6f complex might be regulated in response to the stromal redox poise via a TRX-mediated mechanism (Johnson 2003). As the induction of qE-dependent NPQ is delayed in *C. reinhardtii*, shifting the rate-limiting step of photosynthetic electron transfer from the PSI acceptor side to the Cyt b_6f complex is critical, in particular for the short-term acclimation to high-light stress (Chaux et al. 2015). The decrease in lumenal pH might also diminish the rate of electron transfer between the oxidizing side of PSI and the Cyt b_6f complex, as PC binds tighter to PSI and unbinds slower at lower pH (see Sect. 1.1), thereby additionally contributing to the avoidance of PSI acceptor side limitation. A secondary effect of constraining the rate of photosynthetic electron transfer at the Cyt b_6f complex (termed "photosynthetic control") is an enhanced back pressure on PSII at the level of the PQ pool, which provokes PSII photoinhibition: Relaxation of singlet-excited P680 via the triplet-excited state promotes the formation of $^1O_2$ irreversibly damaging the D1 subunit and thereby inactivating the PSII reaction centre. Since the high turnover rate of the D1 protein facilitates a fast recovery of PSII from photooxidative damage, it is considered as "predetermined breaking point" of the electron transport chain, being essential for the protection of downstream components (Sonoike 2011; Murata et al. 2012; Järvi et al. 2015). In *C. reinhardtii*, integral components involved in D1 turnover are the ATP-dependent zinc metalloprotease FtsH1, which degrades damaged D1 fragments (Malnoë et al. 2014) and TEF30, contributing to PSII repair (Muranaka et al. 2016).

2.4 Pmf Partitioning

As introduced in the preceding paragraphs, the transmembrane proton gradient induces photoprotective mechanisms, i.e. qE-dependent NPQ and photosynthetic control. Still, excessive lumenal acidification results in PSII inactivation (Krieger and Weis 1993). Likewise, as reported lately, an elevated electric field component of the pmf induces PSII photodamage (Davis et al. 2016). Therefore, a tight regulation of pmf partitioning is essential. Recently, the critical role of pmf partitioning modulation via counter ion fluxes balancing proton fluxes has been demonstrated in vascular plants: A Ca^{2+}-dependent two-pore K^+ efflux channel (TPK3), a K^+/H^+ antiport (KEA3) and Cl^- channels (voltage-dependent AtVCCN1/AtBest and AtCLCe) have been established as integral players being

involved in this mechanism and thereby sustaining photosynthetic efficiency (Carraretto et al. 2013; Armbruster et al. 2014, 2016; Kunz et al. 2014; Duan et al. 2016; Herdean et al. 2016a, b). Although in *C. reinhardtii,* such ion channels have not been described yet, pmf partitioning modulation constitutes another potential mechanism impacting the ΔpH component of the pmf and thereby regulating ATP synthesis, photosynthetic electron transfer and light harvesting.

As mentioned in this section, LEF alone is not sufficient to equilibrate the ATP to NADPH ratio. Diverse auxiliary electron flow pathways, addressed in the subsequent sections, sustain the redox homeostasis of the chloroplast and contribute to the transmembrane photochemical proton gradient, having been introduced as essential regulatory photoprotective component in this section.

3 CEF Operation

Starting from NADPH or reduced FDX, electrons may be recycled to a component of the photosynthetic electron transport chain upstream of PSI, thereby completing a cycle around PSI. CEF around PSI operates via two distinct pathways: NDH-dependent and FQR-dependent CEF (Eberhard et al. 2008; Alric 2010; Cardol et al. 2011). The physiological significance of CEF has emerged over the last decade, not least via investigation of the PGR5 (proton gradient regulation 5)/PGRL1 (PGR5-like photosynthetic phenotype 1) knockout mutants. The recycling of electrons via CEF around PSI creates a regulatory feedback loop between the stroma and upstream components of the photosynthetic electron transport chain and contributes to the transmembrane electrochemical proton gradient. Hence, CEF sustains the redox poise of the photosynthetic electron transport chain and is involved in the equilibration of the ATP to NADPH ratio (Kramer et al. 2004a; Alric 2010). Since the habitat of *C. reinhardtii* is prone to hypoxia/anoxia, CEF and H_2 production play an essential role as electron sinks alleviating enhanced stromal redox pressure and sustaining photosynthetic CO_2 fixation (Hemschemeier and Happe 2011; Ghysels et al. 2013; Clowez et al. 2015; Godaux et al. 2015) (see chapters "Chlamydomonas: Anoxic Acclimation and Signaling" and "Chlamydomonas: Hydrogenase and Hydrogen Production"). FQR-dependent CEF, often related to as PGRL1/PGR5-dependent CEF, has been reported to be the major CEF pathway in anoxic conditions in *C. reinhardtii* (Alric 2014). To what extent CEF is directly responsible for the onset of photosynthetic control and the induction of qE-dependent NPQ via acidification of the thylakoid lumen is an issue of controversy: While both LEF and CEF modulate proton influx, proton efflux is mediated by the ATPase. Therefore, mechanisms regulating the ATPase conductivity (g_{H^+}), potentially via stromal P_i levels, have been proposed to account for the initiation of these photoprotective mechanisms as well (Johnson 2004; Kramer et al. 2004b).

3.1 NDH-Dependent CEF

In *C. reinhardtii*, a type II-NDH complex (Nda2) accounts for NDH-dependent CEF, i.e. the light-dependent non-photochemical reduction of PQ (Mus et al. 2005; Jans et al. 2008). Nda2 is non-electrogenic and anchored to the stromal side of the thylakoid membrane. It features two Rossmann-fold domains (β-sheet–-α-helix–β-sheet): one binding the FMN cofactor and the other binding NADP(H). In vitro, recombinant Nda2 mediates the reduction of PQ with NADH as preferential substrate (Desplats et al. 2009; Peltier et al. 2016). In vivo, the transhydrogenase may convert NADPH, the predominant reducing equivalent in the chloroplast, to NADH, being favoured by Nda2 (Terashima et al. 2010). Harbouring two EF hands, Nda2 activity is potentially regulated via Ca^{2+} (Hochmal et al. 2015). Furthermore, Nda2 is subjected to posttranslational modifications in the form of phosphorylations (Wagner et al. 2007). Besides mediating NDH-dependent CEF, Nda2 facilitates the light-independent reduction of PQ, constituting the initial part of chlororespiration (see Sect. 5.2). This pathway creates a light-independent feedback loop between the stromal redox poise and the PQ pool redox state and thus potentially predetermines the balance of light harvesting by state transitions and the partitioning of photosynthetic electron transfer at the onset of illumination by poising of intersystem electron carriers (Nawrocki et al. 2014). Recently, chlororespiration has been proposed to be critical for the adjustment of the intracellular N/C ratio in response to N_2 deprivation (Wei et al. 2014; Saroussi et al. 2016). Furthermore, Nda2 provides access to NAD(P)H derived from endogenous carbon sources, which is, for instance, essential for sustained PSII-independent H_2 photoproduction (Grossman et al. 2011; Baltz et al. 2014) (see chapter "Chlamydomonas: Hydrogenase and Hydrogen Production").

3.2 FQR-Dependent CEF

While NDH-dependent CEF in *C. reinhardtii* relies on NAD(P)H as electron source [in contrast to vascular plants, where FDX is the electron donor of an electrogenic type I-NDH multisubunit complex (NDH1) being associated with PSI (Peng et al. 2008; Yamamoto et al. 2011; Peltier et al. 2016)], FQR-dependent CEF involves the FDX-dependent reduction of PQ. The precise molecular mechanism of FQR-dependent CEF, at least in *C. reinhardtii*, is still elusive, as there is no definite evidence which component supplies the required FQR activity. In this context, it has been proposed in vascular plants that upon association of FNR with the Cyt b_6f complex (Clark et al. 1984; Zhang et al. 2001), PQ might be reduced at the Q_i site according to a modified Q-cycle process involving concerted electron transfer from FDX or FNR, potentially via heme c_i, and from heme b_h to PQ (Joliot and Joliot 2006; Baniulis et al. 2008; Johnson 2011). However, PGR5 and PGRL1 have been identified as factors impacting FQR-dependent CEF efficiency. PGR5 is associated

with the stromal side of the thylakoid membrane and likely positively charged under physiological conditions (Munekage et al. 2002). PGRL1 exhibits two transmembrane domains and features a negatively charged N-terminal loop, which presumably interacts with the positively charged regions of PGR5, resulting in heterodimerization. Furthermore, PGRL1 forms homodimers being destabilized in the presence of TRX. Accumulation of PGR5 requires the presence of PGRL1, whereas PGR5 promotes PGRL1 stability. (DalCorso et al. 2008). Furthermore, PGRL1 performs iron-dependent redox-induced conformational changes and features six redox-active cysteine residues, which mediate diverse intra- and intermolecular interactions via thiol-disulphide transitions (Petroutsos et al. 2009; Hertle et al. 2013). Four of these cysteines form a rubredoxin-fold, which may facilitate the binding of an iron-containing cofactor (Petroutsos et al. 2009). The four cysteines potentially involved in the binding of this cofactor are also required for heterodimerization (Hertle et al. 2013). Copurification implicates the PGRL1-PGR5 complex associates with PSI. Moreover, split-ubiquitin and yeast two-hybrid assays revealed that PGRL1 interacts with FDX and FNR, whereas both PGRL1 and PGR5 interact with the Cyt b_6f complex, as confirmed by co-immunoprecipitation assays (DalCorso et al. 2008; Hertle et al. 2013). In addition, BiFC studies demonstrated PGRL1 interacts with ANR1 and CAS (Terashima et al. 2012). Leister and his group demonstrated in vitro that PGRL1 exhibits the required features of an FQR: PGRL1 accepts electrons from FDX in a PGR5-dependent way and donates electrons to PQ. The redox-dependent interaction of PGRL1 with PGR5 may induce a conformational change enabling electron transfer from FDX to PGRL1 (Hertle et al. 2013). However, in *C. reinhardtii* mechanistic evidence is lacking that PGRL1 in fact acts as FQR in vivo. While on the molecular level, the function of PGRL1 and PGR5 is elusive, the phenotype of PGRL1/PGR5 knockout mutants has been studied in detail.

The photosynthetic phenotype of *C. reinhardtii* PGR5 and/or PGRL1 knockout mutants strongly resembles the one described for *A. thaliana* (Munekage et al. 2002, 2004; Nandha et al. 2007; DalCorso et al. 2008; Suorsa et al. 2012): Both *pgrl1* and *pgr5* fail to induce qE-dependent NPQ in response to high light (Tolleter et al. 2011; Johnson et al. 2014) and FQR-dependent CEF in anoxia, where both the stroma and the PQ pool tend to be reduced (Tolleter et al. 2011; Alric 2014; Johnson et al. 2014; Godaux et al. 2015). Likewise, both mutants feature diminished electron transfer rates (Petroutsos et al. 2009; Dang et al. 2014; Johnson et al. 2014) and are extremely susceptible to PSI photodamage in response to high light (Johnson et al. 2014; Kukuczka et al. 2014). Both the deficient induction of qE-dependent NPQ and the enhanced PSI photoinhibition related to impaired photosynthetic control likely arise from insufficient acidification of the thylakoid lumen, i.e. perturbation of the regulatory feedback loop linking metabolic capacity and excitation flux. This lost capability to fine-tune the transmembrane proton gradient may arise from reduced proton influx and/or enhanced proton efflux. In fact, in vivo ECS absorption spectroscopy indicated, in response to high light, the pmf in *A. thaliana pgr5* is diminished due to an increased g_H^+ of the ATPase (Avenson et al. 2005; Wang et al. 2015). Such alterations of the ATPase conductivity imply a potential direct

involvement of PGR5 in mechanisms regulating the ATPase (Tikkanen et al. 2015). Otherwise, the ATP deficit resulting from reduced CEF efficiency entails the accumulation of P_i in the thylakoid stroma, which in turn may increase g_H^+ (Kramer et al. 2004a). The fact that low CO_2 conditions restore the ability of *pgr5* plants to induce qE-dependent NPQ (Nandha et al. 2007; Munekage et al. 2008) corroborate this notion, as the reduced assimilatory capacity results in decreased ATP consumption. Another interesting insight was obtained with the ATPase PGR5 double mutant in *C. reinhardtii*: The high-light-sensitive phenotype arising from over-acidification of the thylakoid lumen in the ATPase single mutant is alleviated in *ΔATPase pgr5*. Likewise, electron transfer is restored, as the additional absence of PGR5 in the double mutant mitigates the intense photosynthetic control in the ATPase single mutant. Both findings confirm the perturbation of the transmembrane proton gradient in the PGR5 single mutant and point to an impact on proton influx as opposed to proton efflux via the ATPase (Johnson et al. 2014). Recent reports even indicate a surprisingly high contribution of ΔpH (relative to ΔΨ) to the reduced total pmf in *A. thaliana pgr5*, suggesting the existence of a yet unknown compensatory mechanism, still failing to trigger qE-dependent NPQ and photosynthetic control in this mutant (Shikanai and Yamamoto 2016; Yamamoto et al. 2016). Another intriguing aspect of potential PGRL1 functions has been revealed investigating the acclimation of a PGRL1 knockdown mutant to iron deficiency, a condition where both PGR5 and PGRL1 expression are induced in the wild type. In this mutant, the response to iron deprivation is perturbed: The ATP deficit arising from the impaired induction of FQR-dependent CEF is compensated by enhanced respiration. However, the augmented mitochondrial activity potentially results in intensified iron redistribution to sustain the activity of respiratory complexes, resulting in reduced photosynthetic activity. Moreover, the PGRL1 knockdown mutant features iron deficiency symptoms at higher iron concentrations than the wild type. Therefore, the authors proposed PGRL1 plays a dual role in both iron sensing/redistribution and electron transfer partitioning (Petroutsos et al. 2009). Similar to the phenomenon observed during iron starvation, further compensatory mechanisms are induced to cope with the reducing power accumulating at the PSI acceptor side in the absence of PGR5 and/or PGRL1: In *pgrl1* an increased cooperation between chloroplast and mitochondria was observed, facilitating a dissipation of excess reducing power in the mitochondria (Petroutsos et al. 2009; Tolleter et al. 2011; Dang et al. 2014). In addition, the expression of flavodiiron NAD(P)H:O_2 oxidoreductases (FLVA/B) is enhanced in *pgrl1* in response to high-light and low-CO_2 conditions (Dang et al. 2014). In line with this finding, overexpression of *Physcomitrella patens* FLVA and FLVB abolishes PSI acceptor side limitation in *A. thaliana pgr5* plants (Yamamoto et al. 2016). Finally, *pgr5, pgrl1* and *pgr5pgrl1* feature enhanced H_2 production in short-term and long-term anoxia/sulphur deprivation (Tolleter et al. 2011; Godaux et al. 2015; Steinbeck et al. 2015; Chen et al. 2016). Addition of the uncoupling agent FCCP elevates H_2 production in the wild type to a similar level as in *pgrl1*, reflecting the perturbation of the transmembrane proton gradient in the mutant (Tolleter et al. 2011). An accelerated transition to anoxia and efficient O_2 consumption due to increased mitochondrial respiration and

enhanced ROS-scavenging enzyme activity in the mutants during sulphur deprivation even sustains the activity of PSII, since it is more efficiently protected from photodamage (Steinbeck et al. 2015; Chen et al. 2016).

4 CEF Regulation

Emerging concepts for the regulation of CEF, in particular in relation to LEF, range from a dynamic competition between electron flow pathways to a structural and thermodynamic segregation (Eberhard et al. 2008). In a freely diffusing system, reaction kinetics have to be considered. While the rate-limiting step of LEF is the oxidation of PQH_2 at the Q_o site of the Cyt b_6f complex, the reduction of PQ has been considered as the rate-limiting step of CEF, since LEF and CEF compete at this point (Alric 2010). Furthermore, the stromal redox poise and in particular the redox state of the $NADP^+$/NADPH pool have been proposed to modulate CEF operation relative to LEF activity (Hald et al. 2008; Alric et al. 2010; Johnson 2011). In addition, FNR and reduced FDX may play an essential role in electron flow partitioning (Breyton et al. 2006; Goss and Hanke 2014). As LEF and CEF coincide at various points but compete at others, a varying extent of spatial separation has been predicted. In vascular plants, which feature extensive lateral heterogeneity, restricted diffusion of PQ in compartmentalized pools may confine CEF to unstacked areas, whereas LEF might predominate in stacked regions (Kirchhoff 2014). Since in *C. reinhardtii*, lateral heterogeneity is not as pronounced as in vascular plants, further concepts suggesting the formation of multiprotein complexes directing electrons towards distinct routes might be more relevant in this context. According to the FNR model, the association of FNR with PSI (or soluble FNR in the thylakoid stroma) might promote LEF, whereas following the association of FNR with the Cyt b_6f complex, CEF may operate preferentially (Joliot and Joliot 2006; Johnson 2011; Goss and Hanke 2014). A potential CEF supercomplex has been isolated from *C. reinhardtii* upon sucrose density gradient centrifugation of solubilized thylakoids (Iwai et al. 2010a; Terashima et al. 2012). In vascular plants, such a multiprotein complex remained elusive (Breyton et al. 2006), until it has been identified in a recent electron microscopy-based study (Yadav et al. 2017). The formation of the putative CEF supercomplex in *C. reinhardtii* is induced in response to alterations of the chloroplast redox poise as upon shifts to anoxia or high light (Takahashi et al. 2013; Bergner et al. 2015), i.e. reducing conditions where CEF is induced to dissipate stromal redox pressure (Alric 2014). The multiprotein complex comprises major components of the electron transport chain such as the Cyt b_6f complex, PSI and FNR, both LHCI and LHCII as well as PGRL1, PETO (Iwai et al. 2010a; Takahashi et al. 2013), PGR5 (*unpublished data*), ANR1 and CAS (Terashima et al. 2012). Knockdown of PETO, ANR1 and CAS results in impaired CEF induction upon a shift to anoxia, as well as in high-light sensitivity in the case of ANR1 and CAS (Terashima et al. 2012;

Takahashi et al. 2016). Association of the Ca^{2+}-sensor CAS with the putative CEF supercomplex points to a Ca^{2+}-dependent regulation of FQR-dependent CEF in *C. reinhardtii* (Terashima et al. 2012; Chen et al. 2015).

5 Auxiliary Electron Transport Pathways

In addition to the "classical" linear and cyclic electron transport pathways, there exists a multitude of pathways which are all more or less directly interconnected with the regulation and function of the major photosynthetic complexes. These "auxiliary" pathways are mainly thought to optimize photosynthetic function as well as ensure continued operation of the system in an ever-changing environment. Accordingly, the processes discussed in the following sections are most prominent when organisms experience harsh growth conditions.

5.1 Ferredoxins

FDX is a small, soluble, [2Fe-2S]-type iron-sulphur cluster-bearing protein located in the chloroplast stroma. In LEF, it functions as the major electron acceptor of PSI, transferring electrons to FNR for NADPH synthesis (see Sect. 1.1). However, FDX is also involved as electron mediator in a wide variety of metabolic pathways other than LEF, most of which are dependent on electrons derived from the electron transport chain. Specific distribution of photosynthesis-derived electrons between the various metabolic pathways is thought to be achieved by the presence of different pathway-specific FDX isoforms. Consistent with this hypothesis, 13 potential FDX isoforms are encoded in the genome of *C. reinhardtii* (Yang et al. 2015b), with 11 of these being predicted to be targeted to the chloroplast. Out of these, six isoforms have been studied in more detail (FDX1–FDX6) so far. Phylogenetic analysis places FDX1 and FDX5 close to the photosynthetically active, so called leaf-type FDXs and FDX2 close to the non-photosynthetic root-type FDXs of vascular plants (Terauchi et al. 2009). FDX3, FDX4 and FDX6 seem to be more evolutionary divergent, as they cluster with neither of the two groups and are therefore further referred to as microbial-type FDXs.

FDX1 is the by far most abundant isoform under standard growth conditions, where FDX1 mRNA constitutes 98% of the FDX transcript pool. This amount is subjected to changes depending on the environmental conditions, with copper deficiency representing the condition triggering the most dramatic changes so far, under which the FDX1 transcript amount still accounts for 50% of the pool (Terauchi et al. 2009). Being the most abundant, it is not surprising that this isoform is also the one which is thought to be the most diverse in terms of its involvement in different metabolic pathways. Its most prominent function is the support of photosynthetic electron flow, provided by its efficient interaction with FNR and also

hydrogenase, which is necessary to support LEF under anaerobic conditions (Godaux et al. 2015) (see chapter "Chlamydomonas: Hydrogenase and Hydrogen Production"). A recent study aimed at establishing an interaction network for the various FDX isoforms in *C. reinhardtii* uncovered a vast number of potential interaction partners (Peden et al. 2013). Highlighting some results being of particular interest for this chapter, FDX1 was found to be involved in TRX signalling and thereby in all related processes amongst which are ROS signalling, ROS detoxification and alternative electron flow linked to the Mehler reaction (see Sect. 5.3), as well as the regulation of carbon metabolism and redox exchange between chloroplast and other cellular compartments. Furthermore, a possible involvement of FDX1 in fatty acid biosynthesis, nitrogen assimilation and fermentation was inferred.

Although clustering with the non-photosynthetic root-type FDXs, FDX2 is structurally highly similar to FDX1 (Boehm et al. 2015). The redox potential of FDX2 is increased by about 70 mV compared to FDX1, narrowing the number of potential interaction partners. Nevertheless, the two isoforms share, amongst others, FNR and hydrogenase as targets. Regarding the interaction with hydrogenase, in vitro assays show lower rates for electron transfer via FDX2 when compared to FDX1 (Peden et al. 2013; Boehm et al. 2015). For electron donation from either of the two FDX isoforms to FNR, the situation is less clear, with a report claiming lower rates achieved by FDX2 when compared to FDX1 (Peden et al. 2013), which is contrasted by another report claiming similar rates for both isoforms but a markedly higher affinity of *C. reinhardtii* FNR for FDX2, making it the more efficient electron donor (Boehm et al. 2015). Regarding these conflicting results, it should be kept in mind that the amount of FDX1 present in vivo dramatically outweighs that of FDX2 in all conditions analysed so far, so that an increased affinity for FDX2 could represent a mean of ensuring ongoing interaction with both isoforms if they have to compete for FNR. Further functional differences between the two isoforms include a potential involvement of FDX2 in nitrogen assimilation as it is a more efficient electron donor to the nitrate reductase than FDX1. ANR1, a protein shown to be upregulated in anaerobic conditions and being involved in CEF (Terashima et al. 2010), was identified as another potential interaction partner of FDX2, although a direct involvement of the isoform under these conditions remains to be shown. Interestingly, and consistent with its classification as root-type FDX, FDX2 shows a six-times higher catalytic efficiency in accepting electrons from FNR than FDX1, suggesting a role in non-photosynthetic metabolism (Terauchi et al. 2009).

Although clustering with the leaf-type FDXs, FDX5 plays a major role in photosynthesis-independent dark metabolism, more specifically in sustaining thylakoid membrane identity and allowing growth of *C. reinhardtii* cells maintained in darkness (Yang et al. 2015b). Together with previous results showing that FDX5 is inefficient in electron donation to FNR or hydrogenase (Jacobs et al. 2009), a direct involvement of this isoform in photosynthetic processes seems to be highly unlikely at this point.

The three microbial-type FDXs are less well characterized than the isoforms related to vascular plant FDXs, with the least information being available for FDX6. Isoforms 3 and 4 show no function in supporting LEF, as they are inefficient in electron donation to FNR or hydrogenase. FDX4 could however indirectly affect the function of the electron transport chain, as glycolytic enzymes and Ch-PRX1 (see Sect. 5.3.3) have been identified as potential interaction partners (Peden et al. 2013).

5.2 Chlororespiration

Chlororespiration, defined as a respiratory process within the chloroplast oxidizing NAD(P)H at the expense of O_2 and involving changes in the redox state of the PQ pool, was demonstrated by Pierre Bennoun as early as 1982 (Bennoun 1982). Subsequent studies led to the identification of plastid terminal oxidase (PTOX) (Carol et al. 1999; Wu et al. 1999), a diiron oxidase located at the stromal side of the thylakoid membrane (Lennon et al. 2003). Sequence analysis revealed a distant relationship with the alternative oxidase (AOX) found at the n-side of the inner mitochondrial membrane. Single copies of the *PTOX* gene were reported in the genomes of most vascular plant and cyanobacteria species. Within the taxa of red, brown or green algae, species carrying two copies of *PTOX*, including *C. reinhardtii*, were described. PTOX shows high affinity for PQH_2 as a substrate, utilizing the extracted electrons for the reduction of O_2 to H_2O (Josse et al. 2003; Yu et al. 2014). While PTOX oxidizes the PQ pool, the pool is reduced, as discussed above, via Nda2. A phenomenon illustrating the strong link of chlororespiration with overall cellular metabolism is the fact that in dark incubated *C. reinhardtii* cultures, the redox state of PQ is strongly dependent on the aeration of the sample. While the PQ pool in aerated cells is estimated to be 70% oxidized (Houille-Vernes et al. 2011), it is largely reduced when O_2 is withdrawn (Bennoun 1982). An explanation is given by considering the "Pasteur effect", i.e. the induction of glycolysis and starch breakdown upon ATP limitation induced through the shift to anaerobiosis. In *C. reinhardtii*, the "upper half" of glycolysis is localized in the chloroplast, leading to an increase in the stromal NADPH concentration through the catalytic activity of the glyceraldehyde-phosphate-dehydrogenase (Terashima et al. 2011; Johnson and Alric 2012). Via the action of Nda2, this results in reduction of the PQ pool, which additionally cannot be oxidized anymore by PTOX activity as O_2 is absent.

Chlororespiration forms an important link between chloroplast and overall cellular metabolism, as has been recently demonstrated by a pair of studies conducted on nitrogen-limited *C. reinhardtii* cultures (Wei et al. 2014; Saroussi et al. 2016). Photoheterotrophic nitrogen starvation (in the presence of acetate as a carbon source) leads to a progressive loss of the cell's ability to fix carbon, which is achieved by downregulation of Rubisco, the key enzyme of the CBB cycle, and of the Cyt b_6f complex, which is elementary for photosynthetic electron flow. Under

these conditions, the cellular content of Nda2 and PTOX2 increases together with the chlororespiratory activity. This combined effect has been interpreted as a switch in the function of the thylakoid membrane from a photosynthetic towards a respiratory mode in an effort to maintain a balanced availability of nitrogen and carbon resources (Wei et al. 2014).

In contrast to the situation observed for photoheterotrophic nitrogen limitation, photoautotrophic conditions do not result in a downregulation of photosynthetic carbon fixation. Nevertheless, PTOX and Nda2 levels as well as the chlororespiratory activity are also found to be upregulated under these conditions (Saroussi et al. 2016). As the photosynthetic electron transport chain is still fully functional, the role of the chlororespiratory enzymes under these conditions can be expanded to a more direct involvement in photosynthetic electron flow (discussed below).

Further indications for the critical role of the chlororespiratory enzymes in adjusting the dark state of the photosynthetic electron transport chain were given by studies observing chlorophyll fluorescence kinetics and low-temperature fluorescence spectra in a *ptox* mutant (Houille-Vernes et al. 2011; Takahashi et al. 2013). The *ptox* mutant strains exhibit an overall increased reduction of the PQ pool in darkness, leading to an altered distribution of the mobile LHCIIs between the photosystems, modulated through the activity of the Stt7 kinase (Depège et al. 2003): Whereas in darkness, the majority of the mobile antenna is connected to PSII in the wild type (state I), it is connected to PSI in *ptox* (state II). Also, upon a transition from darkness to light, the quantum yield of PSII is drastically lowered in *ptox* due to the reduction of the PSII primary electron acceptor PQ, limiting the efficiency of PSII. Whether these phenotypic differences are accompanied by reduced fitness under growth conditions in which they are expected to have the strongest impact, e.g. fluctuating light, remains to be investigated. Taken together, these results implicate a dual role of chlororespiration in darkness, which would be (1) a direct involvement in cellular metabolism and (2) priming dark incubated cells to ensure a photosynthetic function appropriate to the potential onset of light. As a complicating matter, these two tasks cannot be seen as being separate. In fact, there seems to be a tight interconnection between overall metabolism and photosynthetic function and regulation. For instance, the magnitude of CEF has been hypothesized to rely upon the cellular redox state (Takahashi et al. 2013), with the chlororespiratory enzymes being critical elements involved in such a regulatory network.

5.2.1 Chlororespiratory Enzymes in Light-Driven Electron Transport

While there is clear experimental evidence for the role of the chlororespiratory enzymes in dark metabolism, the presence of light-driven electron transport enhances the complexity of the PQ pool redox state. Hence, the role of Nda2 and especially PTOX in photosynthetic electron transport is still a matter of intense scientific debate.

Chlororespiration in *C. reinhardtii* itself is contributing to the buildup of the pmf, by removing protons from the stroma to reduce PQ, as both enzymes are located at the stromal face of the thylakoid membrane (although no charges are transferred across the membrane due to their specific activity). Furthermore, both Nda2 and PTOX can be part of pmf-building pathways when cooperating with major components of the photosynthetic electron transport chain. For Nda2, this would be PQ reduction and subsequent oxidation by the Cyt b_6f complex, coupled to the Q-cycle in which electrons and protons are translocated by Cyt b_6f complex activity (for a review, see Baniulis et al. 2008). In the context of overall photosynthetic electron transfer, taking into account PSI as the driving force behind Cyt b_6f activity as well as supplying the NADPH which is reinjected into the electron transport chain by Nda2, this pathway constitutes one possible route of CEF around PSI (see Sect. 3). The "other" route, depending on the proteins PGR5 and PGRL1, is generally seen as the major CEF pathway in *C. reinhardtii*. However, recent evidence suggests that under certain conditions, the bulk of CEF is actually carried out via Nda2 (Saroussi et al. 2016).

To be engaged in an electrogenic pathway, PTOX would need to work in conjunction with PSII, oxidizing PQH_2 and thereby being involved in a "short-circuit" water-to-water cycle. The first part of this reaction sequence would be PSII-catalysed H_2O oxidation coupled to proton release into the thylakoid lumen, electron transfer across the membrane and PQ reduction at the stromal site of the photosystem. PTOX would then oxidize PQH_2, thereby reducing O_2 and releasing H_2O into the stroma. Such a water-to-water cycle would of course be inferior to any pathway involving the Cyt b_6f complex in terms of establishment of a proton gradient necessary for ATP synthesis as well as acidification of the lumen required for efficient photoprotection via qE-dependent NPQ.

5.2.2 Potential PTOX Functions in Light-Driven Electron Transfer

Regardless its seeming ineffectiveness, light-driven O_2 reduction by PTOX has been shown to operate at physiological significant levels in a strain of the marine alga *Ostreococcus* (Cardol et al. 2008), which has low amounts of PSI, likely resulting from a permanent adaptation to low iron availability in its habitat. Further observations across various species show rising PTOX levels correlated with the application of abiotic stresses like high light (Trouillard et al. 2012; Laureau et al. 2013) or high salinity (Stepien and Johnson 2009), in line with a phylogenetic analysis illustrating that a number of halotolerant species have undergone PTOX gene duplication (Nawrocki et al. 2014). Consequently, a role of PTOX in stress responses, more specifically as a "safety valve" preventing the photosynthetic electron transport chain from over-reduction and ensuing oxidative damage by providing an additional electron sink, has been speculated. The safety valve hypothesis is a matter of controversial scientific debate. The major criticism arises from a closer consideration of PTOX turnover rates in the context of overall light-driven electron flow. In kinetic assays, in vivo rates spanning from 0.3 e^- s^{-1} $PSII^{-1}$ in tomato plants

(Trouillard et al. 2012) to 5 e^- s^{-1} $PSII^{-1}$ in *C. reinhardtii* (Houille-Vernes et al. 2011) have been reported, while the overall rate of steady-state photosynthesis under saturating light is estimated to be around 150 e^- s^{-1} $PSII^{-1}$ (Alric et al. 2010). The disproportion between these rates has led to the assessment that PTOX can in fact not act as an efficient release for electrons in the case of strong reducing pressure (Trouillard et al. 2012; Nawrocki et al. 2014). This conclusion is supported by an early study demonstrating that chlororespiration is outcompeted by light-driven electron transport at the onset of illumination (Peltier et al. 1987).

Contrasting the low turnover rates estimated from in vivo spectroscopic assays, rather high activities were reported from an in vitro analysis of the enzyme (Yu et al. 2014), reaching up to 320 e^- s^{-1} $PTOX^{-1}$. Together with the observation that PTOX1 from *C. reinhardtii* overexpressed in tobacco is associated with the thylakoid membrane in leaves exposed to high light, but not in low-light-grown leaves (Feilke et al. 2015), a consolidating hypothesis has been proposed (Krieger-Liszkay and Feilke 2016): In this model, PTOX associates with the thylakoid membrane in a pH-dependent manner—high light would lead to the buildup of a strong pH gradient across the membrane, elevating the stromal pH and thereby triggering PTOX association and activity. In low light, the stromal pH would be more acidic, resulting in the enzyme being soluble and therefore inactive, as it would have no access to its substrate PQH_2. The model could explain the discrepancies between the in vitro and the in vivo data. However, further evidence supporting it is needed, as in its current state it is largely based on observations in tobacco plants overexpressing PTOX1 from *C. reinhardtii*, and a universality of enzymatic characteristics cannot be taken for granted across species.

Along with the debate about the impact of PTOX on light-driven electron transport, the safety valve hypothesis has also been questioned based on reports demonstrating the potential of the enzyme to contribute to the generation of cytotoxic ROS. This capability for ROS production could arise from two potential sources, assuming a catalytic mechanism analogous to that proposed for O_2 reduction by AOX (Moore et al. 2013) and taking into account evidence based on the in vitro characterization of PTOX from *Oryza sativa* that both reactions in principle can take place (Yu et al. 2014): At pH 8, a semiquinone radical would be stabilized and trigger ROS formation, while lower pH values coinciding with a limitation of PQH_2 would lead to prolonged lifetimes of a superoxo intermediate formed at the diiron centre, ultimately giving rise to $O_2^{\bullet -}$.

Initial studies focused on potential photoprotecting properties of PTOX, aiming at increased stress tolerance by overexpression of the protein. Contrary to the expectations, elevated PTOX levels did not increase plant fitness (Rosso et al. 2006), with overexpression of foreign PTOX isoforms in *Nicotiana tabacum* even leading to enhanced photoinhibition and ROS production in plants exposed to high light (Heyno et al. 2009; Ahmad et al. 2012; Feilke et al. 2015). Given these results, ROS production would need to be tightly controlled when considering a differential membrane association hypothesis for PTOX. Otherwise, the function of the enzyme as a safety valve would be excluded by its ROS-producing characteristics. It should be kept in mind that ROS are not anymore just seen as potentially detrimental

agents but are also known to be critically involved in signalling mechanisms allowing, amongst other cellular responses, stress acclimation (Baxter et al. 2014).

At this point, the question about the involvement of PTOX in light-driven photosynthetic electron transfer cannot be answered conclusively. Given the data available at present, similar to the situation in darkness, a dual role for PTOX in light-driven electron transfer could arise: (1) as a starting point for ROS signalling (Nawrocki et al. 2014; Krieger-Liszkay and Feilke 2016), thereby initiating a rather long-term acclimatory response, and (2) as a valve releasing reducing pressure from the PQ pool in conditions where the routine electron transport pathways reach their limit.

5.2.3 Carotenoid Biosynthesis

PTOX, originally called IMMUTANS, was identified in *A. thaliana* plants exhibiting a light-dependent variegated phenotype (Carol et al. 1999; Wu et al. 1999). This variegation is thought to be caused by the involvement of the PQ pool and PTOX in carotenoid biosynthesis. In short, the desaturation of the carotenoid precursor phytoene by the phytoene desaturase requires PQ as electron acceptor. Consequently, the absence of PTOX during plastid development results in a strong reduction of the PQ pool, thereby blocking the synthesis of carotenoids (Sandmann 2009). As a result, PTOX-less plastids exposed to light experience enhanced oxidative stress, hindering their maturation.

In green algae containing single chloroplasts, the plastids divide together with their host cells, with each emerging cell inheriting a chloroplast with a functional photosynthetic machinery, providing light-dependent PQH_2 oxidation activity. As carotenoid accumulation in *C. reinhardtii* corresponds with the onset of illumination when grown in a 12-h light-12-h dark photoperiod (Janero and Barrnett 1982), the impact of PTOX on carotenoid synthesis is expected to be minor (Nawrocki et al. 2014). Indeed, a knockout of PTOX2 does not yield a difference in carotenoid accumulation. On the other hand, *ptox2* mutants do not even show a carotenoid phenotype if grown under heterotrophic conditions in darkness. The presence of PTOX1, the second isoform in *C. reinhardtii*, has been speculated to provide sufficient PQH_2 oxidation for driving carotenoid synthesis under these conditions in the mutant (Houille-Vernes et al. 2011). Although PTOX1 shows much lower turnover rates than PTOX2, these observations imply that the oxidase could be necessary for carotenoid synthesis in the alga, at least under specific conditions like dark heterotrophy.

5.3 Oxygen Reduction at the Stromal Face of PSI

The capacity for the photosynthetic consumption of O_2 resulting in the formation of H_2O_2, and, most important at the time, the fact that this reaction is not immediately

linked to H_2O splitting, was first described by Mehler in 1951 (Mehler 1951). In principle, the reduction of O_2 resulting in the formation of ROS can occur at any place of the electron transport chain where highly reducing intermediates are formed and have access to O_2 (Rutherford et al. 2012). In the case of the reaction observed by Mehler, this interface would likely be the terminal electron accepting iron-sulphur cluster F_B at the stromal side of PSI.

From there, O_2 reduction results in the formation of $O_2^{\bullet -}$, which is subsequently converted to H_2O_2 and O_2 by a chloroplast superoxide dismutase (SOD). Alternatively, a reduction of O_2 at the stromal face of PSI can be facilitated by flavodiiron proteins (FDPs) which avoid ROS formation. In any way, utilizing the full linear electron transport chain from H_2O splitting at PSII through the Cyt b_6f complex to O_2 reduction to H_2O at PSI, these water-to-water cycles contribute to the buildup of the trans-thylakoid proton gradient and therefore support all mechanisms requiring this gradient like ATP synthesis or photoprotection but do not result in NAD(P)H formation.

5.3.1 Superoxide Dismutase

Various isoforms of the metal-bearing SODs exist throughout all kingdoms of life, the most common containing iron (FeSOD), manganese (MnSOD), combined copper and zinc (Cu/ZnSOD) or nickel (NiSOD) as cofactors. FeSODs and MnSODs are evolutionary closely related, whereas neither Cu/ZnSODs nor NiSODs have a close relationship to the other SODs (Fink and Scandalios 2002; Priya et al. 2007). Most photosynthetic organisms contain combinations of Cu/ZnSODs with FeSODs and MnSODs, a notable exception being the chlorophyte green algae, including *C. reinhardtii*, which lack Cu/ZnSODs (Asada et al. 1977). So far, the consequence of this difference in the composition of primary antioxidant enzymes is unclear: For Cu/ZnSODs, very high enzymatic activities have been reported, and the enzymes are estimated to be present in stoichiometric amounts when compared to PSI. Furthermore, immune-labelling experiments in spinach chloroplasts illustrate a thylakoid membrane association leading to the formation of ROS-scavenging microdomains at the stromal face of PSI, leading to immediate $O_2^{\bullet -}$ disproportionation when generated at the photosystem (Ogawa et al. 1995). On the other hand, FeSODs have also been found associated with the thylakoid membrane (Friso et al. 2010), and overexpression of FeSODs but not Cu/ZnSODs in tobacco facilitates higher tolerance to methyl viologen-stimulated, light-dependent oxidative stress (Van Camp et al. 1996). *C. reinhardtii* retains FeSOD levels even under iron limitation, while PSI and other iron-containing chloroplast proteins are degraded. Moreover, an additional chloroplast-localized MnSOD is induced under these conditions, stretching the importance of the antioxidant defence system in general and specifically under conditions in which the electron transport chain is restructured (Page et al. 2012).

The H_2O_2 arising from the activity of SODs is less reactive than other ROS and, potentially for this matter, is also an important signalling molecule. However, there

is a need for further processing of the compound, as it is still a strong oxidant and has been shown to inhibit key biochemical pathways, most importantly CO_2 fixation by the CBB cycle (Kaiser 1976). A variety of chloroplast-localized enzymes function in H_2O_2 detoxification, namely, ascorbate peroxidase (APX), glutathione peroxidase (GPX) and peroxiredoxins (PRXs). It should be kept in mind that H_2O_2 is membrane permeable to a small extent, can be transported across membranes (Bienert et al. 2006) and is indicated to diffuse out of the chloroplast (Takeda et al. 1997). Therefore, the scavenging of ROS produced at the photosynthetic electron transport chain might not be confined to the compartment of its generation.

5.3.2 Ascorbate Peroxidase

In plants, the H_2O_2-scavenging enzyme catalase is present in peroxisomes but not in the chloroplast. A major step towards solving the puzzle of ROS detoxification in the photosynthetic compartment was the discovery of thylakoid-bound APX (Groden and Beck 1979) and soluble APX in the stroma (Kelly and Latzko 1979) in the late 1970s. Together with findings of enzymes involved in glutathione and ascorbate metabolism in the chloroplast (Foyer and Halliwell 1976, 1977), the glutathione-ascorbate or Foyer-Halliwell-Asada cycle was established. The first step in this cycle is the reduction of H_2O_2 with electrons derived from ascorbate, leading to the formation of H_2O and monodehydroascorbate (MDA). MDA is then re-reduced to ascorbate, either with electrons derived from FDX or from NAD(P)H, or a spontaneous disproportionation leads to the formation of dehydroascorbate (DHA). In this case, DHA can be re-reduced to ascorbate via a glutathione (GSH)-dependent system which ultimately derives its electrons from NAD(P)H as well.

APX belongs to the family of class I heme-bearing peroxidases (Raven et al. 2004). In *C. reinhardtii*, it is localized in the chloroplast stroma, but in contrast to vascular plants, no thylakoid membrane-associated isoform seems to be present (Takeda et al. 1997). This difference is especially noteworthy, as the membrane-bound APX of vascular plants is expected to be co-located with SOD in ROS-scavenging microdomains around PSI (Asada 2000), which would therefore not be present in the alga. Further comparison based on in vitro analysis of the *C. reinhardtii* enzyme showed an elevated affinity for ascorbate but lower catalytic turnover (Takeda et al. 1997). Regarding the affinity, these results could point towards an adaptation of the enzyme to lower substrate levels [intracellular ascorbate levels up to 1 mM have been reported in *C. reinhardtii* (Urzica et al. 2012), in contrast to levels between 20 mM and 300 mM in vascular plant chloroplasts (Smirnoff 2000)]. In line with this hypothesis are reports describing an inactivation of plant APX at low ascorbate availability (Chen and Asada 1989), whereas the isolated algal APX was much more stable under these conditions.

5.3.3 Peroxiredoxins and Glutathione Peroxidases

As an alternative to H_2O_2 detoxification by APX, photosynthetic organisms contain a set of thiol peroxidases. These include the enzyme families of GPXs and PRXs, which are evolutionary distinct (Dietz 2016), but function according to a similar reaction mechanism. H_2O_2 can be targeted by these enzymes; however, they have a broader range of potential targets, including alkyl hydroperoxides and peroxynitrite. The general mechanism consists of a reduction of the targeted peroxide by an active cysteine, leading to the formation of sulfenic acid. The sulfenic acid is then converted to a disulphide by intra- or intermolecular reaction with another catalytic cysteine residue. Subsequently, the active (reduced) form of the enzyme is restored through reduction by GSH, a TRX or a glutaredoxin, with the electrons ultimately being derived from NAD(P)H or reduced FDX generated by photosynthetic electron transfer. Deviating from this mechanism are selenocysteine-containing GPX (selenoGPX) and monomeric, single cysteine-containing PRX (1-cysPRX) (Dayer et al. 2008; Dietz 2011).

Two recent studies based on genome analyses revealed the presence of seven PRX and five GPX sequences (Dayer et al. 2008) or seven PRX and nine GPX sequences (Pitsch et al. 2010) in the *C. reinhardtii* genome. Based on EST screening, at least six of these PRXs and five of the GPXs are expressed. Of those expressed, three PRXs and three GPXs are potentially targeted to the chloroplast.

The PRX family is further divided into the subgroups of 2-cys PRXs, type II-PRXs and PRXQs, of which one of each is expressed and likely targeted to the chloroplast, as well as 1-cys PRXs, which seems to be absent in *C. reinhardtii*. Out of these, the 2-cys PRX Ch-PRX1 is the first and so far only PRX from the alga which has been isolated and characterized in vitro (Goyer et al. 2002). As described for other members of this group, Ch-PRX1 is present as a functional dimer with each monomer bearing one of the cysteine residues necessary for the reaction mechanism. Strengthening the notion of an involvement in detoxification of photo-generated ROS, Ch-PRX1 gene expression was found to depend on light and/or oxidative stress. The implemented isolation procedure took advantage of the affinity of TRX for Ch-PRX1, implicating that its active form is restored by the TRX system once oxidized. In a recent publication, efficient electron transfer between Ch-PRX1 and calredoxin (CRX), a calcium-dependent TRX has been demonstrated (Hochmal et al. 2016). All the peroxide-scavenging reaction cascades are inherently implicated to influence cellular ROS signalling. Consequently, the novel CRX is at the crossroad between ROS and Ca^{2+} signalling (Hochmal et al. 2015). In line, downregulation of CRX expression by an amiRNA strategy or insertional mutagenesis leads to increased lipid peroxidation in *C. reinhardtii* (Hochmal et al. 2015). Regarding the function in ROS signalling, an interesting feature of 2-cys PRXs is their reversible inactivation by hyperoxidation. This transient inactivation is thought to support ROS signalling and allow cellular acclimation in situations of excessive peroxide formation (Dietz 2011). In addition, 2-cys PRXs from multiple organisms from yeast to vascular plants have been

shown to form multimeres which have been described to adopt chaperone functions and protect other proteins from degradation under stress conditions (Jang et al. 2004; Aran et al. 2008; Kim et al. 2009).

Out of the PRX variants, 2-cys PRX was shown to be by far most abundant within the chloroplast stroma in *A. thaliana* (Peltier 2005). Given the fact that Ch-PRX1 is so far the only PRX which could be isolated from *C. reinhardtii,* this is likely to hold true for the alga as well. Evidence of physiological relevance of the two other PRX types found in the chloroplast, the type II-PRX Ch-PRX5 and the PRXQ Ch-PRX6 (in the nomenclature of Dayer et al.) is scarce (Dayer et al. 2008). Studies from vascular plants indicate that PRXQ is associated with the thylakoid membrane in the vicinity of PSII (Lamkemeyer et al. 2006) and/or could even be targeted to the lumen (Petersson et al. 2006). Judging from the phenotype of *A. thaliana* plants with altered PRXQ content, the function of the enzyme may be related to photosynthesis. In contrast to 2-cys PRX and PRXQ, chloroplast type II-PRX of *A. thaliana* was characterized as a soluble protein in the stroma (Dietz et al. 2006). In the cyanobacterium *Synechocystis* sp. strain PCC6803, this type of PRX was shown to be crucial for the growth of cultures when photosynthesizing in the presence of O_2 even at comparably low light intensities (Kobayashi et al. 2004). Based on the data available so far, a contribution of each type of PRX present in the chloroplast to a light-driven water-to-water cycle seems possible.

The same holds true for the potentially chloroplast-localized GPXs described so far. Two out of these three enzymes, Ch-GPX1 and Ch-GPX2, are selenocysteine-containing GPXs (selenoGPXs). Selenocysteine-containing proteins are widespread amongst organisms but absent from yeast, some animals and embryophytes. Hypothetically, the low redox potential of selenocysteine led to selection pressure against its utilization once the O_2 concentration in the atmosphere was increasing, whereas an O_2-buffering aquatic environment led to organisms retaining these enzymes (Lobanov et al. 2007). Non-selenocysteine-containing GPXs (NS-GPXs) and selenoGPXs show high sequence similarity, but the selenocysteine in their active site is replaced by a cysteine. Regarding the reaction sequence, selenoGPXs are reduced by GSH in a two-step mechanism not involving disulphide formation within the enzyme or with another subunit (Johansson et al. 2005). In contrast, NS-GPXs act via the standard PRX/GPX reaction mechanism described above, and like PRX their reduction is rather dependent on TRX than on GSH. Based on their redox properties, their peroxidase activities should be lower than those of selenoGPXs. One NS-GPX, Ch-GPX5, might be present in two isoforms, one of which is potentially located in the chloroplast and one in the cytosol. Based on EST analysis, this is also the most highly expressed GPX isoform in *C. reinhardtii* (Dayer et al. 2008).

Transcription studies firmly established an involvement of Ch-GPX5 in ROS response. Expression of the corresponding gene is increased in response to singlet oxygen- and organic peroxide-induced oxidative stress (Leisinger et al. 2001), amongst other stresses likely leading to intracellular formation of these compounds (Ledford et al. 2004; Fischer et al. 2006). Conversely, mutants screened for high Ch-GPX5 expression show coinciding elevated singlet oxygen production (Fischer

et al. 2010). The notion that the enzyme is involved in ROS protection is further underpinned when looking at the protein level, where Ch-GPX5 overexpression lines show enhanced tolerance to oxidative stress (Ledford et al. 2007; Fischer et al. 2012). For the selenoGPX isoforms, the situation is less clear: So far, CrGPX1 has been reported to be upregulated on transcript level in sulphur-starved cells (Zhang et al. 2004). Earlier reports show strong dependency of scavenging of externally added H_2O_2 on a selenite-containing GPX in cultures supplemented with sodium selenite (Takeda et al. 1997). However, the identity of the GPX causing this effect was not revealed.

5.3.4 Flavodiiron Proteins

The presence of an additional pathway for PSI-driven O_2 photoreduction is implicated by the presence of flavodiiron proteins (FDPs) in the chloroplast of *C. reinhardtii*. Evidence for an involvement of this type of enzyme in photosynthesis was first found in the cyanobacterium Synechocystis, where electron transport upon a dark to light transition is strongly dependent on O_2 as electron acceptor. Knockout mutants of the encoding genes *FLV1* and/or *FLV3* show multiple related phenotypes like inhibition of light-driven O_2 uptake, acceptor side limitation of PSI and increased reduction of the electron transport chain upon a transition to light in dark-adapted cells (Helman et al. 2003). In the same line, the mutants also exhibit a decrease of PSI levels, likely due to ROS-induced photodamage, accompanied by a severe growth phenotype, when grown under fluctuating light (Allahverdiyeva et al. 2013). FDPs are capable of direct O_2 reduction without intermediate ROS formation, a mechanism which is consequently termed Mehler-like reaction. Evolutionary, FDPs share homologies with a-type flavoproteins charged with the detoxification of O_2 or NO in anaerobic archaea and bacteria. They are present in a multitude of eukaryotic organisms but notably absent from diatoms, haptophytes and vascular plants (Peltier et al. 2010). Despite the absence from vascular plants, a recent study, in which FDPs originating from the moss *P. patens* were heterologously expressed in *A. thaliana*, illustrated that these enzymes can still functionally interact with the electron transfer chain in the chloroplasts of angiosperms and even show potential to increase plant fitness under certain conditions as fluctuating light or in the *pgr5* background (Yamamoto et al. 2016). In photosynthetic organisms, a NAD(P)H:flavin oxidoreductase is fused C-terminally to the FDP, placing NAD(P)H at the intersection between thylakoid membrane-embedded electron transport and this mechanism of O_2 reduction (Vicente et al. 2002).

In the genome of *C. reinhardtii*, two genes encoding FLVA and FLVB are present (Peltier et al. 2010). Protein abundance was found to be elevated in *pgrl1* strains (Dang et al. 2014), where they potentially function as additional electron sink, thereby decreasing the elevated redox pressure on PSI caused by the mutation (see Sect. 3.2). In wildtype *C. reinhardtii* cells, transcript and protein levels were shown to change depending on growth light and/or CO_2 availability and also transiently increase upon a shift to sulphur-limited medium (Jokel et al. 2015).

Changes in light or CO_2 availability are expected to modulate the redox pressure exerted on the photosynthetic electron transport chain. FDPs would play a role as a safety valve downstream of PSI, similar as is discussed for PTOX downstream of PSII. A similar role can be inferred during the initial phase of sulphur starvation, but additionally, the transient induction seems to advance the acclimation process by driving light-dependent O_2 uptake before the O_2-sensitive hydrogenase and fermentation take over.

6 Concluding Remarks

The primary function of photosynthesis is the conversion of light energy into chemical energy. At the first glance, this task seems readily achieved by performing photosynthetic linear electron transfer (LEF, Fig. 1a), providing reducing equivalents in the form of NADPH and an electrochemical proton gradient across the thylakoid membrane which is utilized to build up high-energy compounds in the form of ATP. NADPH and ATP are then consumed by carbon fixation via the Calvin-Benson-Bassham (CBB) cycle, using these primary products to build up organic compounds necessary for cell growth and long-term energy storage. The CBB cycle demands ATP and NADPH in a fixed ratio of 1.5, while LEF itself can only provide these compounds at a ratio of 1.38, so that "simply" running LEF is not sufficient for organisms to thrive based on light energy alone (Allen 2002). Generally, the ATP demand can be satisfied by utilizing some of the captured light energy to run cyclic electron flow around photosystem I (CEF, Fig. 1b), which is considered to be the major auxiliary pathway allowing balanced photosynthetic energy conversion. But photosynthesis is inextricably linked with the widely branched network of cellular metabolism, and in their natural habitats, organisms experience a large variety of different stresses, coping with each of which requires the consumption of some form of energy. Diverting electrons towards various metabolic pathways at the level of ferredoxin (FDX) represents one mechanism to address this issue. Furthermore, the light-capturing machinery itself is able to react in a highly flexible manner depending on external stimuli. Even in the absence of light, chlororespiration provides a way to integrate cellular metabolism to the status of the photosynthetic electron transport chain through the consumption of reducing equivalents (Fig. 1c). During illumination, a challenge is posed by the fluctuating availability and quality of the primary energy source itself, especially in combination with the task of carrying out redox reactions in an O_2-rich atmosphere. Photosystems have evolved to minimize the occurrence of hazardous direct O_2 reduction; state transitions and non-photochemical quenching (NPQ) allow the regulation of energy influx in response to different light availabilities. Further down the line, the electrochemical proton gradient resulting from light-driven electron transfer itself functions as a feedback system implemented through the mechanisms of photosynthetic control and pmf partitioning. In the case of limited availability of the oxidized primary electron acceptor $NADP^+$, the presence of

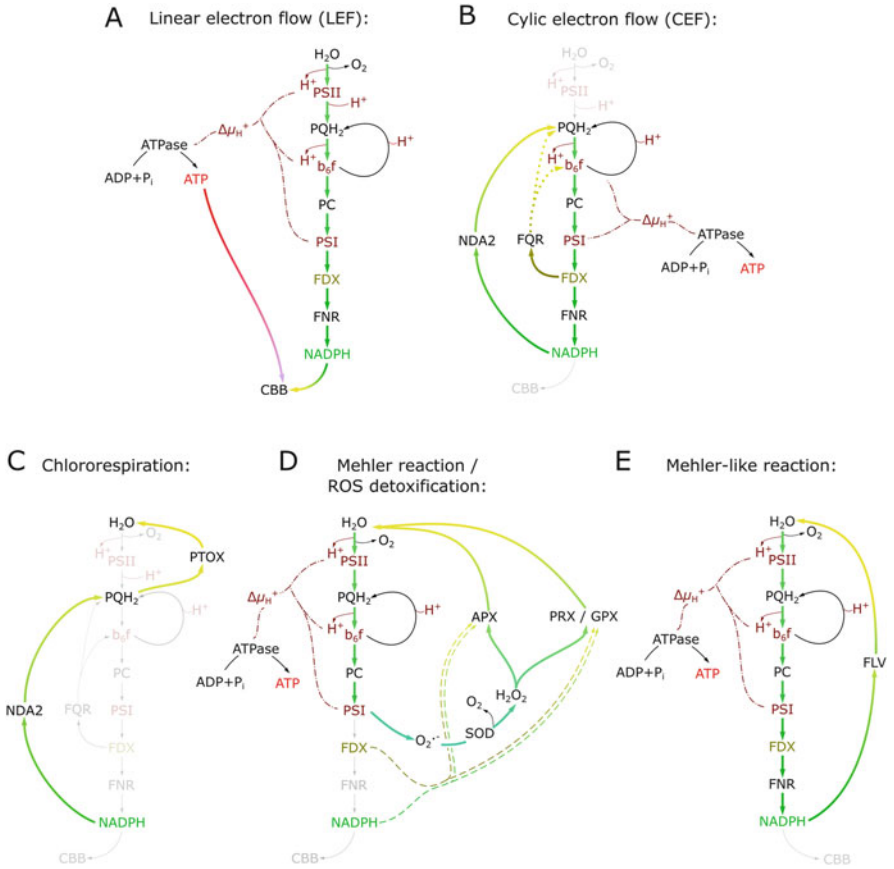

Fig. 1 Overview of the various electron transfer/metabolic pathways described in this chapter. Reaction steps contributing to the buildup of reducing power are depicted in a colour gradient towards *dark green*. Reaction steps leading to consumption of reducing power are depicted in colour gradients towards *yellow*. Protons translocated from the stroma to the thylakoid lumen and enzyme complexes contributing to the buildup of the proton motive force ($\Delta\mu_H^+$ or pmf) are shown in *wine red*. In **a**, ATP consumption in the Calvin-Benson-Bassham (CBB) cycle is highlighted by a colour gradient from *red* to *blue*. For detailed description, refer to text. **a**, **b**, **c**, **d** and **e**, depiction of LEF, CEF, chlororespiration, Mehler reaction/ROS detoxification and Mehler-like reactions

flavodiiron proteins (FDPs) in *C. reinhardtii* allows for safe utilization of O_2 as an alternative electron acceptor (Fig. 1e) while still allowing buildup of the trans-thylakoid proton gradient for ATP synthesis. Despite all these security measures, generation of ROS still occurs, amongst others, through the Mehler reaction at the stromal face of PSI. In this case, reducing power is diverted towards detoxification mechanisms to prevent excessive damage within the chloroplast and the whole cell (Fig. 1d; Table 1).

The mechanisms described in this chapter only represent a fraction of all the mechanisms necessary to allow a safe utilization of light energy, and to this day, the

Table 1 Summary of the discussed electron transfer pathways with their respective electron donors, electron carriers, electron acceptors and products

Electron transfer pathway	Electron donor	Electron carriers	Electron acceptor	Product
Linear electron flow (LEF) (A)	H_2O	PSII, PQ, Cyt b_6f, PC, PSI, FDX, FNR	$NADP^+$	O_2, NADPH, ATP
FQR-dependent CEF (B)	FDX(?)	FNR?	PQ	ATP
NDH-dependent CEF (B)	NAD(P)H	NDA2	PQ	ATP
Chlororespiration (C)	NAD(P)H	NDA2, PTOX	O_2	H_2O
Mehler (D)-, Mehler (E)-like reactions	PSI: F_B NADPH	– FLV	O_2 O_2	$O_2^{\bullet -}$, H_2O, ATP
$O_2^{\bullet -}$ detoxification (D)	$O_2^{\bullet -}$ (a)	SOD	$O_2^{\bullet -}$ (b)	O_2 (a) H_2O_2 (b)
H_2O_2 detoxification (D)	Ascorbate FDX/NADPH	APX GPX/PRX	H_2O_2	H_2O, MDA/DHA
H_2 production	FDX	Hydrogenase	H^+	H_2, ATP

interconnections between the resulting metabolic networks and the exact molecular mechanisms behind them are not fully understood. However, our current knowledge implies that in photosynthesis, a substantial amount of the captured energy is utilized to ensure a safe functioning of the process itself, and, as a direct result of this conclusion, a deepened knowledge of the underlying mechanisms will open a wide variety of possibilities to ultimately improve the utilization of the sun as an energy source.

Acknowledgments The research of MH is funded by the Deutsche Forschungsgemeinschaft (Grant no. HI 739/13-1).

References

Ahmad N, Michoux F, Nixon PJ (2012) Investigating the production of foreign membrane proteins in tobacco chloroplasts: expression of an algal plastid terminal oxidase. PLoS One. doi:10.1371/journal.pone.0041722

Allahverdiyeva Y, Mustila H, Ermakova M, Bersanini L, Richaud P, Ajlani G, Battchikova N, Cournac L, Aro E-M (2013) Flavodiiron proteins Flv1 and Flv3 enable cyanobacterial growth and photosynthesis under fluctuating light. Proc Natl Acad Sci U S A 110:4111–4116

Allen JF (2002) Photosynthesis of ATP – electrons, proton pumps, rotors, and poise. Cell 110:273–276

Allorent G, Tokutsu R, Roach T, Peers G, Cardol P, Girard-Bascou J, Seigneurin-Berny D, Petroutsos D, Kuntz M, Breyton C et al (2013) A dual strategy to cope with high light in Chlamydomonas reinhardtii. Plant Cell 25:545–557

Allorent G, Lefebvre-legendre L, Chappuis R, Kuntz M, Truong TB (2016) UV-B photoreceptor-mediated protection of the photosynthetic machinery in Chlamydomonas reinhardtii. 1–6

Alric J (2010) Cyclic electron flow around photosystem I in unicellular green algae. Photosynth Res 106:47–56

Alric J (2014) Redox and ATP control of photosynthetic cyclic electron flow in Chlamydomonas reinhardtii: (II) involvement of the PGR5-PGRL1 pathway under anaerobic conditions. Biochim Biophys Acta 1837:825–834

Alric J, Lavergne J, Rappaport F (2010) Redox and ATP control of photosynthetic cyclic electron flow in Chlamydomonas reinhardtii (I) aerobic conditions. Biochim Biophys Acta 1797:44–51

Aran M, Caporaletti D, Senn AM, Tellez De Iñon MT, Girotti MR, Llera AS, Wolosiuk RA (2008) ATP-dependent modulation and autophosphorylation of rapeseed 2-Cys peroxiredoxin. FEBS J 275:1450–1463

Armbruster U, Carrillo RL, Venema K, Pavlovic L, Schmidtmann E, Kornfeld A, Jahns P, Berry JA, Kramer DM, Jonikas MC (2014) Ion antiport accelerates photosynthetic acclimation in fluctuating light environments. Nat Commun 5:5439

Armbruster U, Leonelli L, Galvis VC, Strand D, Quinn EH, Jonikas MC, Niyogi KK (2016) Regulation and levels of the thylakoid K+/H+ antiporter KEA3 shape the dynamic response of photosynthesis in fluctuating light. Plant Cell Physiol 57:1557–1567

Asada K (2000) The water-water cycle as alternative photon and electron sinks. Philos Trans R Soc Lond Ser B Biol Sci 355:1419–1431

Asada K, Kanematsu S, Uchida K (1977) Superoxide dismutases in photosynthetic organisms: absence of the cuprozinc enzyme in eukaryotic algae. Arch Biochem Biophys 179:243–256

Avenson TJ, Cruz JA, Kanazawa A, Kramer DM (2005) Regulating the proton budget of higher plant photosynthesis. Proc Natl Acad Sci 102(27):9709–9713

Baker NR (2008) Chlorophyll fluorescence: a probe of photosynthesis in vivo. Annu Rev Plant Biol 59:89–113

Ballottari M, Truong TB, De Re E, Erickson E, Stella GR, Fleming GR, Bassi R, Niyogi KK (2016) Identification of pH-sensing sites in the light harvesting complex stress-related 3 protein essential for triggering non-photochemical quenching in Chlamydomonas reinhardtii. J Biol Chem 291(14):7334–7346. doi:10.1074/jbc.M115.704601

Baltz A, Dang K-V, Beyly A, Auroy P, Richaud P, Cournac L, Peltier G (2014) Plastidial expression of type II NAD(P)H dehydrogenase increases the reducing state of plastoquinones and hydrogen photoproduction rate by the indirect pathway in Chlamydomonas reinhardtii1. Plant Physiol 165:1344–1352

Baniulis D, Yamashita E, Zhang H, Hasan SS, Cramer WA (2008) Review structure–function of the cytochrome b 6 f complex. Photochem Photobiol 84:1349–1358

Baxter A, Mittler R, Suzuki N (2014) ROS as key players in plant stress signalling. J Exp Bot 65:1229–1240

Bennoun P (1982) Evidence for a respiratory chain in the chloroplast. Proc Natl Acad Sci U S A 79:4352–4356

Ben-Shem A, Frolow F, Nelson N (2003) Crystal structure of plant photosystem I. Nature 426:630–635

Bergner SV, Scholz M, Trompelt K, Barth J, Gäbelein P, Steinbeck J, Xue H, Clowez S, Fucile G, Goldschmidt-Clermont M et al (2015) State transition7-dependent phosphorylation is modulated by changing environmental conditions and its absence triggers remodeling of photosynthetic protein complexes. Plant Physiol 168:615–634

Bienert GP, Schjoerring JK, Jahn TP (2006) Membrane transport of hydrogen peroxide. Biochim Biophys Acta Biomembr 1758:994–1003

Boehm M, Alahuhta M, Mulder DW, Peden EA, Long H, Brunecky R, Lunin VV, King PW, Ghirardi ML, Dubini A (2015) Crystal structure and biochemical characterization of Chlamydomonas FDX2 reveal two residues that, when mutated, partially confer FDX2 the redox potential and catalytic properties of FDX1. Photosynth Res 128:45–57

Bonente G, Passarini F, Cazzaniga S, Mancone C, Buia MC, Tripodi M, Bassi R, Caffarri S (2008) The occurrence of the psbs gene product in Chlamydomonas reinhardtii and in other

photosynthetic organisms and its correlation with energy quenching. Photochem Photobiol 84:1359–1370
Breyton C, Nandha B, Johnson GN, Joliot P, Finazzi G (2006) Redox modulation of cyclic electron flow around photosystem I in C3 plants. Biochemistry 45:13465–13475
Busch A, Hippler M (2011) The structure and function of eukaryotic photosystem I. Biochim Biophys Acta 1807:864–877
Cardol P, Bailleul B, Rappaport F, Derelle E, Béal D, Breyton C, Bailey S, Wollman FA, Grossman A, Moreau H et al (2008) An original adaptation of photosynthesis in the marine green alga Ostreococcus. Proc Natl Acad Sci U S A 105:7881–7886
Cardol P, Alric J, Girard-Bascou J, Franck F, Wollman FA, Finazzi G (2009) Impaired respiration discloses the physiological significance of state transitions in Chlamydomonas. Proc Natl Acad Sci U S A 106:15979–15984
Cardol P, Forti G, Finazzi G (2011) Regulation of electron transport in microalgae. Regul Electron Transp Chloroplasts 1807:912–918
Carol P, Stevenson D, Bisanz C, Breitenbach J, Sandmann G, Mache R, Coupland G, Kuntz M (1999) Mutations in the Arabidopsis gene IMMUTANS cause a variegated phenotype by inactivating a chloroplast terminal oxidase associated with phytoene desaturation. Plant Cell 11:57–68
Carraretto L, Formentin E, Teardo E, Checchetto V, Tomizioli M, Morosinotto T, Giacometti GM, Finazzi G, Szabó I (2013) A thylakoid-located two-pore K+ channel controls photosynthetic light utilization in plants. Science 342:114–118
Chaux F, Peltier G, Johnson X (2015) A security network in PSI photoprotection: regulation of photosynthetic control, NPQ and O2 photoreduction by cyclic electron flow. Front Plant Sci 6:1–7
Chen G, Asada K (1989) Ascorbate peroxidase in tea leaves: occurrence of two isozymes and the differences in their enzymatic and molecular properties. Plant Cell Physiol 30:987–998
Chen H, Hu J, Qiao Y, Chen W, Rong J, Zhang Y, He C, Wang Q (2015) Ca2+-regulated cyclic electron flow supplies ATP for nitrogen starvation-induced lipid biosynthesis in green alga. Sci Rep 5:15117
Chen M, Zhang J, Zhao L, Xing J, Peng L, Kuang T, Rochaix J-D, Huang F (2016) Loss of algal proton gradient regulation 5 increases ROS scavenging an H2 evolution. J Integr Plant Biol:6772–6772
Clark RD, Hawkesford MJ, Coughlan SJ, Bennett J, Hind G (1984) Association of ferredoxin-NADP+ oxidoreductase with the chloroplast cytochrome b-f complex. FEBS Lett 174:137–142
Clowez S, Godaux D, Cardol P, Wollman F-A, Rappaport F (2015) The involvement of hydrogen-producing and ATP-dependent NADPH consuming pathways in setting the redox poise in the chloroplast of Chlamydomonas reinhardtii in anoxia. J Biol Chem 290:8666–8676
Correa-Galvis V, Redekop P, Guan K, Grieß A, Truong TB, Wakao S, Niyogi KK, Jahns P (2016) Photosystem II subunit PsbS is involved in the induction of LHCSR-dependent energy dissipation in Chlamydomonas reinhardtii. J Biol Chem jbc.M116.737312
DalCorso G, Pesaresi P, Masiero S, Aseeva E, Schünemann D, Finazzi G, Joliot P, Barbato R, Leister D (2008) A complex containing PGRL1 and PGR5 is involved in the switch between linear and cyclic electron flow in Arabidopsis. Cell 132:273–285
Dang K-V, Plet J, Tolleter D, Jokel M, Cuiné S, Carrier P, Auroy P, Richaud P, Johnson X, Alric J et al (2014) Combined increases in mitochondrial cooperation and oxygen photoreduction compensate for deficiency in cyclic electron flow in Chlamydomonas reinhardtii. Plant Cell 26:1–16
Davis GA, Kanazawa A, Schöttler MA, Kohzuma K, Froehlich JE, Rutherford AW, Satoh-Cruz M, Minhas D, Tietz S, Dhingra A et al (2016) Limitations to photosynthesis by proton motive force-induced photosystem II photodamage. elife 5:1–27
Dayer R, Fischer BB, Eggen RIL, Lemaire SD (2008) The peroxiredoxin and glutathione peroxidase families in Chlamydomonas reinhardtii. Genetics 179:41–57

Delosme R, Olive J, Wollman F-A (1996) Changes in light energy distribution upon state transitions: an in vivo photoacoustic study of the wild type and photosynthesis mutants from Chlamydomonas reinhardtii. Biochim Biophys Acta Bioenerg 1273:150–158

Depège N, Bellafiore S, Rochaix J-D (2003) Role of chloroplast protein kinase Stt7 in LHCII phosphorylation and state transition in Chlamydomonas. Science 299:1572–1575

Desplats C, Mus F, Cuiné S, Billon E, Cournac L, Peltier G (2009) Characterization of Nda2, a plastoquinone-reducing type II NAD(P)H dehydrogenase in chlamydomonas chloroplasts. J Biol Chem 284:4148–4157

Dietz K-J (2011) Peroxiredoxins in plants and cyanobacteria. Antioxid Redox Signal 15:1129–1159

Dietz K-J (2016) Thiol-based peroxidases and ascorbate peroxidases: why plants rely on multiple peroxidase systems in the photosynthesizing chloroplast? Mol Cells 39:20–25

Dietz K-J, Stork T, Finkemeier I, Lamkemeyer P, Li W-X, El-Tayeb MA, Michel K-P, Pistorius E, Baier M (2006) Photoprotection, photoinhibition, gene regulation, and environment. In: Demmig-Adams B, Adams WW, Mattoo AK (eds) Advances in photosynthesis and respiration. Springer Netherlands, Dordrecht, pp 303–319

Drop B, Webber-Birungi M, Fusetti F, Kouřil R, Redding KE, Boekema EJ, Croce R (2011) Photosystem I of Chlamydomonas reinhardtii contains nine light-harvesting complexes (Lhca) located on one side of the core. J Biol Chem 286:44878–44887

Drop B, Webber-Birungi M, Yadav SKN, Filipowicz-Szymanska A, Fusetti F, Boekema EJ, Croce R (2014a) Light-harvesting complex II (LHCII) and its supramolecular organization in Chlamydomonas reinhardtii. Biochim Biophys Acta 1837:63–72

Drop B, Yadav SKN, Boekema EJ, Croce R (2014b) Consequences of state transitions on the structural and functional organization of Photosystem I in the green alga Chlamydomonas reinhardtii. Plant J:181–191

Duan Z, Kong F, Zhang L, Li W, Zhang J (2016) A bestrophin-like protein modulates the proton motive force across the thylakoid membrane in Arabidopsis. J Integr Plant Biol:1–32

Eberhard S, Finazzi G, Wollman FA (2008) The dynamics of photosynthesis. Annu Rev Genet 42:463–515

Fan M, Li M, Liu Z, Cao P, Pan X, Zhang H, Zhao X, Zhang J, Chang W (2015) Crystal structures of the PsbS protein essential for photoprotection in plants. Nat Struct Mol Biol 22:729–735

Feilke K, Streb P, Gabriel C, Perreau F, Kruk J, Krieger-Liszkay A (2015) Effect of Chamydomonas plastid terminal oxidase 1 expressed in tobacco on photosynthetic electron transfer. Plant J 85:219–228

Finazzi G, Rappaport F (1998) In vivo characterization of the electrochemical proton gradient generated in darkness in green algae and its kinetic effects on cytochrome b6f turnover. Biochemistry 37:9999–10005

Finazzi G, Sommer F, Hippler M (2005) Release of oxidized plastocyanin from photosystem I limits electron transfer between photosystem I and cytochrome b6f complex in vivo. Proc Natl Acad Sci 102(19):7031–7036

Fink RC, Scandalios JG (2002) Molecular evolution and structure–function relationships of the superoxide dismutase gene families in angiosperms and their relationship to other eukaryotic and prokaryotic superoxide dismutases. Arch Biochem Biophys 399:19–36

Fischer BB, Eggen RIL, Trebst A, Krieger-Liszkay A (2006) The glutathione peroxidase homologous gene Gpxh in Chlamydomonas reinhardtii is upregulated by singlet oxygen produced in photosystem II. Planta 223:583–590

Fischer BB, Eggen RIL, Niyogi KK (2010) Characterization of singlet oxygen-accumulating mutants isolated in a screen for altered oxidative stress response in Chlamydomonas reinhardtii. BMC Plant Biol 10:279

Fischer BB, Ledford HK, Wakao S, Huang SG, Casero D, Pellegrini M, Merchant SS, Koller A, Eggen RIL, Niyogi KK (2012) SINGLET OXYGEN RESISTANT 1 links reactive electrophile signaling to singlet oxygen acclimation in Chlamydomonas reinhardtii. Proc Natl Acad Sci USA 109:E1302–E1311

Foyer CH, Halliwell B (1976) The presence of glutathione and glutathione reductase in chloroplasts: a proposed role in ascorbic acid metabolism. Planta 133:21–25

Foyer CH, Halliwell B (1977) Purification and properties of dehydroascorbate reductase from spinach leaves. Phytochemistry 16:1347–1350

Friso G, Majeran W, Huang M, Sun Q, van Wijk KJ (2010) Reconstruction of metabolic pathways, protein expression, and homeostasis machineries across maize bundle sheath and mesophyll chloroplasts: large-scale quantitative proteomics using the first maize genome assembly. Plant Physiol 152:1219–1250

Ghysels B, Godaux D, Matagne RF, Cardol P, Franck F (2013) Function of the chloroplast hydrogenase in the microalga Chlamydomonas: the role of hydrogenase and state transitions during photosynthetic activation in anaerobiosis. PLoS One. doi:10.1371/journal.pone.0064161

Godaux D, Bailleul B, Berne N, Cardol P (2015) Induction of photosynthetic carbon fixation in anoxia relies on hydrogenase activity and PGRL1-mediated cyclic electron flow in Chlamydomonas reinhardtii. Plant Physiol 168:00105.2015

Goldschmidt-Clermont M, Bassi R (2015) Sharing light between two photosystems: mechanism of state transitions. Curr Opin Plant Biol 25:71–78

Goss T, Hanke GT (2014) The end of the line: can ferredoxin and ferredoxin NADP (H) oxidoreductase determine the fate of photosynthetic electrons? Curr Protein Pept Sci 15:385–393

Goyer A, Haslekås C, Miginiac-Maslow M, Klein U, Le Marechal P, Jacquot JP, Decottignies P (2002) Isolation and characterization of a thioredoxin-dependent peroxidase from Chlamydomonas reinhardtii. Eur J Biochem 269:272–282

Groden D, Beck E (1979) H2O2 destruction by ascorbate-dependent systems from chloroplasts. BBA-Bioenergetics 546:426–435

Grossman AR, Catalanotti C, Yang W, Dubini A, Magneschi L, Subramanian V, Posewitz MC, Seibert M (2011) Multiple facets of anoxic metabolism and hydrogen production in the unicellular green alga Chlamydomonas reinhardtii. New Phytol 190:279–288

Haehnel W, Jansen T, Gause K, Klösgen RB, Stahl B, Michl D, Huvermann B, Karas M, Herrmann RG (1994) Electron transfer from plastocyanin to photosystem I. EMBO J 13:1028–1038

Hald S, Nandha B, Gallois P, Johnson GN (2008) Feedback regulation of photosynthetic electron transport by NADP(H) redox poise. Biochim Biophys Acta 1777:433–440

Helman Y, Tchernov D, Reinhold L, Shibata M, Ogawa T, Schwarz R, Ohad I, Kaplan A (2003) Genes encoding A-type flavoproteins are essential for photoreduction of O2 in cyanobacteria. Curr Biol 13:230–235

Hemschemeier A, Happe T (2011) Alternative photosynthetic electron transport pathways during anaerobiosis in the green alga Chlamydomonas reinhardtii. Biochim Biophys Acta 1807:919–926

Herdean A, Nziengui H, Zsiros O, Solymosi K, Garab G, Lundin B, Spetea C (2016a) The arabidopsis thylakoid chloride channel AtCLCe functions in chloride homeostasis and regulation of photosynthetic electron transport. Front Plant Sci 7:1–15

Herdean A, Teardo E, Nilsson AK, Pfeil BE, Johansson ON, Ünnep R, Nagy G, Zsiros O, Dana S, Solymosi K et al (2016b) A voltage-dependent chloride channel fine-tunes photosynthesis in plants. Nat Commun 7:11654

Hertle AP, Blunder T, Wunder T, Pesaresi P, Pribil M, Armbruster U, Leister D (2013) PGRL1 is the elusive ferredoxin-plastoquinone reductase in photosynthetic cyclic electron flow. Mol Cell 49:511–523

Heyno E, Gross CM, Laureau C, Culcasi M, Pietri S, Krieger-Liszky A (2009) Plastid alternative oxidase (PTOX) promotes oxidative stress when overexpressed in tobacco. J Biol Chem 284:31174–31180

Hippler M, Reichert J, Sutter M, Zak E, Altschmied L, Schröer U, Herrmann RG, Haehnel W (1996) The plastocyanin binding domain of photosystem I. EMBO J 15:6374–6384

Hippler M, Drepper F, Farah J, Rochaix J (1997) Fast electron transfer from cytochrome c6 and plastocyanin to photosystem I of Chlamydomonas reinhardtii requires PsaF. Biochemistry 36:6343–6349

Hippler M, Drepper F, Haehnel W, Rochaix J-D (1998) The N-terminal domain of PsaF: precise recognition site for binding and fast electron transfer from cytochrome c6 and plastocyanin to photosystem I of Chlamydomonas reinhardtii. Proc Natl Acad Sci U S A 95:7339–7344

Hochmal AK, Schulze S, Trompelt K, Hippler M (2015) Calcium-dependent regulation of photosynthesis. Biochim Biophys Acta 1847:993–1003

Hochmal AK, Zinzius K, Charoenwattanasatien R, Gäbelein P, Mutoh R, Tanaka H, Schulze S, Liu G, Scholz M, Nordhues A et al (2016) Calredoxin represents a novel type of calcium-dependent sensor-responder connected to redox regulation in the chloroplast. Nat Commun. doi:10.1038/ncomms11847

Houille-Vernes L, Rappaport F, Wollman F-A, Alric J, Johnson X (2011) Plastid terminal oxidase 2 (PTOX2) is the major oxidase involved in chlororespiration in Chlamydomonas. Proc Natl Acad Sci 108:20820–20825

Iwai M, Takizawa K, Tokutsu R, Okamuro A, Takahashi Y, Minagawa J (2010a) Isolation of the elusive supercomplex that drives cyclic electron flow in photosynthesis. Nature 464:1210–1213

Iwai M, Yokono M, Inada N, Minagawa J (2010b) Live-cell imaging of photosystem II antenna dissociation during state transitions. Proc Natl Acad Sci U S A 107:2337–2342

Jacobs J, Pudollek S, Hemschemeier A, Happe T (2009) A novel, anaerobically induced ferredoxin in Chlamydomonas reinhardtii. FEBS Lett 583:325–329

Janero DR, Barrnett R (1982) Thylakoid membrane biogenesis in Chlamydomonas reinhardtii 137+. II. Cell-cycle variations in the synthesis and assembly of pigment. J Cell Biol 93:411–416

Jang HH, Lee KO, Chi YH, Jung BG, Park SK, Park JH, Lee JR, Lee SS, Moon JC, Yun JW et al (2004) Two enzymes in one: two yeast peroxiredoxins display oxidative stress-dependent switching from a peroxidase to a molecular chaperone function. Cell 117:625–635

Jans F, Mignolet E, Houyoux P-A, Cardol P, Ghysels B, Cuiné S, Cournac L, Peltier G, Remacle C, Franck F (2008) A type II NAD(P)H dehydrogenase mediates light-independent plastoquinone reduction in the chloroplast of Chlamydomonas. Proc Natl Acad Sci U S A 105:20546–20551

Järvi S, Suorsa M, Aro EM (2015) Photosystem II repair in plant chloroplasts – regulation, assisting proteins and shared components with photosystem II biogenesis. Biochim Biophys Acta Bioenerg 1847:900–909

Johansson L, Gafvelin G, Arnér ESJ (2005) Selenocysteine in proteins – properties and biotechnological use. Biochim Biophys Acta - Gen Subj 1726:1–13

Johnson GN (2003) Thiol regulation of the thylakoid electron transport chain – a missing link in the regulation of photosynthesis? Biochemistry 42:3040–3044

Johnson GN (2004) Controversy remains: regulation of pH gradient across the thylakoid membrane. Trends Plant Sci 9:570–571

Johnson GN (2011) Reprint of: physiology of PSI cyclic electron transport in higher plants. Biochim Biophys Acta 1807:906–911

Johnson X, Alric J (2012) Interaction between starch breakdown, acetate assimilation, and photosynthetic cyclic electron flow in Chlamydomonas reinhardtii. J Biol Chem 287:26445–26452

Johnson X, Steinbeck J, Dent RM, Takahashi H, Richaud P, Ozawa S-I, Houille-Vernes L, Petroutsos D, Rappaport F, Grossman AR et al (2014) Proton gradient regulation 5-mediated cyclic electron flow under ATP- or redox-limited conditions: a study of ΔATpase pgr5 and ΔrbcL pgr5 mutants in the green alga Chlamydomonas reinhardtii. Plant Physiol 165:438–452

Jokel M, Kosourov S, Battchikova N, Tsygankov AA, Aro EM, Allahverdiyeva Y (2015) Chlamydomonas flavodiiron proteins facilitate acclimation to anoxia during sulfur deprivation. Plant Cell Physiol 56:1598–1607

Joliot P, Joliot A (2006) Cyclic electron flow in C3 plants. Biochim Biophys Acta 1757:362–368

Josse EM, Alcaraz JP, Labouré AM, Kuntz M (2003) In vitro characterization of a plastid terminal oxidase (PTOX). Eur J Biochem 270:3787–3794

Kaiser W (1976) The effect of hydrogen peroxide on CO2 fixation of isolated intact chloroplasts. BBA-Bioenergetics 440:476–482

Kelly GJ, Latzko E (1979) Soluble ascorbate peroxidase: detection in plants and use in vitamim C estimation. Naturwissenschaften 66:617–619

Kim SY, Jang HH, Lee JR, Sung NR, Lee HB, Lee DH, Park DJ, Kang CH, Chung WS, Lim CO et al (2009) Oligomerization and chaperone activity of a plant 2-Cys peroxiredoxin in response to oxidative stress. Plant Sci 177:227–232

Kirchhoff H (2014) Diffusion of molecules and macromolecules in thylakoid membranes. Biochim Biophys Acta Bioenerg 1837:495–502

Kobayashi M, Ishizuka T, Katayama M, Kanehisa M, Bhattacharyya-Pakrasi M, Pakrasi HB, Ikeuchi M (2004) Response to oxidative stress involves a novel peroxiredoxin gene in the unicellular cyanobacterium Synechocystis sp. PCC 6803. Plant Cell Physiol 45:290–299

Kramer DM, Avenson TJ, Edwards GE (2004a) Dynamic flexibility in the light reactions of photosynthesis governed by both electron and proton transfer reactions. Trends Plant Sci 9:349–357

Kramer DM, Avenson TJ, Edwards GE (2004b) Response to Johnson: Controversy remains: regulation of pH gradient across thylakoid membrane. Trends Plant Sci 9:571–572

Krieger A, Weis E (1993) The role of calcium in the pH-dependent control of Photosystem II. Photosynth Res 37:117–130

Krieger-Liszkay A, Feilke K (2016) The dual role of the plastid terminal oxidase PTOX: between a protective and a pro-oxidant function. Front Plant Sci 6:2015–2017

Kuhlgert S, Drepper F, Fufezan C, Sommer F, Hippler M (2012) Residues PsaB Asp612 and PsaB Glu613 of photosystem I confer pH-dependent binding of plastocyanin and cytochrome c(6). Biochemistry 51:7297–7303

Kukuczka B, Magneschi L, Petroutsos D, Steinbeck J, Bald T, Powikrowska M, Fufezan C, Finazzi G, Hippler M (2014) Proton gradient regulation5-like1-mediated cyclic electron flow is crucial for acclimation to anoxia and complementary to nonphotochemical quenching in stress adaptation. Plant Physiol 165:1604–1617

Kunz HH, Gierth M, Herdean A, Satoh-Cruz M, Kramer DM, Spetea C, Schroeder JI (2014) Plastidial transporters KEA1, -2, and -3 are essential for chloroplast osmoregulation, integrity, and pH regulation in Arabidopsis. Proc Natl Acad Sci USA 111:7480–7485

Kurisu G, Kusunoki M, Katoh E, Yamazaki T, Teshima K, Onda Y, Kimata-Ariga Y, Hase T (2001) Structure of the electron transfer complex between ferredoxin and ferredoxin-NADP(+) reductase. Nat Struct Biol 8:117–121

Kurisu G, Zhang H, Smith JL, Cramer WA (2003) Structure of the cytochrome b6f complex of oxygenic photosynthesis: tuning the cavity. Science 302:1009–1014

Lamkemeyer P, Laxa M, Collin V, Li W, Finkemeier I, Schöttler MA, Holtkamp V, Tognetti VB, Issakidis-Bourguet E, Kandlbinder A et al (2006) Peroxiredoxin Q of Arabidopsis thaliana is attached to the thylakoids and functions in context of photosynthesis. Plant J 45:968–981

Laureau C, De Paepe R, Latouche G, Moreno-Chacón M, Finazzi G, Kuntz M, Cornic G, Streb P (2013) Plastid terminal oxidase (PTOX) has the potential to act as a safety valve for excess excitation energy in the alpine plant species Ranunculus glacialis L. Plant Cell Environ 36:1296–1310

Ledford HK, Baroli I, Shin JW, Fischer BB, Eggen RIL, Niyogi KK (2004) Comparative profiling of lipid-soluble antioxidants and transcripts reveals two phases of photo-oxidative stress in a xanthophyll-deficient mutant of Chlamydomonas reinhardtii. Mol Gen Genomics 272:470–479

Ledford HK, Chin BL, Niyogi KK (2007) Acclimation to singlet oxygen stress in Chlamydomonas reinhardtii. Eukaryot Cell 6:919–930

Leisinger U, Rüfenacht K, Fischer B, Pesaro M, Spengler A, Zehnder AJ, Eggen RI (2001) The glutathione peroxidase homologous gene from Chlamydomonas reinhardtii is transcriptionally up-regulated by singlet oxygen. Plant Mol Biol 46:395–408

Lemeille S, Willig A, Depège-Fargeix N, Delessert C, Bassi R, Rochaix J-D (2009) Analysis of the chloroplast protein kinase Stt7 during state transitions. PLoS Biol 7:e45

Lennon AM, Prommeenate P, Nixon PJ (2003) Location, expression and orientation of the putative chlororespiratory enzymes, Ndh and IMMUTANS, in higher-plant plastids. Planta 218:254–260

Li XP, Björkman O, Shih C, Grossman AR, Rosenquist M, Jansson S, Niyogi KK (2000) A pigment-binding protein essential for regulation of photosynthetic light harvesting. Nature 403:391–395

Li XP, Gilmore AM, Caffarri S, Bassi R, Golan T, Kramer D, Niyogi KK (2004) Regulation of photosynthetic light harvesting involves intrathylakoid lumen pH sensing by the PsbS protein. J Biol Chem 279:22866–22874

Liguori N, Roy LM, Opacic M, Durand G, Croce R, Roy LM (2013) Regulation of light harvesting in the green alga Chlamydomonas reinhardtii: the C-terminus of LHCSR is the knob of a dimmer switch. J Am Chem Soc 135:18339–18342

Lobanov AV, Fomenko DE, Zhang Y, Sengupta A, Hatfield DL, Gladyshev VN (2007) Evolutionary dynamics of eukaryotic selenoproteomes: large selenoproteomes may associate with aquatic life and small with terrestrial life. Genome Biol 8:R198

Lucker B, Kramer DM (2013) Regulation of cyclic electron flow in Chlamydomonas reinhardtii under fluctuating carbon availability. Photosynth Res. doi:10.1007/s11120-013-9932-0

Malnoë A, Wang F, Girard-Bascou J, Wollman FA, de Vitry C (2014) Thylakoid FtsH protease contributes to photosystem II and cytochrome b6f remodeling in Chlamydomonas reinhardtii under stress conditions. Plant Cell 26:373–390

Maruyama S, Tokutsu R, Minagawa J (2014) Transcriptional regulation of the stress-responsive light harvesting complex genes in Chlamydomonas reinhardtii. Plant Cell Physiol 55:1304–1310

Mehler AH (1951) Studies on reactions of illuminated chloroplasts. II. Stimulation and inhibition of the reaction with molecular oxygen. Arch Biochem Biophys 34:339–351

Meyer Zu Tittingdorf JMW, Rexroth S, Schäfer E, Schlichting R, Giersch C, Dencher NA, Seelert H (2004) The stoichiometry of the chloroplast ATP synthase oligomer III in Chlamydomonas reinhardtii is not affected by the metabolic state. Biochim Biophys Acta Bioenerg 1659:92–99

Mitchell P (1961) Coupling of phosphorylation to electron and hydrogen transfer by a chemiosmotic type of mechanism. Nature 191(4784):144–148

Moore AL, Shiba T, Young L, Harada S, Kita K, Ito K (2013) Unraveling the heater: new insights into the structure of the alternative oxidase. Annu Rev Plant Biol 64:637–663

Müller P, Li XP, Niyogi KK (2001) Non-photochemical quenching. A response to excess light energy. Plant Physiol 125:1558–1566

Munekage Y, Hojo M, Meurer J, Endo T, Tasaka M, Shikanai T (2002) PGR5 is involved in cyclic electron flow around photosystem I and is essential for photoprotection in Arabidopsis. Cell 110:361–371

Munekage YN, Genty B, Peltier G (2008) Effect of PGR5 impairment on photosynthesis and growth in Arabidopsis thaliana. Plant Cell Physiol 49(11):1688–1698

Munekage Y, Hashimoto M, Miyake C, Tomizawa K, Endo T, Tasaka M, Shikanai T (2004) Cyclic electron flow around photosystem I is essential for photosynthesis. Nature 429:579–582

Muranaka LS, Rütgers M, Bujaldon S, Heublein A, Geimer S, Wollman FA, Schroda M (2016) TEF30 interacts with photosystem II monomers and is involved in the repair of photodamaged photosystem II in *Chlamydomonas reinhardtii*. Plant Physiol 170:821–840

Murata N, Allakhverdiev SI, Nishiyama Y (2012) The mechanism of photoinhibition in vivo: re-evaluation of the roles of catalase, α-tocopherol, non-photochemical quenching, and electron transport. Biochim Biophys Acta Bioenerg 1817:1127–1133

Mus F, Cournac L, Cardettini V, Caruana A, Peltier G (2005) Inhibitor studies on non-photochemical plastoquinone reduction and H(2) photoproduction in Chlamydomonas reinhardtii. Biochim Biophys Acta 1708:322–332

Nagy G, Unnep R, Zsiros O, Tokutsu R, Takizawa K, Porcar L, Moyet L, Petroutsos D, Garab G, Finazzi G et al (2014) Chloroplast remodeling during state transitions in Chlamydomonas reinhardtii as revealed by noninvasive techniques in vivo. Proc Natl Acad Sci U S A 111:5042–5047

Nandha B, Finazzi G, Joliot P, Hald S, Johnson GN (2007) The role of PGR5 in the redox poising of photosynthetic electron transport. Biochim Biophys Acta Bioenerg 1767:1252–1259

Nawrocki WJ, Tourasse NJ, Taly A, Rappaport F, Wollman F-A (2014) The plastid terminal oxidase: its elusive function points to multiple contributions to plastid physiology. Annu Rev Plant Biol 66:150112150216002

Nawrocki WJ, Santabarbara S, Mosebach L, Wollman FA, Rappaport F (2016) State transitions redistribute rather than dissipate energy between the two photosystems in Chlamydomonas. Nat Plants 2:16031

Nelson N, Ben-Shem A (2004) The complex architecture of oxygenic photosynthesis. Nat Rev Mol Cell Biol 5:971–982

Nelson N, Yocum CF (2006) Structure and function of photosystems I and II. Annu Rev Plant Biol 57:521–565

Nordling M, Sigfridsson K, Young S, Lundberg LG, Hansson Ö (1991) Flash-photolysis studies of the electron transfer from genetically modified spinach plastocyanin to photosystem I. FEBS Lett 291:327–330

Ogawa K, Kanematsu S, Takabe K, Asada K (1995) Attachment of CuZn-superoxide dismutase to thylakoid membranes at the site of superoxide generation (PSI) in spinach chloroplasts: detection by immuno-gold labeling after rapid freezing and substitution method. Plant Cell Physiol 36:565–573

Page MD, Allen MD, Kropat J, Urzica EI, Karpowicz SJ, Hsieh SI, Loo JA, Merchant SS (2012) Fe sparing and Fe recycling contribute to increased superoxide dismutase capacity in iron-starved Chlamydomonas reinhardtii. Plant Cell 24:2649–2665

Peden EA, Boehm M, Mulder DW, Davis R, Old WM, King PW, Ghirardi ML, Dubini A (2013) Identification of global ferredoxin interaction networks in chlamydomonas reinhardtii. J Biol Chem 288:35192–35209

Peers G, Truong TB, Ostendorf E, Busch A, Elrad D, Grossman AR, Hippler M, Niyogi KK (2009) An ancient light-harvesting protein is critical for the regulation of algal photosynthesis. Nature 462:518–521

Peltier J-B (2005) The oligomeric stromal proteome of Arabidopsis thaliana chloroplasts. Mol Cell Proteomics 5:114–133

Peltier G, Ravenel J, Verméglio A (1987) Inhibition of a respiratory activity by short saturating flashes in Chlamydomonas: evidence for a chlororespiration. BBA-Bioenergetics 893:83–90

Peltier G, Tolleter D, Billon E, Cournac L (2010) Auxiliary electron transport pathways in chloroplasts of microalgae. Photosynth Res 106:19–31

Peltier G, Aro EM, Shikanai T (2016) NDH-1 and NDH-2 plastoquinone reductases in oxygenic photosynthesis. Annu Rev Plant Biol 67:6.1–6.26

Peng L, Shimizu H, Shikanai T (2008) The chloroplast NAD(P)H dehydrogenase complex interacts with photosystem I in Arabidopsis. J Biol Chem 283:34873–34879

Petersson UA, Kieselbach T, García-Cerdán JG, Schröder WP (2006) The Prx Q protein of Arabidopsis thaliana is a member of the luminal chloroplast proteome. FEBS Lett 580:6055–6061

Petroutsos D, Terauchi AM, Busch A, Hirschmann I, Merchant SS, Finazzi G, Hippler M (2009) PGRL1 participates in iron-induced remodeling of the photosynthetic apparatus and in energy metabolism in Chlamydomonas reinhardtii. J Biol Chem 284:32770–32781

Petroutsos D, Busch A, Janssen I, Trompelt K, Bergner SV, Weinl S, Holtkamp M, Karst U, Kudla J, Hippler M (2011) The chloroplast calcium sensor CAS is required for photoacclimation in Chlamydomonas reinhardtii. Plant Cell 23:2950–2963

Petroutsos D, Tokutsu R, Maruyama S, Flori S, Greiner A, Magneschi L, Cusant L, Kottke T, Mittag M, Hegemann P et al (2016) A blue-light photoreceptor mediates the feedback regulation of photosynthesis. Nature 537:563–566

Pitsch NT, Witsch B, Baier M (2010) Comparison of the chloroplast peroxidase system in the chlorophyte Chlamydomonas reinhardtii, the bryophyte Physcomitrella patens, the lycophyte Selaginella moellendorffii and the seed plant Arabidopsis thaliana. BMC Plant Biol 10:133

Priya B, Premanandh J, Dhanalakshmi RT, Seethalakshmi T, Uma L, Prabaharan D, Subramanian G (2007) Comparative analysis of cyanobacterial superoxide dismutases to discriminate canonical forms. BMC Genomics 8:435

Raven EL, Lad L, Sharp KH, Mewies M, Moody PC (2004) Defining substrate specificity and catalytic mechanism in ascorbate peroxidase. Biochem Soc Symp 38:27–38

Rochaix J-D (2014) Regulation and dynamics of the light-harvesting system. Annu Rev Plant Biol 65:287–309

Rosso D, Ivanov AG, Fu A, Geisler-Lee J, Hendrickson L, Geisler M, Stewart G, Krol M, Hurry V, Rodermel SR et al (2006) IMMUTANS does not act as a stress-induced safety valve in the protection of the photosynthetic apparatus of Arabidopsis during steady-state photosynthesis. Plant Physiol 142:574–585

Rott M, Martins NF, Thiele W, Lein W, Bock R, Kramer DM, Schöttler M a (2011) ATP synthase repression in tobacco restricts photosynthetic electron transport, CO2 assimilation, and plant growth by overacidification of the thylakoid lumen. Plant Cell 23:304–321

Rutherford AW, Osyczka A, Rappaport F (2012) Back-reactions, short-circuits, leaks and other energy wasteful reactions in biological electron transfer: redox tuning to survive life in O2. FEBS Lett 586:603–616

Sandmann G (2009) Evolution of carotene desaturation: the complication of a simple pathway. Arch Biochem Biophys 483:169–174

Saroussi SI, Wittkopp TM, Grossman AR (2016) The type II NADPH dehydrogenase facilitates cyclic electron flow, energy dependent quenching and chlororespiratory metabolism during acclimation of Chlamydomonas reinhardtii to nitrogen deprivation. Plant Physiol pp 02014 (2015)

Shikanai T, Yamamoto H (2016) Contribution of cyclic and pseudo-cyclic electron transport to the formation of proton motive force in chloroplasts. Mol Plant. doi:10.1016/j.molp.2016.08.004

Singh SK, Hasan SS, Zakharov SD, Naurin S, Whitelegge JP, Cramer WA, Lafayette W, Pasarow T, Spectrometry M, Angeles L et al (2016) Trans-membrane signaling in photosynthetic state transitions: redox- and structure-dependent interaction in vitro between Stt7 kinase and cytochrome b6f complex. J Biol Chem. doi:10.1074/jbc.M116.732545

Smirnoff N (2000) Ascorbate biosynthesis and function in photoprotection. Philos Trans R Soc Lond Ser B Biol Sci 355:1455–1464

Sommer F, Drepper F, Hippler M (2002) The luminal helix l of PsaB is essential for recognition of plastocyanin or cytochrome c6 and fast electron transfer to photosystem I in Chlamydomonas reinhardtii. J Biol Chem 277:6573–6581

Sommer F, Drepper F, Haehnel W, Hippler M (2004) The hydrophobic recognition site formed by residues PsaA-Trp651 and PsaB-Trp627 of photosystem I in Chlamydomonas reinhardtii confers distinct selectivity for binding of plastocyanin and cytochrome c 6. J Biol Chem 279:20009–20017

Sonoike K (2011) Photoinhibition of photosystem I. Physiol Plant 142:56–64

Steinbeck J, Nikolova D, Weingarten R, Johnson X, Richaud P, Peltier G, Hermann M, Magneschi L, Hippler M (2015) Deletion of Proton Gradient Regulation 5 (PGR5) and PGR5-Like 1 (PGRL1) proteins promote sustainable light-driven hydrogen production in Chlamydomonas reinhardtii due to increased PSII activity under sulfur deprivation. Front Plant Sci 6:1–11

Stepien P, Johnson GN (2009) Contrasting responses of photosynthesis to salt stress in the glycophyte Arabidopsis and the halophyte thellungiella: role of the plastid terminal oxidase as an alternative electron sink. Plant Physiol 149:1154–1165

Stiehl HH, Witt HT (1969) Quantitative treatment of the function of plastoquinone in photosynthesis. Zeitschrift fur Naturforsch – Sect B J Chem Sci 24:1588–1598

Stroebel D, Choquet Y, Popot J-L, Picot D (2003) An atypical haem in the cytochrome b(6)f complex. Nature 426:413–418

Suorsa M, Järvi S, Grieco M, Nurmi M, Pietrzykowska M, Rantala M, Kangasjärvi S, Paakkarinen V, Tikkanen M, Jansson S et al (2012) PROTON GRADIENT REGULATION5 is essential for proper acclimation of Arabidopsis photosystem I to naturally and artificially fluctuating light conditions. Plant Cell 24:2934–2948

Takahashi H, Clowez S, Wollman F-A, Vallon O, Rappaport F (2013) Cyclic electron flow is redox-controlled but independent of state transition. Nat Commun 4:1954

Takahashi H, Okamuro A, Minagawa J, Takahashi Y (2014) Biochemical characterization of photosystem I-associated light-harvesting complexes I and II isolated from state 2 cells of chlamydomonas reinhardtii. Plant Cell Physiol 55:1437–1449

Takahashi H, Schmollinger S, Lee J-H, Schroda M, Rappaport F, Wollman F-A, Vallon O (2016) The PETO protein interacts with other effectors of cyclic electron flow in Chlamydomonas. Mol Plant. doi:10.1016/j.molp.2015.12.017

Takeda T, Ishikawa T, Shigeoka S (1997) Metabolism of hydrogen peroxide by the scavenging system in Chlamydomonas reinhardtii. Physiol Plant 99:49–55

Terashima M, Specht M, Naumann B, Hippler M (2010) Characterizing the anaerobic response of Chlamydomonas reinhardtii by quantitative proteomics. Mol Cell Proteomics 9:1514–1532

Terashima M, Specht M, Hippler M (2011) The chloroplast proteome: a survey from the Chlamydomonas reinhardtii perspective with a focus on distinctive features. Curr Genet 57:151–168

Terashima M, Petroutsos D, Hüdig M, Tolstygina I, Trompelt K, Gäbelein P, Fufezan C, Kudla J, Weinl S, Finazzi G et al (2012) Calcium-dependent regulation of cyclic photosynthetic electron transfer by a CAS, ANR1, and PGRL1 complex. Proc Natl Acad Sci U S A 109:17717–17722

Terauchi AM, Lu S-F, Zaffagnini M, Tappa S, Hirasawa M, Tripathy JN, Knaff DB, Farmer PJ, Lemaire SD, Hase T et al (2009) Pattern of expression and substrate specificity of chloroplast ferredoxins from Chlamydomonas reinhardtii. J Biol Chem 284:25867–25878

Tibiletti T, Auroy P, Peltier G, Caffarri S (2016) Chlamydomonas reinhardtii PsbS protein is functional and accumulates rapidly and transiently under high light. Plant Physiol pp. 00572 (2016)

Tikkanen M, Rantala S, Aro E-M (2015) Electron flow from PSII to PSI under high light is controlled by PGR5 but not by PSBS. Front Plant Sci 6

Tokutsu R, Minagawa J (2013) Energy-dissipative supercomplex of photosystem II associated with LHCSR3 in Chlamydomonas reinhardtii. Proc Natl Acad Sci U S A 110:10016–10021

Tokutsu R, Kato N, Bui KH, Ishikawa T, Minagawa J (2012) Revisiting the supramolecular organization of photosystem II in Chlamydomonas reinhardtii. J Biol Chem 287:31574–31581

Tolleter D, Ghysels B, Alric J, Petroutsos D, Tolstygina I, Krawietz D, Happe T, Auroy P, Adriano J-M, Beyly A et al (2011) Control of hydrogen photoproduction by the proton gradient generated by cyclic electron flow in Chlamydomonas reinhardtii. Plant Cell 23:2619–2630

Trouillard M, Shahbazi M, Moyet L, Rappaport F, Joliot P, Kuntz M, Finazzi G (2012) Kinetic properties and physiological role of the plastoquinone terminal oxidase (PTOX) in a vascular plant. Biochim Biophys Acta Bioenerg 1817:2140–2148

Ünlü C, Drop B, Croce R, van Amerongen H (2014) State transitions in Chlamydomonas reinhardtii strongly modulate the functional size of photosystem II but not of photosystem I. Proc Natl Acad Sci U S A 111:3460–3465

Ünlü C, Polukhina I, Van Amerongen H (2015) Origin of pronounced differences in 77 K fluorescence of the green alga Chlamydomonas reinhardtii in state 1 and 2. Eur Biophys J. doi:10.1007/s00249-015-1087-9

Urzica EI, Adler LN, Page MD, Linster CL, Arbing MA, Casero D, Pellegrini M, Merchant SS, Clarke SG (2012) Impact of oxidative stress on ascorbate biosynthesis in Chlamydomonas via regulation of the VTC2 gene encoding a GDP-L-galactose phosphorylase. J Biol Chem 287:14234–14245

Van Camp W, Capiau K, Van Montagu M, Inzé D, Slooten L (1996) Enhancement of oxidative stress tolerance in transgenic tobacco plants overproducing Fe-superoxide dismutase in chloroplasts. Plant Physiol 112:1703–1714

Vicente JB, Gomes CM, Wasserfallen A, Teixeira M (2002) Module fusion in an A-type flavoprotein from the cyanobacterium Synechocystis condenses a multiple-component pathway in a single polypeptide chain. Biochem Biophys Res Commun 294:82–87

Vinyard DJ, Ananyev GM, Dismukes CG (2013) Photosystem II: the reaction center of oxygenic photosynthesis. Annu Rev Biochem 82:577–606

Wagner V, Ullmann K, Mollwo A, Kaminski M, Mittag M, Kreimer G (2007) The phosphoproteome of a Chlamydomonas reinhardtii eyespot fraction includes key proteins of the light signaling pathway. Plant Physiol 146:772–788

Wang C, Yamamoto H, Shikanai T (2015) Role of cyclic electron transport around photosystem I in regulating proton motive force. Biochim Biophys Acta Bioenerg 1847(9):931–938

Wang L, Yamano T, Takane S, Niikawa Y, Toyokawa C, Ozawa S, Tokutsu R, Takahashi Y, Minagawa J, Kanesaki Y et al (2016) Chloroplast-mediated regulation of CO_2-concentrating mechanism by Ca^{2+}-binding protein CAS in the green alga *Chlamydomonas reinhardtii*. Proc Natl Acad Sci 113:201606519

Wei L, Derrien B, Gautier A, Houille-Vernes L, Boulouis A, Saint-Marcoux D, Malnoë A, Rappaport F, de Vitry C, Vallon O et al (2014) Nitric oxide-triggered remodeling of chloroplast bioenergetics and thylakoid proteins upon nitrogen starvation in Chlamydomonas reinhardtii. Plant Cell 26:353–372

Whatley FR, Tagawa K, Arnon DI (1962) Separation of the light and dark reactions in electron transfer during photosynthesis. Biochemistry 49:266–270

Wobbe L, Bassi R, Kruse O (2015) Multi-level light capture control in plants and green algae. Trends Plant Sci xx:1–14

Wu D, Wright DA, Wetzel C, Voytas DF, Rodermel S (1999) The IMMUTANS variegation locus of Arabidopsis defines a mitochondrial alternative oxidase homolog that functions during early chloroplast biogenesis. Plant Cell 11:43–55

Xue H, Tokutsu R, Bergner SV, Scholz M, Minagawa J, Hippler M (2014) PSBR is required for efficient binding of LHCSR3 to photosystem II – light-harvesting supercomplexes in Chlamydomonas reinhardtii. Plant Physiol 167:1566–1578

Yadav KNS, Semchonok DA, Nosek L, Kouřil R, Fucile G, Boekema EJ, Eichacker LA (2017) Supercomplexes of plant photosystem I with cytochrome b6f, light-harvesting complex II and NDH. Biochim Biophys Acta Bioenerg 1858:12–20

Yamamoto H, Peng L, Fukao Y, Shikanai T (2011) An Src homology 3 domain-like fold protein forms a ferredoxin binding site for the chloroplast NADH dehydrogenase-like complex in Arabidopsis. Plant Cell 23:1480–1493

Yamamoto H, Takahashi S, Badger MR, Shikanai T (2016) Artificial remodelling of alternative electron flow by flavodiiron proteins in Arabidopsis. Nat Plants 2:16012

Yang W, Catalanotti C, Wittkopp TM, Posewitz MC, Grossman AR (2015a) Algae after dark: mechanisms to cope with anoxic/hypoxic conditions. Plant J 82:481–503

Yang W, Wittkopp TM, Li X, Warakanont J, Dubini A, Catalanotti C, Kim RG, Nowack ECM, Mackinder LCM, Aksoy M et al (2015b) Critical role of Chlamydomonas reinhardtii ferredoxin-5 in maintaining membrane structure and dark metabolism. Proc Natl Acad Sci U S A 112:14978–14983

Yu Q, Feilke K, Krieger-Liszkay A, Beyer P (2014) Functional and molecular characterization of plastid terminal oxidase from rice (Oryza sativa). Biochim Biophys Acta Bioenerg 1837:1284–1292

Zhang H, Whitelegge JP, Cramer WA (2001) Ferredoxin:NADP+ oxidoreductase is a subunit of the chloroplast cytochrome b6f complex. J Biol Chem 276:38159–38165

Zhang Z, Shrager J, Jain M, Vallon O, Grossman AR, Chang C (2004) Insights into the survival of Chlamydomonas reinhardtii during sulfur starvation based on microarray analysis of gene expression insights into the survival of Chlamydomonas reinhardtii during sulfur starvation based on microarray analysis of gene expression. Eukaryot Cell 3:1331–1348

Zito F, Finazzi G, Delosme R, Nitschke W, Picot D, Wollman F a (1999) The Qo site of cytochrome b6f complexes controls the activation of the LHCII kinase. EMBO J 18:2961–2969

Chlamydomonas: Bioenergetic Pathways—Regulation of Photosynthesis

State Transitions and qE Quenching

Jun Minagawa

Abstract Plants and algae have acquired the ability to acclimate to ever-changing environments to survive. During photosynthesis, light energy is converted into electrochemical energy by several membrane protein supercomplexes, which is used to fix CO_2. The efficiency of photosynthesis is modulated by many environmental factors, including temperature, drought, CO_2 concentration, and light. Recently, our understanding of such regulations of photosynthesis and the underlying molecular mechanisms has increased considerably. The photosynthetic supercomplexes undergo supramolecular reorganizations within a short time after receiving environmental cues. Two such representative reorganization events include state transitions that balance the excitation of the two photosystems and qE quenching that thermally dissipates excess energy at the level of the light-harvesting antenna. This chapter will focus on recent findings regarding the environmental regulation of photosynthesis in model organisms, paying particular attention to the unicellular green alga *Chlamydomonas reinhardtii*, illustrating the dynamic behavior of the photosynthetic machineries in nature.

Abbreviation

Chl	Chlorophyll
Cyt *bf*	Cytochrome b_6f complex
DCCD	Dicyclohexylcarbodiimide
DCMU	3-(3,4-Dichlorophenyl)-1,1-dimethylurea
Fd	Ferredoxin
HL	High light
LHCI and LHCII	Light-harvesting complex protein I and II
LL	Low light
NPQ	Non-photochemical quenching

J. Minagawa (✉)
Division of Environmental Photobiology, National Institute for Basic Biology, 38 Nishigonaka, Okazaki 444-8585, Aichi, Japan
e-mail: minagawa@nibb.ac.jp

M. Hippler (ed.), *Chlamydomonas: Molecular Genetics and Physiology*, Microbiology Monographs 30, DOI 10.1007/978-3-319-66365-4_5

PQ	Plastoquinone
PSI and PSII	Photosystem I and II
RNAi	RNA interference
Vx	Violaxanthin
WT	Wild type
Zx	Zeaxanthin
α-DM	*n*-Dodecyl-α-D-maltoside
β-DM	*n*-Dodecyl-β-D-maltoside

1 Introduction

Photosynthesis is initiated by harvesting light, which leads to the electron transport and the concomitant generation of proton motive force across the thylakoid membranes. The NADPH generated with the electron flow and the ATP produced with the proton motive force are required for assimilating carbon dioxide in the Calvin-Benson cycle. Photosystem I (PSI) and photosystem II (PSII) represent charge-separation devices on the thylakoid membranes that drive electron flow using light energy. These two photosystems originated from a common prototype, but today's PSI and PSII complexes are specialized and have differences in the organization of their light-harvesting systems, pigment compositions, electron acceptors and donors, and several other features. This chapter begins with introducing the current knowledge of the components and the structures of the two photosystems in *Chlamydomonas reinhardtii* under normal conditions and then describes their regulation and how they are reorganized upon environmental cues.

PSII and its light-harvesting complex proteins (LHCIIs) constitute a large chlorophyll (Chl)-protein supercomplex that is made up of more than 30 subunits. Light energy captured by LHCIIs is transferred to the central dimeric core complex, where it is trapped and used to drive electron flow from water to plastoquinone. In green plants, LHCIIs are formed of two layers, the major trimeric and the minor monomeric LHCII proteins (Dekker and Boekema 2005). In the green alga *C. reinhardtii*, there are four major LHCII proteins (types I–IV) with 5, 1, 2, and 1 isoforms (LHCBM3, -4, -6, -8, and -9; LHCBM5; LHCBM2 and -7; LHCBM1), respectively (Minagawa and Takahashi 2004), whereas in the vascular plant *Arabidopsis thaliana*, there are three major trimeric LHCII proteins (types I–III) with 5, 4, and 1 isoforms (LHCB1.1–1.5, LHCB2.1–2.4, and LHCB3.1), respectively (Jansson 1999). The two minor LHCII proteins CP29 and CP26 are encoded by the *LHCB4* and *LHCB5*, respectively, in *C. reinhardtii* (Teramoto et al. 2001; Minagawa 2009), whereas *A. thaliana* contains another minor LHCII protein CP24 encoded by the *LHCB6*.

Single-particle image analysis of electron micrographs revealed that these LHCII proteins are bound to both sides of the central dimeric core complex, with the core and the major LHCII trimers bordered by a few minor LHCII monomers (Dekker and Boekema 2005) (Fig. 1). When spinach (*Spinacia oleracea*) thylakoid

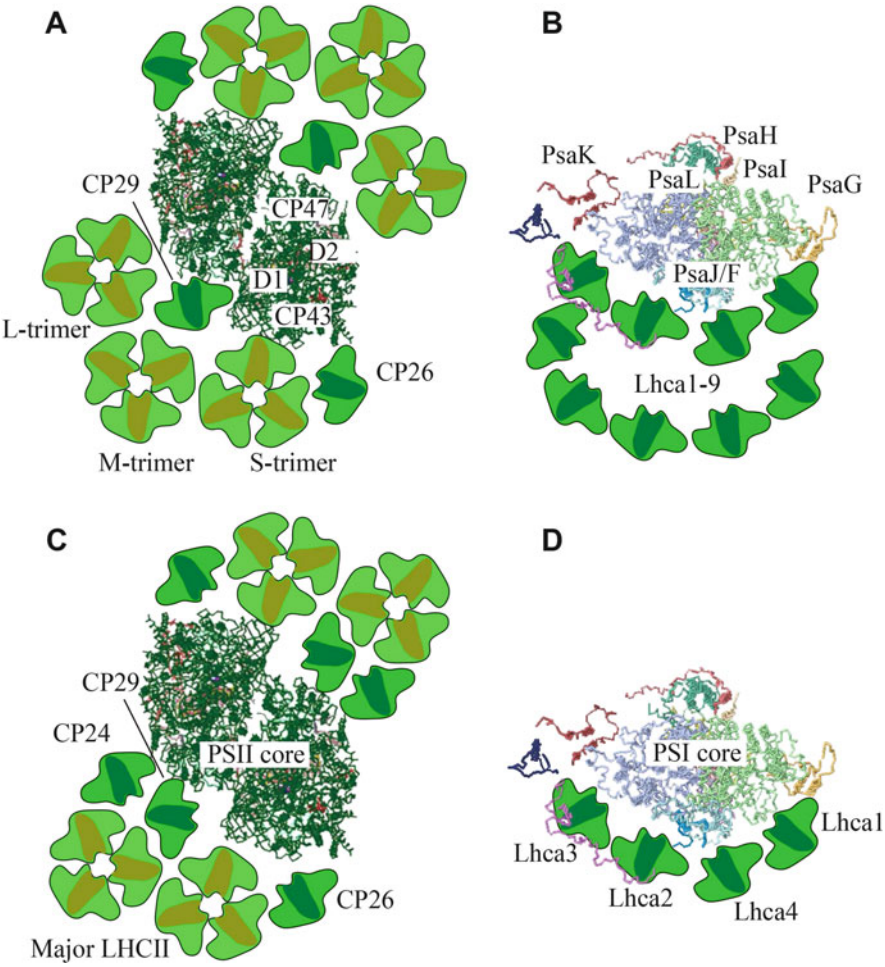

Fig. 1 Supramolecular organization of PSII-LHCII and PSI-LHCI supercomplexes in green algae and vascular plants. Top views of the PSII-LHCII supercomplex (**a**) and the PSI-LHCI supercomplex (**b**) from *C. reinhardtii* based on single-particle image analysis by Tokutsu et al. (2012) and Drop et al. (2011), respectively. Top views of the PSII-LHCII supercomplex from spinach (**c**) and the PSI-LHCI supercomplex from pea (**d**) based on single-particle image analysis by Dekker and Boekema (2005) and crystallography of the PSI-LHCI supercomplex (Amunts et al. 2010), respectively. All top-view images are from the lumenal side. The crystal coordinates were obtained from the Protein Data Bank: PSII core, 3ARC; PSI-LHCI, 2WSC

membranes are solubilized with *n*-dodecyl-β-D-maltoside (β-DM) (Boekema et al. 1995, 1998; Hankamer et al. 1997; Nield et al. 2000b), one LHCII trimer is bound strongly to each side of the core (C_2S_2 PSII-LHCII supercomplex). However, when the membranes are solubilized with *n*-dodecyl-α-D-maltoside (α-DM), the PSII-LHCII supercomplexes are organized as $C_2S_2M_{1-2}$ L_{0-1} or $C_2S_2M_0L_{1-2}$, wherein one to two moderately bound LHCII trimers and/or one loosely bound LHCII trimer

or one to two loosely bound LHCII trimers are associated with the C_2S_2-type supercomplex (Boekema et al. 1999; Yakushevska et al. 2001). When *A. thaliana* thylakoid membranes are solubilized with α-DM, the $C_2S_2M_2$ organization is the largest type observed (Ruban et al. 2003; Caffarri et al. 2009) (Fig. 1c). These results from single-particle analysis were confirmed through the direct observation of the thylakoid membranes by cryoelectron tomography (Daum et al. 2010; Kouřil et al. 2011). When the PSII-LHCII supercomplex from the green alga *C. reinhardtii* was prepared with high concentrations of β-DM (50 mM; 2.6%), the C_2S_2 organization appeared as in vascular plants (Nield et al. 2000a). The lack of M- and L-trimers in *C. reinhardtii* in earlier reports was ascribed to the absence in this alga of CP24 (Minagawa and Takahashi 2004), which was presumed to serve as a linker between PSII core subunits and an M-trimer in *A. thaliana* (Kovács et al. 2006; de Bianchi et al. 2008). However, both trimers were found in a more recent single-particle analysis of the α-DM-solubilized PSII-LHCII supercomplex from *C. reinhardtii*, in which three LHCII trimers were attached to each side of the core (the $C_2S_2M_2L_2$ PSII-LHCII supercomplex) (Tokutsu et al. 2012) (Fig. 1a).

The supercomplex formed by PSI and its light-harvesting complex proteins (LHCI) is also a large Chl-protein complex that is made up of nearly 20 subunits. The PSI supercomplex collects light energy and drives electron flow from plastocyanin to ferredoxin (Fd). The association of LHCIs with a monomeric PSI core was determined by 2.8–3.3 Å crystal structures of the PSI-LHCI supercomplex from pea (*Pisum sativum*), in which the side of the PsaF/J subunits was occupied by the crescent-shaped LHCI belt (Amunts et al. 2010; Qin et al. 2015) (Fig. 1d). The other side of the core is unoccupied under normal conditions, exposing the PsaH/I/L subunits, but it can dock the mobile LHCII(s) under "State 2" conditions as described below. In vascular plants, the LHCI belt is formed by the four LHCI proteins in the order of Lhca1, -4, -2, and -3 (Fig. 1d). In *C. reinhardtii*, however, 9 LHCI proteins in total, encoded by the *LHCA1–9* genes (Stauber et al. 2003; Minagawa 2009), form a double-layered LHCI belt attached to the side of the PsaJ/F/G subunits when grown under low light (LL) conditions (Drop et al. 2011) (Fig. 1b). Proteomic studies demonstrated that the LHCI belt is in fact heterogeneously composed and several LHCI proteins are not present stoichiometrically (Tokutsu et al. 2004; Stauber et al. 2009). The composition of LHCI proteins is known to be variable in response to environmental changes, where downregulation, degradation, or processing of LHCI polypeptides were reported, in particular iron deficient conditions (Moseley et al. 2002; Nield et al. 2004; Tokutsu et al. 2004).

Because plants and algae typically do not have means to escape from adverse environments such as high light (HL) or LL, cold or hot temperatures, drought, or low CO_2 concentration, their ability to acclimate to such conditions is crucial for survival in their niches. The central unit of the photosystems, the core complex, conducts charge separations. The components of these charge-separation devices are almost completely conserved among cyanobacteria, eukaryotic algae, moss, and vascular plants, likely because the process was sufficiently optimized when cyanobacteria originally acquired the ability to oxidize water 2.7 billion years ago by employing the system of a series of enzymes for oxygenic photosynthesis

that remains in use today (Brocks et al. 1999; Summons et al. 1999). Furthermore, this core system is invariable in changing environments. The only exception is the so-called photoinhibition, which is a multistep process of D1 protein degradation upon HL illumination and the replacement of damaged D1 with a newly synthesized D1 polypeptide (Nixon et al. 2010). Photoinhibition is, in one sense, a deleterious event for PSII because it loses the activity, but, in another, it could save all the downstream components from the events even more devastating, namely, the production of more dangerous reactive oxygen species (Asada 1999). Therefore, photoinhibition can be considered as a safety valve for the photosynthetic electron transport.

In contrast to the core complex, the surrounding light-harvesting antenna is diverse, flexible, and dynamic. Different photosynthetic organisms generally have different antenna systems to take advantage of the light environment in their own niches. Moreover, the light-harvesting performance of the antenna system in a single species can be dynamically adjusted to different light regimes. The capabilities of the light-harvesting antenna to acclimate are especially important for photosynthetic organisms to optimize their photosynthetic performance and to protect their photosynthetic machinery from the photooxidative damage in the natural environment, where the quality and quantity of light fluctuates over time.

This chapter presents an overview of the two representative acclimation events of photosystems in *C. reinhardtii*, state transitions, and qE quenching. These acclimation events are accompanied by reorganization of photosystem supercomplexes and super-supercomplexes.

2 State Transitions

2.1 Introduction

Each of the two charge-separation devices—PSI and PSII—in the thylakoid membranes has a distinct pigment system with unique absorption characteristics. Thus, an imbalance of energy distribution between the two photosystems tends to occur in natural environments (Allen 1992; Bellafiore et al. 2005). Because the two photosystems are functionally connected in series under normal conditions, plants and algae must constantly balance their excitation levels to ensure the optimal efficiency of electron flow. State transitions are engaged in balancing the light-harvesting capacities of the two photosystems. State 1 occurs when PSI is preferentially excited and the light-harvesting capacities of PSII and PSI are increased and decreased, respectively; this state is indicated by a higher Chl fluorescence yield at room temperature. Conversely, State 2 occurs when PSII is preferentially excited and the light-harvesting capacities of PSII and PSI are decreased and increased, respectively, to readjust the excitation balance; this state can be monitored as a lower Chl fluorescence yield at room temperature (Minagawa 2011) (Fig. 2).

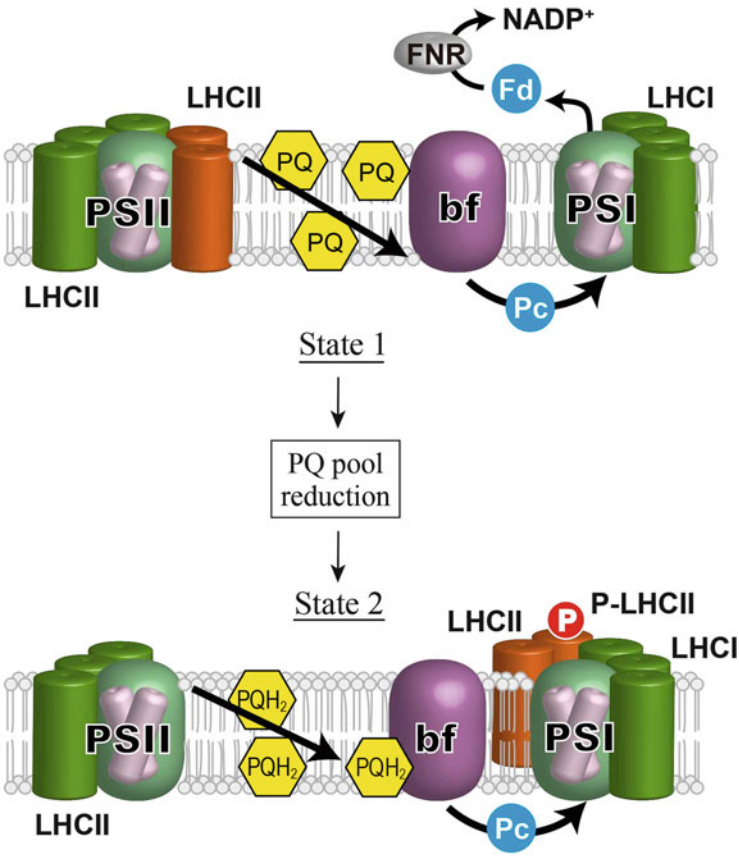

Fig. 2 Schematic representation of state transitions; a transition from State 1 to State 2. *Upper*, when PSI is preferentially excited, the stroma of chloroplast and the PQ pool are oxidized. Under these conditions, LHCIIs are bound to PSII (State 1). *Lower*, when the PQ pool is reduced, migration of the mobile LHCIIs from PSII to PSI occurs to establish State 2. bf, Cyt *bf*; Fd, ferredoxin; Pc, plastocyanin

The core concept of state transitions has been documented, an instant redistribution of the light-harvesting systems of the two photosystems (Bonaventura and Myers 1969; Murata 1969) and of the molecular mechanisms that regulate the redistribution, including the involvement of cytochrome b_6f (Cyt *bf*) (Wollman and Lemaire 1988), the binding of PQH_2 to the Qo-site of Cyt *bf* (Vener et al. 1997; Zito et al. 1999), and the phosphorylation of LHCII by redox-dependent kinase (s) (Depège et al. 2003). Moreover, evidence for the molecular events occurring at PSII and PSI are rapidly accumulating owing to advances in genetic and biochemical techniques using the green alga *C. reinhardtii*. This progress is due, in part, to a unique ability of this alga, where much more LHCII (as much as 67%) is involved in state transitions (Delosme et al. 1996) as compared with vascular plants (only 20–25%) (Allen 1992).

2.2 *Reorganization of the PSII Supercomplex During State Transitions*

The PSII supercomplex was hypothesized to be subjected to the large-scale reorganization during a transition from State 1 to State 2, such that a large number of LHCIIs forming the peripheral antenna for PSII are undocked upon their phosphorylation (Haldrup et al. 2001; Iwai et al. 2008). However, recent studies employing in vivo measurements and high-resolution biochemistry have presented an alternative view of state transitions at the PSII side. By measuring small-angle neutron scattering in living *C. reinhardtii* cells during state transitions, Nagy and coworkers detected a strong periodicity of the thylakoids in State 1 with characteristic repeat distances of approximately 200 Å, which was almost completely lost in State 2 (Nagy et al. 2014). However, circular dichroism corresponding to the long-range order arrangement of the Chl-protein complexes, namely, the arrays of the PSII-LHCII supercomplexes, was only reduced by ~20% upon a transition to State 2 (Nagy et al. 2014). Therefore, ~80% of the PSII-LHCII supercomplex array was preserved during this transition. Nevertheless, the maximal room temperature fluorescence from PSII decreased significantly. This decrease suggests that the energy absorbed by LHCIIs was dissipated as heat, while they were physically associated with PSII (Nagy et al. 2014). Ünlü and coworkers observed some increase of both amplitude and lifetime of the fluorescence due to PSI, but it was indeed far smaller than that reported in the literature (Delosme et al. 1996) and concluded that only a fraction of LHCII recoupled to PSI under State 2 conditions and the rest of them stayed detached and exhibited shortened excited state lifetime (Ünlü et al. 2014). By measuring the electrochromic shift of the thylakoid pigments, which reflects a change in the membrane potential due to charge separations, Nagy et al. also showed that the enhancement of PSI antenna size during State 1 to State 2 transition was not commensurate to the decrease in PSII antenna size (Nagy et al. 2014). On the contrary, a more recent study by Nawrocki et al. demonstrated a larger increase in the PSI antenna size (~35%) and a smaller decrease in the PSII antenna size (~38%) based on their measurements of the electrochromic shift, with which they concluded that the PSI antenna size was commensurate with the decrease in the PSII antenna size so that most of the mobile LHCII were recoupled to PSI (Nawrocki et al. 2016). It is thus still controversial how much PSII and PSI antenna size changes during state transitions, whether the changes in the two antenna size were comparable and whether there is energy-quenching LHCIIs under State 2 conditions.

The possibility of energy quenching within the phosphorylated LHCII was previously suggested by monitoring the effects of state transitions on the lifetimes of the LHCII fluorescence in the cells (Iwai et al. 2010). While the cells were in State 1, the dominant component of the fluorescence lifetime was 170 ps, and it shifted to 250 ps under State 2 conditions. Because this lifetime shift was not observed in the *stt7* mutant, which is incapable of state transitions, and because the

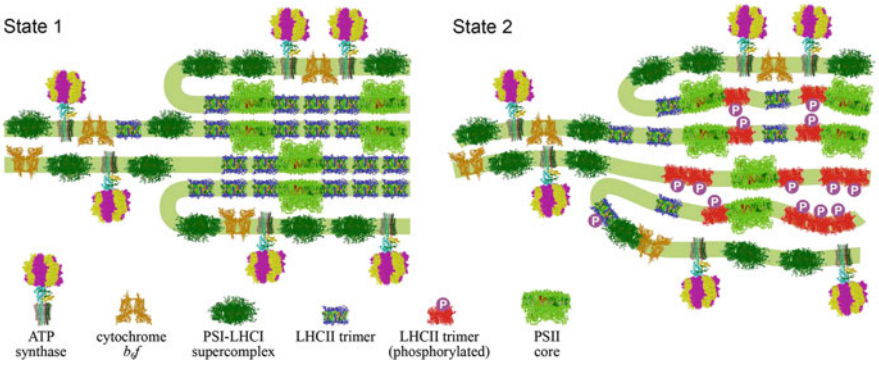

Fig. 3 A model for the remodeling of the photosynthetic supercomplexes in the thylakoid membranes during state transitions in *C. reinhardtii*. Side views of the membrane planes showing alterations in the thylakoid ultrastructure and photosystem supercomplex composition: State 1 (*left*): thylakoids are more stacked, and large arrays of PSII-LHCII supercomplexes reside in the appressed regions. The periodicity of thylakoid membranes is well defined. PSI-LHCI supercomplexes, Cyt *bf*, and ATP synthases are in the non-appressed regions. State 2 (*right*): a number of LHCII proteins are phosphorylated, and the thylakoids are partially unstacked and undulated. The periodicity of the thylakoid membranes is weak. Many of the phosphorylated LHCIIs (*red*) are in the energy-quenching state and remain associated with PSII, so that a large part of the PSII-LHCII supercomplex array is preserved. Some of the phosphorylated LHCIIs (*red*) are aggregated, and in the energy-quenching state, the other phosphorylated LHCIIs are associated with PSI-LHCI supercomplex. The unphosphorylated LHCIIs (*blue*) stay on PSII and act as light-harvesting antenna for PSII

appearance of the 250 ps component was paralleled by the activation of LHCII phosphorylation and the formation of LHCII aggregates, the 250 ps component was ascribed to the aggregated phospho-LHCIIs in the thylakoid membranes in State 2. If the LHCIIs were simply dissociated from the PSII core and existing as free form, the lifetime would be >1 ns.

In Fig. 3, the two possible types of state-transition events in *C. reinhardtii* are illustrated; one is the canonical antenna migration-type state transition, and another is the green algae-specific antenna quenching-type state transition. Although the former type causes reduction and elevation of the excitation of PSII and PSI, respectively, the latter type only causes reduction of the excitation of PSII. The LHCII migration between the two photosystems explains a 10–20% reduction of the PSII light-harvesting capacity in *C. reinhardtii*, where such biochemical evidence has been reported previously (Kargul et al. 2005; Takahashi et al. 2006; Tokutsu et al. 2009); green algae and vascular plants thus seem to share the antenna migration-type state transition. The quenching-type state transition may explain why a large change in the antenna size of PSII is often observed in *C. reinhardtii* (Delosme et al. 1996). The reason why the quenching-type state transition was developed in green algae is not clear at present. One might link these variances in the molecular mechanisms to the variances in the platforms for the photosynthetic machineries, namely, thylakoid supra-structures. It is well known that morphological domains of the thylakoid membranes

are different in vascular plants and most of green algae (Nevo et al. 2009). In vascular plants, grana and stroma-lamellae regions are clearly separated. While 10–20 layers of the thylakoid membranes are stacked in grana region, only a single or a few membrane stacks are present in the stroma-lamellae region (Mustárdy and Garab 2003; Mullineaux 2005; Shimoni et al. 2005). Many green algae have areas of appressed thylakoid membranes, which we also call grana, but do not have the highly structured multiple membrane layers as the grana in vascular plants (Bertos and Gibbs 1998; Engel et al. 2015). It is thus plausible that variances in the molecular mechanism for state transitions and the other photoacclimation events of photosynthetic machineries could be due to such differences in the thylakoid supra-structures. These problems need to be clarified in future studies.

2.3 *Reorganization of the PSI Supercomplex During State Transitions*

Vascular plants without PsaH and PsaL (Lunde et al. 2000) and those without PsaO (Jensen et al. 2004) are deficient in state transitions. Because these small PSI subunits are located on the opposite side of the LHCI belt (Amunts et al. 2010; Qin et al. 2015) (Fig. 1), they were hypothesized to constitute a binding site for the mobile LHCII(s). Further information regarding the reorganization of PSI upon a transition from State 1 to State 2 was provided in a study on *C. reinhardtii*, wherein the PSI-LHCI-LHCII supercomplex from the State 2 cells contained two minor monomeric LHCII proteins, CP26 and CP29, and one major trimeric LHCII protein, LHCBM5, suggesting a pivotal role for the minor monomeric LHCII in state transitions, at least in green algae (Takahashi et al. 2006, 2014). The significance of the minor LHCII in state transitions in *C. reinhardtii* was further supported by an RNA interference (RNAi) study in which the level of CP29 or CP26 was individually reduced (Tokutsu et al. 2009). Both the CP29 and CP26 RNAi mutants underwent reductions in the PSII antenna size during a State 1-to-State 2 transition. However, the LHCIIs undocked from PSII did not reassociate with PSI in the CP29-RNAi mutant. By contrast, the mobile LHCIIs in the CP26-RNAi mutant did reassociate with PSI, such that a PSI-LHCI-LHCII supercomplex could be visualized on a sucrose density gradient (Tokutsu et al. 2009).

These results thus clarified that CP29, but not CP26, is crucial for the classical antenna migration-type state transitions in *C. reinhardtii*. The 2D structures of such a PSI-LHCI-LHCII supercomplex were recently visualized by single-particle analysis of electron micrographs in *C. reinhardtii* (Drop et al. 2014) and in *A. thaliana* (Galka et al. 2012), where two LHCII trimers/one LHCII monomer (in *C. reinhardtii*) and one LHCII trimer (in *A. thaliana*) were found near the PsaH/I/L subunits.

3 qE Quenching

3.1 Introduction

In nature, unexpected increases in light intensity can lead to overexcitation of the photosystems, resulting in the accumulation of harmful reactive oxygen species (Li et al. 2009). Plants and algae have developed non-photochemical quenching (NPQ) mechanisms that alleviate such photooxidative stress. Among these mechanisms, the rapid deexcitation of the light-harvesting antenna of PSII that thermally dissipates excess light energy as heat is called qE quenching (Govindjee et al. 1967; Murata and Sugahara 1969). This type of NPQ is dependent upon ΔpH across the thylakoid membranes (Wraight and Crofts 1971), and its extent and kinetics are affected by the accumulation of a xanthophyll zeaxanthin (Zx) (Demmig et al. 1987). Further genetic studies paved the way for elucidating the molecular mechanism of qE (Horton et al. 2008; Li et al. 2009; de Bianchi et al. 2010).

3.2 Xanthophylls

Zx is accumulated in the thylakoid membranes under HL conditions by reversible de-epoxidation of violaxanthin (Vx) in a process called xanthophyll cycle (Yamamoto et al. 1962), which is activated by the acidification of the thylakoid lumen (Demmig-Adams and Adams III 1992; Demmig-Adams et al. 1996). The *npq1* mutant, which is deficient in the conversion of Vx into Zx, was reported first in *C. reinhardtii* (Niyogi et al. 1997b) and then in *A. thaliana* (Niyogi et al. 1998). Unlike the plant-type enzyme that catalyze the Vx-Zx conversion, the counterpart enzyme in *C. reinhardtii* is located on the stromal side of the thylakoid membrane and seems to be evolved from an ancient de-epoxidase that was present in the common ancestor of green algae and plants (Li et al. 2016).

Because the overaccumulation of Zx elevates the level of qE in vascular plants (Niyogi et al. 1998; de Bianchi et al. 2010), Zx has been attributed to a quenching site for qE. Fleming and coworkers reported that energy dissipation occurs via charge transfer between Chl-Zx in the thylakoids (Holt et al. 2005) and in the reconstituted CP29 protein (Ahn et al. 2008). The increased Chl-Zx interaction was directly correlated with qE in LHCII (Bode et al. 2009). The triplet-*minus*-singlet spectra of carotenoids in leaves and the isolated LHC complexes showed a characteristic redshift in the presence of Zx (Dall'Osto et al. 2012). However, Wachtveitl and coworkers demonstrated that the presence of Vx or Zx cation radicals in LHCII made no difference to the excitation lifetimes of Chls (Amarie et al. 2007). Alternatively, Zx (Johnson et al. 2011), together with PsbS (Kereiche et al. 2010), was hypothesized to decrease the ordered semicrystalline arrays of PSII supercomplexes,

leading to an increase in the fluidity of the thylakoid membranes and the promotion of the energy-dissipative aggregation of LHCIIs (Goral et al. 2012).

In contrast to the *npq1* mutant of vascular plants, the *npq1* mutant in *C. reinhardtii*, which is a different allele as described above, showed only a minor effect on qE, indicating a possibility that the majority of photoprotection can be achieved without Zx in this alga (Niyogi et al. 1997a, b). Although the lack of the plant-type Vx de-epoxidation activity showed little photoinhibition under HL conditions, an additional mutation in *npq1* that inhibits lutein synthesis (*lor1*) caused severe photoinhibition, suggesting that lutein, a central structural component of LHCIIs, largely contributes to qE quenching in *C. reinhardtii* (Niyogi et al. 1997a).

3.3 qE Effectors

The *npq4* mutant, which is deficient in the rapid induction of qE despite the normal xanthophyll cycle and normal lumenal acidification, has been reported in both *A. thaliana* and *C. reinhardtii*, but the alleles were mapped to different gene—the four-helix LHC family protein PsbS in *A. thaliana* (Li et al. 2000) and the three-helix LHC family protein LHCSR3 in *C. reinhardtii* (Peers et al. 2009). Again, the same phenotype with different genotypes indicates that plants and algae perform qE quenching in different ways. In PsbS, although one Chl molecule was identified in its crystal structure (Fan et al. 2015), all of the canonical pigment-binding sites identified in the LHCII crystal structure (Liu et al. 2004) are not conserved. PsbS is not stably associated with the PSII-LHCII supercomplex (Caffarri et al. 2009) but shows stronger association with LHCII trimer upon monomerization under HL conditions (Correa-Galvis et al. 2016a). Several lines of evidence suggested that PsbS in *A. thaliana* controls the macro-organization of the thylakoid membranes through acidification of the lumen (Kiss et al. 2008; Kereiche et al. 2010; Goral et al. 2012). Such a membrane "phase transition" is thought to facilitate the dissociation of several LHCII proteins, including CP24, CP29, and the LHCII M-trimer from PSII (Betterle et al. 2009); moreover, their aggregation (Kiss et al. 2008; Johnson et al. 2011) likely allows for the conformational change within major LHCII (Ruban et al. 2007) and/or minor LHCII (Ahn et al. 2008) to generate energy-quenching site(s). Alternatively, Wilk and colleagues reported that PsbS directly interacts with LHCII and induces energy dissipation (Wilk et al. 2013). A further study on Chl lifetimes showed that PsbS does not affect the relaxation dynamics of the Chl excited state but changes the amount and the initial induction rate of quenching (Sylak-Glassman et al. 2014).

Although both Zx and PsbS are thought to be crucial for qE quenching in vascular plants, the green alga *C. reinhardtii* does not express the PSBS protein at least under normal conditions (Finazzi et al. 2006; Bonente et al. 2008), and a mutant deficient in Vx de-epoxidase activity still exhibits qE quenching (Niyogi

et al. 1997a, b). The PSBS protein encoded in the genome of *C. reinhardtii* shares 45% identity over 180 amino acids with *A. thaliana* PsbS (Minagawa and Takahashi 2004), including the putative pH-sensing Glu residues (Li et al. 2004). Because PSBS is constitutively present even in LL-grown plants (Demmig-Adams et al. 2006), it provides instant photoprotection for vascular plants when they are shifted to HL. The activation of qE in *C. reinhardtii*, however, requires prolonged exposure to HL (Niyogi et al. 1997b), suggesting that algae have a largely different mechanism for qE induction.

The *C. reinhardtii npq4* mutant was mapped to an "ancient" LHC protein, LHCSR3 (Peers et al. 2009). The genes for LHCSR3 (*Lhcsr3.1* and *Lhcsr3.2*), formerly known as LI818 (Gagne and Guertin 1992), encode a 25–26 kDa integral membrane protein whose expression was induced under HL (Richard et al. 2000), low CO_2 (Miura et al. 2004), or low iron (Naumann et al. 2007) conditions. Although PsbS binds few pigments, LHCSR3 is capable of binding Chl *a* and *b*, as well as xanthophylls (Bonente et al. 2011). A recombinant LHCSR3 polypeptide reconstituted with Chls and xanthophylls dissipated excitation energy in a low-pH buffer, suggesting that this protein is a quenching site in *C. reinhardtii* (Bonente et al. 2011). In addition to this "HL-specialized" antenna protein involved in quenching, genetic analysis in *C. reinhardtii* has led to the identification of other LHCs related to quenching. Depletion of one of the major trimeric LHCII proteins, LHCBM1, in the *npq5* mutant decreased its capacity for thermal energy dissipation (Elrad et al. 2002). There is also an LHCSR3 homologue, called LHCSR1 (Minagawa 2009). A recent study reported an intriguing feature of this protein, which is not observed in LHCSR3, namely, LHCSR1 which acts as low-pH sensor, whose small amount induces thermal dissipation of a large array of the excited LHCII (Dinc et al. 2016). Furthermore, very recent studies detected a rapid and transient expression of PSBS, suggesting this plant-type qE effector could also be involved in the algal-type qE, but the details still need to be clarified (Correa-Galvis et al. 2016b; Tibiletti et al. 2016).

3.4 Current Model for the Induction of qE Quenching in C. reinhardtii

Recently, signal transduction pathway(s) for LHCSR3 expression have been becoming clarified. Hippler and coworkers reported that a chloroplast-localized calcium sensor protein (CAS) affected the HL-dependent LHCSR3 expression (Petroutsos et al. 2011), where a knockdown mutant of CAS did not express LHCSR3 under HL conditions unless a high concentration of calcium was supplemented. They also found that calmodulin antagonist W7 inhibited the HL-dependent accumulation of LHCSR3 (Petroutsos et al. 2011), suggesting that

HL-dependent LHCSR3 expression is mediated by calmodulin and/or calmodulin-affected calcium transients. More recently, the gene expression of *LHCSR3.1* and *LHCSR3.2* as well as *LHCSR1* was studied by quantitative PCR, confirming that transcription of all the three *LHCSR* genes was induced by HL (Maruyama et al. 2014). However, their sensitivities to the inhibitors varied. The expressions of *LHCSR3.1* and *LHCSR3.2* were almost completely inhibited by an inhibitor of photosynthesis, 3-(3,4-dichlorophenyl)-1,1-dimethylurea (DCMU), or W7, whereas that of *LHCSR1* was only partially inhibited by W7 and was insensitive to DCMU (Maruyama et al. 2014). Furthermore, Petroutsos et. al. determined the spectral requirement for the induction of LHCSR3 and figured out that blue light sensing by phototropin is crucial together with photosynthetic electron transport (Petroutsos et al. 2016). On the other hand, Ulm, Goldschmidt-Clermont and their coworkers revealed that LHCSR1 was induced by UV-B by means of UVRB (Allorent et al. 2016; Tilbrook et al. 2016). These studies on the *LHCSR* gene expression indicate there is always a few hours before the LHCSR proteins are expressed under HL conditions. The cells are thus inevitably exposed to HL without qE quenching in the first few hours. *C. reinhardtii* cells can actually alleviate such initial HL stress by operating state transitions (Allorent et al. 2013).

Although LHCSR3 is necessary to activate qE quenching in *C. reinhardtii*, where and how the LHCSR3 protein contributes has remained unclear. A recent study clarified where LHCSR3 is localized in the thylakoid membranes and how it dissipates excess energy (Tokutsu and Minagawa 2013). By comparing the PSII-LHCII supercomplex isolated from wild-type (WT) *C. reinhardtii* cells and that from *npq4*, Tokutsu and Minagawa found LHCSR3 was present only in the PSII supercomplex from HL-grown WT cultures and not in that from LL-grown WT or HL-grown *npq4*. The purified PSII-LHCII-LHCSR3 supercomplex was in a high-fluorescence (light-harvesting) state at a neutral pH (7.5). However, the complex was in a low-fluorescence (energy-dissipative) state at pH 5.5 (Tokutsu and Minagawa 2013). This switching from a light-harvesting state to an energy-dissipative state was sensitive to dicyclohexylcarbodiimide (DCCD), a protein-modifying agent specific to protonatable amino acid residues. The molecular site of this pH switch was localized to the C-terminus of LHCSR3 (Liguori et al. 2013). A possible model for the induction of qE quenching in *C. reinhardtii* would be, (1) HL-induced expression of *LHCSR3* gene, (2) association of LHCSR3 with the PSII-LHCII supercomplex, and (3) a conformational change in the C-terminus induced by lumenal acidification (Fig. 4).

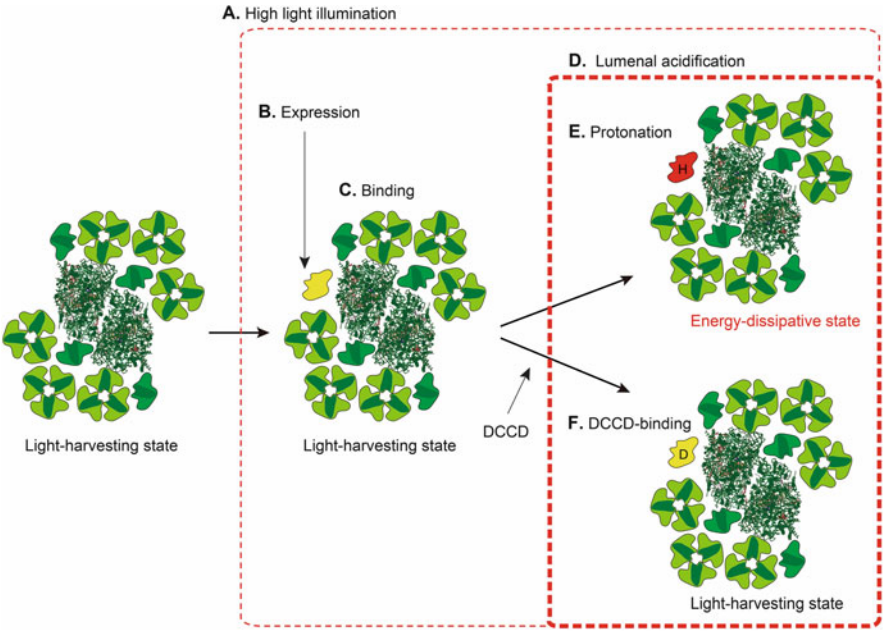

Fig. 4 A model for the induction of qE quenching in *C. reinhardtii*. When *C. reinhardtii* cells are exposed to HL for a few hours (**a**), the expression of LHCSR3 is induced (**b**). LHCSR3 (*yellow*) is then associated with the PSII-LHCII supercomplex to form the PSII-LHCII-LHCSR3 supercomplex (**c**). Though the PSII-LHCII-LHCSR3 supercomplex is still in a light-harvesting state under dark or LL conditions, the lumen of the thylakoid membranes was acidified under HL conditions (**d**), which causes a conformational change in its C-terminal region (*red*; "H" denotes protonation) (**e**) to transform it into energy-dissipative state. When DCCD binds to LHCSR3 (*yellow*; "D" denotes DCCD), the PSII-LHCII-LHCSR3 supercomplex is not protonated (**f**). The crystal coordinates were obtained from the Protein Data Bank: PSII core, 3ARC; LHCII, 2NHW; and PSI-LHCI supercomplex, 2WSC

Acknowledgments The work conducted in my laboratory was supported by the Japan Society for the Promotion of Science and the Japan Science and Technology Agency.

References

Ahn TK, Avenson TJ, Ballottari M, Cheng Y-C, Niyogi KK, Bassi R, Fleming GR (2008) Architecture of a charge-transfer state regulating light harvesting in a plant antenna protein. Science 320:794–797

Allen JF (1992) Protein phosphorylation in regulation of photosynthesis. Biochim Biophys Acta 1098:275–335

Allorent G, Tokutsu R, Roach T, Peers G, Cardol P, Girard-Bascou J, Seigneurin-Berny D, Petroutsos D, Kuntz M, Breyton C, Franck F, Wollman FA, Niyogi KK, Krieger-Liszkay A, Minagawa J, Finazzi G (2013) A dual strategy to cope with high light in *Chlamydomonas reinhardtii*. Plant Cell 25:545–557

Allorent G, Lefebvre-Legendre L, Chappuis R, Kuntz M, Truong TB, Niyogi KK, Ulm R, Goldschmidt-Clermont M (2016) UV-B photoreceptor-mediated protection of the photosynthetic machinery in Chlamydomonas reinhardtii. Proc Natl Acad Sci U S A 113:14864–14869

Amarie S, Standfuss J, Barros T, Kuhlbrandt W, Dreuw A, Wachtveitl J (2007) Carotenoid radical cations as a probe for the molecular mechanism of nonphotochemical quenching in oxygenic photosynthesis. J Phys Chem B 111:3481–3487

Amunts A, Toporik H, Borovikova A, Nelson N (2010) Structure determination and improved model of plant photosystem I. J Biol Chem 285:3478–3486

Asada K (1999) The water-water cycle in chloroplasts: scavenging of active oxygens and dissipation of excess photons. Annu Rev Plant Physiol Plant Mol Biol 50:601–639

Bellafiore S, Barneche F, Peltier G, Rochaix J-D (2005) State transitions and light adaptation require chloroplast thylakoid protein kinase STN7. Nature 433:892–895

Bertos NR, Gibbs SP (1998) Evidence for a lack of photosystem segregation in *Chlamydomonas reinhardtii* (Chlorophyceae). J Phycol 34:1009–1016

Betterle N, Ballottari M, Zorzan S, de Bianchi S, Cazzaniga S, Dall'Osto L, Morosinotto T, Bassi R (2009) Light-induced dissociation of an antenna hetero-oligomer is needed for non-photochemical quenching induction. J Biol Chem 284:15255–15266

Bode S, Quentmeier CC, Liao PN, Hafi N, Barros T, Wilk L, Bittner F, Walla PJ (2009) On the regulation of photosynthesis by excitonic interactions between carotenoids and chlorophylls. Proc Natl Acad Sci U S A 106:12311–12316

Boekema EJ, Hankamer B, Bald D, Kruip J, Nield J, Boonstra AF, Barber J, Rögner M (1995) Supramolecular structure of the photosystem II complex from green plants and cyanobacteria. Proc Natl Acad Sci U S A 92:175–179

Boekema EJ, Nield J, Hankamer B, Barber J (1998) Localization of the 23-kDa subunit of the oxygen-evolving complex of photosystem II by electron microscopy. Eur J Biochem 252:268–276

Boekema EJ, Van Roon H, Van Breemen JF, Dekker JP (1999) Supramolecular organization of photosystem II and its light-harvesting antenna in partially solubilized photosystem II membranes. Eur J Biochem 266:444–452

Bonaventura C, Myers J (1969) Fluorescence and oxygen evolution from *Chlorella pyrenoidosa*. Biochim Biophys Acta 189:366–383

Bonente G, Howes BD, Caffarri S, Smulevich G, Bassi R (2008) Interactions between the photosystem II subunit PsbS and xanthophylls studied in vivo and in vitro. J Biol Chem 283:8434–8445

Bonente G, Ballottari M, Truong TB, Morosinotto T, Ahn TK, Fleming GR, Niyogi KK, Bassi R (2011) Analysis of LhcSR3, a protein essential for feedback de-excitation in the green alga *Chlamydomonas reinhardtii*. PLoS Biol 9:e1000577

Brocks JJ, Logan GA, Buick R, Summons RE (1999) Archean molecular fossils and the early rise of eukaryotes. Science 285:1033–1036

Caffarri S, Kouril R, Kereiche S, Boekema EJ, Croce R (2009) Functional architecture of higher plant photosystem II supercomplexes. EMBO J 28:3052–3063

Correa-Galvis V, Poschmann G, Melzer M, Stühler K, Jahns P (2016a) PsbS interactions involved in the activation of energy dissipation in *Arabidopsis*. Nat Plants 2:15225

Correa-Galvis V, Redekop P, Guan K, Griess A, Truong TB, Wakao S, Niyogi KK, Jahns P (2016b) Photosystem II subunit PsbS is involved in the induction of LHCSR-dependent energy dissipation in *Chlamydomonas reinhardtii*. J Biol Chem 291(33):17478–17487

Dall'Osto L, Holt NE, Kaligotla S, Fuciman M, Cazzaniga S, Carbonera D, Frank HA, Alric J, Bassi R (2012) Zeaxanthin protects plant photosynthesis by modulating chlorophyll triplet yield in specific light-harvesting antenna subunits. J Biol Chem 287:41820–41834

Daum B, Nicastro D, Austin J II, McIntosh JR, Kühlbrandt W (2010) Arrangement of photosystem II and ATP synthase in chloroplast membranes of spinach and pea. Plant Cell 22:1299–1312

de Bianchi S, Dall'Osto L, Tognon G, Morosinotto T, Bassi R (2008) Minor antenna proteins CP24 and CP26 affect the interactions between photosystem II subunits and the electron transport rate in grana membranes of *Arabidopsis*. Plant Cell 20:1012–1028

de Bianchi S, Ballottari M, Dall'osto L, Bassi R (2010) Regulation of plant light harvesting by thermal dissipation of excess energy. Biochem Soc Trans 38:651–660

Dekker JP, Boekema EJ (2005) Supramolecular organization of thylakoid membrane proteins in green plants. Biochim Biophys Acta 1706:12–39

Delosme R, Olive J, Wollman F-A (1996) Changes in light energy distribution upon state transitions: an *in vivo* photoacoustic study of the wild type and photosynthesis mutants from *Chlamydomonas reinhardtii*. Biochim Biophys Acta 1273:150–158

Demmig B, Winter K, Kruger A, Czygan FC (1987) Photoinhibition and zeaxanthin formation in intact leaves: a possible role of the xanthophyll cycle in the dissipation of excess light energy. Plant Physiol 84:218–224

Demmig-Adams B, Adams WW III (1992) Photoprotection and other responses of plants to high light stress. Annu Rev Plant Physiol Plant Mol Biol 43:599–626

Demmig-Adams B, Adams Iii WW, Barker DH, Logan BA, Bowling DR, Verhoeven AS (1996) Using chlorophyll fluorescence to assess the fraction of absorbed light allocated to thermal dissipation of excess excitation. Physiol Plant 98:253–264

Demmig-Adams B, Ebbert V, Mellman DL, Mueh KE, Schaffer L, Funk C, Zarter CR, Adamska I, Jansson S, Adams WW (2006) Modulation of PsbS and flexible vs sustained energy dissipation by light environment in different species. Physiol Plant 127:670–680

Depège N, Bellafiore S, Rochaix J-D (2003) Role of chloroplast protein kinase Stt7 in LHCII phosphorylation and state transition in *Chlamydomonas*. Science 299:1572–1575

Dinc E, Tian L, Roy LM, Roth R, Goodenough U, Croce R (2016) LHCSR1 induces a fast and reversible pH-dependent fluorescence quenching in LHCII in Chlamydomonas reinhardtii cells. Proc Natl Acad Sci U S A 113:7673–7678

Drop B, Webber-Birungi M, Fusetti F, Kouril R, Redding KE, Boekema EJ, Croce R (2011) Photosystem I of *Chlamydomonas reinhardtii* is composed of nine light-harvesting complexes (Lhca) located on one side of the core. J Biol Chem 286:44878–44887

Drop B, Yadav KNS, Boekema EJ, Croce R (2014) Consequences of state transitions on the structural and functional organization of photosystem I in the green alga *Chlamydomonas reinhardtii*. Plant J 78:181–191

Elrad D, Niyogi KK, Grossman AR (2002) A major light-harvesting polypeptide of photosystem II functions in thermal dissipation. Plant Cell 14:1801–1816

Engel BD, Schaffer M, Kuhn Cuellar L, Villa E, Plitzko JM, Baumeister W (2015) Native architecture of the *Chlamydomonas* chloroplast revealed by in situ cryo-electron tomography. elife 4:e04889

Fan M, Li M, Liu Z, Cao P, Pan X, Zhang H, Zhao X, Zhang J, Chang W (2015) Crystal structures of the PsbS protein essential for photoprotection in plants. Nat Struct Mol Biol 22:729–735

Finazzi G, Johnson GN, Dall'Osto L, Zito F, Bonente G, Bassi R, Wollman F-A (2006) Nonphotochemical quenching of chlorophyll fluorescence in *Chlamydomonas reinhardtii*. Biochemistry 45:1490–1498

Gagne G, Guertin M (1992) The early genetic response to light in the green unicellular alga *Chlamydomonas eugametos* grown under light/dark cycles involves genes that represent direct responses to light and photosynthesis. Plant Mol Biol 18:429–445

Galka P, Santabarbara S, Khuong TT, Degand H, Morsomme P, Jennings RC, Boekema EJ, Caffarri S (2012) Functional analyses of the plant photosystem I-light-harvesting complex II supercomplex reveal that light-harvesting complex II loosely bound to photosystem II is a very efficient antenna for photosystem I in state II. Plant Cell 24:2963–2978

Goral TK, Johnson MP, Duffy CD, Brain AP, Ruban AV, Mullineaux CW (2012) Light-harvesting antenna composition controls the macrostructure and dynamics of thylakoid membranes in *Arabidopsis*. Plant J 69:289–301

Govindjee, Papageorgiou G, Rabinowitch E (1967) Chlorophyll fluorescence and photosynthesis. In: Guilbault GG (ed) Fluorescence; Theory, instrumentation and practice. Marcel Dekker, New York, pp 511–564

Haldrup A, Jensen PE, Lunde C, Scheller HV (2001) Balance of power: a view of the mechanism of photosynthetic state transitions. Trends Plant Sci 6:301–305

Hankamer B, Nield J, Zheleva D, Boekema E, Jansson S, Barber J (1997) Isolation and biochemical characterisation of monomeric and dimeric photosystem II complexes from spinach and their relevance to the organisation of photosystem II *in vivo*. Eur J Biochem 243:422–429

Holt NE, Zigmantas D, Valkunas L, Li XP, Niyogi KK, Fleming GR (2005) Carotenoid cation formation and the regulation of photosynthetic light harvesting. Science 307:433–436

Horton P, Johnson MP, Perez-Bueno ML, Kiss AZ, Ruban AV (2008) Photosynthetic acclimation: does the dynamic structure and macro-organisation of photosystem II in higher plant grana membranes regulate light harvesting states? FEBS J 275:1069–1079

Iwai M, Takahashi Y, Minagawa J (2008) Molecular remodeling of photosystem II during state transitions in *Chlamydomonas reinhardtii*. Plant Cell 20:2177–2189

Iwai M, Yokono M, Inada N, Minagawa J (2010) Live-cell imaging of photosystem II antenna dissociation during state transitions. Proc Natl Acad Sci U S A 107:2337–2342

Jansson S (1999) A guide to the *Lhc* genes and their relatives in *Arabidopsis*. Trends Plant Sci 4:236–240

Jensen PE, Haldrup A, Zhang S, Scheller HV (2004) The PSI-O subunit of plant photosystem I is involved in balancing the excitation pressure between the two photosystems. J Biol Chem 279:24212–24217

Johnson MP, Goral TK, Duffy CD, Brain AP, Mullineaux CW, Ruban AV (2011) Photoprotective energy dissipation involves the reorganization of photosystem II light-harvesting complexes in the grana membranes of spinach chloroplasts. Plant Cell 23:1468–1479

Kargul J, Turkina MV, Nield J, Benson S, Vener AV, Barber J (2005) Light-harvesting complex II protein CP29 binds to photosystem I of *Chlamydomonas reinhardtii* under State 2 conditions. FEBS J 272:4797–4806

Kereiche S, Kiss AZ, Kouril R, Boekema EJ, Horton P (2010) The PsbS protein controls the macro-organisation of photosystem II complexes in the grana membranes of higher plant chloroplasts. FEBS Lett 584:759–764

Kiss AZ, Ruban AV, Horton P (2008) The PsbS protein controls the organization of the photosystem II antenna in higher plant thylakoid membranes. J Biol Chem 283:3972–3978

Kouřil R, Oostergetel GT, Boekema EJ (2011) Fine structure of granal thylakoid membrane organization using cryo electron tomography. Biochim Biophys Acta 1807:368–374

Kovács L, Damkjær J, Kereïche S, Ilioaia C, Ruban AV, Boekema EJ, Jansson S, Horton P (2006) Lack of the light-harvesting complex CP24 affects the structure and function of the grana membranes of higher plant chloroplasts. Plant Cell 18:3106–3120

Li XP, Björkman O, Shih C, Grossman AR, Rosenquist M, Jansson S, Niyogi KK (2000) A pigment-binding protein essential for regulation of photosynthetic light harvesting. Nature 403:391–395

Li XP, Gilmore AM, Caffarri S, Bassi R, Golan T, Kramer D, Niyogi KK (2004) Regulation of photosynthetic light harvesting involves intrathylakoid lumen pH sensing by the PsbS protein. J Biol Chem 279:22866–22874

Li Z, Peers G, Dent RM, Bai Y, Yang SY, Apel W, Leonelli L, Niyogi KK (2016) Evolution of an atypical de-epoxidase for photoprotection in the green lineage. Nat Plants 2:16140

Li Z, Wakao S, Fischer BB, Niyogi KK (2009) Sensing and responding to excess light. Annu Rev Plant Biol 60:239–260

Liguori N, Roy LM, Opacic M, Durand G, Croce R (2013) Regulation of light harvesting in the green alga *Chlamydomonas reinhardtii*: the C-terminus of LHCSR is the knob of a dimmer switch. J Am Chem Soc 135:18339–18342

Liu Z, Yan H, Wang K, Kuang T, Zhang J, Gui L, An X, Chang W (2004) Crystal structure of spinach major light-harvesting complex at 2.72 Å resolution. Nature 428:287–292

Lunde C, Jensen PE, Haldrup A, Knoetzel J, Scheller HV (2000) The PSI-H subunit of photosystem I is essential for state transitions in plant photosynthesis. Nature 408:613–615

Maruyama S, Tokutsu R, Minagawa J (2014) Transcriptional regulation of the stress-responsive light harvesting complex genes in *Chlamydomonas reinhardtii*. Plant Cell Physiol 55:1304–1310

Minagawa J (2009) Light-harvesting proteins. In: Stern D, Harris EH (eds) Chlamydomonas sourcebook. Springer, Amsterdam, pp 503–540

Minagawa J (2011) State transitions—the molecular remodeling of photosynthetic supercomplexes that controls energy flow in the chloroplast. Biochim Biophys Acta 1807:897–905

Minagawa J, Takahashi Y (2004) Structure, function and assembly of photosystem II and its light-harvesting proteins. Photosynth Res 82:241–263

Miura K, Yamano T, Yoshioka S, Kohinata T, Inoue Y, Taniguchi F, Asamizu E, Nakamura Y, Tabata S, Yamato KT, Ohyama K, Fukuzawa H (2004) Expression profiling-based identification of CO_2-responsive genes regulated by CCM1 controlling a carbon-concentrating mechanism in *Chlamydomonas reinhardtii*. Plant Physiol 135:1595–1607

Moseley JL, Allinger T, Herzog S, Hoerth P, Wehinger E, Merchant S, Hippler M (2002) Adaptation to Fe-deficiency requires remodeling of the photosynthetic apparatus. EMBO J 21:6709–6720

Mullineaux CW (2005) Function and evolution of grana. Trends Plant Sci 10:521–525

Murata N (1969) Control of excitation transfer in photosynthesis. I. Light-induced change of chlorophyll *a* fluoresence in *Porphyridium cruentum*. Biochim Biophys Acta 172:242–251

Murata N, Sugahara K (1969) Control of excitation transfer in photosynthesis. III. Light-induced decrease of chlorophyll *a* fluorescence related to photophosphorylation system in spinach chloroplasts. Biochim Biophys Acta 189:182–192

Mustárdy L, Garab G (2003) Granum revisited. A three-dimensional model – where things fall into place. Trends Plant Sci 8:117–122

Nagy G, Unnep R, Zsiros O, Tokutsu R, Takizawa K, Porcar L, Moyet L, Petroutsos D, Garab G, Finazzi G, Minagawa J (2014) Chloroplast remodeling during state transitions in *Chlamydomonas reinhardtii* as revealed by noninvasive techniques in vivo. Proc Natl Acad Sci U S A 111:5042–5047

Naumann B, Busch A, Allmer J, Ostendorf E, Zeller M, Kirchhoff H, Hippler M (2007) Comparative quantitative proteomics to investigate the remodeling of bioenergetic pathways under iron deficiency in *Chlamydomonas reinhardtii*. Proteomics 7:3964–3979

Nawrocki WJ, Santabarbara S, Mosebach L, Wollman F-A, Rappaport F (2016) State transitions redistribute rather than dissipate energy between the two photosystems in *Chlamydomonas*. Nat Plants 2:16031

Nevo R, Chuartzman SG, Tsabari O, Reich Z, Charuvi D, Shimoni E (2009) Architecture of thylakoid membrane networks. In: Wada H, Murata N (eds) Lipids in photosynthesis: essential and regulatory functions. Springer, Doredrecht, pp 295–328

Nield J, Orlova EV, Morris EP, Gowen B, van Heel M, Barber J (2000a) 3D map of the plant photosystem II supercomplex obtained by cryoelectron microscopy and single particle analysis. Nat Struct Biol 7:44–47

Nield J, Kruse O, Ruprecht J, da Fonseca P, Büchel C, Barber J (2000b) Three-dimensional structure of *Chlamydomonas reinhardtii* and *Synechococcus elongatus* photosystem II complexes allows for comparison of their oxygen-evolving complex organization. J Biol Chem 275:27940–27946

Nield J, Redding K, Hippler M (2004) Remodeling of light-harvesting protein complexes in *Chlamydomonas* in response to environmental changes. Eukaryot Cell 3:1370–1380

Nixon PJ, Michoux F, Yu J, Boehm M, Komenda J (2010) Recent advances in understanding the assembly and repair of photosystem II. Ann Bot 106:1–16

Niyogi KK, Björkman O, Grossman AR (1997a) The roles of specific xanthophylls in photoprotection. Proc Natl Acad Sci U S A 94:14162–14167

Niyogi KK, Björkman O, Grossman AR (1997b) *Chlamydomonas* xanthophyll cycle mutants identified by video imaging of chlorophyll fluorescence quenching. Plant Cell 9:1369–1380

Niyogi KK, Grossman AR, Björkman O (1998) *Arabidopsis* mutants define a central role for the xanthophyll cycle in the regulation of photosynthetic energy conversion. Plant Cell 10:1121–1134

Peers G, Truong TB, Ostendorf E, Busch A, Elrad D, Grossman AR, Hippler M, Niyogi KK (2009) An ancient light-harvesting protein is critical for the regulation of algal photosynthesis. Nature 462:518–521

Petroutsos D, Busch A, Janssen I, Trompelt K, Bergner SV, Weinl S, Holtkamp M, Karst U, Kudla J, Hippler M (2011) The chloroplast calcium sensor CAS is required for photoacclimation in *Chlamydomonas reinhardtii*. Plant Cell 23:2950–2963

Petroutsos D, Tokutsu R, Maruyama S, Flori S, Greiner A, Magneschi L, Cusant L, Kottke T, Mittag M, Hegemann P, Finazzi G, Minagawa J (2016) A blue-light photoreceptor mediates the feedback regulation of photosynthesis. Nature 537:563–566

Qin X, Suga M, Kuang T, Shen J-R (2015) Structural basis for energy transfer pathways in the plant PSI-LHCI supercomplex. Science 348:989–995

Richard C, Ouellet H, Guertin M (2000) Characterization of the LI818 polypeptide from the green unicellular alga *Chlamydomonas reinhardtii*. Plant Mol Biol 42:303–316

Ruban AV, Wentworth M, Yakushevska AE, Andersson J, Lee PJ, Keegstra W, Dekker JP, Boekema EJ, Jansson S, Horton P (2003) Plants lacking the main light-harvesting complex retain photosystem II macro-organization. Nature 421:648–652

Ruban AV, Berera R, Ilioaia C, van Stokkum IH, Kennis JT, Pascal AA, van Amerongen H, Robert B, Horton P, van Grondelle R (2007) Identification of a mechanism of photoprotective energy dissipation in higher plants. Nature 450:575–578

Shimoni E, Rav-Hon O, Ohad I, Brumfeld V, Reich Z (2005) Three-dimensional organization of higher-plant chloroplast thylakoid membranes revealed by electron tomography. Plant Cell 17:2580–2586

Stauber EJ, Fink A, Markert C, Kruse O, Johanningmeier U, Hippler M (2003) Proteomics of *Chlamydomonas reinhardtii* light-harvesting proteins. Eukaryot Cell 2:978–994

Stauber EJ, Busch A, Naumann B, Svatos A, Hippler M (2009) Proteotypic profiling of LHCI from *Chlamydomonas reinhardtii* provides new insights into structure and function of the complex. Proteomics 9:398–408

Summons RE, Jahnke LL, Hope JM, Logan GA (1999) 2-Methylhopanoids as biomarkers for cyanobacterial oxygenic photosynthesis. Nature 400:554–557

Sylak-Glassman EJ, Malnoe A, De Re E, Brooks MD, Fischer AL, Niyogi KK, Fleming GR (2014) Distinct roles of the photosystem II protein PsbS and zeaxanthin in the regulation of light harvesting in plants revealed by fluorescence lifetime snapshots. Proc Natl Acad Sci U S A 111:17498–17503

Takahashi H, Iwai M, Takahashi Y, Minagawa J (2006) Identification of the mobile light-harvesting complex II polypeptides for state transitions in *Chlamydomonas reinhardtii*. Proc Natl Acad Sci U S A 103:477–482

Takahashi H, Okamuro A, Minagawa J, Takahashi Y (2014) Biochemical characterization of photosystem I associating light-harvesting complexes I and II isolated from State-2 cells of *Chlamydomonas reinhardtii*. Plant Cell Physiol 55:1437–1449

Teramoto H, Ono T-A, Minagawa J (2001) Identification of *Lhcb* gene family encoding the light-harvesting chlorophyll-*a*/*b* proteins of photosystem II in *Chlamydomonas reinhardtii*. Plant Cell Physiol 42:849–856

Tibiletti T, Auroy P, Peltier G, Caffarri S (2016) *Chlamydomonas reinhardtii* PsbS protein is functional and accumulates rapidly and transiently under high light. Plant Physiol 171:2717–2730

Tilbrook K, Dubois M, Crocco CD, Yin R, Chappuis R, Allorent G, Schmid-Siegert E, Goldschmidt-Clermont M, Ulm R (2016) UV-B perception and acclimation in Chlamydomonas reinhardtii. Plant Cell 28(4):966–983

Tokutsu R, Minagawa J (2013) Energy-dissipative supercomplex of photosystem II associated with LHCSR3 in *Chlamydomonas reinhardtii*. Proc Natl Acad Sci U S A 110:10016–10021

Tokutsu R, Teramoto H, Takahashi Y, Ono T-A, Minagawa J (2004) The light-harvesting complex of photosystem I in *Chlamydomonas reinhardtii:* protein composition, gene structures and phylogenic implications. Plant Cell Physiol 45:138–145

Tokutsu R, Iwai M, Minagawa J (2009) CP29, a monomeric light-harvesting complex II protein, is essential for state transitions in *Chlamydomonas reinhardtii*. J Biol Chem 284:7777–7782

Tokutsu R, Kato N, Bui KH, Ishikawa T, Minagawa J (2012) Revisiting the supramolecular organization of photosystem II in *Chlamydomonas reinhardtii*. J Biol Chem 287:31574–31581

Ünlü C, Drop B, Croce R, van Amerongen H (2014) State transitions in *Chlamydomonas reinhardtii* strongly modulate the functional size of photosystem II but not of photosystem I. Proc Natl Acad Sci U S A 111:3460–3465

Vener AV, van Kan PJ, Rich PR, Ohad II, Andersson B (1997) Plastoquinol at the quinol oxidation site of reduced cytochrome *bf* mediates signal transduction between light and protein phosphorylation: thylakoid protein kinase deactivation by a single-turnover flash. Proc Natl Acad Sci U S A 94:1585–1590

Wilk L, Grunwald M, Liao PN, Walla PJ, Kuhlbrandt W (2013) Direct interaction of the major light-harvesting complex II and PsbS in nonphotochemical quenching. Proc Natl Acad Sci U S A 110:5452–5456

Wollman F-A, Lemaire C (1988) Studies on kinase-controlled state transitions in photosystem II and b_6f mutants from *Chlamydomonas reinhardtii* which lack quinone-binding proteins. Biochim Biophys Acta 933:85–94

Wraight CA, Crofts AR (1971) Delayed fluorescence and the high-energy state of chloroplasts. Biochim Biophys Acta 19:386–397

Yakushevska AE, Jensen PE, Keegstra W, van Roon H, Scheller HV, Boekema EJ, Dekker JP (2001) Supermolecular organization of photosystem II and its associated light-harvesting antenna in *Arabidopsis thaliana*. Eur J Biochem 268:6020–6028

Yamamoto HY, Nakayama TO, Chichester CO (1962) Studies on the light and dark interconversions of leaf xanthophylls. Arch Biochem Biophys 97:168–173

Zito F, Finazzi G, Delosme R, Nitschke W, Picot D, Wollman F-A (1999) The Qo site of cytochrome b_6f complexes controls the activation of the LHCII kinase. EMBO J 18:2961–2969

Chlamydomonas: Anoxic Acclimation and Signaling

Anja Hemschemeier

Abstract Chlamydomonas is a soil-dwelling freshwater alga that probably encounters hypoxic or anoxic conditions frequently in its natural habitat. Its repertoire of fermentative enzymes is remarkably complex and flexible. Despite this adaptability, at least under laboratory conditions, Chlamydomonas does not tolerate dark anoxia very well. It appears to respond to this condition by a state of quiescence, but still does not survive without light and molecular oxygen (O_2) longer than a couple of days. The amounts of hundreds of transcripts change in anoxic algal cultures, but not much is known about the regulation of the anoxic response in Chlamydomonas. The phenotypes of mutants deficient for one or the other fermentative enzyme indicate a significant level of control by metabolic signals, and a subset of genes is coordinately regulated in copper and O_2 deficiency by the copper response regulator1 (CRR1). However, the majority of genes that are differentially expressed in anaerobic Chlamydomonas cells are regulated CRR1 independently. While details on O_2 sensing in Chlamydomonas remain elusive, principles and patterns begin to emerge, such as a possible influence of light and the involvement of nitric oxide (NO) as a signaling molecule. This chapter summarizes knowledge on the anoxic metabolism and its regulation in Chlamydomonas and hypothesizes on putative signaling pathways based on existing reports and observations.

Abbreviations

ACK	Acetate kinase
ADH	Alcohol dehydrogenase
ADH1, ADHE	Bifunctional acetaldehyde-alcohol dehydrogenase
AMP, ADP, ATP	Adenosine mono-, di-, triphosphate
ARC	Amidoxime reducing component

A. Hemschemeier (✉)
Faculty of Biology and Biotechnology, Department of Plant Biochemistry, Workgroup Photobiotechnology, Ruhr-University of Bochum, Universitätsstr. 150, 44801 Bochum, Germany
e-mail: anja.hemschemeier@rub.de

M. Hippler (ed.), *Chlamydomonas: Molecular Genetics and Physiology*,
Microbiology Monographs 30, DOI 10.1007/978-3-319-66365-4_6

cGMP	Cyclic guanosine monophosphate
CRR1	Copper response regulator 1
D-LDH	D-Lactate dehydrogenase
FNR	Fumarate and nitrate reduction (regulatory protein)
GK	Glycerol kinase
G3P	Glycerol-3-phosphate
GPD	G3P dehydrogenase
GPP	G3P phosphatase
HP	Hypophosphite
L-NAME	Nω-Nitro-L-arginine methyl ester
NAD(P)H	Nicotinamide adenine dinucleotide (phosphate)
NIT1	Nitrate reductase (of Chlamydomonas)
NO	Nitric oxide
NOS	NO synthase
PAT	Phosphate acetyltransferase
PDC	Pyruvate decarboxylase
PEP	Phosphoenolpyruvate
PFL	Pyruvate-formate lyase
PflA	PFL activase
PFR	Pyruvate ferredoxin oxidoreductase
RNA-Seq	RNA sequencing
ROS	Reactive oxygen species
RNS	Reactive nitrogen species
SAM	*S*-adenosylmethionine
sGC	Soluble guanylate cyclase
THB	Truncated hemoglobin

1 Introduction

Approximately 2.3 billion years ago, molecular oxygen (O_2) accumulated in the Earth's atmosphere (Bekker et al. 2004; Goldblatt et al. 2006), a process also known as the "oxygen catastrophe." It is widely accepted that the evolutionary invention of oxygenic photosynthesis by early cyanobacteria was responsible for the emergence of an oxygenated atmosphere (Lyons 2007; Buick 2008). Notwithstanding of being the cause for one of the Earth's mass extinction events, the accumulation of the reactive and oxidizing gas is assumed to have allowed the evolution of complex multicellular life forms (Hedges et al. 2004; Falkowski et al. 2005). One important reason for this is the high energy yield of aerobic respiration. However, the availability of the O_2 molecule also resulted in the emergence of much more complex biochemical networks (Raymond and Segre 2006) due to the evolution of enzymes that utilize O_2 as a substrate or reactant (Goldfine 1965; Raymond and Blankenship 2004). Not least, reactive oxygen and nitrogen species (ROS, RNS)

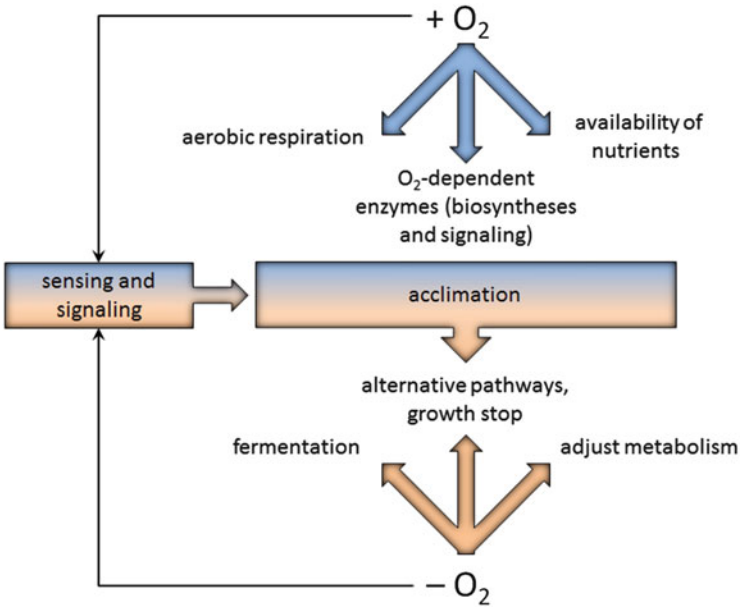

Fig. 1 Overview on important O_2-dependent processes and their counterparts under anoxia that are induced in the framework of acclimatory processes upon sensing and signaling the shortage of O_2

that result from O_2 chemistry are employed in signaling pathways as well as for pathogen defense (Halliwell 2006; Thannickal 2009). The flip side of the coin is that many higher eukaryotes that probably evolved with the help of O_2 are now dependent on the molecule. Most animals and higher plants are aerobes and cannot survive O_2 deficiency for an extended period of time. In contrast, facultative anaerobes such as the bacterium *Escherichia coli* make use of the benefits of O_2 in its presence, but they can also grow in its absence. In any case, when the O_2 concentrations are below those needed for the normal operation of aerobic pathways (hypoxia) or in the complete absence of O_2 (anoxia), the metabolism has to be adjusted (Fig. 1). Many organisms can switch from aerobic to anaerobic respiration and utilize electron acceptors other than O_2 while still generating adenosine triphosphate (ATP) through electron transport phosphorylation (Amend and Shock 2001; Ginger et al. 2010; Müller et al. 2012). In the absence of suitable electron acceptors or in organisms incapable of anaerobic respiration, O_2 deficiency induces fermentation, during which ATP is generated through substrate-level phosphorylation, yielding much less energy compared to respiration. Additionally, fermentation results in the accumulation and often secretion of reduced end products, because the reducing equivalents [mostly reduced nicotinamide adenine dinucleotide (phosphate) (NAD(P)H)] that are produced during the oxidative degradation of the substrate have to be reoxidized in order to allow a continuous substrate flow.

Generating sufficient energy while simultaneously maintaining a healthy equilibrium of the redox status, the pH, and potentially toxic end products such as ethanol is a central issue of fermentation. Additionally, in anoxia, aerobes face the challenge of sustaining their repertoire of cellular components. For example, both the biosynthesis and the degradation of tetrapyrroles include O_2-dependent steps in plants and algae (Hörtensteiner and Kräutler 2011; Tanaka et al. 2011), whereas some bacterial species possess O_2-independent enzymes for the same steps (Brzezowski et al. 2015). The switch from aerobic to hypoxic or anaerobic metabolism can occur on the level of substrate fluxes. A well-known example is the regulation of the glycolytic enzyme phosphofructokinase, which is activated by adenosine diphosphate (ADP) and (in eukaryotes) inhibited by ATP (Schöneberg et al. 2013). However, an important response to a shift from aerobic to anaerobic conditions is the differential expression of hundreds of genes in most organisms (Mustroph et al. 2010).

Oxygenic phototrophs produce O_2 in the light, but they can encounter hypoxic or anoxic conditions frequently. Higher plants can be challenged by O_2 shortage during floods and in water-logged soil (Bailey-Serres and Voesenek 2008). *Chlamydomonas reinhardtii* (Chlamydomonas in the following) is a freshwater alga and was often isolated from soil (Harris 2001). Its habitats tend to become hypoxic due to the respiratory activity of surrounding organisms, especially in low light or in darkness (Steunou et al. 2006). Chlamydomonas has long been used as a model organism for studying plant or animal processes; however, not least the research on its anaerobic metabolism has revealed that the microalga has its particularities and is far from being only a model. This chapter will give an overview about the anaerobic response of Chlamydomonas on the metabolic level and about what is known about anoxic gene regulation. It should be noted that the hypoxic or anaerobic response of Chlamydomonas is studied in different systems, usually depending on the scientific question. Hypoxia in the light can be achieved by purging illuminated cells with argon or nitrogen (N_2) gas and is mostly applied to study state transitions and cyclic electron flow (e.g., Terashima et al. 2012). Starving illuminated Chlamydomonas cells for nutrients can result in endogenously established hypoxia, and this system, which is mainly based on a decrease of photosynthetic O_2 evolution, is being studied extensively with regard to photobio (techno)logical production of molecular hydrogen (H_2) (e.g., Dubini and Ghirardi 2015) (also see chapter "Chlamydomonas: Hydrogenase and Hydrogen Production"). The fermentative metabolism of the alga is usually analyzed in dark-anoxic cells, for example, by purging a concentrated cell suspension with O_2-free gas (e.g., Philipps et al. 2011) or by transferring a culture to sealed flasks in the dark, and let the cells consume the dissolved O_2 by respiratory activity, dubbed "self-anaerobization" (Hemschemeier et al. 2013a). Here, mainly results from analyzing dark-anoxic cells will be summarized, with references to other systems indicated.

2 The Anaerobic Metabolism of Chlamydomonas

Anaerobic respiration has not been described in Chlamydomonas, but it has a surprisingly versatile and flexible repertoire of fermentative pathways (Atteia et al. 2013; Catalanotti et al. 2013) (Fig. 2). According to the current state of knowledge, this complexity makes Chlamydomonas stand out even from other microalgae (Atteia et al. 2013). In contrast to plants and animals that usually resort to ethanol or lactate homofermentation, the pattern of fermentative end products of Chlamydomonas can best be described as a mixed acid fermentation. The major compounds that are secreted by the wild type are formate, ethanol, and acetate (Gfeller and Gibbs 1984; Kreuzberg 1984). This pattern is typical for a pyruvate fermentation pathway initiated by pyruvate formate lyase (PFL) (EC 2.3.1.54). Additionally, the gases carbon dioxide (CO_2) and H_2 are evolved in significant quantities by anoxic Chlamydomonas cultures. D-Lactate, succinate, malate, and glycerol are secreted to low amounts by wild-type algae (Gfeller and Gibbs 1984; Kreuzberg 1984; Mus et al. 2007; Dubini et al. 2009), but can become major end products in mutants (see below).

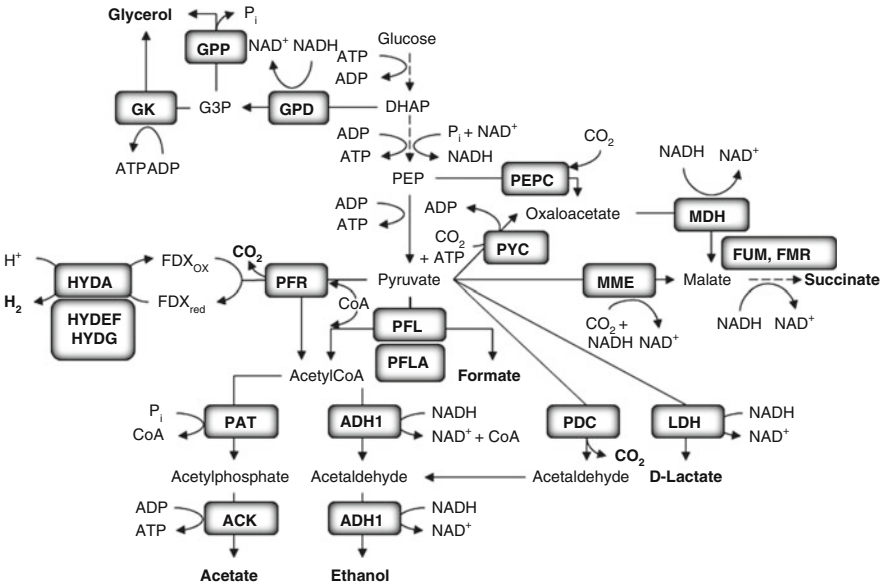

Fig. 2 Schematic overview on fermentative pathways of Chlamydomonas that are discussed in the text. *ACK* acetate kinase, *ADH1* acetaldehyde alcohol dehydrogenase (DH), *DHAP* dihydroxyacetone phosphate, *FDX* ferredoxin, *FMR* fumarate reductase, *FUM* fumarase, *GK* glycerol kinase, *G3P* glycerol-3-phosphate, *GPD* G3P DH, *GPP* G3P phosphatase, *HYDA* [FeFe]-hydrogenase, *HYDEF, HYDG* HYDA maturases, *LDH* lactate DH, *MDH* malate DH, *MME* malic enzyme, *PAT* phosphate acetyltransferase, *PDC* pyruvate decarboxylase, *PEP* phosphoenolpyruvate, *PEPC* PEP carboxylase, *PFL* pyruvate formate lyase, *PFLA* PFL activase, *PFR* pyruvate ferredoxin oxidoreductase, *PYC* pyruvate carboxylase

2.1 Fermentation Through Pyruvate Formate Lyase

According to the pattern and amount of end products, PFL is the major fermentative enzyme of wild-type Chlamydomonas cells. PFL is present in many prokaryotic and some eukaryotic species (Stairs et al. 2011), and the enzyme from *Escherichia coli* is well analyzed. PFL catalyzes the non-oxidative homolytic cleavage of pyruvate to acetyl-CoA and formate and employs a glycyl radical and two conserved cysteines (Cys) for this reaction (Buis and Broderick 2005 and references therein). The glycyl radical is introduced into the PFL polypeptide posttranslationally by the radical *S*-adenosylmethionine (SAM) enzyme PFL activase (PflA) (EC 1.97.1.4) (Buis and Broderick 2005; Shisler and Broderick 2014) and makes the PFL enzyme sensitive toward O_2-induced cleavage at the site of the radical (Wagner et al. 1992). In Chlamydomonas, besides the typical fermentation pattern, further results indicating the activity of a PFL enzyme were enzyme assays using cell extracts (Kreuzberg et al. 1987) and the fact that the formate analogue and mechanism-based PFL inhibitor hypophosphite (HP) (Knappe et al. 1984) inhibits formate secretion by the cells (Kreuzberg 1984). On the transcript and protein level, Chlamydomonas PFL was first described 2006 (Atteia et al. 2006). PFL activity was confirmed on the biochemical level using the recombinant protein, and the algal *PFL1* gene (*Cre01.g044800*) is able to complement an *E. coli pfl* mutant (Hemschemeier et al. 2008). To date, the Chlamydomonas PflA has only been identified on the transcript level (Atteia et al. 2006; Hemschemeier et al. 2008) (GenBank: AAW32935, AJ620192).

The algal PFL1 was detected in the chloroplast and the mitochondrial fraction both on the activity (Kreuzberg et al. 1987) and the protein level (Atteia et al. 2006; Terashima et al. 2010). As only a single PFL-encoding gene can be found in the alga's genome, the enzyme appears to be dually targeted, probably by the approximately 70-amino acid-long N-terminus which has no homology to bacterial enzymes and which is dispensable for catalytic activity (Hemschemeier et al. 2008). It is noteworthy that although the PFL fermentation system of Chlamydomonas is highly similar to that of *E. coli*, the microalga does not appear to reutilize formate in a similar way. *E. coli* reimports formate and converts it into H_2 and CO_2 via the formate hydrogen lyase (FHL) complex (Sawers 2005), which is not present in Chlamydomonas. In fermenting Chlamydomonas cells, formate does not accumulate intracellularly (Hemschemeier et al. 2008), but in the medium (Gfeller and Gibbs 1984; Kreuzberg 1984).

The second product of PFL, acetyl-CoA, can be converted either to acetate, allowing the additional production of ATP via substrate-level phosphorylation, or to ethanol, resulting in the reoxidation of two NAD(P)H molecules (Fig. 2). For the former reaction, Chlamydomonas most likely employs phosphate acetyltransferase (PAT; EC 2.3.1.8) and acetate kinase (ACK; EC 2.7.2.1) like many prokaryotes (Wolfe 2005). The microalga contains two genes for each enzyme. *ACK1* (*Cre09.g396700*) and *PAT2* (*Cre09.g396650*) lie directly adjacent on chromosome 9, while *ACK2* (*Cre17.g709850*) and *PAT1* (*Cre17.g699000*) lie separated on

chromosome 17. ACK1 and PAT2 are chloroplast localized; ACK2 and PAT1 were detected in the mitochondria (Atteia et al. 2009; Terashima et al. 2010; Yang et al. 2014). For the acclimation of Chlamydomonas to anoxia in the dark, the chloroplast system might be more important: *ack1* and *pat2* mutants show a slightly reduced survival after prolonged dark-anoxic incubation when compared to the wild type or an *ack2* mutant, and only mutations in the *ack1* or *pat2* genes result in significantly reduced acetate secretion (Yang et al. 2014). Notably, even an *ack1ack2* double mutant still secretes acetate, suggesting the presence of additional pathways of acetate formation from acetyl-CoA (Atteia et al. 2013; Yang et al. 2014).

Ethanol production from acetyl-CoA requires acetaldehyde dehydrogenase (EC 1.2.1.10) and alcohol dehydrogenase (ADH; EC 1.1.1.1) activity. In *E. coli*, both activities lie on one single polypeptide, the AdhE protein, whose ADH domain belongs to the iron (Fe)-containing ADHs (Kessler et al. 1991). Chlamydomonas possesses at least one protein with high homology to the *E. coli* AdhE (ADH1; *Cre17.g746997*) (Atteia et al. 2006) which is constitutively present (Hemschemeier et al. 2008; Magneschi et al. 2012) although it might be as O_2 sensitive as other Fe-containing ADHs (Cabiscol et al. 1994; Echave et al. 2003). Chlamydomonas possesses additional Fe-binding ADHs and also homologues to zinc (Zn)-containing ADHs; however, an *adh1* mutant does not secrete detectable amounts of ethanol, indicating that ADH1 is the only (fermentatively) active ADH of the alga (Magneschi et al. 2012).

2.2 *Pyruvate Oxidation by Pyruvate Ferredoxin Oxidoreductase*

Chlamydomonas also contains a pyruvate ferredoxin oxidoreductase (PFR, often also abbreviated as PFOR; EC 1.2.7.1) encoded by the gene *Cre02.g095137*. Like PFL, PFR enzymes are mostly found in prokaryotes and some protists (Atteia et al. 2006; Hug et al. 2010). PFR decarboxylates pyruvate and converts it to acetyl-CoA, reducing ferredoxin or flavodoxin at the same time (Fig. 2). PFR enzymes contain three [4Fe4S] clusters and thiamine pyrophosphate (TPP) (Chabrière et al. 1999; Ragsdale 2003). In vitro, several PFR proteins can utilize other keto acids than pyruvate, such as 2-oxobutyrate or α-ketoglutarate (Meinecke et al. 1989; Fukuda et al. 2001; Park et al. 2006). Chlamydomonas PFR was analyzed in the recombinant form and has characteristics typical for the bacterial enzymes: it contains FeS clusters and a TPP radical, is able to reduce ferredoxins, and is O_2 sensitive as most PFR proteins analyzed so far (Noth et al. 2013; van Lis et al. 2013). In several anaerobic parasitic protists such as *Trichomonas vaginalis* or *Tritrichomonas foetus*, reduced ferredoxin is reoxidized by hydrogenases which utilize the electrons to form H_2 (Müller et al. 2012; Makiuchi and Nozaki 2014). Chlamydomonas, as

many prokaryotes, some anaerobic protists, and other species of unicellular green algae (Vignais and Billoud 2007; Peters et al. 2015), contains hydrogenases of the [FeFe] type (also see chapter "Chlamydomonas: Hydrogenase and Hydrogen Production" on hydrogenases and hydrogen production). The isoform HydA1 and probably also the isoform HydA2 are located in the chloroplast (Happe et al. 1994; Forestier et al. 2003; Terashima et al. 2010). HydA1 accepts electrons from reduced ferredoxin and thereby from photosynthetic electron transport (Winkler et al. 2009; Hemschemeier and Happe 2011; Ghysels et al. 2013). During fermentation in the dark, Chlamydomonas evolves relatively low but significant amounts of H_2 (Gfeller and Gibbs 1984; Kreuzberg 1984; Philipps et al. 2011), probably through the reaction catalyzed by PFR: in vitro, a coupled enzyme assay including Chlamydomonas PFR, ferredoxin, and HydA1 and the substrates pyruvate and coenzyme A evolves H_2 (Noth et al. 2013) (Fig. 2). Notably, also oxaloacetate, but not α-ketoglutarate, can be utilized by the algal PFR besides pyruvate.

Whether the PFR-ferredoxin-HydA1 pathway operates in vivo is not clear yet, as no *pfr1* mutant has been published to date. Because PFR and PFL utilize the same substrate, it was hypothesized that reduced PFL activity would enhance pyruvate turnover by PFR and thus ferredoxin reduction and H_2 production. However, analyses in different laboratories and of different strains yielded conflicting results: H_2 production in darkness was higher in a *pfl1* mutant and the HP-treated wild type in one study (Philipps et al. 2011), but lower in allelic *pfl1* mutants (Catalanotti et al. 2012) or after HP treatment of the wild type in another study (Kreuzberg 1984). Catalanotti et al. (2012) suggested the higher CO_2 and ethanol levels determined in *pfl1* mutant cultures to be due to pyruvate decarboxylase (PDC; EC 4.1.1.1) (Fig. 2). Indeed, Chlamydomonas has PDC activity (Kreuzberg et al. 1987), and a protein of the expected size can be detected using an antibody against *Pisum sativum* PDC (Hemschemeier et al. 2008). PDC is probably encoded by the gene *PDC3* (*Cre03.g165700*) whose product is localized in the cytosol (Burgess et al. 2016). In the *pfl1* mutant described by Catalanotti et al. (2012), the *PDC3* transcript is higher abundant than in the wild type, while *PFR* transcript and PFR protein are less abundant. Because the only ethanol producing fermentative enzyme of Chlamydomonas is probably the ADH1 enzyme (see above, Magneschi et al. 2012), it would also have to oxidize the acetaldehyde produced by PDC. AdhE enzymes indeed are able to convert acetaldehyde directly (Kessler et al. 1991; Bruchhaus and Tannich 1994), and the *pfl1* mutant has higher *ADH1* transcript levels (Catalanotti et al. 2012).

The different experimental outcomes regarding H_2 evolution might be explained by different incubation conditions. Higher H_2 yields in algae with impaired PFL1 activity were observed in cells that were concentrated in full medium (Philipps et al. 2011), while lower H_2 yields were observed analyzing allelic *pfl1* mutants (Catalanotti et al. 2012) or the wild type treated with HP (Kreuzberg 1984) that were both anaerobically incubated in buffer. The amounts of PFR protein are indeed much lower in anoxic cells incubated in buffer versus

full medium (van Lis et al. 2013). Another factor might be that different Chlamydomonas strains were analyzed. The community becomes increasingly aware of the fact that Chlamydomonas strains isolated at different locations or even the same strain kept for years in one or the other laboratory show genetic and/or phenotypic differences that can be quite significant (Chochois et al. 2010; Jang and Ehrenreich 2012; Flowers et al. 2015; Gallaher et al. 2015).

2.3 *Fermentation in Chlamydomonas Is Flexible*

To date, several Chlamydomonas mutants deficient for individual fermentative enzymes have been discovered. Their examination revealed that the alga is capable to adjust its fermentative metabolism, usually secreting another end product in higher amounts. For example, *pfl1* mutants secrete no formate, more ethanol, and less acetate than the wild type. Most interestingly, however, is the fact that these mutants secrete significant amounts of D-lactate, which is usually hardly detectable in the supernatant of wild-type cultures (Kreuzberg 1984; Philipps et al. 2011; Burgess et al. 2012; Catalanotti et al. 2012). This indicates that constitutively present D-lactate dehydrogenase activity (D-LDH; EC 1.1.1.28) (Husic and Tolbert 1985; Kreuzberg et al. 1987; Burgess et al. 2016) takes over and converts the pyruvate that accumulates in cells with impaired PFL activity (Kreuzberg 1984) (Fig. 2). Notably, Chlamydomonas transformants in which the gene for the protein with the highest homology to D-LDH enzymes (gene *LDH1*, *Cre07.g324550*) is posttranscriptionally downregulated still excrete wild-type amounts of D-lactate upon inhibition of PFL1 with HP, suggesting either a high substrate flux through LDH1 or alternative D-LDH generating pathways (Burgess et al. 2016).

An *adh1* mutant, which does not secrete ethanol and which is therefore probably incapable of utilizing acetyl-CoA for the reoxidation of NAD(P)H, also secretes D-lactate, but additionally significant amounts of glycerol (Magneschi et al. 2012), a fermentative end product usually not detected in Chlamydomonas wild-type cultures (Gfeller and Gibbs 1984; Kreuzberg 1984). Fermentative glycerol generation might occur as in *S. cerevisiae* or *T. vaginalis* via glycerol-3-phosphate (G3P) dehydrogenase (GPD; EC 1.1.1.8 or 1.1.1.94) which reduces dihydroxyacetone phosphate to G3P and G3P phosphatase (GPP; EC 3.1.3.21) (Steinbüchel and Müller 1986; Ansell et al. 1997; Påhlman et al. 2001). G3P could also be used by glycerol kinase (GK; EC 2.7.1.30) to generate ATP (Fig. 2). In most organisms, GK is utilized for the reverse reaction, because the thermodynamic equilibrium is in favor of G3P production. However, the unicellular parasite *Trypanosoma brucei* uses GK in anaerobiosis for ATP production (Hammond et al. 1985). Chlamydomonas has several genes encoding putative GPDs as well as a GPP and a GK gene, none of which are significantly upregulated on the transcriptional level in the *adh1* mutant (Magneschi et al. 2012).

Yet another strategy is employed by a de facto Chlamydomonas hydrogenase mutant, in which the cofactor of the [FeFe]-hydrogenases cannot be assembled due to a mutation in a gene encoding for the specific maturase *HYDEF* (Posewitz et al. 2004a) (also see chapter "Chlamydomonas: Hydrogenase and Hydrogen Production") and which is incapable of producing H_2. The *hydef* mutant secretes less formate, ethanol, and acetate, no CO_2, but—again in contrast to the wild type—succinate (Dubini et al. 2009). This mutant probably converts phosphoenolpyruvate (PEP) or pyruvate to oxaloacetate or malate and then employs reverse reactions of the tricarboxylic acid or glyoxylate cycle (Fig. 2). Some transcripts coding for enzymes that would be involved in these reactions are indeed upregulated in the *hydef* mutant, such as PEP carboxylase (EC 4.1.1.31), pyruvate carboxylase (EC 6.4.1.1), malic enzyme (EC 1.1.1.38 or 1.1.1.40), fumarase (EC 4.2.1.2), and fumarate reductase (EC 1.3.1.6) (Dubini et al. 2009).

It is noteworthy that many of the fermentative enzymes of Chlamydomonas are located in the chloroplast (Happe et al. 1994; Atteia et al. 2006; Terashima et al. 2010; van Lis et al. 2013; Yang et al. 2014; Burgess et al. 2016), although some of them are extremely O_2 sensitive. Most analyses of the alga's fermentative metabolism were conducted in dark-adapted and thus probably completely anoxic cells, but H_2 production and fermentation can also be observed under conditions of nutrient deficiency in the light (Melis et al. 2000; Tsygankov et al. 2002; Winkler et al. 2002; Hemschemeier et al. 2008; Philipps et al. 2012) which results in hypoxia in sealed cultures mainly due to a decreased activity of photosystem II (PSII) (Wykoff et al. 1998; Melis et al. 2000; Batyrova et al. 2012; Philipps et al. 2012; Volgusheva et al. 2015). However, PSII remains active on a low level (e.g., Melis et al. 2000; Philipps et al. 2012). It is unclear whether the O_2-sensitive enzymes such as the [FeFe]-hydrogenases, PFL, and PFR are protected from the photosynthetically evolved O_2, e.g., by O_2-binding or O_2-scavenging proteins, by compartmentalization, or by respiratory activities in- and outside the chloroplast (e.g., Steinbeck et al. 2015), or if they are destroyed but constantly resynthesized.

An induction on the transcript or protein level of some fermentative enzymes has also been observed under conditions that are not typically associated with fermentation. For example, the dual function alcohol/acetaldehyde dehydrogenase ADH1 shows a higher abundance under Fe deficiency in the light (Urzica et al. 2012; Höhner et al. 2013). The physiological significance of this was revealed in an *adh1* mutant in which the typical responses of the photosynthetic apparatus to Fe deficiency were less pronounced, while stress responses were enhanced, and it was discussed that the ADH1 enzyme might be necessary to maintain the redox poise of the chloroplast (Höhner et al. 2013). Notably, ADH1 as well as PFL1 also accumulate under copper (Cu) and Zn deficiency (Hsieh et al. 2013). Cu deficiency does not result in reduced photosynthetic activity in the Chlamydomonas wild type (see Sect. 3.2), but the *HYDA1* and *PFR1* genes are also induced on the transcriptional and protein level under this condition (Castruita et al. 2011; Hsieh et al. 2013).

2.4 Anaerobic Survival of Chlamydomonas

Most higher plants or their organs are not very tolerant against hypoxia or anaerobiosis (e.g., Drew 1997; Fukao and Bailey-Serres 2004; Bailey-Serres and Voesenek 2008). The plenty of fermentative routes of Chlamydomonas and the flexibility of the alga in dealing with the failure of fermentative subsystems should indicate that the microalga can thrive well in O_2 deficiency. Furthermore, the availability of a hydrogenase coupled to photosynthetic electron transport helps the alga to restart photosynthetic electron transport after dark-anoxic incubation, which is also an important aspect of dealing with periods of anoxia in its natural environment. HydA1 serves as a transient electron acceptor until sufficient amounts of ATP are produced by linear and cyclic electron flow for the Calvin cycle to take over as the major electron sink (Ghysels et al. 2013; Godaux et al. 2015). However, Chlamydomonas does not grow under anoxic conditions unless supplied with light (Graves et al. 1990; Hemschemeier et al. 2013a). Arrested growth in the dark is accompanied by a significant decrease of the amounts of transcripts involved in various aspects of cell growth and division (DNA biosynthesis, replication, and structure, general transcription, and translation) (Hemschemeier et al. 2013a). This response appears to be a "power save mode," similar to the quiescence of several plant species exposed to hypoxia (Bailey-Serres and Voesenek 2008). Whether or how long this response can ensure the survival of Chlamydomonas in the long term is not clear yet, because different observations were published. For example, Magneschi et al. (2012) concentrated Chlamydomonas cell suspensions in buffer, purged the suspension with argon, and then incubated them anoxically in the dark. These cells, when dropped on agar plates and transferred back to light, showed reduced growth already after 6 h and hardly any growth after 18 h of dark anoxia, indicating that most of the cells died (Magneschi et al. 2012). After a similar treatment, but concentration and incubation in high salt medium, the algal cells showed a reduced growth only after 18 h of dark anoxia (Yang et al. 2014). In yet another study, cells grew after several days of dark anaerobic incubation. Here, cells were spotted on full medium agar plates, kept in an N_2-H_2 atmosphere in the dark and then transferred back to normoxia (Whitney et al. 2011). The latter study additionally indicated that the tolerance of the cells changed depending on the time of day at which they were shifted to darkness and anoxia. After self-anaerobization and transfer of the liquid cultures back to normoxia and light, cells incubated without O_2 in the dark for 24 h bleach, but green afterwards (Hemschemeier 2013). Even after 72 h of dark anoxia, cells green again, although this takes considerably longer compared to cells treated for 24 h. Taken together, these results show that many parameters influence the vitality of Chlamydomonas under O_2 deprivation in the dark, such as nutrient availability, cell density, time of day, and maybe also the speed at which anaerobiosis sets in.

3 O_2-Responsive Gene Expression in Chlamydomonas

Transcripts of several genes that code for enzymes known to be involved in the anaerobic metabolism of Chlamydomonas accumulate under anoxic conditions, such as *HYDA1* and *HYDA2* (Happe and Kaminski 2002; Forestier et al. 2003), *PFR* (Mus et al. 2007; Catalanotti et al. 2012), or *PFL1* (Atteia et al. 2006). In case of the hydrogenases (Happe and Kaminski 2002; Forestier et al. 2003) and PFR (Catalanotti et al. 2012; van Lis et al. 2013), this transcriptional induction is accompanied by an accumulation of protein, while the amounts of PFL1 protein stay rather constant (Atteia et al. 2006; Catalanotti et al. 2012; Magneschi et al. 2012). It is noteworthy, though, that in several studies, a double-band pattern can be observed in PFL1 immunoblots testing cell extracts from anoxic cells, whereby an additional, slightly lower band appears (Atteia et al. 2006; Catalanotti et al. 2012; Magneschi et al. 2012). This band pattern would be consistent with an O_2-induced cleavage of the PFL polypeptide at the site of the glycyl radical (Wagner et al. 1992). Although this has not been analyzed on the biochemical level in Chlamydomonas yet, one might speculate that PFL is regulated mostly on the posttranslational level via its conversion from the inactive form to the glycyl-harboring active enzyme.

In addition to results on individual known genes, transcriptomics applying microarray or RNA sequencing (RNA-Seq) analyses have revealed that the abundance of hundreds of transcripts changes in dark-hypoxic or dark-anoxic Chlamydomonas cells (Mus et al. 2007; Dubini et al. 2009; Hemschemeier et al. 2013a). In the context of anoxic gene regulation, it is noteworthy that the results of the independent transcriptome analyses revealed only a relatively small number of genes that were similarly regulated in all studies. Although the utilization of different technologies (microarray versus RNA-Seq) and possibly also the progress of the Chlamydomonas genome annotation (Blaby et al. 2014) are probably in part responsible for these differences, the different treatment of the algal cells (cell suspensions concentrated in buffer and purged with argon versus self-anaerobization) will certainly have contributed to the different outcomes. From these studies, but also from single-gene analyses, one can assume that many "anoxia-responsive" genes are not directly or not solely regulated by the absence of the O_2 molecule, but also by other factors (see below).

Many O_2 sensing and signaling components are known from various organism groups (Bien and Espenshade 2010; Bailey-Serres et al. 2012; Butler 2013; Green et al. 2014; Taabazuing et al. 2014), but not much is known on the factors that regulate anoxia-responsive genes in Chlamydomonas. Although the fermentative enzymes of the microalga show clear homology to their counterparts in other organism groups, the associated O_2 sensors or transcription factors were in most cases not identified in its genome. However, considering the large number of "unknown" genes in Chlamydomonas, it might well be that a known principle of O_2 sensing is carried out by a protein with no or no clear homology to a known O_2 sensor.

3.1 Principles of O_2 Sensing

In general, O_2 sensors can be described to be direct or indirect sensors, depending on if they interact with the O_2 molecule or if they register a physiological consequence of O_2 deficiency. Known direct O_2 sensors contain an O_2-binding moiety such as heme, a diiron center, or iron sulfur (FeS) clusters (Taabazuing et al. 2014). A well-studied example for a direct O_2 sensor is the FNR (fumarate and nitrate reduction) transcription factor of *E. coli*, which harbors a [4Fe4S] cluster under anaerobic and a [2Fe2S] cluster under aerobic conditions, while only the [4Fe4S] protein can form homodimers and bind to its DNA target sequences (Green et al. 2014, and references therein). Most FeS clusters are sensitive toward O_2 unless protected by the protein (Imlay 2006), so although Chlamydomonas does not contain a clear FNR homologue, an FeS protein without any homology to FNR might carry out a similar function. PFL activase, whose active FeS cluster is only formed under anaerobic conditions in *E. coli* (Yang et al. 2009), might be such a protein, although it would probably be responsible for activating the PFL protein only.

Another direct O_2 sensor is FixL which is part of a two-component system in diazotrophic bacteria. It consists of a histidine kinase and a heme-binding PAS (Per Arnt Sim) domain. Under microaerobic or anoxic conditions, when no O_2 molecule binds to the heme group, the kinase is activated and phosphorylates the response regulator FixJ (Rodgers and Lukat-Rodgers 2005). Nine putative heme-binding homologues of the FixL PAS domain were identified in Chlamydomonas, and two of these, when analyzed in their recombinant forms, bind O_2 with low affinity, making them plausible candidates for O_2 sensors (Murthy et al. 2012). In dark-anoxic algal cells, several transcripts encoding PAS domain containing proteins accumulate, among them *FXL5* (*Cre08.g373200*) that was shown by Murthy et al. (2012) to bind heme and O_2 (Mus et al. 2007; Hemschemeier et al. 2013a). To date, it is not known if these proteins are involved in regulating the anoxic response of Chlamydomonas. They are all transmembrane proteins, but lack further domains clearly hinting to a function (e.g., a kinase domain) (Murthy et al. 2012).

Indirect O_2 sensing registers the metabolic consequences of O_2 deficiency. For example, through redox reactions of Cys residues, the ArcB transmembrane sensor kinase from *E. coli*, part of the ArcAB two component system, registers the redox state of quinones and thereby indirectly the respiratory electron flow (Bueno et al. 2012 and references therein).

Somewhere in between direct and indirect O_2 sensing are signals arising from O_2-dependent pathways. Several organisms make a virtue out of necessity and utilize the inability of O_2-dependent enzymes to carry out catalysis as means of sensing the O_2 status. The readout can be the product of a biosynthetic pathway that involves O_2-dependent steps or the direct modification of an effector. In *S. cerevisiae*, the cellular heme concentration decreases in anoxia (Zagorec and

Labbe-Bois 1986; Hon et al. 2003). Heme levels are registered by the transcription factor Hap1p that activates genes involved in the aerobic metabolism only in a heme-bound state (Zhang et al. 1998; Mense and Zhang 2006). In the fission yeast *Schizosaccharomyces pombe* and other fungi, an SREBP (sterol regulatory element-binding protein) transcription factor activates various genes involved in the hypoxic response when sterol and O_2 levels are low (Todd et al. 2006; Lee et al. 2009; Bien and Espenshade 2010; Butler 2013). *S. pombe* cannot take up sterols from the environment and is thus dependent on its de novo biosynthesis, which is impaired in anoxia (Hughes et al. 2005). In metazoa, a central transcription factor of the hypoxic response is the hypoxia-inducible factor 1 (HIF1), a heterodimeric transcription factor consisting of HIF1α and HIF1β. Regulation occurs to a large extent by stabilization of HIF1α. Although the regulation of HIF1α is very complex and occurs on various levels (Fábián et al. 2016), one major regulatory step is carried out by prolyl-4-hydroxylases. These enzymes O_2-dependently hydroxylate specific residues of the HIF1α polypeptide (Willam et al. 2004), which is thereby targeted for proteasomal degradation (Robinson and Ohh 2014). The HIF1α hydroxylases have a relatively low affinity for O_2, resulting in reduced hydroxylation activity in hypoxia and a stabilization of HIF1α which then becomes available for activating genes involved in the hypoxic metabolism (Semenza 2004, 2012).

In Arabidopsis, group VII ethylene-responsive factors (ERFs) are redundantly involved in hypoxic gene expression and are stabilized in hypoxia (Bailey-Serres et al. 2012; van Dongen and Licausi 2015). These ERFs are regulated through the N-end rule, which refers to the lifetime of proteins in dependence of their N-terminal amino acid. Several group VII ERFs feature a conserved N-terminal sequence (MCGGAI) with a Cys directly following the methionine (Met). The Met residue is probably constitutively removed by a Met aminopeptidase, exposing the reactive Cys residue and allowing its O_2-dependent conversion to sulfinic acid by Cys dioxygenases (Weits et al. 2014). This is in turn recognized by an arginyltransferase, and the arginylated N-terminus is a target for the protein degradation pathway (Bailey-Serres et al. 2012; van Dongen and Licausi 2015).

In dark-anoxic Chlamydomonas cultures, more than 30 transcripts accumulate that code for O_2-dependent enzymes, including O_2-dependent tetrapyrrole biosynthetic enzymes and prolyl-4-hydroxylases (Mus et al. 2007; Hemschemeier et al. 2013a), indicating that pathways that depend on the O_2 molecule are responsive to anoxia on the gene regulatory level. However, Chlamydomonas lacks clear homologues of the well-studied executing regulators Hap1p, SREBP, or HIF1α. The alga contains at least 20 APETALA2/ethylene-responsive element-binding protein-domain transcription factors (Dietz et al. 2010, plus own BlastP analyses on Phytozome), but according to the current annotation, none starts with the conserved MCGGAI motive or has a Cys at the second position. Obviously, if Chlamydomonas makes use of this type of O_2 sensing, the actual signal transducing components are different.

3.2 Shared Anoxia and Copper-Responsive Gene Expression

To date, there is only one relatively well-studied example of an "anoxia-responsive" transcription factor, which, however, was initially discovered due to its essential role in the acclimation of Chlamydomonas to Cu deficiency. It was noted that several genes that are induced upon Cu deficiency are also induced by a lack of O_2 and that both responses share signal transduction components and require the same genetic locus (Wood 1978; Quinn et al. 2000, 2002). The responsible transcription factor was termed copper response regulator 1 (CRR1) because Chlamydomonas *crr1* mutants hardly grow under Cu deficiency, whereas the wild type grows well even if the growth medium is essentially Cu-free (Eriksson et al. 2004; Kropat et al. 2005). Similarly, Chlamydomonas grows well in an anoxic atmosphere in the light, but the *crr1* mutant does not (Eriksson et al. 2004; Hemschemeier et al. 2013a). All responses of the wild type to a lack of Cu studied to date are absent in the *crr1* mutant, such as the replacement of the Cu-binding soluble photosynthetic electron transport protein plastocyanin by the heme-protein cytochrome c_6 (CYC6) (Merchant and Bogorad 1986; Eriksson et al. 2004) or the transcriptional induction of Cu transporter-encoding genes (Page et al. 2009).

3.2.1 The Principles of Gene Regulation by CRR1

The CRR1 transcription factor is a huge protein of 1232 amino acids which binds to its target sequences through its *SQUAMOSA* promoter-binding protein (SBP) domain (Kropat et al. 2005; Sommer et al. 2010), a plant-type DNA-binding domain made of two Zn fingers (Yamasaki et al. 2004). The core DNA-binding motive of SBP domain transcription factors is a highly conserved 5′-GTAC-3′ sequence, but flanking nucleotides also play a role (Quinn et al. 2000, 2002; Birkenbihl et al. 2005; Kropat et al. 2005; Liang et al. 2008). The transcriptional activation of all Chlamydomonas CRR1 targets analyzed to date accordingly depends on the presence of GTAC motives in their promoters, but the numbers and positions of these target sites vary. The *CYC6* core promoter (Quinn and Merchant 1995) contains three GTAC motives, but only two of these confer Cu-responsive gene expression and were therefore termed CuREs (copper response elements). Notably, they can fulfil this function individually (i.e., mutations in one of them do not abolish the expression of a reporter gene as long as the other one is present) (Quinn et al. 2000). Two GTAC sites were analyzed in the promoter of the gene encoding the aerobic coproporphyrinogen III oxidase CPX1, and only the distal element allows Cu-responsive transcriptional activation (Quinn et al. 1999, 2000), while in the promoter of the Cu transporter encoding *CTR1* gene, the proximal of two analyzed GTAC sites is needed for Cu-dependent regulation (Page et al. 2009). From the three GTAC motives present in the promoter of the *CRD1* gene coding for magnesium-protoporphyrin IX monomethyl ester (oxidative) cyclase, two are required in concert for a significant expression of a reporter

gene under Cu deficiency (Allen et al. 2008), and the same is true for the promoter of the gene encoding the ferredoxin isoform FDX5 (Lambertz et al. 2010). All of the CuREs analyzed so far are also necessary for the induction of CRR1 target genes under anaerobiosis; however, the transcriptional activation of the *CPX1* gene requires an additional GTAC motive, which was therefore termed HyRE (hypoxia response element) (Quinn et al. 2002).

The varying positions and relevance of the GTAC motives show that CRR1 targets are not regulated by exactly the same mechanism. This notion was further supported by ChIP (chromatin immunoprecipitation) and FAIRE (formaldehyde-assisted isolation of regulatory elements) experiments that revealed that Cu deficiency results in changes of the nucleosome occupancy and in histone modifications in the promoters of the three CRR1 target genes *CYC6*, *CPX1*, and *CRD1* (Strenkert et al. 2011). The patterns were consistent with a loosening of the chromatin structure, and significant changes were dependent on the wild-type *CRR1* gene. However, the results were distinct for each target gene and indicated that the DNA of the *CYC6* promoter is tightly packed (and thus essentially inactive) in the non-induced state, while the *CRD1* promoter is rather loosely packed even under non-activating conditions and the status of the *CPX1* promoter is somewhere in between (Strenkert et al. 2011). This fits to transcript level analyses showing that *CYC6* mRNA cannot be detected by RNA hybridization analyses in non-induced cells, whereas low amounts of *CPX1* and *CRD1* can (Merchant et al. 1991; Hill and Merchant 1992; Quinn et al. 2002).

To date, additional putative CRR1 targets have been identified by comparing the transcriptomes of *crr1* mutants with those of the wild type in Cu (Castruita et al. 2011; Blaby-Haas et al. 2016) or O_2 deficiency (Hemschemeier et al. 2013a). Motive-enrichment analyses showed indeed an overrepresentation of GTAC sites upstream of targets in Cu-depleted cells (Castruita et al. 2011). The CRR1 targets in anoxic cells overlap only partially with those of Cu-deficient cells (Hemschemeier et al. 2013a; Blaby-Haas et al. 2016), which might indicate distinct functions of CRR1 under both conditions. However, the target genes remain to be analyzed in detail. Furthermore, while the CRR1 targets mentioned above are essentially all-or-nothing targets that are not activated at all in the *crr1* mutant, there seem to be intermediate responses, too, and those can get easily overlooked in RNA-Seq analyses in which certain cutoffs have to be set.

So far, only one example for such an intermediate response has been analyzed. Notably, this is the *HYDA1* gene, which is induced in Cu-deficient cells, too, resulting in an accumulation of transcript and protein (Castruita et al. 2011; Pape et al. 2012; Hsieh et al. 2013). The involvement of CRR1 in *HYDA1* regulation was discovered by chance in a reporter gene screening for mutants affected in *HYDA1* promoter activation under anoxia (Pape et al. 2012). The thereby identified allelic *crr1* mutant and the *crr1* mutant originally isolated in the lab of Sabeeha Merchant (Eriksson et al. 2004) have about half the amount of *HYDA1* transcripts as well as hydrogenase activity compared to the parental strains (Pape et al. 2012). The *HYDA1* promoter contains two GTAC sites, and a mutation of both is required to reduce reporter gene activity to 50% under hypoxic conditions in the light, while

they appear to have a stronger impact in Cu-deficient cells (Pape et al. 2012). In electrophoretic mobility shift assays, the SBP domain of CRR1 can bind the one GTAC motive tested, and mercury ions inhibit *HYDA1* gene induction (Pape et al. 2012). Mercury probably disturbs the binding of the CRR1 SBP domain to DNA (Sommer et al. 2010) and inhibits the induction of several CRR1 targets (Hill et al. 1991; Quinn et al. 2002). *HYDA1* transcript accumulation is less sensitive to mercury than the *CPX1* gene (Quinn et al. 2002), which is consistent with its partial regulation by CRR1.

To date, the varying responses of CRR1 targets to limitations in Cu or O_2 are not understood. Most probably, CRR1 interacts with other proteins for a fine-tuning of gene regulation. For example, the results regarding the chromatin and histone status mentioned above suggest that CRR1 recruits histone modifying enzymes to its target promoters (Strenkert et al. 2011). The size and architecture of the CRR1 polypeptide make such functions likely. With a length of ca. 80 amino acids, the SBP domain constitutes only a small part of the protein. In its N-terminus, CRR1 has an AHA (*aromatic*, *hydrophobic*, *acidic*) domain which might be involved in transcription transactivation in SBP box transcription factors from Arabidopsis and *Physcomitrella patens* (Riese et al. 2007), but which does not appear to have an essential function in CRR1 (Sommer et al. 2010). C-terminal of the SBP domain, CRR1, and other SBP box factors feature a conserved domain which was termed IRPGC domain according to highly conserved amino acids (Kropat et al. 2005; Riese et al. 2007) and which might be involved in the homodimerization of Arabidopsis SPL7 (Garcia-Molina et al. 2014). The C-terminus of CRR1 contains ankyrin repeats which are often involved in protein-protein interactions (Mosavi et al. 2004). CRR1 without ankyrin repeats restores growth, photosynthetic activity, and *CYC6* expression in the Cu-deficient *crr1* mutant, but not *CYC6* induction in anaerobiosis (Sommer et al. 2010). It is therefore possible that CRR1 needs to form homodimers or to interact with other proteins for *CYC6* induction in anaerobiosis, but not in Cu deficiency. At the very C-terminus of CRR1 lies a Cys-rich domain which has similarities to metallothioneins and the Cu^{1+}-binding domain of metal-responsive transcription factor1 from *Drosophila melanogaster* (Kropat et al. 2005; Sommer et al. 2010). Besides their role in coordinating metal ions, cysteines are also known for their redox-related functions, and some anoxia-responsive sensors indeed make use of the redox properties of Cys residues (Malpica et al. 2006; Bueno et al. 2012). Therefore, the Cys-rich C-terminus of CRR1 is an interesting candidate for both metal and anoxia sensing. Similar to the observations regarding the CRR1 ankyrin repeats, the *crr1* mutant equipped with a CRR1 protein without the Cys-rich C-terminus (termed *crr1*ΔCys) shows restored growth, photosynthesis, and *CYC6* induction in the absence of Cu, but *CYC6* transcript levels do not change in anoxia. Additionally, in contrast to the wild type, this strain does hardly accumulate Cu in O_2 deficiency, but overaccumulates Zn under all conditions tested (Sommer et al. 2010). The comparison of the transcriptomes of dark-anoxic *crr1* mutants, *crr1*ΔCys strains, and the wild type showed that 23 of the anoxic CRR1 targets were not misregulated in *crr1*ΔCys strains, and in contrast to the *crr1* mutant, the cells can grow in an anoxic atmosphere in the light, although not as

well as the wild type (Hemschemeier et al. 2013a). This indicates that the Cys-rich C-terminus of CRR1 plays no essential and/or no O_2-specific role in anoxia. It was discussed that it is rather involved in sensing the Zn status, which is also connected to the Cu availability (see below) (Sommer et al. 2010).

A noteworthy feature of the CRR1-mediated transcriptional response of Chlamydomonas is its inducibility by nickel (Ni) ions. To date, no biological role of Ni is known in the microalga, and its effects are thus probably pharmacological (Quinn et al. 2003; Blaby-Haas et al. 2016). The comparison of the transcriptomes of *CRR1*, *crr1*, and *crr1*ΔCys genotypes under Cu and O_2 deficiency as well as Ni addition revealed that the CRR1-dependent transcriptional response to Ni addition is very similar to that to Cu deficiency, while its overlap with the hypoxia-responsive transcriptome is significantly lower, again hinting to the involvement of different additional factors (Blaby-Haas et al. 2016). Also, the Cys-rich C-terminus of CRR1 seems to be needed for the most part of the Ni response, while its role in the hypoxic response is less pronounced (Hemschemeier et al. 2013a; Blaby-Haas et al. 2016). From their observations, Blaby-Haas et al. (2016) concluded that Ni might interfere with a co-regulator of CRR1, which binds to the Cys-rich region. Based on similarities to mammals, in which Ni inhibits the abovementioned prolyl-4-hydroxylases, whose activity is also compromised by low O_2 levels, it was suggested that this co-regulator might be regulated by prolyl-4-hydroxylases in a similar fashion as HIF1α (Blaby-Haas et al. 2016).

3.2.2 The Role of Coordinated Cu- and O_2-Responsive Gene Expression

RNA-Seq analyses showed that in dark-anoxic Chlamydomonas wild-type cells, the amounts of over 400 transcripts changed at least fourfold (Hemschemeier et al. 2013a), while under Cu deficiency, the amounts of ca. 150 transcripts changed at least twofold (Castruita et al. 2011; Blaby-Haas et al. 2016). This difference indicates that the acclimation to Cu deficiency is less demanding for the cell than that to O_2 deficiency, although the different timescales of the experiments have to be considered. Hemschemeier et al. (2013a) incubated the cells for 6 h while Castruita et al. (2011) incubated them for several days, so the former study might have captured a more transient and the latter study a more stationary transcriptome. Nevertheless, the Chlamydomonas wild type grows undisturbed in the absence of Cu, while it seems to tolerate dark anoxia less well (see above), suggesting that anoxia requires a more drastic acclimation and results in more stress. Indeed, about 800 transcripts change in the Cu-deficient *crr1* mutant, and this higher number compared to the wild type was interpreted to be a stress response (Castruita et al. 2011).

From the 150 transcripts whose amounts change significantly in Cu-deficient cells, 83 were also differentially expressed in dark anoxia, and not all of these were assigned CRR1 targets (Castruita et al. 2011; Hemschemeier et al. 2013a). The biological reason for the coordinated response to Cu and O_2 deficiency in Chlamydomonas is still not known. The most obvious explanation lies in the

chemistry of Cu, which becomes reduced in anoxia and then tends to form insoluble complexes that are hardly bioavailable. It would therefore make sense for an organism to anticipate Cu deficiency in anoxia and vice versa. However, at least in the laboratory, anoxic Chlamydomonas cells accumulate Cu (Sommer et al. 2010) and still produce plastocyanin holoprotein (Quinn et al. 2002), indicating that the cells do not experience intracellular Cu shortage. Still, it seems plausible that the oxidation state of the cellular Cu pool changes under anoxic conditions and that this is registered by the Cu sensor (Quinn et al. 2002). This model is supported by the observations that Cu^{2+} (present in aerobiosis) prevents the CRR1 SBP domain from binding to its target sequence, but Cu^{1+} (probably present in anoxic cells) does not (Sommer et al. 2010).

Another shared experience of Cu-depleted and anoxic cells is probably a change in the overall metal status or its regulation. CRR1 is needed for a proper response to Fe deficiency, probably via the biosynthesis of the Cu-containing ferroxidase FOX1 (La Fontaine et al. 2002; Eriksson et al. 2004; Chen et al. 2008). The responses of Chlamydomonas to Cu and Zn deficiency are interwoven, too. Zn-depleted cells overaccumulate Cu^{1+} in bodies similar to lysosomes, termed cuprosomes, in a CRR1-dependent manner (Hong-Hermesdorf et al. 2014). These cells obviously experience intracellular Cu deficiency, because CYC6 accumulates and the plastocyanin amount decreases (Hong-Hermesdorf et al. 2014). In anoxia, the solubility and thus likely the bioavailability of many metal ions change. For example, Zn and molybdenum, like Cu, are less and manganese and Fe more soluble in low O_2 environments (Anbar 2008). The abundance of several transcripts encoding components of metal assimilation pathways change in dark-anoxic Chlamydomonas cells (Hemschemeier et al. 2013a). Six thereof are also regulated under Cu deficiency, and four (*CTR1* to *CTR3* and the putative Fe transporter-encoding gene *IRT2*) are CRR1 targets. Yet another and, for the time being, speculative explanation for the coordinated response to Cu and O_2 deficiency might be the compromised respiratory activity of both anoxic and Cu-deficient cells. While the former lack the electron acceptor, the latter cannot fully maintain the synthesis of the Cu-containing cytochrome *c* oxidase (Kropat et al. 2015).

In most cases, the physiological function of the enzymes encoded by Cu- and O_2-responsive genes remains elusive in at least one of the two conditions. For example, the cytochrome c_6 encoding *CYC6* transcript accumulates strongly under both conditions (Quinn et al. 2000), but whereas the function of CYC6 as a replacement of plastocyanin under Cu deficiency is clear (Wood 1978; Eriksson et al. 2004), its role in anoxia is not known, especially as anoxia does not result in a degradation of plastocyanin (Moseley et al. 2000; Quinn et al. 2002). Two further well-analyzed examples of coordinate expression under both Cu and O_2 deficiency are the *CPX1* and the *CRD1* genes (Hill and Merchant 1995; Quinn et al. 2000, 2002; Moseley et al. 2002b). CPX1 is an enzyme in the tetrapyrrole biosynthesis pathway, CRD1 is part of the chlorophyll-specific branch, and the catalysis of both enzymes is O_2 dependent. It was suggested that under Cu deficiency, higher amounts of CPX1 would allow the biosynthesis of sufficient amounts of heme for the CYC6 protein. In hypoxia, it might be a strategy to catch the limited O_2

molecules. In yeast, the corresponding gene *HEM13* is also induced in hypoxia, and the HEM13 protein is rate limiting under this condition (Zagorec and Labbe-Bois 1986; Zagorec et al. 1988). In case of CRD1, a physiological function under both Cu and O_2 deficiency has been shown, because *crd1* mutants are chlorotic under both conditions (Moseley et al. 2000, 2002b; Quinn et al. 2002). In Cu-free medium, photosynthetic electron transport of the *crd1* mutant is disturbed, and the amounts of photosystem I (PSI) and light-harvesting complexes (LHC) I and II are strongly reduced (Moseley et al. 2000, 2002b). Notably, *CRD1* is expressed reciprocally to the *CTH1* gene, encoding an isoform that shares 67% identical amino acids with CRD1 (Moseley et al. 2002b), but basal amounts of *CRD1* transcript are also detected under standard growth conditions (in the presence of Cu and O_2), and the CRD1 protein has a constitutive function. Low-temperature (77K) chlorophyll fluorescence emission spectra and isolation and characterization of PSI complexes indicate that in *crd1* mutants, the LHCI antennae are permanently uncoupled from PSI (Moseley et al. 2002a, b). Because of the similarity of the photosynthetic apparatus of the *crd1* mutant in full medium to that of the wild type under Fe deficiency, it was hypothesized that the CRD1 enzyme, which belongs to the class of diiron-carboxylate proteins, plays a role in sensing the Fe status and transmits this signal via chlorophyll biosynthesis and the PSI subunit PsaK to the PSI-LHCI complex (Moseley et al. 2002a). Why higher amounts of CRD1 are needed when Cu and O_2 are limited is not known. A mutant deficient for light-dependent protochlorophyllide reductase that has a similarly reduced chlorophyll concentration as the Cu- or O_2-deficient *crd1* mutant does not exhibit a disturbed chlorophyll fluorescence pattern in Cu-free medium (Moseley et al. 2000). A *crd1* suppressor strain in which, contrary to the wild type, the CTH1 protein is present in the absence of Cu and O_2, is not chlorotic under these conditions, but 77K chlorophyll fluorescence spectra are still different from those of the wild type (Moseley et al. 2002b). These results indicate that CRD1 and CTH1 do not solely function as chlorophyll biosynthetic enzymes but that they have other, only partially overlapping roles.

As noted above, one of the shared targets of Cu and O_2 deficiency is the *HYDA1* gene. Notably, further genes encoding (O_2-intolerant) enzymes known to be involved in the anoxic metabolism of Chlamydomonas are induced on the transcript and/or protein level in fully aerated Cu-deficient cells, such as the [FeFe]-hydrogenase maturases HydEF and HydG, PFR, PFL1, or PAT2 (Castruita et al. 2011; Hsieh et al. 2013). Although this has not been analyzed yet, it is unlikely that the extremely O_2-sensitive HydA1 (Stripp et al. 2009) is active in aerated Cu-deficient cells, unless there are protective mechanisms. The physiological role of Cu- and O_2-responsive genes becomes even more puzzling in view of recent results about the ferredoxin encoding *FDX5* gene. The gene is strongly induced in anoxia and Cu deficiency (Mus et al. 2007; Jacobs et al. 2009; Terauchi et al. 2009; Lambertz et al. 2010) and is a CRR1 target (Lambertz et al. 2010; Castruita et al. 2011; Hemschemeier et al. 2013a). Fdx5 is a plant-type [2Fe2S]-ferredoxin located in the chloroplast (Jacobs et al. 2009; Terashima et al. 2010; Yang et al. 2015). In in vitro enzyme assays, Fdx5 does not mediate NADPH photoproduction via

ferredoxin-$NADP^+$ reductase, H_2 production via HydA1, or pyruvate oxidation via PFR (Jacobs et al. 2009; Noth et al. 2013; Peden et al. 2013; van Lis et al. 2013). However, it seems to play a major and essential role under dark-oxic conditions, probably as an electron donor to fatty acid desaturases (Yang et al. 2015). This raises the question as to why the gene is so strongly induced by a lack of Cu and O_2. Several fatty acid desaturase transcripts are induced upon Cu limitations or anoxia, some of them CRR1 dependently (Castruita et al. 2011; Hemschemeier et al. 2013a). In Cu-deficient cells, the induction of fatty acid desaturase genes is accompanied by an increased desaturation level of several fatty acids in the wild type but not in the *crr1* mutant, and it was discussed that Cu-deficient cells need to restructure their membranes (Castruita et al. 2011). In contrast, the general desaturation status of the fatty acids in anoxic cells does not change significantly (Hemschemeier et al. 2013a). This might be interpreted in a way that anoxic cells also attempt to restructure their membrane fatty acid profile but cannot do so because of the absence of the reactant O_2, or that the O_2-dependent fatty acid desaturases are induced as a compensatory measure to catch the few available O_2 molecules, or that the cells prepare for reoxygenation. The *FDX5* gene, because of its close physiological connection to fatty acid desaturases (Yang et al. 2015), might be regulated due to the same reasons.

3.3 *Potential Mechanisms of Indirect O_2 Sensing in Chlamydomonas*

Roughly 10% of the transcriptional changes in dark-anoxic cells were assigned CRR1 targets, showing that additional signal transduction pathways must be present (Hemschemeier et al. 2013a). The (direct or indirect) O_2 sensors or transcription factors involved are not known yet, but in the following, several stimuli that are plausible based on observations in dark-anoxic Chlamydomonas cells are discussed (Fig. 3).

Metabolic signals can be concluded from the studies of Chlamydomonas mutants deficient for individual fermentative enzymes. In Chlamydomonas *pfl1* mutants, some transcripts encoding fermentative enzymes accumulate differentially compared to the wild type, especially *HYDA1* and *PFR* (Philipps et al. 2011; Catalanotti et al. 2012). The mechanism behind this phenomenon is not known. A regulatory role of formate as known from *E. coli* (Sawers 2005) is certainly possible, although externally added formate does not restore *HYDA1* expression in Chlamydomonas (Philipps et al. 2011) and the alga does not have a homologue of the *E. coli* formate-binding transcription factor FhlA. In the *hydef* (de facto hydrogenase) mutant that, in contrast to the wild type, secretes succinate under anoxic conditions, the amounts of several transcripts are different from those in the wild type, too, such as *PFR*, *PFL1*, and *MME4* (Dubini et al. 2009). Several genes are also differentially expressed in an *adh1* mutant, especially the *PFR* gene (Magneschi et al. 2012).

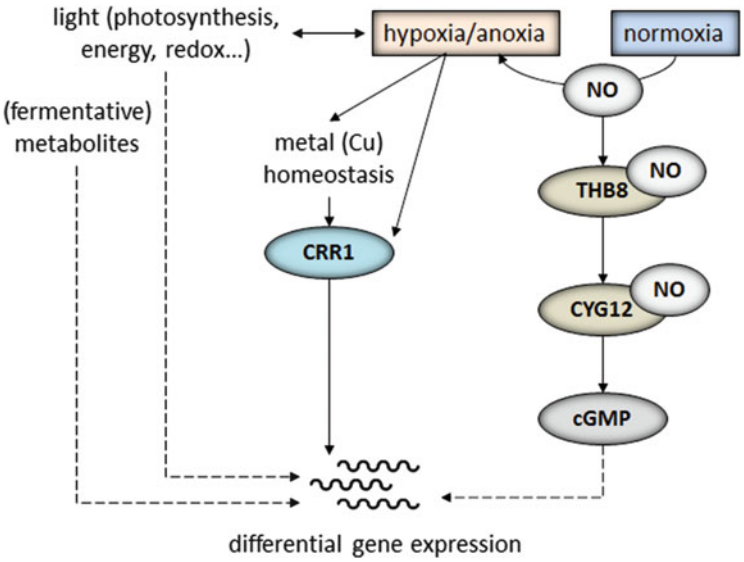

Fig. 3 Schematic overview on possible ways of O_2 sensing and signaling in Chlamydomonas that are discussed in the text. Except for the known role of CRR1, the depicted processes and pathways are deduced from mutant phenotypes or physiological observations and remain to be confirmed and understood in molecular detail, respectively

Although the nature of the responsible signals remains to be elucidated, it is possible that they originate from changes in the energy, redox, or metabolite status (Fig. 3).

In a eukaryotic photosynthetic organism, signals originating in the plastid are well known to influence gene expression, such as intermediates of tetrapyrrole and/or chlorophyll biosynthesis, metabolites, the redox state, or ROS (Fey et al. 2005; Kleine et al. 2009; Duanmu et al. 2013; Erickson et al. 2015). In Arabidopsis, the gene regulatory responses to darkness, sucrose starvation, or anoxia indeed overlap (Branco-Price et al. 2008; Schröder et al. 2011; Juntawong and Bailey-Serres 2012). In dark-anoxic Chlamydomonas cells, the amounts of several "photosynthetic transcripts" in the widest sense decrease, such as transcripts coding for chlorophyll-binding proteins, chlorophyll biosynthetic enzymes, or components of the carbon-concentrating mechanism (CCM) (Hemschemeier et al. 2013a). However, many "photosynthetic transcripts" are generally lower in darkness, independent from the presence or absence of O_2, indicating that not anoxia but darkness (or any metabolic consequence of the absence of light) is the stimulus (Duanmu et al. 2013; Hemschemeier et al. 2013a; Zones et al. 2015). Notably, several anoxia-responsive transcripts such as *HYDA1*, *HYDA2*, *HYDEF*, and *HYDG* accumulate transiently in cells transferred to darkness in the presence of O_2, but their amounts decrease again upon prolonged dark-oxic incubation (Hemschemeier et al. 2013a). Additional studies showed that *HYDA1* and *HYDA2* (and further "fermentative") transcript amounts are higher in dark- versus light-incubated cells (Duanmu et al. 2013), and a diel rhythm in synchronized cells

can be observed (Whitney et al. 2011; Zones et al. 2015). However, it is not known whether the genes are regulated by the circadian clock. Because the effect of darkness is also seen in not synchronized cells (Duanmu et al. 2013; Hemschemeier et al. 2013a), it is well possible that the photosynthetic activity and the resulting O_2 content of the cells (Whitney et al. 2011) influence the expression of "anaerobic genes". Experiments that utilized the PSII inhibitor 3-(3,4-dichlorophenyl)-1,1-dimethylurea (DCMU) to test the effect of a sudden drop of photosynthetic O_2 evolution resulted in mixed responses depending on the target gene analyzed. While the *HYDA1*, *HYDEF*, and *PFR* transcripts did not significantly respond to DCMU treatment of Chlamydomonas in the light and still responded to darkness, other dark-responsive transcripts (e.g., of genes putatively involved in amino acid catabolism) were strongly induced by DCMU in the light (Hemschemeier et al. 2013a). This suggests that different stimuli are responsible for the dark-induced accumulation of different subsets of transcripts, such as the relative O_2 content, the redox potential, or the carbohydrate or energy status (Fig. 3). The Chlamydomonas *HYDA1* gene can be induced in aerobic cells by adding the monothiol reductant β-mercaptoethanol to the cells (Hemschemeier et al. 2013a), HydA1 amounts are lower in the anaerobic response 1 (*anr1*)-deficient mutant impaired in cyclic electron flow under anoxic conditions (Terashima et al. 2012), and *HYDA1* transcript levels are lower in dark-anoxic starchless mutants deficient for isoamylase (STA7) or ADP-glucose pyrophosphorylase (STA6) (Posewitz et al. 2004b). Other signals emerging from the photosynthetic apparatus influence HydA1 on the level of the absolute enzymatic activity (i.e., the maximal enzymatic activity detectable in the cells, for example, by proton/deuterium (H/D) isotope exchange measurements (Jouanneau et al. 1980) which is independent from physiological electron supply). Usually, this maximum activity follows the transcript and protein amounts (Happe et al. 1994; Forestier et al. 2003). H/D exchange activity is hardly detectable in the dark-anoxic *sta6* mutant, consistent with the transcript data shown by Posewitz et al. (2004b), but reaches significant values under anoxia in the light (Chochois et al. 2009). In contrast, the H/D exchange activity of the anoxic wild type is rather similar in the dark or in the light. DCMU has no significant effect on hydrogenase enzyme activity, while an inhibitor of the cytochrome b_6f complex (2,5-dibromo-3-methyl-6-isopropyl-*p*-benzoquinone (DBMIB)) as well as the uncoupler carbonyl cyanide-*p*-trifluoromethoxyphenylhydrazone (FCCP) result in strongly reduced H/D exchange activity. It was therefore discussed that the proton gradient which results from cyclic electron flow is involved in the regulation of the synthesis or stabilization of active hydrogenase (Chochois et al. 2009).

Hypothetically, the alga might also employ pathways involved in retrograde plastid-to-nucleus signaling under dark anoxia. Signals emerging from tetrapyrrole metabolism are implied to result in differential expression of nuclear genes (Duanmu et al. 2013; Brzezowski et al. 2015). Tetrapyrrole biosynthesis and/or degradation involve several O_2-dependent steps which are probably impaired in hypoxia. For example, bilin was reported to play a role in retrograde signaling in

Chlamydomonas, and its synthesis from heme is catalyzed by the O_2-dependent enzyme heme oxygenase (Duanmu et al. 2013).

3.4 Nitric Oxide as a Second Messenger

While with the exception of CRR1, the components of O_2 sensing and signaling in Chlamydomonas are as yet unknown, a role of nitric oxide (NO) as a second messenger is emerging. The NO molecule, a gas and free radical, is a ubiquitous product of many enzymatic and chemical reactions within a cell (Blokhina and Fagerstedt 2010; Stern and Zhu 2014). In higher concentrations, NO is toxic, and it is indeed generated by activated macrophages as part of the pathogen defense (Fang 2004; Stern and Zhu 2014). However, it is also employed as a signaling molecule, and NO-dependent processes in animals include neuronal communication, vasodilation, and the immune response (Bryan et al. 2009). According to ongoing research, it appears that NO is employed in signaling pathways in all organism groups (Besson-Bard et al. 2008; Poyton et al. 2009; Moreau et al. 2010; Baudouin 2011; Baudouin and Hancock 2014; Stern and Zhu 2014). It is therefore not surprising that it also plays important roles in Chlamydomonas. The responses of the alga to Cu stress and Fe starvation appear to involve NO-regulated processes (Zhang et al. 2008; Liping et al. 2013). Upon nitrogen starvation, the cytochrome b_6f complex of Chlamydomonas is degraded in a regulated process which also involves NO (Wei et al. 2014). Especially well analyzed is the role of NO in regulating nitrate assimilation in the microalga (de Montaigu et al. 2010; Sanz-Luque et al. 2013, 2015), and it also plays a role in the hypoxic or anoxic response of Chlamydomonas (see below). As is the case in plants (Baudouin and Hancock 2014), the molecular mechanisms of NO signaling in Chlamydomonas are in most cases not understood, with the exception of emerging details on NO production and detoxification in the context of nitrate assimilation (see below).

3.4.1 NO Signaling in Animals and Plants

In the context of the well-studied "classical" NO-signaling pathway in animals (Martínez-Ruiz et al. 2011), NO synthases (NOSs) produce NO in an NADPH- and O_2-dependent reaction from L-arginine (Arg), which is converted to L-citrulline (Daff 2010; Santolini 2011). Two of the three NOSs of mammals are regulated by calcium (Ca^{2+}) and calmodulin (Daff 2010). Additional relevant NO sources in animals are nitrate and nitrite (Lundberg et al. 2008; Lundberg and Weitzberg 2010), which can be converted to NO nonenzymatically or enzymatically, the latter, for example, by hemoglobins (Cosby et al. 2003; Rassaf et al. 2007). Important mediators of NO signaling in animals are the soluble guanylate cyclases (sGCs), also termed heme/NO-binding guanylate cyclases (Bryan et al. 2009; Martínez-Ruiz et al. 2011). In mammals, sGCs are usually αβ-heterodimers sharing one

N-terminal heme group. The heterodimerization of α- and β-monomers is obligatory in most cases, because individual heme-binding or catalytically essential residues are contributed from only one monomer (Derbyshire and Marletta 2012). An exception is the rat β2-subunit, which contains all essential residues within its monomer sequence and can form functional homodimers (Koglin et al. 2001; Derbyshire and Marletta 2012). The basic principle of sGC-mediated signaling is the stimulation of guanylate cyclase activity by the binding of NO to the heme group and possibly additional sites of the enzyme (Fernhoff et al. 2009; Derbyshire and Marletta 2012; Underbakke et al. 2014). The cyclic guanosine monophosphate (cGMP) produced by sGCs acts as the downstream second messenger and influences mostly cGMP-dependent protein kinases and cGMP-dependent phosphodiesterases (PDEs) as well as cGMP-gated ion channels (Lucas et al. 2000; Hofmann 2005; Bryan et al. 2009). PDEs are also responsible for removing cGMP. NO can also directly, or after reaction with ROS, in the form of a reactive nitrogen species (RNS) perform regulatory roles. For example, NO is a competitive inhibitor of the respiratory cytochrome *c* oxidase and thereby influences the mitochondrial metabolism which can result in higher ROS production or an increased AMP:ATP ratio (Erusalimsky and Moncada 2007). An important regulatory role of NO is conveyed through posttranslational modifications of proteins, mostly in the form of Cys *S*-nitrosylation or tyrosine nitration (Hess et al. 2005; Abello et al. 2009; Martínez-Ruiz et al. 2011; Nakamura and Lipton 2013).

The number of reports about NO-dependent acclimatory processes in plants has increased over the years, indicating that the plant employs NO signaling under various conditions and throughout its life cycle (Perazzolli et al. 2006; Hebelstrup et al. 2013; Baudouin and Hancock 2014; Domingos et al. 2015). Plant NO signaling shares similarities with that in animals in that, for example, cross talk with other second messengers (Ca^{2+}, cGMP) or protein *S*-nitrosylation occurs (Besson-Bard et al. 2008; Courtois et al. 2008; Astier et al. 2012). However, NOSs have not been identified in plants yet (Jeandroz et al. 2016). Arg-dependent NO production sensitive to pharmaceuticals interfering with animal NOSs such as L-NAME (Nω-nitro-L-arginine methyl ester) has been reported to occur in plants (Gas et al. 2009; Gupta et al. 2011); however, these observations might be due to other Arg-dependent pathways (Planchet and Kaiser 2006; Besson-Bard et al. 2008; Winter et al. 2015). For example, polyamines, whose synthesis requires Arg, are involved in NO production (Tun et al. 2006; Wimalasekera et al. 2011). An important source for NO in plants is nitrite, which can be converted to NO chemically and by various enzymes such as nitrate reductase, plasma membrane-bound nitrite-NO reductase, xanthine oxidoreductase, cytochrome *c* oxidase, or hemoglobins (Stöhr and Stremlau 2006; Wilson et al. 2008; Gupta et al. 2011; Gupta and Igamberdiev 2011; Tiso et al. 2012). To date, no homologues to animal sGCs have been detected in plants, although pattern-matching searches have identified some Arabidopsis proteins putatively having sGC-like functions (Mulaudzi et al. 2011; Domingos et al. 2015). It is possible that posttranslational modifications through NO play major roles in plants (Serpa et al. 2007; Tada et al. 2008; Baudouin 2011; Astier et al. 2012; Astier and Lindermayr 2012; Tavares et al. 2014).

3.4.2 NO Signaling in Chlamydomonas

NO signaling in Chlamydomonas appears to employ both plant and animal strategies (Fig. 4). Although some algal species contain NOS homologues, Chlamydomonas is not among those (Jeandroz et al. 2016). However, in contrast to plants, the microalga contains six genes encoding sGC homologues (de Montaigu et al. 2010). The deduced polypeptides each contain all amino acid residues described in Derbyshire and Marletta (2012) to be important for heme-binding and catalytic activity (de Montaigu et al. 2010; plus own alignments and manual inspection), indicating that they can function as homodimers. The isoform Cre16.g688901 (de Montaigu et al. 2010) and the cyclase domain of the Chlamydomonas CYG12 protein (Winger et al. 2008) are indeed catalytically active in the homodimeric form. The role of NO in the regulation of nitrate assimilation in Chlamydomonas is the best analyzed, and the involvement of an sGC, cGMP, and Ca^{2+} in this process was shown (de Montaigu et al. 2010; Sanz-Luque et al. 2013, 2015; Chamizo-Ampudia et al. 2016). The NO-dependent signaling pathway was discovered through a screen for ammonium-insensitive mutants which, in contrast to the wild type, express genes of the nitrate assimilation pathway in the presence of ammonium (de Montaigu et al. 2010). In one

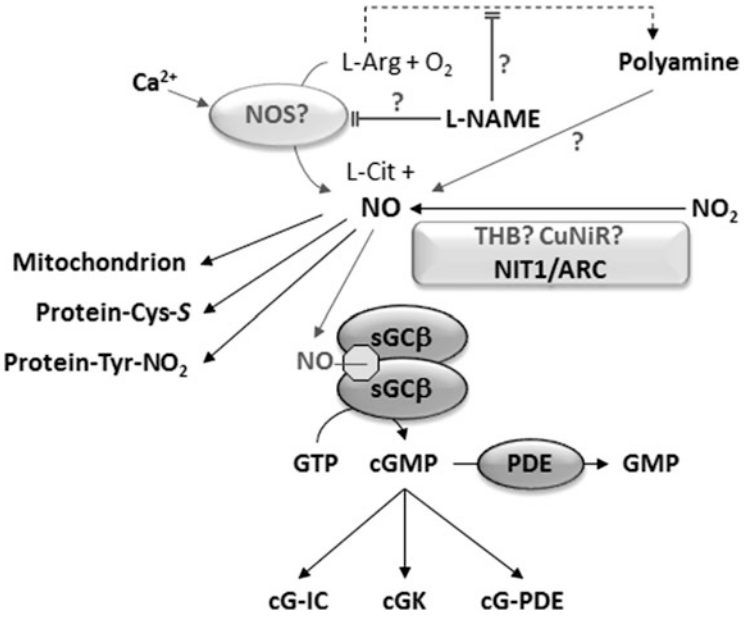

Fig. 4 Overview on putative NO production and signaling pathways in Chlamydomonas in the context of the known pathways in animals. Details are explained in the text. *ARC* amidoxime reducing component, *cG-IC* cGMP-gated ion channel, *cGK* cGMP-dependent kinase, *(cG-)PDE* (cGMP-dependent) phosphodiesterase, *CuNiR* Cu-binding nitrite NO reductase, *L-Cit* L-citrulline, *L-NAME* Nω-nitro-L-arginine methyl ester, *NOS* NO synthase, *THB* truncated hemoglobin

mutant, a gene coding for a putative sGC is affected (*Cre16.g688901*; note that the gene was formerly known as *CYG56*, but in the current genome version, another protein containing an adenylate/guanylate cyclase domain, Cre13.g603350, is termed CYG56). The phenotype of the mutant is consistent with analyses of the Chlamydomonas wild type, in which NO and cGMP accumulate in conditions of ammonium repression (de Montaigu et al. 2010), and in which NO donors, cGMP analogues, and PDE inhibitors result in the repression of the nitrate reductase (NIT1)-encoding gene in the absence of ammonium, whereas sGC inhibitors or an NO scavenger result in its derepression in the presence of ammonium (de Montaigu et al. 2010). NO also regulates ammonium and nitrate assimilation sGC- and cGMP-independently (Sanz-Luque et al. 2013). The high-affinity transport of ammonium, nitrate, and nitrite as well as NIT1 activity are rapidly and reversibly inhibited by the external addition of an NO donor, a process independent from inhibitors of sGCs or PDEs (Sanz-Luque et al. 2013). Here, NO appears to act through posttranslational modification, possibly *S*-nitrosylation, which is a process also occurring in Chlamydomonas as shown by its *S*-nitrosoproteome (Morisse et al. 2014). Notably, the inhibitory effect of NO on NIT1 was only observed in whole Chlamydomonas cells, but not in cell extracts, not in *E. coli* cells heterologously synthesizing NIT1, and not in the purified enzyme (Sanz-Luque et al. 2013). This indicates that the putative posttranslational modification by NO is mediated by organism-specific cellular structures. Because NO signaling is ubiquitous and involved in different acclimatory processes in most organisms, there must be means of providing specificity to the NO signal, for example, by spatiotemporal patterns, protein-protein interactions, and cross talks with other molecules or conditions (Kone et al. 2003; Hess et al. 2005; Anand and Stamler 2012; Nakamura and Lipton 2013).

In Chlamydomonas as in plants, no NOS was identified yet, so that other chemical or enzymatic reactions must be responsible for NO production. Similar to plants, nitrate reductase seems to be a major source of NO. Nitrite and NIT1-dependent NO production was shown (Sakihama et al. 2002), and very recently it was revealed that the molybdoenzyme amidoxime reducing component (ARC) is involved in this process (Chamizo-Ampudia et al. 2016) (Fig. 4). Like its homologue in humans, Chlamydomonas ARC can be reduced by cytochrome b_5 and an associated reductase (Chamizo-Ampudia et al. 2011), but also by the diaphorase domain of NIT1, allowing NO production from nitrite (Chamizo-Ampudia et al. 2016). In plants, both nitrate reductase-dependent and -independent processes have been described (Baudouin 2011; Fröhlich and Durner 2011), and this probably applies to Chlamydomonas, too, because NO-dependent processes have been reported for Chlamydomonas *nit1* mutants (Hemschemeier et al. 2013b; Liping et al. 2013; Wei et al. 2014). The ammonium-induced repression of *NIT1* can be mimicked by Ca^{2+} ionophores (see above: certain animal NOSs are activated by calmodulin), whereas L-NAME relieves ammonium repression. Additionally, Ca^{2+} ionophores induce and L-NAME impairs NO accumulation within the algal cells (de Montaigu et al. 2010). This suggests (a) Ca^{2+}-sensitive, Arg-dependent pathway (s) as reported for plants.

3.4.3 NO Signaling in the Anaerobic Response of Chlamydomonas

The acclimation of Chlamydomonas to anoxic conditions also involves NO-dependent processes. In the presence of the chemical NO scavenger PTIO (2-phenyl-4,4,5,5-tetramethylimidazoline-1-oxyl 3-oxide), growth of the wild type in an anoxic but not in an aerobic atmosphere in the light is strongly impaired, and the *HYDA1* and *HYDA2* transcripts accumulate in aerobic cells treated with an NO donor (Hemschemeier et al. 2013b). Additionally, the amounts of two sGC-encoding transcripts, *CYG11* (*Cre07.g320700*) and *CYG12* (*Cre07.g320750*), increase in dark-anoxic *C. reinhardtii* cells (Hemschemeier et al. 2013a).

Details on the putative NO-dependent hypoxic signaling pathway remain to be elucidated. The experiments in anoxia were conducted with a Chlamydomonas strain (CC-124) that has a *nit1 nit2* genetic background and is thus deficient for NIT1 and the central regulator of the nitrate regulon, NIT2 (Camargo et al. 2007). The mechanism of NO production under this condition (or in this strain) must therefore be different from the NIT1-ARC system described above. Similarly, the involvement of NO in the degradation of the cytochrome b_6f complex was observed in *nit1* mutants, however, by comparing Chlamydomonas strains with different genetic backgrounds regarding nitrate and nitrite reductase activity, nitrite as the NO source was proposed (Wei et al. 2014). Although speculative for the time being, one might think of several routes. Given an intracellular source of nitrite, its reduction to NO might occur by hemoglobins (see below) or by ERM3 (Cre08.g360550), a homologue of Cu-binding nitrite reductases from bacteria and fungi whose transcript accumulates in dark-anoxic Chlamydomonas cells (Hemschemeier et al. 2013a). The observed effect of L-NAME on the regulation of nitrate assimilation (de Montaigu et al. 2010) suggests other Arg-dependent pathways. For example, NO generation from polyamines, involving amine oxidases, was reported for Arabidopsis (Tun et al. 2006; Wimalasekera et al. 2011, 2015). Transcripts for two flavin containing and one Cu amine oxidase (*AOF1*, *AOF2*, *AMX2*) accumulate in dark-anoxic Chlamydomonas cultures (Hemschemeier et al. 2013a). Also, a scenario can be envisioned in which the above described ARC component reduces intracellular nitrite utilizing cytochrome b_5 instead of NIT1 as the reducing partner. In the Chlamydomonas CC-124 *nit1 nit2* strain, the transcripts encoding cytochrome b_5-1 (Cre16.g659350) and cytochrome b_5 reductase (CBR1, Cre03.g145547) determined by Chamizo-Ampudia et al. (2011), to reduce ARC, are present at reasonably high levels (Hemschemeier et al. 2013a).

Not least, hemoglobins might be involved in the (anoxic) NO metabolism of Chlamydomonas. The microalga contains 12 genes coding for so-called truncated hemoglobins (THBs) (Vinogradov et al. 2011; Hemschemeier et al. 2013b). THBs feature a truncated version of the three-helices-on-three-helices (3/3)-fold of the "classical" hemoglobins and myoglobins that results in an overall two-helices-on-two-helices (2/2)-fold (Lecomte et al. 2005; Nardini et al. 2007; Johnson and Lecomte 2013; Pesce et al. 2013). Hemoglobins are widespread and found in every kingdom (Vinogradov et al. 2011, 2013a, b; Vázquez-Limón et al. 2012).

Although the first and probably best studied hemoglobins are the O_2 transporting hemoglobins and myoglobins, hemoglobins are recognized today as versatile proteins that fulfil various functions as enzymes or sensors (Hoy and Hargrove 2008; Vinogradov and Moens 2008; Reeder 2010; Martínková et al. 2013). Several enzymatic activities of hemoglobins involve nitrogen compounds, such as NO dioxygenation, reduction of hydroxylamine and peroxynitrite, and nitrite to NO reduction (Gladwin et al. 2003; Gardner 2005; Ascenzi et al. 2008, 2009; De Marinis et al. 2009; Sturms et al. 2011a, b). Notably, many hemoglobins are capable of catalyzing various reactions in vitro, so that their in vivo function cannot directly be inferred from biochemical analyses. Different reaction kinetics and affinities, however, can give clues. For example, the class 1 nonsymbiotic 3/3 hemoglobins of plants usually have very high affinities and very low dissociation constants for O_2, making their function as O_2 transport proteins unlikely (Hoy and Hargrove 2008; Smagghe et al. 2009). The function of a hemoglobin can additionally change depending on the environment or on protein partners. For example, animal hemoglobin and myoglobin can reduce nitrite to NO under hypoxic conditions (Cosby et al. 2003; Rassaf et al. 2007; Totzeck et al. 2012). The NO dioxygenase activity of hemoglobins requires a reducing system that converts the heme group, which is left oxidized after catalysis, back to the reactive reduced form (Smagghe et al. 2008). Some, but not all hemoglobins, can be directly reduced by NADPH or $FADH_2$ (Perazzolli et al. 2004; Sainz et al. 2013).

In Chlamydomonas, no 3/3 hemoglobins have been identified yet, which is in contrast to plants which often contain both 3/3 hemoglobins and THBs (Vázquez-Limón et al. 2012). The high number of *THB* genes in Chlamydomonas is rather unusual, although some protists and *Caenorhabditis elegans* have also numerous hemoglobin-encoding genes (Hoogewijs et al. 2004; Tilleman et al. 2011; Vinogradov et al. 2013a). The domain architecture of the annotated Chlamydomonas THBs indicates additional functions of the proteins, because most of them have considerably elongated N- or C-termini with so far unknown roles (Vinogradov et al. 2011; Hemschemeier et al. 2013b; Huwald et al. 2015). To date, only two of the genes have been studied on the physiological level, *THB1* and *Cre16.g661200* [termed *THB8* in Hemschemeier et al. (2013b)]. THB1, which is the shortest of all Chlamydomonas hemoglobins, has been analyzed most extensively and is well characterized biochemically and structurally (Johnson and Lecomte 2013, 2014; Johnson et al. 2014; Ciaccio et al. 2015; Rice et al. 2015). Transcript and protein levels are high only in Chlamydomonas strains that possess the global nitrate assimilation regulator NIT2 and that are cultivated in the presence of nitrate (Johnson et al. 2014; Sanz-Luque et al. 2015). *THB1* transcript levels can be further enhanced by treating the cells with NO (Sanz-Luque et al. 2015), and the protein has NO dioxygenase activity (Johnson et al. 2014; Sanz-Luque et al. 2015). Notably, the diaphorase domain of NIT1 is able to reduce THB1 so that in vitro, several cycles of NO dioxygenation are possible (Sanz-Luque et al. 2015). Probably by abstracting electrons, THB1 protein reduces NIT1 activity in cell extracts, and in strains with posttranscriptionally reduced *THB1* transcript amounts, NIT1 activity is inversely proportional to *THB1* transcript levels (Sanz-Luque et al. 2015). A dual

function of THB1 in both NO detoxification and modulation of NIT1 activity was therefore proposed, forming a kind of feedback loop, in which the accumulation of nitrite (e.g., due to low photosynthetic activity) would cause an NO burst, which in turn would result in electron abstraction from NIT1 through THB1 and thus in lower nitrite levels (Sanz-Luque et al. 2015).

Cre16.g661200 (*THB8*) is strongly upregulated in dark-anoxic Chlamydomonas cells and plays a vital role for the anoxic acclimation of the alga. Strains in which the *THB8* gene is posttranscriptionally downregulated do hardly grow in an anoxic atmosphere in the light (Hemschemeier et al. 2013b). The function of the THB8 protein is yet unknown. In view of the effects of NO on anoxic growth and expression of "anaerobic genes" in Chlamydomonas in addition to the observation that applying the NO scavenger PTIO to the *THB8* knockdown strains prevented their anoxic growth completely, it was postulated that THB8 might be involved in an NO-dependent signaling pathway. Since also externally added NO did not rescue the anoxic growth of the knockdown strains, and because treating the recombinant THB8 protein with NO resulted in spectra consistent with protein nitrosylation, it was suggested that THB8 might function as an NO carrier (or transnitrosylase) (Hemschemeier et al. 2013b). The *THB8* knockdown strains also showed aberrant transcript amounts of some anoxia-responsive genes, among those the *CYG12* gene that encodes one of the sGCs of Chlamydomonas (Hemschemeier et al. 2013b). Though speculative for the time being, this might indicate a feedback loop between two genes that are most probably both involved in an NO-dependent process.

Whether further THBs play a role in the acclimation of Chlamydomonas to hypoxia or anoxia remains to be elucidated. Several additional *THB* genes are transcriptionally upregulated in dark-anoxic but also in dark-oxic algae (Hemschemeier et al. 2013a; Huwald et al. 2015). Although only about half of the THBs of Chlamydomonas have been analyzed and most of them only in vitro, the observations so far indicate that their functions are not redundant. This is apparent in Chlamydomonas knockdown transformants that show a clear phenotype (Hemschemeier et al. 2013b; Sanz-Luque et al. 2015), but is also suggested by differences in their biochemistry and structure (Johnson et al. 2014; Ciaccio et al. 2015; Huwald et al. 2015; Rice et al. 2015). Hemoglobins are good candidates for playing roles in the hypoxic or anoxic metabolism. NO metabolism is a plausible scenario in view of the numerous reports on NO chemistry catalyzed by hemoglobins also in plants, where they are supposed to act as NO scavengers and to modulate NO levels in signaling cascades (Perazzolli et al. 2006; Hill 2012; Hebelstrup et al. 2013). Because NO dioxygenation consumes electrons, NO scavenging under hypoxic conditions would also contribute to the redox balance (Igamberdiev and Hill 2004). Chlamydomonas THB1, THB2, and THB4 have nitrite reductase activity in vitro (Ciaccio et al. 2015), so they might be responsible for nitrite-dependent NO production. Certainly, a function in O_2 concentration or transport as reported for bacterial hemoglobins (Stark et al. 2011; Davidge and Dikshit 2013) but also for plant nonsymbiotic hemoglobins (Vigeolas et al. 2011) is possible. Hemoglobins might even function as O_2 scavengers and protect the O_2-labile fermentative enzymes of Chlamydomonas in the natural habitat, which is probably rather hypoxic

than completely anoxic. A further possibility is O_2 sensing, although the extensions of Chlamydomonas THBs do not show the typical domains of globin-coupled sensors such as kinases or cyclases (Martínková et al. 2013).

3.5 Conclusions and Outlook

Research on the anoxic metabolism of Chlamydomonas has revealed many details on its remarkable complexity and flexibility. However, just as many and more questions remain. For example, most enzymes of the fermentative metabolism remain poorly characterized, and it is not known how the observed flexibility of fermentative pathways is regulated. Additional metabolic acclimation strategies such as the utilization of fermenting substrates other than starch are just emerging to be revealed, and little is known about the cross talks between the organelles in which fermentative enzymes have been detected. Also the players and mechanisms of O_2 sensing and signaling are largely unknown to date. In view of the long history of research on Chlamydomonas and the tools available for its analysis and manipulation, the alga is well suited for the analysis of anoxic signaling strategies, despite or perhaps precisely because of its particularities that make Chlamydomonas an organism somewhere in between animals, plants, and bacteria. Apart from being a model, the adaptable alga is in itself a fascinating organism, and new insights into its (dark) anoxic metabolism and its regulation will not least result in a deeper understanding of ecosystems which are dependent on healthy O_2 producers.

References

Abello N, Kerstjens HA, Postma DS, Bischoff R (2009) Protein tyrosine nitration: selectivity, physicochemical and biological consequences, denitration, and proteomics methods for the identification of tyrosine-nitrated proteins. J Proteome Res 8:3222–3238

Allen MD, Kropat J, Merchant SS (2008) Regulation and localization of isoforms of the aerobic oxidative cyclase in *Chlamydomonas reinhardtii*. Photochem Photobiol 84:1336–1342

Amend JP, Shock EL (2001) Energetics of overall metabolic reactions of thermophilic and hyperthermophilic Archaea and bacteria. FEMS Microbiol Rev 25:175–243

Anand P, Stamler JS (2012) Enzymatic mechanisms regulating protein S-nitrosylation: implications in health and disease. J Mol Med (Berl) 90:233–244

Anbar AD (2008) Oceans. Elements and evolution. Science 322:1481–1483

Ansell R, Granath K, Hohmann S, Thevelein JM, Adler L (1997) The two isoenzymes for yeast NAD^+-dependent glycerol 3-phosphate dehydrogenase encoded by *GPD1* and *GPD2* have distinct roles in osmoadaptation and redox regulation. EMBO J 16:2179–2187

Ascenzi P, De Marinis E, Coletta M, Visca P (2008) H_2O_2 and NO scavenging by *Mycobacterium leprae* truncated hemoglobin O. Biochem Biophys Res Commun 373:197–201

Ascenzi P, De Marinis E, Visca P, Ciaccio C, Coletta M (2009) Peroxynitrite detoxification by ferryl *Mycobacterium leprae* truncated hemoglobin O. Biochem Biophys Res Commun 380:392–396

Astier J, Lindermayr C (2012) Nitric oxide-dependent posttranslational modification in plants: an update. Int J Mol Sci 13:15193–15208

Astier J, Kulik A, Koen E, Besson-Bard A, Bourque S, Jeandroz S, Lamotte O, Wendehenne D (2012) Protein S-nitrosylation: what's going on in plants? Free Radic Biol Med 53:1101–1110

Atteia A, van Lis R, Gelius-Dietrich G, Adrait A, Garin J, Joyard J, Rolland N, Martin W (2006) Pyruvate formate-lyase and a novel route of eukaryotic ATP synthesis in *Chlamydomonas* mitochondria. J Biol Chem 281:9909–9918

Atteia A, Adrait A, Brugière S, Tardif M, van Lis R, Deusch O, Dagan T, Kuhn L, Gontero B, Martin W, Garin J, Joyard J, Rolland N (2009) A proteomic survey of *Chlamydomonas reinhardtii* mitochondria sheds new light on the metabolic plasticity of the organelle and on the nature of the α-proteobacterial mitochondrial ancestor. Mol Biol Evol 26:1533–1548

Atteia A, van Lis R, Tielens AG, Martin WF (2013) Anaerobic energy metabolism in unicellular photosynthetic eukaryotes. Biochim Biophys Acta 1827:210–223

Bailey-Serres J, Voesenek LA (2008) Flooding stress: acclimations and genetic diversity. Annu Rev Plant Biol 59:313–339

Bailey-Serres J, Fukao T, Gibbs DJ, Holdsworth MJ, Lee SC, Licausi F, Perata P, Voesenek LA, van Dongen JT (2012) Making sense of low oxygen sensing. Trends Plant Sci 17:129–138

Batyrova KA, Tsygankov AA, Kosourov SN (2012) Sustained hydrogen photoproduction by phosphorus-deprived *Chlamydomonas reinhardtii* cultures. Int J Hydrog Energy 37:8834–8839

Baudouin E (2011) The language of nitric oxide signalling. Plant Biol (Stuttg) 13:233–242

Baudouin E, Hancock J (2014) Nitric oxide signalling in plants. Front Plant Sci 4:553

Bekker A, Holland HD, Wang PL, Rumble D III, Stein HJ, Hannah JL, Coetzee LL, Beukes NJ (2004) Dating the rise of atmospheric oxygen. Nature 427:117–120

Besson-Bard A, Pugin A, Wendehenne D (2008) New insights into nitric oxide signaling in plants. Annu Rev Plant Biol 59:21–39

Bien CM, Espenshade PJ (2010) Sterol regulatory element binding proteins in fungi: hypoxic transcription factors linked to pathogenesis. Eukaryot Cell 9:352–359

Birkenbihl RP, Jach G, Saedler H, Huijser P (2005) Functional dissection of the plant-specific SBP-domain: overlap of the DNA-binding and nuclear localization domains. J Mol Biol 352:585–596

Blaby IK, Blaby-Haas CE, Tourasse N, Hom EF, Lopez D, Aksoy M, Grossman A, Umen J, Dutcher S, Porter M, King S, Witman GB, Stanke M, Harris EH, Goodstein D, Grimwood J, Schmutz J, Vallon O, Merchant SS, Prochnik S (2014) The *Chlamydomonas* genome project: a decade on. Trends Plant Sci 19:672–680

Blaby-Haas CE, Castruita M, Fitz-Gibbon ST, Kropat J, Merchant SS (2016) Ni induces the CRR1-dependent regulon revealing overlap and distinction between hypoxia and Cu deficiency responses in *Chlamydomonas reinhardtii*. Metallomics 8(7):679–691. doi:10.1039/c1036mt00063k

Blokhina O, Fagerstedt KV (2010) Oxidative metabolism, ROS and NO under oxygen deprivation. Plant Physiol Biochem 48:359–373

Branco-Price C, Kaiser KA, Jang CJ, Larive CK, Bailey-Serres J (2008) Selective mRNA translation coordinates energetic and metabolic adjustments to cellular oxygen deprivation and reoxygenation in *Arabidopsis thaliana*. Plant J 56:743–755

Bruchhaus I, Tannich E (1994) Purification and molecular characterization of the NAD^+-dependent acetaldehyde/alcohol dehydrogenase from *Entamoeba histolytica*. Biochem J 303:743–748

Bryan NS, Bian K, Murad F (2009) Discovery of the nitric oxide signaling pathway and targets for drug development. Front Biosci 14:1–18

Brzezowski P, Richter AS, Grimm B (2015) Regulation and function of tetrapyrrole biosynthesis in plants and algae. Biochim Biophys Acta 1847:968–985

Bueno E, Mesa S, Bedmar EJ, Richardson DJ, Delgado MJ (2012) Bacterial adaptation of respiration from oxic to microoxic and anoxic conditions: redox control. Antioxid Redox Signal 16:819–852

Buick R (2008) When did oxygenic photosynthesis evolve? Philos Trans R Soc Lond Ser B Biol Sci 363:2731–2743

Buis JM, Broderick JB (2005) Pyruvate formate-lyase activating enzyme: elucidation of a novel mechanism for glycyl radical formation. Arch Biochem Biophys 433:288–296

Burgess SJ, Tredwell G, Molnàr A, Bundy JG, Nixon PJ (2012) Artificial microRNA-mediated knockdown of pyruvate formate lyase (PFL1) provides evidence for an active 3-hydroxybutyrate production pathway in the green alga *Chlamydomonas reinhardtii*. J Biotechnol 162:57–66

Burgess SJ, Taha H, Yeoman JA, Iamshanova O, Chan KX, Boehm M, Behrends V, Bundy JG, Bialek W, Murray JW, Nixon PJ (2016) Identification of the elusive pyruvate reductase of *Chlamydomonas reinhardtii* chloroplasts. Plant Cell Physiol 57:82–94

Butler G (2013) Hypoxia and gene expression in eukaryotic microbes. Annu Rev Microbiol 67:291–312

Cabiscol E, Aguilar J, Ros J (1994) Metal-catalyzed oxidation of Fe^{2+} dehydrogenases. Consensus target sequence between propanediol oxidoreductase of *Escherichia coli* and alcohol dehydrogenase II of *Zymomonas mobilis*. J Biol Chem 269:6592–6597

Camargo A, Llamas A, Schnell RA, Higuera JJ, González-Ballester D, Lefebvre PA, Fernández E, Galván A (2007) Nitrate signaling by the regulatory gene *NIT2* in *Chlamydomonas*. Plant Cell 19:3491–3503

Castruita M, Casero D, Karpowicz SJ, Kropat J, Vieler A, Hsieh SI, Yan W, Cokus S, Loo JA, Benning C, Pellegrini M, Merchant SS (2011) Systems biology approach in *Chlamydomonas* reveals connections between copper nutrition and multiple metabolic steps. Plant Cell 23:1273–1292

Catalanotti C, Dubini A, Subramanian V, Yang W, Magneschi L, Mus F, Seibert M, Posewitz MC, Grossman AR (2012) Altered fermentative metabolism in *Chlamydomonas reinhardtii* mutants lacking pyruvate formate lyase and both pyruvate formate lyase and alcohol dehydrogenase. Plant Cell 24:692–707

Catalanotti C, Yang W, Posewitz MC, Grossman AR (2013) Fermentation metabolism and its evolution in algae. Front Plant Sci 4:150

Chabrière E, Charon MH, Volbeda A, Pieulle L, Hatchikian EC, Fontecilla-Camps JC (1999) Crystal structures of the key anaerobic enzyme pyruvate:ferredoxin oxidoreductase, free and in complex with pyruvate. Nat Struct Biol 6:182–190

Chamizo-Ampudia A, Galván A, Fernández E, Llamas A (2011) The *Chlamydomonas reinhardtii* molybdenum cofactor enzyme crARC has a Zn-dependent activity and protein partners similar to those of its human homologue. Eukaryot Cell 10:1270–1282

Chamizo-Ampudia A, Sanz-Luque E, Llamas A, Ocaña-Calahorro F, Mariscal V, Carreras A, Barroso JB, Galván A, Fernández E (2016) A dual system formed by the ARC and NR molybdoenzymes mediates nitrite-dependent NO production in *Chlamydomonas*. Plant Cell Environ 39(10):2097–2107. doi:10.1111/pce.12739

Chen JC, Hsieh SI, Kropat J, Merchant SS (2008) A ferroxidase encoded by *FOX1* contributes to iron assimilation under conditions of poor iron nutrition in *Chlamydomonas*. Eukaryot Cell 7:541–545

Chochois V, Dauvillée D, Beyly A, Tolleter D, Cuiné S, Timpano H, Ball S, Cournac L, Peltier G (2009) Hydrogen production in *Chlamydomonas*: photosystem II-dependent and -independent pathways differ in their requirement for starch metabolism. Plant Physiol 151:631–640

Chochois V, Constans L, Dauvillée D, Beyly A, Solivérès M, Ball S, Peltier G, Cournac L (2010) Relationships between PSII-independent hydrogen bioproduction and starch metabolism as evidenced from isolation of starch catabolism mutants in the green alga *Chlamydomonas reinhardtii*. Int J Hydrog Energy 35:10731–10740

Ciaccio C, Ocaña-Calahorro F, Droghetti E, Tundo GR, Sanz-Luque E, Polticelli F, Visca P, Smulevich G, Ascenzi P, Coletta M (2015) Functional and spectroscopic characterization of *Chlamydomonas reinhardtii* truncated hemoglobins. PLoS One 10:e0125005

Cosby K, Partovi KS, Crawford JH, Patel RP, Reiter CD, Martyr S, Yang BK, Waclawiw MA, Zalos G, Xu X, Huang KT, Shields H, Kim-Shapiro DB, Schechter AN, Cannon RO III, Gladwin MT (2003) Nitrite reduction to nitric oxide by deoxyhemoglobin vasodilates the human circulation. Nat Med 9:1498–1505

Courtois C, Besson A, Dahan J, Bourque S, Dobrowolska G, Pugin A, Wendehenne D (2008) Nitric oxide signalling in plants: interplays with Ca^{2+} and protein kinases. J Exp Bot 59:155–163

Daff S (2010) NO synthase: structures and mechanisms. Nitric Oxide 23:1–11

Davidge KS, Dikshit KL (2013) Haemoglobins of Mycobacteria: structural features and biological functions. Adv Microb Physiol 63:147–194

De Marinis E, Casella L, Ciaccio C, Coletta M, Visca P, Ascenzi P (2009) Catalytic peroxidation of nitrogen monoxide and peroxynitrite by globins. IUBMB Life 61:62–73

de Montaigu A, Sanz-Luque E, Gálvan A, Fernández E (2010) A soluble guanylate cyclase mediates negative signaling by ammonium on expression of nitrate reductase in *Chlamydomonas*. Plant Cell 22:1532–1548

Derbyshire ER, Marletta MA (2012) Structure and regulation of soluble guanylate cyclase. Annu Rev Biochem 81:533–559

Dietz KJ, Vogel MO, Viehhauser A (2010) AP2/EREBP transcription factors are part of gene regulatory networks and integrate metabolic, hormonal and environmental signals in stress acclimation and retrograde signalling. Protoplasma 245:3–14

Domingos P, Prado AM, Wong A, Gehring C, Feijo JA (2015) Nitric oxide: a multitasked signaling gas in plants. Mol Plant 8:506–520

Drew MC (1997) Oxygen deficiency and root metabolism: injury and acclimation under hypoxia and anoxia. Annu Rev Plant Physiol Plant Mol Biol 48:223–250

Duanmu D, Casero D, Dent RM, Gallaher S, Yang W, Rockwell NC, Martin SS, Pellegrini M, Niyogi KK, Merchant SS, Grossman AR, Lagarias JC (2013) Retrograde bilin signaling enables *Chlamydomonas* greening and phototrophic survival. Proc Natl Acad Sci U S A 110:3621–3626

Dubini A, Ghirardi ML (2015) Engineering photosynthetic organisms for the production of biohydrogen. Photosynth Res 123:241–253

Dubini A, Mus F, Seibert M, Grossman AR, Posewitz MC (2009) Flexibility in anaerobic metabolism as revealed in a mutant of *Chlamydomonas reinhardtii* lacking hydrogenase activity. J Biol Chem 284:7201–7213

Echave P, Tamarit J, Cabiscol E, Ros J (2003) Novel antioxidant role of alcohol dehydrogenase E from *Escherichia coli*. J Biol Chem 278:30193–30198

Erickson E, Wakao S, Niyogi KK (2015) Light stress and photoprotection in *Chlamydomonas reinhardtii*. Plant J 82:449–465

Eriksson M, Moseley JL, Tottey S, Del Campo JA, Quinn J, Kim Y, Merchant S (2004) Genetic dissection of nutritional copper signaling in *Chlamydomonas* distinguishes regulatory and target genes. Genetics 168:795–807

Erusalimsky JD, Moncada S (2007) Nitric oxide and mitochondrial signaling: from physiology to pathophysiology. Arterioscler Thromb Vasc Biol 27:2524–2531

Fábián Z, Taylor CT, Nguyen LK (2016) Understanding complexity in the HIF signaling pathway using systems biology and mathematical modeling. J Mol Med (Berl) 94:377–390

Falkowski PG, Katz ME, Milligan AJ, Fennel K, Cramer BS, Aubry MP, Berner RA, Novacek MJ, Zapol WM (2005) The rise of oxygen over the past 205 million years and the evolution of large placental mammals. Science 309:2202–2204

Fang FC (2004) Antimicrobial reactive oxygen and nitrogen species: concepts and controversies. Nat Rev Microbiol 2:820–832

Fernhoff NB, Derbyshire ER, Marletta MA (2009) A nitric oxide/cysteine interaction mediates the activation of soluble guanylate cyclase. Proc Natl Acad Sci U S A 106:21602–21607

Fey V, Wagner R, Bräutigam K, Pfannschmidt T (2005) Photosynthetic redox control of nuclear gene expression. J Exp Bot 56:1491–1498

Flowers JM, Hazzouri KM, Pham GM, Rosas U, Bahmani T, Khraiwesh B, Nelson DR, Jijakli K, Abdrabu R, Harris EH, Lefebvre PA, Hom EF, Salehi-Ashtiani K, Purugganan MD (2015) Whole-genome resequencing reveals extensive natural variation in the model green alga *Chlamydomonas reinhardtii*. Plant Cell 27:2353–2369

Forestier M, King P, Zhang LP, Posewitz M, Schwarzer S, Happe T, Ghirardi ML, Seibert M (2003) Expression of two [Fe]-hydrogenases in *Chlamydomonas reinhardtii* under anaerobic conditions. Eur J Biochem 270:2750–2758

Fröhlich A, Durner J (2011) The hunt for plant nitric oxide synthase (NOS): is one really needed? Plant Sci 181:401–404

Fukao T, Bailey-Serres J (2004) Plant responses to hypoxia – is survival a balancing act? Trends Plant Sci 9:449–456

Fukuda E, Kino H, Matsuzawa H, Wakagi T (2001) Role of a highly conserved YPITP motif in 2-oxoacid: ferredoxin oxidoreductase: heterologous expression of the gene from *Sulfolobus* sp. strain 7, and characterization of the recombinant and variant enzymes. Eur J Biochem 268:5639–5646

Gallaher SD, Fitz-Gibbon ST, Glaesener AG, Pellegrini M, Merchant SS (2015) *Chlamydomonas* genome resource for laboratory strains reveals a mosaic of sequence variation, identifies true strain histories, and enables strain-specific studies. Plant Cell 27:2335–2352

Garcia-Molina A, Xing S, Huijser P (2014) Functional characterisation of Arabidopsis SPL7 conserved protein domains suggests novel regulatory mechanisms in the Cu deficiency response. BMC Plant Biol 14:231

Gardner PR (2005) Nitric oxide dioxygenase function and mechanism of flavohemoglobin, hemoglobin, myoglobin and their associated reductases. J Inorg Biochem 99:247–266

Gas E, Flores-Pérez U, Sauret-Güeto S, Rodríguez-Concepción M (2009) Hunting for plant nitric oxide synthase provides new evidence of a central role for plastids in nitric oxide metabolism. Plant Cell 21:18–23

Gfeller RP, Gibbs M (1984) Fermentative metabolism of *Chlamydomonas reinhardtii*: I. Analysis of fermentative products from starch in dark and light. Plant Physiol 75:212–218

Ghysels B, Godaux D, Matagne RF, Cardol P, Franck F (2013) Function of the chloroplast hydrogenase in the microalga *Chlamydomonas*: the role of hydrogenase and state transitions during photosynthetic activation in anaerobiosis. PLoS One 8:e64161

Ginger ML, Fritz-Laylin LK, Fulton C, Cande WZ, Dawson SC (2010) Intermediary metabolism in protists: a sequence-based view of facultative anaerobic metabolism in evolutionarily diverse eukaryotes. Protist 161:642–671

Gladwin MT, Lancaster JR Jr, Freeman BA, Schechter AN (2003) Nitric oxide's reactions with hemoglobin: a view through the SNO-storm. Nat Med 9:496–500

Godaux D, Bailleul B, Berne N, Cardol P (2015) Induction of photosynthetic carbon fixation in anoxia relies on hydrogenase activity and proton-gradient regulation-like1-mediated cyclic electron flow in *Chlamydomonas reinhardtii*. Plant Physiol 168:648–658

Goldblatt C, Lenton TM, Watson AJ (2006) Bistability of atmospheric oxygen and the great oxidation. Nature 443:683–686

Goldfine H (1965) The evolution of oxygen as a biosynthetic reagent. J Gen Physiol 49 (Suppl):253–274

Graves DA, Spradlin GM, Greenbaum E (1990) Effect of oxygen on photoautotrophic and heterotrophic growth of *Chlamydomonas reinhardtii* in an anoxic atmosphere. Photochem Photobiol 52:585–590

Green J, Rolfe MD, Smith LJ (2014) Transcriptional regulation of bacterial virulence gene expression by molecular oxygen and nitric oxide. Virulence 5:794–809

Gupta KJ, Igamberdiev AU (2011) The anoxic plant mitochondrion as a nitrite: NO reductase. Mitochondrion 11:537–543

Gupta KJ, Fernie AR, Kaiser WM, van Dongen JT (2011) On the origins of nitric oxide. Trends Plant Sci 16:160–168

Halliwell B (2006) Reactive species and antioxidants. Redox biology is a fundamental theme of aerobic life. Plant Physiol 141:312–322

Hammond DJ, Aman RA, Wang CC (1985) The role of compartmentation and glycerol kinase in the synthesis of ATP within the glycosome of *Trypanosoma brucei*. J Biol Chem 260:15646–15654

Happe T, Kaminski A (2002) Differential regulation of the Fe-hydrogenase during anaerobic adaptation in the green alga *Chlamydomonas reinhardtii*. Eur J Biochem 269:1022–1032

Happe T, Mosler B, Naber JD (1994) Induction, localization and metal content of hydrogenase in the green alga *Chlamydomonas reinhardtii*. Eur J Biochem 222:769–774

Harris EH (2001) *Chlamydomonas* as a model organism. Annu Rev Plant Physiol Plant Mol Biol 52:363–406

Hebelstrup KH, Shah JK, Igamberdiev AU (2013) The role of nitric oxide and hemoglobin in plant development and morphogenesis. Physiol Plant 148:457–469

Hedges SB, Blair JE, Venturi ML, Shoe JL (2004) A molecular timescale of eukaryote evolution and the rise of complex multicellular life. BMC Evol Biol 4:2

Hemschemeier A (2013) Photo-bleaching of *Chlamydomonas reinhardtii* after dark-anoxic incubation. Plant Signal Behav 8(11):e27263

Hemschemeier A, Happe T (2011) Alternative photosynthetic electron transport pathways during anaerobiosis in the green alga *Chlamydomonas reinhardtii*. Biochim Biophys Acta 1807:919–926

Hemschemeier A, Jacobs J, Happe T (2008) Biochemical and physiological characterization of the pyruvate formate-lyase Pfl1 of *Chlamydomonas reinhardtii*, a typically bacterial enzyme in a eukaryotic alga. Eukaryot Cell 7:518–526

Hemschemeier A, Casero D, Liu B, Benning C, Pellegrini M, Happe T, Merchant SS (2013a) Copper response regulator1-dependent and -independent responses of the *Chlamydomonas reinhardtii* transcriptome to dark anoxia. Plant Cell 25:3186–3211

Hemschemeier A, Düner M, Casero D, Merchant SS, Winkler M, Happe T (2013b) Hypoxic survival requires a 2-on-2 hemoglobin in a process involving nitric oxide. Proc Natl Acad Sci U S A 110:10854–10859

Hess DT, Matsumoto A, Kim SO, Marshall HE, Stamler JS (2005) Protein *S*-nitrosylation: purview and parameters. Nat Rev Mol Cell Biol 6:150–166

Hill RD (2012) Non-symbiotic haemoglobins – what's happening beyond nitric oxide scavenging? AoB Plants 2012:pls004

Hill KL, Merchant S (1992) In vivo competition between plastocyanin and a copper-dependent regulator of the *Chlamydomonas reinhardtii* cytochrome c_6 gene. Plant Physiol 100:319–326

Hill KL, Merchant S (1995) Coordinate expression of coproporphyrinogen oxidase and cytochrome c_6 in the green alga *Chlamydomonas reinhardtii* in response to changes in copper availability. EMBO J 14:857–865

Hill KL, Li HH, Singer J, Merchant S (1991) Isolation and structural characterization of the *Chlamydomonas reinhardtii* gene for cytochrome c_6. Analysis of the kinetics and metal specificity of its copper-responsive expression. J Biol Chem 266:15060–15067

Hofmann F (2005) The biology of cyclic GMP-dependent protein kinases. J Biol Chem 280:1–4

Höhner R, Barth J, Magneschi L, Jaeger D, Niehues A, Bald T, Grossman A, Fufezan C, Hippler M (2013) The metabolic status drives acclimation of iron deficiency responses in *Chlamydomonas reinhardtii* as revealed by proteomics based hierarchical clustering and reverse genetics. Mol Cell Proteomics 12:2774–2790

Hon T, Dodd A, Dirmeier R, Gorman N, Sinclair PR, Zhang L, Poyton RO (2003) A mechanism of oxygen sensing in yeast. Multiple oxygen-responsive steps in the heme biosynthetic pathway affect Hap1 activity. J Biol Chem 278:50771–50780

Hong-Hermesdorf A, Miethke M, Gallaher SD, Kropat J, Dodani SC, Chan J, Barupala D, Domaille DW, Shirasaki DI, Loo JA, Weber PK, Pett-Ridge J, Stemmler TL, Chang CJ, Merchant SS (2014) Subcellular metal imaging identifies dynamic sites of Cu accumulation in *Chlamydomonas*. Nat Chem Biol 10:1034–1042

Hoogewijs D, Geuens E, Dewilde S, Moens L, Vierstraete A, Vinogradov S, Vanfleteren J (2004) Genome-wide analysis of the globin gene family of *C. elegans*. IUBMB Life 56:697–702

Hörtensteiner S, Kräutler B (2011) Chlorophyll breakdown in higher plants. Biochim Biophys Acta 1807:977–988

Hoy JA, Hargrove MS (2008) The structure and function of plant hemoglobins. Plant Physiol Biochem 46:371–379

Hsieh SI, Castruita M, Malasarn D, Urzica E, Erde J, Page MD, Yamasaki H, Casero D, Pellegrini M, Merchant SS, Loo JA (2013) The proteome of copper, iron, zinc, and manganese micronutrient deficiency in *Chlamydomonas reinhardtii*. Mol Cell Proteomics 12:65–86

Hug LA, Stechmann A, Roger AJ (2010) Phylogenetic distributions and histories of proteins involved in anaerobic pyruvate metabolism in eukaryotes. Mol Biol Evol 27:311–324

Hughes AL, Todd BL, Espenshade PJ (2005) SREBP pathway responds to sterols and functions as an oxygen sensor in fission yeast. Cell 120:831–842

Husic DW, Tolbert NE (1985) Anaerobic formation of D-lactate and partial purification and characterization of a pyruvate reductase from *Chlamydomonas reinhardtii*. Plant Physiol 78:277–284

Huwald D, Schrapers P, Kositzki R, Haumann M, Hemschemeier A (2015) Characterization of unusual truncated hemoglobins of *Chlamydomonas reinhardtii* suggests specialized functions. Planta 242:167–185

Igamberdiev AU, Hill RD (2004) Nitrate, NO and haemoglobin in plant adaptation to hypoxia: an alternative to classic fermentation pathways. J Exp Bot 55:2473–2482

Imlay JA (2006) Iron-sulphur clusters and the problem with oxygen. Mol Microbiol 59:1073–1082

Jacobs J, Pudollek S, Hemschemeier A, Happe T (2009) A novel, anaerobically induced ferredoxin in *Chlamydomonas reinhardtii*. FEBS Lett 583:325–329

Jang H, Ehrenreich IM (2012) Genome-wide characterization of genetic variation in the unicellular, green alga *Chlamydomonas reinhardtii*. PLoS One 7:e41307

Jeandroz S, Wipf D, Stuehr DJ, Lamattina L, Melkonian M, Tian Z, Zhu Y, Carpenter EJ, Wong GK, Wendehenne D (2016) Occurrence, structure, and evolution of nitric oxide synthase-like proteins in the plant kingdom. Sci Signal 9:re2

Johnson EA, Lecomte JT (2013) The globins of cyanobacteria and algae. Adv Microb Physiol 63:195–272

Johnson EA, Lecomte JT (2014) Characterization of the truncated hemoglobin THB1 from protein extracts of *Chlamydomonas reinhardtii*. F1000Res 3:294

Johnson EA, Rice SL, Preimesberger MR, Nye DB, Gilevicius L, Wenke BB, Brown JM, Witman GB, Lecomte JT (2014) Characterization of THB1, a *Chlamydomonas reinhardtii* truncated hemoglobin: linkage to nitrogen metabolism and identification of lysine as the distal heme ligand. Biochemistry (Mosc) 53:4573–4589

Jouanneau Y, Kelley BC, Berlier Y, Lespinat PA, Vignais PM (1980) Continuous monitoring, by mass spectrometry, of H_2 production and recycling in *Rhodopseudomonas capsulata*. J Bacteriol 143:628–636

Juntawong P, Bailey-Serres J (2012) Dynamic light regulation of translation status in *Arabidopsis thaliana*. Front Plant Sci 3:66

Kessler D, Leibrecht I, Knappe J (1991) Pyruvate-formate-lyase-deactivase and acetyl-CoA reductase activities of *Escherichia coli* reside on a polymeric protein particle encoded by *adhE*. FEBS Lett 281:59–63

Kleine T, Voigt C, Leister D (2009) Plastid signalling to the nucleus: messengers still lost in the mists? Trends Genet 25:185–192

Knappe J, Neugebauer FA, Blaschkowski HP, Gänzler M (1984) Post-translational activation introduces a free radical into pyruvate formate-lyase. Proc Natl Acad Sci U S A 81:1332–1335

Koglin M, Vehse K, Budaeus L, Scholz H, Behrends S (2001) Nitric oxide activates the β_2 subunit of soluble guanylyl cyclase in the absence of a second subunit. J Biol Chem 276:30737–30743

Kone BC, Kuncewicz T, Zhang W, Yu ZY (2003) Protein interactions with nitric oxide synthases: controlling the right time, the right place, and the right amount of nitric oxide. Am J Physiol Renal Physiol 285:F178–F190

Kreuzberg K (1984) Starch fermentation via a formate producing pathway in *Chlamydomonas reinhardii*, *Chlorogonium elongatum* and *Chlorella fusca*. Physiol Plant 61:87–94

Kreuzberg K, Klöck G, Grobheiser D (1987) Subcellular distribution of pyruvate-degrading enzymes in *Chlamydomonas reinhardtii* studied by an improved protoplast fractionation procedure. Physiol Plant 69:481–488

Kropat J, Tottey S, Birkenbihl RP, Depege N, Huijser P, Merchant S (2005) A regulator of nutritional copper signaling in *Chlamydomonas* is an SBP domain protein that recognizes the GTAC core of copper response element. Proc Natl Acad Sci U S A 102:18730–18735

Kropat J, Gallaher SD, Urzica EI, Nakamoto SS, Strenkert D, Tottey S, Mason AZ, Merchant SS (2015) Copper economy in *Chlamydomonas*: prioritized allocation and reallocation of copper to respiration vs. photosynthesis. Proc Natl Acad Sci U S A 112:2644–2651

La Fontaine S, Quinn JM, Nakamoto SS, Page MD, Gohre V, Moseley JL, Kropat J, Merchant S (2002) Copper-dependent iron assimilation pathway in the model photosynthetic eukaryote *Chlamydomonas reinhardtii*. Eukaryot Cell 1:736–757

Lambertz C, Hemschemeier A, Happe T (2010) Anaerobic expression of the ferredoxin-encoding *FDX5* gene of *Chlamydomonas reinhardtii* is regulated by the Crr1 transcription factor. Eukaryot Cell 9:1747–1754

Lecomte JT, Vuletich DA, Lesk AM (2005) Structural divergence and distant relationships in proteins: evolution of the globins. Curr Opin Struct Biol 15:290–301

Lee CYS, Stewart EV, Hughes BT, Espenshade PJ (2009) Oxygen-dependent binding of Nro1 to the prolyl hydroxylase Ofd1 regulates SREBP degradation in yeast. EMBO J 28:135–143

Liang X, Nazarenus TJ, Stone JM (2008) Identification of a consensus DNA-binding site for the *Arabidopsis thaliana* SBP domain transcription factor, AtSPL14, and binding kinetics by surface plasmon resonance. Biochemistry (Mosc) 47:3645–3653

Liping Z, Hongbo S, Xiaohua L, Zhaopu L (2013) Gene regulation of iron-deficiency responses is associated with carbon monoxide and heme oxydase 1 in *Chlamydomonas reinhardtii*. PLoS One 8:e53835

Lucas KA, Pitari GM, Kazerounian S, Ruiz-Stewart I, Park J, Schulz S, Chepenik KP, Waldman SA (2000) Guanylyl cyclases and signaling by cyclic GMP. Pharmacol Rev 52:375–414

Lundberg JO, Weitzberg E (2010) NO-synthase independent NO generation in mammals. Biochem Biophys Res Commun 396:39–45

Lundberg JO, Weitzberg E, Gladwin MT (2008) The nitrate-nitrite-nitric oxide pathway in physiology and therapeutics. Nat Rev Drug Discov 7:156–167

Lyons TW (2007) Palaeoclimate: oxygen's rise reduced. Nature 448:1005–1006

Magneschi L, Catalanotti C, Subramanian V, Dubini A, Yang W, Mus F, Posewitz MC, Seibert M, Perata P, Grossman AR (2012) A mutant in the *ADH1* gene of *Chlamydomonas reinhardtii* elicits metabolic restructuring during anaerobiosis. Plant Physiol 158:1293–1305

Makiuchi T, Nozaki T (2014) Highly divergent mitochondrion-related organelles in anaerobic parasitic protozoa. Biochimie 100:3–17

Malpica R, Sandoval GR, Rodriguez C, Franco B, Georgellis D (2006) Signaling by the arc two-component system provides a link between the redox state of the quinone pool and gene expression. Antioxid Redox Signal 8:781–795

Martínez-Ruiz A, Cadenas S, Lamas S (2011) Nitric oxide signaling: classical, less classical, and nonclassical mechanisms. Free Radic Biol Med 51:17–29

Martínková M, Kitanishi K, Shimizu T (2013) Heme-based globin-coupled oxygen sensors: linking oxygen binding to functional regulation of diguanylate cyclase, histidine kinase, and methyl-accepting chemotaxis. J Biol Chem 288:27702–27711

Meinecke B, Bertram J, Gottschalk G (1989) Purification and characterization of the pyruvate-ferredoxin oxidoreductase from *Clostridium acetobutylicum*. Arch Microbiol 152:244–250

Melis A, Zhang L, Forestier M, Ghirardi ML, Seibert M (2000) Sustained photobiological hydrogen gas production upon reversible inactivation of oxygen evolution in the green alga *Chlamydomonas reinhardtii*. Plant Physiol 122:127–136

Mense SM, Zhang L (2006) Heme: a versatile signaling molecule controlling the activities of diverse regulators ranging from transcription factors to MAP kinases. Cell Res 16:681–692

Merchant S, Bogorad L (1986) Regulation by copper of the expression of plastocyanin and cytochrome c_{552} in *Chlamydomonas reinhardtii*. Mol Cell Biol 6:462–469

Merchant S, Hill K, Howe G (1991) Dynamic interplay between two copper-titrating components in the transcriptional regulation of cyt *c6*. EMBO J 10:1383–1389

Moreau M, Lindermayr C, Durner J, Klessig DF (2010) NO synthesis and signaling in plants – where do we stand? Physiol Plant 138:372–383

Morisse S, Zaffagnini M, Gao XH, Lemaire SD, Marchand CH (2014) Insight into Protein S-nitrosylation in *Chlamydomonas reinhardtii*. Antioxid Redox Signal 21:1271–1284

Mosavi LK, Cammett TJ, Desrosiers DC, Peng ZY (2004) The ankyrin repeat as molecular architecture for protein recognition. Protein Sci 13:1435–1448

Moseley J, Quinn J, Eriksson M, Merchant S (2000) The *Crd1* gene encodes a putative di-iron enzyme required for photosystem I accumulation in copper deficiency and hypoxia in *Chlamydomonas reinhardtii*. EMBO J 19:2139–2151

Moseley JL, Allinger T, Herzog S, Hoerth P, Wehinger E, Merchant S, Hippler M (2002a) Adaptation to Fe-deficiency requires remodeling of the photosynthetic apparatus. EMBO J 21:6709–6720

Moseley JL, Page MD, Alder NP, Eriksson M, Quinn J, Soto F, Theg SM, Hippler M, Merchant S (2002b) Reciprocal expression of two candidate di-iron enzymes affecting photosystem I and light-harvesting complex accumulation. Plant Cell 14:673–688

Mulaudzi T, Ludidi N, Ruzvidzo O, Morse M, Hendricks N, Iwuoha E, Gehring C (2011) Identification of a novel *Arabidopsis thaliana* nitric oxide-binding molecule with guanylate cyclase activity *in vitro*. FEBS Lett 585:2693–2697

Müller M, Mentel M, van Hellemond JJ, Henze K, Woehle C, Gould SB, Yu RY, van der Giezen M, Tielens AG, Martin WF (2012) Biochemistry and evolution of anaerobic energy metabolism in eukaryotes. Microbiol Mol Biol Rev 76:444–495

Murthy UM, Wecker MS, Posewitz MC, Gilles-Gonzalez MA, Ghirardi ML (2012) Novel FixL homologues in *Chlamydomonas reinhardtii* bind heme and O_2. FEBS Lett 586:4282–4288

Mus F, Dubini A, Seibert M, Posewitz MC, Grossman AR (2007) Anaerobic acclimation in *Chlamydomonas reinhardtii*: anoxic gene expression, hydrogenase induction, and metabolic pathways. J Biol Chem 282:25475–25486

Mustroph A, Lee SC, Oosumi T, Zanetti ME, Yang H, Ma K, Yaghoubi-Masihi A, Fukao T, Bailey-Serres J (2010) Cross-kingdom comparison of transcriptomic adjustments to low-oxygen stress highlights conserved and plant-specific responses. Plant Physiol 152:1484–1500

Nakamura T, Lipton SA (2013) Emerging role of protein-protein transnitrosylation in cell signaling pathways. Antioxid Redox Signal 18:239–249

Nardini M, Pesce A, Milani M, Bolognesi M (2007) Protein fold and structure in the truncated (2/2) globin family. Gene 398:2–11

Noth J, Krawietz D, Hemschemeier A, Happe T (2013) Pyruvate: ferredoxin oxidoreductase is coupled to light-independent hydrogen production in *Chlamydomonas reinhardtii*. J Biol Chem 288:4368–4377

Page MD, Kropat J, Hamel PP, Merchant SS (2009) Two *Chlamydomonas* CTR copper transporters with a novel Cys-Met motif are localized to the plasma membrane and function in copper assimilation. Plant Cell 21:928–943

Påhlman AK, Granath K, Ansell R, Hohmann S, Adler L (2001) The yeast glycerol 3-phosphatases Gpp1p and Gpp2p are required for glycerol biosynthesis and differentially involved in the cellular responses to osmotic, anaerobic, and oxidative stress. J Biol Chem 276:3555–3563

Pape M, Lambertz C, Happe T, Hemschemeier A (2012) Differential expression of the *Chlamydomonas* [FeFe]-hydrogenase-encoding *HYDA1* gene is regulated by the copper response regulator1. Plant Physiol 159:1700–1712

Park YJ, Yoo CB, Choi SY, Lee HB (2006) Purifications and characterizations of a ferredoxin and its related 2-oxoacid:ferredoxin oxidoreductase from the hyperthermophilic archaeon, *Sulfolobus solfataricus* P1. J Biochem Mol Biol 39:46–54

Peden EA, Boehm M, Mulder DW, Davis R, Old WM, King PW, Ghirardi ML, Dubini A (2013) Identification of global ferredoxin interaction networks in *Chlamydomonas reinhardtii*. J Biol Chem 288:35192–35209

Perazzolli M, Dominici P, Romero-Puertas MC, Zago E, Zeier J, Sonoda M, Lamb C, Delledonne M (2004) Arabidopsis nonsymbiotic hemoglobin AHb1 modulates nitric oxide bioactivity. Plant Cell 16:2785–2794

Perazzolli M, Romero-Puertas MC, Delledonne M (2006) Modulation of nitric oxide bioactivity by plant haemoglobins. J Exp Bot 57:479–488

Pesce A, Bolognesi M, Nardini M (2013) The diversity of 2/2 (truncated) globins. Adv Microb Physiol 63:49–78

Peters JW, Schut GJ, Boyd ES, Mulder DW, Shepard EM, Broderick JB, King PW, Adams MW (2015) [FeFe]- and [NiFe]-hydrogenase diversity, mechanism, and maturation. Biochim Biophys Acta 1853:1350–1369

Philipps G, Krawietz D, Hemschemeier A, Happe T (2011) A pyruvate formate lyase-deficient *Chlamydomonas reinhardtii* strain provides evidence for a link between fermentation and hydrogen production in green algae. Plant J 66:330–340

Philipps G, Happe T, Hemschemeier A (2012) Nitrogen deprivation results in photosynthetic hydrogen production in *Chlamydomonas reinhardtii*. Planta 235:729–745

Planchet E, Kaiser WM (2006) Nitric oxide production in plants: facts and fictions. Plant Signal Behav 1:46–51

Posewitz MC, King PW, Smolinski SL, Zhang L, Seibert M, Ghirardi ML (2004a) Discovery of two novel radical *S*-adenosylmethionine proteins required for the assembly of an active [Fe] hydrogenase. J Biol Chem 279:25711–25720

Posewitz MC, Smolinski SL, Kanakagiri S, Melis A, Seibert M, Ghirardi ML (2004b) Hydrogen photoproduction is attenuated by disruption of an isoamylase gene in *Chlamydomonas reinhardtii*. Plant Cell 16:2151–2163

Poyton RO, Castello PR, Ball KA, Woo DK, Pan N (2009) Mitochondria and hypoxic signaling: a new view. Ann N Y Acad Sci 1177:48–56

Quinn JM, Merchant S (1995) Two copper-responsive elements associated with the *Chlamydomonas Cyc6* gene function as targets for transcriptional activators. Plant Cell 7:623–628

Quinn JM, Nakamoto SS, Merchant S (1999) Induction of coproporphyrinogen oxidase in *Chlamydomonas* chloroplasts occurs via transcriptional regulation of *Cpx1* mediated by copper response elements and increased translation from a copper deficiency-specific form of the transcript. J Biol Chem 274:14444–14454

Quinn JM, Barraco P, Eriksson M, Merchant S (2000) Coordinate copper- and oxygen-responsive *Cyc6* and *Cpx1* expression in *Chlamydomonas* is mediated by the same element. J Biol Chem 275:6080–6089

Quinn JM, Eriksson M, Moseley JL, Merchant S (2002) Oxygen deficiency responsive gene expression in *Chlamydomonas reinhardtii* through a copper-sensing signal transduction pathway. Plant Physiol 128:463–471

Quinn JM, Kropat J, Merchant S (2003) Copper response element and Crr1-dependent Ni^{2+}-responsive promoter for induced, reversible gene expression in *Chlamydomonas reinhardtii*. Eukaryot Cell 2:995–1002

Ragsdale SW (2003) Pyruvate ferredoxin oxidoreductase and its radical intermediate. Chem Rev 103:2333–2346

Rassaf T, Flogel U, Drexhage C, Hendgen-Cotta U, Kelm M, Schrader J (2007) Nitrite reductase function of deoxymyoglobin: oxygen sensor and regulator of cardiac energetics and function. Circ Res 100:1749–1754

Raymond J, Blankenship RE (2004) Biosynthetic pathways, gene replacement and the antiquity of life. Geobiology 2:199–203

Raymond J, Segre D (2006) The effect of oxygen on biochemical networks and the evolution of complex life. Science 311:1764–1767

Reeder BJ (2010) The redox activity of hemoglobins: from physiologic functions to pathologic mechanisms. Antioxid Redox Signal 13:1087–1123

Rice SL, Boucher LE, Schlessman JL, Preimesberger MR, Bosch J, Lecomte JT (2015) Structure of *Chlamydomonas reinhardtii* THB1, a group 1 truncated hemoglobin with a rare histidine-lysine heme ligation. Acta Crystallogr F Struct Biol Commun 71:718–725

Riese M, Höhmann S, Saedler H, Münster T, Huijser P (2007) Comparative analysis of the SBP-box gene families in *P. patens* and seed plants. Gene 401:28–37

Robinson CM, Ohh M (2014) The multifaceted von Hippel-Lindau tumour suppressor protein. FEBS Lett 588:2704–2711

Rodgers KR, Lukat-Rodgers GS (2005) Insights into heme-based O_2 sensing from structure-function relationships in the FixL proteins. J Inorg Biochem 99:963–977

Sainz M, Pérez-Rontomé C, Ramos J, Mulet JM, James EK, Bhattacharjee U, Petrich JW, Becana M (2013) Plant hemoglobins may be maintained in functional form by reduced flavins in the nuclei, and confer differential tolerance to nitro-oxidative stress. Plant J 76:875–887

Sakihama Y, Nakamura S, Yamasaki H (2002) Nitric oxide production mediated by nitrate reductase in the green alga *Chlamydomonas reinhardtii*: an alternative NO production pathway in photosynthetic organisms. Plant Cell Physiol 43:290–297

Santolini J (2011) The molecular mechanism of mammalian NO-synthases: a story of electrons and protons. J Inorg Biochem 105:127–141

Sanz-Luque E, Ocaña-Calahorro F, Llamas A, Galván A, Fernández E (2013) Nitric oxide controls nitrate and ammonium assimilation in *Chlamydomonas reinhardtii*. J Exp Bot 64:3373–3383

Sanz-Luque E, Ocaña-Calahorro F, de Montaigu A, Chamizo-Ampudia A, Llamas A, Galván A, Fernández E (2015) THB1, a truncated hemoglobin, modulates nitric oxide levels and nitrate reductase activity. Plant J 81:467–479

Sawers RG (2005) Formate and its role in hydrogen production in *Escherichia coli*. Biochem Soc Trans 33:42–46

Schöneberg T, Kloos M, Brüser A, Kirchberger J, Sträter N (2013) Structure and allosteric regulation of eukaryotic 6-phosphofructokinases. Biol Chem 394:977–993

Schröder F, Lisso J, Müssig C (2011) EXORDIUM-LIKE1 promotes growth during low carbon availability in Arabidopsis. Plant Physiol 156:1620–1630

Semenza GL (2004) Hydroxylation of HIF-1: oxygen sensing at the molecular level. Physiology 19:176–182

Semenza GL (2012) Hypoxia-inducible factors: mediators of cancer progression and targets for cancer therapy. Trends Pharmacol Sci 33:207–214

Serpa V, Vernal J, Lamattina L, Grotewold E, Cassia R, Terenzi H (2007) Inhibition of AtMYB2 DNA-binding by nitric oxide involves cysteine *S*-nitrosylation. Biochem Biophys Res Commun 361:1048–1053

Shisler KA, Broderick JB (2014) Glycyl radical activating enzymes: structure, mechanism, and substrate interactions. Arch Biochem Biophys 546:64–71

Smagghe BJ, Trent JT 3rd, Hargrove MS (2008) NO dioxygenase activity in hemoglobins is ubiquitous *in vitro*, but limited by reduction *in vivo*. PLoS One 3:e2039

Smagghe BJ, Hoy JA, Percifield R, Kundu S, Hargrove MS, Sarath G, Hilbert JL, Watts RA, Dennis ES, Peacock WJ, Dewilde S, Moens L, Blouin GC, Olson JS, Appleby CA (2009) Review: Correlations between oxygen affinity and sequence classifications of plant hemoglobins. Biopolymers 91:1083–1096

Sommer F, Kropat J, Malasarn D, Grossoehme NE, Chen X, Giedroc DP, Merchant SS (2010) The CRR1 nutritional copper sensor in *Chlamydomonas* contains two distinct metal-responsive domains. Plant Cell 22:4098–4113

Stairs CW, Roger AJ, Hampl V (2011) Eukaryotic pyruvate formate lyase and its activating enzyme were acquired laterally from a Firmicute. Mol Biol Evol 28:2087–2099

Stark BC, Dikshit KL, Pagilla KR (2011) Recent advances in understanding the structure, function, and biotechnological usefulness of the hemoglobin from the bacterium *Vitreoscilla*. Biotechnol Lett 33:1705–1714

Steinbeck J, Nikolova D, Weingarten R, Johnson X, Richaud P, Peltier G, Hermann M, Magneschi L, Hippler M (2015) Deletion of Proton Gradient Regulation 5 (PGR5) and PGR5-Like 1 (PGRL1) proteins promote sustainable light-driven hydrogen production in *Chlamydomonas reinhardtii* due to increased PSII activity under sulfur deprivation. Front Plant Sci 6:892

Steinbüchel A, Müller M (1986) Glycerol, a metabolic end product of *Trichomonas vaginalis* and *Tritrichomonas foetus*. Mol Biochem Parasitol 20:45–55

Stern AM, Zhu J (2014) An introduction to nitric oxide sensing and response in bacteria. Adv Appl Microbiol 87:187–220

Steunou AS, Bhaya D, Bateson MM, Melendrez MC, Ward DM, Brecht E, Peters JW, Kühl M, Grossman AR (2006) *In situ* analysis of nitrogen fixation and metabolic switching in unicellular thermophilic cyanobacteria inhabiting hot spring microbial mats. Proc Natl Acad Sci U S A 103:2398–2403

Stöhr C, Stremlau S (2006) Formation and possible roles of nitric oxide in plant roots. J Exp Bot 57:463–470

Strenkert D, Schmollinger S, Sommer F, Schulz-Raffelt M, Schroda M (2011) Transcription factor-dependent chromatin remodeling at heat shock and copper-responsive promoters in *Chlamydomonas reinhardtii*. Plant Cell 23:2285–2301

Stripp ST, Goldet G, Brandmayr C, Sanganas O, Vincent KA, Haumann M, Armstrong FA, Happe T (2009) How oxygen attacks [FeFe] hydrogenases from photosynthetic organisms. Proc Natl Acad Sci U S A 106:17331–17336

Sturms R, DiSpirito AA, Fulton DB, Hargrove MS (2011a) Hydroxylamine reduction to ammonium by plant and cyanobacterial hemoglobins. Biochemistry (Mosc) 50:10829–10835

Sturms R, DiSpirito AA, Hargrove MS (2011b) Plant and cyanobacterial hemoglobins reduce nitrite to nitric oxide under anoxic conditions. Biochemistry (Mosc) 50:3873–3878

Taabazuing CY, Hangasky JA, Knapp MJ (2014) Oxygen sensing strategies in mammals and bacteria. J Inorg Biochem 133:63–72

Tada Y, Spoel SH, Pajerowska-Mukhtar K, Mou Z, Song J, Wang C, Zuo J, Dong X (2008) Plant immunity requires conformational changes of NPR1 via S-nitrosylation and thioredoxins. Science 321:952–956

Tanaka R, Kobayashi K, Masuda T (2011) Tetrapyrrole metabolism in *Arabidopsis thaliana*. Arabidopsis Book 9:e0145

Tavares CP, Vernal J, Delena RA, Lamattina L, Cassia R, Terenzi H (2014) S-nitrosylation influences the structure and DNA binding activity of AtMYB30 transcription factor from *Arabidopsis thaliana*. Biochim Biophys Acta 1844:810–817

Terashima M, Specht M, Naumann B, Hippler M (2010) Characterizing the anaerobic response of *Chlamydomonas reinhardtii* by quantitative proteomics. Mol Cell Proteomics 9:1514–1532

Terashima M, Petroutsos D, Hüdig M, Tolstygina I, Trompelt K, Gäbelein P, Fufezan C, Kudla J, Weinl S, Finazzi G, Hippler M (2012) Calcium-dependent regulation of cyclic photosynthetic electron transfer by a CAS, ANR1, and PGRL1 complex. Proc Natl Acad Sci U S A 109:17717–17722

Terauchi AM, Lu SF, Zaffagnini M, Tappa S, Hirasawa M, Tripathy JN, Knaff DB, Farmer PJ, Lemaire SD, Hase T, Merchant SS (2009) Pattern of expression and substrate specificity of chloroplast ferredoxins from *Chlamydomonas reinhardtii*. J Biol Chem 284:25867–25878

Thannickal VJ (2009) Oxygen in the evolution of complex life and the price we pay. Am J Respir Cell Mol Biol 40:507–510

Tilleman L, Germani F, De Henau S, Geuens E, Hoogewijs D, Braeckman BP, Vanfleteren JR, Moens L, Dewilde S (2011) Globins in *Caenorhabditis elegans*. IUBMB Life 63:166–174

Tiso M, Tejero J, Kenney C, Frizzell S, Gladwin MT (2012) Nitrite reductase activity of nonsymbiotic hemoglobins from *Arabidopsis thaliana*. Biochemistry (Mosc) 51:5285–5292

Todd BL, Stewart EV, Burg JS, Hughes AL, Espenshade PJ (2006) Sterol regulatory element binding protein is a principal regulator of anaerobic gene expression in fission yeast. Mol Cell Biol 26:2817–2831

Totzeck M, Hendgen-Cotta UB, Rammos C, Petrescu AM, Meyer C, Balzer J, Kelm M, Rassaf T (2012) Assessment of the functional diversity of human myoglobin. Nitric Oxide 26:211–216

Tsygankov A, Kosourov S, Seibert M, Ghirardi ML (2002) Hydrogen photoproduction under continuous illumination by sulfur-deprived, synchronous *Chlamydomonas reinhardtii* cultures. Int J Hydrog Energy 27:1239–1244

Tun NN, Santa-Catarina C, Begum T, Silveira V, Handro W, Floh EI, Scherer GF (2006) Polyamines induce rapid biosynthesis of nitric oxide (NO) in *Arabidopsis thaliana* seedlings. Plant Cell Physiol 47:346–354

Underbakke ES, Iavarone AT, Chalmers MJ, Pascal BD, Novick S, Griffin PR, Marletta MA (2014) Nitric oxide-induced conformational changes in soluble guanylate cyclase. Structure 22:602–611

Urzica EI, Casero D, Yamasaki H, Hsieh SI, Adler LN, Karpowicz SJ, Blaby-Haas CE, Clarke SG, Loo JA, Pellegrini M, Merchant SS (2012) Systems and *trans*-system level analysis identifies conserved iron deficiency responses in the plant lineage. Plant Cell 24:3921–3948

van Dongen JT, Licausi F (2015) Oxygen sensing and signaling. Annu Rev Plant Biol 66:345–367

van Lis R, Baffert C, Couté Y, Nitschke W, Atteia A (2013) *Chlamydomonas reinhardtii* chloroplasts contain a homodimeric pyruvate:ferredoxin oxidoreductase that functions with FDX1. Plant Physiol 161:57–71

Vázquez-Limón C, Hoogewijs D, Vinogradov SN, Arredondo-Peter R (2012) The evolution of land plant hemoglobins. Plant Sci 191-192:71–81

Vigeolas H, Hühn D, Geigenberger P (2011) Nonsymbiotic hemoglobin-2 leads to an elevated energy state and to a combined increase in polyunsaturated fatty acids and total oil content when overexpressed in developing seeds of transgenic Arabidopsis plants. Plant Physiol 155:1435–1444

Vignais PM, Billoud B (2007) Occurrence, classification, and biological function of hydrogenases: an overview. Chem Rev 107:4206–4272

Vinogradov SN, Moens L (2008) Diversity of globin function: enzymatic, transport, storage, and sensing. J Biol Chem 283:8773–8777

Vinogradov SN, Fernández I, Hoogewijs D, Arredondo-Peter R (2011) Phylogenetic relationships of 3/3 and 2/2 hemoglobins in Archaeplastida genomes to bacterial and other eukaryote hemoglobins. Mol Plant 4:42–58

Vinogradov SN, Bailly X, Smith DR, Tinajero-Trejo M, Poole RK, Hoogewijs D (2013a) Microbial eukaryote globins. Adv Microb Physiol 63:391–446

Vinogradov SN, Tinajero-Trejo M, Poole RK, Hoogewijs D (2013b) Bacterial and archaeal globins – a revised perspective. Biochim Biophys Acta 1834:1789–1800

Volgusheva A, Kukarskikh G, Krendeleva T, Rubin A, Mamedov F (2015) Hydrogen photoproduction in green algae *Chlamydomonas reinhardtii* under magnesium deprivation. RSC Adv 5:5633–5637

Wagner AF, Frey M, Neugebauer FA, Schäfer W, Knappe J (1992) The free radical in pyruvate formate-lyase is located on glycine-734. Proc Natl Acad Sci U S A 89:996–1000

Wei L, Derrien B, Gautier A, Houille-Vernes L, Boulouis A, Saint-Marcoux D, Malnoë A, Rappaport F, de Vitry C, Vallon O, Choquet Y, Wollman FA (2014) Nitric oxide-triggered remodeling of chloroplast bioenergetics and thylakoid proteins upon nitrogen starvation in *Chlamydomonas reinhardtii*. Plant Cell 26:353–372

Weits DA, Giuntoli B, Kosmacz M, Parlanti S, Hubberten HM, Riegler H, Hoefgen R, Perata P, van Dongen JT, Licausi F (2014) Plant cysteine oxidases control the oxygen-dependent branch of the N-end-rule pathway. Nat Commun 5:3425

Whitney LA, Loreti E, Alpi A, Perata P (2011) Alcohol dehydrogenase and hydrogenase transcript fluctuations during a day-night cycle in *Chlamydomonas reinhardtii*: the role of anoxia. New Phytol 190:488–498

Willam C, Nicholls LG, Ratcliffe PJ, Pugh CW, Maxwell PH (2004) The prolyl hydroxylase enzymes that act as oxygen sensors regulating destruction of hypoxia-inducible factor alpha. Adv Enzym Regul 44:75–92

Wilson ID, Neill SJ, Hancock JT (2008) Nitric oxide synthesis and signalling in plants. Plant Cell Environ 31:622–631

Wimalasekera R, Villar C, Begum T, Scherer GF (2011) *COPPER AMINE OXIDASE1* (*CuAO1*) of *Arabidopsis thaliana* contributes to abscisic acid- and polyamine-induced nitric oxide biosynthesis and abscisic acid signal transduction. Mol Plant 4:663–678

Wimalasekera R, Schaarschmidt F, Angelini R, Cona A, Tavladoraki P, Scherer GF (2015) *POLYAMINE OXIDASE2* of *Arabidopsis* contributes to ABA mediated plant developmental processes. Plant Physiol Biochem 96:231–240

Winger JA, Derbyshire ER, Lamers MH, Marletta MA, Kuriyan J (2008) The crystal structure of the catalytic domain of a eukaryotic guanylate cyclase. BMC Struct Biol 8:42

Winkler M, Hemschemeier A, Gotor C, Melis A, Happe T (2002) [Fe]-hydrogenases in green algae: photo-fermentation and hydrogen evolution under sulfur deprivation. Int J Hydrog Energy 27:1431–1439

Winkler M, Kuhlgert S, Hippler M, Happe T (2009) Characterization of the key step for light-driven hydrogen evolution in green algae. J Biol Chem 284:36620–36627

Winter G, Todd CD, Trovato M, Forlani G, Funck D (2015) Physiological implications of arginine metabolism in plants. Front Plant Sci 6:534

Wolfe AJ (2005) The acetate switch. Microbiol Mol Biol Rev 69:12–50

Wood PM (1978) Interchangeable copper and iron proteins in algal photosynthesis. Studies on plastocyanin and cytochrome *c*-552 in *Chlamydomonas*. Eur J Biochem 87:9–19

Wykoff DD, Davies JP, Melis A, Grossman AR (1998) The regulation of photosynthetic electron transport during nutrient deprivation in *Chlamydomonas reinhardtii*. Plant Physiol 117:129–139

Yamasaki K, Kigawa T, Inoue M, Tateno M, Yamasaki T, Yabuki T, Aoki M, Seki E, Matsuda T, Nunokawa E, Ishizuka Y, Terada T, Shirouzu M, Osanai T, Tanaka A, Seki M, Shinozaki K, Yokoyama S (2004) A novel zinc-binding motif revealed by solution structures of DNA-binding domains of *Arabidopsis* SBP-family transcription factors. J Mol Biol 337:49–63

Yang J, Naik SG, Ortillo DO, García-Serres R, Li M, Broderick WE, Huynh BH, Broderick JB (2009) The iron-sulfur cluster of pyruvate formate-lyase activating enzyme in whole cells: cluster interconversion and a valence-localized $[4Fe\text{-}4S]^{2+}$ state. Biochemistry (Mosc) 48:9234–9241

Yang W, Catalanotti C, D'Adamo S, Wittkopp TM, Ingram-Smith CJ, Mackinder L, Miller TE, Heuberger AL, Peers G, Smith KS, Jonikas MC, Grossman AR, Posewitz MC (2014) Alternative acetate production pathways in *Chlamydomonas reinhardtii* during dark anoxia and the dominant role of chloroplasts in fermentative acetate production. Plant Cell 26:4499–4518

Yang W, Wittkopp TM, Li X, Warakanont J, Dubini A, Catalanotti C, Kim RG, Nowack EC, Mackinder LC, Aksoy M, Page MD, D'Adamo S, Saroussi S, Heinnickel M, Johnson X, Richaud P, Alric J, Boehm M, Jonikas MC, Benning C, Merchant SS, Posewitz MC, Grossman AR (2015) Critical role of *Chlamydomonas reinhardtii* ferredoxin-5 in maintaining membrane structure and dark metabolism. Proc Natl Acad Sci U S A 112:14978–14983

Zagorec M, Labbe-Bois R (1986) Negative control of yeast coproporphyrinogen oxidase synthesis by heme and oxygen. J Biol Chem 261:2506–2509

Zagorec M, Buhler JM, Treich I, Keng T, Guarente L, Labbe-Bois R (1988) Isolation, sequence, and regulation by oxygen of the yeast *HEM13* gene coding for coproporphyrinogen oxidase. J Biol Chem 263:9718–9724

Zhang L, Hach A, Wang C (1998) Molecular mechanism governing heme signaling in yeast: a higher-order complex mediates heme regulation of the transcriptional activator HAP1. Mol Cell Biol 18:3819–3828

Zhang LP, Mehta SK, Liu ZP, Yang ZM (2008) Copper-induced proline synthesis is associated with nitric oxide generation in *Chlamydomonas reinhardtii*. Plant Cell Physiol 49:411–419

Zones JM, Blaby IK, Merchant SS, Umen JG (2015) High-resolution profiling of a synchronized diurnal transcriptome from *Chlamydomonas reinhardtii* reveals continuous cell and metabolic differentiation. Plant Cell 27:2743–2769

Chlamydomonas: Regulation Toward Metal Deficiencies

Eugen I. Urzica

Abstract The green alga, *Chlamydomonas reinhardtii*, is an ideal organism to study cellular responses related to metal deficiencies. The biology of *C. reinhardtii* is relevant to both animals and photosynthetic organisms, since many genes are derived from the common plant–animal ancestor. By studying *C. reinhardtii*, important questions in trace metal homeostasis have been answered; however, many aspects remain to be discovered. To cope with the effects of metal deficiencies or excess, *C. reinhardtii* has developed mechanisms to tightly regulate metal homeostasis. Here we describe the *C. reinhardtii* requirements for trace metals, the intracellular distribution of these micronutrients, and their assimilation mechanisms. We further discuss the impact of trace metals deficiencies on the metabolism and how the regulation is achieved.

1 Introduction

Although transition metals are essential for life, they could also be toxic. The same chemical reactivity used for specific reactions could damage the macromolecules when it is present in excess. Therefore, the organisms have developed mechanisms that help to maintain the intracellular homeostasis and control the nutrient intracellular levels. The nutrient assimilation pathways are induced at low nutrient concentrations and turned off at high nutrient concentrations. Metal homeostasis serves to ensure that the metal ions are accessible and the apoproteins only interact with the right metal.

Metal ions are simple protein cofactors, and copper, zinc, iron, and manganese, in particular, can play a role in many and often essential reactions within the cell. To utilize metal ions as catalysts is imperative for the cell to overcome the unique challenge of metal specificity and selectively. The interaction between a protein and a different metal is generally unproductive, and with few exceptions, proteins

E.I. Urzica (✉)
Institute of Plant Biology and Biotechnology, Westfaelische Wilhelms Universitaet, Muenster, 48143 Muenster, Germany
e-mail: eugen.urzica@uni-muenster.de

M. Hippler (ed.), *Chlamydomonas: Molecular Genetics and Physiology*,
Microbiology Monographs 30, DOI 10.1007/978-3-319-66365-4_7

have evolved to exploit the properties of a specific metal. However, many metalloproteins bind Cu^{2+} with higher affinity than they do bind Zn^{2+}, followed by Fe^{2+} and then Mn^{2+} (Williams 2001). To ensure that each protein binds the correct metal and to exclude the "wrong" one, the cells have developed specific mechanisms to avoid mismetalation. When an imbalance between metal availability and apoprotein abundance occurs, mismetalation is inevitable. In eukaryotes, an additional mechanism to maintain metal homeostasis is the storage of metals in intracellular organelles. Plant and yeast vacuoles are well-established organelles to sequester and mobilize metals (Martinoia et al. 2007, 2012). More recently, other compartments like acidocalcisomes and other lysosome-related organelles emerged as important players of metal homeostasis (Blaby-Haas and Merchant 2014; Hong-Hermesdorf et al. 2014).

Transition metals due to the capacity to reversibly change their oxidation states are often found as cofactors in many enzymes. *C. reinhardtii* as a photosynthetic organism uses many metals in its photosynthetic and respiratory electron chains. In the chloroplast many enzymes are present that require metals as cofactors. For example, the photosynthetic electron chain requires the use of manganese, iron, and copper. Several other metal-containing enzymes are localized in the chloroplast like Mn-dependent enzymes (MnSOD3), Zn-dependent carbonic anhydrases (CAH8), and many Fe-dependent enzymes (e.g., FeSOD, ADH1, FDX1–6, or fatty acid desaturases like FAB2). Carotenoid and chlorophyll biosynthesis, two pathways that take place in the chloroplast, are also requiring several metal-dependent enzymes, mostly being Fe-containing proteins. Likewise, mitochondrial respiratory electron chain requires the use of many Fe-dependent proteins (subunits of Complexes I, II, III, and IV), the Cu-dependent cytochrome oxidase, and the Mn-dependent MnSOD2.

The green alga, *C. reinhardtii*, is an ideal organism to study cellular responses to metal deficiencies, since its biology is relevant to both animals and photosynthetic organisms, many genes being derived from the plant–animal common ancestor (Merchant et al. 2007). Advantages of using *C. reinhardtii* as a model organism include the possibility of growth in a defined medium of inorganic salts, where the metal content is more easily controlled and buffered (Merchant et al. 2006). *C. reinhardtii* possesses a well-characterized compartmentalization of metal metabolism (i.e., the chloroplast for photosynthesis and the mitochondria for respiration). Both the photosynthetic and respiratory electron chains are rich in metals ions.

In this chapter, we will describe the requirements of the green alga *C. reinhardtii* for micronutrients (Fe, Cu, Zn, and Mn) and detail their key functions in the metabolism. Hereafter, the nutrient assimilation pathways, the members of the intracellular metals trafficking, and the potential metal-binding chaperones will be described. We will review the impact of nutrient deficiency and the acclimation mechanisms acting at the organelle, cellular, and organism levels to preserve the photosynthetic and respiratory functions under nutrient deficiency.

2 Iron Deficiency and Regulation

2.1 Iron Nutrition

Based on the expression of sentinel genes, chlorophyll content, growth, and sensitivity to high light, four stages of iron nutrition were defined in *C. reinhardtii*. Iron replete, with 20 μM Fe in the medium, corresponds to the iron content of standard laboratory growth medium (Harris 2009). The second stage is iron deficiency with around 1–3 μM Fe (depending on the strain) when the cells are preparing for the onset of iron limitation by upregulating iron transporters and adjusting their biochemistry to minimize iron utilization, but their chlorophyll content is not or only marginally affected. Fluorescence kinetics and low-temperature fluorescence studies indicate an impact on PSI light harvesting as well as electron transfer (Moseley et al. 2002a). Iron-limited cultures (with iron concentrations bellow 0.5 μM Fe) are visibly chlorotic and show an N-terminal processing of LHCA3 which correlates with the drop in the excitation energy transfer efficiency between LHCI and PSI as evidenced by low-temperature fluorescence emission spectroscopy (Moseley et al. 2002a; Naumann et al. 2005). The effect on chlorophyll biosynthesis visualized by chlorosis could be attributed to a di-iron aerobic cyclase encoded by CHL27 in chlorophyll biosynthesis (Tottey et al. 2003). Finally, in the iron-excess situation (200 μM Fe), the cells are phenotypically indistinguishable from iron-replete cells at normal light intensities but are sensitive to excess excitation energy (500 μmol photons m^{-2} s^{-1}) (Long and Merchant 2008). Even though the high-affinity iron-uptake system is downregulated under iron-excess situation, it has been shown that *C. reinhardtii* cells hyperaccumulate iron under both photoheterotrophic and photoautotrophic conditions (Terauchi et al. 2010). The iron is most likely entering the cells using the low-affinity pathway, evidenced by the increased IRT1 transcript levels (see below) (Long and Merchant 2008).

2.2 Iron Assimilation

Iron-deficient *C. reinhardtii* cells assimilate iron from environment primarily using a high-affinity pathway that is common to the iron-uptake strategy I in non-graminaceous plants (reduction strategy) and to the one described in baker's yeast *Saccharomyces cerevisiae*. This high-affinity reduction iron-uptake system in *C. reinhardtii* comprises a ferric reductase (FRE1) and a multicopper ferroxidase (FOX1) that provides the iron in the right oxidation state to be imported into the cells by the FTR1 permease (La Fontaine et al. 2002; Allen et al. 2007a; Kosman 2003; Philpott 2006). Two additional ZIP family members (IRT1 and IRT2) that showed an increased expression specifically in iron-deficient cells (Allen et al. 2007a;

Hanikenne 2008) might be involved in low-affinity uptake of ferrous iron. In the high-affinity iron assimilation pathway, FRE1 is reducing the ferric iron (Fe^{3+}) to ferrous iron (Fe^{2+}). The soluble Fe^{2+} produced by the FRE1 ferric reductase is reoxidized by the plasma membrane ferroxidase (FOX1), and the Fe^{3+} produced by FOX1 serves as a substrate for the ferric permease FTR1 (Table 1). An important feature of this high-affinity iron acquisition system is that Fe^{3+} alone cannot serve as a substrate for uptake by FTR1. It has been shown in yeast that the permeation of iron is coupled to ferroxidation via a substrate channeling mechanism in which the Fe^{3+} substrate of Ftr1p is handed off directly from the ferroxidase Fet3p (Terzulli and Kosman 2009, 2010). Residues involved in iron channeling from Fet3p to Ftr1p have been identified in both proteins. It is most likely that the same mechanism is taking place also in the green alga *C. reinhardtii* (Chen et al. 2008).

C. reinhardtii grown under low-iron nutrition showed induced transcript and protein levels of two algal-specific periplasmic proteins, FEA1 and FEA2. It has been proposed that these two proteins might play a role in concentrating the iron ions in the vicinity of the iron transporters. Overexpression of *C. reinhardtii* FEA1 in *S. cerevisiae* and *A. thaliana* showed that the protein can facilitate ferrous (Fe^{2+}) uptake. *C. reinhardtii* FEA1 can complement the *irt1* mutant in *A. thaliana*, as well as Δ*ftr1* mutant in *S. cerevisiae*. Moreover, it has been demonstrated that FEA1 specifically facilitates the uptake of iron, since the FEA1 protein does not increase sensitivity to toxic concentrations of competing nonferrous metals nor facilitate their (cadmium) accumulation (Narayanan et al. 2011).

The low-affinity iron uptake in *C. reinhardtii* comprises two members of the ZIP family of transporters, IRT1 and IRT2 (Allen et al. 2007a). They are similar to the IRT1/2 from *A. thaliana* and have been shown that in *C. reinhardtii*, the IRT1/2 mRNA levels are upregulated in response to iron deficiency (Allen et al. 2007a; Urzica et al. 2012). In non-graminaceous plants, iron uptake involves the reduction of Fe^{3+} to Fe^{2+} by the plasma membrane ferrireductase FRO2, followed by the import of ferrous iron into the roots by IRT1. Iron uptake in *A. thaliana* is preceded by the solubilization of iron mainly mediated by the root plasma membrane H+-ATPase, AHA2, which pumps protons resulting in rhizosphere acidification (Brumbarova et al. 2015; Jeong and Guerinot 2009; Santi and Schmidt 2009).

Grasses acquire iron using the chelation mechanism (Strategy II), in which phytosiderophores (PS) such as mugineic acids are secreted and released to chelate Fe^{3+}. The PS–Fe^{3+} chelates are then transported into the roots via the yellow stripe-like (YSL) transporters (Curie et al. 2009). Grasses can also take up Fe^{2+} in addition to Fe^{3+}–PS chelates. Rice, a Strategy II plant, and its wild relatives are well adapted for growth under submerged conditions, in which Fe^{2+} is more abundant than Fe^{3+}. However, unlike Strategy I in non-graminaceous plants, neither H^+-ATPase nor ferrireductase activities are induced under iron deficiency. Ishimaru et al. found that *Oryza sativa* encodes two IRT transporters (OsIRT1 and OsIRT2), both being localized at the plasma membrane. OsIRT1 and OsIRT2 are induced under low-iron nutrition, and both can rescue the growth defects of a yeast iron-uptake mutant suggesting that OsIRT1 and OsIRT2 are involved in the uptake of Fe^{2+}. This probably reflects an adaptation to flooded rice paddies, where Fe^{2+} is

Table 1 Known and putative proteins involved in iron assimilation and distribution of intracellular iron

Transcript name	Gene name	Defline	Domain
Iron assimilation			
Cre04.g227400.t1.2	*FRE1*	Ferric-chelate reductase/oxidoreductase	Ferric reductase-like transmembrane component, FAD-binding domain; ferric reductase NAD-binding domain
Cre09.g393150.t1.2	*FOX1*	Multicopper ferroxidase	Multicopper oxidase
Cre03.g192050.t1.1	*FTR1*	Iron permease, membrane protein	Iron permease FTR1 family
Cre12.g546550.t1.1	*FEA1*	Iron-assimilating protein 1	Low iron-inducible periplasmic protein
Cre12.g546600.t1.1	*FEA2*	Iron-assimilating protein 2	Low iron-inducible periplasmic protein
Cre12.g530400.t1.2	*IRT1*	Iron-nutrition-responsive ZIP family transporter	ZIP zinc transporter
Cre12.g530350.t1.1	*IRT2*	Iron-nutrition-responsive ZIP family transporter	ZIP zinc transporter
Intracellular iron transport			
Cre12.g546500.t1.2	*TEF22*	DOMON domain, cytochrome b_{561}/ferric reductase transmembrane domain	DOMON domain, eukaryotic cytochrome b_{561}
Cre05.g241400.t1.1		Putative ferric reductase like transmembrane component	Ferric reductase-like transmembrane component, FAD-binding domain
Cre16.g695950.t1.2	*MFL1*	Mitoferrin-like protein	Mitochondrial carrier protein
Cre05.g248300.t1.1	*NRAMP4*	Natural resistance-associated macrophage domain protein	Natural resistance-associated macrophage protein
Cre02.g099500.t1.1	*CVL1*	Similar to yeast CCC1 and plant VIT1	VIT family
Cre02.g107550.t1.2	*CVL2*	Similar to yeast CCC1 and plant VIT1	VIT family
Cre16.g687000.t1.1	*FPN1*	Similar to ferroportin	Ferroportin1 (FPN1)

(continued)

Table 1 (continued)

Transcript name	Gene name	Defline	Domain
Cre12.g538350.t1.1	*FTX1*	Frataxin	Frataxin-like domain
Cre11.g467759.t1.1	*PIC1*	PIC1 permease	Protein of unknown function (DUF3611)
Ferritins			
Cre09.g387800.t1.2	*FER1*	Pre-apoferritin	Ferritin-like domain
Cre13.g574500.t1.1	*FER2*	Ferritin subunit	Ferritin-like domain
Cre01.g033300.t1.2		Ferritin-like domain protein (ferritin2)	Ferritin2 domain
Unknown function			
Cre12.g531200.t1.1	*FOX2*	Multicopper oxidase	Multicopper oxidase
Cre03.g188300.t1.1	*RBOL1*	Respiratory burst oxidase	Ferric reductase-like transmembrane component, FAD-binding domain
Cre03.g188400.t1.1	*RBOL2*	Respiratory burst oxidase	Ferric reductase-like transmembrane component, FAD-binding domain

more abundant than Fe^{3+} owing to reduced levels of oxygen (Ishimaru et al. 2006; Thomine and Vert 2013; Walker and Connolly 2008).

2.3 *Intracellular Iron Distribution*

After its import into Chlamydomonas cell, iron most likely binds to diverse low-molecular-weight biological ligands forming the labile iron pool. From this labile pool, iron is distributed to the chloroplast, mitochondria where it is needed for photosynthesis and respiration, and for Fe–S clusters and heme synthesis or is sequestered into the vacuole. Iron-deficient *C. reinhardtii* cells upregulate several gene-encoding transporters with the potential to function in intracellular metal distribution. These include a transporter of the natural resistance-associated macrophage proteins NRAMP4, Cre16.g687000 protein with sequence homology to plant and mammalian ferroportins, CVL1 and CVL2 which are two putative transporters

similar to vacuolar plant VIT1 and yeast CCC1-like transporters, and two putative ferric reductases (TEF22 and Cre05.g241400) (Table 1) (Urzica et al. 2012).

The NRAMP proteins are conserved from bacteria to humans, and they catalyze the H^+-dependent transport of divalent metal ions, such as Mn^{2+}, Fe^{2+}, Co^{2+}, Zn^{2+}, Ni^{2+}, or Cd^{2+} (Courville et al. 2006; Nevo and Nelson 2006). The yeast genome codes for three NRAMP transporters (Sm1p, Smf2p, and Smf3p), of which Smf3p is vacuolar membrane localized and its expression is regulated by iron nutrition, whereas mammals have two, SLC11A1 and SLC11A2 (Portnoy et al. 2000; Singh et al. 2007). Mammalian SCL11A2 (also called DCT1/DMT1) functions in iron import into enterocytes, after reduction of ferric iron by ferric reductase at the apical membrane, and in Fe^{2+} transport from the endosome during the transferrin cycle (Andrews 2000; Riedel et al. 1995). NRAMP3 and NRAMP4 in Arabidopsis are both induced by iron deficiency (Thomine et al. 2000) and function to mobilize iron from vacuoles during seed germination (Lanquar et al. 2005). The *C. reinhardtii* genome codes for four NRAMPs (NRAMP1, NRAMP2, RET1, and NRAMP4). *C. reinhardtii* NRAMP4 is induced by iron deficiency under both photoheterotrophic and photoautotrophic conditions, and these changes in NRAMP4 mRNA abundances are specific to iron-deficient/iron-limited cells, whereas the NRAMP1 and NRAMP2 genes are induced specifically in manganese-starved cells (Urzica et al. 2012). NRAMP4 from *C. reinhardtii* is more closely related to Arabidopsis NRAMP3/NRAMP4 and mammalian DCT1 than to the other *C. reinhardtii* NRAMP proteins. Therefore, it seems likely that *C. reinhardtii* NRAMP4 is involved in remobilization of vacuolar iron stores needed for essential processes (photosynthesis and mitochondrial respiration) during low-iron nutrition. A compartment called the acidocalcisome has been described in *C. reinhardtii* (Ruiz et al. 2001). This compartment contains polyphosphate and metals and is a specialized vacuolar structure based on proteomic analysis of *Cyanidioschyzon merolae* acidocalcisomes that identified V-ATPase subunits (Yagisawa et al. 2009). In addition, at least two candidate metal transporters, including a protein related to *S. cerevisiae* Ccc1p and a cation diffusion facilitator family member (putative Zn transporter), were described. CVL1 and CVL2 are two proteins related to *S. cerevisiae* Ccc1p and Arabidopsis VIT1 that are involved in the iron export from the vacuole into the cytosol (Kim et al. 2006; Li et al. 2001). Although the increasing transcript levels of *C. reinhardtii* CCVL1/CCVL2 seem counterintuitive, it is possible that under iron deficiency, they function to only transiently store the potentially toxic iron released from degraded or damaged iron–sulfur proteins into the vacuoles prior to its redistribution to intracellular compartments. A similar pattern of expression and function has been documented for a vacuolar zinc transporter in *S. cerevisiae* (ZRC1) (MacDiarmid et al. 2003).

Cre16.g687000 encodes a ferroportin-like protein (FPN1), and similar increasing expression profiles during iron deficiency have been observed for a plant ferroportin IREG2/FPN2, whereas another plant ferroportin IREG3/MAR1 is downregulated under iron deficiency in *A. thaliana* (Buckhout et al. 2009; Colangelo and Guerinot 2004; Long et al. 2010; Kong and Yang 2010; Zheng

et al. 2009). *A. thaliana* FPN2 is localized to vacuolar membranes and MAR1 to the plastid envelope membranes. The proteins can apparently transport divalent cations like Fe^{2+}, Co^{2+}, and Ni^{2+} (Conte et al. 2009; Morrissey et al. 2009; Schaaf et al. 2006). Since the overexpression of MAR1 in *A. thaliana* confers chlorosis which can be rescued by excess iron, it has been suggested that MAR1 has a function in iron import into the chloroplasts. In addition MAR1 can transport multiple aminoglycoside antibiotics (Conte et al. 2009). On the other hand, FPN2 is playing a role in sequestering other divalent cations to the vacuole. The latter function is necessary in iron-deficient cells because members of the ZIP family (like IRT1/IRT2, which are induced) are not as selective for iron as is the FTR1/FOX1 pathway and may bring in unwanted, potentially toxic ions. For instance, plant IRT proteins are known to transport Cd^{2+} (Connolly et al. 2002).

Another induced gene in iron-deficient/iron-limited *C. reinhardtii* is *Cre05.g241400* and encodes for a ferric reductase-like protein. This putative ferrireductase could function to reduce intracellular ferric to ferrous prior to transport into the vacuole or the chloroplast, by analogy to Fre6p in yeast or FRO7 in Arabidopsis (Jeong et al. 2008; Singh et al. 2007).

C. reinhardtii genome also encodes for three cytochrome b_{561} family proteins (TEF22, Cre14.g609900, and Cre13.g586600). TEF22 and Cre14.g609900 possess a DOMON domain fused to a cytochrome b_{561} ferric reductase domain and are more related to mammalian FRRS-like ferric reductases than they are to the plant homologs (Urzica et al. 2012). Mouse, rat, human, and *Drosophila melanogaster* SDR2 (FRRS1) are indeed functional ferric reductases, and mouse SDR2 is also regulated by iron (Vargas et al. 2003). Expression of mammalian duodenal cytochrome *b* (Dcytb), which generates the Fe^{2+} used by DCT1/DMT1, is likewise regulated by iron nutrition (McKie 2008; McKie et al. 2001), and two other mammalian cytochrome b_{561} homologs from chromaffin granules and lysosomes function as ascorbate-dependent ferric reductases (Fleming et al. 1997; Fleming and Kent 1991; Njus et al. 1987; Su and Asard 2006; Zhang et al. 2006). These cytochrome b_{561} ferric reductases each possess four conserved histidine residues involved in coordination of two heme molecules and conserved sites for ascorbate and monodehydroascorbate binding (Su and Asard 2006; Takeuchi et al. 2004; Trost et al. 2000). The *C. reinhardtii* proteins retain the conserved residues, making them likely to be true ferric reductases (Urzica et al. 2012). Proteomic studies indicated that TEF22 is in the mitochondrion (Allmer et al. 2006; Atteia et al. 2009) suggesting that TEF22 might be a ferric reductase involved in supplying ferrous iron for mitochondrial respiratory complexes. Cre14.g609900 may function together with FRE1 at the plasma membrane, whereas Cre13.g586600, whose monodehydroascorbate and ascorbate binding sites are well conserved, might be involved in ascorbate regeneration from monodehydroascorbate at the plasma membrane or vacuolar membrane (Urzica et al. 2012). Members of the mitochondrial solute carrier (MSC) family can transport multiple substrates across the inner mitochondrial membrane. Some of them are involved in iron import into mitochondria, like MIT from rice (Bashir et al. 2011a, b), Mrs3p and Mrs4p in yeast (Froschauer et al. 2009; Muhlenhoff et al. 2003), or mitoferrins 1 and 2 in zebrafish

and mouse (Shaw et al. 2006). *C. reinhardtii* encodes for a mitoferrin homolog (MFL1) that is potentially involved in iron import into the algal mitochondria (Table 1) (Blaby-Haas and Merchant 2012).

Another key player in the iron homeostasis is played by the ferritin. Due to its ability to store large quantities of iron, ferritin is the major, and perhaps only, iron storage protein (Koorts and Viljoen 2007; Theil 1987). Ferritin is a multimeric complex, consisting of 24 subunits that form a shell around a core that can hold up to 4500 Fe(III) atoms as an insoluble iron–oxyhydroxide mineral (Harrison and Arosio 1996; Theil 1987). When iron is needed, reduction leads to release of the metal from the complex, but the mechanism is not yet fully understood (Harrison and Arosio 1996). Even though its three-dimensional structure is conserved, mammalian and plant ferritins differ in their subunit composition and the cellular localization. In mammals, the ferritin complex is localized in the cytosol (Harrison and Arosio 1996) and is composed of the H and L subunits in a tissue-dependent stoichiometry. The H chain carries ferroxidase active sites that oxidize ferrous to ferric iron, a prerequisite for mineralization in the core (Chasteen 1998). The L chain that is present only in vertebrates does not have a ferroxidase site but is able to form a complex and bind iron at neutral but not acidic pH (Levi et al. 1989). Therefore changes in the ratio of H/L subunits, e.g., in response to iron nutrition or in particular cell types, can affect the iron storage capability of ferritin (Koorts and Viljoen 2007). In vascular plants, ferritin is located in the plastids rather than in the cytosol and is the source of iron for de novo synthesis of the cytochromes and FeS proteins in the photosynthetic apparatus during chloroplast development (Lobréaux and Briat 1991).

Recently, ferritin was also found in plant mitochondria, and it was suggested that this might be a consequence of dual targeting of one of the preproteins (Zancani et al. 2004). Although ferritin is encoded by a multigene family in plants [four FER genes in Arabidopsis (Petit et al. 2001); three in *Lupinus luteus* (Strozycki et al. 2010)], the subunits are all of one type with a ferroxidase active site and characteristics of both the H and the L chains (Wade et al. 1993). During the early stages of plant development, ferritin is mostly detected in the nongreen plastids of seeds and developing organs, such as young leaves, where it serves as an iron pool (Lobréaux and Briat 1991), whereas in the chloroplasts, it is only found during senescence (Buchanan-Wollaston and Ainsworth 1997). The elevated protein level sequestered iron at the expense of the iron-rich photosynthetic machinery and led to an iron-deficient phenotype of the chloroplasts, evidenced by an increase in root ferric reductase activity and in leaf iron content (Van Wuytswinkel et al. 1998).

Two genes *FER1* and *FER2* encoding ferritin subunits were identified in the *C. reinhardtii* genome with 49% identity between the FER1 and FER2 subunits. Both ferritin subunits are plastid localized, but FER1 is quantitatively recovered in soluble extracts of cells, while FER2 is found associated with the particulate fraction. Both FER1 and FER2 transcripts are increased in abundance as iron nutrition is decreased, but the pattern for each gene is distinct (Long et al. 2008; Urzica et al. 2012). The increased abundance of FER1 mRNAs in iron deficiency (La Fontaine et al. 2002) is counterintuitive for an iron storage protein, and it has

been suggested that plastid ferritin1 plays a role in buffering iron or holding it transiently as it was released from PSI by degradation (Moseley et al. 2002a). However, the iron content of the FER1 complex is decreased suggesting that increased expression results in increased capacity for iron binding in the chloroplast of iron-limited cells, which supports a role for FER1 as an iron buffer (Long et al. 2008). Busch et al. showed that there is a strong correlation between the induction of the FER1 protein levels and the degree of PSI degradation under iron-limited conditions. The PSI level can be fully restored within 24 h after iron repletion at the expense of the accumulated ferritin, indicating that the ferritin-stored iron allows fast adjustment of the photosynthetic apparatus with respect to iron availability (Busch et al. 2008). Reducing the amount of FER1 protein using RNAi results in a significant delay in the degradation of PSI under iron limitation, and these strains are more susceptible to photooxidative stress under high-light conditions. This suggests that it plays also a protective role under photooxidative stress conditions (Busch et al. 2008).

On the other hand, FER2 protein levels are decreased in iron-deprived cells, suggesting that there is an iron-nutrition-responsive regulation at the translational or posttranslational level for FER2. Partial purification of the FER1 complex indicates that the two ferritins are associated in distinct complexes but they do not coassemble. The ratio of FER1 to FER2 is 70:1 in iron-replete cells, suggesting a more dominant role of FER1 in iron homeostasis (Long et al. 2008).

2.3.1 Photoautotrophic Versus Photoheterotrophic Growth Conditions

C. reinhardtii cells can grow autotrophically on CO_2 and heterotrophically using acetate. In either case, metabolism depends on abundant iron proteins, the autotrophic growth on proteins of the photosynthetic apparatus in the chloroplast whereas the heterotrophic growth on mitochondrial respiratory complex proteins. The responses of Chlamydomonas cells to iron-deficient conditions are specific depending on the trophic status. Chlamydomonas cells grown photoheterotrophically under iron-limited conditions grow faster than the autotrophic grown cells. As already pointed out, photoheterotrophic cells suppress photosynthesis while maintaining relatively high rates of respiration, whereas the photoautotrophic cells still perform efficiently photosynthesis while respiration is lost (Hohner et al. 2013; Terauchi et al. 2010). Iron-limited, photoheterotrophically grown Chlamydomonas cells have less chlorophyll, lower quantum efficiency of PSII (Fv/Fm), and lower non-photochemical quenching (NPQ) compared to phototrophically iron-limited grown cells (Hohner et al. 2013; Naumann et al. 2007; Terauchi et al. 2010). Also degradation of PSI subunits is faster in cells grown under photoheterotrophic iron-limited conditions. Iron limitation has a major impact on respiratory rates in cells grown in iron-limited conditions and in the presence of acetate. Respiratory oxygen rates do not decrease significantly under photoheterotrophic low-iron conditions, and comparative proteomics showed that the subunits of the respiratory complexes were only slightly diminished or even increased under similar conditions but

strongly diminished under autotrophic low-iron nutrition (Hohner et al. 2013; Naumann et al. 2007; Terauchi et al. 2010). This indicates a hierarchical reallocation of iron from one organelle to another in a Chlamydomonas cell which is dependent on the metabolic status of the cell.

Interestingly, when the Chlamydomonas cells are cultivated phototrophically, they accumulate approximately twice as much iron when compared to photoheterotrophically grown cells in both iron-replete and iron-limited conditions (Terauchi et al. 2010). It is possible that the excess iron is stored inside ferritin or inside the vacuoles and will become available when needed. This is supported by the delayed degradation of PSI and by the delayed induction of the iron-uptake system (e.g., ferroxidase) (Busch et al. 2008; Terauchi et al. 2010).

2.4 Iron Sparing and Recycling

Cells are able to acclimate to poor iron nutrition by activating an iron-sparing mechanism. Cells could decide that some iron-binding proteins are not synthesized, synthesized at a much lower rate, or eventually degraded before they can compete for iron. Once iron is assimilated or remobilized from cellular stores, it can further be selectively used for less dispensable iron-dependent functions, such as DNA repair/synthesis at the expense of other nonessential iron-dependent processes (Sanvisens et al. 2011).

The common examples of iron sparing have been described in bacteria and yeast. Iron sparing in *Escherichia coli* is accomplished with RhyB (a small regulatory RNA), in *Bacillus subtilis* with the sRNA FsrA, and with the RNA-binding protein Cth2 in *Saccharomyces cerevisiae*. Common targets include succinate dehydrogenase (Complex II), aconitase (tricarboxylic acid cycle enzyme containing a [4Fe–4S]), and glutamate synthase (glutamate and nitrogen metabolism, two [4Fe–4S] and one [3Fe–4S]). Although analogous sRNAs or RNA-binding proteins remain to be discovered in plants and algae, iron-responsive microRNAs have been found in Arabidopsis (Kong and Yang 2010).

While iron sparing is well characterized in model bacterial and fungal organisms, how this strategy occurs and how it is regulated in plants and algae are relatively limited. Several plant transcriptome studies in low-iron nutrition revealed transcripts with reduced abundance in response to poor iron nutrition and among them are several mRNAs encoding iron-dependent proteins, and these are potential targets of iron sparing. In Arabidopsis these genes encode cytochrome P450s (heme), peroxidases (heme), Rieske [Fe–S] domain-containing proteins, 2OG–Fe (II) oxygenase family proteins, and the iron-dependent superoxide dismutase, FSD1, in the plastid (Dinneny et al. 2008; Long et al. 2010).

In *C. reinhardtii*, several transcripts of iron-containing proteins were shown to be repressed in a recent transcriptome study using RNA-Seq on cells grown in iron-sufficient (20 μM Fe), iron-deficient (1 μM Fe), and iron-limited (0.25 μM Fe) media in the presence (photoheterotrophic) or absence of acetate

(photoautotrophic) (Urzica et al. 2012). During the iron-limited state, several examples of putative iron-sparing events were found for both trophic conditions. During photoheterotrophic iron-limited growth, at least 25 transcripts encoding known or putative iron-dependent proteins are reduced twofold or more in abundance. The most highly decreased of these are linked to anaerobic growth, including hybrid-cluster proteins (HCP4, 28-fold; HCP1 20-fold), pyruvate–ferredoxin oxidoreductase (PRF1, 15-fold), hydrogenase assembly factors (HYDG, 15-fold; HYDEF, 11-fold), and ferredoxin–sulfite reductase (SIR1, 6-fold) (Urzica et al. 2012). Under the photoautotrophic iron-limited condition, at least ten transcripts encoding known or putative iron-dependent proteins are reduced in abundance. Seven transcripts encoding iron-dependent proteins are reduced in both iron-limited trophic conditions; these transcripts may represent core iron-sparing targets. Correlated reduction in protein abundance was confirmed using two independent quantitative proteomic studies for a protein similar to MitoNEET ([2Fe–2S]), the classic ferredoxin PETF ([2Fe–2S]), aconitase (4Fe–4S]), the hybrid-cluster protein HCP3 ([4Fe–4S], [4Fe–3O–3S]), glutamate synthase, NADH-dependent (GSN1, [3Fe–4S]), and an adenylylphosphosulfate reductase (APR1, [4Fe–4S]) (Hohner et al. 2013; Hsieh et al. 2013; Urzica et al. 2012).

On the other hand, there are few examples where the iron-containing proteins are degraded in response to low-iron nutrition as another mechanism to economize iron. Moseley et al. observed that in *C. reinhardtii* the subunits of the iron-rich PSI and cytochrome b_6f complexes are reduced in abundance within 24 h of iron starvation (Moseley et al. 2002a). The transcripts of these subunits, however, had roughly the same pattern of expression regardless of iron supply, leading the authors to conclude that reduction in complex abundance is not due to absence of transcript. The reduction in PSI and cytochrome b_6f could be due to programmed iron-deficiency-responsive proteolysis, since the authors also found protease activity specific to iron-starved cells, which was responsible for degrading some light-harvesting proteins (Moseley et al. 2002a).

A comparison between the transcriptome and proteome study revealed a decrease in the protein content of several iron-containing proteins but without any evident downregulation of the corresponding transcripts. These are L-ascorbate peroxidase (APX4, heme), 4-hydroxy-3-methylbut-2-enyl diphosphate reductase (IDS1, [4Fe–4S]), and 3-isopropylmalate dehydratase (LEU1L, [4Fe–4S]). The decrease of these proteins is either a response to poor iron nutrition-induced proteolysis or they may degrade because of the lack of the cofactor (Hsieh et al. 2013; Urzica et al. 2012).

While iron-sparing mechanism is supported by downregulation of gene expression, transcript degradation, and initiation of proteolysis, there are also some indispensable iron-dependent proteins that are preferentially maintained. This involves the increase in gene expression that leads to an induction of the corresponding mRNA levels in response to low-iron nutrition. Also mechanisms that prevent proteolysis and increasing the translation of the prioritized protein might be involved as well. On the other hand, the absence of mutilation could lead

to no enzymatic activity, which could have a regulatory feedback on the respective pathway leading to increase in transcript levels.

In *C. reinhardtii*, the best-characterized example of prioritizing one Fe-dependent enzyme over others is the chloroplast Fe-dependent superoxide dismutase (FeSOD). Page et al. showed that there is a hierarchical allocation of iron to chloroplast proteins. For example, the protein levels of cytochrome *f*, magnesium protoporphyrin monomethyl ester cyclase (a di-iron cyclase), and ferredoxin1 (FDX1) were severely reduced in response to iron limitation, whereas the protein abundance of FeSOD could be maintained under the same conditions. This raised the question how FeSOD is preferentially maintained when other Fe-containing proteins are all reduced in abundance. By monitoring the abundance of these chloroplast Fe-containing proteins over 5 days of iron starvation, the authors could demonstrate that FeSOD and the other Fe-dependent chloroplast proteins decreased in abundance in the first 24 h of Fe starvation, but while the protein levels of cytochrome *f*, di-iron cyclase, and FDX1 were constantly decreasing over the 5-day period, the FeSOD protein abundance started to recover and was fully restored to normal levels by day 5. Not only the protein levels were recovered but also the FeSOD activity, suggesting that FeSOD in the first 24 h is degraded due to lack of iron, but FeSOD is preferentially resynthesized and metalated over the other chloroplast Fe-containing proteins (Page et al. 2012).

2.5 Regulation of Iron-Deficiency Responses

To date there is no information on how iron homeostasis is regulated in *C. reinhardtii*. In higher plants, a number of transcription factors have been identified as components of the iron signaling response, including FIT1/FER, POPEYE (PYE), bHLH115, and ILR3 (Bauer et al. 2007; Brumbarova et al. 2008; Colangelo and Guerinot 2004; Ling et al. 2002). In addition, there is a posttranslational component involving an E3-ubiquitin ligase BRUTUS (BTS) (Long et al. 2010; Selote et al. 2015).

In the last years, several bHLH proteins have been identified as regulators of iron-deficiency responses in plants. In tomato, the bHLH protein, FER, was the first characterized factor that controls the iron-deficiency responses, and its mutant failed to activate iron acquisition strategy I (Ling et al. 2002). FIT1, a homolog of FER in *A. thaliana*, is required for the regulation of ferric-chelate reductase activity and Fe transport into the plant root, and its mutation was lethal when plants were grown in normal soils (Colangelo and Guerinot 2004; Jakoby et al. 2004; Yuan et al. 2005). Studies have indicated that FIT is dually regulated by iron starvation: at the transcriptional level, FIT is induced by iron deficiency (Colangelo and Guerinot 2004; Jakoby et al. 2004; Yuan et al. 2005), whereas at the posttranscriptional level, FIT is actively destabilized and degraded by the 26S proteasome during iron limitation (Meiser et al. 2011). Both FIT and bHLH38/39/100/101 function as positive regulators. In contrast, PYE was identified as a negative

regulator of iron-deficiency responses in *A. thaliana* (Long et al. 2010). PYE transcript levels were elevated under low-iron conditions, and its direct targets are several genes involved in metal homeostasis, such as nicotianamine synthase 4 (NAS4), FRO3, and zinc-induced facilitator 1 (ZIF1). In a *pye-1* mutant, the expression of these target genes is significantly upregulated in iron-deficient conditions, suggesting that PYE functions as a negative regulator. It is unclear how plants perceive iron status and transmit signals to downstream pathways. In mammals, FBXL5 functions as an iron sensor and contains a hemerythrin domain (HHE) for Fe binding and an F-box domain for ubiquitination and degradation of IRP2. The proteins IRP1 and IRP2 govern cellular iron homeostasis by regulation of translation and stability of mRNAs involved in iron homeostasis (Salahudeen et al. 2009; Vashisht et al. 2009). Interestingly the *A. thaliana* BRUTUS (BTS) and its rice orthologs, HRZ1 and HRZ2, possess HHE domains for binding Fe. Although they lack an F-box domain similar to that in FBXL5, BTS and HRZ1/HRZ2 have RING domains that can mediate the ubiquitination reaction. Functional analysis revealed that BTS and HRZ1/HRZ2 negatively regulate iron-deficiency responses in plants (Kobayashi et al. 2013; Selote et al. 2015). Given that BTS and HRZ1/HRZ2 are structurally and functionally similar to FBXL5, they are thought to be potential iron sensors in plants. Although no substrates for HRZ1/HRZ2 have been found, it is established that BTS interacts with three PYE-like proteins (bHLH104, bHLH105/ILR3, and bHLH115) and facilitates 26S proteasome-mediated degradation of bHLH105/IAA-LEUCINE RESISTANT3 (ILR3) and bHLH115 in the absence of Fe in vitro (Selote et al. 2015). Recently, Zhang et al. (2015) revealed that bHLH104 and bHLH105 positively regulate iron homeostasis by directly activating transcription of bHLH38/39/100/101 and PYE. Recent studies demonstrated that bHLH34 and bHLH104 play major roles in regulating iron homeostasis by activating the transcription of bHLH38/39/100/101 under iron-deficiency conditions (Li et al. 2016).

In *C. reinhardtii* most of the highly regulated genes (*FOX1*, *FTR1*, *FEA1*, and *MSD3*) are controlled at transcriptional level (Allen et al. 2007a; Page et al. 2012; Urzica et al. 2012). Using deletion analyses, two different iron response elements (FeREs) were identified in the 5′-flanking regions of the *FOX1*, *FTR1*, *FEA1*, and *ATX1* genes (Deng and Eriksson 2007; Fei and Deng 2007; Fei et al. 2009, 2010). These distinctive cis-acting elements are CAC(G/A)CG in the promoter regions of *FOX1*, *FEA2*, or *FER1* and TG(G/C)CA in the promoters of *FEA1*, *FRE1*, and *ATX1*. An unsupervised promoter analysis on different iron-deficiency gene sets showed that for short promoters, CACGCG is the most overrepresented 6mer, both for genes induced under both photoheterotrophic and photoautotrophic conditions (Urzica et al. 2012). Besides the FeREs, little else is known about the regulation of iron-deficient responses in *C. reinhardtii*. The *C. reinhardtii* Cre24.g770450 protein is similar to the *A. thaliana* group IV transcription factors (ILR3, bHLH34, bHLH104, and bHLH115), and its expression is increased in iron-poor conditions in both photoheterotrophically and photoautotrophically grown cells. Several other transcription factors are induced at the transcript level under iron-deficient and iron-limited conditions, and among them three MYB-like transcription factors (MYB4, MYB16, and Cre12.g514400) were identified (Urzica et al. 2012). MYB-like

transcription factors have been previously associated with iron deficiency in plants, where they might function as regulators of iron-deficiency responses (Chen et al. 2006; Ogo et al. 2006; Shen et al. 2008). Whether any of these genes can regulate the iron-deficiency responses in *C. reinhardtii* remains to be experimentally elucidated.

3 Copper Deficiency and Regulation

3.1 Copper Assimilation and Copper Chaperones

Copper can exist in two oxidation states (Cu^{+} and Cu^{2+}) and like iron can be found as a cofactor in many electron transfer proteins and different enzymes such as cytochrome oxidase, ferroxidase, or CuZn superoxide dismutase; thus copper is an essential micronutrient for most organisms. Copper homeostasis must be tightly regulated to maintain proper intracellular levels. Transporters that can import copper have been identified in several organisms. The *S. cerevisiae* Ctr1 and Ctr3 are plasma membrane copper transporters with redundant functions; only deletion of both could abolish the high-affinity copper uptake. The Fe^{3+}/Cu^{2+} reductase, FRE1, is required for maximal copper uptake, indicating that Cu^{+} is the substrate for the Ctr1 and Ctr3. The third CTR transporter in baker's yeast, Ctr2p, plays a role in mobilization of copper stores from the vacuole under conditions of copper deficiency (Rees et al. 2004).

CTR type of transporters was also identified in humans and plants. For example, hCTR1 is transporting Cu^{+} across the plasma membrane, and deletion of CTR1 homolog in mice is lethal (Lee et al. 2001). Once imported into the cells, copper is bound to cytosolic chaperones that deliver the metal to target proteins. In *A. thaliana*, the CTR-type transporters belong to a six-gene family of copper transporters (COPT1–6) (Penarrubia et al. 2010; Pilon et al. 2006). Of these, COPT1 and COPT2 are plasma membrane localized and can fully complement the Δ*ctr1* growth phenotype in yeast (Sancenon et al. 2003). COPT3 and COPT5 can only partially rescue defective mutants in copper transport, suggesting that they might be involved in intracellular copper transport. In plants, Cu must also be distributed to the chloroplast, and in *A. thaliana* the P-type ATPase transporters PAA1 and PAA2 translocate Cu across the envelope and thylakoid membranes, respectively (Abdel-Ghany et al. 2005; Shikanai et al. 2003).

C. reinhardtii genome encodes for four CTR-type transporters (COPT1 and CTR1–3) (Table 2). Besides the CTR type of transporters, the *C. reinhardtii* possesses five candidate copper-transporting P-type ATPases (CTP1–4 and HMA1) that are potentially involved in intracellular copper transport (Table 2). In *C. reinhardtii* the transcript levels of *CTR1*, *CTR2*, and *CTR3* are highly upregulated in response to copper deficiency. On the other hand, the abundance of CTP1–4, COPT1, and HMA1 was not significantly changed in copper-deficient cells (Castruita et al. 2011; Page et al. 2009).

Table 2 Known and putative copper transporters or potentially to be involved in copper acquisition

Transcript name	Gene name	Defline	Domain
Cre13.g570600.t1.2	*CTR1*	CTR-type copper ion transporter	Ctr copper transporter family
Cre10.g434350.t1.1	*CTR2*	CTR-type copper ion transporter	Ctr copper transporter family
Cre10.g434650.t1.1	*CTR3*	Copper transport related	
Cre05.g247050.t1.2	*COPT1*	CTR-type copper ion transporter	Ctr copper transporter family
Cre16.g682369.t1.1	*CTP1*	Heavy-metal-transporting ATPase	Heavy-metal-associated domain; E1–E2 ATPase; haloacid dehalogenase-like hydrolase
Cre10.g424775.t1.1	*CTP2*	Heavy-metal-transporting ATPase	Heavy-metal-associated domain; E1–E2 ATPase; haloacid dehalogenase-like hydrolase
Cre09.g406400.t1.1	*CTP3*	Heavy-metal-transporting ATPase	Heavy-metal-associated domain; E1–E2 ATPase; haloacid dehalogenase-like hydrolase
Cre10.g422201.t1.1	*CTP4*	Heavy-metal-transporting ATPase	Heavy-metal-associated domain; E1–E2 ATPase
Cre17.g720400.t1.1	*HMA1*	Heavy-metal-transporting ATPase	E1-E2 ATPase; haloacid dehalogenase-like hydrolase
Cre02.g082350.t1.1	*CUTA1*	Copper-binding protein CutA	CutA1 divalent ion tolerance protein
Cre17.g732700.t1.2	*CUTC*	Copper homeostasis protein cutC homolog	CutC family
Cre09.g392467.t1.1	*ATX1*	Copper chaperone	Heavy-metal-associated domain
Cre05.g248600.t1.2	*PCC1*	Copper ATPase	Heavy-metal-associated domain

Once copper is imported into the cell, it has to be incorporated into the major copper-containing proteins, ferroxidase (FOX1), plastocyanin in the chloroplast and cytochrome oxidase in the mitochondria. Since these cuproproteins are located in different cellular compartments, distinct pathways are used for copper delivery. The plasma membrane-localized ferroxidase has an extracellular active site with six

copper atoms. The copper chaperone ATX1 is predicted to deliver the copper to the Cu^{+}-transporting P-type ATPase (CTP1) in the trans-Golgi compartment where FOX1 is matured (Blaby-Haas and Merchant 2012; Merchant and Bogorad 1986b).

In *A. thaliana* copper transport into the chloroplasts depends on the HMA proteins P-type ATPase of Arabidopsis 1 (PAA1 or HMA6) and PAA2 (or HMA8), and analyses of chloroplast copper proteins in the *paa1* and *paa2* mutants demonstrate that both ATPases are required for copper delivery to plastocyanin (Puig et al. 2007). In *C. reinhardtii*, plastocyanin, with a single copper at its active site, is located in the thylakoid lumen, and the copper delivery to this compartment requires the related Cu+-transporting ATPases PAA1 and PAA2 (CTP2/Cre10.g424775 and CTP4/Cre10.g422201 in Chlamydomonas) in the envelope and thylakoid membranes, respectively (Pilon et al. 2006). Based on similarity to Arabidopsis PAA1 and PAA2, the Chlamydomonas protein CTP2 is predicted to pump copper across the inner membrane, and CTP4 is predicted to pump copper across the thylakoid membrane. Recently, a plant-specific copper chaperone has been identified to deliver Cu with specificity to PAA1. This Cu chaperone evolved early in the plant lineage by alternative-splicing event of the PAA1 pre-mRNA (Blaby-Haas et al. 2014).

Cytochrome oxidase is localized to the inner mitochondrial membrane and has three copper atoms associated with integral membrane subunits COX1 and COX2. In Chlamydomonas, COX2 consists of two domains, a membrane component COX2A and a soluble extramembrane domain COX2B, whose accumulation is used as a proxy for the whole complex. Cox17 is most likely involved in Cu trafficking toward mitochondrial cytochrome c oxidase (COX) as seen in yeast (Cobine et al. 2006).

3.2 Backup Proteins

Even that *C. reinhardtii* genome codes for several candidate cuproproteins, the transcriptome and proteome analyses indicate that the copper quota of the cell is dependent largely on only a few copper-containing proteins (Castruita et al. 2011). Plastocyanin is a blue copper protein that is required for photosynthesis and involved in transferring the electrons from cytochrome b_6f complex to PSI (Merchant and Sawaya 2005). *PCY1* mRNA which encodes the plastocyanin in *C. reinhardtii* is one of the most abundant transcripts in the cell (top 10 of >17,000 genes), consistent with the abundance of plastocyanin ($\sim 8 \times 10^6$ molecules per cell) (Castruita et al. 2011). The PCY1 gene is constitutively expressed, but the protein accumulates only in the presence of copper in the medium; in copper-deficient cells, plastocyanin is rapidly degraded (Merchant and Bogorad 1986a, b). A potential protease involved in plastocyanin degradation is RSEP1, a protein related to bacterial membrane metalloproteases. *RSEP1* expression is tightly regulated by copper nutrition (highly induced in response to copper deficiency) and dependent on the copper response regulator1 (CRR1) (Castruita et al. 2011). The

CYC6 gene which encodes for the heme-containing cyt c_6 is transcribed only in copper-deficient *C. reinhardtii* cells, and its expression replaces the loss of plastocyanin function, thus reducing the copper quota (Merchant and Bogorad 1986b). A remarkable feature is that in *C. reinhardtii*, plastocyanin and cyt c_6 are almost functionally equally efficient in reducing PSI (Hippler et al. 1997).

Other abundant transcripts include FOX1, encoding the copper-containing ferroxidase required for iron assimilation and hence more heavily expressed in iron-deficient cells; COX2A and COX2B, encoding one of two copper-binding subunits of cytochrome oxidase, which is essential for respiration in the mitochondria; and UOX1 encoding urate oxidase, which functions in nitrogen metabolism. The dominance of plastocyanin over other cuproproteins (e.g., 100-fold higher than urate oxidase) has been confirmed using quantitative proteomics of soluble *C. reinhardtii* fractions (Hsieh et al. 2013).

3.3 Regulation of Copper Homeostasis

Under copper-limiting conditions, to sustain photosynthesis and electron transport, *C. reinhardtii* replaces the copper-containing plastocyanin with the heme-containing cytochrome c_6. This replacement is transcriptionally activated via the copper-responsive elements (CuREs) present in the promoter sequence of *CYC6* gene. Responsible for the activation is the copper response regulator 1 (CRR1) (Kropat et al. 2005; Quinn and Merchant 1995). CRR1 is a member of the plant-specific squamosa promoter-binding protein (SBP) family of transcription factors. CRR1 possesses also ankyrin repeats, which are known protein–protein interaction modules, and a C-terminal Cys-rich region similar to metallothionein (Kropat et al. 2005). In Arabidopsis, the copper-responsive regulator is SPL7 which is the functional equivalent of CRR1 (Yamasaki et al. 2009). In *C. reinhardtii* the CRR1 binds to the CuREs and recognizes the GTAC core of these elements via its SBP domain (Quinn et al. 2000). The genes required for the acclimation to copper deficiency, like the assimilatory CTR transporters, Cyt c_6, and others, must possess in their 5′ UTRs the CuREs to allow the copper-deficient cells to maintain the essential metabolic pathways. CRR1 can bind copper ions via the SBP domain, but the copper-deficiency phenotype can be mimicked by additional Ni^{2+} ions which can induce the CRR1 regulon (Blaby-Haas et al. 2016).

Copper response defect 1 (CRD1) and copper target homolog 1 (CTH1) are two paralogues encoding alternatively regulating oxidative cyclases involved in the tetrapyrrole biosynthesis (Allen et al. 2008). The pattern of expression of these two cyclases is reciprocal*:* CRD1 accumulates in copper-deficient conditions and hypoxia, whereas CTH1 abundance is increased in copper-sufficient conditions (Moseley et al. 2002b). Regulation of cyclase accumulation is complex: in copper-replete conditions, a 2.1 kb *CTH1* mRNA is produced, and CTH1 protein accumulates. On the other hand, in copper deficiency, a 3.1 kb *CTH1* mRNA and the *CRD1* mRNA are produced, but only CRD1 protein accumulates (Moseley et al.

2002b). Deletion of *CRD1* results in a strong chlorotic phenotype under copper deficiency due to loss of PSI polypeptides (Moseley et al. 2000, 2002b). In addition to CRD1, it has been shown that several other genes (Cyt c_6 and coproporphyrinogen oxidase *CPX1*) are upregulated in both Cu-deficient conditions and hypoxia and are targets of the transcriptional regulator (Eriksson et al. 2004; Quinn et al. 2000, 2002).

Recently, a transcriptome survey of copper-deficient wild-type and *crr1*–2 mutant cells identified the main CRR1 targets. This study identified 63 CRR1 targets plus another 86 copper-responsive genes (Castruita et al. 2011). Among the CRR1 targets, several putative plastid proteins could be identified: a highly conserved protein CGL78, ferredoxins FDX5 and FDX6, and a thylakoid membrane protease RSEP1. As mentioned, RSEP1 might play a role in plastocyanin degradation. The role of CRR1 target genes under hypoxia is essential for cells, since the *crr1* mutant has a severe growth defect in hypoxic conditions in the light. Genes known to be important for the copper deficiency response of *C. reinhardtii* are activated in hypoxia, and genes known to be responsive to O_2 limitation, such as iron-hydrogenase subunit *HYDA1* and pyruvate/ferredoxin oxidoreductase *PFR1*, are also induced in copper-deficient cells (Castruita et al. 2011; Eriksson et al. 2004; Hemschemeier et al. 2013).

4 Other Metals

4.1 Zinc

In addition to iron and copper, zinc is an another essential micronutrient since many enzymes contain zinc as a cofactor, usually coordinated via the zinc-binding domains (Andreini et al. 2006). Intracellular zinc content must be regulated to ensure that zinc-containing proteins can function; therefore, the zinc uptake must be tightly regulated. The intracellular zinc status controls the expression of low- and high-affinity transporters at the plasma membrane. Zinc compartmentalization is also important; specific transporters can sequester zinc in the vacuole (in fungi, plants), lysosome-related compartments (in *Caenorhabditis elegans*), or zincosomes (in mammalian cells) in a situation of excess (Ehrensberger and Bird 2011; Eide 2009; Sinclair and Kramer 2012).

Two families of transporters have been implicated in zinc assimilation and compartmentalization: the ZIP (Zrt-, Irt-like protein) family and the CDF (cation diffusion facilitator) family. The ZIP transporters usually play a role in moving either zinc or iron into the cytoplasm, whereas the CDF type of transporters functions primarily to move zinc out of the cytoplasm (Blaby-Haas and Merchant 2012). *C. reinhardtii* genome encodes for 14 members of ZIP family transporters based on the homology to known plant, yeast, and human transporters (Table 3).

Table 3 Known and putative zinc transporters or known to be involved in zinc assimilation and trafficking

Transcript name	Gene name	Defline	Domain
Cre03.g145087.t1.1	*MTP1*	CDF transporter	Cation efflux family
Cre02.g087400.t1.2	*ZIL1*	ZIP family transporter-like	ZIP zinc transporter
Cre06.g281900.t1.2	*ZIL2*	ZIP family transporter-like	ZIP zinc transporter
Cre07.g355100.t1.2	*ZIP1*	ZIP family transporter	ZIP zinc transporter
Cre13.g576050.t1.1	*ZIP2*	ZIP family transporter	ZIP zinc transporter
Cre03.g189500.t1.2	*ZIP3*	ZIP family transporter	NUDIX domain
Cre09.g392060.t1.1	*ZIP4*	ZIP family transporter	ZIP zinc transporter
Cre06.g299600.t1.2	*ZIP6*	ZIP family transporter	ZIP zinc transporter
Cre07.g351950.t1.1	*ZRT1*	Zinc-nutrition responsive transporter	ZIP zinc transporter
Cre01.g000150.t1.2	*ZRT2*	Zinc-nutrition responsive transporter	ZIP zinc transporter
Cre13.g573950.t1.1	*ZRT3*	Zinc-nutrition responsive transporter	ZIP zinc transporter
Cre01.g066187.t1.1	*ZRT4*	Zinc-nutrition responsive transporter	ZIP zinc transporter
Cre07.g355150.t1.1	*ZRT5*	Zinc-nutrition responsive transporter	ZIP zinc transporter
Cre12.g536900.t1.1	*ZCP1*	Zinc-responsive COG0523 domain-containing protein	CobW/HypB/UreG, nucleotide-binding domain
Cre02.g118400.t1.1	*ZCP2*	Zinc-responsive COG0523 domain-containing protein	CobW/HypB/UreG, nucleotide-binding domain

In *C. reinhardtii* four nutritional zinc conditions have been identified: toxic, replete, deficient, and limited. Growth is inhibited in zinc-limited and zinc-toxic cells relative to zinc replete cells, whereas zinc deficiency can only be distinguished by the accumulation of transcripts encoding ZIP family transporters. In a recent transcriptome study, the mechanisms to zinc acclimation and the targets of different zinc nutritional conditions were analyzed (Malasarn et al. 2013). The authors found out that five ZIP transporters (ZRT1-5) and two potentially zinc chaperones (ZCP1–2) (zinc-responsive COG0523 domain-containing protein) are significantly changed in abundance under zinc-limited conditions. In addition, zinc deficiency has an impact on two other regulatory pathways, the carbon concentrating mechanism (CCM) and the nutritional copper regulon. Targets of transcription factor Ccm1 and various genes coding for carbonic anhydrases are upregulated in zinc deficiency. As a consequence, Chlamydomonas cells are not able to grow photoautotrophically under zinc-limiting conditions. As mentioned above, Crr1 regulon responds to copper limitation but is also turned on in zinc deficiency, and Crr1 is required for growth in zinc-limiting conditions. Zinc-deficient cells are functionally copper deficient, and they hyperaccumulate copper up to 20-fold over normal levels (Malasarn et al. 2013). The copper accumulates in lysosome-related acidic organelles called acidocalcisomes and it co-localizes with calcium as visualized per confocal microscopy (Hong-Hermesdorf et al. 2014). Elemental analysis of these compartments that overaccumulate under zinc-limited conditions revealed increased Ca and Cu content when isolated from zinc-deficiency conditions. The copper that hyperaccumulates in the cells under zinc limitation is bioavailable, since it can be remobilized from the acidic compartments and can be sensed by the copper-transcriptional regulator CRR1 and used for the synthesis of plastocyanin (Hong-Hermesdorf et al. 2014).

4.2 Manganese

Manganese is an essential micronutrient for phototrophic growth, since it is present in the polynuclear cluster in PSII and required for the water-splitting reaction (Merchant and Sawaya 2005). The main enzymes in algae that use manganese are the superoxide dismutases (MnSOD). The assimilation of manganese in eukaryotes is performed by the members of the NRAMP family. In *A. thaliana* the NRAMP1 is located at the plasma membrane and induced by manganese deficiency. An nramp1-1 mutant in *A. thaliana* has impaired growth and less manganese levels compared to wild type under limiting manganese concentrations suggesting that is the major high-affinity manganese transporter (Cailliatte et al. 2010). In addition, the *A. thaliana NRAMP1* transcript is induced also by iron deficiency and fails to rescue a yeast mutant defective in the *FET3* and *FET4* (*fet3fet4*) iron importers, suggesting that NRAMP1 can also take up iron (Curie et al. 2000). At least two other members of the NRAMP family (NRAMP3 and NRAMP4) are involved in intracellular distribution of manganese in *A. thaliana*. Both are localized in the

Table 4 Known and putative manganese transporters

Transcript name	Gene name	Defline	Domain
Cre17.g707700.t1.2	*NRAMP1*	Natural resistance-associated macrophage protein	NRAMP
Cre07.g321951.t1.1	*NRAMP2*	Natural resistance-associated macrophage protein	NRAMP
Cre03.g160800.t1.2	*MTP2*	CDF transporter, membrane protein	Cation efflux family
Cre03.g160750.t1.1	*MTP3*	CDF transporter, membrane protein	Cation efflux family
Cre03.g160550.t1.1	*MTP4*	CDF transporter, membrane protein	Cation efflux family
Cre06.g289150.t1.1	*MTP5*	CDF transporter, membrane protein	Cation efflux family

vacuolar membrane, and in addition to manganese release from the vacuole, they also transport iron (Lanquar et al. 2005, 2010). In *C. reinhardtii* four members of the NRAMP family have been identified (NRAMP1, NRAMP2, RET1, and NRAMP4). NRAMP1 and NRAMP2 are bacterial-like MntH class of Mn–Fe transporters, while NRAMP4 is similar to the eukaryotic-type AtNRAMP3 and AtNRAMP4 from Arabidopsis (Blaby-Haas and Merchant 2012).

The members of a second family, cation diffusion facilitator (CDF), are also predicted to play a role in manganese transport. *C. reinhardtii* CDF proteins MTP2, MTP3, and MTP4 are predicted to transport manganese based on phylogenetic relationships, while *MTP2* and *MTP5* transcripts are three- and fivefold more abundant in manganese-limited conditions (Allen et al. 2007b). Under conditions of manganese deficiency, cells show a slower growth, and the activity of PSII is compromised (decreased photosynthesis quantum efficiency). The oxygen evolving enhancer proteins (OEE1–3) are slightly decreased under manganese deprivation, but they are not localized anymore to the membrane, suggesting that manganese is mostly required to stabilize the complex on the membrane (Allen et al. 2007b; Hsieh et al. 2013) (Table 4).

Low-manganese nutrition has an impact on the activity of the major MnSOD in *C. reinhardtii*, and the cells are sensitive to peroxide stress, most likely do to the loss of MnSOD activities, known to possess antioxidant functions. Manganese deficiency also leads to secondary iron deficiency and contains less intracellular iron content, which might suggest that mechanisms to reduce iron levels in order to protect the cells from increased oxidative stress are active (Allen et al. 2007b). A proteome study of manganese-deficient and manganese-limited cells indicated that the components of the 20S and 26S proteasomes and the T-complex chaperonin were increased in low-manganese nutrition relative to the replete situation. This increase in the proteasome levels suggests an overall increase in the amount of proteolysis occurring in manganese-deficient cells, possibly due to increased levels of oxidative damage (Hsieh et al. 2013).

5 Conclusions and Perspective

The micronutrient ions described in this chapter (Fe, Cu, Zn, and Mn) fulfil multiple key functions in *Chlamydomonas reinhardtii* cell. In particular the chloroplast and mitochondria have important requirements for these metals. Recent work revealed that complex acclimation mechanisms evolved to allow maintenance of the photosynthetic function under metals deficiency. Several transcription factors that coordinate the deficiency responses have been identified or proposed to play a role in the regulation of metal homeostasis. However, further work will be required to determine how the metal status is sensed in the Chlamydomonas cell and how it is signaled to other compartments to adapt uptake and trafficking in the cell.

Except for copper, the uptake systems for other metals (e.g., iron, zinc, manganese) in chloroplasts and mitochondria remain to be identified.

Recent studies started to shed light on the interactions between metal homeostases of chloroplasts, mitochondria, and/or vacuoles. For example, copper that hyperaccumulates in the cells under zinc limitation can be remobilized from the acidic compartments and can be sensed by the copper-transcriptional regulator CRR1 and used for the synthesis of plastocyanin indicating that it is bioavailable (Hong-Hermesdorf et al. 2014).

In conclusion, many open questions remain regarding the metal homeostasis inside the organelles and the crosstalk of metals between organelles and represent topical avenues for future investigations.

Acknowledgments The research of EIU is funded by the Deutsche Forschungsgemeinschaft (Grant no. UR 269/1-1).

References

Abdel-Ghany SE, Muller-Moule P, Niyogi KK, Pilon M, Shikanai T (2005) Two P-type ATPases are required for copper delivery in Arabidopsis thaliana chloroplasts. Plant Cell 17 (4):1233–1251. doi:10.1105/tpc.104.030452

Allen MD, del Campo JA, Kropat J, Merchant SS (2007a) FEA1, FEA2, and FRE1, encoding two homologous secreted proteins and a candidate ferrireductase, are expressed coordinately with FOX1 and FTR1 in iron-deficient Chlamydomonas reinhardtii. Eukaryot Cell 6 (10):1841–1852. doi:10.1128/EC.00205-07

Allen MD, Kropat J, Tottey S, Del Campo JA, Merchant SS (2007b) Manganese deficiency in Chlamydomonas results in loss of photosystem II and MnSOD function, sensitivity to peroxides, and secondary phosphorus and iron deficiency. Plant Physiol 143(1):263–277. doi:10.1104/pp.106.088609

Allen MD, Kropat J, Merchant SS (2008) Regulation and localization of isoforms of the aerobic oxidative cyclase in Chlamydomonas reinhardtii. Photochem Photobiol 84(6):1336–1342. doi:10.1111/j.1751-1097.2008.00440.x

Allmer J, Naumann B, Markert C, Zhang M, Hippler M (2006) Mass spectrometric genomic data mining: novel insights into bioenergetic pathways in *Chlamydomonas reinhardtii*. Proteomics 6(23):6207–6220

Andreini C, Banci L, Bertini I, Rosato A (2006) Zinc through the three domains of life. J Proteome Res 5(11):3173–3178. doi:10.1021/pr0603699

Andrews NC (2000) Iron homeostasis: insights from genetics and animal models. Nat Rev Genet 1 (3):208–217

Atteia A, Adrait A, Brugiere S, Tardif M, van Lis R, Deusch O, Dagan T, Kuhn L, Gontero B, Martin W, Garin J, Joyard J, Rolland N (2009) A proteomic survey of *Chlamydomonas reinhardtii* mitochondria sheds new light on the metabolic plasticity of the organelle and on the nature of the alpha-proteobacterial mitochondrial ancestor. Mol Biol Evol 26 (7):1533–1548

Bashir K, Ishimaru Y, Nishizawa NK (2011a) Identification and characterization of the major mitochondrial Fe transporter in rice. Plant Signal Behav 6(10):1591–1593. doi:10.4161/psb.6.10.17132

Bashir K, Ishimaru Y, Shimo H, Nagasaka S, Fujimoto M, Takanashi H, Tsutsumi N, An G, Nakanishi H, Nishizawa NK (2011b) The rice mitochondrial iron transporter is essential for plant growth. Nat Commun 2:322. doi:10.1038/ncomms1326

Bauer P, Ling HQ, Guerinot ML (2007) FIT, the FER-like iron deficiency induced transcription factor in Arabidopsis. Plant Physiol Biochem 45(5):260–261

Blaby-Haas CE, Merchant SS (2012) The ins and outs of algal metal transport. Biochim Biophys Acta 1823(9):1531–1552. doi:10.1016/j.bbamcr.2012.04.010

Blaby-Haas CE, Merchant SS (2014) Lysosome-related organelles as mediators of metal homeostasis. J Biol Chem 289(41):28129–28136. doi:10.1074/jbc.R114.592618

Blaby-Haas CE, Padilla-Benavides T, Stube R, Arguello JM, Merchant SS (2014) Evolution of a plant-specific copper chaperone family for chloroplast copper homeostasis. Proc Natl Acad Sci U S A 111(50):E5480–E5487. doi:10.1073/pnas.1421545111

Blaby-Haas CE, Castruita M, Fitz-Gibbon ST, Kropat J, Merchant SS (2016) Ni induces the CRR1-dependent regulon revealing overlap and distinction between hypoxia and Cu deficiency responses in Chlamydomonas reinhardtii. Metallomics. doi:10.1039/c6mt00063k

Brumbarova T, Matros A, Mock HP, Bauer P (2008) A proteomic study showing differential regulation of stress, redox regulation and peroxidase proteins by iron supply and the transcription factor FER. Plant J 54(2):321–334

Brumbarova T, Bauer P, Ivanov R (2015) Molecular mechanisms governing Arabidopsis iron uptake. Trends Plant Sci 20(2):124–133. doi:10.1016/j.tplants.2014.11.004

Buchanan-Wollaston V, Ainsworth C (1997) Leaf senescence in Brassica napus: cloning of senescence related genes by subtractive hybridisation. Plant Mol Biol 33(5):821–834

Buckhout TJ, Yang TJ, Schmidt W (2009) Early iron-deficiency-induced transcriptional changes in Arabidopsis roots as revealed by microarray analyses. BMC Genomics 10:147

Busch A, Rimbauld B, Naumann B, Rensch S, Hippler M (2008) Ferritin is required for rapid remodeling of the photosynthetic apparatus and minimizes photo-oxidative stress in response to iron availability in Chlamydomonas reinhardtii. Plant J 55(2):201–211. doi:10.1111/j.1365-313X.2008.03490.x

Cailliatte R, Schikora A, Briat JF, Mari S, Curie C (2010) High-affinity manganese uptake by the metal transporter NRAMP1 is essential for Arabidopsis growth in low manganese conditions. Plant Cell 22(3):904–917. doi:10.1105/tpc.109.073023

Castruita M, Casero D, Karpowicz SJ, Kropat J, Vieler A, Hsieh SI, Yan W, Cokus S, Loo JA, Benning C, Pellegrini M, Merchant SS (2011) Systems biology approach in Chlamydomonas reveals connections between copper nutrition and multiple metabolic steps. Plant Cell 23 (4):1273–1292. doi:10.1105/tpc.111.084400

Chasteen ND (1998) Ferritin. Uptake, storage, and release of iron. Met Ions Biol Syst 35:479–514

Chen YH, Wu XM, Ling HQ, Yang WC (2006) Transgenic expression of DwMYB2 impairs iron transport from root to shoot in *Arabidopsis thaliana*. Cell Res 16(10):830–840

Chen JC, Hsieh SI, Kropat J, Merchant SS (2008) A ferroxidase encoded by FOX1 contributes to iron assimilation under conditions of poor iron nutrition in Chlamydomonas. Eukaryot Cell 7 (3):541–545. doi:10.1128/EC.00463-07

Cobine PA, Pierrel F, Winge DR (2006) Copper trafficking to the mitochondrion and assembly of copper metalloenzymes. Biochim Biophys Acta 1763(7):759–772. doi:10.1016/j.bbamcr.2006.03.002

Colangelo EP, Guerinot ML (2004) The essential basic helix-loop-helix protein FIT1 is required for the iron deficiency response. Plant Cell 16(12):3400–3412

Connolly EL, Fett JP, Guerinot ML (2002) Expression of the IRT1 metal transporter is controlled by metals at the levels of transcript and protein accumulation. Plant Cell 14(6):1347–1357

Conte S, Stevenson D, Furner I, Lloyd A (2009) Multiple antibiotic resistance in Arabidopsis is conferred by mutations in a chloroplast-localized transport protein. Plant Physiol 151(2):559–573. doi:10.1104/pp.109.143487

Courville P, Chaloupka R, Cellier MF (2006) Recent progress in structure-function analyses of Nramp proton-dependent metal-ion transporters. Biochem Cell Biol 84(6):960–978

Curie C, Alonso JM, Le Jean M, Ecker JR, Briat JF (2000) Involvement of NRAMP1 from Arabidopsis thaliana in iron transport. Biochem J 347(Pt 3):749–755

Curie C, Cassin G, Couch D, Divol F, Higuchi K, Le Jean M, Misson J, Schikora A, Czernic P, Mari S (2009) Metal movement within the plant: contribution of nicotianamine and yellow stripe 1-like transporters. Ann Bot 103(1):1–11. doi:10.1093/aob/mcn207

Deng X, Eriksson M (2007) Two iron-responsive promoter elements control expression of *FOX1* in *Chlamydomonas reinhardtii*. Eukaryot Cell 6(11):2163–2167

Dinneny JR, Long TA, Wang JY, Jung JW, Mace D, Pointer S, Barron C, Brady SM, Schiefelbein J, Benfey PN (2008) Cell identity mediates the response of Arabidopsis roots to abiotic stress. Science 320(5878):942–945

Ehrensberger KM, Bird AJ (2011) Hammering out details: regulating metal levels in eukaryotes. Trends Biochem Sci 36(10):524–531. doi:10.1016/j.tibs.2011.07.002

Eide DJ (2009) Homeostatic and adaptive responses to zinc deficiency in Saccharomyces cerevisiae. J Biol Chem 284(28):18565–18569. doi:10.1074/jbc.R900014200

Eriksson M, Moseley JL, Tottey S, Del Campo JA, Quinn J, Kim Y, Merchant S (2004) Genetic dissection of nutritional copper signaling in chlamydomonas distinguishes regulatory and target genes. Genetics 168(2):795–807. doi:10.1534/genetics.104.030460

Fei X, Deng X (2007) A novel Fe deficiency-responsive element (FeRE) regulates the expression of *atx1* in *Chlamydomonas reinharditii*. Plant Cell Physiol 48(10):1496–1503

Fei X, Eriksson M, Yang J, Deng X (2009) An Fe deficiency responsive element with a core sequence of TGGCA regulates the expression of *FEA1* in *Chlamydomonas reinhardtii*. J Biochem 146(2):157–166

Fei X, Eriksson M, Li Y, Deng X (2010) A novel negative Fe-deficiency-responsive element and a TGGCA-type-like FeRE control the expression of *FTR1* in *Chlamydomonas reinhardtii*. J Biomed Biotechnol 2010:790247

Fleming PJ, Kent UM (1991) Cytochrome b_{561}, ascorbic acid, and transmembrane electron transfer. Am J Clin Nutr 54(6 Suppl):1173S–1178S

Fleming MD, Trenor CC III, Su MA, Foernzler D, Beier DR, Dietrich WF, Andrews NC (1997) Microcytic anaemia mice have a mutation in Nramp2, a candidate iron transporter gene. Nat Genet 16(4):383–386

Froschauer EM, Schweyen RJ, Wiesenberger G (2009) The yeast mitochondrial carrier proteins Mrs3p/Mrs4p mediate iron transport across the inner mitochondrial membrane. Biochim Biophys Acta 1788(5):1044–1050. doi:10.1016/j.bbamem.2009.03.004

Hanikenne M, Merchant SS, Hamel PP (2008) Transition metal nutrition: a balance between deficiency and toxicity. The Chlamydomonas sourcebook, vol 2, 2nd edn. Academic, San Diego

Harris EH (2009) The Chlamydomonas sourcebook, 2nd edn. Academic, San Diego

Harrison PM, Arosio P (1996) The ferritins: molecular properties, iron storage function and cellular regulation. Biochim Biophys Acta 1275(3):161–203

Hemschemeier A, Casero D, Liu B, Benning C, Pellegrini M, Happe T, Merchant SS (2013) Copper response regulator1-dependent and -independent responses of the Chlamydomonas

reinhardtii transcriptome to dark anoxia. Plant Cell 25(9):3186–3211. doi:10.1105/tpc.113.115741

Hippler M, Drepper F, Farah J, Rochaix JD (1997) Fast electron transfer from cytochrome c6 and plastocyanin to photosystem I of Chlamydomonas reinhardtii requires PsaF. Biochemistry 36 (21):6343–6349. doi:10.1021/bi970082c

Hohner R, Barth J, Magneschi L, Jaeger D, Niehues A, Bald T, Grossman A, Fufezan C, Hippler M (2013) The metabolic status drives acclimation of iron deficiency responses in Chlamydomonas reinhardtii as revealed by proteomics based hierarchical clustering and reverse genetics. Mol Cell Proteomics 12(10):2774–2790. doi:10.1074/mcp.M113.029991

Hong-Hermesdorf A, Miethke M, Gallaher SD, Kropat J, Dodani SC, Chan J, Barupala D, Domaille DW, Shirasaki DI, Loo JA, Weber PK, Pett-Ridge J, Stemmler TL, Chang CJ, Merchant SS (2014) Subcellular metal imaging identifies dynamic sites of Cu accumulation in Chlamydomonas. Nat Chem Biol 10(12):1034–1042. doi:10.1038/nchembio.1662

Hsieh SI, Castruita M, Malasarn D, Urzica E, Erde J, Page MD, Yamasaki H, Casero D, Pellegrini M, Merchant SS, Loo JA (2013) The proteome of copper, iron, zinc, and manganese micronutrient deficiency in Chlamydomonas reinhardtii. Mol Cell Proteomics 12(1):65–86. doi:10.1074/mcp.M112.021840

Ishimaru Y, Suzuki M, Tsukamoto T, Suzuki K, Nakazono M, Kobayashi T, Wada Y, Watanabe S, Matsuhashi S, Takahashi M, Nakanishi H, Mori S, Nishizawa NK (2006) Rice plants take up iron as an Fe3+-phytosiderophore and as Fe2+. Plant J 45(3):335–346. doi:10.1111/j.1365-313X.2005.02624.x

Jakoby M, Wang HY, Reidt W, Weisshaar B, Bauer P (2004) *FRU* (*BHLH029*) is required for induction of iron mobilization genes in *Arabidopsis thaliana*. FEBS Lett 577(3):528–534

Jeong J, Guerinot ML (2009) Homing in on iron homeostasis in plants. Trends Plant Sci 14 (5):280–285. doi:10.1016/j.tplants.2009.02.006

Jeong J, Cohu C, Kerkeb L, Pilon M, Connolly EL, Guerinot ML (2008) Chloroplast Fe(III) chelate reductase activity is essential for seedling viability under iron limiting conditions. Proc Natl Acad Sci U S A 105(30):10619–10624

Kim SA, Punshon T, Lanzirotti A, Li L, Alonso JM, Ecker JR, Kaplan J, Guerinot ML (2006) Localization of iron in Arabidopsis seed requires the vacuolar membrane transporter VIT1. Science 314(5803):1295–1298

Kobayashi T, Nagasaka S, Senoura T, Itai RN, Nakanishi H, Nishizawa NK (2013) Iron-binding haemerythrin RING ubiquitin ligases regulate plant iron responses and accumulation. Nat Commun 4:2792. doi:10.1038/ncomms3792

Kong WW, Yang ZM (2010) Identification of iron-deficiency responsive microRNA genes and cis-elements in Arabidopsis. Plant Physiol Biochem 48(2-3):153–159. doi:10.1016/j.plaphy.2009.12.008

Koorts AM, Viljoen M (2007) Ferritin and ferritin isoforms I: structure-function relationships, synthesis, degradation and secretion. Arch Physiol Biochem 113(1):30–54. doi:10.1080/13813450701318583

Kosman DJ (2003) Molecular mechanisms of iron uptake in fungi. Mol Microbiol 47 (5):1185–1197

Kropat J, Tottey S, Birkenbihl RP, Depege N, Huijser P, Merchant S (2005) A regulator of nutritional copper signaling in Chlamydomonas is an SBP domain protein that recognizes the GTAC core of copper response element. Proc Natl Acad Sci U S A 102(51):18730–18735. doi:10.1073/pnas.0507693102

La Fontaine S, Quinn JM, Nakamoto SS, Page MD, Gohre V, Moseley JL, Kropat J, Merchant S (2002) Copper-dependent iron assimilation pathway in the model photosynthetic eukaryote Chlamydomonas reinhardtii. Eukaryot Cell 1(5):736–757

Lanquar V, Lelievre F, Bolte S, Hames C, Alcon C, Neumann D, Vansuyt G, Curie C, Schroder A, Kramer U, Barbier-Brygoo H, Thomine S (2005) Mobilization of vacuolar iron by AtNRAMP3 and AtNRAMP4 is essential for seed germination on low iron. EMBO J 24(23):4041–4051. doi:10.1038/sj.emboj.7600864

Lanquar V, Ramos MS, Lelievre F, Barbier-Brygoo H, Krieger-Liszkay A, Kramer U, Thomine S (2010) Export of vacuolar manganese by AtNRAMP3 and AtNRAMP4 is required for optimal photosynthesis and growth under manganese deficiency. Plant Physiol 152(4):1986–1999. doi:10.1104/pp.109.150946

Lee J, Prohaska JR, Thiele DJ (2001) Essential role for mammalian copper transporter Ctr1 in copper homeostasis and embryonic development. Proc Natl Acad Sci U S A 98(12):6842–6847. doi:10.1073/pnas.111058698

Levi S, Salfeld J, Franceschinelli F, Cozzi A, Dorner MH, Arosio P (1989) Expression and structural and functional properties of human ferritin L-chain from Escherichia coli. Biochemistry 28(12):5179–5184

Li L, Chen OS, McVey Ward D, Kaplan J (2001) CCC1 is a transporter that mediates vacuolar iron storage in yeast. J Biol Chem 276(31):29515–29519

Li XL, Zhang HM, Ai Q, Liang G, Yu D (2016) Two bHLH transcription factors, bHLH34 and bHLH104, regulate iron homeostasis in *Arabidopsis thaliana*. Plant Physiol. doi:10.1104/pp.15.01827

Ling HQ, Bauer P, Bereczky Z, Keller B, Ganal M (2002) The tomato *fer* gene encoding a bHLH protein controls iron-uptake responses in roots. Proc Natl Acad Sci U S A 99(21):13938–13943

Lobréaux S, Briat JF (1991) Ferritin accumulation and degradation in different organs of pea (*Pisum sativum*) during development. Biochem J 274(Pt 2):601–606

Long JC, Merchant SS (2008) Photo-oxidative stress impacts the expression of genes encoding iron metabolism components in Chlamydomonas. Photochem Photobiol 84(6):1395–1403. doi:10.1111/j.1751-1097.2008.00451.x

Long JC, Sommer F, Allen MD, Lu SF, Merchant SS (2008) FER1 and FER2 encoding two ferritin complexes in Chlamydomonas reinhardtii chloroplasts are regulated by iron. Genetics 179 (1):137–147. doi:10.1534/genetics.107.083824

Long TA, Tsukagoshi H, Busch W, Lahner B, Salt DE, Benfey PN (2010) The bHLH transcription factor POPEYE regulates response to iron deficiency in Arabidopsis roots. Plant Cell 22 (7):2219–2236

MacDiarmid CW, Milanick MA, Eide DJ (2003) Induction of the ZRC1 metal tolerance gene in zinc-limited yeast confers resistance to zinc shock. J Biol Chem 278(17):15065–15072

Malasarn D, Kropat J, Hsieh SI, Finazzi G, Casero D, Loo JA, Pellegrini M, Wollman FA, Merchant SS (2013) Zinc deficiency impacts CO2 assimilation and disrupts copper homeostasis in Chlamydomonas reinhardtii. J Biol Chem 288(15):10672–10683. doi:10.1074/jbc.M113.455105

Martinoia E, Maeshima M, Neuhaus HE (2007) Vacuolar transporters and their essential role in plant metabolism. J Exp Bot 58(1):83–102. doi:10.1093/jxb/erl183

Martinoia E, Meyer S, De Angeli A, Nagy R (2012) Vacuolar transporters in their physiological context. Annu Rev Plant Biol 63:183–213. doi:10.1146/annurev-arplant-042811-105608

McKie AT (2008) The role of Dcytb in iron metabolism: an update. Biochem Soc Trans 36 (Pt 6):1239–1241

McKie AT, Barrow D, Latunde-Dada GO, Rolfs A, Sager G, Mudaly E, Mudaly M, Richardson C, Barlow D, Bomford A, Peters TJ, Raja KB, Shirali S, Hediger MA, Farzaneh F, Simpson RJ (2001) An iron-regulated ferric reductase associated with the absorption of dietary iron. Science 291(5509):1755–1759

Meiser J, Lingam S, Bauer P (2011) Posttranslational regulation of the iron deficiency basic helix-loop-helix transcription factor FIT is affected by iron and nitric oxide. Plant Physiol 157 (4):2154–2166. doi:10.1104/pp.111.183285

Merchant S, Bogorad L (1986a) Rapid degradation of apoplastocyanin in Cu(II)-deficient cells of Chlamydomonas reinhardtii. J Biol Chem 261(34):15850–15853

Merchant S, Bogorad L (1986b) Regulation by copper of the expression of plastocyanin and cytochrome c552 in Chlamydomonas reinhardtii. Mol Cell Biol 6(2):462–469

Merchant S, Sawaya MR (2005) The light reactions: a guide to recent acquisitions for the picture gallery. Plant Cell 17(3):648–663. doi:10.1105/tpc.105.030676

Merchant SS, Allen MD, Kropat J, Moseley JL, Long JC, Tottey S, Terauchi AM (2006) Between a rock and a hard place: trace element nutrition in Chlamydomonas. Biochim Biophys Acta 1763(7):578–594. doi:10.1016/j.bbamcr.2006.04.007

Merchant SS, Prochnik SE, Vallon O, Harris EH, Karpowicz SJ, Witman GB, Terry A, Salamov A, Fritz-Laylin LK, Marechal-Drouard L, Marshall WF, Qu LH, Nelson DR, Sanderfoot AA, Spalding MH, Kapitonov VV, Ren Q, Ferris P, Lindquist E, Shapiro H, Lucas SM, Grimwood J, Schmutz J, Cardol P, Cerutti H, Chanfreau G, Chen CL, Cognat V, Croft MT, Dent R, Dutcher S, Fernandez E, Fukuzawa H, Gonzalez-Ballester D, Gonzalez-Halphen D, Hallmann A, Hanikenne M, Hippler M, Inwood W, Jabbari K, Kalanon M, Kuras R, Lefebvre PA, Lemaire SD, Lobanov AV, Lohr M, Manuell A, Meier I, Mets L, Mittag M, Mittelmeier T, Moroney JV, Moseley J, Napoli C, Nedelcu AM, Niyogi K, Novoselov SV, Paulsen IT, Pazour G, Purton S, Ral JP, Riano-Pachon DM, Riekhof W, Rymarquis L, Schroda M, Stern D, Umen J, Willows R, Wilson N, Zimmer SL, Allmer J, Balk J, Bisova K, Chen CJ, Elias M, Gendler K, Hauser C, Lamb MR, Ledford H, Long JC, Minagawa J, Page MD, Pan J, Pootakham W, Roje S, Rose A, Stahlberg E, Terauchi AM, Yang P, Ball S, Bowler C, Dieckmann CL, Gladyshev VN, Green P, Jorgensen R, Mayfield S, Mueller-Roeber B, Rajamani S, Sayre RT, Brokstein P, Dubchak I, Goodstein D, Hornick L, Huang YW, Jhaveri J, Luo Y, Martinez D, Ngau WC, Otillar B, Poliakov A, Porter A, Szajkowski L, Werner G, Zhou K, Grigoriev IV, Rokhsar DS, Grossman AR (2007) The Chlamydomonas genome reveals the evolution of key animal and plant functions. Science 318(5848):245–250. doi:10.1126/science.1143609

Morrissey J, Baxter IR, Lee J, Li L, Lahner B, Grotz N, Kaplan J, Salt DE, Guerinot ML (2009) The ferroportin metal efflux proteins function in iron and cobalt homeostasis in Arabidopsis. Plant Cell 21(10):3326–3338

Moseley J, Quinn J, Eriksson M, Merchant S (2000) The Crd1 gene encodes a putative di-iron enzyme required for photosystem I accumulation in copper deficiency and hypoxia in Chlamydomonas reinhardtii. EMBO J 19(10):2139–2151. doi:10.1093/emboj/19.10.2139

Moseley JL, Allinger T, Herzog S, Hoerth P, Wehinger E, Merchant S, Hippler M (2002a) Adaptation to Fe-deficiency requires remodeling of the photosynthetic apparatus. EMBO J 21(24):6709–6720

Moseley JL, Page MD, Alder NP, Eriksson M, Quinn J, Soto F, Theg SM, Hippler M, Merchant S (2002b) Reciprocal expression of two candidate di-iron enzymes affecting photosystem I and light-harvesting complex accumulation. Plant Cell 14(3):673–688

Muhlenhoff U, Stadler JA, Richhardt N, Seubert A, Eickhorst T, Schweyen RJ, Lill R, Wiesenberger G (2003) A specific role of the yeast mitochondrial carriers MRS3/4p in mitochondrial iron acquisition under iron-limiting conditions. J Biol Chem 278 (42):40612–40620. doi:10.1074/jbc.M307847200

Narayanan NN, Ihemere U, Chiu WT, Siritunga D, Rajamani S, Singh S, Oda S, Sayre RT (2011) The iron assimilatory protein, FEA1, from *Chlamydomonas reinhardtii* facilitates iron-specific metal uptake in yeast and plants. Front Plant Sci 2:67. doi:10.3389/fpls.2011.00067

Naumann B, Stauber EJ, Busch A, Sommer F, Hippler M (2005) N-terminal processing of Lhca3 Is a key step in remodeling of the photosystem I-light-harvesting complex under iron deficiency in Chlamydomonas reinhardtii. J Biol Chem 280(21):20431–20441. doi:10.1074/jbc.M414486200

Naumann B, Busch A, Allmer J, Ostendorf E, Zeller M, Kirchhoff H, Hippler M (2007) Comparative quantitative proteomics to investigate the remodeling of bioenergetic pathways under iron deficiency in Chlamydomonas reinhardtii. Proteomics 7(21):3964–3979. doi:10.1002/pmic.200700407

Nevo Y, Nelson N (2006) The NRAMP family of metal-ion transporters. Biochim Biophys Acta 1763(7):609–620

Njus D, Kelley PM, Harnadek GJ, Pacquing YV (1987) Mechanism of ascorbic acid regeneration mediated by cytochrome b_{561}. Ann N Y Acad Sci 493:108–119

Ogo Y, Itai RN, Nakanishi H, Inoue H, Kobayashi T, Suzuki M, Takahashi M, Mori S, Nishizawa NK (2006) Isolation and characterization of IRO2, a novel iron-regulated bHLH transcription factor in graminaceous plants. J Exp Bot 57(11):2867–2878

Page MD, Kropat J, Hamel PP, Merchant SS (2009) Two Chlamydomonas CTR copper transporters with a novel cys-met motif are localized to the plasma membrane and function in copper assimilation. Plant Cell 21(3):928–943. doi:10.1105/tpc.108.064907

Page MD, Allen MD, Kropat J, Urzica EI, Karpowicz SJ, Hsieh SI, Loo JA, Merchant SS (2012) Fe sparing and Fe recycling contribute to increased superoxide dismutase capacity in iron-starved Chlamydomonas reinhardtii. Plant Cell 24(6):2649–2665. doi:10.1105/tpc.112.098962

Penarrubia L, Andres-Colas N, Moreno J, Puig S (2010) Regulation of copper transport in Arabidopsis thaliana: a biochemical oscillator? J Biol Inorg Chem 15(1):29–36. doi:10.1007/s00775-009-0591-8

Petit JM, Briat JF, Lobreaux S (2001) Structure and differential expression of the four members of the Arabidopsis thaliana ferritin gene family. Biochem J 359(Pt 3):575–582

Philpott CC (2006) Iron uptake in fungi: a system for every source. Biochim Biophys Acta 1763 (7):636–645

Pilon M, Abdel-Ghany SE, Cohu CM, Gogolin KA, Ye H (2006) Copper cofactor delivery in plant cells. Curr Opin Plant Biol 9(3):256–263. doi:10.1016/j.pbi.2006.03.007

Portnoy ME, Liu XF, Culotta VC (2000) *Saccharomyces cerevisiae* expresses three functionally distinct homologues of the Nramp family of metal transporters. Mol Cell Biol 20 (21):7893–7902

Puig S, Andres-Colas N, Garcia-Molina A, Penarrubia L (2007) Copper and iron homeostasis in Arabidopsis: responses to metal deficiencies, interactions and biotechnological applications. Plant Cell Environ 30(3):271–290. doi:10.1111/j.1365-3040.2007.01642.x

Quinn JM, Merchant S (1995) Two copper-responsive elements associated with the Chlamydomonas Cyc6 gene function as targets for transcriptional activators. Plant Cell 7 (5):623–628. doi:10.1105/tpc.7.5.623

Quinn JM, Barraco P, Eriksson M, Merchant S (2000) Coordinate copper- and oxygen-responsive Cyc6 and Cpx1 expression in Chlamydomonas is mediated by the same element. J Biol Chem 275(9):6080–6089

Quinn JM, Eriksson M, Moseley JL, Merchant S (2002) Oxygen deficiency responsive gene expression in Chlamydomonas reinhardtii through a copper-sensing signal transduction pathway. Plant Physiol 128(2):463–471. doi:10.1104/pp.010694

Rees EM, Lee J, Thiele DJ (2004) Mobilization of intracellular copper stores by the Ctr2 vacuolar copper transporter. J Biol Chem 279(52):54221–54229

Riedel HD, Remus AJ, Fitscher BA, Stremmel W (1995) Characterization and partial purification of a ferrireductase from human duodenal microvillus membranes. Biochem J 309 (Pt 3):745–748

Ruiz FA, Marchesini N, Seufferheld M, Govindjee, Docampo R (2001) The polyphosphate bodies of *Chlamydomonas reinhardtii* possess a proton-pumping pyrophosphatase and are similar to acidocalcisomes. J Biol Chem 276(49):46196–46203

Salahudeen AA, Thompson JW, Ruiz JC, Ma HW, Kinch LN, Li Q, Grishin NV, Bruick RK (2009) An E3 ligase possessing an iron-responsive hemerythrin domain is a regulator of iron homeostasis. Science 326(5953):722–726

Sancenon V, Puig S, Mira H, Thiele DJ, Penarrubia L (2003) Identification of a copper transporter family in Arabidopsis thaliana. Plant Mol Biol 51(4):577–587

Santi S, Schmidt W (2009) Dissecting iron deficiency-induced proton extrusion in Arabidopsis roots. New Phytol 183(4):1072–1084. doi:10.1111/j.1469-8137.2009.02908.x

Sanvisens N, Bano MC, Huang M, Puig S (2011) Regulation of ribonucleotide reductase in response to iron deficiency. Mol Cell 44(5):759–769. doi:10.1016/j.molcel.2011.09.021

Schaaf G, Honsbein A, Meda AR, Kirchner S, Wipf D, von Wirén N (2006) *AtIREG2* encodes a tonoplast transport protein involved in iron-dependent nickel detoxification in *Arabidopsis thaliana* roots. J Biol Chem 281(35):25532–25540

Selote D, Samira R, Matthiadis A, Gillikin JW, Long TA (2015) Iron-binding E3 ligase mediates iron response in plants by targeting basic helix-loop-helix transcription factors. Plant Physiol 167(1):273–286. doi:10.1104/pp.114.250837

Shaw GC, Cope JJ, Li L, Corson K, Hersey C, Ackermann GE, Gwynn B, Lambert AJ, Wingert RA, Traver D, Trede NS, Barut BA, Zhou Y, Minet E, Donovan A, Brownlie A, Balzan R, Weiss MJ, Peters LL, Kaplan J, Zon LI, Paw BH (2006) Mitoferrin is essential for erythroid iron assimilation. Nature 440(7080):96–100. doi:10.1038/nature04512

Shen J, Xu X, Li T, Cao D, Han Z (2008) An MYB transcription factor from *Malus xiaojinensis* has a potential role in iron nutrition. J Integr Plant Biol 50(10):1300–1306

Shikanai T, Muller-Moule P, Munekage Y, Niyogi KK, Pilon M (2003) PAA1, a P-type ATPase of Arabidopsis, functions in copper transport in chloroplasts. Plant Cell 15(6):1333–1346

Sinclair SA, Kramer U (2012) The zinc homeostasis network of land plants. Biochim Biophys Acta 1823(9):1553–1567. doi:10.1016/j.bbamcr.2012.05.016

Singh A, Kaur N, Kosman DJ (2007) The metalloreductase Fre6p in Fe-efflux from the yeast vacuole. J Biol Chem 282(39):28619–28626

Strozycki PM, Szymanski M, Szczurek A, Barciszewski J, Figlerowicz M (2010) A new family of ferritin genes from Lupinus luteus – comparative analysis of plant ferritins, their gene structure, and evolution. Mol Biol Evol 27(1):91–101. doi:10.1093/molbev/msp196

Su D, Asard H (2006) Three mammalian cytochromes b_{561} are ascorbate-dependent ferrireductases. FEBS J 273(16):3722–3734

Takeuchi F, Hori H, Obayashi E, Shiro Y, Tsubaki M (2004) Properties of two distinct heme centers of cytochrome b_{561} from bovine chromaffin vesicles studied by EPR, resonance Raman, and ascorbate reduction assay. J Biochem 135(1):53–64

Terauchi AM, Peers G, Kobayashi MC, Niyogi KK, Merchant SS (2010) Trophic status of Chlamydomonas reinhardtii influences the impact of iron deficiency on photosynthesis. Photosynth Res 105(1):39–49. doi:10.1007/s11120-010-9562-8

Terzulli AJ, Kosman DJ (2009) The Fox1 ferroxidase of Chlamydomonas reinhardtii: a new multicopper oxidase structural paradigm. J Biol Inorg Chem 14(2):315–325. doi:10.1007/s00775-008-0450-z

Terzulli A, Kosman DJ (2010) Analysis of the high-affinity iron uptake system at the Chlamydomonas reinhardtii plasma membrane. Eukaryot Cell 9(5):815–826. doi:10.1128/EC.00310-09

Theil EC (1987) Ferritin: structure, gene regulation, and cellular function in animals, plants and microorganisms. Annu Rev Biochem 56:289–315

Thomine S, Vert G (2013) Iron transport in plants: better be safe than sorry. Curr Opin Plant Biol 16(3):322–327. doi:10.1016/j.pbi.2013.01.003

Thomine S, Wang R, Ward JM, Crawford NM, Schroeder JI (2000) Cadmium and iron transport by members of a plant metal transporter family in Arabidopsis with homology to Nramp genes. Proc Natl Acad Sci U S A 97(9):4991–4996

Tottey S, Block MA, Allen M, Westergren T, Albrieux C, Scheller HV, Merchant S, Jensen PE (2003) Arabidopsis CHL27, located in both envelope and thylakoid membranes, is required for the synthesis of protochlorophyllide. Proc Natl Acad Sci U S A 100(26):16119–16124. doi:10.1073/pnas.2136793100

Trost P, Bèrczi A, Sparla F, Sponza G, Marzadori B, Asard H, Pupillo P (2000) Purification of cytochrome b_{561} from bean hypocotyls plasma membrane. Evidence for the presence of two heme centers. Biochim Biophys Acta 1468(1–2):1–5

Urzica EI, Casero D, Yamasaki H, Hsieh SI, Adler LN, Karpowicz SJ, Blaby-Haas CE, Clarke SG, Loo JA, Pellegrini M, Merchant SS (2012) Systems and trans-system level analysis identifies conserved iron deficiency responses in the plant lineage. Plant Cell 24(10):3921–3948. doi:10.1105/tpc.112.102491

Van Wuytswinkel O, Vansuyt G, Grignon N, Fourcroy P, Briat JF (1998) Iron homeostasis alteration in transgenic tobacco overexpressing ferritin. Plant J 17(1):93–97

Vargas JD, Herpers B, McKie AT, Gledhill S, McDonnell J, van den Heuvel M, Davies KE, Ponting CP (2003) Stromal cell-derived receptor 2 and cytochrome b_{561} are functional ferric reductases. Biochim Biophys Acta 1651(1-2):116–123

Vashisht AA, Zumbrennen KB, Huang X, Powers DN, Durazo A, Sun D, Bhaskaran N, Persson A, Uhlen M, Sangfelt O, Spruck C, Leibold EA, Wohlschlegel JA (2009) Control of iron homeostasis by an iron-regulated ubiquitin ligase. Science 326(5953):718–721

Wade VJ, Treffry A, Laulhere JP, Bauminger ER, Cleton MI, Mann S, Briat JF, Harrison PM (1993) Structure and composition of ferritin cores from pea seed (Pisum sativum). Biochim Biophys Acta 1161(1):91–96

Walker EL, Connolly EL (2008) Time to pump iron: iron-deficiency-signaling mechanisms of higher plants. Curr Opin Plant Biol 11(5):530–535. doi:10.1016/j.pbi.2008.06.013

Williams RJP (2001) Chemical selection of elements by cells. Coord Chem Rev 216–217:583–595. doi:10.1016/S0010-8545(00)00398-2

Yagisawa F, Nishida K, Yoshida M, Ohnuma M, Shimada T, Fujiwara T, Yoshida Y, Misumi O, Kuroiwa H, Kuroiwa T (2009) Identification of novel proteins in isolated polyphosphate vacuoles in the primitive red alga *Cyanidioschyzon merolae*. Plant J 60(5):882–893

Yamasaki H, Hayashi M, Fukazawa M, Kobayashi Y, Shikanai T (2009) SQUAMOSA promoter binding protein-like7 is a central regulator for copper homeostasis in Arabidopsis. Plant Cell 21 (1):347–361. doi:10.1105/tpc.108.060137

Yuan YX, Zhang J, Wang DW, Ling HQ (2005) *AtbHLH29* of *Arabidopsis thaliana* is a functional ortholog of tomato *FER* involved in controlling iron acquisition in strategy I plants. Cell Res 15 (8):613–621

Zancani M, Peresson C, Biroccio A, Federici G, Urbani A, Murgia I, Soave C, Micali F, Vianello A, Macri F (2004) Evidence for the presence of ferritin in plant mitochondria. Eur J Biochem 271(18):3657–3664. doi:10.1111/j.1432-1033.2004.04300.x

Zhang DL, Su D, Bérczi A, Vargas A, Asard H (2006) An ascorbate-reducible cytochrome b_{561} is localized in macrophage lysosomes. Biochim Biophys Acta 1760(12):1903–1913

Zhang J, Liu B, Li M, Feng D, Jin H, Wang P, Liu J, Xiong F, Wang J, Wang HB (2015) The bHLH transcription factor bHLH104 interacts with IAA-LEUCINE RESISTANT3 and modulates iron homeostasis in Arabidopsis. Plant Cell 27(3):787–805. doi:10.1105/tpc.114.132704

Zheng L, Huang F, Narsai R, Wu J, Giraud E, He F, Cheng L, Wang F, Wu P, Whelan J, Shou H (2009) Physiological and transcriptome analysis of iron and phosphorus interaction in rice seedlings. Plant Physiol 151(1):262–274

Calcium-Dependent Signalling Processes in Chlamydomonas

Glen L. Wheeler

Abstract Like all organisms, the motile green alga Chlamydomonas has evolved an array of sensory mechanisms to enable it to detect and respond to an array of abiotic and biotic stimuli. It is clear that Ca^{2+}-dependent signalling mechanisms are central to many responses in Chlamydomonas, from flagella function through to stress signalling and photosynthesis. Chlamydomonas has long been used as a model organism for flagella function and this aspect of signalling has received much attention, with well-characterised roles for Ca^{2+} in flagella beat, phototaxis, mating and deflagellation. Recent progress has identified a series of ion channels and Ca^{2+}-sensor kinases that underpin these responses and direct imaging of flagella Ca^{2+} in Chlamydomonas cells has demonstrated the highly dynamic nature of Ca^{2+} signalling in these organelles. The role of Ca^{2+} in other signalling processes in Chlamydomonas has been less well explored, although exciting recent developments have demonstrated novel Ca^{2+}-dependent signalling processes associated with the regulation of photosynthesis. These developments highlight the diverse roles of Ca^{2+} in Chlamydomonas physiology and the potential for the discovery of novel Ca^{2+} signalling mechanisms within this organism.

1 Introduction

All organisms must sense and respond to their environment to ensure their survival. As a motile soil-dwelling photosynthetic green alga, Chlamydomonas is likely to experience rapid changes in light, osmotic stress and nutrient availability and possesses diverse signalling mechanisms to help the cell respond to these stimuli. In eukaryotes, Ca^{2+} acts a versatile second messenger, amplifying and propagating intracellular signals in response to diverse environmental stimuli. Eukaryote cells maintain a very low cytosolic concentration of Ca^{2+} (100 nM), resulting in a large inward concentration gradient. The activation of Ca^{2+}-permeable channels localised to the plasma membrane or internal membranes results in rapid Ca^{2+} influx, leading to elevations in cytosolic Ca^{2+} ($[Ca^{2+}]_{cyt}$). Ca^{2+} efflux proteins such

G.L. Wheeler (✉)
Marine Biological Association, The Laboratory, Citadel Hill, Plymouth PL1 2PB, UK
e-mail: glw@mba.ac.uk

M. Hippler (ed.), *Chlamydomonas: Molecular Genetics and Physiology*,
Microbiology Monographs 30, DOI 10.1007/978-3-319-66365-4_8

as Ca^{2+} ATPases or Ca^{2+}/H^{+} exchangers return $[Ca^{2+}]_{cyt}$ to its resting level and therefore play an important role in shaping the Ca^{2+} transient (McAinsh and Pittman 2009). Diverse Ca^{2+}-binding proteins, such as calmodulin (CaM), the calcium-dependent protein kinases (CDPKs) or the calcineurin B-like (CBL) calcium sensor proteins and their CBL-interacting protein kinases (CIPKs), respond to the changes in cytosolic Ca^{2+} by eliciting a host of downstream responses (Edel and Kudla 2015; Zhu et al. 2015). As $[Ca^{2+}]_{cyt}$ elevations are generated by a wide variety of stimuli, specificity in Ca^{2+} signalling is conveyed by the spatial and temporal dynamics of each $[Ca^{2+}]_{cyt}$ elevation. For example, $[Ca^{2+}]_{cyt}$ elevations can take the form of brief localised spikes lasting <1 s or large whole cell $[Ca^{2+}]_{cyt}$ elevations that persist for minutes or even hours. In combination with the broad range of downstream responders, the distinct spatiotemporal dynamics of $[Ca^{2+}]_{cyt}$ elevations enable the cell to use Ca^{2+} signalling in response to many different stimuli. Ca^{2+} has been implicated in many different signalling processes in Chlamydomonas. Many of these relate to flagella function, reflecting the extensive use of Chlamydomonas as a model organism for the study of this organelle, but emerging evidence suggests that Ca^{2+} plays a central role in many other cellular processes. This review aims to highlight the different roles of Ca^{2+} within the cell and identify some of the key recent developments that are now providing insight into the underlying cellular mechanisms.

2 Ca^{2+} Signalling in Flagella Motility

2.1 Ca^{2+}-Sensitive Elements Involved in Flagellar Beat

Ca^{2+} signalling plays a central role in regulating swimming motility in Chlamydomonas, and this aspect of signalling is the most extensively characterised in this alga. Research into flagellar signalling mechanisms has had a significant wider impact, exemplified by the discovery of the novel light-gated ion channel channelrhodopsin. Chlamydomonas has two flagella that beat at 50–70 Hz in a breaststroke motion. This results in a helical swimming path, in which the cell moves forwards at a velocity of 100–200 μm s^{-1}, whilst the cell body rotates about its longitudinal axis at 2 Hz. Swimming Chlamydomonas cells exhibit two very characteristic responses to light, photoshock and phototaxis. In the photoshock response, sudden exposure to high light results in a rapid but transient (duration 500 ms) switch to an undulating flagellar waveform, resulting in a brief period of backwards swimming (Fig. 1). In the phototactic response, differential activation of the *cis* (closest to eyespot)- and *trans* (furthest from eyespot)-flagella enables a change in swimming direction towards or away from a directional light source.

Experiments using demembranated cell models (cells permeabilised with a non-ionic detergent) demonstrated that Ca^{2+} plays a direct role in controlling the beat frequency and waveform of the flagella. Changing Ca^{2+} in the medium from

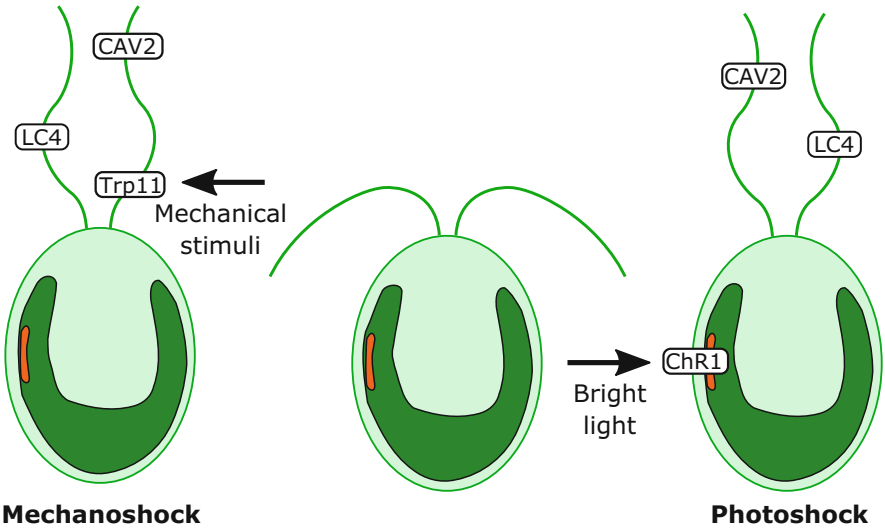

Fig. 1 Cellular mechanisms underlying the phobic motile responses. The scheme illustrates the major proteins identified in phobic swimming responses of Chlamydomonas cells. In the mechanoshock response, the flagella-localised mechanosensitive ion channel TRP11 is proposed to activate the voltage-gated Ca^{2+} channel CAV2. In the photoshock response, bright light activates channelrhodopsin (ChR1), leading to a whole cell depolarisation and activation of CAV2 in the flagella membrane. In both responses, the resultant intraflagellar Ca^{2+} elevations are likely sensed by LC4 in the outer dynein arm, which causes the switch to the undulating waveform and the onset of backwards swimming

$<10^{-6}$ M to 10^{-4} M resulted in a shift from the breaststroke waveform of cell models to the undulating waveform observed during photoshock (Bessen et al. 1980; Hyams and Borisy 1978). Smaller changes in Ca^{2+} were observed to modulate the breaststroke waveform differently between the two flagella. The *cis*-flagellum beats strongest at low Ca^{2+} ($<10^{-7}$ M), whereas the *trans*-flagellum beats strongest at higher Ca^{2+} concentrations (Kamiya and Witman 1984). These findings indicated that phototaxis, as well as the photoshock response, is directly mediated by changes in intraflagellar Ca^{2+}. In support of this, a mutant strain was isolated (*ptx1*) which lacks the Ca^{2+}-dependent shift in flagellar dominance and shows very little phototactic ability (Horst and Witman 1993; Okita et al. 2005).

Ca^{2+} modulates the flagellar beat patterns by binding directly to a range of axonemal proteins, although the modes of regulation are likely to be complex. Of the 650 proteins that are known to comprise the flagella axoneme in Chlamydomonas, 27 are predicted to bind Ca^{2+} (DiPetrillo and Smith 2013; Pazour et al. 2005). Flagellar beat is driven by the axonemal dyneins, which are arranged in the inner and outer dynein arms. Outer dynein arm mutants exhibit a defective photoshock response, with little or no backwards swimming (Kamiya and Okamoto 1985). Two Ca^{2+}-binding proteins have been characterised in the outer dynein arm, LC4 and DC3. The docking complex protein DC3 has two consensus EF hands and

oda14 mutants, which lack DC3 and show defects in the photoshock response (Casey et al. 2003a). However, this phenotype is most likely due to defects in outer arm assembly in *oda14* rather than Ca^{2+} binding by DC3, as complementation of *oda14* with a modified DC3 protein that does not bind Ca^{2+} restored the assembly of the outer dynein arms and the photoshock response (Casey et al. 2003b). LC4 is also related to calmodulin and undergoes a conformational change on binding Ca^{2+}. The affinity of LC4 for Ca^{2+} and its interactions with other outer dynein arm proteins makes it the prime candidate to act as the major Ca^{2+} sensor in the outer dynein arm and mediate the waveform conversion observed during the photoshock response (Sakato et al. 2007).

Calmodulin (CaM) also plays an important role in modifying flagellar beat, by regulating dynein-driven microtubule sliding through interactions with the central pair of microtubules and the radial spokes (Smith 2002). CaM-containing complexes associated with either the radial spokes or the central pair have been purified from Chlamydomonas flagella, indicating the CaM acts in multiple roles (Dymek and Smith 2007; Patel-King et al. 2004). A further CaM-containing complex was isolated in high Ca^{2+} buffer, suggesting that changes in intraflagellar Ca^{2+} cause CaM to form additional regulatory complexes (DiPetrillo and Smith 2010, 2013).

2.2 Light-Dependent Signalling Pathways

The photoshock and phototactic responses are both mediated by channelrhodopsin, a light-gated ion channel localised to the plasma membrane adjacent to the eyespot. The eyespot is composed of a series of carotenoid-rich lipid globules in the chloroplast and is positioned approximately half way along the longitudinal axis of the cell. The eyespot acts as a quarter-wave stack antenna, reflecting light onto the plasma membrane adjacent to the eyespot where the receptor (channelrhodopsin) is situated (Foster and Smyth 1980). Electrophysiological approaches have enabled the extensive characterisation of the light-dependent ion currents in Chlamydomonas. A flash of light results in an initial inward current (the photocurrent, PC or *I*p) in the region of the eyespot. The photocurrent rises with virtually no delay at saturating light intensities and was initially shown to be carried largely by Ca^{2+} (Harz and Hegemann 1991; Holland et al. 1996). However, when the driving force is sufficiently large, H^+, Na^+ and K^+ can also contribute significantly to the photocurrent (Ehlenbeck et al. 2002; Holland et al. 1996; Nonnengasser et al. 1996). The lack of a delay in the rise of the photocurrent (<500 μs) suggested that the light receptor and the ion channel were either very tightly linked or represented the same protein. The discovery of two genes (ChR1 and ChR2) encoding a novel light-gated ion channel (channelrhodopsin) demonstrated that the latter hypothesis was correct. When expressed in *Xenopus* oocytes, both ChR1 and ChR2 elicit large light-dependent H^+ conductances (Nagel et al. 2002, 2003). However, unlike the voltage-gated H^+ channels that exhibit a near-perfect selectivity for H^+ (DeCoursey 2013), channelrhodopsins are much less

selective for H^+ (Berthold et al. 2008; Schneider et al. 2013). As the relative external concentrations of other cations is often much greater than that of H^+, particularly at alkaline pH, the photocurrent may be carried by Ca^{2+}, Na^+ or K^+ even though channelrhodopsins exhibit a greater permeability for H^+ (Berthold et al. 2008). The discovery and subsequent optogenetic application of channelrhodopsin have revolutionised the study of neuroscience, by enabling non-invasive activation of transgenic neurons expressing channelrhodopsins.

Studies using anti-sense knockdown of channelrhodopsins suggested that ChR1 and ChR2 may perform different roles within the cell, with ChR1 responsible primarily for responses to high light, e.g. photoshock, and ChR2 responsible for low-light responses such as phototaxis (Sineshchekov et al. 2002). However, a more recent study using gametes of *cw2*, which exhibit very little ChR2 expression, demonstrated that RNAi knockdown of ChR1 almost completely prevented the photocurrent and strongly inhibited the photoshock and the phototactic responses (Berthold et al. 2008). This suggests that ChR1 alone can contribute to both of these processes. The requirement for two functional channelrhodopsins in Chlamydomonas therefore remains unclear.

The intensity of the light stimulus determines the amplitude of the photocurrent, which causes depolarisation of the membrane potential. If the extent of depolarisation reaches a certain threshold, voltage-gated Ca^{2+} channels in the flagella membrane are activated, leading to Ca^{2+} influx into the flagella (Harz and Hegemann 1991). The flagella current is carried by Ca^{2+} and has two clear components: a fast transient current (I_{FF}) lasting a few ms that coincides with the switch to the undulating waveform and a slower sustained flagella current (I_{FS}) that has a much smaller amplitude and lasts around 600 ms, similar to the duration of the backwards swimming (Holland et al. 1997). The fast flagella current represents an action potential, as it is an all-or-nothing response that is triggered when a threshold depolarisation is reached. In the presence of 100 μM Ba^{2+}, the slow flagella current has a much larger amplitude and leads to a sustained and erratic photophobic response (Holland et al. 1996). This suggests that the slow flagella current is normally regulated by feedback inhibition from the intraflagellar Ca^{2+} concentration, allowing maintenance of a similar intraflagellar Ca^{2+} concentration throughout the duration of the photophobic response (Holland et al. 1996). Characterisation of a mutant, *ppr2*, which is defective in the photophobic response but not in phototaxis, revealed that this phenotype was due to a defect in *CAV2*, a homologue of the mammalian four-domain voltage-gated Ca^{2+} channels (Fujiu et al. 2009). CAV2 localises to the distal region of the flagella and appears to play a major role in mediating the flagellar Ca^{2+} influx during the photophobic response.

The electrophysiological characterisation of the photoshock response not only provides important information on the molecular mechanisms of Ca^{2+} signalling in Chlamydomonas but also demonstrates an important environmental aspect of this signalling mechanism. The imperfect H^+ selectivity of ChR1 and ChR2 allows the photocurrent to be carried by other cations, such as Na^+ or Ca^{2+} at alkaline pH environments where the concentration of H^+ is much lower. The feedback inactivation of the resultant flagella current by the intraflagellar Ca^{2+} concentration ensures

that the flagella response is very similar even in a wide range of external Ca^{2+} concentrations. Thus, even if the cell encounters aquatic environments with a significantly different ionic composition, which is highly likely for a freshwater/soil organism, the cell is able to generate a robust and reproducible photoshock response.

Whilst it is clear that the photoshock response is mediated by light-induced depolarisation of the plasma membrane, the mechanism through which channelrhodopsin directs phototaxis is less clear. Channelrhodopsin is clearly the sensor for phototaxis, as demonstrated by RNAi knockdown of ChR1 (Berthold et al. 2008). However, phototaxis can be observed at low light intensities where the photocurrent is only sufficient to depolarise the cellular membrane potential by 1 mV, which elicits no measurable flagella current (Hegemann and Berthold 2009). The *ppr2* mutant, which lacks the flagella-localised voltage-gated Ca^{2+} channel CAV2, exhibits normal phototaxis (Matsuda et al. 1998). These findings suggest that phototaxis does not rely on changes in flagella membrane potential and that additional signalling mechanisms are required in order to transmit information from the sensory region (the eyespot) to the flagella.

2.3 Other Motile Responses

Chlamydomonas exhibits a mechanoshock response, where the flagella briefly switch to an undulating waveform on encountering a solid surface, causing a brief period (<1 s) of backwards swimming. The swimming response during mechanoshock is similar to that of photoshock, although clearly the sensory mechanisms are different. In addition to the mechanoshock response, Chlamydomonas also exhibits a Ca^{2+}-dependent increase in swimming velocity following a mechanical stimulus, such as shear stress induced by vortexing a population of swimming cells (Wakabayashi et al. 2009). By applying suction to flagella using a micropipette, Yoshimura (1996) demonstrated that Chlamydomonas flagella are directly mechanosensitive. Suction induced a series of repetitive inward Ca^{2+} currents in flagella that were sensitive to Gd^{3+} and Ba^{2+} (Yoshimura 1996). Chlamydomonas flagella possess a number of candidate mechanosensitive ion channels, most notably a range of transient receptor potential (TRP) channels, which are known to play a role in mechanosensation in animal cells (Huang et al. 2007). A study of the localisation of a range of TRP channels indicated that TRP11 was localised exclusively to the flagella with the greatest abundance at the proximal region (Fujiu et al. 2011). RNAi-mediated knockdown of *TRP11* expression resulted in a greatly reduced mechanoshock response (Fujiu et al. 2011). The mechanoshock response is absent in the *ppr2* mutant, suggesting that activation of TRP11 by mechanical stimulation leads to a depolarisation of the flagella membrane and activation of CAV2 (Fujiu et al. 2009). Mechanoshock responses have been characterised in other motile green algae such as *Spermatozopsis*, although in this case the alga responds by a very rapid acceleration

in swimming velocity (Kreimer and Witman 1994). Patch clamp recordings using reconstituted liposomes from *Spermatozopsis* flagella membranes indicated the presence of a voltage-gated Ca^{2+} channel that most likely underlies the avoidance response (Hill et al. 2000).

Chlamydomonas also demonstrates tactic responses to stimuli other than light. Vegetative cells exhibit chemotaxis towards ammonium and sugars (Ermilova et al. 1998; Sjoblad and Frederikse 1981), and gametes also exhibit chemotactic responses to peptone and tryptone (Govorunova and Sineshchekov 2003, 2005). Chemotaxis towards ammonium is dependent on external Ca^{2+}, and chemotactic responses towards sugars can be blocked by Ca^{2+} channel blockers (Ermilova et al. 1998; Sjoblad and Frederikse 1981). There is some evidence for integration between the chemotaxis and phototaxis signalling pathways, as the addition of tryptone to gametes temporarily inhibits the channelrhodopsin-mediated photocurrent (Govorunova and Sineshchekov 2003). Chlamydomonas also demonstrates negative gravitaxis, i.e. a tendency to swim upwards, in the absence of light and other stimuli. Gravitaxis was found to be normal in the *ptx1* mutant and was unaffected by the removal of Ca^{2+}, suggesting that gravitaxis does not involve Ca^{2+}-dependent signalling mechanisms (Kam et al. 1999; Yoshimura et al. 2003).

3 Other Ca^{2+} Signalling Processes Related to Flagella Function

3.1 Mating

Signal transduction during fertilisation has been extensively explored in Chlamydomonas. The signalling pathway is initiated by contact between agglutinins on the flagella of gametes of opposite mating types. This results in a signalling cascade that leads to activation of an adenylyl cyclase and a rise of cyclic AMP (cAMP) (Wang and Snell 2003). The accumulation of cAMP results in shedding of the cell walls and activation of mating structures, followed by cell fusion and formation of the quadriflagellate cell. The elevation of cAMP is central to this signalling pathway, as mating responses can be induced in gametes by the application of cell-permeable cAMP analogue, dibutyryl cAMP, in the presence of the phosphodiesterase inhibitor IBMX (Brownlee 1994; Pan and Snell 2000). The role of Ca^{2+} signalling during mating is less clear. Inhibition of Ca^{2+} signalling with CaM antagonists (trifluoperazine and W-7) or Ca^{2+} channel blockers (e.g. La^{3+} or Cd^{2+}) had no effect on flagella agglutination but prevented the rise in cAMP and inhibited mating (Goodenough et al. 1993; Pasquale and Goodenough 1987). Mating could be rescued by the addition db-cAMP + IBMX, suggesting that Ca^{2+} acts upstream of the activation of adenylyl cyclase. Mating efficiency is reduced but not completely inhibited in the absence of external Ca^{2+}, suggesting that a Ca^{2+} influx across the plasma membrane and/or the flagella membrane contributes to the signalling

pathway (Goodenough et al. 1993). In combination, these results suggest that flagella agglutination may trigger a flagellar Ca^{2+} elevation, which could contribute to the activation of adenylyl cyclase and the rise in cAMP. Support for this hypothesis came from the characterisation of PKD2 in Chlamydomonas, a homologue of a mammalian Ca^{2+}-permeable TRP channel. PKD2 is highly expressed in the flagella of gametes, and RNAi-mediated knockdown of PKD2 resulted in an inhibition of mating (Huang et al. 2007). The mating defect could be rescued by the addition of db-cAMP and papaverine (a phosphodiesterase inhibitor), suggesting that PKD2 acts upstream of the adenylyl cyclase and may therefore contribute to flagellar Ca^{2+} signalling following flagella adhesion (Huang et al. 2007).

3.2 Gliding

In addition to swimming, Chlamydomonas flagella can also support an alternative form of cellular motility. The flagella membrane of Chlamydomonas contains an abundant glycoprotein (FMG-1B), which enables the flagella to adhere to a solid substrate (Bloodgood 1981; Bloodgood and Workman 1984). The regulated movement of FMG-1B in the flagella membrane allows the adherent flagella pull the cell body forwards and results in the two flagella becoming orientated at 180° to each other. The movement of FMG-1B in the flagella membrane can also be observed using microspheres (Bloodgood 1995; Shih et al. 2013). Microspheres move along the flagellum at a rate similar to gliding motility but this movement differs in that the beads move back and forth, whereas gliding flagella only move forwards (Bloodgood 1981). Adhesion of FMG-1B to a solid substrate, such as a microsphere or a glass surface during gliding motility, results in cross-linking of the flagellar glycoprotein. Bead movement and gliding motility require the presence of micromolar free Ca^{2+} in the medium, suggesting that the movement of FMG-1B in the flagella membrane is directly regulated by Ca^{2+} (Bloodgood 1995; Bloodgood and Salomonsky 1990).

As the flagella of gliding cells are arranged at 180° and pull the cell body in opposite directions, there is clearly a need to coordinate the motive force generated by each flagellum. Direct imaging of intraflagellar Ca^{2+} ($[Ca^{2+}]_{fla}$) indicated that no $[Ca^{2+}]_{fla}$ elevations were observed in the leading flagellum during gliding motility but a $[Ca^{2+}]_{fla}$ elevation was consistently observed in the trailing flagellum at the onset of dragging motion (Fig. 2) (Collingridge et al. 2013). This was puzzling as it had been previously assumed that Ca^{2+} signalling was linked to the initiation of force generation by the microtubule motor proteins in the leading flagellum (Bloodgood 2009). However, this discrepancy was resolved by the discovery that the retrograde IFT motor cytoplasmic dynein provides the motive force for gliding motility (Collingridge et al. 2013; Shih et al. 2013). Direct observation of fluorescently tagged IFT particles during gliding motility demonstrated that retrograde IFT particles accumulate in the leading flagellum and are able to drive the flagellum forward, presumably through a direct interaction with FMG-1B (Collingridge et al.

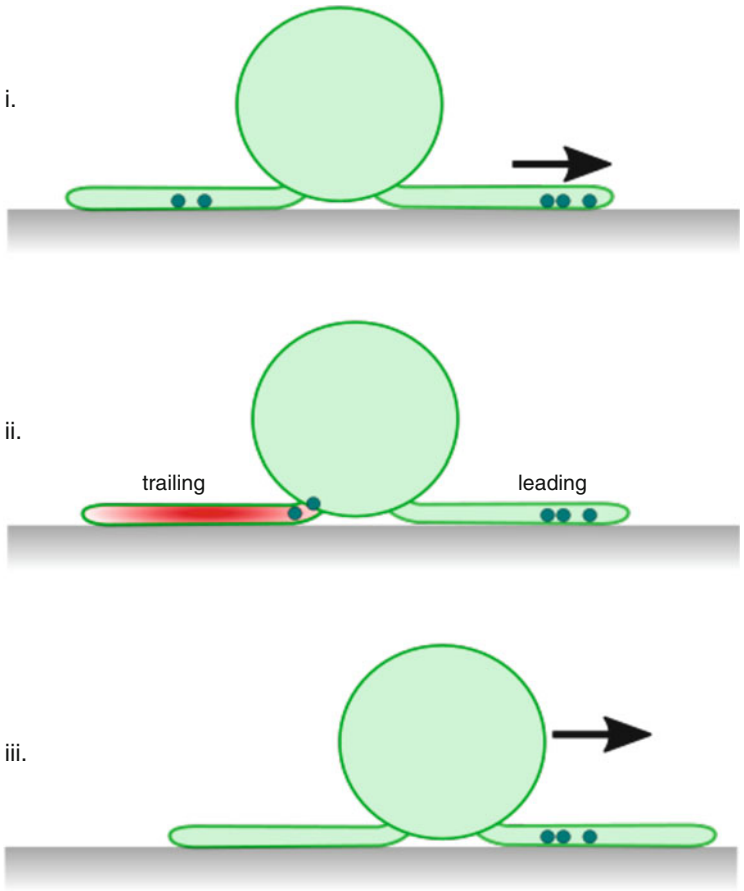

Fig. 2 Flagellar Ca^{2+} signalling during gliding. Chlamydomonas cells adhere to solid substrates via their flagella and glide along the surface due to the movement of adherent flagella membrane glycoproteins. (i) Retrograde IFT particles accumulate in adherent flagella and provide the motive force to pull the cell body forwards. (ii) As the leading flagellum begins to move forwards, a intraflagellar Ca^{2+} elevation occurs in the trailing flagellum only, which disrupts the interaction between the IFT particles and the flagella membrane in the trailing flagellum. (iii) This prevents a futile tug-of-war between the two flagella and allows the leading flagellum to pull the cell body forwards

2013; Shih et al. 2013). In the trailing flagellum, the $[Ca^{2+}]_{fla}$ elevations caused by the dragging motion disrupt the accumulated retrograde IFT particles, which are returned to the cell body by retrograde IFT (Collingridge et al. 2013). This suggests that the interaction between the retrograde IFT particle and FMG-1B is sensitive to Ca^{2+}. The absence of external Ca^{2+} inhibits $[Ca^{2+}]_{fla}$ elevations and leads to a massive accumulation of IFT particles in the regions of the flagellum that are in contact with the solid surface (Collingridge et al. 2013). In contrast, Shih et al. (2013) demonstrated that IFT trains pause less frequently in the absence of external

Ca^{2+} and proposed that Ca^{2+} was required to initiate the interaction between the IFT particle and FMG-1B. However, this proposal seems at odds with the direct observations of $[Ca^{2+}]_{fla}$ and IFT.

The ability to directly observe $[Ca^{2+}]_{fla}$ in Chlamydomonas has highlighted some important properties relating to these signalling pathways. Firstly, $[Ca^{2+}]_{fla}$ elevations are very rapid (often <1 s) and they occur simultaneously along the length of the flagellum, suggesting that changes in membrane potential and activation of voltage-gated Ca^{2+} channels are likely to be involved in their generation. Secondly, the two flagella are able to act as independent Ca^{2+} signalling entities, which is essential for the coordination of gliding motility. Thirdly, $[Ca^{2+}]_{fla}$ elevations are directly linked to the movement of microtubule motor proteins, which has interesting parallels with other cellular processes, such as the Ca^{2+}-dependent movement of mitochondria along microtubules (Saotome et al. 2008). Although the molecular identity of the Ca^{2+} channels involved in the flagellar signalling pathway has not yet been confirmed, it is likely that the dragging motion of the trailing flagellum is sensed initially by a mechanosensitive ion channel, which leads to membrane depolarisation and activation of voltage-gated Ca^{2+} channels along the length of the flagellum (Collingridge et al. 2013). Further characterisation of the signal transduction pathway regulating gliding motility is likely to yield important broader insights into the nature of ciliary signalling.

3.3 Deflagellation

The process of flagellar excision is another flagella-related signalling pathway that has been extensively characterised in Chlamydomonas. Cells exposed to various stressors including chemicals (such as dibucaine and mastoparan), pH shock, elevated temperature and mechanical shear rapidly shed both flagella by precise severing of the nine outer doublet microtubules at the distal end of the flagella transition zone (Quarmby 2004). This process has been much exploited by Chlamydomonas researchers in order to obtain large quantities of flagella for biochemical characterisation of their component proteins. It is presumed that deflagellation contributes to survival in unfavourable conditions, e.g. by reducing the surface area of exposed cellular membranes, although there is little experimental evidence to support this. The microtubule-severing activity is directly dependent on Ca^{2+}, as axonemal severing can be induced in purified axonemes/basal bodies exposed to 1 μM Ca^{2+} (Lohret et al. 1998). How exactly Ca^{2+} triggers the severing process is not yet clear. The Ca^{2+}-binding protein centrin may contribute to flagellar excision through contraction of the stellate fibres in the distal flagella transition zone. However, the centrin mutant *vfl2* deflagellates normally suggesting that the activity of centrin alone does not induce microtubule severing (Quarmby 2004). Katanin is a likely candidate for the microtubule-severing protein, although katanin likely plays further roles in the cell and conclusive evidence supporting a role for katanin in deflagellation is lacking (Lohret et al. 1998; Rasi et al. 2009).

Treatment of Chlamydomonas cells with organic acids, such as benzoate or acetate, results in cytosolic acidification, which rapidly leads to deflagellation (Braun and Hegemann 1999; Quarmby 1996). Quarmby and Hartzell (1994) demonstrated that acid-induced deflagellation is completely dependent on a Ca^{2+} influx across the plasma membrane and does not occur in the absence of external Ca^{2+}. Cytosolic acidification due to organic acids also causes activation of phospholipase C and an accumulation of inositol triphosphate (IP_3), which may play a role in the deflagellation signalling pathway (Quarmby et al. 1992). Mastoparan, a G-protein agonist that stimulates intracellular Ca^{2+} release through elevation of IP_3, deflagellates cells in the absence of external Ca^{2+}, suggesting that deflagellation can also result from the release of Ca^{2+} from internal stores (Quarmby and Hartzell 1994). However, the evidence for the role of IP_3 in the signalling pathway remains inconclusive (Quarmby 2004).

Direct imaging of cytosolic Ca^{2+} demonstrates that organic acids cause a rapid and sustained elevation in $[Ca^{2+}]_{cyt}$ throughout the cytosol, which coincides with the timing of flagellar excision (Braun and Hegemann 1999; Wheeler et al. 2008). The *adf1* mutant, which is defective in acid-induced deflagellation but deflagellates normally in response to other stimuli, does not exhibit a Ca^{2+} influx in response to acid or demonstrate the $[Ca^{2+}]_{cyt}$ elevation (Finst et al. 2000; Quarmby and Hartzell 1994; Wheeler et al. 2008). The absence of a Ca^{2+} influx led to proposals that *ADF1* encodes a H^+-stimulated Ca^{2+} channel localised to the apical region of the cell (Quarmby and Hartzell 1994). Recently, a combination of genetic mapping and whole genome sequencing of *adf1* mutants identified Adf1 as a member of the TRP family of ion channels (Hilton et al. 2016). Closer examination of the *adf1* mutant revealed that a small percentage of cells do deflagellate during benzoate addition, and in each of these instances, a localised transient $[Ca^{2+}]_{cyt}$ elevation was observed in the apical region of the cell coinciding with deflagellation (Wheeler et al. 2008). Assuming Adf1 is a Ca^{2+}-permeable ion channel, its reduced activity in the *adf1-1* mutant may result in greatly reduced Ca^{2+} influx in the apical region, leading to a transient localised $[Ca^{2+}]_{cyt}$ elevation that is sufficient to cause flagellar excision but does not trigger further Ca^{2+} release from intracellular stores. This indicates that deflagellation can be induced solely by a localised $[Ca^{2+}]_{cyt}$ elevation in the region around the basal body and does not require the whole cell $[Ca^{2+}]_{cyt}$ elevation normally observed in wild-type cells. It is likely that additional inputs are required in the signalling pathway before Ca^{2+} can act to trigger flagellar excision. Rapid addition of 20 mM external Ca^{2+} to Chlamydomonas causes a series of repetitive $[Ca^{2+}]_{cyt}$ elevations and leads to deflagellation (Fig. 3) (Wheeler et al. 2008). However, whilst each deflagellation event was observed to coincide with a $[Ca^{2+}]_{cyt}$ elevation, many cells exhibited multiple $[Ca^{2+}]_{cyt}$ elevations prior to flagellar excision indicating that $[Ca^{2+}]_{cyt}$ elevations alone do not induce deflagellation in an intact cell. One additional component of the deflagellation signalling pathway is the aurora protein kinase CALK, which has a role in the regulating flagellar length and assembly. CALK is phosphorylated during acid-induced deflagellation, and RNAi-mediated knockdown of CALK led to defects in deflagellation (Pan et al. 2004), although how CALK interacts with the Ca^{2+} signalling pathway is not known. As

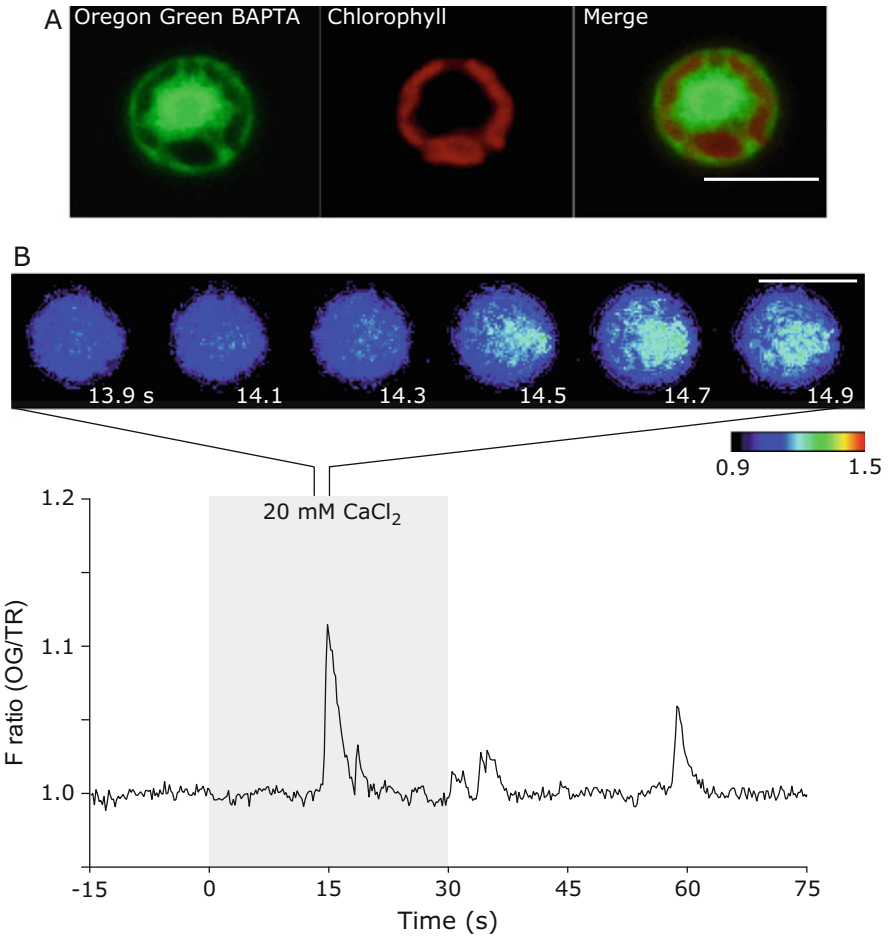

Fig. 3 Imaging $[Ca^{2+}]_{cyt}$ elevations in Chlamydomonas. (**a**) Confocal microscopic images of a Chlamydomonas cell loaded with the Ca^{2+}-responsive dye Oregon Green BAPTA dextran. The dextran-conjugated dye demonstrates diffuse cytoplasmic loading, with no compartmentalisation. Chlorophyll autofluorescence is also shown. Bar = 10 μm. (**b**) An example of the $[Ca^{2+}]_{cyt}$ elevations induced by adding 20 mM external Ca^{2+} to a Chlamydomonas cell. The *upper images* show changes in Oregon Green BAPTA fluorescence viewed by epifluorescent microscopy. Images are generated by dividing each image by a rolling median image ($n = 20$ images) and are pseudo-coloured to illustrate relative changes in fluorescence. The *lower graph* shows the corresponding changes in the fluorescence ratio of Oregon Green BAPTA (OG) and a non-responsive dye, Texas Red (TR), for the same cell. Perfusion of the cell with 20 mM external Ca^{2+} for 30 s results in a series of $[Ca^{2+}]_{cyt}$ elevations that persist after the cell is returned to the initial external Ca^{2+} (300 μM). Bar = 10 μm

$[Ca^{2+}]_{cyt}$ elevations are linked to many different stress responses, understanding their interactions with other signalling components is critical in determining the specificity of Ca^{2+} signalling.

3.4 The Role of Ca^{2+} in Flagellar Length

In addition to its central role in the process of flagellar excision, Ca^{2+} also contributes to the regulation of gene expression during flagellar regrowth (Cheshire and Keller 1991). Acid-induced deflagellation is followed by the rapid accumulation of transcripts for many flagella-related genes, and the increase is dependent on external Ca^{2+} (Evans and Keller 1997). The induction of gene expression is also greatly reduced in the presence of inhibitors of Ca^{2+} channels and in the *adf1* mutant, although these also exhibit decreased deflagellation (Evans and Keller 1997). However, deflagellation of Chlamydomonas cells by mechanical shear in the absence of Ca^{2+} prevents the upregulation of flagella-related gene transcripts, indicating that Ca^{2+} entry is required for the transcriptional response (Cheshire et al. 1994; Cheshire and Keller 1991).

There is also a direct requirement for Ca^{2+} in flagellar regrowth and length control. In low external Ca^{2+} (<0.15 μM), deflagellated cells do not regrow flagella at all until Ca^{2+} is restored to c. >0.5 μM (Cheshire and Keller 1991; Liang and Pan 2013). Ca^{2+} also appears to be required for the maintenance of flagellar length, as cells placed in very low Ca^{2+} media containing 25 mM Na^+ or K^+ will resorb their flagella (Lefebvre et al. 1978). Chlamydomonas *pf18* (paralysed flagella) cells have longer flagella when grown in elevated Ca^{2+} (2 mM), but they also produce longer flagella in the presence of Ca^{2+} channel blockers (La^{3+} and Cd^{2+}), which makes this result difficult to interpret (Tuxhorn et al. 1998). However, mammalian IMCD (immortalised kidney-collecting duct) cells treated with 30 μM Gd^{3+} (a non-specific blocker of Ca^{2+} channels) also show elongated cilia, suggesting that the effect of lanthanides on ciliary length may be conserved in eukaryotes (Besschetnova et al. 2010). Whilst it is not clear exactly how intraflagellar Ca^{2+} acts to regulate flagellar length in Chlamydomonas, significant recent progress has been made in identifying a requirement for Ca^{2+} sensor kinases. Chlamydomonas contains an expanded family of 14 Ca^{2+}-dependent protein kinases (CDPK), which possess an N-terminal serine/threonine kinase and 4 Ca^{2+}-binding EF hands at the C-terminus (Edel and Kudla 2015). Three CDPKs (CDPK1, CDPK3 and CDPK11) were identified in the flagellar proteome, suggesting a probable role in flagella function (Liang and Pan 2013; Pazour et al. 2005). RNAi knockdown strains for CDPK3 showed slow regrowth of flagella at low concentrations of external Ca^{2+}, but flagellar length, motility and mating were unaffected (Liang and Pan 2013). In contrast, RNAi knockdown of CDPK1 led to significantly reduced flagellar length and defects in IFT (Liang et al. 2014). CDPK1 acts to phosphorylate the FLA8 subunit of the microtubule motor protein kinesin-II, which disrupts the interaction between kinesin and the IFT-B subunit of the IFT particle. The phosphorylation of FLA8 by CDPK1 appears to block entry of kinesin into the flagella but also promotes dissociation of kinesin from the IFT-B particle at the flagellar tip. As a consequence, CDPK1 RNAi strains accumulate FLA8 and components of the IFT particle at the flagellar tip (Liang et al. 2014). These findings indicate that Ca^{2+} sensor kinases play an important role in flagellar length assembly and length control. As Ca^{2+} plays a direct role in the

regulation of IFT during gliding motility (Collingridge et al. 2013), it will be interesting to determine whether the directed movement of IFT particles also contributes to flagellar length control.

4 Cytosolic Ca^{2+} Signalling During Stress Responses

Compared to the wealth of evidence examining the diverse roles of Ca^{2+} in flagella function, there is relatively little information on the nature of the Ca^{2+}-dependent signalling processes in the cell body. However, there has been some important recent progress, most notably in examining the link between Ca^{2+} and photosynthesis. In land plants, Ca^{2+} signalling plays a central role in the response to many different environmental stimuli, including osmotic stress, oxidative stress, temperature and biotic stimuli, and the dynamics of the $[Ca^{2+}]_{cyt}$ elevations associated with each stimulus have been characterised in detail (Kiegle et al. 2000; Knight et al. 1997; Takahashi et al. 1997). In contrast, there have been very few studies involving direct imaging of $[Ca^{2+}]_{cyt}$ in green algae, and our understanding of the nature of $[Ca^{2+}]_{cyt}$ elevations in Chlamydomonas remains in its infancy (Bauer et al. 1997; Braun and Hegemann 1999; Thompson et al. 2007). A recent study demonstrated that different osmotic stimuli give rise to distinct $[Ca^{2+}]_{cyt}$ elevations in Chlamydomonas, although $[Ca^{2+}]_{cyt}$ elevations were not observed in response to oxidative stress from hydrogen peroxide (Bickerton et al. 2016). Hyperosmotic shock through the addition of NaCl resulted in a single $[Ca^{2+}]_{cyt}$ elevation that originated in the apex of the cell and rapidly propagated to the rest of the cytoplasm, resembling the well-characterised Ca^{2+} waves observed in animal cells. The timing and amplitude of the $[Ca^{2+}]_{cyt}$ elevation were dependent on the intensity of the stimulus. In contrast, hypoosmotic shocks induced by very dilute media or deionised water resulted in a series of repetitive $[Ca^{2+}]_{cyt}$ elevations (Bickerton et al. 2016). Hypoosmotic shock also induced repetitive $[Ca^{2+}]_{fla}$ elevations, but these did not coincide with the $[Ca^{2+}]_{cyt}$ elevations, suggesting that the flagella and the cytosol can respond independently to this stimulus (Bickerton et al. 2016). The requirement for Ca^{2+} in the osmotic signalling response appears to be conserved between Chlamydomonas and land plants, although the spatial and temporal nature of the resultant $[Ca^{2+}]_{cyt}$ elevations is distinct.

The $[Ca^{2+}]_{cyt}$ elevations observed in response to NaCl stress and hypoosmotic shock were both severely inhibited in the absence of external Ca^{2+}, suggesting an important role for Ca^{2+} entry across the plasma membrane in the initiation of the signalling response. However, it is likely that these $[Ca^{2+}]_{cyt}$ elevations involve further release of Ca^{2+} from intracellular stores following the initial Ca^{2+} entry (e.g. during propagation of the Ca^{2+} wave). A major internal store of Ca^{2+} in Chlamydomonas is likely to be the acidocalcisomes, which play a direct role in Ca^{2+} signalling in a range of other protists (Docampo and Huang 2016; Ruiz et al. 2001). Acidocalcisomes are numerous small low-pH vesicles that are rich in polyphosphate, Ca^{2+} and a range of other metal ions. Recent evidence in Chlamydomonas suggests that the

acidocalcisomes play an important role in cell survival during nutrient deficiency (sulphate, nitrate, phosphate) and are also used for the storage of metals such as zinc and copper (Aksoy et al. 2014; Hong-Hermesdorf et al. 2014). In trypanosomes and apicomplexan parasites, Ca^{2+} entry into acidocalcisomes is mediated by the action of Ca^{2+} ATPases, although it is likely that Ca^{2+}/H^+ antiporters also contribute to Ca^{2+} uptake (Docampo and Huang 2016). Chlamydomonas possesses three CAX Ca^{2+}/H^+ antiporters (Emery et al. 2012), although it is not known whether any of these localise to the acidocalcisomes. Characterisation of Chlamydomonas CAX1 identified some unusual properties, as CAX1 exhibits Na^+/H^+ exchange activity in addition to Ca^{2+}/H^+ exchange (Pittman et al. 2009). CAX1 may therefore contribute to Na^+ efflux during salt stress, in addition to its likely role in Ca^{2+} homeostasis. However, CAX1 expression was repressed by high concentrations of Ca^{2+} or Na^+, suggesting that it is unlikely to function primarily in the sequestration of excess Na^+ or Ca^{2+} (Pittman et al. 2009).

5 Ca^{2+} Signalling and Photosynthesis

One emerging area of significant interest in Chlamydomonas is the role of Ca^{2+} in regulating photosynthesis. An early report suggested that Ca^{2+} and CaM played a role in regulating the biosynthesis of chlorophyll by contributing to the transcriptional regulation of glutamate-1-semialdehyde aminomutase by blue light (Im et al. 1996). More recently, a direct link to Ca^{2+}-dependent regulation of photosynthesis has emerged through studies of the Ca^{2+}-sensor protein, CAS. CAS was initially identified in land plants as a sensor of external Ca^{2+} but was subsequently shown to localise to the thylakoid membranes and play a major role in the modulation of $[Ca^{2+}]_{cyt}$ elevations in stomatal guard cells (Nomura et al. 2008; Weinl et al. 2008). CAS also localises to the thylakoid membranes in Chlamydomonas and plays an important role in photoprotection through its role in the accumulation of LHCSR3 in high light (Petroutsos et al. 2011). LHCSR3 is a light-harvesting protein that is required for the dissipation of excess light energy through non-photochemical quenching (NPQ). CAS RNAi knockdown strains exhibit low levels of LHCSR3 and defects in NPQ, although both of these phenotypes can be rescued by the addition of 3 mM Ca^{2+} in the external media (Petroutsos et al. 2011). LHCSR3 is encoded by two genes *LHCSR3.1* and *LHCSR3.2* that produce an identical amino acid product, and both genes appear to be transcriptionally regulated by Ca^{2+} (Maruyama et al. 2014). Under anoxic conditions, CAS RNAi knockdown strains show a strong inhibition of cyclic electron flow (CEF) in photosystem I, which in wild-type cells is required for the generation of the pH gradient across the thylakoid membrane during NPQ (Terashima et al. 2012). CAS was shown to form a complex with a novel protein ANR1 and with PGR5-Like 1 (PGRL1), a protein that is required for normal CEF in land plants (Terashima et al. 2012). Recently, a novel class of Ca^{2+}-sensor proteins has also been described in Chlamydomonas. Calredoxin (CRX) possesses a unique combination of four Ca^{2+}-binding EF hands at the N-terminus and a

C-terminal thioredoxin domain and was localised to the chloroplast stroma (Hochmal et al. 2016). CRX interacts with a 2-cys peroxiredoxin in a Ca^{2+}-dependent manner in order to drive the detoxification of hydrogen peroxide. CRX mutant and RNAi knockdown strains are not defective in the induction of *LHCSR3* expression under high light but exhibit increased CEF (Hochmal et al. 2016). Together, these findings illustrate that Chlamydomonas is a very useful model to study the Ca^{2+}-dependent regulation of photosynthesis and its associated photoprotective mechanisms.

6 Evolution of the Ca^{2+} Signalling Toolkit

The sequencing of the Chlamydomonas genome and further advances in algal genomics have provided important insight into the evolution of the Ca^{2+} signalling in the green algae. Land plant genomes lack clear homologues of several classes of ion channel that are central to Ca^{2+} signalling in animal cells, including the four-domain voltage-dependent Ca^{2+} channels (VDCC), transient receptor potential (TRP) channels and the inositol triphosphate receptor (IP_3R) (Edel and Kudla 2015; Verret et al. 2010; Wheeler and Brownlee 2008). Instead, land plants possess an extended family of cyclic nucleotide-gated channels and ionotropic glutamate receptors (Swarbreck et al. 2013). In contrast, green algae possess multiple homologues of the well-characterised 'animal-like' Ca^{2+} channels that are absent from land plants, and experimental evidence indicates that members of the VDCC and TRP classes of ion channel play important roles in signal transduction in Chlamydomonas (Arias-Darraz et al. 2015; Fujiu et al. 2009, 2011; Huang et al. 2007; Merchant et al. 2007; Wheeler and Brownlee 2008). The broad distribution of these channels in the green algae and other eukaryote lineages suggests that they have been specifically lost in the land plants. Identification of their functional roles in Chlamydomonas and other green algae will be important in understanding the evolutionary processes leading to the loss of these Ca^{2+} channels in the land plants.

The mechanisms through which Ca^{2+} signals are generated in green algae are therefore very different from those found in land plants. Significant differences in the mechanisms that sense $Ca^{2+}$are also found between these lineages. Land plants have an expanded family of CaMs and CaM-like (CML) proteins, with a total of 58 proteins present in Arabidopsis. Whilst CaM is highly conserved amongst eukaryotes, CML is absent from animals and this family has become greatly expanded in the land plants. Chlamydomonas possesses a CaM homologue and eight CMLs belonging to 1c and III (Zhu et al. 2015). This complement is similar to the charophyte *Klebsormidium* suggesting that the major diversification of the CMLs into multiple subgroups occurred after this lineage diverged from the land plants (Zhu et al. 2015). Land plants also possess an expanded repertoire of Ca^{2+}-sensor kinases. For example, Arabidopsis has 34 CDPKs, 26 CIPKs and 10 CBLs (Edel and Kudla 2015). Whilst Chlamydomonas has 15 CDPKs, the CIPKs and their binding partner the CBLs appear to be absent, along with the CCaMKs. CIPKs/

CBLs are not specific to the land plants though, as a single CIPK and a CBL are present in *Ostreococcus* (Edel and Kudla 2015). This suggests that the CIPKs may have been lost in an ancestor of Chlamydomonas, although greater taxonomic sampling of other green algal lineages is required to resolve this. One of the Chlamydomonas CDPKs has unique domain architecture, possessing a C2 domain at the N-terminus (Hamel et al. 2014). C2 domains are often involved in Ca^{2+}-dependent membrane interactions, and this unique C2-CDPK was only found in other members of the Volvocales, suggesting that a single gene fusion event gave rise to this novel protein (Hamel et al. 2014).

7 Technical Considerations for the Study of Ca^{2+} Signalling in Chlamydomonas

The studies listed above illustrate just how many diverse processes are regulated by Ca^{2+} in Chlamydomonas. Whilst significant progress has now been made in characterising these signalling pathways, a fuller understanding of the role of Ca^{2+} in these signalling pathways has been hampered by the technical issues associated with Ca^{2+} imaging in Chlamydomonas. As with many plant and algal cells, loading of Ca^{2+}-responsive fluorescent dyes via membrane-permeant acetoxymethyl (AM) esters is problematic, due to unequal loading and dye compartmentalisation (Braun and Hegemann 1999). For example, the AM ester of the Ca^{2+}-responsive dye Fluo-4 was found to localise to the acidocalcisomes in Chlamydomonas (Hong-Hermesdorf et al. 2014). Because of these problems, the use of ester-loaded dyes for the examination of $[Ca^{2+}]_{cyt}$ dynamics, particularly over longer timescales or in fluorimetric approaches (rather than direct single cell imaging), is not recommended. Dextran-conjugated dyes are not subject to compartmentalisation as they are membrane impermeable, but they require specialised techniques in order to load them into intact cells. Microinjection is clearly not appropriate for small algal cells, but a biolistic delivery method for dextran-conjugated dyes into Chlamydomonas has been developed that provides robust and reproducible cytoplasmic dye loading (Bothwell et al. 2006; Wheeler and Brownlee 2008). Although this technique has proven to be reliable, there are clearly some disadvantages associated with this delivery method, such as the equipment and technical expertise required and the low proportion of cells that are loaded. Therefore, the future development of genetically encoded calcium indicators in Chlamydomonas is of top priority in order to advance this field. GECIs not only allow for simple routine imaging of $[Ca^{2+}]_{cyt}$, they may also be targeted to specific cellular locations (e.g. the mitochondria or the chloroplast) to enable the study of localised or intra-organellar $[Ca^{2+}]_{cyt}$ elevations. It is important to note that GECIs will be an important additional tool to be used alongside Ca^{2+}-responsive fluorescent dyes in Chlamydomonas, as the properties (e.g. Ca^{2+} dissociation kinetics, pH sensitivity) of certain dyes may make them a preferred choice for certain applications, such as

the observation of the very rapid flagellar Ca^{2+} elevations (Chen et al. 2013; Hendel et al. 2008). Whilst the development of further robust protocols for Ca^{2+} imaging is likely to be of greatest benefit in this field, the ability to perform electrophysiological studies in Chlamydomonas should not be overlooked. Much of our knowledge on flagellar signalling in Chlamydomonas originates from these approaches, and their application led to the discovery of channelrhodopsin.

8 Concluding Remarks

The broad scope of this review demonstrates the wide-reaching influence of Ca^{2+}-dependent signalling processes on the cell biology of Chlamydomonas. Significant progress has now been made in identifying the molecular mechanisms and physiological processes associated with diverse signalling pathways. However, there is clearly much to be learnt and our knowledge of Ca^{2+} signalling in Chlamydomonas remains limited. In particular, whilst individual components of some signalling pathways have now been identified, e.g. the ion channels, the Ca^{2+} elevations or the Ca^{2+} sensors, there are very few examples where all of these aspects have been characterised and compiled into working knowledge of the whole pathway. To some extent, this is partially true for the land plants, where the molecular identification of the specific Ca^{2+} channels responsible for well-characterised ion currents and Ca^{2+} elevations has proven to be problematic (Swarbreck et al. 2013). The reduced complexity of the Ca^{2+} signalling toolkit in Chlamydomonas may allow for simpler resolution of these issues. Chlamydomonas has already proven to be an important model for the study of signalling processes relating to flagella and photosynthesis. Studies in Chlamydomonas have also contributed important information on the evolution of Ca^{2+} signalling. Together these studies have revealed many surprising and novel aspects of the Ca^{2+}-dependent signalling pathways in Chlamydomonas, and there are likely to be many more exciting discoveries in the future.

References

Aksoy M, Pootakham W, Grossman AR (2014) Critical function of a *Chlamydomonas reinhardtii* putative polyphosphate polymerase subunit during nutrient deprivation. Plant Cell 26:4214–4229

Arias-Darraz L, Cabezas D, Colenso CK, Alegria-Arcos M, Bravo-Moraga F, Varas-Concha I, Almonacid DE, Madrid R, Brauchi S (2015) A transient receptor potential ion channel in Chlamydomonas shares key features with sensory transduction-associated TRP channels in mammals. Plant Cell 27:177–188

Bauer CS, Plieth C, Hansen UP, Sattelmacher B, Simonis W, Schonknecht G (1997) Repetitive Ca^{2+} spikes in a unicellular green alga. FEBS Lett 405:390–393

Berthold P, Tsunoda SP, Ernst OP, Mages W, Gradmann D, Hegemann P (2008) Channelrhodopsin-1 initiates phototaxis and photophobic responses in Chlamydomonas by immediate light-induced depolarization. Plant Cell 20:1665–1677

Besschetnova TY, Kolpakova-Hart E, Guan Y, Zhou J, Olsen BR, Shah JV (2010) Identification of signaling pathways regulating primary cilium length and flow-mediated adaptation. Curr Biol 20:182–187

Bessen M, Fay RB, Witman GB (1980) Calcium control of waveform in isolated flagellar axonemes of Chlamydomonas. J Cell Biol 86:446–455

Bickerton P, Sello S, Brownlee C, Pittman JK, Wheeler GL (2016) Spatial and temporal specificity of Ca^{2+} signalling in *Chlamydomonas reinhardtii* in response to osmotic stress. New Phytol 212 (4):920–933

Bloodgood RA (1981) Flagella-dependent gliding motility in Chlamydomonas. Protoplasma 106:183–192

Bloodgood RA (1995) Flagellar surface motility: gliding and microsphere movements. Methods Cell Biol 47:273–279

Bloodgood RA (2009) The *Chlamydomonas* flagellar membrane and its dynamic properties. In: Witman GB (ed) The Chlamydomonas sourcebook. Academic, Oxford, pp 309–368

Bloodgood RA, Salomonsky NL (1990) Calcium influx regulates antibody-induced glycoprotein movements within the Chlamydomonas flagellar membrane. J Cell Sci 96(Pt 1):27–33

Bloodgood RA, Workman LJ (1984) A flagellar surface glycoprotein mediating cell-substrate interaction in Chlamydomonas. Cell Motil 4:77–87

Bothwell JHF, Brownlee C, Hetherington AM, Ng CKY, Wheeler GL, McAinsh MR (2006) Biolistic delivery of Ca^{2+} dyes into plant and algal cells. Plant J 46:327–335

Braun FJ, Hegemann P (1999) Direct measurement of cytosolic calcium and pH in living Chlamydomonas reinhardtii cells. Eur J Cell Biol 78:199–208

Brownlee C (1994) Tansley review No-70 – signal-transduction during fertilization in algae and vascular plants. New Phytol 127:399–423

Casey DM, Inaba K, Pazour GJ, Takada S, Wakabayashi K, Wilkerson CG, Kamiya R, Witman GB (2003a) DC3, the 21-kDa subunit of the outer dynein arm-docking complex (ODA-DC), is a novel EF-hand protein important for assembly of both the outer arm and the ODA-DC. Mol Biol Cell 14:3650–3663

Casey DM, Yagi T, Kamiya R, Witman GB (2003b) DC3, the smallest subunit of the Chlamydomonas flagellar outer dynein arm-docking complex, is a redox-sensitive calcium-binding protein. J Biol Chem 278:42652–42659

Chen TW, Wardill TJ, Sun Y, Pulver SR, Renninger SL, Baohan A, Schreiter ER, Kerr RA, Orger MB, Jayaraman V et al (2013) Ultrasensitive fluorescent proteins for imaging neuronal activity. Nature 499:295–300

Cheshire JL, Keller LR (1991) Uncoupling of Chlamydomonas flagellar gene expression and outgrowth from flagellar excision by manipulation of Ca^{2+}. J Cell Biol 115:1651–1659

Cheshire JL, Evans JH, Keller LR (1994) Ca^{2+} signaling in the Chlamydomonas flagellar regeneration system: cellular and molecular responses. J Cell Sci 107(Pt 9):2491–2498

Collingridge P, Brownlee C, Wheeler GL (2013) Compartmentalized calcium signaling in cilia regulates intraflagellar transport. Curr Biol 23:2311–2318

DeCoursey TE (2013) Voltage-gated proton channels: molecular biology, physiology, and pathophysiology of the H(V) family. Physiol Rev 93:599–652

DiPetrillo CG, Smith EF (2010) Pcdp1 is a central apparatus protein that binds Ca(2+)-calmodulin and regulates ciliary motility. J Cell Biol 189:601–612

DiPetrillo CG, Smith EF (2013) Methods for analysis of calcium/calmodulin signaling in cilia and flagella. Methods Enzymol 524:37–57

Docampo R, Huang G (2016) Acidocalcisomes of eukaryotes. Curr Opin Cell Biol 41:66–72

Dymek EE, Smith EF (2007) A conserved CaM- and radial spoke associated complex mediates regulation of flagellar dynein activity. J Cell Biol 179:515–526

Edel KH, Kudla J (2015) Increasing complexity and versatility: how the calcium signaling toolkit was shaped during plant land colonization. Cell Calcium 57:231–246

Ehlenbeck S, Gradmann D, Braun FJ, Hegemann P (2002) Evidence for a light-induced H(+) conductance in the eye of the green alga *Chlamydomonas reinhardtii*. Biophys J 82:740–751

Emery L, Whelan S, Hirschi KD, Pittman JK (2012) Protein phylogenetic analysis of Ca(2+)/cation antiporters and insights into their evolution in plants. Front Plant Sci 3:1

Ermilova E, Zalutskaya Z, Munnik T, van den Ende H, Gromov B (1998) Calcium in the control of chemotaxis in Chlamydomonas. Biologia 53:577–581

Evans JH, Keller LR (1997) Calcium influx signals normal flagellar RNA induction following acid shock of *Chlamydomonas reinhardtii*. Plant Mol Biol 33:467–481

Finst RJ, Kim PJ, Griffis ER, Quarmby LM (2000) Fa1p is a 171 kDa protein essential for axonemal microtubule severing in Chlamydomonas. J Cell Sci 113(Pt 11):1963–1971

Foster KW, Smyth RD (1980) Light antennas in phototactic algae. Microbiol Rev 44:572–630

Fujiu K, Nakayama Y, Yanagisawa A, Sokabe M, Yoshimura K (2009) Chlamydomonas CAV2 encodes a voltage- dependent calcium channel required for the flagellar waveform conversion. Curr Biol 19:133–139

Fujiu K, Nakayama Y, Iida H, Sokabe M, Yoshimura K (2011) Mechanoreception in motile flagella of Chlamydomonas. Nat Cell Biol 13:630–632

Goodenough UW, Shames B, Small L, Saito T, Crain RC, Sanders MA, Salisbury JL (1993) The role of calcium in the *Chlamydomonas reinhardtii* mating reaction. J Cell Biol 121:365–374

Govorunova EG, Sineshchekov OA (2003) Integration of photo- and chemosensory signaling pathways in Chlamydomonas. Planta 216:535–540

Govorunova EG, Sineshchekov OA (2005) Chemotaxis in the green flagellate alga Chlamydomonas. Biochemistry (Mosc) 70:717–725

Hamel LP, Sheen J, Seguin A (2014) Ancient signals: comparative genomics of green plant CDPKs. Trends Plant Sci 19:79–89

Harz H, Hegemann P (1991) Rhodopsin-regulated calcium currents in Chlamydomonas. Nature 351:489–491

Hegemann P, Berthold P (2009) Sensory photoreceptors and light control of flagellar activity. In: Witman GB (ed) The Chlamydomonas sourcebook. Academic, Oxford, pp 395–429

Hendel T, Mank M, Schnell B, Griesbeck O, Borst A, Reiff DF (2008) Fluorescence changes of genetic calcium indicators and OGB-1 correlated with neural activity and calcium in vivo and in vitro. J Neurosci 28:7399–7411

Hill K, Hemmler R, Kovermann P, Calenberg M, Kreimer G, Wagner R (2000) A Ca(2+)- and voltage-modulated flagellar ion channel is a component of the mechanoshock response in the unicellular green alga *Spermatozopsis similis*. Biochim Biophys Acta 1466:187–204

Hilton LK, Meili F, Buckoll PD, Rodriguez-Pike JC, Choutka CP, Kirschner JA, Warner F, Lethan M, Garces FA, Qi J, Quarmby LM (2016) A forward genetic screen and whole genome sequencing identify deflagellation defective mutants in Chlamydomonas, including assignment of ADF1 as a TRP channel. G3 6(10):3409–3418

Hochmal AK, Zinzius K, Charoenwattanasatien R, Gabelein P, Mutoh R, Tanaka H, Schulze S, Liu G, Scholz M, Nordhues A et al (2016) Calredoxin represents a novel type of calcium-dependent sensor-responder connected to redox regulation in the chloroplast. Nat Commun 7:11847

Holland EM, Braun FJ, Nonnengasser C, Harz H, Hegemann P (1996) Nature of rhodopsin-triggered photocurrents in Chlamydomonas.1. Kinetics and influence of divalent ions. Biophys J 70:924–931

Holland EM, Harz H, Uhl R, Hegemann P (1997) Control of phobic behavioral responses by rhodopsin-induced photocurrents in Chlamydomonas. Biophys J 73:1395–1401

Hong-Hermesdorf A, Miethke M, Gallaher SD, Kropat J, Dodani SC, Chan J, Barupala D, Domaille DW, Shirasaki DI, Loo JA et al (2014) Subcellular metal imaging identifies dynamic sites of Cu accumulation in Chlamydomonas. Nat Chem Biol 10:1034–1042

Horst CJ, Witman GB (1993) ptx1, a nonphototactic mutant of Chlamydomonas, lacks control of flagellar dominance. J Cell Biol 120:733–741

Huang K, Diener DR, Mitchell A, Pazour GJ, Witman GB, Rosenbaum JL (2007) Function and dynamics of PKD2 in *Chlamydomonas reinhardtii* flagella. J Cell Biol 179:501–514

Hyams JS, Borisy GG (1978) Isolated flagellar apparatus of Chlamydomonas: characterization of forward swimming and alteration of waveform and reversal of motion by calcium ions in vitro. J Cell Sci 33:235–253

Im CS, Matters GL, Beale SI (1996) Calcium and calmodulin are involved in blue light induction of the gsa gene for an early chlorophyll biosynthetic step in Chlamydomonas. Plant Cell 8:2245–2253

Kam V, Moseyko N, Nemson J, Feldman LJ (1999) Gravitaxis in *Chlamydomonas reinhardtii*: characterization using video microscopy and computer analysis. Int J Plant Sci 160:1093–1098

Kamiya R, Okamoto M (1985) A mutant of *Chlamydomonas reinhardtii* that lacks the flagellar outer dynein arm but can swim. J Cell Sci 74:181–191

Kamiya R, Witman GB (1984) Submicromolar levels of calcium control the balance of beating between the 2 flagella in demembranated models of Chlamydomonas. J Cell Biol 98:97–107

Kiegle E, Moore CA, Haseloff J, Tester MA, Knight MR (2000) Cell-type-specific calcium responses to drought, salt and cold in the Arabidopsis root. Plant J 23:267–278

Knight H, Trewavas AJ, Knight MR (1997) Calcium signalling in *Arabidopsis thaliana* responding to drought and salinity. Plant J 12:1067–1078

Kreimer G, Witman GB (1994) Novel touch-induced, Ca(2+)-dependent phobic response in a flagellate green alga. Cell Motil Cytoskeleton 29:97–109

Lefebvre PA, Nordstrom SA, Moulder JE, Rosenbaum JL (1978) Flagellar elongation and shortening in Chlamydomonas. IV. Effects of flagellar detachment, regeneration, and resorption on the induction of flagellar protein synthesis. J Cell Biol 78:8–27

Liang Y, Pan J (2013) Regulation of flagellar biogenesis by a calcium dependent protein kinase in *Chlamydomonas reinhardtii*. PLoS One 8:e69902

Liang Y, Pang Y, Wu Q, Hu Z, Han X, Xu Y, Deng H, Pan J (2014) FLA8/KIF3B phosphorylation regulates kinesin-II interaction with IFT-B to control IFT entry and turnaround. Dev Cell 30:585–597

Lohret TA, McNally FJ, Quarmby LM (1998) A role for katanin-mediated axonemal severing during Chlamydomonas deflagellation. Mol Biol Cell 9:1195–1207

Maruyama S, Tokutsu R, Minagawa J (2014) Transcriptional regulation of the stress-responsive light harvesting complex genes in *Chlamydomonas reinhardtii*. Plant Cell Physiol 55:1304–1310

Matsuda A, Yoshimura K, Sineshchekov OA, Hirono M, Kamiya R (1998) Isolation and characterization of novel Chlamydomonas mutants that display phototaxis but not photophobic response. Cell Motil Cytoskeleton 41:353–362

McAinsh MR, Pittman JK (2009) Shaping the calcium signature. New Phytol 181:275–294

Merchant SS, Prochnik SE, Vallon O, Harris EH, Karpowicz SJ, Witman GB, Terry A, Salamov A, Fritz-Laylin LK, Marechal-Drouard L et al (2007) The Chlamydomonas genome reveals the evolution of key animal and plant functions. Science 318:245–250

Nagel G, Ollig D, Fuhrmann M, Kateriya S, Mustl AM, Bamberg E, Hegemann P (2002) Channelrhodopsin-1: a light-gated proton channel in green algae. Science 296:2395–2398

Nagel G, Szellas T, Huhn W, Kateriya S, Adeishvili N, Berthold P, Ollig D, Hegemann P, Bamberg E (2003) Channelrhodopsin-2, a directly light-gated cation-selective membrane channel. Proc Natl Acad Sci U S A 100:13940–13945

Nomura H, Komori T, Kobori M, Nakahira Y, Shiina T (2008) Evidence for chloroplast control of external Ca^{2+}-induced cytosolic Ca^{2+} transients and stomatal closure. Plant J 53:988–998

Nonnengasser C, Holland EM, Harz H, Hegemann P (1996) The nature of rhodopsin-triggered photocurrents in Chlamydomonas. II. Influence of monovalent ions. Biophys J 70:932–938

Okita N, Isogai N, Hirono M, Kamiya R, Yoshimura K (2005) Phototactic activity in Chlamydomonas 'non-phototactic' mutants deficient in Ca^{2+}-dependent control of flagellar dominance or in inner-arm dynein. J Cell Sci 118:529–537

Pan J, Snell WJ (2000) Signal transduction during fertilization in the unicellular green alga, Chlamydomonas. Curr Opin Microbiol 3:596–602

Pan J, Wang Q, Snell WJ (2004) An aurora kinase is essential for flagellar disassembly in Chlamydomonas. Dev Cell 6:445–451

Pasquale SM, Goodenough UW (1987) Cyclic AMP functions as a primary sexual signal in gametes of *Chlamydomonas reinhardtii*. J Cell Biol 105:2279–2292

Patel-King RS, Gorbatyuk O, Takebe S, King SM (2004) Flagellar radial spokes contain a Ca^{2+}-stimulated nucleoside diphosphate kinase. Mol Biol Cell 15:3891–3902

Pazour GJ, Agrin N, Leszyk J, Witman GB (2005) Proteomic analysis of a eukaryotic cilium. J Cell Biol 170:103–113

Petroutsos D, Busch A, Janssen I, Trompelt K, Bergner SV, Weinl S, Holtkamp M, Karst U, Kudla J, Hippler M (2011) The chloroplast calcium sensor CAS is required for photoacclimation in *Chlamydomonas reinhardtii*. Plant Cell 23:2950–2963

Pittman JK, Edmond C, Sunderland PA, Bray CM (2009) A cation-regulated and proton gradient-dependent cation transporter from *Chlamydomonas reinhardtii* has a role in calcium and sodium homeostasis. J Biol Chem 284:525–533

Quarmby LM (1996) Ca^{2+} influx activated by low pH in Chlamydomonas. J Gen Physiol 108:351–361

Quarmby LM (2004) Cellular deflagellation. Int Rev Cytol 233(233):47–91

Quarmby LM, Hartzell HC (1994) Two distinct, calcium-mediated, signal transduction pathways can trigger deflagellation in *Chlamydomonas reinhardtii*. J Cell Biol 124:807–815

Quarmby LM, Yueh YG, Cheshire JL, Keller LR, Snell WJ, Crain RC (1992) Inositol phospholipid-metabolism may trigger flagellar excision in *Chlamydomonas reinhardtii*. J Cell Biol 116:737–744

Rasi MQ, Parker JD, Feldman JL, Marshall WF, Quarmby LM (2009) Katanin knockdown supports a role for microtubule severing in release of basal bodies before mitosis in Chlamydomonas. Mol Biol Cell 20:379–388

Ruiz FA, Marchesini N, Seufferheld M, Govindjee D, R. (2001) The polyphosphate bodies of *Chlamydomonas reinhardtii* possess a proton-pumping pyrophosphatase and are similar to acidocalcisomes. J Biol Chem 276:46196–46203

Sakato M, Sakakibara H, King SM (2007) Chlamydomonas outer arm dynein alters conformation in response to Ca^{2+}. Mol Biol Cell 18:3620–3634

Saotome M, Safiulina D, Szabadkai G, Das S, Fransson A, Aspenstrom P, Rizzuto R, Hajnoczky G (2008) Bidirectional Ca^{2+}-dependent control of mitochondrial dynamics by the Miro GTPase. Proc Natl Acad Sci U S A 105:20728–20733

Schneider F, Gradmann D, Hegemann P (2013) Ion selectivity and competition in channelrhodopsins. Biophys J 105:91–100

Shih SM, Engel BD, Kocabas F, Bilyard T, Gennerich A, Marshall WF, Yildiz A (2013) Intraflagellar transport drives flagellar surface motility. elife 2:e00744

Sineshchekov OA, Jung KH, Spudich JL (2002) Two rhodopsins mediate phototaxis to low- and high-intensity light in *Chlamydomonas reinhardtii*. Proc Natl Acad Sci U S A 99:8689–8694

Sjoblad RD, Frederikse PH (1981) Chemotactic responses of *Chlamydomonas reinhardtii*. Mol Cell Biol 1:1057–1060

Smith EF (2002) Regulation of flagellar dynein by calcium and a role for an axonemal calmodulin and calmodulin-dependent kinase. Mol Biol Cell 13:3303–3313

Swarbreck SM, Colaco R, Davies JM (2013) Plant calcium-permeable channels. Plant Physiol 163:514–522

Takahashi K, Isobe M, Knight MR, Trewavas AJ, Muto S (1997) Hypoosmotic shock induces increases in cytosolic Ca^{2+} in tobacco suspension-culture cells. Plant Physiol 113:587–594

Terashima M, Petroutsos D, Hudig M, Tolstygina I, Trompelt K, Gabelein P, Fufezan C, Kudla J, Weinl S, Finazzi G et al (2012) Calcium-dependent regulation of cyclic photosynthetic electron transfer by a CAS, ANR1, and PGRL1 complex. Proc Natl Acad Sci U S A 109:17717–17722

Thompson SE, Callow JA, Callow ME, Wheeler GL, Taylor AR, Brownlee C (2007) Membrane recycling and calcium dynamics during settlement and adhesion of zoospores of the green alga *Ulva linza*. Plant Cell Environ 30:733–744

Tuxhorn J, Daise T, Dentler WL (1998) Regulation of flagellar length in Chlamydomonas. Cell Motil Cytoskeleton 40:133–146

Verret F, Wheeler G, Taylor AR, Farnham G, Brownlee C (2010) Calcium channels in photosynthetic eukaryotes: implications for evolution of calcium-based signalling. New Phytol 187:23–43

Wakabayashi K, Ide T, Kamiya R (2009) Calcium-dependent flagellar motility activation in *Chlamydomonas reinhardtii* in response to mechanical agitation. Cell Motil Cytoskeleton 66:736–742

Wang Q, Snell WJ (2003) Flagellar adhesion between mating type plus and mating type minus gametes activates a flagellar protein-tyrosine kinase during fertilization in Chlamydomonas. J Biol Chem 278:32936–32942

Weinl S, Held K, Schlucking K, Steinhorst L, Kuhlgert S, Hippler M, Kudla J (2008) A plastid protein crucial for Ca^{2+}-regulated stomatal responses. New Phytol 179:675–686

Wheeler GL, Brownlee C (2008) Ca^{2+} signalling in plants and green algae - changing channels. Trends Plant Sci 13:506–514

Wheeler GL, Joint I, Brownlee C (2008) Rapid spatiotemporal patterning of cytosolic Ca^{2+} underlies flagellar excision in *Chlamydomonas reinhardtii*. Plant J 53:401–413

Yoshimura K (1996) A novel type of mechanoreception by the flagella of Chlamydomonas. J Exp Biol 199:295–302

Yoshimura K, Matsuo Y, Kamiya R (2003) Gravitaxis in *Chlamydomonas reinhardtii* studied with novel mutants. Plant Cell Physiol 44:1112–1118

Zhu X, Dunand C, Snedden W, Galaud JP (2015) CaM and CML emergence in the green lineage. Trends Plant Sci 20:483–489

Chlamydomonas: The Eyespot

Mark D. Thompson, Telsa M. Mittelmeier, and Carol L. Dieckmann

Abstract Vision evolved in motile, single-celled, green algae to enhance photosynthetic capability. A specialized structure within the cell, the eyespot, aids in the detection of light direction and is key to improving the efficiency of phototactic behavior. The *Chlamydomonas reinhardtii* eyespot is the most well-studied photoreceptive structure guiding cellular movement. Crucial features required for function as a light-sensing organelle and signal transducer affecting swimming behavior are (1) a light-signal transduction cascade, i.e., photon capture, membrane depolarization, and flagellar waveform change; (2) a structure that allows discernment of light direction, i.e., the elaborate layered membrane organization of the eyespot; and (3) precise placement of the organelle relative to the flagella, required for coupling the space/time of light reception to the space/time of the flagellar response accurately. Here we summarize what is known about eyespot function, assembly and placement, and highlight the development of new tools and approaches that will aid in illuminating Chlamydomonas eyespot structure and function.

1 Introduction

Vision evolved in motile, single-celled, green algae to enhance photosynthetic capability. Rhodopsin proteins inherited from prokaryotic ancestors absorb photons and change conformation, triggering downstream signaling events that direct swimming to locations optimal for photosynthesis. Phototaxis, or moving in response to light, is a complex behavior that requires many cellular components in addition to the rhodopsin photoreceptors. The cell must be able to crawl or swim. And, it must be able to discern the location of the light source and link motility behavior to that information. A specialized structure within the cell, the eyespot,

Experimental work in the Dieckmann lab was supported by NSF award MCB-1157795 (M.T., T.M. and C.D.) and NIH award T32 GM008659 (M.T.).

M.D. Thompson • T.M. Mittelmeier • C.L. Dieckmann (✉)
Department of Molecular and Cellular Biology, University of Arizona,
Tucson, AZ 85721, USA
e-mail: dieckman@u.arizona.edu

M. Hippler (ed.), *Chlamydomonas: Molecular Genetics and Physiology*,
Microbiology Monographs 30, DOI 10.1007/978-3-319-66365-4_9

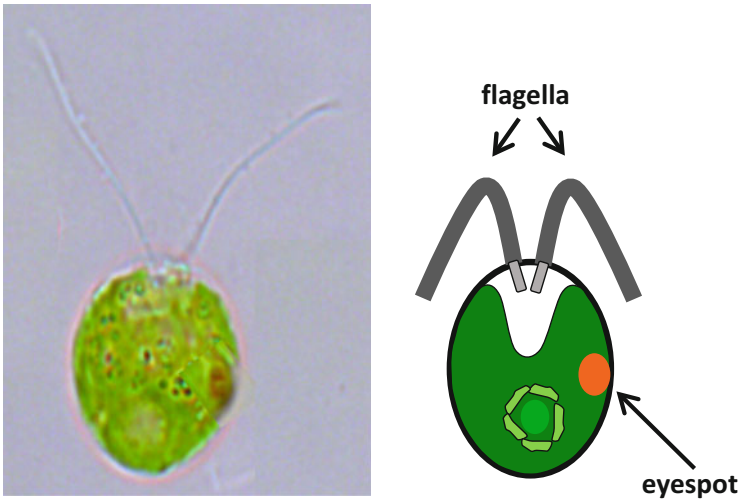

Fig. 1 Chlamydomonas eyespot. Composite color micrograph and diagram highlighting the position of the eyespot relative to the flagella. The *orange eyespot* is visible on the background of the large, *green*, cup-shaped chloroplast. The paired flagella, patterned by the basal bodies (*light gray* in diagram), emanate from the apical pole of the cell. The pyrenoid (*light green circle*) defines the posterior pole

aids in the detection of light direction and is key to improving the efficiency of phototactic behavior.

Many species of algae have eyespots, organelles that have evolved to organize photoreceptors together with other components that enhance directional light reception. Eyespots are likely to have arisen in different lineages independently (Kivic and Walne 1983), but most share the ability to block light from one or more directions in the cell, thereby enhancing detection from a particular direction relative to the cell. The *Chlamydomonas reinhardtii* eyespot is the most well-studied photoreceptive structure guiding cellular movement.

The eyespot is readily apparent by light microscopy as an orange oval within the single, green Chlamydomonas cell (Fig. 1). The approximately 1 μm spot is located at the "equator" of the cell, roughly halfway between the anterior flagellar pole and the posterior pole, defined by the pyrenoid, which stores starch in the chloroplast. The eyespot appears to be associated with the plasma membrane on the outer surface of the cell. Its role in light detection was first verified by Hartshorne (1953), who collected an eyeless mutant strain *(eye1)* that could not phototax. Subsequent studies with additional *eye1* strains confirmed that the eyespot is required for accurate phototactic behavior (Morel-Laurens and Feinleib 1983; Foster et al. 1984).

Collectively, data gathered over several decades by many different researchers has led to a better understanding of Chlamydomonas eyespot structure and function [reviewed in: Foster and Smyth (1980), Witman (1993), Kreimer (1994), Hegemann (1997), Sineshchekov and Govorunova (2001), Nagel et al. (2005) and Kreimer (2009)]. Crucial features required for function as a light-sensing organelle and signal

transducer affecting swimming behavior are (1) a light-signal transduction cascade, i.e., photon capture, membrane depolarization, and flagellar waveform change; (2) a cellular structure that allows discernment of light direction, i.e., the elaborate layered membrane organization of the eyespot; and (3) precise placement of the organelle relative to the flagella, required for coupling the space/time of light reception to the space/time of the flagellar response accurately. Each of these three features will be the focus of a separate section below.

2 Light-Signal Transduction Cascade

Rhodopsin photoreceptors in the eyespot absorb light over a broad range of wavelengths, with maxima in the blue-aqua-green part of the spectrum. Two different proteins with overlapping absorbance spectra, ChR1 and ChR2, govern the phototactic behavior of Chlamydomonas cells (Nagel et al. 2002, 2003; Sineshchekov et al. 2002). These rhodopsin family proteins with seven transmembrane domains are most similar to prokaryotic rhodopsins and form ion channels. Absorption of a photon by the retinal cofactor leads to a conformational change in the opsin, which opens the ion channel and depolarizes the membrane. Thus, the Chlamydomonas receptors, which are cation channels, have been named "channelrhodopsins." Other names for the ChR1 and ChR2 photoreceptors are CsrA and CsrB (Sineshchekov et al. 2002) and Acop-1 and Acop-2 (Suzuki et al. 2003). Innovative work has led to the extensive use of ChR2 for specific control of neurons and other cells in a variety of animals (Boyden et al. 2005). Presently, multiple such channelrhodopsins are available, tuned to different wavelengths of light (Wietek and Prigge 2016). "Optogenetic" control of animal behavior is the most dramatic use of these light-activated Chlamydomonas plasma membrane ion channels.

Membrane depolarization can be detected at the eyespot after light exposure, moving in a wave along the membrane of the cell and flagella (Harz and Hegemann 1991). Details of the ion fluxes at the eyespot and flagella have been analyzed by pipette recording under a variety of conditions (Holland et al. 1996; Nonnengässer et al. 1996). In response to membrane depolarization, high-speed video microscopy has revealed that the primarily symmetric breaststroke beating of the two flagella becomes temporarily asymmetric (Rüffer and Nultsch 1985, 1987). One of the two flagella takes less robust strokes, while the other takes more robust strokes. This uneven pulling turns the cell such that it reorients and swims toward the light (Fig. 2, top row). The differential waveform responses of the two flagella were observed also using demembranated models of flagella and manipulation of the calcium ion concentration (Kamiya and Witman 1984). Depolarization and the change in calcium ion concentration ultimately lead to a change in the complex breaststroke waveform of the Chlamydomonas flagella, likely due to the differential response of the inner arm dynein motors along the length of the flagella (Horst and Witman 1993; Rüffer and Nultsch 1997; King and Dutcher 1997; Okita et al. 2005). Are there three different states for a flagellum during phototaxis: normal stroking,

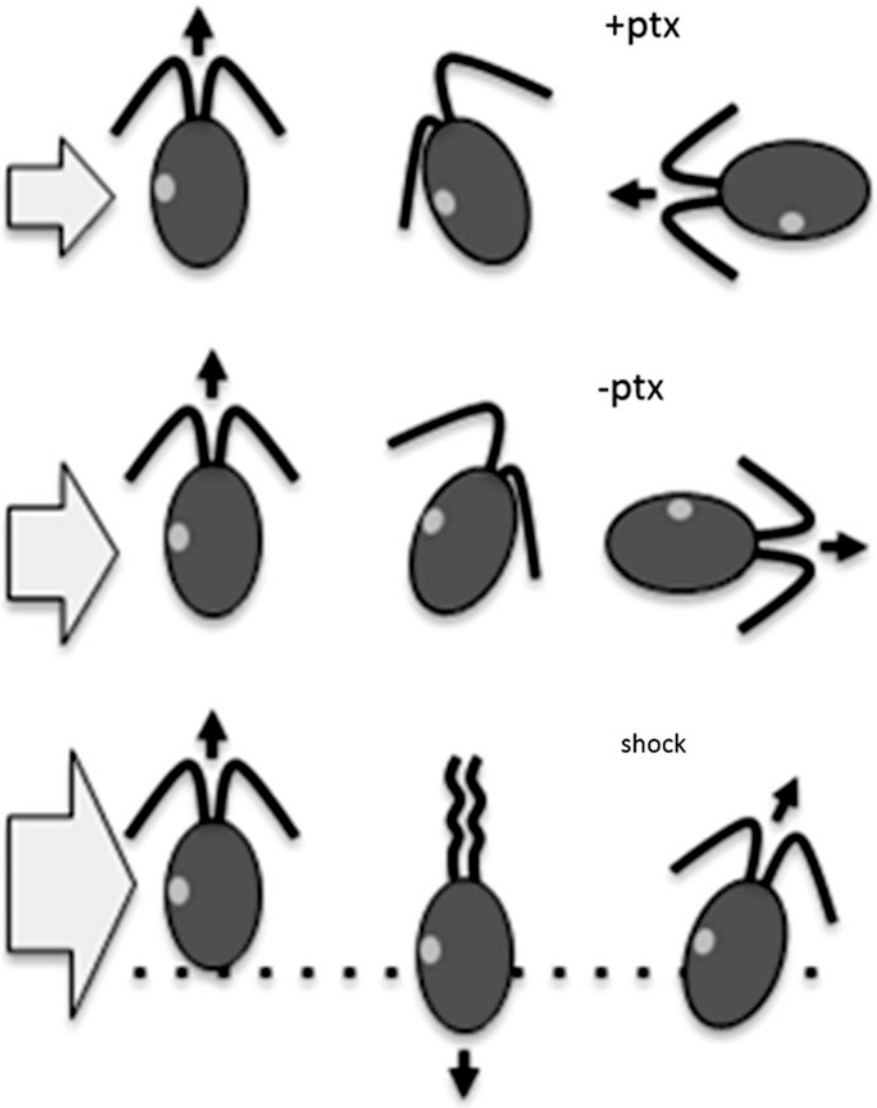

Fig. 2 Responses to light. Three cell cartoons in each *row* represent a time series *from left to right*. Initially the cell is breaststroking forward (*up*). When the light is turned on (*arrow on left*), the cell turns toward the light (+ptx = positive phototaxis). In stronger light (*second row*), the cell turns away from the light (−ptx = negative phototaxis). In very bright light (*third row*), the flagella switch from breaststroking to an undulating waveform (photoshock), which pushes the cell backward (*down*) for a half second, then they resume breaststroking in a randomly chosen direction

overstroking, and understroking, sampled by switching? Or, is flagellar stroking on a continuum governed by some kind of amplitude scalar?

The swimming pattern of Chlamydomonas cells is more complicated than can be described by "breaststroke." When the photoreceptors are not activated, such as in the dark or in red light, the flagella pull the cells forward. However, the strokes of the two flagella are not exact mirror images of one another. The flagellum templated by the older (mother) basal body has a slightly off-plane stroke that causes the cell to spiral slowly at two revolutions for every 60 strokes per second (Rüffer and Nultsch 1987; Fig. 3). The spiral path means that the eyespot, on only one side of the cell, samples the environment in any particular direction twice per second. Though they appear equivalent, there must be an inherent difference between the flagellum templated by the mother *versus* the daughter basal body that is responsible for this refinement in the breaststroke waveform.

Another refinement of the phototactic response is observed when cells are exposed to light of different intensities. Photosynthetic membranes can be damaged by light that is too bright, because the light-harvesting and protective pigment molecules are overwhelmed and free radicals are generated that damage proteins and lipids in the membranes (Schuster et al. 1986). When exposed to light intensities that could damage the membranes, Chlamydomonas cells swim away from light instead of toward it (Fig. 2, middle row). How does this switch in the flagellar response happen? Instead of the mother flagellum overstroking and the daughter understroking as for positive phototaxis, the daughter overstrokes and the mother understrokes. Thus, both flagella can over- or understroke and are not hardwired for one or the other response. Cells exposed to very bright flashes of light exhibit yet another behavior, called the "photophobic" response, in which both flagella lose their breaststroke waveform completely and beat much more similarly to other motile eukaryotic flagella, in an undulation pattern that propels the cell "backward" for a half second (Fig. 2, bottom row). Then, the cell resumes breaststroking forward (Ringo 1967). The "sign" of phototaxis (positive vs. negative) can be switched by manipulating free radical levels (Wakabayashi et al. 2011) or expression of functional domains of the blue-light receptor, phototropin (Trippens et al. 2012), but the mechanisms governing switching and photophobic behavior are still a mystery.

3 Eyespot Structure and Function

Why did carotenoid-pigmented eyespots evolve in green algae? Many different types of experiments have been done over the years to understand why eyespots arose. A strong consensus is that they enhance the ability to detect light direction. Light is directional, i.e., it comes from a source: the sun, a lightning bolt, a fire, a light bulb, or a laser. Motile photosynthetic algae have an advantage if they can adjust their location relative to the sun to optimize photosynthesis, while minimizing damage to the thylakoid membranes. So, how does the eyespot help with detection of light direction?

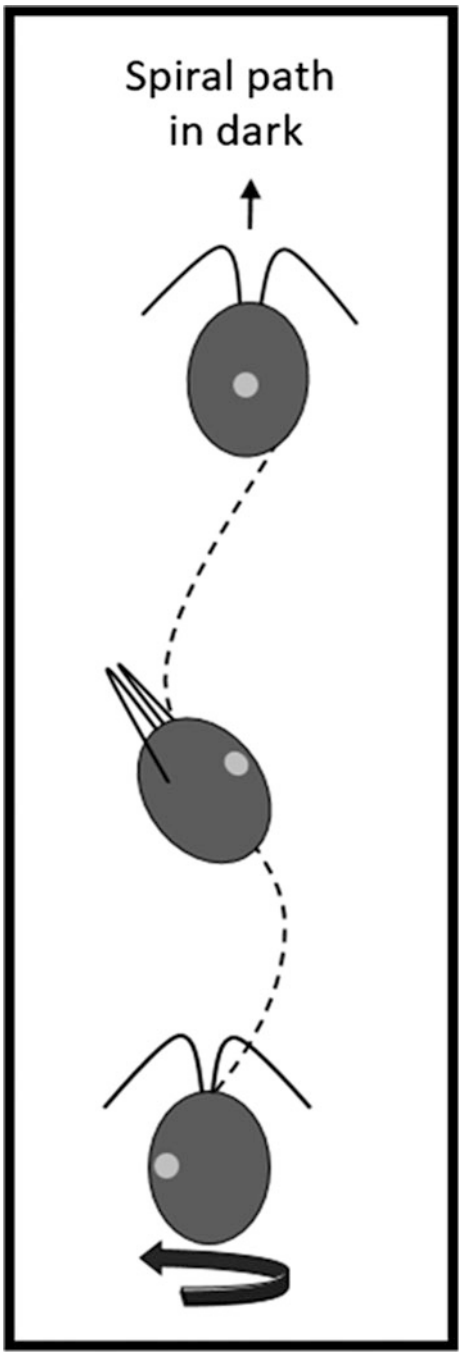

Fig. 3 Chlamydomonas swims in spiral path. Chlamydomonas flagella breaststroke in almost a flat plane relative to each other. However, the *trans* flagellum, on the side away from the eyespot, beats just slightly out of the plane, causing the cell to rotate as it strokes forward. The cell rotates approximately twice per second, while the flagella beat about 60 times and move the cell forward 100–200 μm

The Chlamydomonas eyespot is on/near the surface of the cell. Light shining on the outer surface of the eyespot activates the light-signal transduction cascade governing phototaxis. Light shining on the other side of the cell, and/or through the cell, is absorbed efficiently by the elaborate layered structure of the eyespot, and the cascade is not activated. These observations suggest that the eyespot structure is "sided" and that the plasma membrane side is different from the side toward the cell. Electron microscopy first revealed the complexity of the eyespot structure and the involvement of chloroplast membranes, though the orange eyespot had been observed against the green background of the large cup-shaped chloroplast many years before by light microscopy. As shown in the cryo-EM micrograph (Fig. 4) and 3D reconstruction (Fig. 5), the plasma membrane and both chloroplast envelopes are tightly apposed in the region of the eyespot (Engel et al. 2015). Underlying the inner envelope are rows of carotenoid-filled pigment granules, with each row subtended by a thylakoid. In 1980, Foster and Smyth hypothesized that this periodic arrangement of granules and membranes acted as a quarter-wave plate, absorbing photons traveling through the cell and striking the layers from the "back" and reflecting photons striking the eyespot surface from the outside back toward the

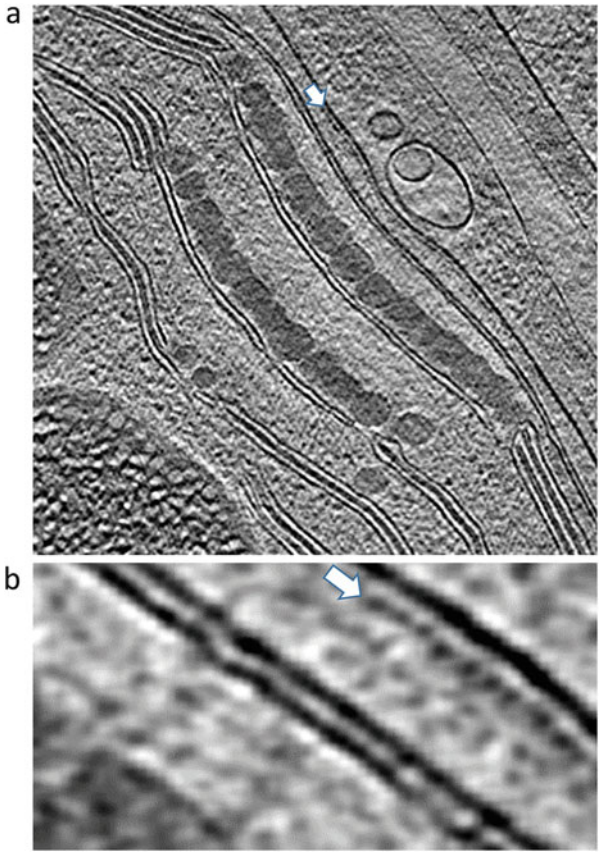

Fig. 4 Cryo-EM section of the eyespot. One section through the eyespot, showing the layered structure. Part (**b**) is an enlargement of a small area of Part (**a**); the *white arrows* are in approximately the same location in the micrographs and point to a row of ordered particles just under the plasma membrane. Reprinted with permission from Ben Engel (Engel et al. 2015)

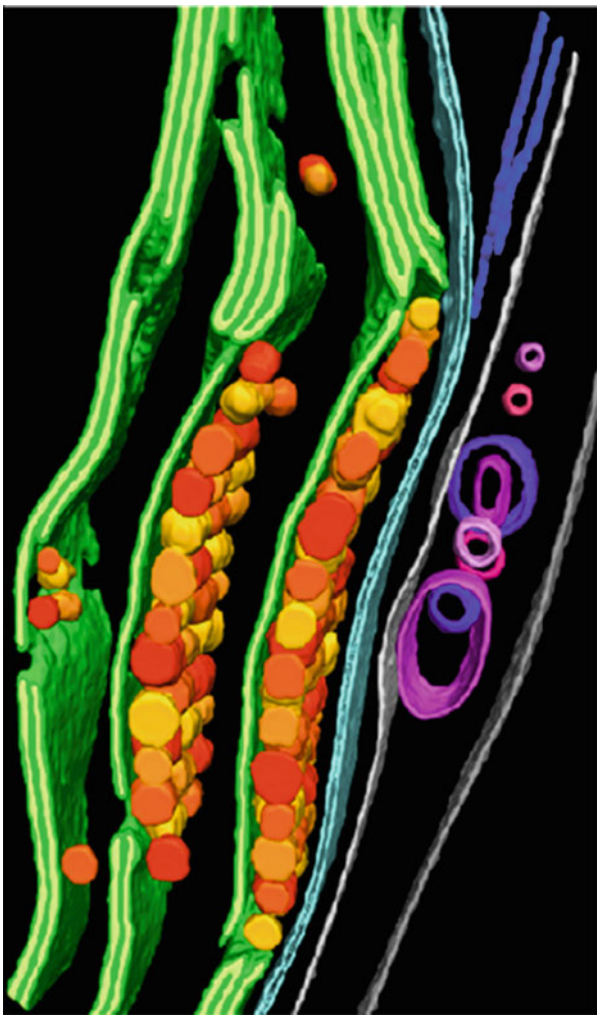

Fig. 5 3D reconstruction of cryo-EM sections through the eyespot. The outside of the cell is on the *right*. *False colors* were used to distinguish the separate parts of the eyespot structure. Moving *leftward* through the layers: the *outer gray ribbon* is part of the cell wall. The *purple* and *pink "bubbles"* between the wall and the plasma membrane were found only at the eyespot but are of unknown function. The *inner gray ribbon* is the plasma membrane. The *bright blue structures* just under the plasma membrane in the *top right* are microtubules, presumably in the D4 rootlet. The *light blue membranes* are the chloroplast outer and inner envelopes. The pigment granules are *various shades of orange*, and the thylakoids are *green*. Reprinted with permission from Ben Engel (Engel et al. 2015)

photoreceptors. Both the abilities of the eyespot to block light from the back (Ueki et al. 2016; Matsunaga et al. 2003) and to reflect light from the outside (Kreimer and Melkonian 1990) have been demonstrated experimentally, lending credence to the quarter-wave plate explanation for how this organelle functions. In recent years, immunofluorescence microscopy has revealed much about the fine structure and function of the eyespot.

The channelrhodopsins are localized in the plasma membrane, positioned to capture photons as they first strike the surface of the cell over the eyespot or secondarily after reflection by the chloroplast layers (Berthold et al. 2008; Mittelmeier et al. 2013). These molecules may be what was visualized long ago by freeze-fracture as the major protein entities in the membranes of the eyespot (Melkonian and Robenek 1980). In 2002–2003, three research groups searched the

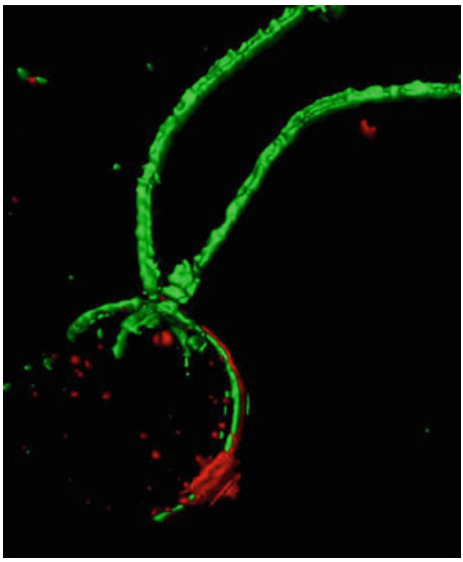

Fig. 6 ChR1 photoreceptors are on the outer surface of the D4 microtubule rootlet. Fluorescence micrograph of a Chlamydomonas cell taken with a structured illumination microscope. Acetylated tubulin monoclonal (*green*) highlights the flagella and four microtubule rootlets. Channelrhodopsin 1 staining (*red*) is apparent along the outer surface of the D4 microtubule rootlet and aggregated at the eyespot

recently available cDNA databases for rhodopsin-like molecules and found cDNAs for ChR1 and ChR2 (Nagel et al. 2002, 2003; Sineshchekov et al. 2002; Suzuki et al. 2003). Knockdown analyses showed that they function redundantly for the most part vis-à-vis phototaxis and photoshock (Sineshchekov et al. 2002, 2009; Govorunova et al. 2004). Antisera specific to each channelrhodopsin were raised and have shown that both proteins are restricted to the plasma membrane of the eyespot (Berthold et al. 2008; Mittelmeier et al. 2013), with small accumulations of ChR1 apparent in pools near the basal bodies and in a stripe on one of the four major microtubule rootlet bundles in the cell body (Mittelmeier et al. 2011, Fig. 6).

What do we know about the specific protein and lipid composition of the eyespot, other than the photoreceptor opsins in the plasma membrane? Two major approaches have been employed to learn about eyespot proteins. A forward genetics approach has yielded a few candidates (Lamb et al. 1999), and a mass spectrometry approach has yielded many more (Schmidt et al. 2006; Wagner et al. 2008; Eitzinger et al. 2015). Here, we have organized what is known about individual eyespot proteins by "layer," based on the experimentally determined or inferred localization of each component.

4 Plasma Membrane Eyespot Proteins

In addition to the genes encoding ChR1 and ChR2 (*COP3* and *COP4*, respectively), six other opsin genes have been identified in the Chlamydomonas genome (Kateriya et al. 2004, Awasthi et al. 2016). COP1 and COP2, products of the same gene by alternative splicing, are abundant and localized at the eyespot, but do not function as light receptors for phototaxis (Deininger et al. 1995; Fuhrmann

et al. 2001). COP2 was found to co-purify with a factor important for photosystem I assembly, Ycf4, and reducing levels of COP2 to 10% of wild type resulted in destabilization of the Ycf4 complex (Ozawa et al. 2009). Perhaps this light receptor governs the assembly of the photosystem (Ozawa et al. 2009; Kreimer 2009). HKR1/COP5, COP6, COP7, and COP8 have the characteristic opsin membrane helices and in addition have histidine kinase domains hypothesized to function in signal transduction cascades as they do in other "two-component" systems (Kateriya et al. 2004; Luck et al. 2012, Awasthi et al. 2016). HKR1 has been localized to the eyespot by immunofluorescence microscopy (Luck et al. 2012), and COP8 to flagella and the eyespot (Awasthi et al. 2016). Phototropin, which functions in blue-light signal transduction, is found in plasma membrane, axonemal, and soluble fractions. At the eyespot, phototropin is likely localized to the plasma membrane and governs the size of the organelle with respect to light fluence; in high light, the eyespot becomes smaller, and in low light, the eyespot becomes larger. And, though levels of ChR1 are decreased in high light, eyespot size determination is not dependent on ChR1, because a *Δcop3* mutant has wild-type eyespot size (Trippens et al. 2012). Phototropin must stimulate/inhibit as yet unknown crucial regulators of eyespot assembly to affect the size changes relative to environmental light levels.

Individual mutant strains that could not phototax were collected and screened for eyespot defects by light microscopy (Lamb et al. 1999). Mutations in the *MIN1* gene, on chromosome XII, were identified in strains with miniature eyespots. Electron microscopy revealed that the *min1* mutant strain had disorganized eyespots. When grown on minimal medium, the pigment granule layers were found "floating" in the stroma of the chloroplast, rather than tightly apposed to the envelope and plasma membrane layers. MIN1 is predicted to be a membrane-spanning protein lacking a chloroplast-targeting signal (Fig. 7). The polypeptide has an N-terminal C2 domain, recognized in other proteins as important for interaction with phospholipid bilayers. In transfection experiments with the large cells of the moss Physcomitrella, a MIN1 C2 domain-YFP fusion protein associated

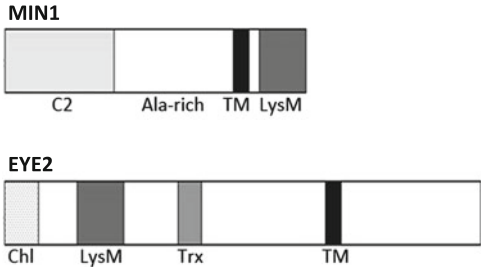

Fig. 7 MIN1 and EYE2 both have transmembrane and LysM domains. Two eyespot proteins, MIN1 and EYE2, both have transmembrane domains (TM) and LysM domains. MIN1 has a C2 domain thought to be important for membrane adhesion and a low complexity region rich in alanine residues. EYE2 has a chloroplast-targeting sequence (Chl) and a thioredoxin-family active site domain (Trx)

with the outer chloroplast envelope (Mittelmeier et al. 2008). Mutation of two conserved aspartate residues to alanine in the C2 domain, thought to coordinate calcium ions important for recognition, abolished the association of the fusion protein with the chloroplast envelope. Collectively, the following features suggest that MIN1 is required for adhesion of the chloroplast components to the outer layers and resides either in the outer chloroplast envelope or the plasma membrane: the disorganized eyespot phenotype of the *min1* mutant strain, the presence of a membrane-interacting domain and a membrane-spanning helix in MIN1, lower levels of photoreceptors in the *min1* mutant strain, and lack of a chloroplast-targeting sequence. Verification of this hypothesis awaits the development of MIN1-specific antibodies.

The MIN1 C-terminal domain belongs to the LysM family, the most extensively characterized eukaryotic members of which are found extracellularly and are involved in recognition between plant roots and nitrogen-fixing bacteria (reviewed in Greeff et al. 2012). The domain has been shown to bind directly to chitin and peptidoglycan in cell walls (Gust 2015), which usually are not found intracellularly, nor at all in Chlamydomonas (Woessner and Goodenough 1994). Interestingly, many such LysM domains are found in Chlamydomonas proteins, particularly several in the eyespot proteome (Schmidt et al. 2006; Wagner et al. 2008; Eitzinger et al. 2015; Table 1). Have these domains been co-opted to function in adhesion between layers in the Chlamydomonas eyespot?

Table 1 Chlamydomonas proteins containing LysM domains

Chlamydomonas proteins containing LysM domains		
Gene name/alias	Phytozome v. 11 Cre#	In eyespot proteome
LMR2	Cre03.g175351	
g4985.t1	Cre04.g227800	
g7058.t1	Cre06.g304913	
AKC2	Cre06.g307100	
g8874.t1	Cre08.g376740	
LMR1	Cre09.g393765	**X**
CEP9	Cre09.g404250	
CEP10	Cre10.g456950	
MIN1	Cre12.g490700	**X**
EYE2	Cre12.g509250	**X**
g14687.t1	Cre14.g609202	
PLP8, PLAP8	Cre14.g611700	**X**
g14905.t1	Cre14.g618641	
ELG36	Cre14.g619850	
CEP13, SRR29	Cre14.g631100	
CEP14	Cre14.g631150	
LMR3	Cre16.g667100	
CEP16	Cre17.g697300	
CEP17	Cre17.g736100	
g18125.t1	Cre19.g750397	

5 Chloroplast Envelope Protein

An eyeless strain from the phototaxis mutant screen, *eye2*, also has a mutation in a gene on chromosome XII, about a million base pairs from *MIN1* (Phytozome v11.0). The EYE2 protein has a chloroplast-targeting signal and, by immunofluorescence microscopy, appears to reside in one of the chloroplast envelopes (Boyd et al. 2011b). It has an interesting combination of recognizable domains (Fig. 7). One small domain in the middle of the polypeptide fits well in the 5′ adenylylsulfate reductase subfamily of thioredoxin superfamily enzymes. These enzymes catalyze the conversion of adenosine 5′ phosphosulfate to sulfite in the cysteine biosynthetic pathway and are primarily found in the stroma of plant chloroplasts (Davidian and Kopriva 2010). Why the reductase activity would be required for eyespot biogenesis was not readily apparent, and mutating the redox active site cysteines to serines had no deleterious effect on eyespot formation and phototaxis (Roberts et al. 2001). Does this domain reside in the Chlamydomonas chloroplast stroma, or another compartment? Localization and orientation in one of two chloroplast envelopes of the eyespot await verification by immuno-electron microscopy. The other recognizable domain in EYE2 is a LysM domain, similar to that in MIN1 and two other eyespot proteins (Table 1).

6 Pigment Granule Proteins

Another *eyeless* locus was identified in our original screen, *EYE3*. The gene encoding EYE3 resides on chromosome II and thus is not part of the eyespot-specific cluster on chromosome XII. Rabbit antiserum raised against an EYE3 peptide sequence was used to show that EYE3 is a constituent of eyespot granules (Boyd et al. 2011b). EYE3 is a Ser-Thr kinase in the ABC1 family (Do et al. 2001), and though the details have yet to be published (Dieckmann lab), mutation of the predicted active site Asp residue in the EYE3 kinase domain causes the loss of eyespot pigment granules, the *eye3* eyeless phenotype readily apparent by light microscopy.

EYE3 is most similar to several kinases found in plastoglobules of Arabidopsis (Lundquist et al. 2012). By comparing the extensive list of Chlamydomonas eyespot proteins generated by proteomic analyses (Schmidt et al. 2006; Wagner et al. 2008; Eitzinger et al. 2015), to the similar list of Arabidopsis plastoglobule proteins, it is clear that eyespot granules or globules are similar to plastoglobules and are likely evolutionarily related (Kreimer 2009; Davidi et al. 2014, 2015). These compartments, bounded by proteins called fibrillins and monolayers of phospholipids, are home to enzymes involved in biosynthesis of hydrophobic molecules required for photosynthetic and other plant functions, such as tocopherols and carotenoids.

Recently, Lohscheider et al. (2016) surveyed all available phosphoproteome data for plastoglobules and found many phospho-sites on the structural fibrillins that bound the globules. They hypothesize that the Ser-Thr ABC1 kinases may be responsible for the phosphorylation of these proteins. Perhaps phosphorylation is required for assembly or stability of the plastoglobule surface, and by analogy, there could be a similar requirement for eyespot granule assembly/stability.

In addition to the EYE3 serine/threonine kinase, other ABC1 homologues of unknown function with respect to eyespot formation and/or photosynthesis were identified in the eyespot proteome and, similar to EYE3, are likely to be constituents of the eyespot pigment granules. The first identified eukaryotic ABC1 kinase, and most well studied, is the yeast mitochondrial ubiquinone biosynthetic factor Coq8, which is required for specific phosphorylation of three enzymes in the multimeric Coq complex, Coq3, Coq5, and Coq7. Phosphorylation has been shown to be required for Coq complex assembly and activity (Xie et al. 2011). In Arabidopsis, the ABC1K1/ABC1K3 complex is required for prenylquinone biosynthesis in plastoglobules, likely through phosphorylation of tocopherol cyclase (reviewed in van Wijk and Kessler 2017). Based on what is known about Coq8 and the similarity of EYE3 to Arabidopsis plastoglobular ABC1K6, EYE3 kinase activity may be required for biosynthesis of some type of quinone in the pigment granules of the Chlamydomonas eyespot, and loss of this activity is deleterious for eyespot granule formation.

Another interesting eyespot component first identified by proteomics, SOUL3, binds hemin and was shown to be a constituent of eyespot granules (Schulze et al. 2013). Knockdown of *SOUL3* expression led to smaller eyespots, suggesting that like EYE3, this granule protein is required also for the integrity of granules and/or the full oval shape of the organelle.

7 Asymmetric Placement of the Eyespot

Chlamydomonas cells appear to be bilaterally symmetric when viewed through the light microscope, with the symmetry axis running from the apical basal bodies to the posterior chloroplast structure called the pyrenoid. The single, orange eyespot is the readily apparent symmetry anomaly (Fig. 1). On closer examination from the flagellar pole perspective, the eyespot is found offset precisely 45° clockwise from the plane of flagellar beating (Fig. 8; Rüffer and Nultsch 1985; Holmes and Dutcher 1989). Presumably a product of the evolutionary refinement of the coupling of light reception to the flagellar response, this position serves the signal transduction pathway optimally. Chlamydomonas cells rotate twice per second as they swim forward (Fig. 3), and the elapsed time from photon capture by ChR's at the eyespot to a change in the symmetric breaststroke waveform is about 62 ms, matching the time it takes for an eighth of a revolution or 45°. This puts the paired under- and overstrokes by the flagella precisely in the position required to swim toward (or away from) the light.

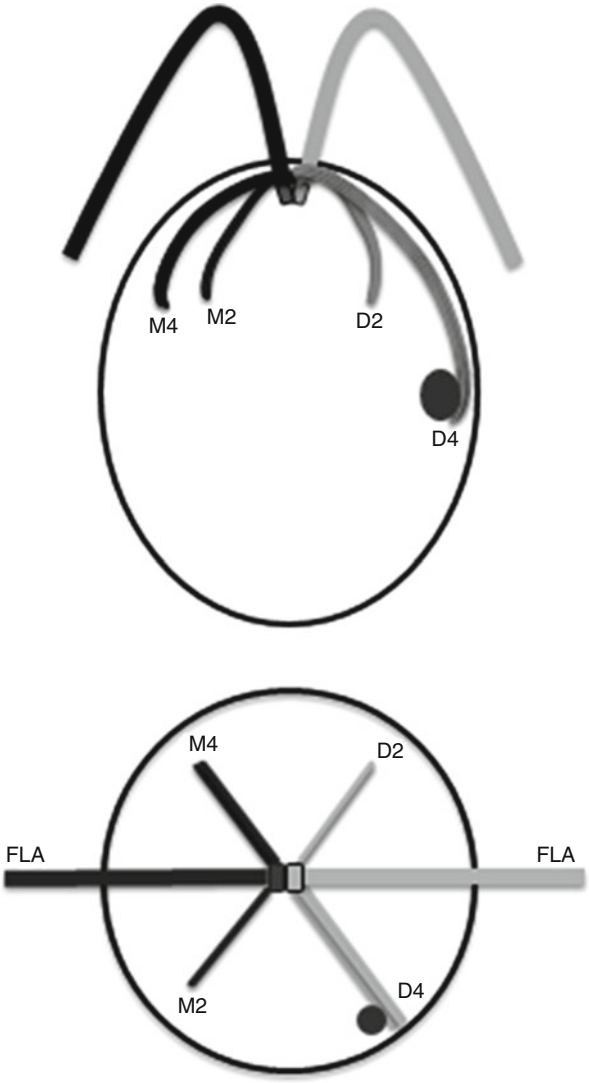

Fig. 8 Asymmetric microtubule cytoskeleton dictates eyespot position. Major elements of the microtubule cytoskeleton are shown in a side view of a cell (*top*) and in a top-down view of the cell (*bottom*). The eyespot is positioned at the equator of the cell (*dark oval*), next to the D4 rootlet, which is longer than the other three. The flagellum and rootlets on the right side of the cell are "**D**aughter" structures (*light gray*), formed since the last cell division. On the *left side* of the cell are "**M**other" structures (*dark gray*/*black*), formed prior to the last division

In addition to the eyespot, other cellular structures, which appear to be symmetric by microscopic analysis of interphase cells, are known to be differentiated by age and composition. For example, the basal bodies differ in age. The mother basal body in a cell is at least one generation older than the daughter, which matures from a pro-basal body just before division. As mentioned above, the flagellum templated by the mother basal body must differ in composition or regulation of the constituent dyneins responsible for waveform, because the stroke differs slightly from that of the daughter. Also, only the mother flagellum is assembled in *uni1*, *uni2*, *and uni3* mutant strains (Huang et al. 1982; Dutcher and Trabuco 1998; Piasecki and Silflow 2009).

Two pairs of microtubule bundles, called rootlets, are associated with the basal bodies. The mother pair, called the M2 and M4 rootlets, comprise two and four microtubules, respectively. And, the daughter pair, D2 and D4, first appears during cell division. Similar to the flagellar microtubules, the microtubules in these four rootlets are highly acetylated and can be distinguished from other microtubules of the cell cortex and spindle utilizing an invaluable monoclonal antibody that recognizes the acetylated form of tubulin coupled with immunofluorescence microscopy (LeDizet and Piperno 1986; Fig. 6).

Holmes and Dutcher (1989) did a beautiful study describing the duplication of the basal bodies and rootlet apparatus during cell division, orienting the structures relative to the position of the eyespot. They found that the eyespot was always associated with the equatorial end of the D4 rootlet. Therefore, though not readily apparent by light microscopy, the microtubule cytoskeleton is asymmetric in age of the basal bodies and associated rootlets. Our hypothesis has been that the eyespot was positioned near the D4 rootlet by "read out" of some unique feature of the asymmetric cytoskeleton.

Trying to understand how the eyespot is positioned relative to the flagellar plane became a serious quest when we isolated the *mlt1* mutant in our original screen for eyespot-defective strains (Lamb et al. 1999). The mutant strain had multiple eyespots, most often two in logarithmically growing cultures. Roughly 40% of the cells had two eyespots on one side of the cell, and another 40% had an eyespot on either side of the cell. In both types of cells, the eyespots appeared to be closer to the anterior pole than wild-type equatorial eyespots. The remainder of the cells in a culture had zero, one, or more than two eyespots. The percentage of cells with more than two eyespots increased as the cultures entered into, or remained in, stationary phase. Single cells from such a culture grow and divide, resulting in a similar distribution of cells with aberrant phenotypes. Thus, *mlt1* mutants are defective in the control of eyespot number and proper placement in the cell.

One early hypothesis was that perhaps, unlike wild type, *mlt1* cells might retain the "old" eyespot during cell division. This proved not to be the case. As shown in Fig. 9, the eyespot in a wild-type mother cell disappears as cell division progresses. Indeed, the plane of division is coincident with the longitude of the eyespot. We found that eyespots in *mlt1* mother cells, regardless of position within the cell, also disappear at division.

A generous gift of antiserum raised against the ChR1 channelrhodopsin (Peter Hegemann, Berlin) launched the analysis of specific eyespot proteins relative to the asymmetric rootlet cytoskeleton by immunofluorescence microscopy. Using a fluorescence microscope purchased in 1999, we observed photoreceptor at the eyespot in wild-type and *min1* mutant cells (Mittelmeier et al. 2008). This was the first evidence that photoreceptor molecules were still associated with the D4 rootlet in cells in which the chloroplast pigment granule layers were disorganized as for *min1*, or absent as for *eye2* and *eye3* mutant cells (Boyd et al. 2011b). However, instead of defining an oval shape of wild-type size, the photoreceptors were seen in small dots or streaks directly on the D4 rootlet.

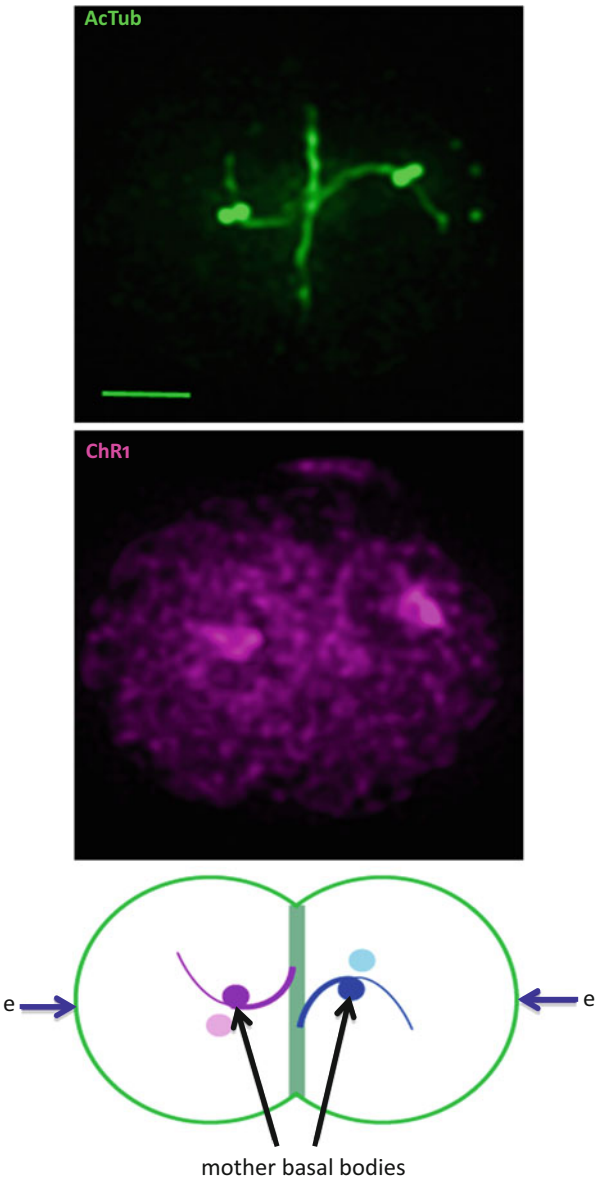

Fig. 9 "Old" eyespots disappear in early cell division. Fluorescence micrograph of a dividing cell viewed from the apical pole shows two pairs of basal bodies (*green dots*) have separated into the daughter cells, retaining the old two- and four-membered rootlets (*green*), now mother rootlets. New D4 rootlets have not begun to grow out to the positions where ChR1 photoreceptors will aggregate at the new eyespots, labeled "e"

Understanding the importance of the D4 to eyespot assembly was enhanced by the acquisition of a deconvolution microscope. Higher resolution and deconvolution allowed the detection of photoreceptor not only in oval shapes at the eyespot in wild-type cells, but all along the cortical surface (outside) of the D4 rootlet (Mittelmeier et al. 2011). In addition, small "pools" or "depots" of photoreceptor

were observed near the apical ends of the four-membered rootlets. Now, images captured by a superresolution microscope have solidified the impression that photoreceptor is found on the "outer" surface of the D4, coincident with the plasma membrane (Fig. 6).

Our current hypothesis, based on the fluorescence microscopy data described above, is that the channelrhodopsins are inserted into the endoplasmic reticulum membrane co-translationally. After trafficking through the Golgi stacks, vesicles travel to the apical "depots" where they fuse with the plasma membrane. From this location, the large, atypical C-terminal domains of the Chlamydomonas photoreceptor molecules are captured by kinesin motors near the minus ends of the D4 microtubules and are trafficked along the rootlet, with the canonical rhodopsin membrane-spanning helices in the N-halves of the molecules embedded in, and "dragged through," the plasma membrane. Alternatively, the vesicles may be trafficked on the microtubules, and fusion with the plasma membrane occurs at the eyespot. However, it is not clear why vesicles would be restricted to the outside surface of the rootlet. Another alternative hypothesis is that photoreceptor is not trafficked on microtubules, but the vesicles fuse with the membrane only over the D4 rootlet and at the eyespot location. Differentiating among these three hypotheses awaits development of live cell microscopy to visualize movement of photoreceptor molecules.

Why do we observe depots of photoreceptor near the minus ends of the D4 and M4 rootlet, but photoreceptor is only trafficked on, or associated with, the D4 rootlet? A breakthrough in understanding the exclusivity of the D4 for photoreceptor association came after a successful third attempt to acquire a useful antiserum to the MLT1 protein (Mittelmeier et al. 2015). The MLT1 antibodies detect the protein exclusively on the D4 rootlet, from the minus ends, all along the rootlet to the apical edge of the eyespot. Most interphase cells have a "tag end" of acetylated rootlet extending beyond the posterior edge of the eyespot, but this tag end of the D4 does not have MLT1 deposition. Therefore, the MLT1 protein on the D4 not only defines the exclusive longitude of the eyespot in the cell needed for phototaxis but also the latitude of the eyespot near the equator of the cell.

Since MLT1 is only observed on the D4 rootlet, what happens when cell division begins and the D4 is soon to become an M4? A careful study of cells going through division showed that as soon as the flagella are resorbed and the new daughter basal bodies are mature enough to stain with the anti-acetylated monoclonal, the MLT1 protein disappears from the D4 (Mittelmeier et al. 2015). Once the two pairs of basal bodies separate from each other into the daughter cells, there is a brief period when only the old rootlets are visible with anti-acetylated tubulin antibody. Once the new D4 and D2 rootlets begin to emanate from near the daughter basal bodies, MLT1 polyclonal antibodies detect the protein on the nascent D4 rootlet. Only later do the daughter rootlets stain with the anti-acetylated monoclonal. Thus, it appears that MLT1 associates with the D4 simultaneously with the growth of the D4 outward from the daughter basal body just under the plasma membrane and in the direction of the equator of the cell. Why it does not associate with the D2 rootlet as

well appears to depend on centrin fibers, because in a centrin mutant strain, *vfl2*, MLT1 associated with the presumptive D2 as well as the D4 rootlet. Centrin must either block MLT1 association with the D2 directly via depositions on the apical portion of the two-membered rootlets (Geimer and Melkonian 2005), or it acts indirectly by maintaining structural features of the basal body complex that are critical for excluding the D2.

Is MLT1 needed absolutely for determining longitude and latitude of the eyespot? The answer is yes and no or "sort of," for longitude. Photoreceptor is still found on four-membered rootlets in *mlt1* mutant cells, but appearance at the eyespot is very delayed after cell division. In wild type, the ChR's arrive at the eyespot simultaneously with the appearance of the EYE2 protein in the underlying chloroplast envelope. In *mlt1* cells, EYE2 arrives with wild-type kinetics, but the ChR's are delayed, and the apical pools of photoreceptor molecules expand into huge aggregations. *mlt1* mutant cells often have two eyespots on the D4 but just as many have an eyespot on the M4 and the D4. Why? Perhaps, photoreceptor transport is so defective in *mlt1* cells that the huge apical pools promote misdirected trafficking down both four-membered rootlets. And, why the more apical positions of the eyespots on the D4 and M4? Perhaps with the delay in trafficking, the position is fixed more anteriorly. Though photoreceptors/eyespots associate with the D4 rootlet eventually in *mlt1* mutant cells, MLT1 must have a key role in promoting eyespot formation, since eyespots form at the ends of both MLT1-decorated rootlets in centrin mutant cells (Mittelmeier et al. 2015).

8 Other Latitude Effectors

In addition to *MLT1*, other genes govern eyespot latitude. A mutation in the *PEY1* (posterior eyespot) gene leads to a more posterior placement of the eyespot in the cell. Immunofluorescence staining of the rootlets showed that the D4 rootlet is longer in general than in wild-type cells (Boyd et al. 2011a). The *cmu1* mutation also results in much more posterior eyespots and very long cytoplasmic microtubules, including the rootlets (Horst et al. 1999). The genes disrupted by these mutations have yet to be identified, and thus the mechanism of rootlet lengthening is unknown. However, the data suggest that the eyespot is more posteriorly positioned because the D4 is longer.

We could also consider the hypothesis that eyespot position affects the length of the D4. During wild-type cell division, the D4 rootlet microtubules "grow" toward the equator of the cell, where the new eyespot forms. The eyespot appears to become "fixed" at the equator, and for a brief period, the D4 and other rootlets continue extending to the very posterior pole of the cell. This "long rootlet" stage is brief and is followed by recession of the plus ends back toward the anterior of the cell, with the D4 stopping near the posterior edge of the fixed eyespot. Often an aforementioned "tag end" of the D4 can be seen below the eyespot after recession. It is our supposition that further recession of the D4 is blocked by the fixed position

of the eyespot. This idea is strengthened by the recession of the other three rootlets to much more apical positions (Mittelmeier et al. 2011). Thus, one could hypothesize that the latitude of the eyespot and D4 length reflect the relative rates of D4 growth toward the posterior pole, D4 disassembly following the long rootlet stage, and eyespot fixation.

9 Clustering of Eyespot Loci and Similar Cell Cycle Expression Profiles

Several of the genes we have identified through forward genetic screens are located on the left arm of chromosome XII. As shown in Table 2, *MIN1*, *EYE2*, and *MLT1* are within one million base pairs of each other, and *EYE2* and *MLT1* are only 50 kb apart. Also, the *MLT2* locus maps to the region just centromeric of *MLT1*. Thus, four of the six loci we have identified are in this region of the genome. The other two, *EYE3* and a third eyeless locus, are within six map units of each other on the left arm of chromosome II. Why the loci would be clustered is not immediately apparent, but all are expressed with a similar pattern relative to the cell cycle as shown in Fig. 10. The expression data plotted here were published by Zones et al. (2015). New eyespots are assembled shortly after cell division (Holmes and Dutcher 1989); thus it makes sense that these genes are upregulated coordinately at the beginning of the dark phase when the cells start to divide. Though the chromosome XII eyespot genes range over a large section of the left arm, perhaps there is some local effect on transcription rates in this region with respect to the cell cycle. However, eyespot loci unlinked to those on XII are also coordinately upregulated, such as *EYE3* and *COP4* (ChR2) on II and *COP3* (ChR1) on XIV.

Table 2 Locations of genes important for eyespot assembly, placement, and function in the Chlamydomonas genome

Gene	Phytozome v. 11 Cre #	Linkage group	Location on linkage group in base pairs		Gene size
COP4	cre02.g085257	2	1,623,925	1,631,008	7083
EYE3	cre02.g105600	2	5,183,426	5,189,440	6014
PHOT1	cre03.g199000	3	8,321,420	8,329,663	8243
MIN1	cre12.g490700	12	1,096,696	1,100,777	4081
MLT1	cre12.g509850	12	2,044,806	2,056,067	11,261
EYE2	cre12.g509250	12	2,101,188	2,104,358	3170
COP3	cre14.g611300	14	493,380	500,751	7371
SOUL3	cre16.g666550	16	3,217,434	3,229,838	12,404

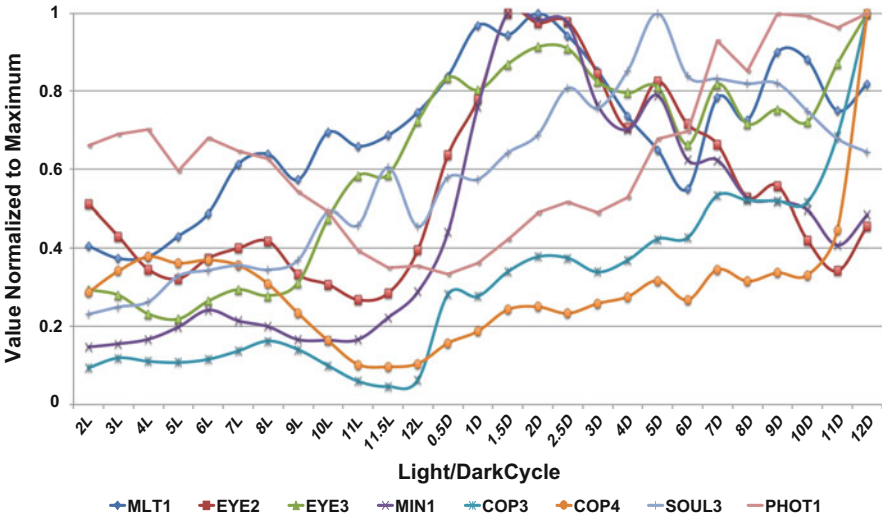

Fig. 10 Expression of genes important for eyespot assembly, placement, and function increases when new eyespots are forming. Changes in expression of Chlamydomonas genes were analyzed over the cell cycle (Zones et al. 2015). Here the data for the subset of genes encoding proteins important for eyespot assembly, placement, and function were plotted as a percentage of the maximum value to reveal the trend of increased expression at cell division, which occurs very early in the dark phase. The cells were exposed to a 12 h light:12 h dark cycle. Gene expression was analyzed every hour of light (L) and dark (D), and every half hour during the transition from light to dark (scale expanded twofold from 11 L to 3D)

10 Future Directions

We predict that our understanding of eyespot biogenesis, placement, and function will progress rapidly in the near future. One of the exciting recent developments that will accelerate all research employing Chlamydomonas as an experimental organism is the availability of insertional mutations in known genes (Li et al. 2016). Coupling this mutational library with eyespot polypeptides identified by proteomics (Eitzinger et al. 2015) may lead quickly to new information about the specific function of individual eyespot proteins and/or provide null strains for the reintroduction of tagged protein constructs or proteins with specific site-directed mutations.

Another continually improving front is the availability of whole-genome sequencing (Lin and Dutcher 2015). This will be an important complement to the insertional library, for analyses of nonlethal point mutations in essential genes, as well as mutations causing more subtle or specific phenotypes in genes for which knockouts are available.

We salute continuing efforts to develop vectors and other methods to successfully avoid the silencing of transgenes in Chlamydomonas, providing reliable

expression of slightly altered native genes, tagged protein constructs for microscopy, or completely foreign genes (Plucinak et al. 2015). These new approaches are critical for establishing and maintaining strains useful for research on the eyespot and other cellular structures. They are also great tools for gene knockdown studies.

Extremely exciting are the many continuing advancements in both fluorescence microscopy and cryoelectron tomography. Absolutely fantastic resolution of the eyespot in Chlamydomonas promises next-generation tools for analysis of eyespot structure and function in wild-type and mutant cells (e.g., Figs. 4 and 5; Engel et al. 2015).

We plan to continue work on several specific eyespot placement and assembly problems. One quest is to visualize photoreceptor movement in live cells. Another is to probe the role of the various domains of the MLT1 protein in exclusive deposition on D4 rootlet microtubules and not others, stimulation of photoreceptor localization, and promotion of eyespot assembly. The assembly of the tightly packed layers of the eyespot is another enigma. Analysis of the LysM domains in MIN1 and EYE2 and that of the C2 domain in MIN1 are particular targets for unraveling the specifics of membrane adhesion. Finally, we still do not know the "master" regulator of eyespot assembly. How is it that EYE2 is localized properly in the chloroplast envelope "under" the plus ends of the D4 microtubule rootlets, when photoreceptors are pooled at the apical pole in dividing *mlt1* mutant cells? There must be a protein(s) associated with the plus ends of the D4 microtubules that signals the proper location for the underlying chloroplast eyespot proteins. We look forward to making progress on these projects and to learning about other studies illuminating Chlamydomonas eyespot structure and function.

References

Awasthi M, Ranjan P, Sharma K, Veetil SK, Kateriya S (2016) The trafficking of bacterial type rhodopsins into the Chlamydomonas eyespot and flagella is IFT mediated. Sci Rep 6:37096

Berthold P, Tsunoda SP, Ernst OP, Mages W, Gradmann D, Hegemann P (2008) Channelrhodopsin-1 initiates phototaxis and photophobic responses in Chlamydomonas by immediate light-induced depolarization. Plant Cell 20:1665–1677

Boyd JS, Gray MM, Thompson MD, Horst CJ, Dieckmann C (2011a) The daughter four-membered microtubule rootlet determines anterior-posterior positioning of the eyespot in *Chlamydomonas reinhardtii*. Cytoskeleton (Hoboken) 68:459–469

Boyd JS, Mittelmeier TM, Lamb MR, Dieckmann C (2011b) Thioredoxin-family protein EYE2 and Ser/Thr kinase EYE3 play interdependent roles in eyespot assembly. Mol Biol Cell 22: 1421–1429

Boyden ES, Zhang F, Bamberg E, Nagel G, Deisseroth K (2005) Millisecond-timescale, genetically targeted optical control of neural activity. Nat Neurosci 8:1263–1268

Davidi L, Shimoni E, Khozin-Goldberg I, Zamir A, Pick U (2014) Origin of β-carotene-rich plastoglobuli in *Dunaliella bardawil*. Plant Physiol 164:2139–2156

Davidi L, Levin Y, Ben-Dor S, Pick U (2015) Proteome analysis of cytoplasmatic and plastidic β-carotene lipid droplets in *Dunaliella bardawil*. Plant Physiol 167:60–79

Davidian JC, Kopriva S (2010) Regulation of sulfate uptake and assimilation--the same or not the same? Mol Plant 3:314–325

Deininger W, Kroger P, Hegemann U, Lottspeich F, Hegemann P (1995) Chlamyrhodopsin represents a new type of sensory photoreceptor. EMBO J 14:5849–5858

Do TQ, Hsu AY, Jonassen T, Lee PT, Clarke CF (2001) A defect in coenzyme Q biosynthesis is responsible for the respiratory deficiency in *Saccharomyces cerevisiae abc1* mutants. J Biol Chem 276:18161–18168

Dutcher SK, Trabuco EC (1998) The *UNI3* gene is required for assembly of basal bodies of Chlamydomonas and encodes delta-tubulin, a new member of the tubulin superfamily. Mol Biol Cell 9:1293–1308

Eitzinger N, Wagner V, Weisheit W, Geimer S, Boness D, Kreimer G, Mittag M (2015) Proteomic analysis of a fraction with intact eyespots of *Chlamydomonas reinhardtii* and assignment of protein methylation. Front Plant Sci 6:1085

Engel BD, Schaffer M, Kuhn Cuellar L, Villa E, Plitzko JM, Baumeister W (2015) Native architecture of the Chlamydomonas chloroplast revealed by *in situ* cryo-electron tomography. eLife 4:3583

Foster KW, Smyth RD (1980) Light antennas in phototactic algae. Microbiol Rev 44:572–630

Foster KW, Saranak J, Patel N, Zarilli G, Okabe M, Kline T, Nakanishi K (1984) A rhodopsin is the functional photoreceptor for phototaxis in the unicellular eukaryote Chlamydomonas. Nature 311:756–759

Fuhrmann M, Stahlberg A, Govorunova E, Rank S, Hegemann P (2001) The abundant retinal protein of the Chlamydomonas eye is not the photoreceptor for phototaxis and photophobic responses. J Cell Sci 114:3857–3863

Geimer S, Melkonian M (2005) Centrin scaffold in *Chlamydomonas reinhardtii* revealed by immunoelectron microscopy. Eukaryot Cell 4:1253–1263

Govorunova EG, Jung K-H, Sineshchekov OA, Spudich JL (2004) Chlamydomonas sensory rhodopsins A and B: cellular content and role in photophobic responses. Biophys J 86: 2342–2349

Greeff C, Roux M, Mundy J, Petersen M (2012) Receptor-like kinase complexes in plant innate immunity. Front Plant Sci 3:1–7

Gust AA (2015) Peptidoglycan perception in plants. PLoS Pathog 11:e1005275

Hartshorne JN (1953) The function of the eyespot in Chlamydomonas. New Phytol 52:292–297

Harz H, Hegemann P (1991) Rhodopsin-regulated calcium currents in Chlamydomonas. Nature 351:489–491

Hegemann P (1997) Vision in microalgae. Planta 203:266–274

Holland EM, Braun FJ, Nonnengässer C, Harz H, Hegemann P (1996) The nature of rhodopsin-triggered photocurrents in Chlamydomonas. I. Kinetics and influence of divalent ions. Biophys J 70:924–931

Holmes JA, Dutcher SK (1989) Cellular asymmetry in *Chlamydomonas reinhardtii*. J Cell Sci 94(Pt 2):273–285

Horst CJ, Witman GB (1993) *ptx1*, a nonphototactic mutant of Chlamydomonas, lacks control of flagellar dominance. J Cell Biol 120:733–741

Horst CJ, Fishkind DJ, Pazour GJ, Witman GB (1999) An insertional mutant of *Chlamydomonas reinhardtii* with defective microtubule positioning. Cell Motil Cytoskeleton 44:143–154

Huang B, Ramanis Z, Dutcher SK, Luck DJ (1982) Uniflagellar mutants of Chlamydomonas: evidence for the role of basal bodies in transmission of positional information. Cell 29:745–753

Kamiya R, Witman G (1984) Submicromolar levels of calcium control the balance of beating between the two flagella in demembranated models of Chlamydomonas. J Cell Biol 98:97–107

Kateriya S, Nagel G, Bamberg E, Hegemann P (2004) "Vision" in single-celled algae. News Physiol Sci 19:133–137

King SJ, Dutcher SK (1997) Phosphoregulation of an inner dynein arm complex in *Chlamydomonas reinhardtii* is altered in phototactic mutant strains. J Cell Biol 136:177–191

Kivic PA, Walne PL (1983) Algal photosensory apparatus probably represent multiple parallel evolutions. Biosystems 16:31–38

Kreimer G (1994) Cell biology of phototaxis in flagellate algae. Int Rev Cytol 148:229–310

Kreimer G (2009) The green algal eyespot apparatus: a primordial visual system and more? Curr Genet 55:19–43
Kreimer G, Melkonian M (1990) Reflection confocal laser scanning microscopy of eyespots in flagellated green algae. Eur J Cell Biol 53:101–111
Lamb MR, Dutcher SK, Worley CK, Dieckmann C (1999) Eyespot-assembly mutants in *Chlamydomonas reinhardtii*. Genetics 153:721–729
LeDizet M, Piperno G (1986) Cytoplasmic microtubules containing acetylated alpha-tubulin in *Chlamydomonas reinhardtii*: spatial arrangement and properties. J Cell Biol 103:13–22
Li X, Zhang R, Patena W, Gang SS, Blum SR, Ivanova N, Yue R, Robertson JM, Lefebvre PA, Fitz-Gibbon ST, Grossman AR, Jonikas MC (2016) An indexed, mapped mutant library enables reverse genetics studies of biological processes in *Chlamydomonas reinhardtii*. Plant Cell 28:367–387
Lin H, Dutcher SK (2015) Genetic and genomic approaches to identify genes involved in flagellar assembly in *Chlamydomonas reinhardtii*. Methods Cell Biol 127:349–386
Lohscheider JN, Friso G, van Wijk KJ (2016) Phosphorylation of plastoglobular proteins in *Arabidopsis thaliana*. J Exp Bot 67(13):3975–3984. doi:10.1093/jxb/erw091
Luck M, Mathes T, Bruun S, Fudim R, Hagedorn R, Tran Nguyen TM, Kateriya S, Kennis JTM, Hildebrandt P, Hegemann P (2012) A photochromic histidine kinase rhodopsin (HKR1) that is bimodally switched by ultraviolet and blue light. J Biol Chem 287:40083–40090
Lundquist PK, Davis JI, van Wijk KJ (2012) ABC1K atypical kinases in plants: filling the organellar kinase void. Trends Plant Sci 17:546–555
Matsunaga S, Watanabe S, Sakaushi S, Miyamura S, Hori T (2003) Screening effect diverts the swimming directions from diaphototactic to positive phototactic in a disk-shaped green flagellate *Mesostigma viride*. Photochem Photobiol 77:324–329
Melkonian M, Robenek H (1980) Eyespot membranes of *Chlamydomonas reinhardii*: a freeze-fracture study. J Ultrastruct Res 72:90–102
Mittelmeier TM, Berthold P, Danon A, Lamb MR, Levitan A, Rice ME, Dieckmann C (2008) C2 domain protein MIN1 promotes eyespot organization in *Chlamydomonas reinhardtii*. Eukaryot Cell 7:2100–2112
Mittelmeier TM, Dieckmann C, Boyd JS, Lamb MR (2011) Asymmetric properties of the *Chlamydomonas reinhardtii* cytoskeleton direct rhodopsin photoreceptor localization. J Cell Biol 193:741–753
Mittelmeier TM, Thompson MD, Oztürk E, Dieckmann C (2013) Independent localization of plasma membrane and chloroplast components during eyespot assembly. Eukaryot Cell 12: 1258–1270
Mittelmeier TM, Thompson MD, Lamb MR, Lin H, Dieckmann C (2015) MLT1 links cytoskeletal asymmetry to organelle placement in Chlamydomonas. Cytoskeleton 72:1–11
Morel-Laurens N, Feinleib ME (1983) Photomovement in an "eyeless" mutant of Chlamydomonas. Photochem Photobiol 37:189–194
Nagel G, Ollig D, Fuhrmann M, Kateriya S, Musti AM, Bamberg E, Hegemann P (2002) Channelrhodopsin-1: a light-gated proton channel in green algae. Science 296:2395–2398
Nagel G, Szellas T, Huhn W, Kateriya S, Adeishvili N, Berthold P, Ollig D, Hegemann P, Bamberg E (2003) Channelrhodopsin-2, a directly light-gated cation-selective membrane channel. Proc Natl Acad Sci U S A 100:13940–13945
Nagel G, Szellas T, Kateriya S, Adeishvili N, Hegemann P, Bamberg E (2005) Channelrhodopsins: directly light-gated cation channels. Biochem Soc Trans 33:863–866
Nonnengässer C, Holland EM, Harz H, Hegemann P (1996) The nature of rhodopsin-triggered photocurrents in Chlamydomonas. II. Influence of monovalent ions. Biophys J 70:932–938
Okita N, Isogai N, Hirono M, Kamiya R, Yoshimura K (2005) Phototactic activity in Chlamydomonas "non-phototactic" mutants deficient in Ca2+−dependent control of flagellar dominance or in inner-arm dynein. J Cell Sci 118:529–537

Ozawa SI, Nield J, Terao A, Stauber EJ, Hippler M, Koike H, Rochaix JD, Takahashi Y (2009) Biochemical and structural studies of the large Ycf4-photosystem I assembly complex of the green alga *Chlamydomonas reinhardtii*. Plant Cell 21:2424–2442

Piasecki BP, Silflow CD (2009) The *UNI1* and *UNI2* genes function in the transition of triplet to doublet microtubules between the centriole and cilium in Chlamydomonas. Mol Biol Cell 20:368–378

Plucinak TM, Horken KM, Jiang W, Fostvedt J, Nguyen ST, Weeks DP (2015) Improved and versatile viral 2A platforms for dependable and inducible high-level expression of dicistronic nuclear genes in *Chlamydomonas reinhardtii*. Plant J 82:717–729

Ringo DL (1967) Flagellar motion and fine structure of the flagellar apparatus in Chlamydomonas. J Cell Biol 33:543–571

Roberts DG, Lamb MR, Dieckmann C (2001) Characterization of the *EYE2* gene required for eyespot assembly in *Chlamydomonas reinhardtii*. Genetics 158:1037–1049

Rüffer U, Nultsch W (1985) High-speed cinematographic analysis of the movement of Chlamydomonas. Cell Motil Cytoskeleton 5:251–263

Rüffer U, Nultsch W (1987) Comparison of the beating of *cis*- and *trans*-flagella of Chlamydomonas cells held on micropipettes. Cell Motil Cytoskeleton 7:87–93

Rüffer U, Nultsch W (1997) Flagellar photoresponses of *ptx1*, a nonphototactic mutant of Chlamydomonas. Cell Motil Cytoskeleton 37:111–119

Schmidt M, Gessner G, Luff M, Heiland I, Wagner V, Kaminski M, Geimer S, Eitzinger N, Reissenweber T, Voytsekh O, Fiedler M, Mittag M, Kreimer G (2006) Proteomic analysis of the eyespot of *Chlamydomonas reinhardtii* provides novel insights into its components and tactic movements. Plant Cell 18:1908–1930

Schulze T, Schreiber S, Iliev D, Boesger J, Trippens J, Kreimer G, Mittag M (2013) The heme-binding protein SOUL3 of *Chlamydomonas reinhardtii* influences size and position of the eyespot. Mol Plant 6:931–944

Schuster G, Dewit M, Staehelin A, Ohad I (1986) Transient inactivation of the thylakoid photosystem II light-harvesting protein kinase system and concomitant changes in intramembrane particle size during photoinhibition of *Chlamydomonas reinhardtii*. J Cell Biol 103:71–80

Sineshchekov OA, Govorunova EG (2001) Rhodopsin receptors of phototaxis in green flagellate algae. Biochemistry (Mosc) 66:1300–1310

Sineshchekov O, Jung K, Spudich J (2002) Two rhodopsins mediate phototaxis to low- and high-intensity light in *Chlamydomonas reinhardtii*. Proc Natl Acad Sci U S A 99:8689–8694

Sineshchekov OA, Govorunova EG, Spudich JL (2009) Photosensory functions of channelrhodopsins in native algal cells. Photochem Photobiol 85:556–563

Suzuki T, Yamasaki K, Fujita S, Oda K, Iseki M, Yoshida K, Watanabe M, Daiyasu H, Toh H, Asamizu E, Tabata S, Miura K, Fukuzawa H, Nakamura S, Takahashi T (2003) Archaeal-type rhodopsins in Chlamydomonas: model structure and intracellular localization. Biochem Biophys Res Commun 301:711–717

Trippens J, Greiner A, Schellwat J, Neukam M, Rottmann T, Lu Y, Kateriya S, Hegemann P, Kreimer G (2012) Phototropin influence on eyespot development and regulation of phototactic behavior in *Chlamydomonas reinhardtii*. Plant Cell 24:4687–4702

Ueki N, Ide T, Mochiji S, Kobayashi Y, Tokutsu R, Ohnishi N, Yamaguchi K, Shigenobu S, Tanaka K, Minagawa J, Hisabori T, Hirono M, Wakabayashi K-I (2016) Eyespot-dependent determination of the phototactic sign in *Chlamydomonas reinhardtii*. Proc Natl Acad Sci U S A 113:5299–5304

van Wijk KJ, Kessler F (2017) Plastoglobuli: plastid microcompartments with integrated functions in metabolism, plastid developmental transitions, and environmental adaptation. Annu Rev Plant Biol 68:253–289

Wakabayashi K, Misawa Y, Mochiji S, Kamiya R (2011) Reduction-oxidation poise regulates the sign of phototaxis in *Chlamydomonas reinhardtii*. Proc Natl Acad Sci U S A 108:11280–11284

Wagner V, Ullmann K, Mollwo A, Kaminski M, Mittag M, Kreimer G (2008) The phosphoproteome of a *Chlamydomonas reinhardtii* eyespot fraction includes key proteins of the light signaling pathway. Plant Physiol 146:772–788

Wietek J, Prigge M (2016) Enhancing channelrhodopsins: an overview. Methods Mol Biol 1408: 141–165

Witman GB (1993) Chlamydomonas phototaxis. Trends Cell Biol 3:403–408

Woessner JP, Goodenough UW (1994) Volvocine cell walls and their constituent glycoproteins: an evolutionary perspective. Protoplasma 181:245–258

Xie LX, Hsieh EJ, Watanabe S, Allan CM, Chen JY, Tran UC, Clarke CF (2011) Expression of the human atypical kinase ADCK3 rescues coenzyme Q biosynthesis and phosphorylation of Coq polypeptides in yeast *coq8* mutants. Biochim Biophys Acta 1811:348–360

Zones JM, Blaby IK, Merchant SS, Umen JG (2015) High-resolution profiling of a synchronized diurnal transcriptome from *Chlamydomonas reinhardtii* reveals continuous cell and metabolic differentiation. Plant Cell 27:2743–2769